

Campbell, T.D. (1975) Strains, deformations and buckling in very thin torispherical pressure vessel ends. PhD thesis, University of Nottingham.

**Access from the University of Nottingham repository:**

<http://eprints.nottingham.ac.uk/13321/1/450631.pdf>

**Copyright and reuse:**

The Nottingham ePrints service makes this work by researchers of the University of Nottingham available open access under the following conditions.

This article is made available under the University of Nottingham End User licence and may be reused according to the conditions of the licence. For more details see:  
[http://eprints.nottingham.ac.uk/end\\_user\\_agreement.pdf](http://eprints.nottingham.ac.uk/end_user_agreement.pdf)

**A note on versions:**

The version presented here may differ from the published version or from the version of record. If you wish to cite this item you are advised to consult the publisher's version. Please see the repository url above for details on accessing the published version and note that access may require a subscription.

For more information, please contact [eprints@nottingham.ac.uk](mailto:eprints@nottingham.ac.uk)

STRAINS, DEFORMATIONS AND BUCKLING IN VERY  
THIN TORISPHERICAL PRESSURE VESSEL ENDS

BY

T. D. CAMPBELL, B.Sc.(Eng.)

Thesis submitted to the University of Nottingham  
for the degree of Doctor of Philosophy  
May 1975

## CONTENTS

Page No.

### ABSTRACT

#### 1. INTRODUCTION

1.1	General	1
1.2	Notation	3
1.3	Basic geometrical relationships	5

#### 2. LITERATURE SURVEY

2.1	General	6
2.2	Theoretical	6
2.2.1	Galletly G.D.	6
2.2.2	Shield R.T. and Drucker D.C.	7
2.2.3	Mescall J.	9
2.2.4	Thurston G.A. and Holston A.A.	9
2.2.5	Rotondo P. and Kraus H.	10
2.2.6	Esztergar E.P. and Kraus H.	11
2.3	Experimental	12
2.3.1	Meesters A.G. and Slaaf C.M.	12
2.3.2	Jones O.	13
2.3.3	Fino A. and Schneider R.W.	13
2.3.4	Adachi J. and Benicek M.	14
2.3.5	Stennet R.	15
2.3.6	Kemper M.J.	15
2.4	Codes and standards	16
2.4.1	British Standards	16
2.4.1.1	B.S. 1500:1958	16
2.4.1.2	B.S. 1515: Part 2: 1968	17
2.4.1.3	B.S. 3915: 1965	17
2.4.2	ASME Code: Section VIII:div. 1: 1971	18

2.5	Other literature	18
3.	MATERIAL AND MANUFACTURE	
3.1	Material	20
3.1.1	General	20
3.1.2	Chemical composition	21
3.1.3	Mechanical properties	21
3.2	Manufacture of ends	21
3.2.1	General	21
3.2.2	"Pressed and spun"	22
3.2.3	"Crown and segment"	22
3.3	Fabrication	23
4.	CHOICE OF ENDS	
4.1	General	24
4.2	54 in diameter test ends	25
4.2.1	End 1	26
4.2.2	End 2	26
4.2.3	End 3	26
4.2.4	End 4	26
4.2.5	End 5	26
4.2.6	End 6	27
4.3	108 in diameter test ends	27
4.3.1	End 7	27
4.3.2	End 8	27
4.3.3	End 9	28
4.3.4	End 10	28
4.3.5	End 11	28
4.3.6	End 12	28
4.3.7	End 13	28

	<u>Page No.</u>
4.4 81. in diameter test ends	29
4.4.1 End 14	29
4.4.2 End 15	29
4.4.3 End 16	29
4.4.4 End 17	30
4.5 Principal sets	30
5. TEST INSTALLATION	
5.1 General	31
5.2 Preparation "cradle" and test stand	31
5.3 Pressurising system	31
5.4 Pole attachment	32
5.5 Strain measuring and recording system	33
5.6 End height growth gauge	35
5.7 Circumferential growth gauge	36
6. VESSEL PREPARATION AND TEST PROCEDURE	
6.1 Vessel preparation	37
6.1.1 General	37
6.1.2 Marking out	37
6.1.3 Thickness measurements	38
6.1.4 Curvature measurements	38
6.1.5 Strain gauging of ends	39
6.1.5.1 Gauge coverage	39
6.1.5.2 Bonding of gauges	40
6.1.5.3 Water-proofing	41
6.1.6 Welding test end to base end	42
6.1.7 Final preparation for test	43
6.1.8 Vessel parting	43
6.2 Test procedure	44

## 7. RESULTS

7.1	Introduction	46
7.2	End No.9	47
7.3	54 in diameter ends	49
7.3.1	End No.1	49
7.3.2	Ends No.2 - 6	49
7.4	108 in and 81 in diameter ends	50
7.4.1	End No. 7 (Crown and segment base end).	50
7.4.2	Ends No. 8, and 10 to 17	50

## 8. DISCUSSION

8.1	Individual ends	53
8.1.1	End No.1	53
8.1.2	End No.2	55
8.1.3	End No.3	57
8.1.4	End No.4	59
8.1.5	End No.5	61
8.1.6	End No.6	62
8.1.7	End No.7	63
8.1.8	End No.8	65
8.1.9	End No.9	67
8.1.10	End No.10	69
8.1.11	End No.11	71
8.1.12	End No.12	72
8.1.13	End No.13	74
8.1.14	End No.14	76
8.1.15	End No.15	78
8.1.16	End No.16	79
8.1.17	End No.17	81

8.2	Shape/Thickness defects	83
8.2.1	General	83
8.2.2	Thickness	83
8.2.2.1	Pressed and spun ends	83
8.2.2.2	Crown and segment ends	84
8.2.3	Curvature	84
8.3	Material properties	85
8.3.1	Test procedure	85
8.3.2	Stress-strain characteristics	86
8.3.3	Overall results	87
8.4	Residual stresses	88
8.4.1	General	88
8.4.2	Procedure	88
8.4.3	Results	89
8.4.4	Residual stresses predicted from pressure test measurements	91
8.4.5	Layer residual stresses	92
8.5	The effect of nominal shape/thickness parameters on end behaviour	94
8.5.1	General	94
8.5.2	Elastic behaviour	94
8.5.3	Post-yield behaviour	96
8.5.4	Buckling behaviour	97
8.6	Computations	98
8.7	Design considerations	100
8.7.1	Comparison with limit pressures and theoretical buckling pressures	100
8.7.2	Alternative approaches	104
8.7.2.1	The knuckle as a ring subjected to external pressure	104
8.7.2.2	The knuckle as a "column" with a transverse elastic support	106

	<u>Page No.</u>
8.7.3 Range of buckling pressures	109
8.7.4 Time-dependence of buckling	110
8.7.5 Materials	111
9. FUTURE WORK	112
10. CONCLUSIONS	113

REFERENCES

ACKNOWLEDGEMENTS

APPENDIX I

Thickness and curvature variations, pressure-strain curves and strain and stress index distributions.

APPENDIX 2

Summary sheets.



## LIST OF FIGURES

- 1.1 Geometry of torispherical end.
- 2.1 Variation of limit pressure with thickness from the formula and graphical data of ref. 15.
- 2.2 Comparison of experimental (ref. 12) and theoretical (refs 10 and 16) elastic buckling pressures.
- 4.1 Test ends.
- 4.2 Base ends-support ring details.
- 4.3 Crown and segment ends - position of knuckle segments.
- 5.1 Test stand.  
Preparation cradle.
- 5.2 Vessel assembly for 54 in diameter ends.
- 5.3 Pressurising system.
- 5.4 Pole attachment.
- 5.5 Strain measuring and recording system.
- 5.6 Flow diagrams of PDP8 data acquisition system.
- 6.1 Curvature measuring device.
- 6.2 Gauge location. End. No.3.
- 6.3 Vessel parting-improved method.  
Vessel parting-cutting machine.
- 7.1 - 7.33 Set of graphs for end No.9.
- 7.34 - 7.38 Examples of buckles produced.
- 8.1 - 8.10 Test history diagrams .
- 8.11 Stress-strain curves of higher proof stress 304 stainless steel.
- 8.12 Change in Vickers hardness number against reduction in thickness.
- 8.13a Proportional limit stress.

- 8.13b 0.01% proof stress.
- 8.14a 0.05% proof stress.
- 8.14b 0.1% proof stress.
- 8.15a 0.2% proof stress.
- 8.15b Ultimate tensile strength.
- 8.16 Residual loads and stresses for end No.10.
- 8.17 Residual loads and stresses for end No.11.
- 8.18 Residual loads and stresses for end No.13.
- 8.19 Residual loads and stresses for Kemper end (ref. 24).
- 8.20 Combined pressure and residual stresses for end No.10.
- 8.21 Combined pressure and residual stresses for end No.11.
- 8.22 Surface hardness in knuckle region.
- 8.23 Derived and measured equivalent residual stresses.
- 8.24 "Layer" residual stress specimen.
- 8.25 The effect of thickness on the peak stress indices  $I_{oc}$  and  $I_{im}$ .
- 8.26 The effect of knuckle radius on the peak stress indices  $I_{oc}$  and  $I_{im}$ .
- 8.27 The effect of crown radius on the peak stress indices  $I_{oc}$  and  $I_{im}$ .
- 8.28 The effect of thickness on limit pressure.
- 8.29 The effect of knuckle radius on limit pressure.
- 8.30 The effect of crown radius on limit pressure.
- 8.31 The effect of thickness on first buckling pressure.
- 8.32 The effect of knuckle radius on first buckling pressure.
- 8.33 The effect of crown radius on first buckling pressure.
- 8.34 End No.4. Distribution of elastic stress indices.
- 8.35 Variation of  $\bar{R}$  with  $t_e/D_i$
- 8.36 Determination of R and N.

## LIST OF TABLES

- 2.1 Details of ends which have failed by buckling.
  
- 4.1 Nominal dimensions and shape parameters.
  
- 6.1 Strain gauge positions - distance from pole in inches on the meridians indicated.
  
- 7.1 Comparison of nominal and measured dimensions.
- 7.2 Elastic strain factors and stress indices.
- 7.3a Post yield behaviour of ends prior to buckling.
- 7.3b Maximum peak strains not given in table 7.3a.
- 7.4 Summary of buckle development.
  
- 8.1 Ratios of experimental buckling pressure to limit pressure (ref. 15) and theoretical buckling pressure (ref. 10).
- 8.2 Other ratios of experimental buckling pressure to limit pressure (ref. 15) and theoretical buckling pressure (ref. 10).
- 8.3 Calculated and measured buckling pressures.
- 8.4 Calculated and measured buckling pressures for other ends.

## ABSTRACT

An experimental study has been made of the behaviour of "very thin" torispherical ends subjected to internal pressure. The seventeen ends tested were full-size production ends made from stainless steel, with thickness to diameter ratios ( $t_e/D_i$ ) varying from 0.002 to 0.001. At each value of  $t_e/D_i$  the knuckle radius ( $r_i$ ) and crown radius ( $R_i$ ) were varied to cover the range of ends frequently used.

Each end was strain gauged on both inner and outer surfaces and then pressurised until buckling occurred in the knuckle region. The strain gauges were monitored throughout each test thus giving a detailed coverage of the strain distribution. High compressive hoop strains, shown to exist on both surfaces of the knuckle, are responsible for the buckling mode of failure.

A shape/thickness survey was performed on each end prior to pressure testing. The effects of thickness reductions and deviations of curvature from the nominal are discussed.

Residual strain measurements were made on three ends and were shown to be significantly large in the pressed and spun manufactured ends. A study of the effect of work hardening on the properties of the material from which the ends were made is also presented. It is shown that the proof stress and Vickers hardness number increases rapidly when the material is work hardened.

The dependence of the elastic stress indices, limit pressures and first buckling pressures on wall thickness, knuckle radius and crown radius has been examined.

The design implications of the study are discussed and a method for predicting the first buckling pressure of production ends given.

CHAPTER 1INTRODUCTION1.1. General

The torispherical end is widely used as a closure for cylindrical pressure vessels and a large volume of literature has been written on its behaviour under internal pressure. Past work includes experimental (ref. 1) and numerical work (2, 3) in the elastic range, limit load studies (4) and shakedown investigations (5).

However, most of the existing literature pertains to relatively thick ends (thickness/diameter ( $t/D$ ) ratio greater than 0.002); "very thin" ends ( $t/D < 0.002$ ) have received sparse attention. (The "very thin" designation has been used previously (6)). Such ends find a very wide application in industry throughout the world and can represent a large capital investment for the companies concerned. They are used in low-pressure (10 - 100 lbf/in<sup>2</sup>) applications such as food processing, brewing and distilling where large, high-quality vessels are essential. There are also applications in reactor installations. In most cases the vessel material is stainless steel; the higher proof stress grades are usually favoured for economy.

The maximum stress due to internal pressure in most ends with  $t/D$  greater than 0.002 is the meridional stress on the inner surface of the knuckle part of the end. The possible failure modes of these ends are well understood and their design is covered by the existing codes and standards.

As the  $t/D$  ratio is reduced towards 0.002 the circumferential stress on the outer surface of the knuckle (which is compressive) increases at a greater rate than the inner surface meridional stress and eventually can become the maximum stress in the end (6, 7). The circumferential stress on the inner surface of the knuckle, which is a relatively small stress in

the thicker ends, also grows until it approaches the outer surface circumferential stress value. These high circumferential compressive stresses result in an additional possible failure mode, viz instability (or "buckling" or "wrinkling") in the knuckle region.

This buckling may occur whilst the knuckle stresses are elastic (elastic buckling) or after the elastic limit has been passed (plastic buckling) but the thinner the end, the more likely it is that the critical pressure will be less than the limit pressure. When this occurs the former should replace the latter as the design basis for the end.

The first report of knuckle buckling appears to be that by Meester and Slaaf (8). Galletly drew attention to the possibility in a well known paper (7) and Fino and Schneider (9) described a notable example in some detail. This mode of failure was also mentioned by Fessler and Stanley (6). The most advanced theoretical treatment (10) predicts buckling pressures about four times greater than those observed for production ends (11). Clearly idealisations and assumptions made in the theoretical work cannot be carried over to production ends. Work with small scale models (12) supported the theoretical work but because important features of production ends were inevitably not reproduced, the work does not provide a satisfactory design basis.

Current British standards do not give recommendations for the design of ends with  $t/D$  less than 0.002. (BS 1515 mentions however that ends with small knuckle radii are prone to buckling in the knuckle region.) Since the recommendations for greater  $t/D$  values are based on failure modes other than buckling simple extrapolation of the existing design curves is not acceptable. The Fino and Schneider end (9) was designed to an early version of the A.S.M.E. code.

It was considered that progress towards the framing of reliable design rules for these ends could not be made without a systematic experimental study of their behaviour. Such a study has been carried out in this project.

The objective of the work was to determine the strain and deformation behaviour of a series of typical, full-size, torispherical end closures, with t/D ratios of 0.002 or less, subjected to internal pressure.

The ends were large diameter "production" ends made from higher proof stress stainless steel by standard manufacturing methods and were typical in every respect of "very thin" ends used in industry. Each vessel was tested at a series of increasing pressures until failure in the form of buckling and/or excessive plastic deformation occurred. Parallel studies of the shape and thickness variations, material properties and residual stresses were also carried out. The work is critically discussed.

## 1.2 Notation

c	suffix - circumferential
	suffix - in cylinder
e	suffix - in end
el	suffix - elastic behaviour of material
h	end height
i	suffix - inner surface
l	gauge length of curvature measuring device
m	suffix - meridional
o	suffix - outer surface
p	pressure
$p_{CR}$	first buckling pressure
$p_{FI}$	pressure at which I and F are determined
$p^L$	lower bound limit pressure
$p_{NL}$	pressure at which pressure-strain curve becomes non-linear
$p_{S\&D}$	Shield and Drucker (ref. 15) limit pressure
$p_{TH}$	Thurston and Holston (ref. 10) buckling pressure

$p^u$	upper bound limit pressure
$r$	knuckle radius
$s$	distance from pole
$t$	thickness
$x$	height indicated by curvature measuring device
$x,y$	coordinates
$C$	curvature
$D$	cylinder diameter
$E$	modulus of elasticity
$F$	strain factor ( $\epsilon \div (pD_i(1-\nu/2)/2t_e E)$ )
$H_v$	Vickers hardness number
$I$	stress index ( $\sigma \div (pD_i/2t_e)$ )
$L$	cylinder length
$M$	moment/unit length of circumference
$N$	force/unit length of circumference
$R$	crown radius
$\alpha$	angle subtended by knuckle at centre of meridional curvature.
$\Delta$	prefix - a small increment
$\epsilon$	strain
$\theta$	suffix - circumferential
$\nu$	Poisson's ratio
$\sigma$	stress
$\phi$	suffix - meridional



### 1.3 Basic Geometrical Relationships

The torispherical end (Fig. 1.1) is an axisymmetric shell formed by combining a toroidal "knuckle" and spherical "crown". Although there is an abrupt change in curvature at the knuckle/crown junction there is no discontinuity in slope

The end shape is defined in terms of the crown and knuckle radii ( $R$  and  $r$ ). The relationship between  $R$ ,  $r$  and the head height ( $h$ ) is :

$$(R - h)^2 + \left(\frac{D}{2} - r\right)^2 = (R - r)^2 \quad 1.1$$

This equation can be written in terms of the shape parameters  $R/D$ ,  $r/D$ , and  $h/D$  as follows :

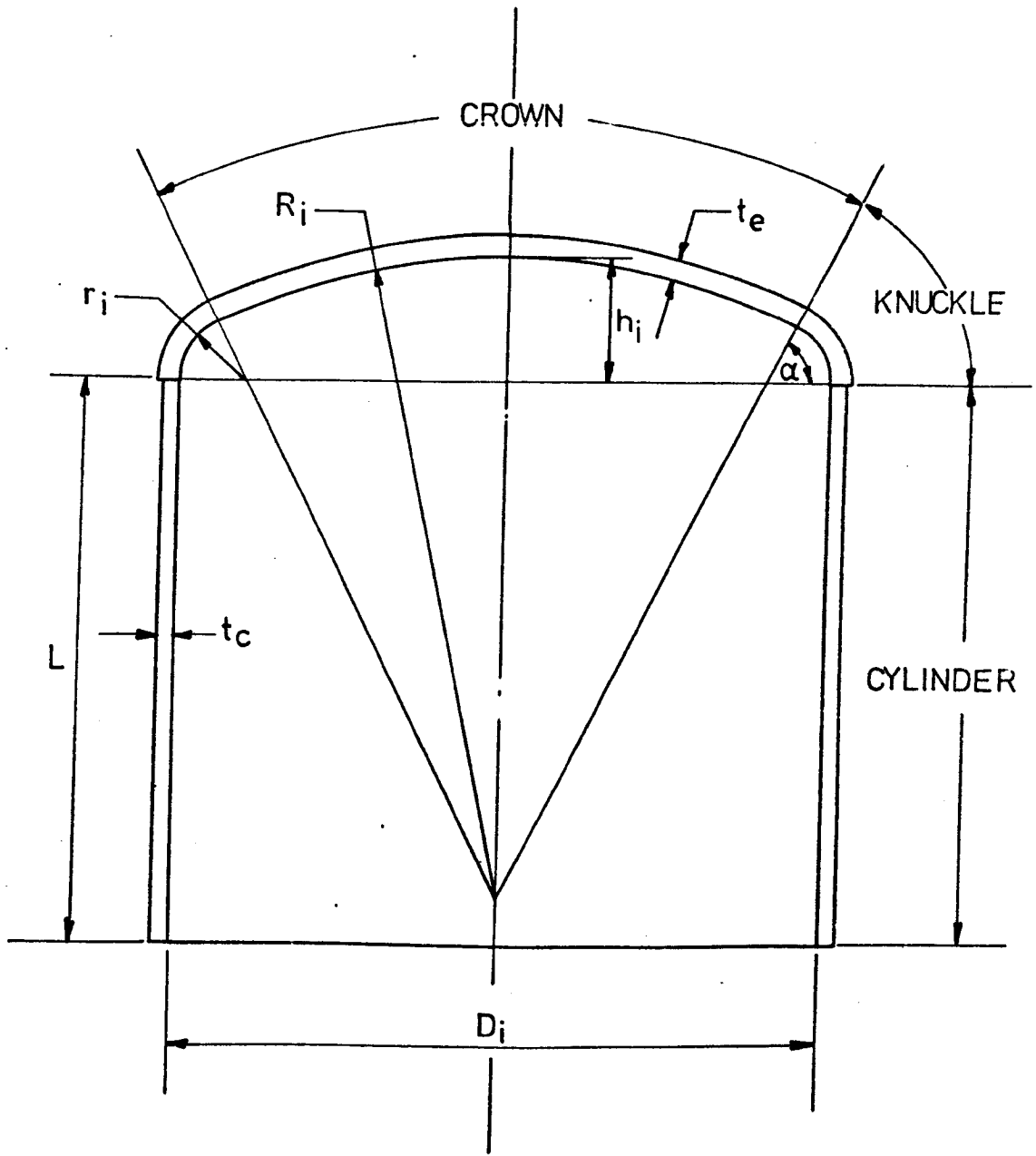
$$\frac{R}{D} = \frac{\frac{1}{4} + \left(\frac{h}{D}\right)^2 - \frac{r}{D}}{2 \left(\frac{h}{D} - \frac{r}{D}\right)} \quad 1.2$$

or 
$$\frac{r}{D} = \frac{2 \frac{R}{D} \frac{h}{D} - \left(\frac{h}{D}\right)^2 - \frac{1}{4}}{2 \frac{R}{D} - 1} \quad 1.3$$

The angle ( $\alpha$ ) subtended by the knuckle at the centre of meridional curvature is given by :

$$\sin \alpha = \frac{\frac{R}{D} - \frac{h}{D}}{\frac{R}{D} - \frac{r}{D}} \quad 1.4$$

The above equations refer to the geometrically perfect end. It is known that in production ends the "real" geometry varies considerably from the nominal.



GEOMETRY OF TORISPHERICAL END.

CHAPTER 2LITERATURE SURVEY.2.1 General

The following survey is a brief summary of the important reports and papers relevant to the present study. The work is divided into three main parts; namely theoretical, experimental and codes. Within each part the items are presented in chronological order.

2.2 Theoretical2.2.1 Galletly G.D. (refs. 2, 7 and 13)

The inadequacy of the then ASME Unfired Pressure Vessel Code was discussed by Galletly in ref. 7 following the collapse of a large pressure vessel during hydrostatic proof testing in America. He compared the results of an accurate stress analysis with values predicted by the code.

In Galletly's analysis the differential equations of equilibrium governing the bending of a shell of revolution with constant thickness and meridional curvature were modified to include the effects of non-uniform internal pressure. The two resulting second-order differential equations were then reduced to a single second-order non-homogeneous differential equation. This equation was specialised to apply to spherical and toroidal shells. Solutions for the cylinder, knuckle and crown, obtained with the aid of a computer, allowed the edge displacements and rotations of the various shells to be calculated in terms of the unknown edge moments and shearing forces. When compatibility equations were applied a set of simultaneous linear algebraic equations for the edge moments and shearing forces was obtained. From the solution of these equations the edge conditions were determined thus enabling the complete elastic stress distribution to be obtained.

In ref. 7 the analysis is applied to a torispherical end with  $t/D_i = 0.00227$ ,  $r_i/D_i = 0.0652$  and  $R_i/D_i = 0.8231$ . At a pressure of

60 lbf/in<sup>2</sup> (the proof test pressure) the American code predicted a maximum stress of 18,000 lbf/in<sup>2</sup>. Stress values obtained by Galletly were :-

maximum circumferential stress	55,000 lbf/in <sup>2</sup> compression (outer surface of knuckle)
maximum mean circumferential stress	45,000 lbf/in <sup>2</sup> compression (knuckle)
maximum meridional stress	48,000 lbf/in <sup>2</sup> tension (inner surface of knuckle)
maximum meridional bending stress	40,000 lbf/in <sup>2</sup>

The material had a yield stress of 30,000 lbf/in<sup>2</sup> and so a "limit pressure" approach to the problem was considered useful. Subsequently Shield and Drucker calculated a collapse pressure of 49 lbf/in<sup>2</sup>.

Galletly high-lighted the shortcomings of the ASME code and concluded that elastic buckling in the knuckle region was a possibility for thin ends made from high yield stress material.

In a second paper (2) the analysis was applied to 125 torispherical ends. The results were tabulated in the form of edge influence coefficients, i.e. the displacement and rotation at an edge due to a unit value of edge moment, edge shearing force or pressure.

Ref. 13 describes how influence coefficients can be used to obtain stress distributions. The method is illustrated by means of two examples.

#### 2.2.2 Shield R.T. and Drucker D.C. (Refs. 4, 14 and 15)

Shield and Drucker have applied the technique of limit analysis to the torispherical end under internal pressure to determine the pressure at which appreciable plastic deformation occurs (i.e. the limit pressure). The analysis is an extension of earlier work by Drucker, Onat, Hodge and Prager. It assumes a perfectly plastic material and a maximum shear stress yielding criterion. In ref. 4 it is assumed that the knuckle is held rigidly at its junctions with the crown and cylinder. The upper bound

limit pressure is derived using a simplified circumscribed yield surface whilst the lower bound limit pressure is assumed to be three quarters of the upper bound value. For design purposes a limit pressure, seven-eighths of the upper bound value is suggested. The analysis is applied to an illustrative example. It is stated that the analysis is not valid for ends with extremely small values of  $t/r$ .

In ref. 14 the analysis is applied to an ASME standard head and it is shown that below a  $t/D$  value of 0.010 a vessel designed to the ASME code may become unsafe.

In their third paper (15) the authors derive upper ( $p^U$ ) and lower ( $p^L$ ) bounds on the limit pressure for a range of ends of different shape and thickness. The results are presented in the form of a series of curves in which the bounds are plotted against the geometric parameters. The following approximate formula is also presented :

$$\frac{np^D}{\sigma_0} = \left( 0.33 + 5.5\frac{r}{D} \right) \frac{t}{R} + 28 \left( 1 - 2.2\frac{r}{D} \right) \left( \frac{t}{R} \right)^2 - 0.0006$$

where  $np^D$  is the limit pressure,  $p^D$  is the design pressure,  $n$  is a factor of safety and  $\sigma_0$  is the yield stress of the material.

Agreement between values of limit pressure derived from the formula and the average of values obtained from the upper and lower bound curves is good (see Fig. 2.1). However it has been shown that for very thin ends (6) the formula does not hold, since the value of  $np^D/\sigma_0$  becomes negative as  $t/D$  approaches zero.

Curves are presented for  $t/D$  values down to 0.002, and can be extrapolated below this but the authors recognise that very thin ends will fail by buckling due to circumferential compression.

The analysis assumes hinge points to exist in the cylinder, knuckle and crown. However for thinner ends the "cylinder" hinge point moves into the knuckle and this has not been taken into account.

It is clearly shown that for constant  $t/D$  and  $R/D$  ratios the limit

pressure decreases as  $r/D$  decreases. Similarly as  $R/D$  decreases the limit pressure increases for constant values of  $t/D$  and  $r/D$ .

### 2.2.3 Mescall J. (ref. 16)

This work appears to be the first attempt to predict theoretically the buckling pressure of a torispherical end.

Linear bending theory based on asymptotic integration was used to calculate the prebuckling stress distribution whilst the buckling pressure was obtained by applying a Rayleigh-Ritz procedure to a potential energy expression.

Results for two shapes of end were given and it is shown that the buckling pressure decreases rapidly as the thickness is reduced. The results are in fairly close agreement with those obtained from the models of Adachi and Benicek (12) (see Fig. 2.2) but serious discrepancies were found between the theoretical and experimental critical pressure values obtained for a large aluminium bulkhead. The bulkhead buckled at  $25 \text{ lbf/in}^2$  whilst the theory predicted a pressure of  $64 \text{ lbf/in}^2$ . Mescall's report stated that stresses very near to yield occurred at  $25 \text{ lbf/in}^2$  and suggested that this may be responsible for the low buckling pressure observed.

### 2.2.4 Thurston G.A. and Holston A.A. (ref. 10)

This report contains the most advanced theoretical analysis of buckling in shallow axisymmetric end closures subjected to internal pressure. In this treatment of the problem non-linear finite deflection theory is used to obtain the prebuckling stress distribution and the elastic buckling pressures are obtained from linearised equations derived from the non-linear strain-displacement relations listed by Sanders (17).

A number of different boundary conditions were used in the determination of the axisymmetric prebuckled stress state. For most of the ends it was assumed that a cylinder of the same material and thickness was attached to the end. However one end shape was also analysed with both membrane (i.e.

no edge transverse shear or moment) and clamped (i.e. no radial deflection or edge rotation) boundary conditions. The results suggest that the buckling pressure is not sensitive to the edge condition used to determine the prebuckling stresses.

For the asymmetric buckling modes only a clamped edge boundary condition was used.

The report illustrates the difference in stress levels obtained by linear and finite deflection theory. For a given pressure the compressive hoop stresses calculated from non-linear theory are lower than those obtained from the linear theory and consequently, the finite deflection analysis predicts higher buckling pressures. However it is shown that the buckling theory used predicts lower critical pressures than those obtained by Mescall (16) for a particular shape of end.

The behaviour of semi-ellipsoidal ends is also described. It is predicted that ends can have an  $h/D$  ratio less than 0.35 ( $\sqrt{2}:1$  ellipsoid) and still not fail by buckling. For example an end with an  $h/D$  ratio of 0.2 will not buckle if the  $t/D$  ratio is greater than 0.0023.

Thurston and Holston have analysed ends with  $t/D$  ratios varying from 0.00017 to 0.00156. However the report does not fully cover the range of ends frequently used. This sparse coverage presents difficulties when attempts are made to interpolate and extrapolate values.

#### 2.2.5 Rotondo P. and Kraus H. (ref. 18)

This paper is the most recent theoretical work published on the buckling of very thin ends.

The theory can only be applied to complete ellipsoidal and clamped semi-ellipsoidal shells. Using the method of adjacent equilibrium, the internal forces and moments are separated into a primary and secondary system corresponding to the prebuckling and buckling pressure systems respectively. The three resulting homogeneous differential equations are

solved by considering the variation of the total energy of the shell. Using the Rayleigh-Ritz method, and assuming that trigonometric functions define the deflected shape, critical buckling pressures are derived.

The results indicate that semi-ellipsoidal ends with  $h/D$  ratios greater than 0.33 will not buckle under internal pressure. It is also shown that as the  $h/D$  ratio is reduced below 0.15 the complete ellipsoid has a higher buckling pressure than the clamped semi-ellipsoid. This is because as the height is reduced the "equator" region is strengthened by the small radius and so the position of the first buckle in the complete ellipsoid moves from the "equator" to the knuckle.

When compared with Thurston and Holston's work (10) this theory predicts lower buckling pressures for semi-ellipsoidal ends when  $h/D$  is greater than 0.15 and higher values when  $h/D$  is less than 0.10. The reason for this is that deeper ends are less sensitive to nonlinearity effects and so the discrepancy is due mainly to the different solutions. For shallower ends the effects of nonlinearity are more significant.

#### 2.2.6 Esztergar E.P. and Kraus H. (ref. 19)

Esztergar and Kraus have described the development of design rules for semi-ellipsoidal ends with  $t/D$  ratios varying from 0.1 to 0.0001. Only ends with an  $h/D$  ratio of 0.25 were considered.

The elastic, plastic and buckling characteristics of ends were described, the main aim of the paper being to show how design procedures could be produced from computer data.

Elastic stress distributions, presented in the form of stress indices, were used together with the Tresca yield criterion to calculate initial yield pressures. They obtained upper bound limit pressures from the work of Gerdeen (20) and lower bound values from the work of Gajewski and Lance (21). Elastic buckling pressures were derived from the work of Rotondo and Kraus (18).



The results show that as the  $t/D$  ratio decreases the strength of the end relative to that of a cylinder of equal thickness decreases. Design rules based on the requirement that the end and cylinder must be of equal strength were proposed. For thinner ends it was shown that the cylinder must be thinner than the end if identical collapse strengths were to be achieved in both.

The work indicated that elastic buckling does not become a problem until the  $t/D$  ratio is less than about 0.000125. This feature contradicts ref. 9, which quotes the example of a semi-ellipsoidal end with a  $t/D$  ratio of 0.00043 and an  $h/D$  ratio of 0.25 buckling under internal pressure.

### 2.3 Experimental

#### 2.3.1 Meesters A.G. and Slaaf C.M. (ref. 8)

These authors have described a test performed on a stainless steel vessel with toripherical ends. The  $t/D$  ratio was 0.00219. Details are given in table 2.1.

The two nominally identical ends were assembled to form a vessel that could be subjected to a hydrostatic pressure test. A support skirt was welded to the knuckle of the lower end. The objective of the test was to determine the safety factor of dished ends.

During the test the pressure was increased in steps of about 14 lbf/in<sup>2</sup> up to a value of 142 lbf/in<sup>2</sup>. At this pressure the test was interrupted for lunch and the vessel left unattended for an interval of one hour. At the end of this period a large number of buckles (45 in the lower end) were found in the knuckle of each end. The buckles took the form of outward radial bulges. In both ends the most prominent buckle formed near a diametrical weld and the authors suggested that weld material and/or residual stresses may be affecting buckling.

A brittle lacquer test was also performed on the ends. This indicated that the peak strains on the outer surface occurred near the knuckle/crown junction.

### 2.3.2 Jones O. (ref 22)

Jones has determined stress levels within a torispherical end by means of electrical resistance strain gauges placed along two meridians. The steel end had a  $t/D_i$  ratio of 0.0018 with shape parameters  $r_i/D_i = 0.059$ ,  $R_i/D_i = 1.014$  and  $h_i/D_i = 0.167$ .

The results illustrate many of the characteristics of the stress distribution in this type of end. The compressive hoop stresses on the outer surface of the knuckle were the highest stresses in the end with the peak stress occurring in the region of the knuckle/crown junction. However the results show some disconcerting features. The meridional stresses, in the knuckle near the cylinder, showed peaks opposite in sign to those normally associated with these ends. Large variations in stresses at corresponding points along the two gauged meridians were also observed. The vessel was only pressurised to 15 lbf/in<sup>2</sup> and so stresses resulting from initial irregularities in shape may have had a large effect on the total stresses recorded at this low pressure. It is unlikely that instability effects would be evident at this pressure.

### 2.3.3 Fino A, and Schneider R.W. (ref 9)

These authors describe the failure of a large (60 ft. diameter) thin semi-ellipsoidal carbon steel end ( $h/D$  ratio of 0.25) designed and manufactured according to the rules of the ASME Unfired Pressure Vessel Code : 1959 edition. Details of the end are given in table 2.1. The end failed by the formation of wrinkles or buckles in the knuckle region at a pressure of 12.5 lbf/in<sup>2</sup> whereas the code test pressure for the end was 19.2 lbf/in<sup>2</sup>. All the buckles occurred on meridional welds in the knuckle. As a result of the failure the end was strengthened by welding a circumferential stiffening angle to the knuckle. The end then withstood the specified test pressure without buckling.

The buckling was an isolated test result and the work was not pursued.

### 2.3.4 Adachi J. and Benicek M. (ref. 12)

Adachi and Benicek performed a series of tests on model torispherical bulkheads as a result of the failure during proof testing of two aluminium bulkheads designed for use in the Jupiter I C B M (Details of these failures are given in table 2.1). This investigation was carried out in conjunction with the theoretical treatment by Mescall (16).

The models used for the tests were made from rigid polyvinyl chloride with a diameter of 10.52 in. They were produced by a moulding procedure which enabled the thickness variation in a portion of the knuckle containing a buckle to be less than 0.0005 in. Model thickness ranged from 0.005 in. up to 0.016 in. The four configurations tested are shown below.

Configuration	r/D	R/D	h/D	$\alpha$
A	0.173	0.741	0.276	55°
B	0.173	0.894	0.251	63°
C	0.173	1.179	0.228	71.1°
D	0.084	0.810	0.215	55°

The following relationship between buckling pressure and thickness was suggested

$$\frac{P}{E} = c \left( \frac{t}{R} \right)^n$$

where c and n are constants for a given end geometry.

The tests showed clearly that buckling pressure increased as the crown radius was reduced. Fig. 2.2 gives a comparison of results obtained with those of refs. 10 and 16. The results of the model work are shown to agree more closely with the Thurston and Holston treatment than with the Mescall treatment.

Configuration A was a 1/10th scale model of the Jupiter I C B M bulkhead. The model work indicated a buckling pressure of 70 lbf/in<sup>2</sup>. compared with the measured buckling pressure of 25 lbf/in<sup>2</sup>. The authors suggested that the failure of the aluminium end was an example of plastic buckling so explaining the difference between the two buckling pressures.

It was also stated that residual stresses might be affecting the buckling of the aluminium ends.

This model coverage was valuable, particularly in confirming the general soundness of the Thurston and Holston approach but the design relevance of the work should not be over-rated. The models did not incorporate the geometrical imperfections and thinning which are inevitable in the manufacture of production ends. Material property changes and residual stresses were also not represented in the models. These factors may have an appreciable influence on the buckling pressure.

#### 2.3.5 Stennet R. (ref. 23)

Stennet has described the failure of two nominally identical torispherical pressure vessel ends by buckling. The vessels were inadvertently overpressurized to  $40 \text{ lbf/in}^2$  in service. Details of the failures are given in table 2.1. The author states that ends of this type are "encountered in sufficient numbers to be a cause for concern". The use of higher proof stress stainless steels may not increase the strength of an end when buckling is considered. The calculated allowable design pressures for these ends from BS 1500 and ASME Section VIII (div. 1) 1968 were  $20 \text{ lbf/in}^2$  and  $26 \text{ lbf/in}^2$  respectively.

#### 2.3.6 Kemper M.J. (refs 11 and 24)

Kemper has described the failure of a number of very thin stainless steel torispherical ends by buckling. Details of the failures are given in table 2.1.

The buckling pressures experienced in practice were shown to be one quarter to one sixth those predicted by Thruston and Holston. It was suggested that limit pressures calculated from the curves of Shield and Drucker gave a closer indication of whether or not buckling was likely to occur.

In Kemper's experience the knuckle of a spun end can thin by about 25% near the knuckle/cylinder junction during the course of manufacture. Hardness measurements taken in the knuckle region of a spun end suggest that the elastic limit of the material could increase threefold. Kemper has also described a residual strain measurement test performed on a 65 in diameter spun end. Strain gauge rosettes were attached to two meridians, four gauges to a meridian. The change in strain was then measured as a 1 in. diameter circle of metal containing each gauge was removed from the end. In this way it was hoped to measure the elastic residual strains. No attempt was made to vary the size of the disc removed or to reduce the thickness of the disc so that "layer" residual strains could be assessed. (The term "layer" residual strains is defined as the strain remaining in the material due to varying levels of yield attained through the thickness) Maximum strains of -0.25% (inner surface meridional) and -0.18% (inner surface circumferential) were recorded in the knuckle. However as the residual strains were low in the region of the knuckle/crown junction where the maximum pressure strains exist, Kemper suggested that residual strains did not have an appreciable effect on the buckling pressure.

From his work, Kemper concludes that errors in shape and the method of manufacture do not seem to have any significant effect.

## 2.4 Codes and Standards

### 2.4.1 British Standards

#### 2.4.1.1 BS 1500: 1958 (ref. 25)

No lower limit on thickness is given by this standard. The shape limitations specified are as follows :-

1.  $R_i \leq D_o$
2. a)  $r_i \geq 0.1 D_i$   
 b)  $r_i \geq 0.06 D_i$  if a) is not practicable.

The required thickness is obtained from the formula

$$t = \frac{p D_o K_1 K_2}{2f JK_3} + C$$

where  $f$  is the design stress,  $J$  is a weld joint factor,  $C$  is a corrosion allowance and  $K_1$ ,  $K_2$  and  $K_3$  are factors defined by the code. The shape factor  $K_1$  is dependant upon  $h_o/D_o$  only.

#### 2.4.1.2 BS 1515 : Part 2 : 1968 (ref. 26)

The standard is only applicable to ends with  $t/D$  ratios  $\geq 0.002$ .

The limitations placed on geometry by the standard are as follows :

1.  $R_i \leq D_o$
2. a)  $r_i \geq 0.1 D_i$   
b)  $r_i \geq 0.06 D_i$  if a) is not practicable.
3.  $r_i \geq 3t$

The standard states that for ends designed to 2b) "consideration should be given to the possibility of buckling in the knuckle region".

The required thickness is obtained from the formula :

$$t = \frac{p D_o K}{2fJ}$$

where  $f$  is the design stress,  $J$  is a weld joint factor and  $K$  is a factor dependant on  $h_E/D_o$  and  $t/D_o$ .  $h_E$  is the effective outside height of an end and is equal to  $h_o$  or  $D_o^2/4R_o$  or  $\sqrt{D_o} r_o/2$ , whichever is the smallest.

It has been ascertained that the  $K$  factor curves for  $t/D = 0.005$  and  $0.002$  were derived by using the Shield and Drucker formula (15) to scale-up an existing ISO curve for  $t/D = 0.01$ .

For design temperatures up to  $50^\circ\text{C}$ ,  $f$  is the smaller of  $\text{UTS}/2.5$  or  $1.0\%$  proof stress/1.5.

#### 2.4.1.3 BS 3915 : 1965 (ref 27)

The design rules described in this standard are similar to those specified by ref. 26. However 2b) is not applicable (i.e. the knuckle radius must not be less than 10 per cent of the inside drum diameter) and no warning about buckling is given.

An additional limitation specified by the standard is that the outside height of the end must not be less than 18 per cent of the outside drum diameter.

This standard is applicable to carbon and low alloy steel pressure vessels used for the primary circuits of nuclear reactors.

#### 2.4.2 ASME Code : Section VIII : div. 1 : 1971 (ref. 28)

No limit on thickness is specified by the code. Shape limitations for unstayed ends are as follows :

1.  $R_i \leq D_o$
2.  $r_i \geq 0.06 D_o$
3.  $r_i \geq 3t$

The end thickness is then obtained from the formula

$$t = \frac{p R_i M}{2fE - 0.2p}$$

where  $M = \frac{1}{4}(3 + \sqrt{\frac{R_i}{r_i}})$ ,  $E$  is a joint efficiency factor and  $f$  is the maximum allowable stress;  $f$  is specified by the code for various materials. For materials having specified minimum tensile strengths greater than 80,000 lbf/in<sup>2</sup> a value of 20,000 lbf/in<sup>2</sup> is used for  $f$ . This stipulation has been introduced into later versions of the code for all torispherical ends and for semi-ellipsoidal ends shallower than 2 : 1.

In contrast with the recommendations in the U.K. standards the thickness is dependant on both knuckle and crown radii and is not directly proportional to the design pressure.

#### 2.5 Other Literature

The failure modes of torispherical ends have been described in papers by Cloud (29) and Langer (30). The possibility of very thin ends buckling under internal pressure is mentioned.

A computer analysis of the elastic stresses in a very thin end with  $t/D = 0.0023$  is given by Fessler and Stanley (6). A compressive hoop

stress on the outer surface of the knuckle, 3.8 times the cylinder hoop stress was predicted. This compares with 4.2 for a similar end analysed by Galletly (7).

Popov, Khojastah-Bakht and Sharifi (31) have produced a finite element elastic-plastic analysis for a number of ends. The progressive yielding through the thickness of several ends is illustrated for  $t/D$  ratios varying from 0.012 to 0.001. For all the ends considered a single hinge circle was found to form in the knuckle.

In ref. 32 Kraus has presented the computed elastic stress distributions for a number of torispherical, ellipsoidal and hemispherical ends. The minimum  $t/D$  ratio considered was 0.0025.

Gill (33) has recently tested three model torispherical ends (diameter 5.3 in) machined from an aluminium alloy.

Model No.	$r/D$	$R/D$	$p_{CR}$ (lbf/in <sup>2</sup> )
1	0.075	1	35
2	0.113	1	55
3	0.170	1	115

The  $t/D$  ratio of each model was 0.0019.

The buckling pressures obtained appear to be more realistic than those obtained by Adachi and Benicek (ref. 12) when compared with results from production ends.

Galletly (34) has also produced buckles in a similar sized model with a  $t/D$  of 0.001.



TABLE 2.1 DETAILS OF ENDS WHICH HAVE FAILED BY BUCKLING

Author	Ref. No.	D (in)	Shape Parameters					Material	Buckling Pressure	
			t/D	r/D	R/D	h/D	$\alpha$		Observed $P_{CR}$ (lb/in <sup>2</sup> )	Predicted from ref. 10 $P_{PTH}$ (lb/in <sup>2</sup> )
Meester & Slaaf	8	107.8	0.00219	0.085	1.0	0.184	63° 15'	Stainless Steel	142	-
Fino & Schneider	9	720	0.00043	0.173	0.905	0.250	63° 30'	ASMESA-212 Grade B	12.5	38
Adachi & Benicek	12	105.2	0.00077	0.173	0.742	0.276	55°	Aluminium	25	68
Stennett	23	76.25	0.00105	0.105	1.0	0.197	63° 46'	Stainless Steel	40	162
Kemper	24	-	0.0012	0.16	0.91	0.241	63° 3'	Stainless Steel	$P_{CR}/P_{TH} = 0.228$	
Kemper	24	-	0.0011	0.163	1.0	0.234	66° 15'	Stainless Steel	$P_{CR}/P_{TH} = 0.212$	
Kemper	24	-	0.0011	0.166	1.0	0.236	66° 24'	Stainless Steel	$P_{CR}/P_{TH} = 0.223$	
Kemper	24	167	0.00095	0.063	1.0	0.171	62° 12'	Stainless Steel	33	159
Kemper	24	-	0.00081	0.075	1.0	0.178	62° 39'	Stainless Steel	$P_{CR}/P_{TH} = 0.161$	

VARIATION OF LIMIT PRESSURE  
 WITH THICKNESS FROM THE FORMULA  
 AND GRAPHICAL DATA OF REF 15

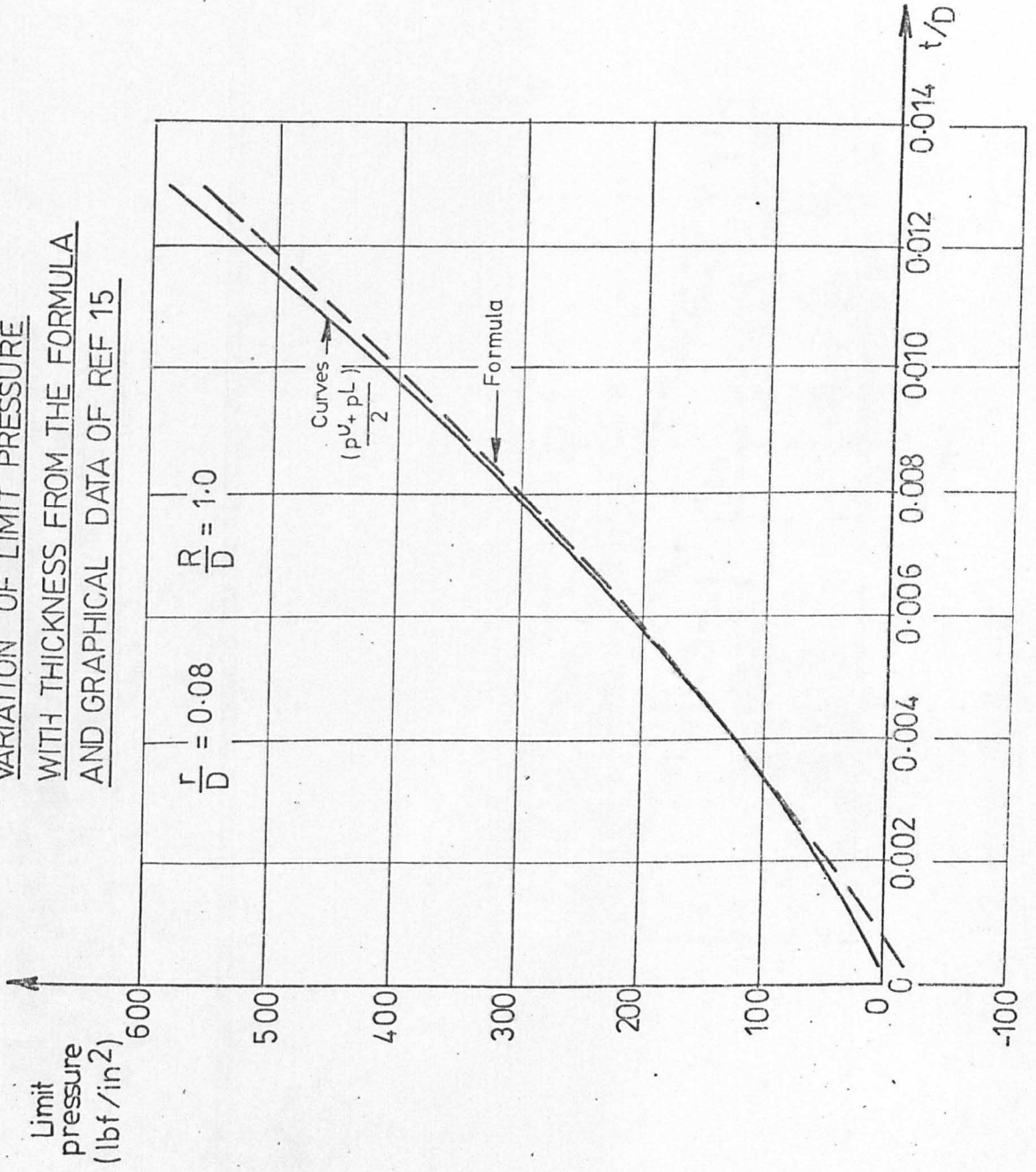


FIG. 2.1

COMPARISON OF EXPERIMENTAL (REF 12)  
AND THEORETICAL ( REFS 10 & 16) ELASTIC  
BUCKLING PRESSURES

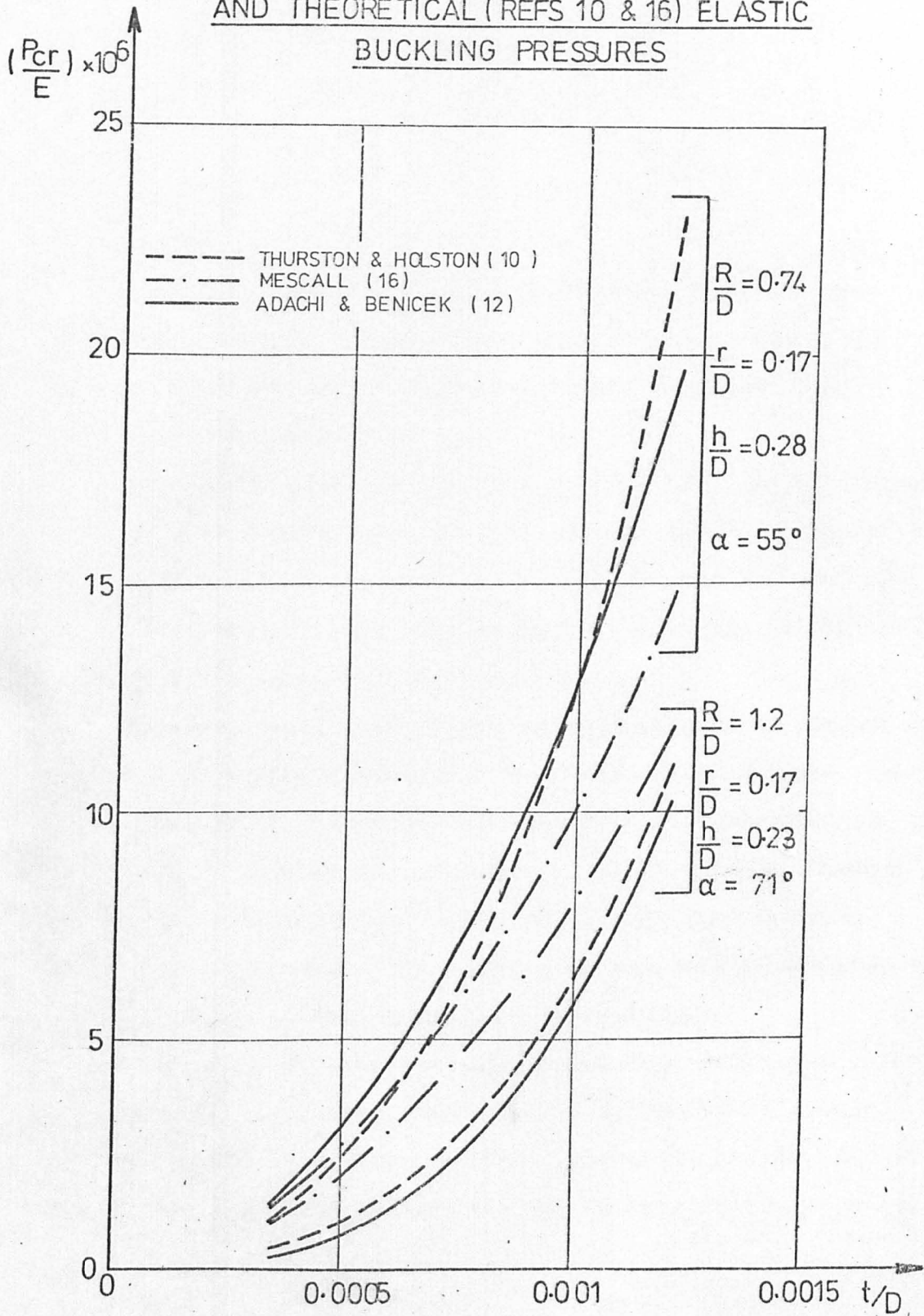


FIG. 2.2

CHAPTER 3

MATERIAL AND MANUFACTURE

3.1 Material

3.1.1 General

The most important applications of vessels of the kind under consideration require stainless steel. Such vessels are occasionally made in other materials but these cases are far outweighed by the stainless steel applications.

The material used in the manufacture of the test ends was a higher proof stress austenitic stainless steel. It was produced by the British Steel Corporation and is known as "Silver Fox, Hi-proof 304" (ref. 35). The material is specified by BS 1501: Part 3: 1973 (Grade 304 S65) and is used for a wide range of stainless steel vessels.

The higher proof stress properties are produced by the addition of controlled quantities of nitrogen to the normal austenitic grade. This is a well known method of improving the strength of austenitic steel and has been described in detail in the literature (ref. 36 and 37). Research has shown that the addition of about 0.20% nitrogen gives the best combination of properties. The corrosion resistance and welding properties are not adversely affected by the presence of nitrogen.

The steel is available in a range of forms (35). The plates used in pressure vessel applications are provided in the softened (i.e. fully annealed) condition. Cold forming causes considerable increases in the hardness and proof stress, without detriment to other mechanical properties.

### 3.1.2 Chemical composition

The composition of the material is as follows:

	%
Carbon	0.06 max
Silicon	1.0 max
Manganese	2.0 max
Chromium	17.5/19.0
Nickel	8.0/11.0
Nitrogen	0.15/0.25

### 3.1.3 Mechanical properties

The manufacturer's guaranteed minimum properties in the fully annealed condition at 20°C are as follows:

Tensile strength	38.0 tonf/in <sup>2</sup>
0.2% Proof stress	19.0 tonf/in <sup>2</sup>
1.0% Proof stress	20.5 tonf/in <sup>2</sup>
Elongation	35%

Detailed mechanical tests on the "as-received" and worked material are described in Chapter 8.

## 3.2 Manufacture of ends

### 3.2.1 General

"Very thin" torispherical ends are usually manufactured by the "pressed and spun" method. However, if a large knuckle radius or a vessel diameter greater than 14 ft is required this method cannot be used and the more expensive "crown and segment" method of construction must be resorted to.

In contrast with what is customary in thicker ends, it is not normal practice to include a cylindrical flange in very thin ends manufactured by either of these methods. The end is welded directly to the cylinder at

the position of the knuckle/cylinder junction.

The ends tested in this project have been manufactured by A.P.V. Company Limited, Crawley, Sussex to normal production standards.

### 3.2.2 "Pressed and spun"

Ends less than about 4ft 6 in diameter can be made from a single sheet of material (maximum width of sheet 6 ft), otherwise the end is produced from two or more sheets welded together. The welds are dressed before commencement of the forming process. The 6 ft 9 in and 9 ft diameter ends (see Chapter 4) used for test purposes had single diametrical welds. The 4 ft 6 in dia ends were made from a single sheet.

The sheet is first pressed to the required crown radius in a concave die by means of a series of press hits. The surface is then hammered in a machine hammer to produce a smooth finish in the crown. The end is rotated about its axis and a knuckle formed by turning the outer edges between rollers. The fixed inner roller acts as a former whilst the outer roller is moved in the meridional direction. In this way the knuckle is formed around the inner roller.

The main characteristics of ends formed by spinning are thinning and work hardening in the knuckle region, and significant residual stresses. Thickness reductions of 25% have been measured and the increase in proof stress may be threefold (11). Further details are given in Chapter 8.

The forming machine used to produce the test ends used in this study was made by the Italian organisation of Boldrini.

### 3.2.3 "Crown and segment"

In these ends the crown and knuckle are formed separately and then welded together to form a complete end.

If possible the crown is made from a single sheet, otherwise two or more

sheets are welded together. The 4ft 6 in and 6 ft 9 in dia test ends had crowns formed from a single sheet. The crown of each 9 ft dia test end had a single diametrical weld. The crown sheet is pressed to form a spherical segment of the required radius by means of a series of press hits. The surface is hammered in a machine hammer to produce a smooth finish.

The knuckle is formed by welding together four or more conical segments (the number depending on the diameter of the end) to form a frustum. The knuckle of each 4 ft 6 in dia test end had four segments. The 6 ft 9 in and 9 ft dia ends had five segments each. The welds are dressed and the knuckle radius is then formed by pressing around the circumference with a lag tool. This process may have to be repeated 20 times (11).

The knuckle and crown are welded together and the weld dressed. The knuckle of the completed end is then hammered in a machine hammer to produce a smooth finish.

The thinning and work hardening produced by this method of manufacture are much less than those associated with the "pressed and spun" method.

### 3.3 Fabrication

The Hi-proof 304 steel used in the manufacture of the test ends is readily weldable. The argon arc welding process was used by the vessel manufacturer whilst welds produced at the University were of the manual arc type.

CHAPTER 4CHOICE OF ENDS4.1 General

At the outset it was decided that the nominal thickness of the test ends should be the minimum sheet thickness normally used for ends of this type; this was 10 gauge (0.128 in). (Thinner sheet is occasionally used but it was considered that such ends would not necessarily exhibit the characteristics of typical production ends.) This decision minimised the cost of the work. The handling facilities in the department and the room available for the test rig and for storage were limited; the upper limit on vessel diameter was about 10 ft. The minimum thickness/maximum diameter combination allowed a minimum  $t_e/D_i$  ratio of about 0.001 to be attained.

The nominal end thickness was constant throughout the series. The different  $t_e/D_i$  ratios of 0.002, 0.0015 and 0.001 were obtained by changing the diameter. The test ends were chosen after careful consideration of the ranges of shapes in common use, the restrictions imposed on the shape of thicker ends by the major codes and standards, and the practical limitations faced by the manufacturer. Important factors were:-

- i) the manufacturer was unable to produce ends with an  $R_i/D_i$  ratio greater than unity.
- ii) it is normal practice to make the  $R_i/D_i$  ratio as close as possible to unity. (This fact is reflected in the choice of test ends in that twelve of the seventeen ends had an  $R_i/D_i$  ratio of 1.00.).
- iii) the ranges of ends manufactured by the two different processes do not "overlap". Consequently a direct comparison of the behaviour of similar ends formed by the two methods was ruled out.



iv) a continuous range of knuckle radii was not available. For spun ends values were available at 2 in intervals.

The test series was planned so as to include sets of ends in which one shape parameter was varied while the others were held constant; the sets through which  $t_e/D_i$  was varied for a constant shape were considered particularly important.

Each end was welded to a cylindrical drum, with a nominal thickness of 0.104 in. In all cases the weld followed the knuckle/drum junction.

The ends of a given diameter were tested in succession. For each diameter, one end (always of crown and segment construction) was used as a "base end", the other ends being welded in turn to this end to form a closed vessel. The base ends were expected to be the strongest ends tested. An angle or channel section ring was welded to the cylinder of each base end so that it could be supported with the axis vertical in a wooden stand. The shape of each base end was repeated in one of the other ends for each diameter. This duplication was not considered uneconomic. The strain gauge coverage on a base end was necessarily sparse.

Details of the ends tested are given in Table 4.1. The test ends are also represented in Fig. 4.1 which is a plot of  $r_i/D_i$  against  $D_i/R_i$  with contours of constant  $h_i/D_i$  included. The series of ends chosen effectively covers the area of the  $r_i/D_i$ ,  $D_i/R_i$  diagram in which the great majority of production ends lie.

#### 4.2 54 in diameter test ends

This was the greatest diameter of spun end that could be made from a single sheet. The resulting  $t_e/D_i$  ratio was 0.00237 based on the nominal thickness and 0.00185 based on an estimated reduced knuckle thickness in

spun ends of 0.100 in. With the exception of the base end all ends of this diameter had a cylinder length of 2 ft. These ends were the first to be tested.

#### 4.2.1 End 1

This is the crown and segment base end, with a crown radius equal to the vessel diameter and the largest knuckle radius normally used for a 54 in diameter end. A 3 in x 3 in x  $\frac{3}{8}$  in angle support ring was welded to the cylinder 21 in from the knuckle/cylinder junction (see Fig. 4.2). The positions of the four knuckle segments are illustrated in Fig. 4.3.

#### 4.2.2 End 2

This end is nominally identical to end 1 and so a direct comparison can be made with it. It was considered useful to obtain an indication of the repeatability of end behaviour in this way. The positions of the four knuckle segments are illustrated in Fig. 4.3.

#### 4.2.3 End 3

This end has a knuckle radius of 6 in, the largest possible for a spun end of this diameter and thickness. The  $R_i/D_i$  ratio is again equal to one.

#### 4.2.4 End 4

A knuckle radius of 4 in is the nearest practical value, for a 54 in diameter end, to the minimum value of 3.24 in ( $r_i/D_i = 0.06$ ) recommended by BS 1515, Part 2. Ends 1, 2, 3 and 4 form a set with constant crown radius. It was anticipated that this would be the weakest of the 54 in diameter ends.

#### 4.2.5 End 5

The knuckle radius of end 4 is repeated for this end whilst the crown radius has been reduced to 45 in. This produces a deeper and therefore probably stronger end.

#### 4.2.6 End 6

End 6 also has the same knuckle radius as end 4 but has a smaller crown radius than end 5. Ends 4, 5 and 6 therefore form a set with a constant knuckle radius.

#### 4.3 108 in diameter test ends

A diameter value of 108 in was chosen because forming tools were available which allowed the same shape parameters (particularly  $r_i/D_i$ ) to be used in these test ends as in the 54 in diameter ends. This diameter was very close to the maximum diameter of vessel that could be handled conveniently in the department.

The resulting  $t_e/D_i$  ratios were 0.00119 based on the nominal thickness and 0.000926 based on an estimated reduced knuckle thickness of 0.100 in.

With the exception of the base end all ends of this diameter had a cylinder length of 4 ft. These ends were the second set to be tested.

##### 4.3.1 End 7

This is the base end for the 9 ft diameter set of ends and has the same shape parameters as ends 1 and 2. It is of crown and segment construction and has an 18 in knuckle, the largest available for this diameter. A 1 ft length of cylinder was welded to the end. A support ring made from 6 in x 3 in mild steel channel (see Fig. 4.2) was welded to the cylinder as close as possible to the knuckle/cylinder junction (approximately  $\frac{1}{2}$  in). This end had therefore an effectively encasté boundary condition. The positions of the five knuckle segments are illustrated in Fig. 4.3.

##### 4.3.2 End 8

The end is geometrically similar to end 3 and has a knuckle radius of 12 in, the largest possible for a spun end of this diameter and thickness.

#### 4.3.3 End 9

End 9 is geometrically similar to end 4 with a knuckle radius of 8 in and a  $R_i/D_i$  ratio of one.

#### 4.3.4 End 10

Geometrically similar in shape to end 5, this end was chosen to study the effect of decreasing the crown radius to 90 in. Ends 9 and 10 have the same knuckle radius.

#### 4.3.5 End 11

This end has a crown radius of 78 in whilst the knuckle radius is the same as that for ends 9 and 10. Ends 9, 10 and 11 therefore form a set with constant knuckle radius. The value of  $R_i/D_i$  used for end 6 was not repeated for this end as experience gained from the earlier tests showed that the shapes used for ends 5 and 6 were too close.

#### 4.3.6 End 12

This end has a knuckle radius of 6 in which is less than 6% of the drum diameter and therefore just outside the recommended limit in BS 1515, Part 2. The tool for a knuckle radius of  $0.06 \times D_i$  (i.e. 6.48 in) was not available. Nevertheless, this was considered a useful choice and interpolation through the constant  $R_i/D_i$  set for intermediate  $r_i$  values would present no difficulties. In any event the existing code recommendations can only be treated as a guide for ends of this type. The crown radius was made equal to the vessel diameter.

#### 4.3.7 End 13

This is a crown and segment end nominally identical to end 7 but with a 4 ft long cylinder welded to it. By comparing the results of ends 7 and 13 it was therefore possible to determine the effect of an encastred condition at the knuckle/cylinder junction. Ends 7, 8, 9, 12 and 13 form a set with a constant crown radius. The positions of the five segments are illustrated in Fig. 4.3.

#### 4.4 81 in diameter test ends

An intermediate diameter was chosen to facilitate interpolation through the  $t_e/D_i$  range between 0.001 and 0.002. The value chosen was the arithmetic mean of the two previous values, giving a  $t_e/D_i$  ratio of 0.00158 based on the nominal thickness and 0.00123 based on an estimated reduced knuckle thickness of 0.100 in. The reciprocal mean value was considered as a possible intermediate diameter but the available forming tool sizes would not permit a useful development of the sets and series built up with the first two diameters.

With the exception of the base end all ends of this diameter had a cylinder length of 2 ft 11 $\frac{1}{2}$  in.

These ends were the last to be tested.

##### 4.4.1 End 14

This is the base end for the 81 in diameter set of ends and has the same shape parameters as the previous base ends. It is of crown and segment construction and has a 13 $\frac{1}{2}$  in knuckle radius, the largest possible. A 10 in length of cylinder was welded to the end and a support ring made from 3 in x 3 in x  $\frac{3}{8}$  in angle was welded to the cylinder (see Fig. 4.2) as close as possible to the knuckle/cylinder junction (approximately  $\frac{1}{2}$  in away). The positions of the five segments are illustrated in Fig. 4.3.

##### 4.4.2 End 15

This is a crown and segment end nominally identical to end 14 but with a 2 ft 11 $\frac{1}{2}$  in long cylinder welded to it. Comparison with end 14 indicates the effect of an encastred condition at the knuckle/cylinder junction. The positions of the five segments are illustrated in Fig. 4.3.

##### 4.4.3 End 16

This spun end has the same shape parameters as ends 4 and 9, a knuckle radius of 6 in and a  $R_i/D_i$  ratio of one. Ends 14, 15 and 16 form a set of constant crown radius.

#### 4.4.4 End 17

Geometrically similar to ends 5 and 10, this spun end was chosen to study the effect of decreasing the crown radius. Ends 16 and 17 form a set with a constant knuckle radius.

#### 4.5 Principal sets

The principal sets in the complete test series (see Fig. 4.1) were:-

	Ends
Varying $t_e/D_i$ ratio,	2, 13, 15
other parameters constant	4, 9, 16
	5, 10, 17
Varying $r_i/D_i$ ratio,	2, 3, 4
other parameters constant	13, 8, 9, 12
Varying $R_i/D_i$ ratio,	4, 5, 6
other parameters constant	9, 10, 11

End No.	$D_i$ (in)	L(in)	$t_c/D_i$	$t_e/D_i$	$r_i/D_i$	$R_i/D_i$	$h_i/D_i$	$\alpha$	Construction
1*	54	30	0.00193	0.00237	0.167	1.0	0.236	66°25'	C & S (4)
2	54	24	0.00193	0.00237	0.167	1.0	0.236	66°25'	C & S (4)
3	54	24	0.00193	0.00237	0.111	1.0	0.201	64°5'	S
4	54	24	0.00193	0.00237	0.074	1.0	0.178	62°37'	S
5	54	24	0.00193	0.00237	0.074	0.833	0.205	55°53'	S
6	54	24	0.00193	0.00237	0.074	0.778	0.218	52°45'	S
7*	108	12	0.00096	0.00119	0.167	1.0	0.236	66°25'	C & S (5)
8	108	48	0.00096	0.00119	0.111	1.0	0.201	64°5'	S
9	108	48	0.00096	0.00119	0.074	1.0	0.178	62°37'	S
10	108	48	0.00096	0.00119	0.074	0.833	0.205	55°53'	S
11	108	48	0.00096	0.00119	0.074	0.722	0.234	48°55'	S
12	108	48	0.00096	0.00119	0.056	1.0	0.167	61°56'	S
13	108	48	0.00096	0.00119	0.167	1.0	0.236	66°25'	C & S (5)
14*	81	10	0.00128	0.00158	0.167	1.0	0.236	66°25'	C & S (5)
15	81	35.5	0.00128	0.00158	0.167	1.0	0.236	66°25'	C & S (5)
16	81	35.5	0.00128	0.00158	0.074	1.0	0.178	62°37'	S
17	81	35.5	0.00128	0.00158	0.074	0.833	0.205	55°53'	S

TABLE 4.1 Nominal Dimensions and Shape Parameters

\* Base end

C & S Crown and segment

S Pressed and spun

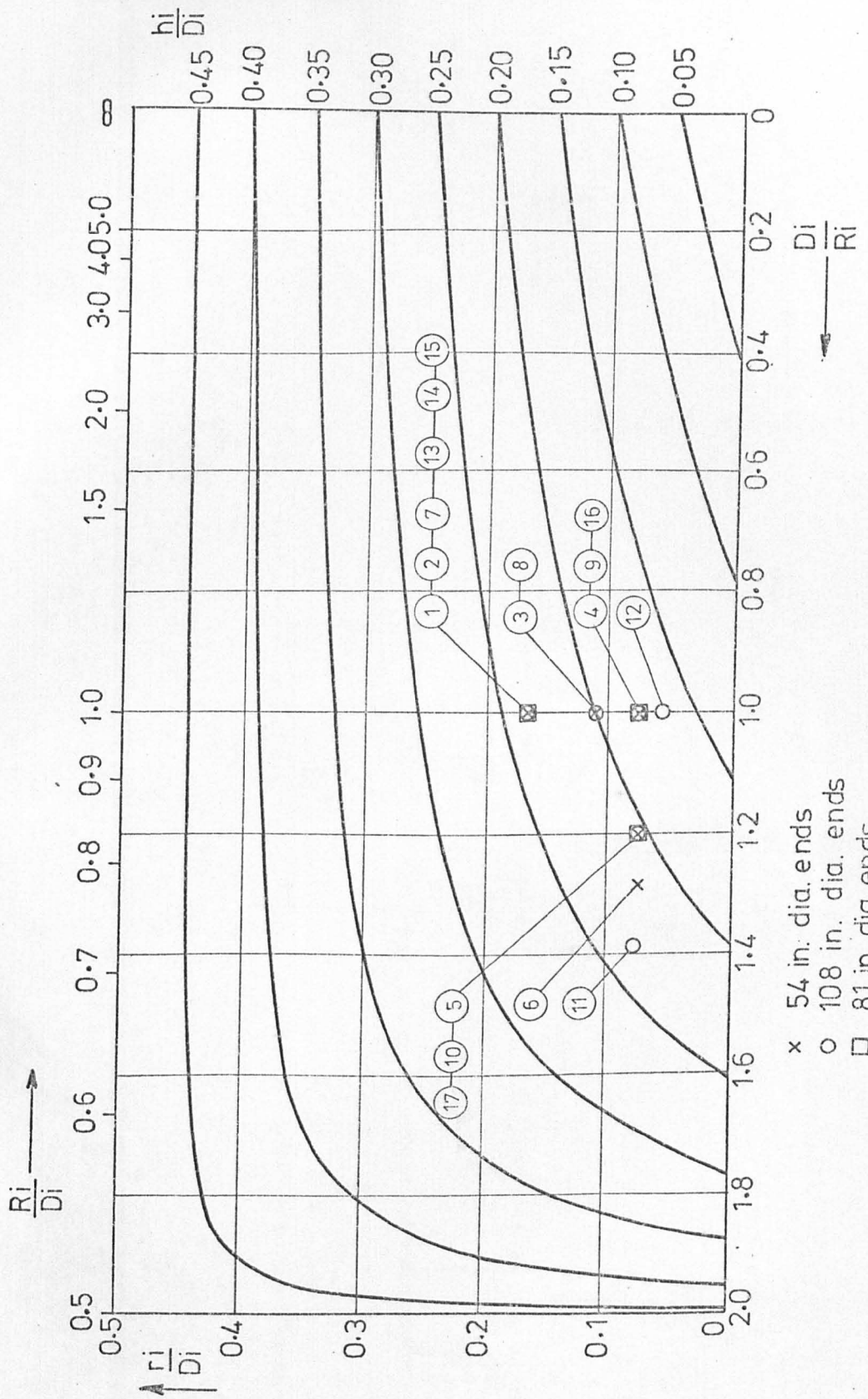


FIG. 4.1



BASE ENDS SUPPORT RING DETAILS

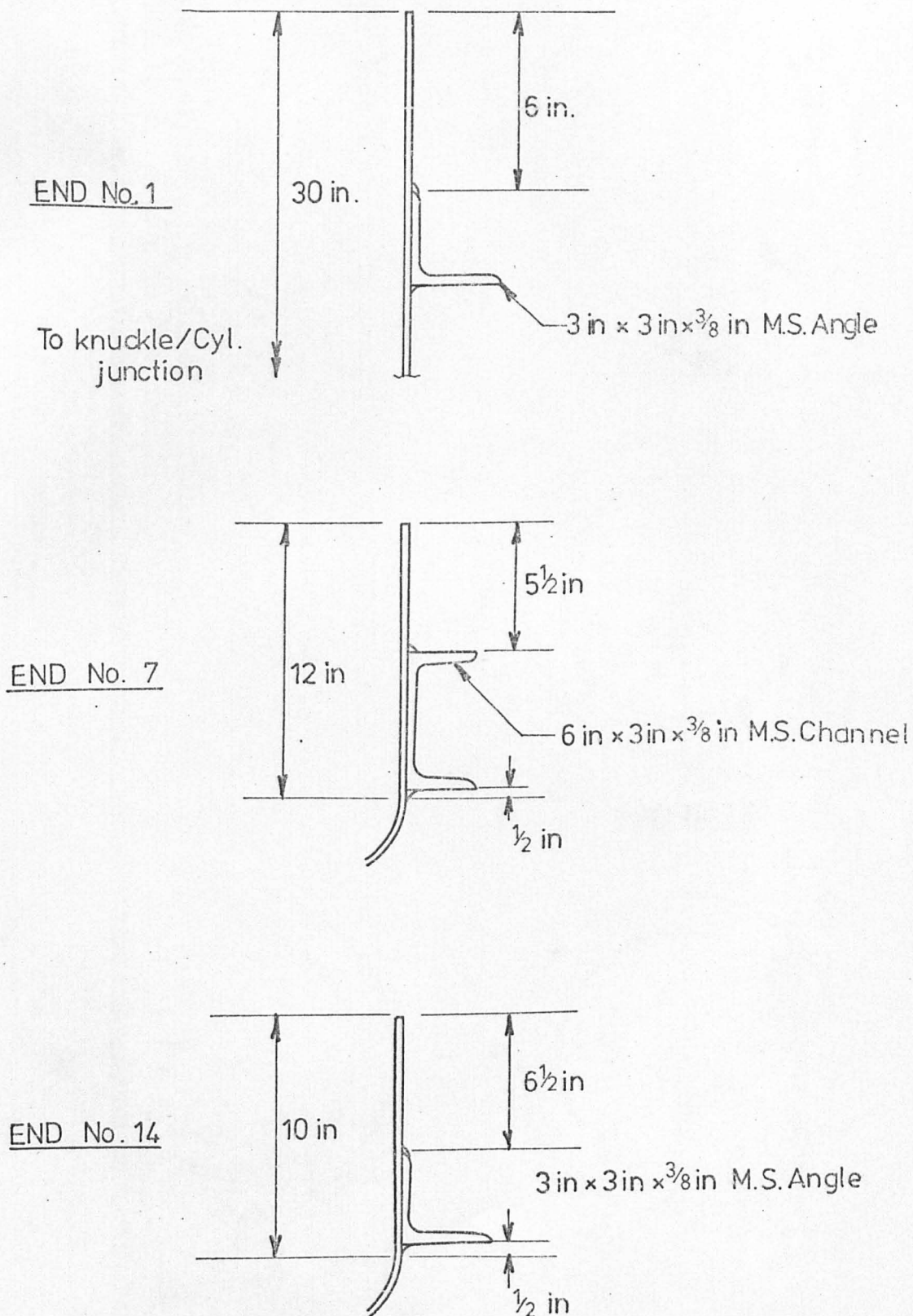
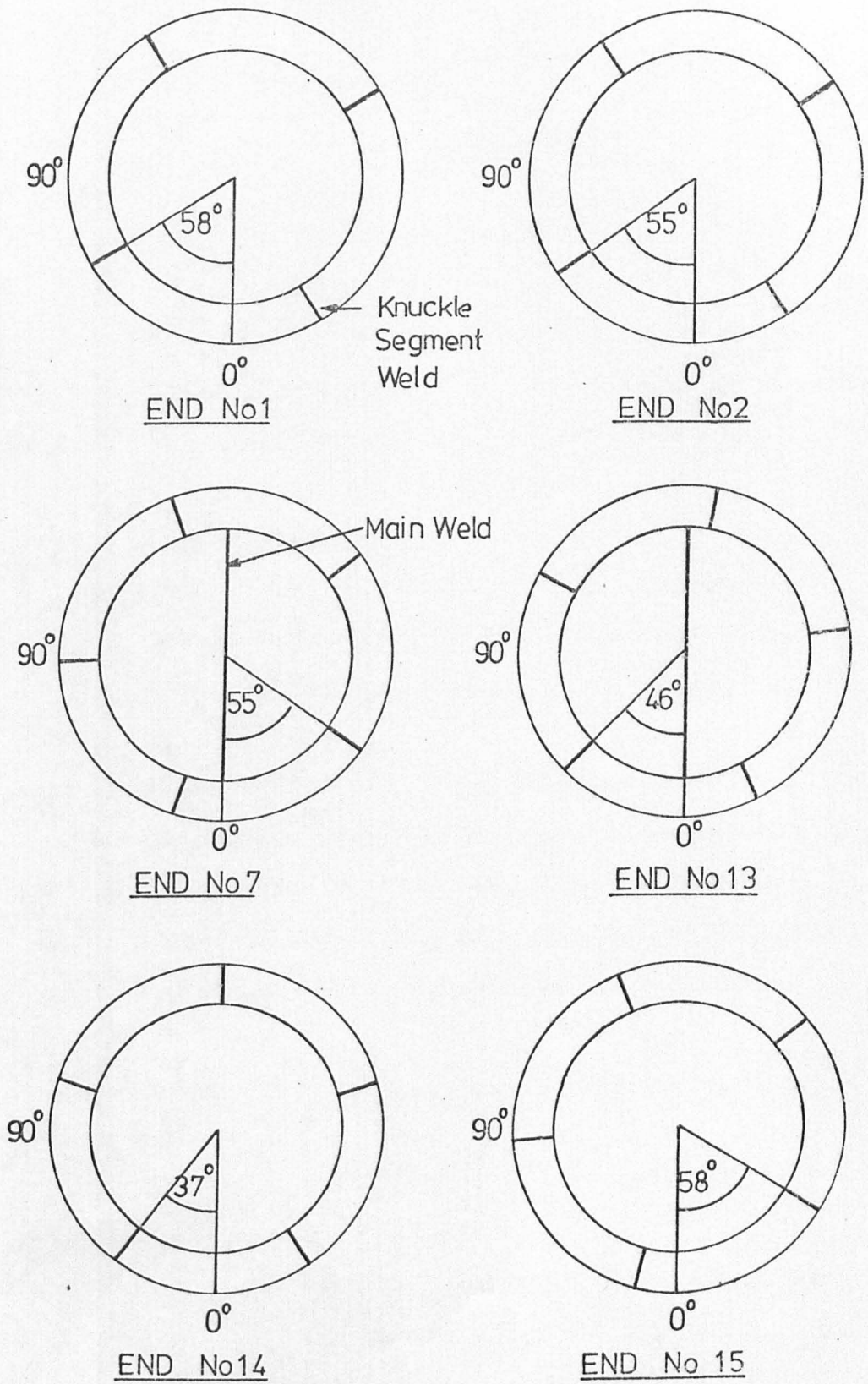


FIG. 4.2



CROWN AND SEGMENT ENDS-POSITION OF KNUCKLE SEGMENTS

## CHAPTER 5

### TEST INSTALLATION

#### 5.1 General

The facilities used for testing the pressure vessel ends were designed and developed during the first year of the project. Considerable time was spent in developing a strain gauge data logging system, using scanning units coupled to a mini-computer for A-D conversion and processing. This and other items of the test installation are described below.

#### 5.2 Preparation "cradle" and test stand

The preparation "cradle" shown in Fig. 5.1, was used for gauging the interior of the test ends, welding the test and base ends together to form a vessel and for the final parting (see chapter 6) of the 54 in diameter vessels.

The stand consisted of channel and I-section girders bolted together to form a firm base. Heavy rubber castors, attached to the stand and in contact with the outer surface of the cylinder, allowed each end to be rotated about its horizontal axis. This assisted in the manipulation of the test ends and was found to be indispensable for the 81 in and 108 in diameter ends.

A stand made from railway sleepers, Figs. 5.1 and 5.2, was used for supporting the test vessels.

#### 5.3 Pressurising system

The test vessels were completely filled with water through an inlet at the pole of the base end. The pole attachment (see section 5.4) on the test end (Fig. 5.4) was loosened so that air within the vessel could escape

as the water level rose. A flexible hydraulic hose was used to connect the vessel to the pressurising system shown in Fig. 5.3. The water was pressurised by means of a small capacity (2.5 gallons/min), high pressure, double acting reciprocating pump manufactured by Oswalds and Ridgway Ltd. Fluctuations in pressure were virtually eliminated by using a Greer Mercer air/water accumulator. The pressure was controlled by a pressure regulator used in conjunction with a relief valve. Shut-off valves were also incorporated in the system to allow the vessel to be isolated from the pressurising system and to enable the pressure within the vessel to be reduced if necessary.

Two high quality standard test pressure gauges of different ranges and sensitivities were also included.

The system was operated by adjusting the relief valve (Fig. 5.3) so that a pressure, slightly higher than that required in the vessel, was built up on the pump side of the pressure regulator. The pressure in the vessel was then increased by adjusting the pressure regulator. At the required pressure the regulator was closed and water from the pump would bypass the vessel and return to the reservoir, via the relief valve. If the pressure in the vessel tended to fall (due to creep deformations or a minor leak) the regulator could be opened slightly to maintain the test pressure. It was found that the test pressure could be held without difficulty even when significant creep deformations were occurring in the vessel.

#### 5.4 Pole attachment

The 200 lead wires from the gauges on the interior of the vessel were brought to the outside through the fitting shown in Fig. 5.4. This

consisted basically of a brass block and conical steel connector held together by means of eight studs and nuts. An O-ring seal at the interface prevented any leakage. The connector was screwed onto a threaded 1 in BSP stub welded to the pole of the test end where there was a 1 in diameter hole in the end. A tapered recess was machined on the "inside" of the brass block and 200 1/16th in diameter holes were drilled through the block at the base of the recess. Insulated strain gauge leads from the interior of the vessel were passed through the holes and soldered to sockets on the outside. The tapered recess was filled with silicone rubber so that the effectiveness of the seal increased as the pressure was applied. With only occasional minor leaks along the insulated leads, which could be tolerated, a pair of these connectors were used without trouble through the whole of the test programme.

### 5.5 Strain measuring and recording system

A data logging system for handling the signals from 200 strain gauges was developed before the testing of the first vessel could commence. A diagram of the system is presented in Fig. 5.5.

The system consists basically of three main sections:

- i) Wheatstone bridge circuitry,
- ii) the scanning unit,
- iii) the recording unit.

The bridge circuit was constructed on the two lead wire, half bridge, apex switching principle. Each active gauge had a corresponding dummy gauge whilst a pair of fixed resistors (strain gauges) common to the 200 gauge pairs completed the Wheatstone bridge circuits. The dummy gauges were bonded to stainless steel plates (pieces of vessel material) which were in turn mounted in a covered frame and positioned alongside the test vessel. The gauges were connected into the bridge circuits using 20 core

screened cable. The active and dummy gauge leads were made the same length and laid together as far as possible to ensure adequate temperature compensation. By using a bridge switching circuit of this type (i.e. switching half bridges in turn) it was ensured that switching resistances did not modify the signal voltages. The bridges were supplied with a 3 volt d.c. input voltage from a stabilised power supply. Bridge balancing, which would have been time-consuming and expensive was unnecessary since zero-pressure bridge readings were taken, stored and subtracted from all subsequent strain gauge readings. Gauge factors were also stored in the computer thus enabling the output to be in the form of strains.

The bridge circuits were switched by four 50 channel Solartron scanner head units (model LU 1976) connected to a Solartron scanner controller (model LU 1975). A PDP8 mini-computer, which incorporated an A-D converter, was used to process the signals. It was situated about 50 yards from but within sight of the test area. The output signals from the bridge circuits were amplified in order to compensate for losses and to match the anticipated maximum bridge output to the maximum acceptable input to the A-D converter, thus utilising its full input range. A Bell and Howell d.c. amplifier with a suitably adjusted gain was used.

For convenience the four scanner units were mounted in one cabinet and the scanner controller, amplifier and bridge power supply in another. The two cabinets were mounted together in a portable trolley; initial interference between the components was eliminated by placing a sheet of Mu-metal between the two cabinets.

After conversion into digital form the output signals from the strain gauges were stored and processed in the mini-computer. A machine code program was required as the relatively small store (4k) of the computer had to be used efficiently to handle large quantities of input data. A flow diagram of the system is shown in Fig. 5.6.

The teletype output was designed to present the results of three consecutive scans through the gauges. For each gauge the three strain values together with the differences between successive readings, were printed out alongside the gauge number. This enabled possible creep effects to be easily assessed. The scanning rate was 8 gauges per second; each scanning sequence being initiated manually. Individual readings were triggered by a timing pulse from the scanner controller when switching was complete and the signal had settled. When the teletype printout was complete, a visual display of selected strain gauge signals could be produced on the oscilloscope attached to the PDP8 computer. In this way it was possible to observe the strain distribution in a group of adjacent gauges (say outer surface circumferential) within a few minutes of the completion of the scan.

If the strain readings had not settled after 3 scans, taken at suitable time intervals, the computer was set up to accept a further series of scans at the same pressure. If the strains had settled, a paper tape recording of the strains in the last scan was obtained from the high speed punch for further processing on an ICL 1906A computer.

#### 5.6 End height growth gauge

On each end (excluding the base ends) an attempt was made to measure the increase in end height with increasing pressure.

For ends 2 to 6, the 54 in diameter ends, a tubular steel cross-bar (Fig. 5.2) was bolted to the pole attachment. Each end of the bar carried a clock gauge which registered on a narrow Araldite block cemented to the vessel at the knuckle/cylinder junction. Both gauges were read as the test proceeded, the average deflection indicating the increase in end height.

As the cylinder deformations became appreciable at the higher pressure levels, the Araldite blocks rotated so giving a clock gauge reading which depended on the distance of the dial gauge pointer from the wall of the cylinder. Although it was possible to take account of this rotation it was decided to change the measuring system used on the larger diameter ends.

End height growths in ends 8 to 13 and 15 to 17 were measured by means of two optical levels sited approximately 20 ft from the vessels. One level was used to measure the displacement of the pole; the other the displacement of the knuckle/cylinder junction. Small graduated scales were cemented to the pole attachment and the cylinder for this purpose; the levels were calibrated on these scales. By subtracting the reading at the knuckle/cylinder junction from that at the pole the growth in the height of the end was determined.

#### 5.7 Circumferential growth gauge

The growth in cylinder circumference was measured at four positions in each test vessel. At each position a thin steel tape was wrapped around the vessel. To the ends of the tape were bolted small aluminium blocks which were held together with springs. A small clock gauge was attached to one block and allowed to register on the other. As the cylinder increased in circumference the growth was measured by the clock gauge. A simple pointer attached to the block on the end of the tape and registering across the gap against the other end of the tape was used for measuring the larger plastic deformations. (The tapes were discarded lengths of graduated surveying tape.)

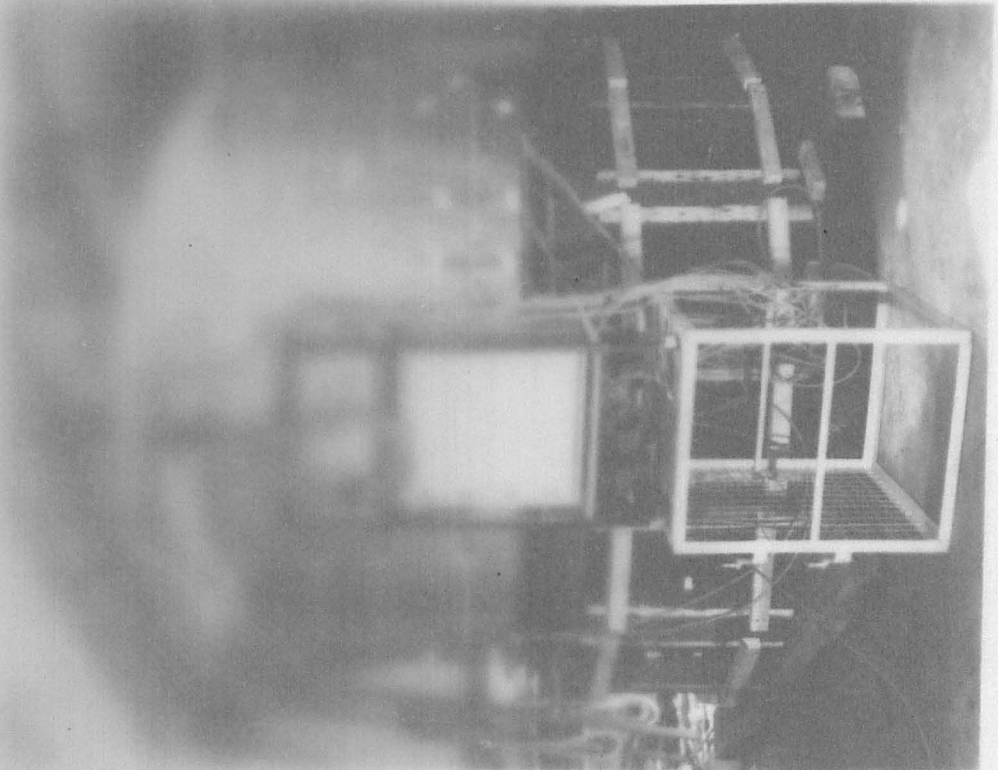


PREPARATION CRADLE

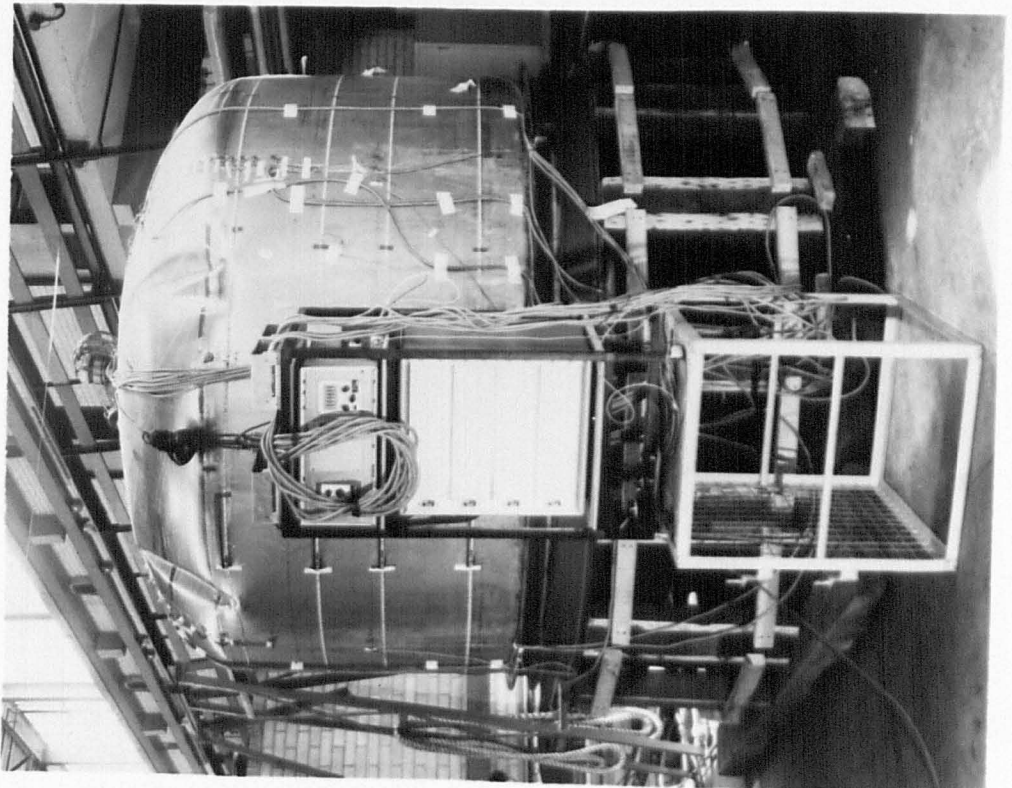
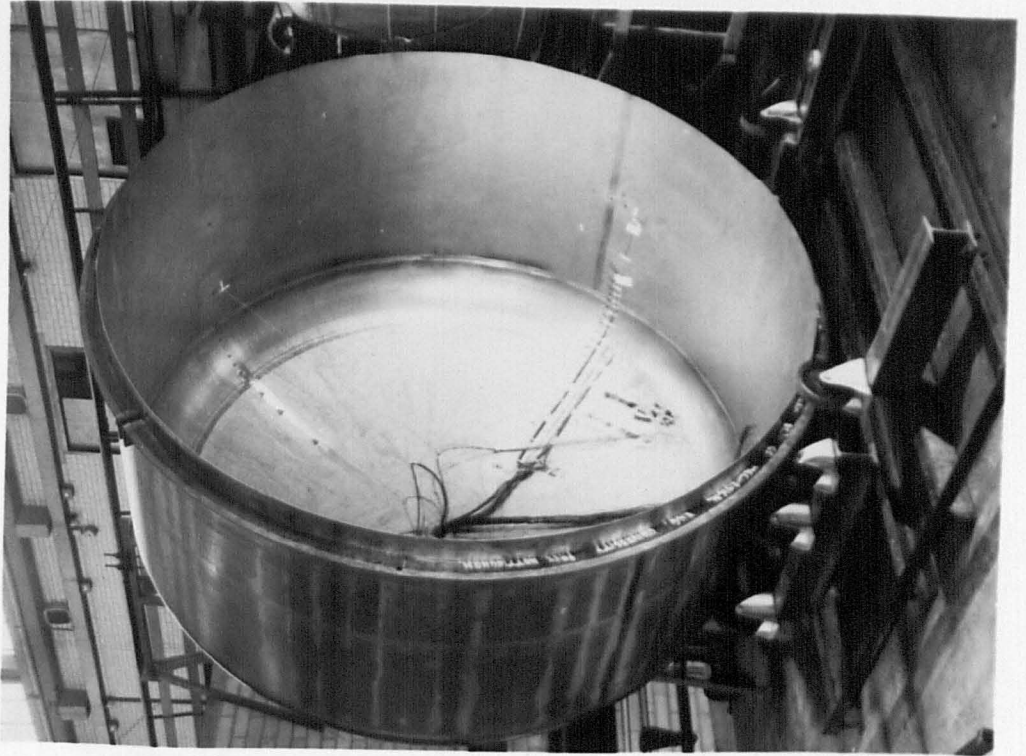
TEST STAND

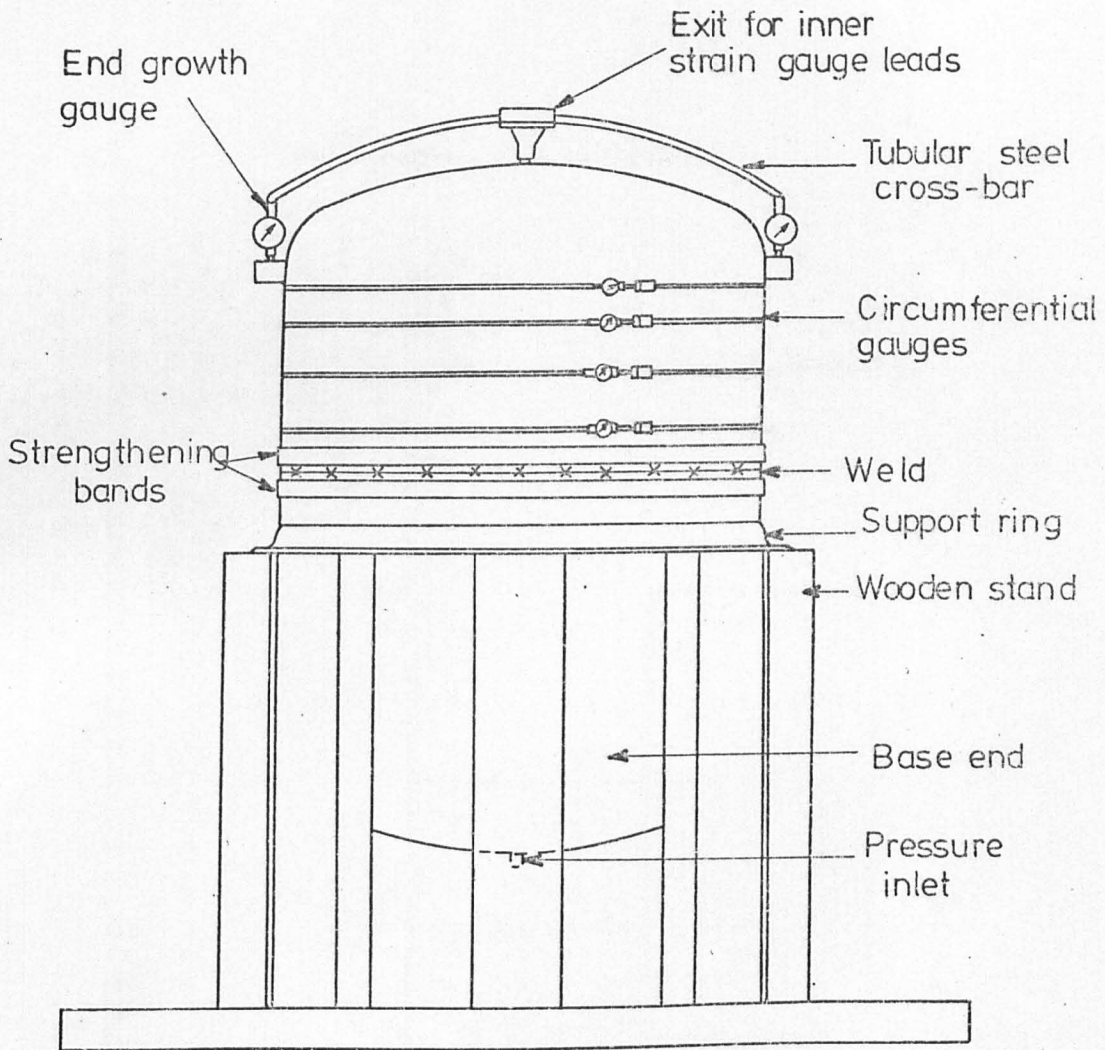


PREPARATION CRADLE



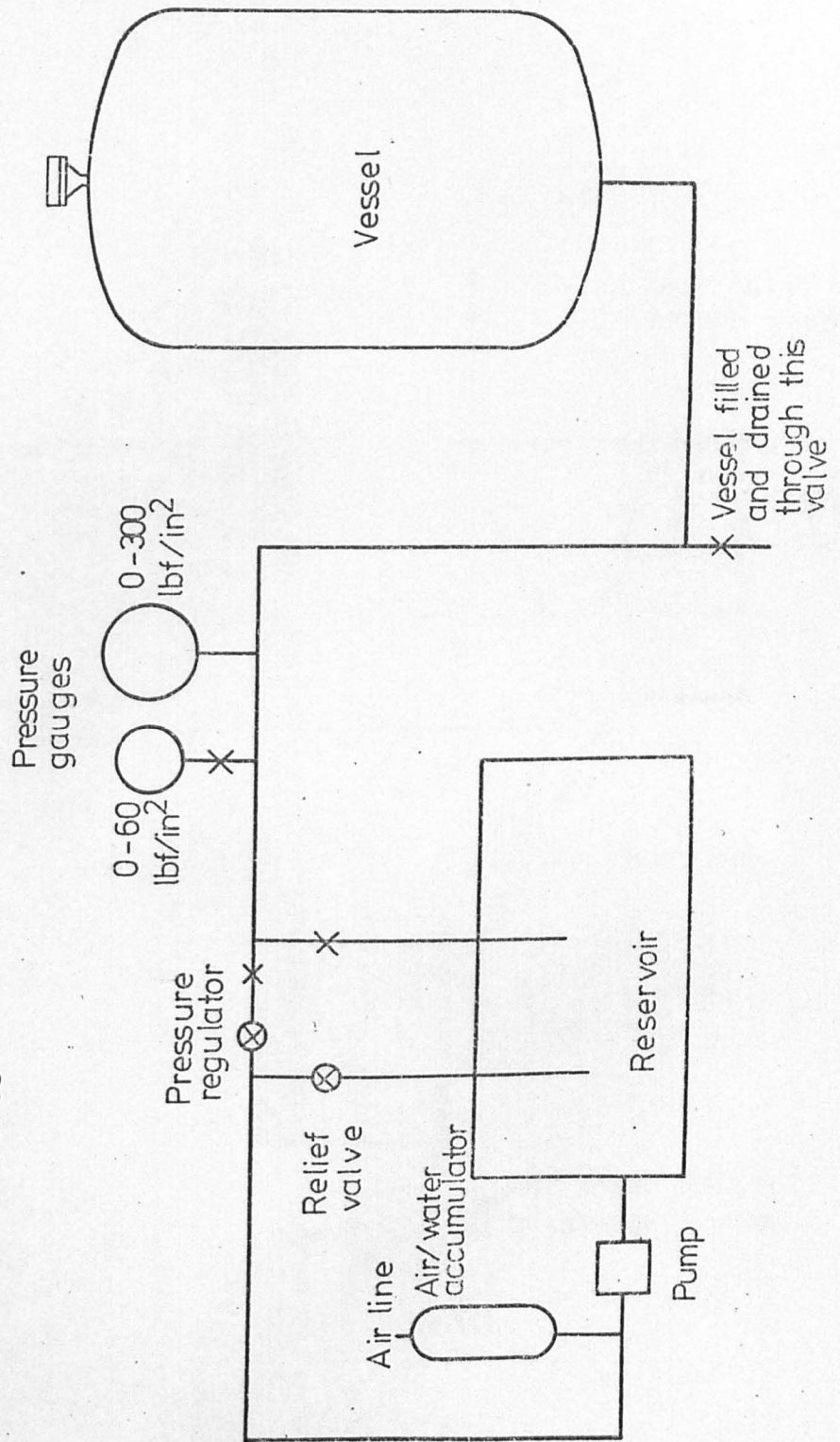
TEST STAND





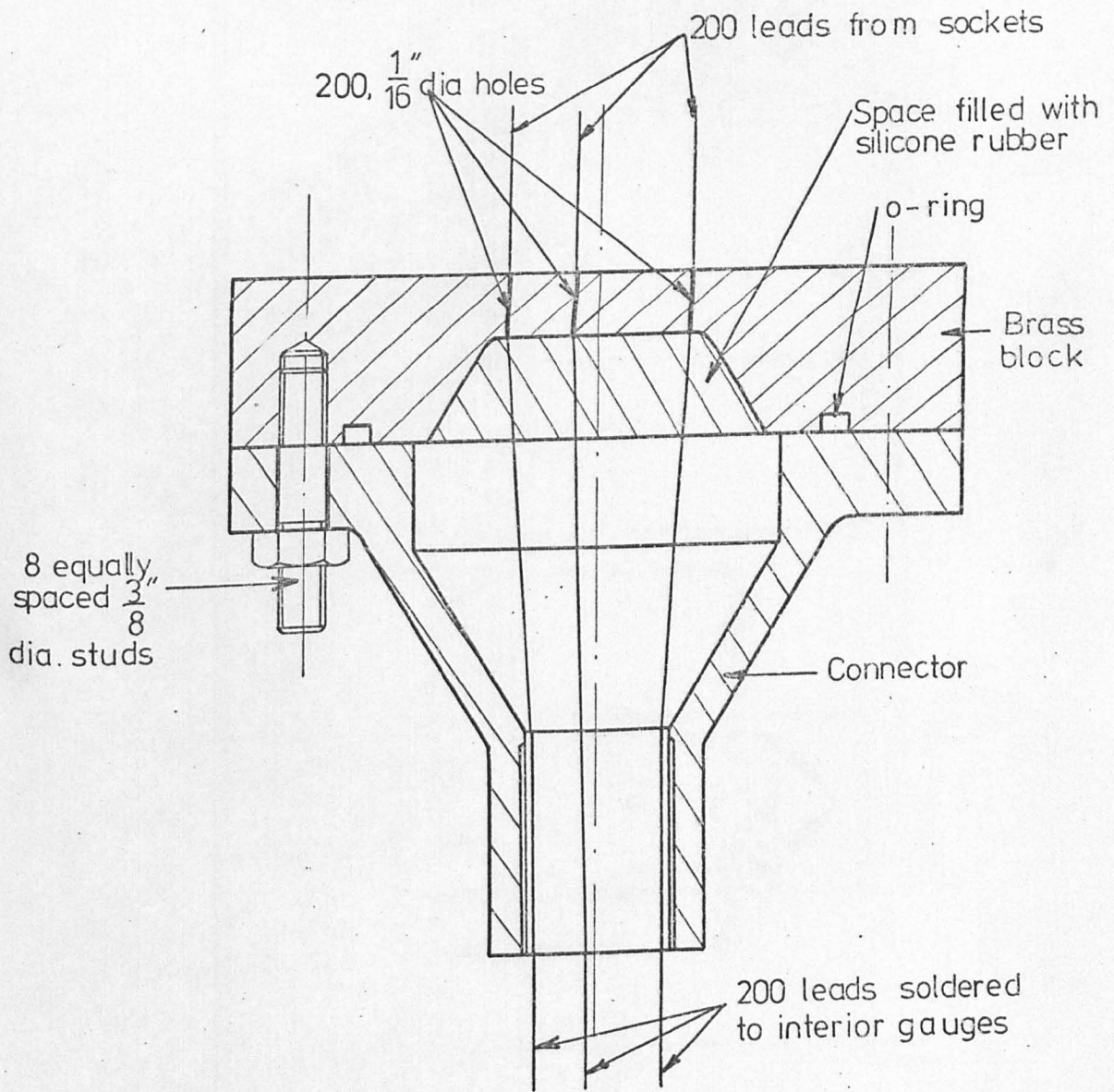
VESSEL ASSEMBLY FOR 54 in. dia. ENDS.

X Shut-off valves

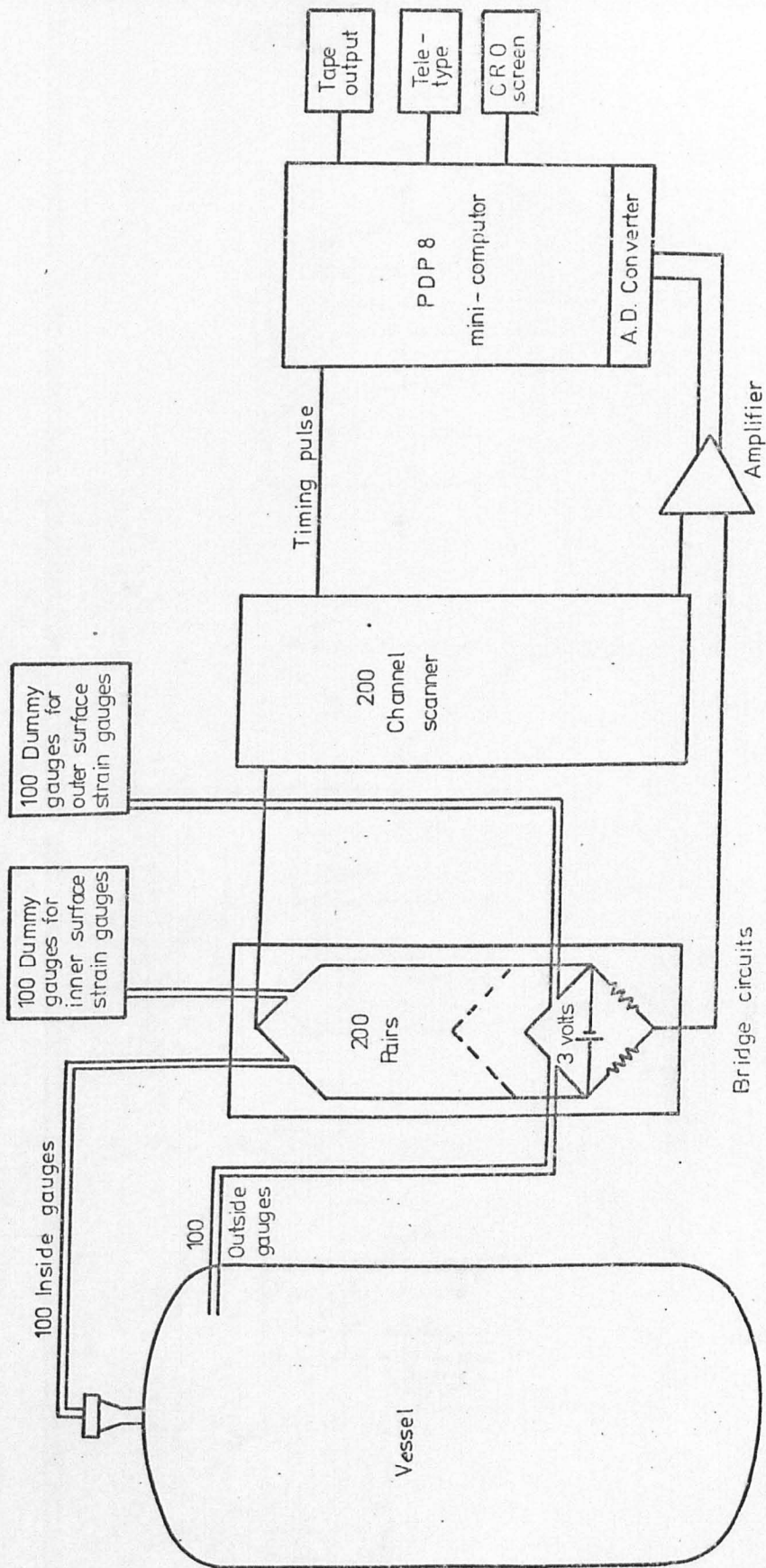


PRESSURISING SYSTEM.

FIG. 5.3



POLE ATTACHMENT



STRAIN MEASURING AND RECORDING SYSTEM.

FIG. 5.5

FLOW DIAGRAM OF PDP 8 DATA ACQUISITION SYSTEM -  
PART A

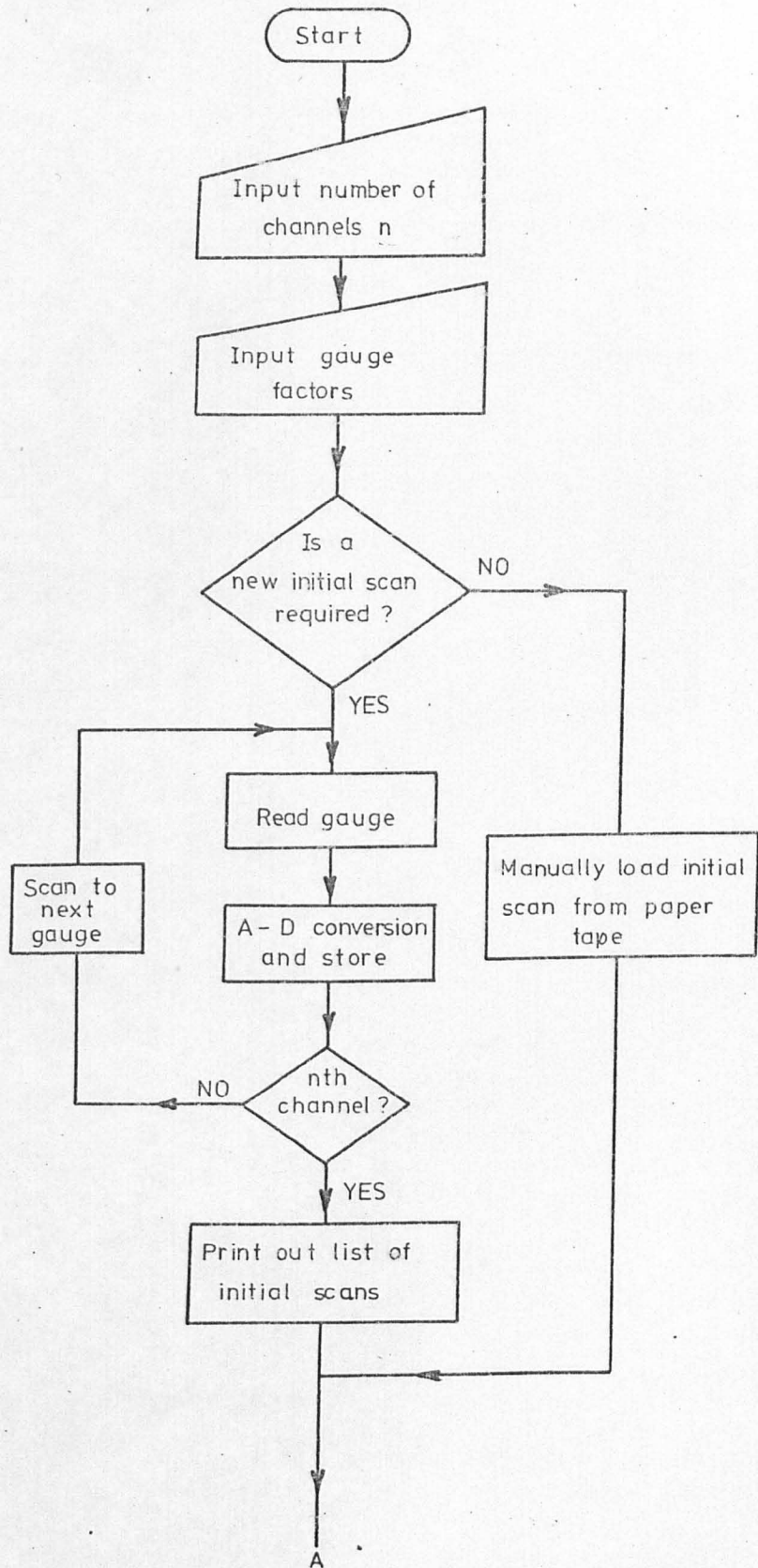


FIG. 5-6 a



FLOW DIAGRAM OF PDP8 DATA ACQUISITION SYSTEM -

PART B

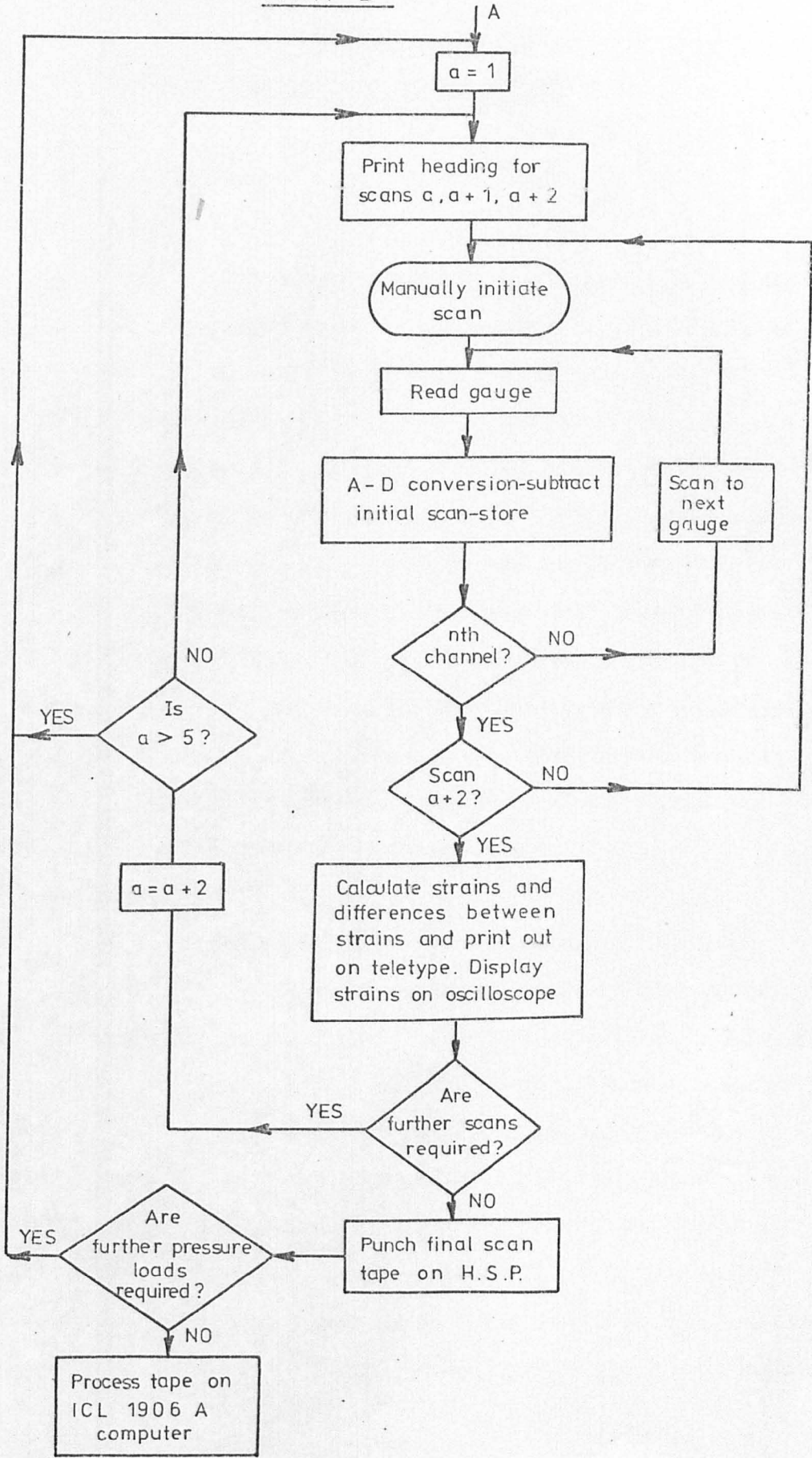


FIG. 5.6 b

## CHAPTER 6

### VESSEL PREPARATION AND TEST PROCEDURE

#### 6.1 Vessel preparation

##### 6.1.1 General

The preliminary measurements and preparatory work on each end called for a considerable amount of time and effort. The successful completion of the test and interpretation of the test results depended, to a large degree, on the quality of this work and all possible care was taken with each operation. The following is a general description of the preparation work performed on each end. It will be appreciated that some details in the preparation work were the outcome of considerable development and, where appropriate, some indication of this is given.

The test program could only be maintained by carefully "overlapping" thickness and curvature measurements, gauging and testing etc. At any given time at least two, and at times three or four, ends were in the course of preparation. Two pole attachments were made to allow one end to be gauged whilst testing another.

##### 6.1.2 Marking out

The outer surface of each test end was marked with eight equally spaced meridional lines, by means of a felt tip pen. The 0° meridian corresponded to the rolling direction of the sheet in all the ends and also to the main diametrical weld in the larger ends. On each meridian about twenty positions were marked, concentrated mainly in the region of the knuckle. The gauge positions were measured from the knuckle/cylinder junction using a surveying tape; the junction line itself was located and marked by measuring up the nominal length of the cylinder from the open end. The tape was graduated in  $\frac{1}{8}$  inches and the gauge positions were marked to within about  $\frac{1}{16}$  in. of the required position. Thickness

measurements were taken at these positions and strain gauges applied subsequently to about 50 of them. Having chosen these strain gauge positions the corresponding positions on the internal surface were similarly marked. The inner surface positions were located by using a small but powerful magnet placed on the outer surface of the vessel to move a few iron filings across the inner surface. Tests on sheet material showed that the corresponding position could be located to within 1/16 in.

#### 6.1.3 Thickness measurements

Prior to pressure testing, the thickness of every end was measured at each position marked on the external surface. An ultrasonic probe developed by the Non-Destructive Testing Centre at Harwell was used for the purpose. The device was a delayed ultrasonic pulse echo thickness gauge and was accurate to within 0.001 in. The ultrasonic signal was transmitted into the vessel material via an acoustic delay line. The signal received consisted of a series of echoes, the first being the reflection from the interface between the delay line and the vessel outer surface followed by smaller echoes reverberating within the material. Errors usually associated with pulse echo thickness gauges, due to coupling the ultrasonic crystal onto the specimen, were eliminated in this equipment by measuring the time of flight of the echoes that had undergone more than one transit within the specimen. After calibration, using specimens of known thickness, a direct digital reading of thickness was displayed, thus enabling a very detailed coverage of each end to be obtained.

#### 6.1.4 Curvature measurements

The curvature of a manufactured end varies considerably from the nominal values and as it was considered important to know the real shape, a curvature survey was carried out on each end prior to testing. Curvature measurements were taken at closely spaced intervals ( $\frac{1}{2}$  in. to

1 in.) along four of the marked meridians.

The curvatures were measured with the 3 legged device illustrated in Fig. 6.1. A number of bases were used thus enabling the gauge length to be varied to suit the radius. The curvature was readily calculated from the dial gauge reading. The formula is shown in the figure, together with an approximate expression for the error ( $\Delta C$ ) in the derived curvature associated with a small error ( $\Delta x$ ) in the clock gauge reading. The greater the gauge length of the instrument the smaller the change in curvature which can be reliably measured. However the curvature obtained was only an average over the gauge length and a compromise was therefore necessary in selecting the gauge length. In general, the gauge length and clock gauge were chosen to allow a change in curvature of less than 4% to be detected.

#### 6.1.5 Strain gauging of ends

##### 6.1.5.1 Gauge coverage

Table 6.1 shows the strain gauge coverage of the individual ends and from this it can be seen that generally a similar gauge coverage was used throughout.

Typically double strain gauges (i.e.  $90^\circ$  pairs) were attached to about 50 gauge positions on the inner and outer surfaces, giving a total of 200 strain gauge readings for each end. The gauges were concentrated mainly in and near the knuckle where the peak stresses were expected to occur.

For the 54 in. diameter test ends (in which there was no diametrical weld) two meridians ( $0^\circ$  and  $90^\circ$ ) had a full coverage at about 21 gauge positions. This used 168 gauges; the remaining 32 were used to measure knuckle and cylinder strains on other meridians. The layout of the gauges for a typical end (No.3) is shown in Fig. 6.2.

For the 108 in. diameter test ends (each had a diametrical weld) one meridian ( $90^\circ$ ) had a full coverage at 20 gauge positions. The  $0^\circ$  and  $180^\circ$  meridians (corresponding to the diametrical weld) had 10 gauge positions each. The gauges were positioned in this way to allow a full coverage along an unwelded meridian, giving a basic strain distribution for the end, and to provide some indication of the differences due to the weld and of weld-to-weld variations. The remaining gauges were attached to other meridians.

Gauges were also mounted on the outer knuckle surfaces of the 54 in. and 108 in. diameter base ends. These gauges were read through a manually switched unit in conjunction with a digital volt meter display.

For the 81 in. diameter base end (the last diameter to be tested) it was considered that a fuller coverage could be afforded by using some of the 200 scanned gauges. Also by using a modified pressure inlet attachment in this end it was possible to bring out gauge leads through this inlet and consequently to use gauges on the inner surface of the base end. Gauges were attached to 20 positions (in corresponding pairs) on both the inner and outer surfaces (80 strain gauge readings). Ten gauge positions were on a meridional weld and ten along the central meridian of a knuckle segment. As a result, the gauge coverage on the first of the 81 in. diameter test ends (No. 16) was reduced to 120; twenty gauge positions being used on the  $90^\circ$  meridian and 10 on the  $0^\circ$  meridian. For the remaining ends of this diameter two meridians had a full coverage of 20 gauge positions each.

#### 6.1.5.2 Bonding of gauges

T.M.L. type (FCA-6-17) temperature compensated foil strain gauges were used throughout the test program. They had a gauge length of 6 mm, were made from a copper-nickel alloy and had a biaxial  $90^\circ$  cross form. The gauges were bonded to the vessel using Micro Measurements

Certified M-Bond 200 adhesive, a modified methyl-2-cyanoacrylate compound. The standard preparation and bonding techniques recommended by Micro Measurements were followed.

The strain gauge wires were soldered to terminal strips bonded to the inner and outer surface adjacent to the gauges.

The inner surface strain gauges were bonded to the end after the marking out, thickness and curvature measurements had been completed. Before water-proofing the gauges, the leads from the pole attachment were soldered to the terminal strips and each gauge tested to ensure that it was connected to the correct leads, that the resistance between grid and vessel was sufficiently high and that no open or short circuits existed.

The outer surface strain gauges were attached after the welding of the end to the base end. Each gauge was tested as previously described for the interior.

#### 6.1.5.3 Water-proofing

As the vessels were pressurised with water it was necessary to water-proof the interior gauges before use. On the first five ends tested siliconerubber was used for this purpose. The terminals and wire ends were sealed with Dow Corning 3145 R.T.V. sealant. After this had cured, the whole area of the gauge was coated with Dow Corning 3140 R.T.V. silicone rubber and this was allowed to cure. The compound is liquid in form and so the vessel had to be positioned carefully to prevent the rubber flowing away from the gauge during the application. Only a few gauges could be treated at any one time. During the course of a typical test about twenty internal gauges failed (excluding those damaged by buckling).

For the larger diameter ends Micro Measurements M-Coat G was used. The gauge area and wire ends were first coated with M-Coat D primer to prevent any slight electrical leakage under the adverse conditions.

The M-Coat G layer was then carefully applied to the gauge area; special attention being paid to the region where the lead wires joined the soldered terminal strips. This layer was allowed to extend beyond the edges of the M-Coat D layer. The coating used did not flow away from the gauges. This allowed all the gauges to be treated at the same time and made careful positioning of the vessel unnecessary. Using this method of waterproofing, typically ten interior gauges failed during a test (excluding those damaged by buckling).

#### 6.1.6 Welding test end to base end

After strain gauging the interior of a test end a number of locating lugs approximately  $\frac{1}{2}$  in. x 2 in. were welded to the open end of its cylinder on the inner surface. Eight to sixteen lugs were used, the number depending on the diameter of vessel to be welded. The function of the lugs was to locate the cylinder of the test end against that of the base end so facilitating the welding work.

The base end was first placed in the test stand and the test end lowered onto it. The lugs, whilst pulling the two cylinders into roughly the same shape, did not completely eliminate radial mismatches between the two cylinders. These radial mismatches were removed by careful levering with crowbars and blows from a rawhide mallet. Any lack of flatness in the rim of the base end due to the parting of the previous vessel was noted and removed by grinding. This process was repeated until the joint between the cylinders was satisfactory for the purpose of welding.

With the test end resting on the base the two cylinders were tack welded together at several points around the circumference. The partially welded vessel was then placed in the preparation cradle which allowed the vessel to be easily rotated. By positioning himself above the vessel (a fork-lift truck was used) the welder was able to weld "downhand"

thus producing a sound and reliable weld. Manual arc welding was used. The electrode (Nicrex NDR) was supplied by Murex Welding Processes Ltd. The weld was visually inspected for any cracks or pin poles and repaired if necessary. Dressing of this weld was unnecessary. During the test programme minor leaks were found in this weld on only two occasions and there was never any major trouble.

After welding, the vessel was placed in the test stand with the axis vertical and test end uppermost.

#### 6.1.7 Final preparation for test

The leads from the data logger, attached to plugs, were connected to the sockets on the pole attachment thus enabling the interior strain gauges to be scanned. The remaining lead wires from the data logger were soldered to the terminal strips of the outer surface strain gauges. The end height growth and the cylinder growth gauges were also attached thus completing the preparation of the test vessel.

#### 6.1.8 Vessel parting

After each test had been completed the vessel was parted so that the base end could be re-used.

For the 54 in. diameter ends the vessel was lifted into the preparation cradle, to which was attached a hand grinder fitted with a  $\frac{1}{8}$  in. thick cutting wheel. As the vessel was slowly rotated by hand the cutting wheel was brought into contact with the cylinder of the base end about  $\frac{1}{2}$  in. from the weld. In this way the vessel was cut into two halves leaving the base end reasonably flat for the welding of the next end. However it was found that distortions in the cylinder, due to buckling, caused the vessel to "wander" slightly and so for the larger vessels a new parting technique was developed.

The pipe fitting at the pole of the base end was located in a thrust bearing placed on the floor whilst the upper end of the vessel was



supported in a brass journal bearing around the cylindrical lower part of the pole attachment. The brass bearing was held in members projecting out from two angle-iron frames fastened to a nearby wall. The vessel was thus free to rotate about its vertical axis. A photograph of this arrangement is shown in Fig. 6.3.

The hand grinder, fitted with a cutting wheel, was clamped to one of the nearby frames so that the wheel could contact the cylinder about  $\frac{1}{2}$  in. below the main circumferential weld (Fig. 6.3). As the vessel was rotated slowly by hand, the cutting wheel was brought into contact with the cylinder, thus cutting the vessel into two halves. The weight of the upper portion was partially taken by an overhead crane thus preventing the gap between the two half vessels from closing as parting neared completion. The flatness of the cut produced on the base end was invariably good enough to allow welding of the next test end without dressing.

## 6.2 Test procedure

The following is a general description of the test procedure used for each test end. Details about pressure increments and the length of time a vessel was held at a particular pressure level varied considerably. They can be determined for each end from the test history diagrams in Chapter 8. Individual tests are described in detail in Chapter 8.

- i) A test was commenced by filling the vessel with water through the opening at the pole of the base end. During filling the eight nuts securing the two halves of the pole attachment (Fig. 5.4) were slackened to allow air to escape.
- ii) An initial scan of the two hundred strain gauges was taken at "zero" pressure and the values stored in the computer and on paper tape. The initial scan reading for each gauge was

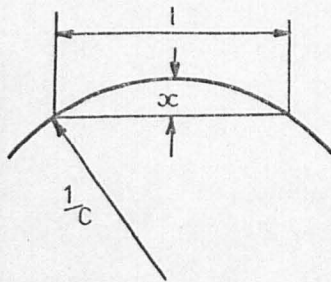
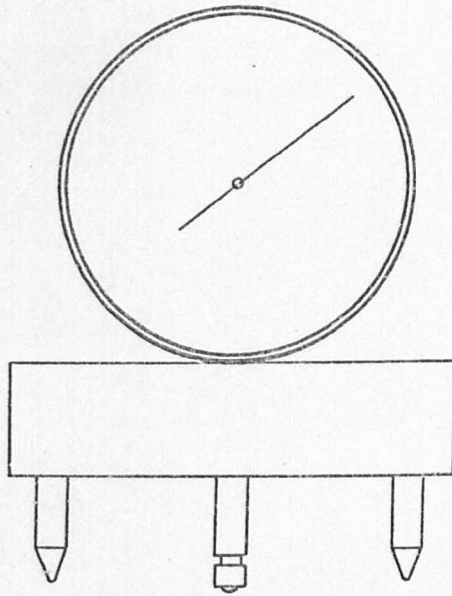
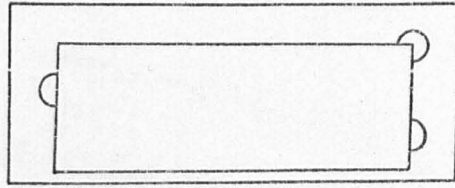
subtracted from all subsequent readings for that gauge. (The "zero" pressure referred to was that occurring when the vessel was full of water with the top open to the atmosphere).

- iii) The strain gauges were then scanned again at "zero" pressure and the zero strain values printed on the teletype as a check.
- iv) The pole deflection devices and circumferential growth gauges were zeroed.
- v) The pressure was slowly increased in suitable steps until the vessel failed by buckling or excessive plastic deformation.
- vi) At each pressure all gauges were scanned at regular intervals. After three scans the strain gauge readings were printed out as strains on the teletype. If the vessel appeared to be creeping, further scans were taken at suitable time intervals until the creeping had effectively ceased. At low pressures three scans were usually sufficient. At high pressures as many as 10 scans were necessary.
- vii) Throughout a test, the vessel was carefully inspected for any signs of buckling.
- viii) The pressure was usually increased above the first buckling pressure to determine the subsequent behaviour of the end. As many as nine buckles were obtained on some ends.

TABLE 6.1 STRAIN GAUGE POSITIONS - DISTANCE FROM POLE IN INCHES ON THE MERIDIANS INDICATED

\* Crown/Knuckle Junction.  
 + Knuckle/Cylinder Junction.

Position No.	1	2	3	4	5	6	7	8	9	10	11	12	13	14	15	16	17	18	19	20	21	
1	7.31 0° 00'	13.31 0° 00'	17.04 0° 00'	19.81 0° 00'	21.12 0° 00'	22.31 0° 00'	23.56 0° 00'	24.87 0° 00'	26.06 0° 00'	27.44 0° 00'	28.81 0° 00'	30.19 0° 24'	31.56 0° 24'	32.94 0° 24'	33.94 0° 24'	34.94 0° 24'	36.04 0° 00'	41.04 0° 00'				
2	7.31 0° 00'	13.31 0° 00'	15.81 0° 00'	17.94 0° 00'	19.81 0° 00'	21.12 0° 00'	22.31 0° 00'	23.56 0° 00'	24.87 0° 00'	26.06 0° 00'	27.44 0° 00'	28.81 0° 00'	30.19 0° 00'	31.56 0° 00'	32.94 0° 00'	33.94 0° 00'	34.94 0° 00'	36.04 0° 00'	41.04 0° 00'	44.94 0° 00'		
3	6.81 0° 00'	11.88 0° 00'	16.88 0° 00'	19.88 0° 00'	21.88 0° 00'	22.75 0° 00'	23.63 0° 00'	24.50 0° 00'	25.38 0° 00'	26.25 0° 00'	27.13 0° 00'	28.00 0° 00'	28.88 0° 00'	29.75 0° 00'	30.63 0° 00'	31.38 0° 00'	32.00 0° 00'	32.63 0° 00'	33.25 0° 00'	35.31 0° 00'	43.31 0° 00'	
4	7.38 0° 00'	13.38 0° 00'	19.38 0° 00'	22.38 0° 00'	24.38 0° 00'	24.88 0° 00'	25.38 0° 00'	25.88 0° 00'	26.38 0° 00'	26.88 0° 00'	27.38 0° 00'	27.88 0° 00'	28.38 0° 00'	28.88 0° 00'	29.13 0° 00'	29.75 0° 00'	30.38 0° 00'	30.88 0° 00'	31.38 0° 00'	31.88 0° 00'	43.31 0° 00'	
5	8.35 0° 00'	17.35 0° 00'	22.35 0° 00'	24.85 0° 00'	25.85 0° 00'	26.35 0° 00'	26.85 0° 00'	27.35 0° 00'	27.85 0° 00'	28.35 0° 00'	28.85 0° 00'	29.35 0° 00'	29.85 0° 00'	29.85 0° 00'	30.88 0° 00'	31.38 0° 00'	31.88 0° 00'	32.88 0° 00'	34.88 0° 00'	42.88 0° 00'	43.31 0° 00'	
6	8.00 0° 00'	17.00 0° 00'	20.40 0° 00'	22.90 0° 00'	25.40 0° 00'	26.31 0° 00'	26.86 0° 00'	27.40 0° 00'	27.94 0° 00'	28.49 0° 00'	29.03 0° 00'	29.57 0° 00'	30.11 0° 00'	30.11 0° 00'	30.66 0° 00'	31.20 0° 00'	31.74 0° 00'	32.29 0° 00'	33.20 0° 00'	35.20 0° 00'	43.20 0° 00'	
7	14.50	26.50	31.50	35.50	38.50	41.50	44.50	47.12	49.75	52.38	55.00	57.63	60.26	62.89	65.51	68.14	70.77	73.40	76.03	78.66	81.29	
8	18.96 0° 00'	30.96 0° 00'	35.96 0° 00'	39.96 0° 00'	42.96 0° 00'	44.96 0° 00'	46.96 0° 00'	48.96 0° 00'	50.96 0° 00'	52.83 0° 00'	54.77 0° 00'	56.71 0° 00'	58.65 0° 00'	60.58 0° 00'	62.52 0° 00'	64.42 0° 00'	66.32 0° 00'	68.22 0° 00'	70.12 0° 00'	72.02 0° 00'	73.92 0° 00'	
9	20.68 0° 00'	38.68 0° 00'	41.68 0° 00'	44.68 0° 00'	46.68 0° 00'	48.68 0° 00'	50.18 0° 00'	51.68 0° 00'	52.95 0° 00'	54.22 0° 00'	55.49 0° 00'	56.76 0° 00'	58.03 0° 00'	59.30 0° 00'	60.57 0° 00'	61.82 0° 00'	63.32 0° 00'	64.23 0° 00'	65.32 0° 00'	66.57 0° 00'	68.57 0° 00'	
10	23.28 0° 00'	41.28 0° 00'	45.28 0° 00'	48.28 0° 00'	50.28 0° 00'	51.41 0° 00'	52.55 0° 00'	53.68 0° 00'	54.81 0° 00'	55.94 0° 00'	57.08 0° 00'	58.21 0° 00'	59.34 0° 00'	60.47 0° 00'	61.60 0° 00'	62.73 0° 00'	64.23 0° 00'	65.46 0° 00'	66.60 0° 00'	68.60 0° 00'	70.57 0° 00'	
11	23.02 0° 00'	42.02 0° 00'	49.02 0° 00'	51.02 0° 00'	53.02 0° 00'	54.02 0° 00'	55.02 0° 00'	56.02 0° 00'	57.01 0° 00'	58.00 0° 00'	59.99 0° 00'	59.98 0° 00'	60.98 0° 00'	61.97 0° 00'	62.96 0° 00'	63.96 0° 00'	65.46 0° 00'	66.23 0° 00'	67.96 0° 00'	69.60 0° 00'	71.57 0° 00'	
12	21.98 0° 00'	39.98 0° 00'	45.98 0° 00'	47.98 0° 00'	49.98 0° 00'	50.98 0° 00'	51.98 0° 00'	52.98 0° 00'	53.92 0° 00'	54.87 0° 00'	55.82 0° 00'	56.76 0° 00'	57.71 0° 00'	58.65 0° 00'	59.60 0° 00'	60.60 0° 00'	62.10 0° 00'	64.10 0° 00'	67.60 0° 00'	70.90 0° 00'	74.90 0° 00'	
13	14.50 0° 00'	26.50 0° 00'	31.50 0° 00'	35.50 0° 00'	38.50 0° 00'	41.50 0° 00'	44.50 0° 00'	47.12 0° 00'	49.75 0° 00'	52.38 0° 00'	55.00 0° 00'	57.63 0° 00'	60.26 0° 00'	62.89 0° 00'	65.51 0° 00'	68.14 0° 00'	70.77 0° 00'	73.40 0° 00'	76.03 0° 00'	78.66 0° 00'	81.29 0° 00'	
14	10.09	19.89	23.64	26.64	28.89	31.14	33.39	35.36	37.34	39.31	41.28	43.26	45.23	47.21	49.18	51.14	53.11	55.08	57.05	59.02	61.00	
15	10.89	19.89	23.64	26.64	28.89	31.14	33.39	35.36	37.34	39.31	41.28	43.26	45.23	47.21	49.18	51.14	53.11	55.08	57.05	59.02	61.00	
16	15.08	29.38	31.63	33.88	35.28	36.78	37.78	38.78	39.74	40.69	41.65	42.61	43.56	44.52	45.47	46.48	47.58	48.68	49.78	50.88	51.98	
17	17.47 0° 00'	30.97 0° 00'	33.97 0° 00'	36.22 0° 00'	37.72 0° 00'	38.57 0° 00'	39.42 0° 00'	40.26 0° 00'	41.13 0° 00'	41.98 0° 00'	42.84 0° 00'	43.69 0° 00'	44.55 0° 00'	45.40 0° 00'	46.25 0° 00'	47.05 0° 00'	47.85 0° 00'	48.65 0° 00'	49.45 0° 00'	50.25 0° 00'	51.05 0° 00'	51.85 0° 00'



$$\text{Curvature } (C) = \left[ \frac{l^2}{8x} + \frac{x}{2} \right]^{-1}$$

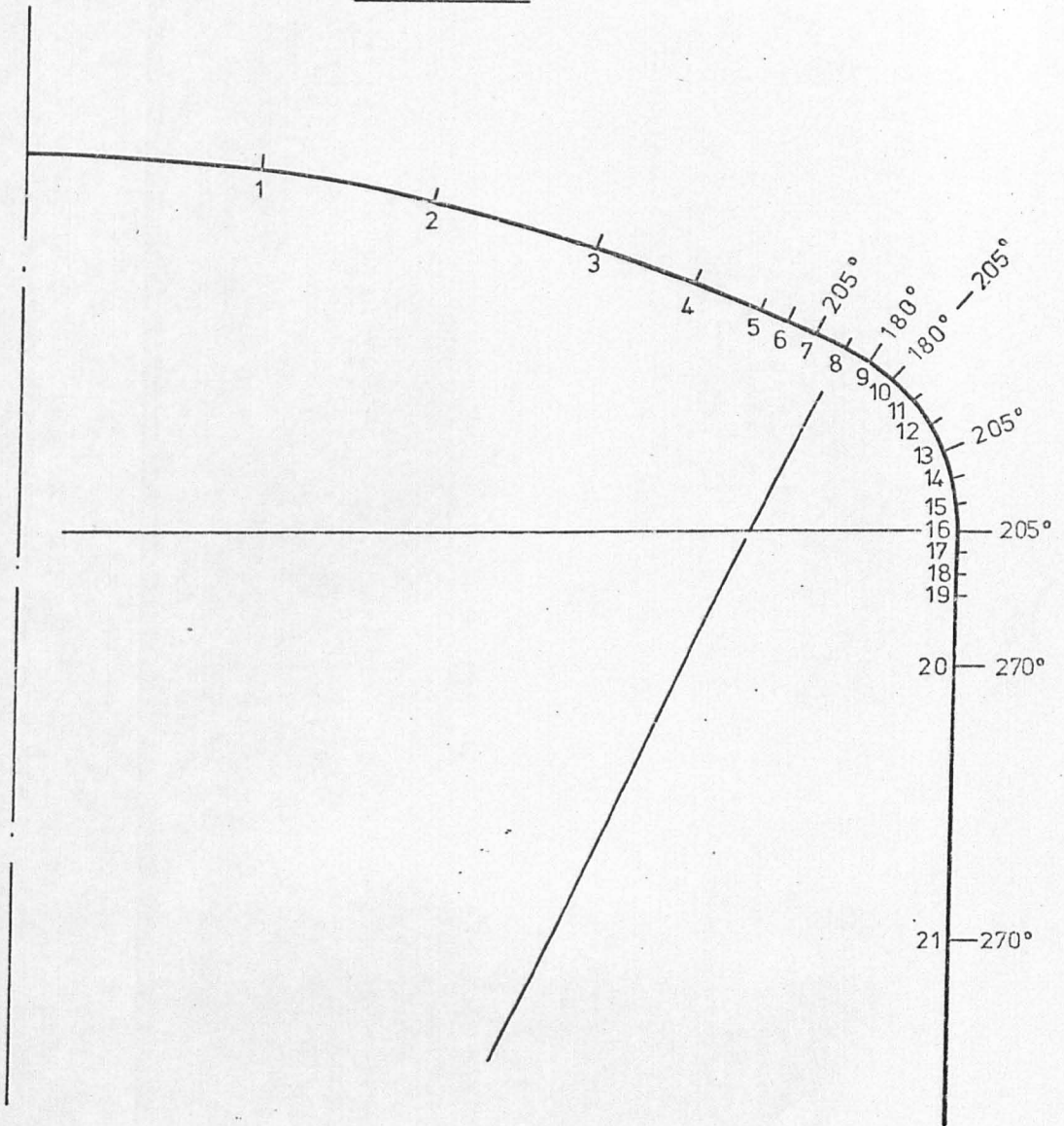
$$\Delta C \approx \frac{8 \Delta x}{l^2}$$

CURVATURE MEASURING DEVICE

FIG. 6.1

# GAUGE LOCATION

## END No. 3



### NOTES.

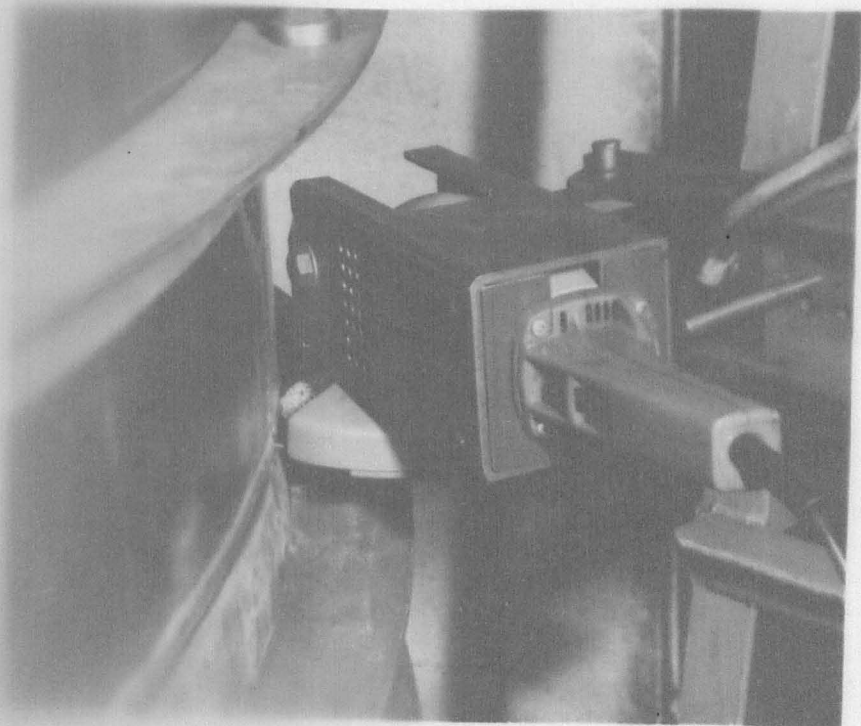
1. Strain gauges are positioned on both surfaces along the  $0^\circ$  and  $90^\circ$  meridians at the 21 positions shown.
2. The positions and meridians of additional gauges are indicated.
3. Individual gauges are identified by position (1-21), inner or outer surface (i or o), meridional or circumferential (m or c) and meridian.

VESSEL PARTING - IMPROVED METHOD

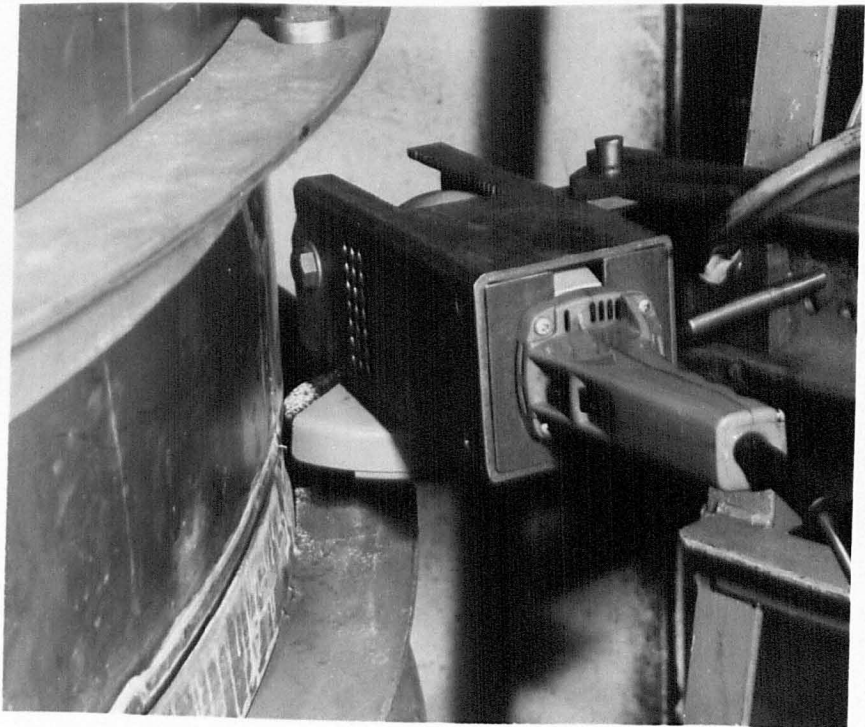
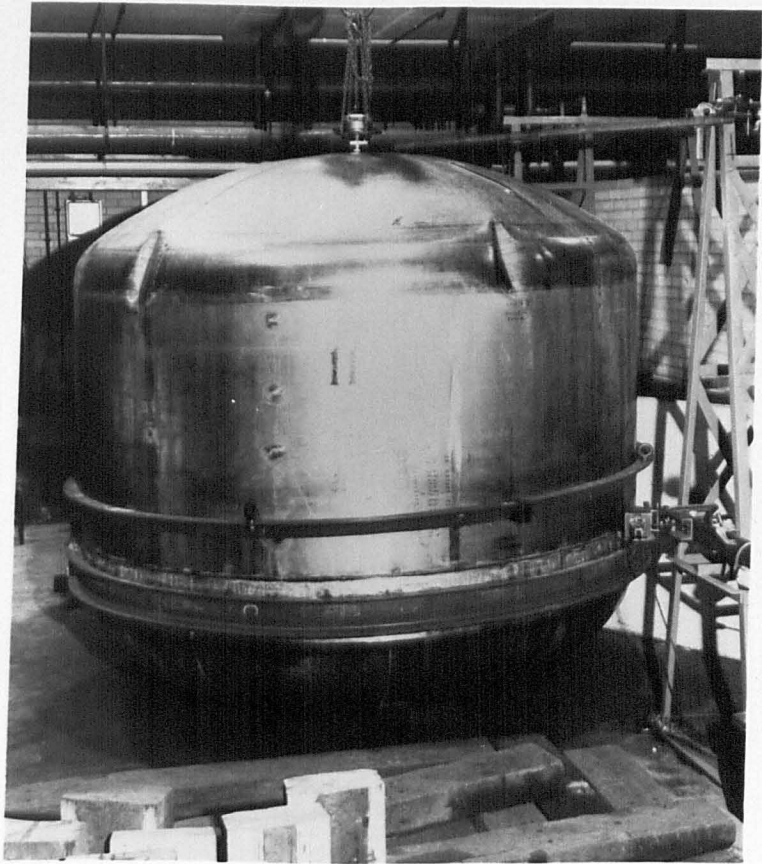
VESSEL PARTING - CUTTING MACHINE



VESSEL PARTING - IMPROVED METHOD



VESSEL PARTING - CUTTING MACHINE





CHAPTER 7RESULTS7.1 Introduction

To illustrate the extent and detail of the measurements recorded during each test, a complete set of results for a typical end (number 9) has been included in this chapter (Figs. 7.1 - 7.33). As it would be impracticable to present a similar set of graphs for each of the seventeen test ends, only a limited number of figures have been included for the sixteen other ends. They have been chosen to illustrate the main features of each end. These graphs are presented in Appendix 1.

In general five types of graph are shown for each end. These are :

1. Thickness against distance from pole(s) along a typical meridian.
2. Curvature against distance from pole(s) along a typical meridian.
3. Pressure against strain plots for individual strain gauges (in general the highest reading) along a typical meridian. The individual gauges are identified by position (1-21), inner or outer surface (i or o) meridional or circumferential (m or c) and meridian.
4. A strain distribution along a typical meridian at a pressure level just below that at which first buckling occurred.
5. A distribution of elastic stress indices along a typical meridian.

For ends containing welds two graphs each of the type 3, 4 and 5 are presented. One meridian chosen corresponds to the main weld whilst the other is at  $90^\circ$  to it. The figure numbers associated with these graphs indicate to which end the graph refers. For example Fig. A1.8.3 can be found in Appendix 1, refers to end number 8, and is the third graph for that end.

It is emphasised at this point that the stresses and strains given

in these figures are for the applied internal pressure only, and do not include the residual stresses and strains present on delivery. These will be discussed separately in chapter 8.

A summary sheet for each end is presented in Appendix 2.

The pressure values quoted in the graphs and text are those occurring at the knuckle/cylinder junction.

## 7.2 End No.9

Fig. 7.1 shows the thickness variation along a typical meridian ( $90^\circ$ ), at twenty positions. Thickness ( $t$ ) is plotted against distance from pole ( $s$ ).

Figs. 7.2 and 7.3 illustrate the variation of curvature with position along two meridians ( $45^\circ$  and  $180^\circ$ ). The nominal crown and knuckle curvatures are also included. The error in curvature ( $\Delta C$ ) indicated on these and other curvature plots is calculated from the formula shown in Fig. 6.1.

Figs. 7.4 to 7.6 are pressure-strain plots for individual strain gauges on the  $0^\circ$ ,  $90^\circ$  and  $180^\circ$  meridians respectively. The  $0^\circ$  and  $180^\circ$  meridians are coincident with a diametrical weld in the end. The gauges chosen are in general those giving the highest readings in the knuckle. The position of each gauge on the end can be identified from Table 6.1. For these and other pressure-strain plots individual gauges are identified by position (1-21), inner or outer surface (i or o), meridional or circumferential (m or c) and meridian.

Figs. 7.7 to 7.21 show the strain distributions along three meridians ( $0^\circ$ ,  $90^\circ$  and  $180^\circ$ ) at various pressures during the test. Strain values are plotted against  $s/D_i$ . The extent of the knuckle and crown is indicated. The elastic strain distributions in the end, at pressures of  $10 \text{ lbf/in}^2$  and  $18 \text{ lbf/in}^2$ , can be seen in Figs. 7.7 to 7.9 and 7.10 to

7.12 respectively. The elastic-plastic strain distributions prior to buckling at pressures of  $38 \text{ lbf/in}^2$  and  $58 \text{ lbf/in}^2$  are shown in Figs. 7.13 to 7.15 and 7.16 to 7.18 respectively. Figs. 7.19 and 7.20 show the strain distributions at the first buckling pressure after the first buckle had occurred. (No graph is given for the  $0^\circ$  meridian as the strain gauges were damaged by the buckle). Fig. 7.21 shows the strain distribution on the  $90^\circ$  meridian at the maximum test pressure, after the occurrence of five buckles.

Figs. 7.22 to 7.27 illustrate the distribution of elastic stress indices along the three gauged meridians at pressures of  $10 \text{ lbf/in}^2$  and  $18 \text{ lbf/in}^2$ . The stress index values used were calculated from the strain readings of Figs. 7.7 to 7.12 and are shown plotted against  $s/D_i$ . They were obtained by dividing the calculated stress at each position by  $pD_i/2t_e$ , the hoop stress in a cylinder with the same thickness to diameter ratio as the end. Stresses for all ends were calculated using  $E = 29 \times 10^6 \text{ lbf/in}^2$  and  $\nu = 0.31$ . These values were obtained from the steel manufacturer's catalogue (Ref. 35).

Fig. 7.28 shows the variation of strain in the knuckle with circumferential angular position just prior to the first buckle. The  $0^\circ$  position corresponds to the eventual "fold line" of the first buckle. Each gauge plotted is the same distance from the pole. The strain gauge readings  $90^\circ$  away from the site of the buckle are also shown.

Figs. 7.29 to 7.31 illustrate the increase in strain with time (creep) at three of the most highly strained positions. At each position the creep at three pressure levels is plotted.

Fig. 7.32 shows the increase in end height with pressure.  $\Delta h/h_i(\%)$  is plotted against pressure.

Fig. 7.33 shows the development of circumferential strain in the cylinder with pressure at four positions. The strain values are calculated from the circumferential growth measured by the steel tape gauges.

### 7.3 54 in. diameter ends

#### 7.3.1 End No.1 (Crown and segment base end)

Figs. Al.1.1 and Al.1.2 show the thickness and curvature variations respectively along the  $0^{\circ}$  meridian of the end.

Fig. Al.1.3 is a plot of pressure against strain for some of the highest reading gauges during the first pressurization. On a subsequent pressurization (prior to the appearance of any buckle) additional strain gauges were attached to the end. From these gauges a distribution of elastic stress indices along the  $0^{\circ}$  meridian was obtained (Fig. Al.1.4).

No strain gauges were attached to the interior of this end.

#### 7.3.2 Ends No. 2 - 6.

Figs. Al.2.1, Al.3.1 ..... Al.6.1 show the variation of thickness along a typical meridian of each end.

Figs. Al.2.2 etc illustrate typical curvature variations along a meridian.

Figs Al.2.3 etc. show the change in strain with increasing pressure for the most interesting (usually the highest reading) strain gauges on one meridian.

Figs. Al.2.4 etc. are strain distributions along typical meridians after the onset of yield but before buckling.

Figs. Al.2.5 etc. show the distribution of elastic stress indices along the meridians indicated. The peak stress indices illustrated are not necessarily the maxima occurring on a given end.

The strain gauges on end 2 used to obtain Figs. Al.2.3 to Al.2.5 were situated well clear of the knuckle segment welds.

#### 7.4 108 in. and 81 in diameter ends

##### 7.4.1 End No.7 (Crown and segment base end)

Fig. Al.7.1 shows the thickness variation along the  $0^\circ$  (crown weld) and  $90^\circ$  meridians.

Fig. Al.7.2 illustrates the variation in curvature along the  $45^\circ$  meridian.

Fig. Al.7.3 shows the change in strain with increasing pressure for individual strain gauges along two gauged meridians. The  $233^\circ$  meridian corresponds to a knuckle weld. The  $268^\circ$  meridian was situated midway along a knuckle segment.

Fig. Al.7.4 illustrates the outer surface strain distribution in the knuckle along the  $233^\circ$  and  $268^\circ$  meridians at a pressure just below that at which the first buckle occurred.

Fig. Al.7.5 shows the distribution of elastic stress indices along the two gauged meridians at a pressure of  $20 \text{ lbf/in}^2$ .

No strain gauges were attached to the interior of this end.

##### 7.4.2 Ends No.8, and 10 to 17

Figs. Al.8.1, Al.10.1 etc. show the variation of thickness along the  $90^\circ$  meridian of each end.

Figs Al.8.2, Al.10.2 etc. show the variation of curvature along the  $90^\circ$  meridian of each end.

Figs. Al.8.3 etc are pressure-strain plots for individual strain gauges situated on welds. The gauges chosen are in general the highest reading gauges in the knuckle.

Fig. Al.8.4 etc. are pressure-strain plots for individual strain gauges situated away from welds. Again the gauges chosen are in general the highest reading gauges in the knuckle.

Figs Al.8.5 etc. show the strain distributions along meridians coincident with welds.

Figs. Al.8.6 etc show the strain distributions along meridians situated away from welds.

Figs. Al.8.7 etc illustrate the distribution of elastic stress indices along meridians coincident with welds.

Figs. Al.8.8 etc illustrate the distribution of elastic stress indices along meridians situated away from welds..

## 7.5 Tables and Photographs

Tables 7.1 to 7.4 attempt to summarise the most important features of each test end.

The thickness and shape characteristics are presented in Table 7.1. The nominal thickness and dimensions are also included. These can be compared with the measured thickness at several positions in the knuckle and the mean radii observed in the crown and knuckle.

Table 7.2 shows the elastic behaviour of each end. Peak strain factors (i.e. strains divided by hoop strain in a cylinder with the same thickness to diameter ratio as the end) and stress indices are presented together with relative end height growths and cylinder strains. The nominal shape parameters are also shown.

Table 7.3 presents the post yield behaviour of each end prior to buckling. Peak strains at the first buckling pressure (prior to buckling) are given. Cylinder strains and end height growths at the same pressure are included. The last part of the table presents various calculated limit pressures, details of which are given in the notes associated with this table.

Table 7.4 shows the pressure at which each buckle occurred. The time at the pressure prior to buckling, the meridian on which the buckle occurred and the type of buckle are also tabulated. The maximum test pressure reached  $p_{MAX}$  and the theoretical buckling pressure  $p_{TH}$  predicted from the work of Thurston and Holston (Ref. 10) are included.

Figs. 7.34 to 7.38 are photographs of buckles produced on the ends. Two buckles are shown for end 13 and one for each other end.

TABLE 7.1 COMPARISON OF NOMINAL AND MEASURED DIMENSIONS

End No.	Construction	Nominal Dimensions (inches)						Measured Dimensions (inches)										Thickness in cyl $t_c$
		$3D_o$	$r_o$	$R_o$	$h_o$	$t_e$	$t_c$	$3D_o$	$4r_o$	$5R_o$	$h_o$	$t_k/crown$	$t_{1/4}$	$t_{1/2}$	$t_{3/4}$	$t_{1 1/2}$ in	$t_k/cyl$	
1	C & S (4)	54.256	9.128	54.128	12.89	0.128	0.104	54.2	10.2	42.8	12.6	0.128+11 -9	0.133+2 -2	0.132+3 -3	0.133+2 -4	0.134+2 -3	0.104+22 -11	0.108+1 -1
2	C & S (4)	54.256	9.128	54.128	12.89	0.128	0.104	54.1	10.8	41.5	12.7	0.130+16 -8	0.131+2 -2	0.131+3 -1	0.131+4 -1	0.132+3 -2	0.098+9 -6	0.106+0 -0
3	S	54.256	6.128	54.128	10.97	0.128	0.104	54.2	7.1	44.7	10.8	0.131+2 -2	0.112+1 -2	0.117+2 -2	0.113+2 -2	0.112+2 -2	0.109+16 -11	0.109+1 -1
4	S	54.256	4.128	54.128	9.73	0.128	0.104	54.2	5.4	47.4	9.6	0.133+3 -2	0.133+3 -4	0.116+2 -2	0.101+2 -2	0.104+2 -2	0.107+2 -3	0.108+1 -1
5	S	54.256	4.128	45.128	11.19	0.128	0.104	54.2	5.1	38.1	11.1	0.136+2 -3	0.117+3 -3	0.107+2 -3	0.115+3 -3	0.114+4 -3	0.098+10 -8	0.108+1 -3
6	S	54.256	4.128	42.128	11.88	0.128	0.104	54.2	4.6	36.0	11.6	0.127+5 -5	0.119+2 -3	0.110+3 -3	0.109+2 -3	0.109+2 -2	0.102+7 -7	0.109+1 -1
7	C & S (5)	108.256	18.128	108.128	25.64	0.128	0.104	108.3	18.9	128.8	25.5	0.125+5 -13	0.130+2 -3	0.128+3 -5	0.128+1 -1	-	-	-
8	S	108.256	12.128	108.128	21.80	0.128	0.104	108.2	14.4	81.6	21.8	0.130+2-1 0.124+1-1	0.120+4-3 0.113+0-0	0.105+1-1 0.099+0-0	0.095+4-2 0.090+1-1	0.093+3-7 0.089+3-3	0.090+10 -12	0.107+1 -2
9	S	108.256	8.128	108.128	19.34	0.128	0.104	108.0	9.8	85.9	19.3	0.131+2-2 0.125+0-0	0.121+1-2 0.115+0-0	0.119+3-3 0.112+0-0	0.114+2-3 0.114+2-2	0.121+2-3 0.114+1-1	0.096+23 -7	0.107+1 -2
10	S	108.256	8.128	90.128	22.25	0.128	0.104	108.2	10.3	75.9	21.8	0.123+4-3 0.117+2-2	0.123+2-2 0.122+4-4	0.119+2-1 0.114+1-1	0.121+3-3 0.118+0-0	0.122+2-1 0.119+1-1	0.095+9 -7	0.107+1 -1
11	S	108.256	8.128	78.128	25.36	0.128	0.104	108.2	11.2	61.1	25.1	0.127+4-7 0.121+3-3	0.116+2-3 0.113+1-1	0.105+1-1 0.103+1-1	0.108+2-1 0.106+2-2	0.110+2-2 0.109+3-3	0.102+2 -8	0.107+3 -3
12	S	108.256	6.128	108.128	18.13	0.128	0.104	107.9	8.5	73.1	18.9	0.131+4-3 0.126+2-2	0.116+4-4 0.114+2-2	0.119+3-4 0.117+0-0	0.120+2-3 0.119+0-0	0.121+2-3 0.119+6-0	0.095+6 -8	0.107+2 -2
13	C & S (5)	108.256	18.128	108.128	25.64	0.128	0.104	108.1	17.9	106.8	25.2	0.124+8 -8	0.134+2 -3	0.133+2 -2	0.134+2 -3	0.116+8 -5	0.092+15 -11	0.108+1 -1
14	C & S (5)	81.256	13.628	81.128	19.26	0.128	0.104	81.2	15.5	69.9	19.1	0.119+8 -10	0.131+4 -3	0.130+4 -3	0.130+5 -3	0.129+6 -6	0.126+10 -20	-
15	C & S (5)	81.256	13.628	81.128	19.26	0.128	0.104	81.1	14.3	75.2	19.0	0.128+2 -2	0.128+2 -2	0.128+2 -2	0.129+4 -3	0.123+6 -4	0.103+14 -11	0.109+1 -1
16	S	81.256	6.128	81.128	14.53	0.128	0.104	81.0	7.2	61.7	14.4	0.135+2-3 0.129+4-4	0.121+1-1 0.116+1-1	0.118+2-1 0.115+1-1	0.119+2-2 0.111+1-1	0.119+2-2 0.112+1-1	0.094+12 -8	0.109+1 -2
17	S	81.256	6.128	67.628	16.72	0.128	0.104	80.9	7.3	51.6	16.6	0.137+2-2 0.131+2-2	0.124+2-3 0.117+1-1	0.118+2-2 0.113+1-1	0.116+2-2 0.114+3-3	0.116+2-2 0.114+3-3	0.106+21 -13	0.110+2 -1

Superscript numbers refer to notes on following page.



NOTES ON TABLE 7.1

1. Base end.
2. C & S ( ). Crown and segment (number of panels in knuckle)  
S. Pressed and spun.
3. The nominal value of  $D_o$  is equal to  $(D_i + 2t_e)$ . The "measured" value of  $D_o$  is calculated from the circumference measurement at the knuckle/cylinder junction.
4. Outer surface knuckle radius, obtained by calculating the reciprocal of the average curvature in the knuckle.
5. Outer surface crown radius, obtained by calculating the reciprocal of the average curvature in the crown.
6. The positions of the thickness quoted are :-
  - a) Knuckle/crown junction.
  - b)  $\frac{1}{4}$ ,  $\frac{1}{2}$  and  $\frac{3}{4}$  of the length of the knuckle arc measured from a).
  - c) In the knuckle  $1\frac{1}{2}$  in. from the knuckle/cylinder junction.
  - d) Knuckle/cylinder junction.

At each position the thickness quoted is the average of several values measured around the knuckle. The range of values observed is also given.

For ends 8, 9, 10, 11, 12, 16 and 17 the first value quoted is away from the welds and the second is on a weld.
7. The position of thickness quoted is midway down the length of the cylinder. At each position the thickness quoted is the average of several values measured around the cylinder. The range of values observed is also given.

TABLE 7.2: ELASTIC STRAIN FACTORS AND STRESS INDICES

End No.	Shape Parameters			Peak strain Factors at PFI						Peak Stress Indices at PFI						PFI	$\frac{2\epsilon_{ah}}{h_1}$	Cylinder Strain Gauge	Hoop Factor Tape	$h_{P_{NL}}$
	$r_i/D_i$	$F_i/D_i$	$h_i/D_i$	$t_e/D_i$	$F_{im}$	$F_{om}$	$F_{ic}$	$F_{oc}$	$I_{im}$	$I_{om}$	$I_{ic}$	$I_{oc}$								
1	0.167	1.0	0.236	0.00237	-	0.58 0°	-	-	-1.42 0°	-	0.20 0°	-	-	-1.10 0°	50.3	-	-	70		
2	0.167	1.0	0.236	0.00237	1.74 90°	0.42 90°	0.76 145°W	-1.27 0°	-2.12 235°W	1.33 90°	1.24 145°W	0.30 90°	-0.88 0°	-1.70 235°W	38.3	-1.29 145°W	0.93	0.88	50	
3	0.111	1.0	0.201	0.00237	3.46 0°	-0.75 90°	-	-3.21 90°	-3.18 90°	2.48 0°	-1.51 90°	-2.21 90°	-3.04 90°	-3.04 90°	58.3	-	0.96	63		
4	0.074	1.0	0.178	0.00237	5.58 45°	-1.72 0°	-5.00 90°	-5.00 90°	-5.00 45°	3.91 45°	-2.84 0°	-3.62 90°	-5.00 45°	-5.00 45°	28.3	-	0.98	28		
5	0.074	0.833	0.205	0.00237	3.74 0°	-0.76 0°	-3.26 180°	-3.40 90°	-3.40 90°	2.64 0°	-1.41 0°	-2.31 180°	-3.16 90°	-3.16 90°	38.3	-	0.95	42		
6	0.074	0.778	0.218	0.00237	4.51 225°	-0.83 225°	-3.87 225°	-3.87 225°	-3.87 225°	3.09 225°	-1.89 225°	-2.51 225°	-3.84 225°	-3.84 225°	43.3	-	0.98	100		
7	0.167	1.0	0.236	0.00119	-	0.48 269°	0.32 233°	-	-2.08 269°	-	-0.16 269°	-	-	-1.83 269°	20.2	-2.70 233°	-	26		
8	0.111	1.0	0.201	0.00119	3.16 90°	0.05 90°	-0.14 0°	-2.76 90°	-3.34 180°W	2.35 90°	2.12 180°W	-0.72 90°	-1.99 90°	-2.29 180°W	18.0	-3.78 0°W	1.02	5.38		
9	0.074	1.0	0.178	0.00119	4.25 90°	0.00 90°	-0.05 0°W	-4.84 90°	-5.06 180°W	2.63 90°	2.59 180°W	-1.22 90°	-3.53 90°	-3.91 180°W	18.0	-5.83 0°W	1.02	22		
10	0.074	0.833	0.205	0.00119	3.49 90°	-0.23 90°	0.00 180°W	-4.47 90°	-4.59 0°W	2.11 90°	1.21 90°	-3.32 90°	-3.54 0°W	-4.12 90°	14.0	-4.19 180°W	0.92	5.33		
11	0.074	0.722	0.234	0.00119	3.37 90°	-4.01 90°	-0.81 180°W	-4.13 90°	-4.18 180°W	2.38 90°	1.92 180°W	-1.80 90°	-2.98 90°	-3.34 180°W	14.0	-4.07 180°W	0.99	41		
12	0.056	1.0	0.167	0.00119	4.47 90°	-0.06 90°	-0.29 0°W	-5.00 90°	-5.46 180°W	2.74 90°	3.21 0°W	-1.40 90°	-3.43 90°	-3.84 180°W	14.0	-5.51 0°W	1.02	15		
13	0.167	1.0	0.236	0.00119	2.44 90°	0.52 90°	0.52 118°W	-2.48 90°	-2.66 118°W	1.46 90°	1.46 118°W	-0.42 90°	-1.59 90°	-1.77 90°	22.0	-2.32 118°W	0.97	22		
14	0.167	1.0	0.236	0.00158	2.59 0°	-0.11 0°	0.22 325°W	-2.12 0°	-2.44 325°W	1.80 0°	1.90 325°W	-0.78 0°	-1.29 325°W	-1.73 325°W	30.2	-2.29 325°W	-	38		
15	0.167	1.0	0.236	0.00158	3.02 338°	-0.29 338°	0.14 86°W	-2.54 338°	-3.12 86°W	2.09 338°	2.76 86°W	-0.97 338°	-1.58 338°	-2.29 86°W	22.6	-2.12 86°W	0.96	36		
16	0.074	1.0	0.178	0.00158	4.78 90°	-0.80 90°	-0.61 0°W	-5.20 90°	-4.97 90°	3.10 90°	3.57 0°W	-1.76 90°	-3.55 90°	-4.15 90°	28.6	-5.79 0°W	1.00	29		
17	0.074	0.833	0.205	0.00158	3.74 90°	-0.72 90°	-0.43 0°W	-4.37 90°	-4.37 90°	2.53 90°	2.78 0°W	-1.76 90°	-2.76 90°	-3.02 0°W	22.6	-4.71 0°W	0.98	39		

Superscript numbers refer to notes on following page.

NOTES ON TABLE 7.2

1. Strain factor is defined as strain divided by  $pD(1-\nu/2)/2t_eE$ , the theoretical hoop strain in a cylinder with the same  $t_e/D$  ratio as the end.

Stress index is defined as stress divided by  $pD/2t_e$ , the theoretical hoop stress in a cylinder with the same  $t_e/D$  ratio as the end.

The position of corresponding peak stresses and strains do not necessarily coincide.

There were no welds in ends 3 to 6, therefore peak values used are the maximum occurring anywhere in an end.

For ends with welds the peak strain factors and stress indices both on and away from welds are given.

The figure beneath each peak strain factor and stress index refers to the meridian on which the factor or index was observed. A 'W' after this figure indicates the meridian is coincident with a weld.

2. The values of  $\Delta h/h_1$  quoted were obtained at  $p_{FI}$ .

3. Cylinder hoop strain factors were determined at a pressure level approximately half the cylinder yield pressure.

4. Interpolated pressure at which the pressure-strain curve for the maximum reading strain gauge (see 5) first departs from the linear.

5. The maximum reading gauge to show appreciable departure from the linear was used for ends 8 and 10.

TABLE 7.2a: POST YIELD BEHAVIOUR OF ENDS PRIOR TO BUCKLING

End No.	Shape Parameters				P <sub>ML</sub>	P <sub>CR</sub>	2 Peak strains at P <sub>CR</sub>						Cylinder strains at P <sub>CR</sub> (Z)		3 h <sub>i</sub> / h <sub>1</sub>	S & D	S <sub>SAVE</sub>	7 (Z)	Limit Pressures									
	r <sub>i</sub> /D <sub>i</sub>	R <sub>i</sub> /D <sub>i</sub>	h <sub>i</sub> /D <sub>i</sub>	t <sub>e</sub> /D <sub>i</sub>			ε <sub>1m</sub>	ε <sub>om</sub>	ε <sub>ic</sub>	ε <sub>oc</sub>	Strain Gauge Value	Tape Value	ε <sub>1</sub>	ε <sub>2</sub>					0.01	0.05	0.1	0.15	0.2	0.5				
1	0.167	1.0	0.236	0.00237	70	280	-	-	-	-	-	-	-	-	104	-	112	124	170	-	-	0.01	0.05	0.1	0.15	0.2	0.5	
2	0.167	1.0	0.236	0.00237	50	278	0.885 0°	0.796 0°	0.749 0°	-0.853 0°	-1.032 145°W	-0.683 0°	-0.489 145°W	3.048	104	196	51	78	140	178	-	-	124	170	178	193	211	-
3	0.111	1.0	0.201	0.00237	63	248	1.125 180°	0.230 180°	0.230 180°	-0.690 180°	-1.075 145°	-0.665 180°	1.517	77	92	80	85	108	124	140	-	-	85	108	124	140	156	-
4	0.074	1.0	0.178	0.00237	28	198	1.340 45°	0.099 45°	0.099 45°	-1.023 45°	-1.075 45°	-1.075 45°	0.432	60	60	41	42	63	75	83	-	-	42	63	75	83	91	134
5	0.074	0.833	0.205	0.00237	42	278	1.293 90°	0.103 90°	0.103 90°	-0.939 90°	-0.730 90°	-0.730 90°	1.867	72	76	58	65	92	111	128	-	-	65	92	111	128	146	-
6	0.074	0.778	0.218	0.00237	100	276	1.800 225°	0.788 225°	0.788 225°	-1.598 225°	-1.251 225°	-1.251 225°	2.150	78	139	126	118	144	158	178	-	-	118	144	158	168	178	-
7	0.167	1.0	0.236	0.00119	26	60	-	0.170 269°	0.179 233°	-	-0.313 269°	-0.260 233°	-	47	40	40	40	-	-	-	-	-	40	-	-	-	-	-
8	0.111	1.0	0.201	0.00119	38	70	0.296 270°	0.067 270°	-0.034 0°W	-0.237 270°	-0.236 0°W	-0.245 270°	0.126	33	-	-	56	-	-	-	-	-	56	-	-	-	-	-
9	0.074	1.0	0.178	0.00119	22	62	0.426 90°	0.325 180°W	0.073 180°W	-0.450 90°	-0.461 180°W	-0.377 90°	0.109	25	-	34	29	40	45	48	-	-	29	40	45	48	51	57
10	0.074	0.833	0.205	0.00119	33	78	0.521 90°	0.561 0°W	0.330 0°W	-0.410 90°	-0.800 0°W	-0.621 90°	0.139	30	-	41	43	58	68	-	-	43	58	68	-	-	-	
11	0.074	0.722	0.234	0.00119	41	86	0.557 90°	0.379 180°W	-0.103 180°W	-0.525 90°	-0.431 180°W	-0.384 90°	0.193	36	65	61	53	70	78	84	-	-	53	70	78	84	-	-
12	0.056	1.0	0.167	0.00119	15	66	0.691 90°	0.497 0°W	0.079 0°W	-0.970 90°	-0.468 0°W	-0.424 90°	0.115	21	45	22	20	28	35	40	-	-	20	28	35	40	45	58
13	0.167	1.0	0.236	0.00119	22	82	0.378 90°	0.337 118°W	0.170 118°W	-0.378 90°	-0.332 118°W	-0.306 90°	0.150	47	41	41	43	70	-	-	-	43	70	-	-	-	-	-
14	0.167	1.0	0.236	0.00158	38	120	0.513 0°	0.580 325°W	0.043 0°	-0.300 0°	-1.003 325°W	-0.368 0°	-	65	-	48	52	77	93	-	-	52	77	93	-	-	-	-
15	0.167	1.0	0.236	0.00158	36	107	0.497 330°	1.265 86°W	0.378 86°W	-0.378 330°	-1.269 86°W	-0.322 330°	0.131	65	-	53	51	70	82	96	-	-	51	70	82	96	106	106
16	0.074	1.0	0.178	0.00158	29	95	0.745 90°	0.511 0°W	0.083 90°	-0.711 90°	-0.449 0°W	-0.416 90°	0.116	36	50	44	41	62	77	-	-	41	62	77	-	-	-	-
17	0.074	0.833	0.205	0.00158	39	107	0.413 90°	0.960 0°W	-0.081 90°	-0.352 90°	-0.856 0°W	-0.461 90°	0.146	43	70	64	55	75	84	-	-	55	75	84	-	-	-	-

Superscript numbers refer to notes on following pages

TABLE 7.3b : MAXIMUM PEAK STRAINS NOT GIVEN IN TABLE 7.3a

End No.	P <sub>CR</sub>	Peak Strains at P <sub>CR</sub>							
		$\epsilon_{im}$		$\epsilon_{om}$		$\epsilon_{ic}$		$\epsilon_{oc}$	
1	280								
2	278								-0.515 235°W
3	248				-0.005 90°				
4	198				0.013 0°				
5	278				-0.015 0°				-0.785 180°
6	278				-0.215 0°				-1.377 180°
7	60								
8	70		0.310 180°W		0.048 90°			-0.256 180°W	-0.295 90°
9	62								
10	78								
11	86								
12	66								
13	82				0.095 0°				-0.371 0°
14	120								
15	95								
16	95								
17	107								

See notes on following pages.

NOTES ON TABLES 7.3a and 7.3b

1. Pressure at which the first buckle occurred.
2. The peak strain values given are those at  $p_{CR}$  prior to buckling. For ends with welds the peak strains both on and away from welds are given.

The figure beneath each peak strain refers to the meridian on which the strain was observed. A 'W' after this figure indicates the meridian is coincident with a weld.

The four peak strains occurring on a given meridian are presented. The maximum of these strains is the highest measured strain. The other peak strains are not necessarily maxima. For example although one meridian may have the highest inner surface circumferential strain, the highest outer surface circumferential strain may occur elsewhere. Where this has occurred the maximum peak strain value is given in table 7.3b.

3. The values of  $\Delta h/h_i$  quoted were obtained at  $p_{cr}$  prior to buckling unless otherwise stated.
4. Limit pressure is defined as the pressure at which appreciable plastic deformations occur.
5. Shield and Drucker limit pressures calculated from the curves given in ref.15. A yield stress of 19 tonf/in<sup>2</sup> and nominal dimensions were used in the calculations.
6. Limit pressure values derived from experimental pressure-strain data by use of Save's definition (ref.38).
7. Limit pressure value derived using the type of construction suggested by Sampayo and Turner (ref.39). For the maximum reading strain gauge a point is obtained on the pressure-strain curve by drawing a line through the origin with seven-eighths the elastic slope. The intersection of

the elastic line with a tangent to the curve at this point defines the limit pressure.

8. Limit pressure values derived from the pressure-strain curve for the maximum reading strain gauge by determining the pressure at which a defined amount of permanent strain exists.

TABLE 7.4: SUMMARY OF BUCKLE DEVELOPMENT

Superscript numbers refer to notes on following page

End No.	Shape Parameters			Buckle Number									Type	$\rho_{MAX}$	$\rho_{PTH}$	Remarks	
	$r_i/D_i$	$R_i/D_i$	$h_i/D_i$	$t_e/D_i$	1	2	3	4	5	6	7	8					9
1	0.167	1.0	0.236	0.00237	Pressure Time	280	280	280	280	280	280	280	280	280	300	2130	3rd and 4th buckles on welds in knuckle
2	0.167	1.0	0.236	0.00237	Meridian	360	530	1480	3280						298	2130	Only partially formed
3	0.111	1.0	0.201	0.00237	Pressure Time	2610									293	1110	
4	0.074	1.0	0.178	0.00237	Meridian	248	198	198	198	198	198	198	198	198	198	440	1st buckle in line with cylinder weld
5	0.074	0.833	0.205	0.00237	Pressure Time	30	198	198	198	198	198	198	198	198	283	-	
6	0.074	0.778	0.218	0.00237	Meridian	1270	2900	2430							298	-	
7	0.167	1.0	0.236	0.00119	Pressure Time	278	283	288	298	298	298	298	298	298	104	430	4th buckle on weld in knuckle
8	0.111	1.0	0.201	0.00119	Meridian	0	2680	1640	510	3280					94	270	1st buckle occurred in region distorted during manufacture
9	0.074	1.0	0.178	0.00119	Pressure Time	70	86	86	86	86	86	86	86	86	78	160	1st & 2nd buckles on welds in knuckle
10	0.074	0.833	0.205	0.00119	Meridian	7	27	19	19	19	19	19	19	19	86	-	1st & 3rd buckles on welds in knuckle
11	0.074	0.722	0.234	0.00119	Pressure Time	1120	3090	1700	2430	350	78	78	78	78	98	-	4th & 6th buckles on welds in knuckle
12	0.056	1.0	0.167	0.00119	Meridian	62	66	70	70	70	70	70	70	70	98	110	3rd & 5th buckles on welds in knuckle
13	0.167	1.0	0.236	0.00119	Pressure Time	1	181	120	297	2520	72	72	72	72	102	430	1st and 2nd buckles on welds in knuckle
14	0.167	1.0	0.236	0.00158	Meridian	0	2680	1640	510	3280					239	950	3rd buckle on weld in knuckle
15	0.167	1.0	0.236	0.00158	Pressure Time	120	126	132	138	144	150	150	150	150	239	950	1st, 3rd & 4th buckles on welds in knuckle
16	0.074	1.0	0.178	0.00158	Meridian	293	1690	380	3360	990	2440	2150	1310	1310	119	230	1st buckle on weld in knuckle
17	0.074	0.833	0.205	0.00158	Pressure Time	107	119	131	143	149	149	161	207	219	199	-	1st buckle on weld in knuckle



NOTES ON TABLE 7.4.

1. Maximum test pressure applied.
2. Values obtained by extrapolation of work by Thurston and Holston (10). They give only an approximate indication of the theoretical buckling pressure.
3. S.I. - Snap inwards type buckle.
4. G.O. - Gradual outwards type buckle.

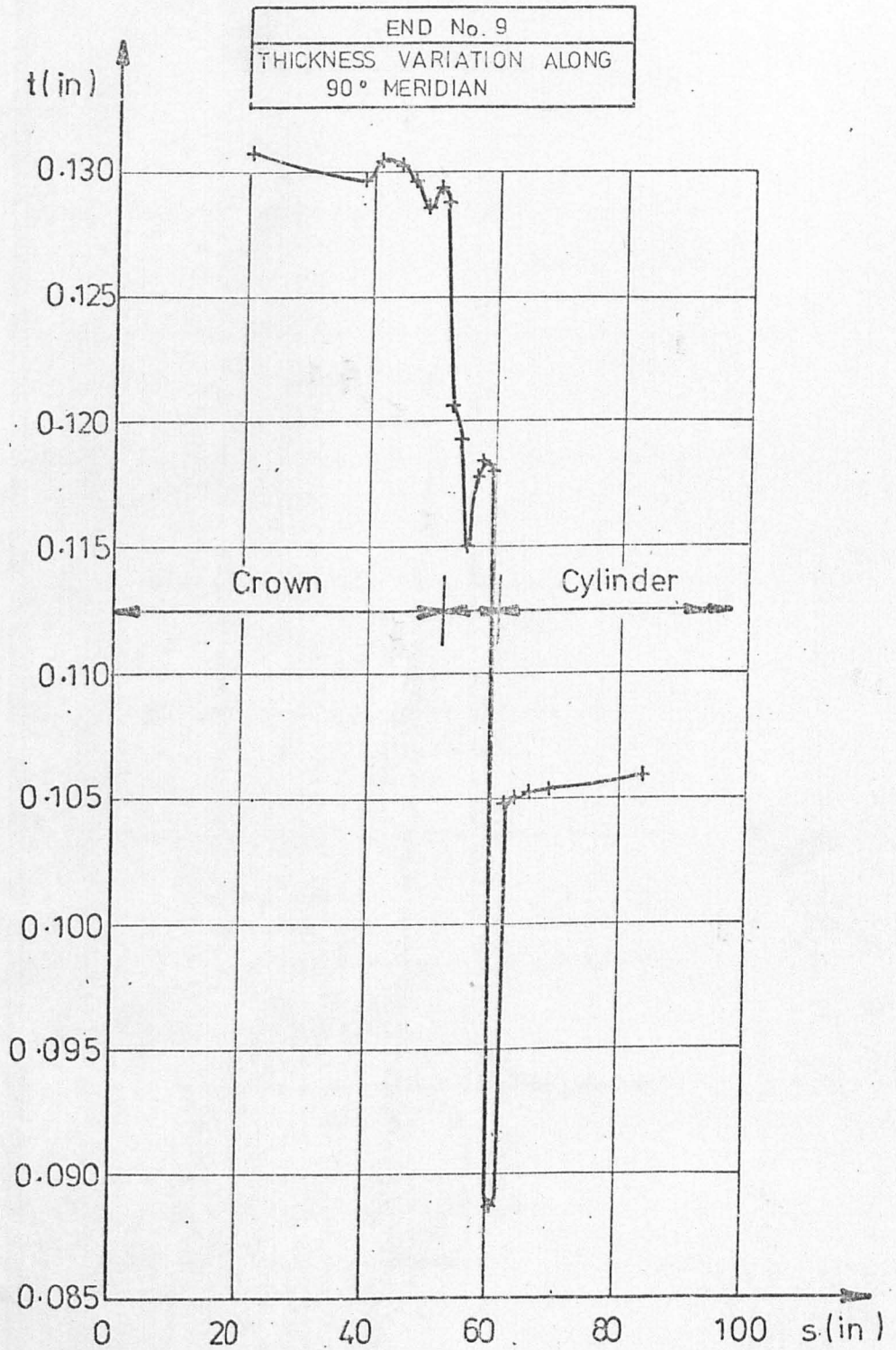


FIG. 7.1

END No.9  
 CURVATURE VARIATION ALONG  
 45° MERIDIAN

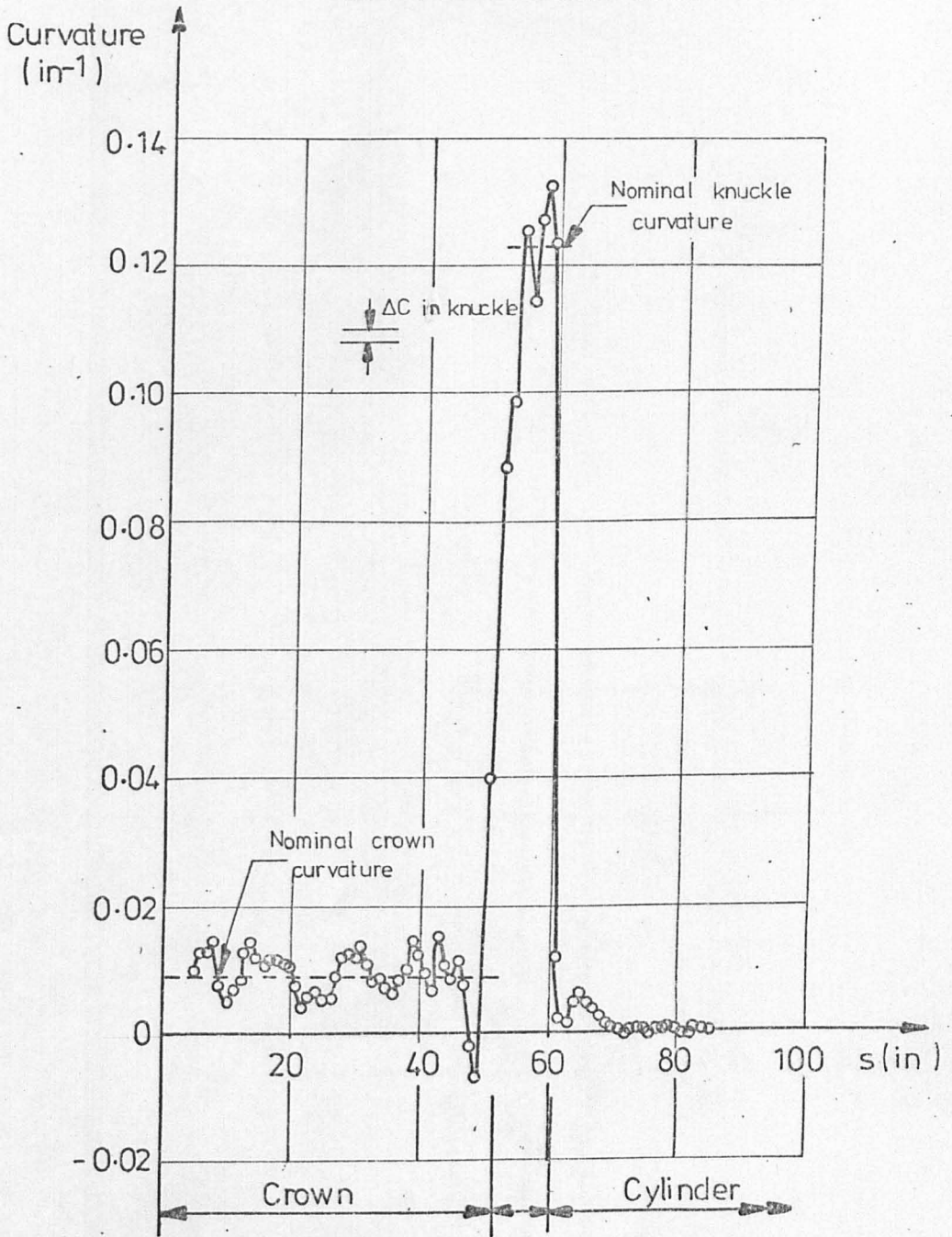


FIG. 7-2

END No.9  
 CURVATURE VARIATION ALONG  
 180° MERIDIAN

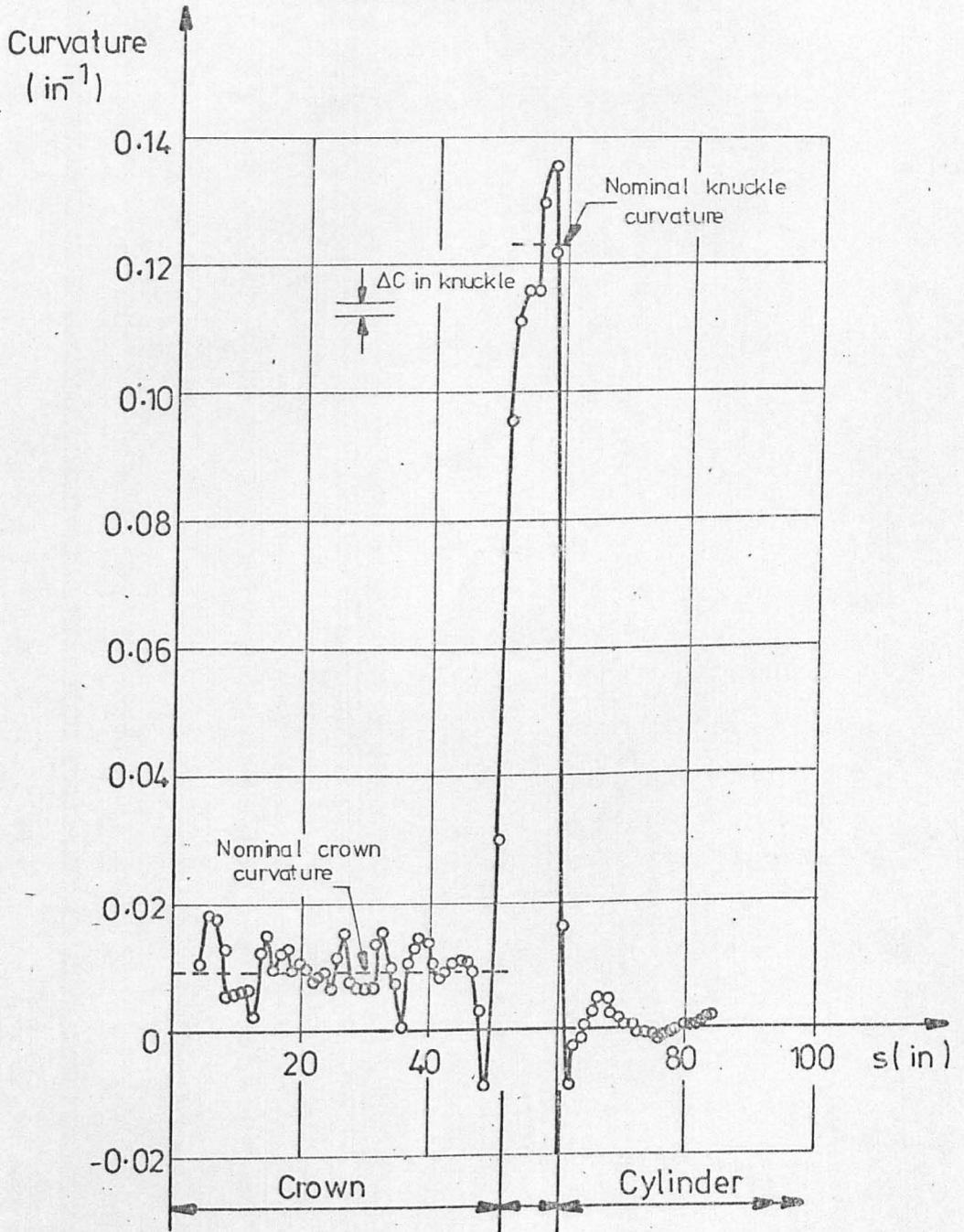


FIG. 7.3

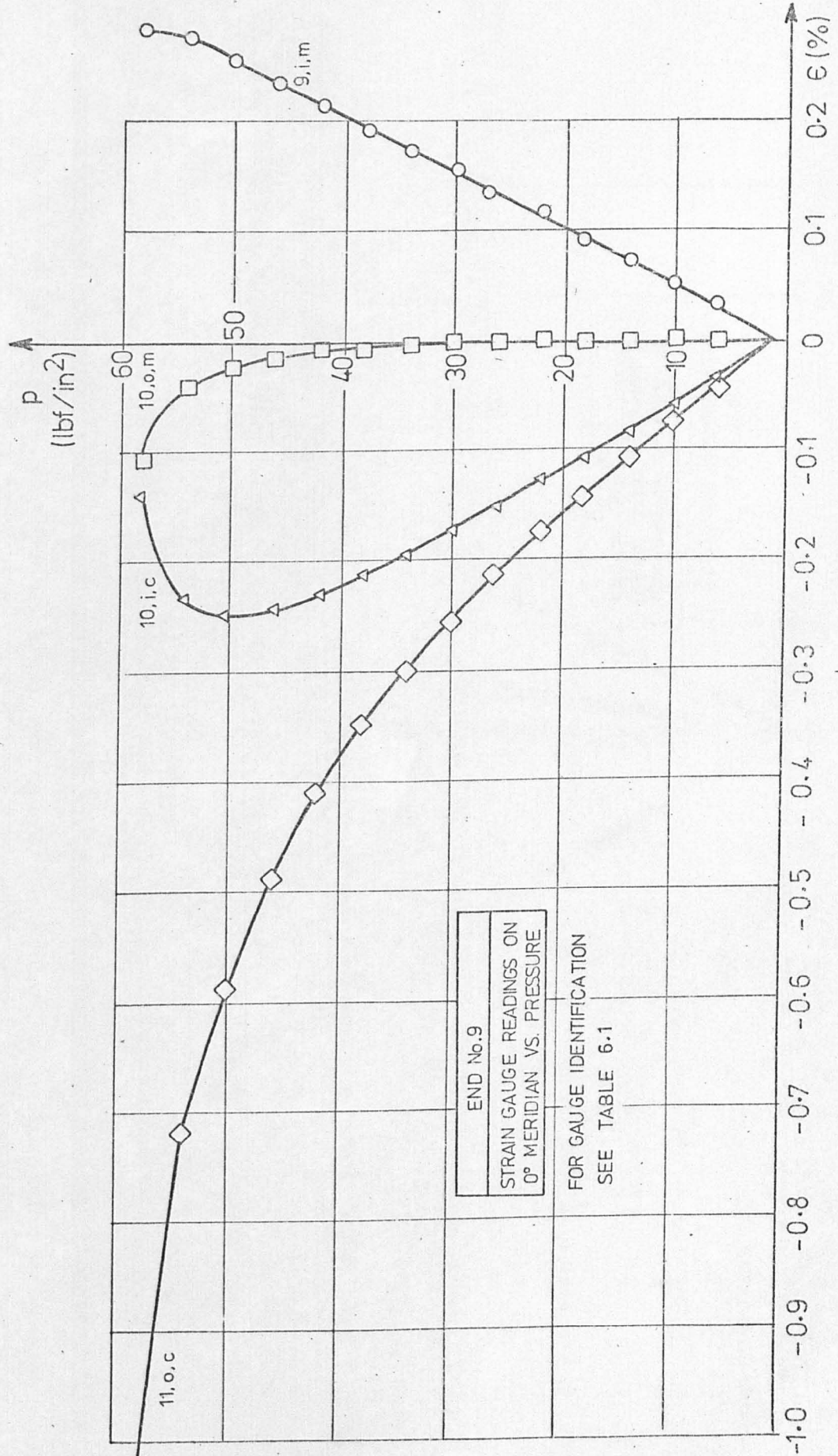


FIG. 7.4

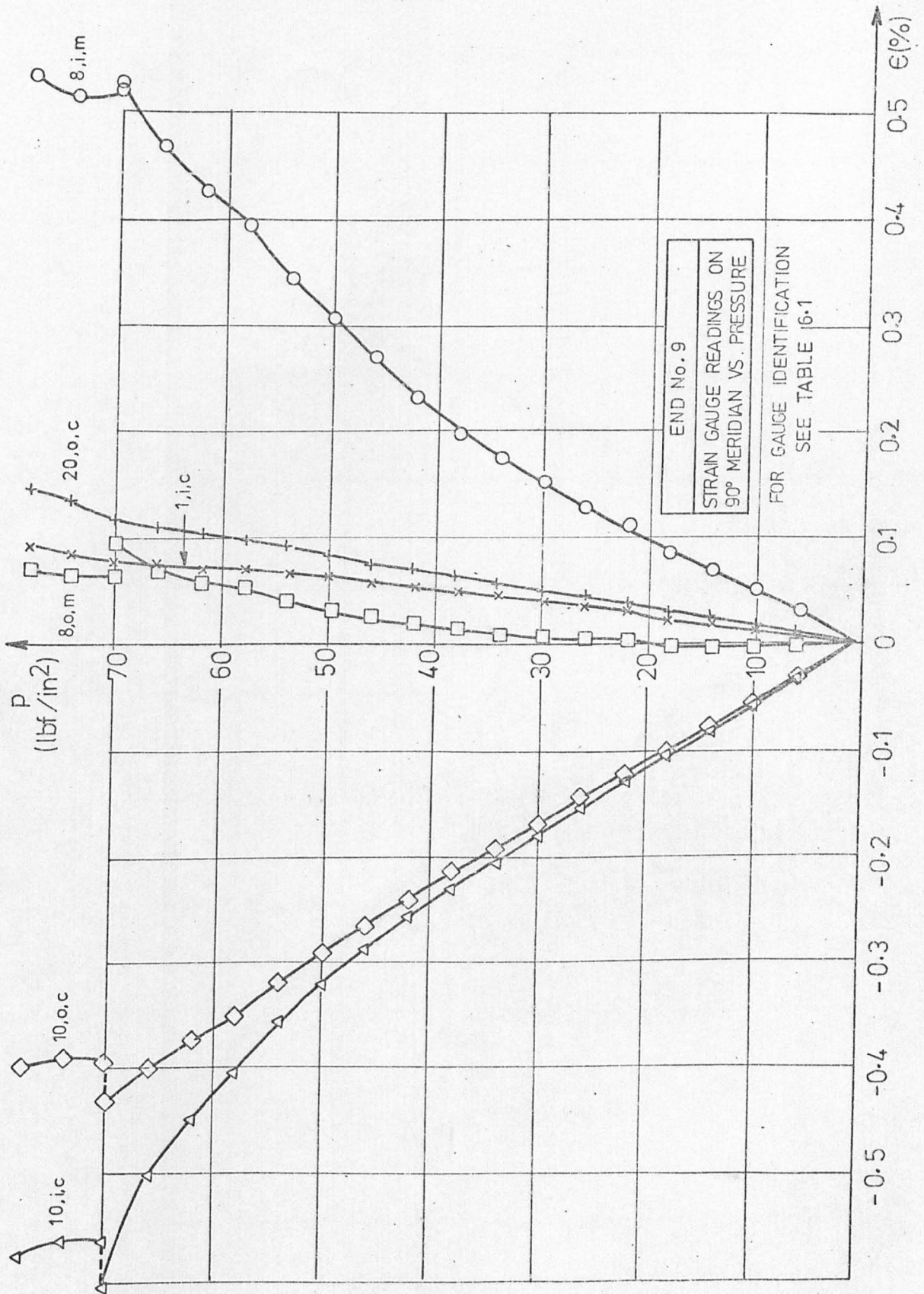


FIG. 7.5

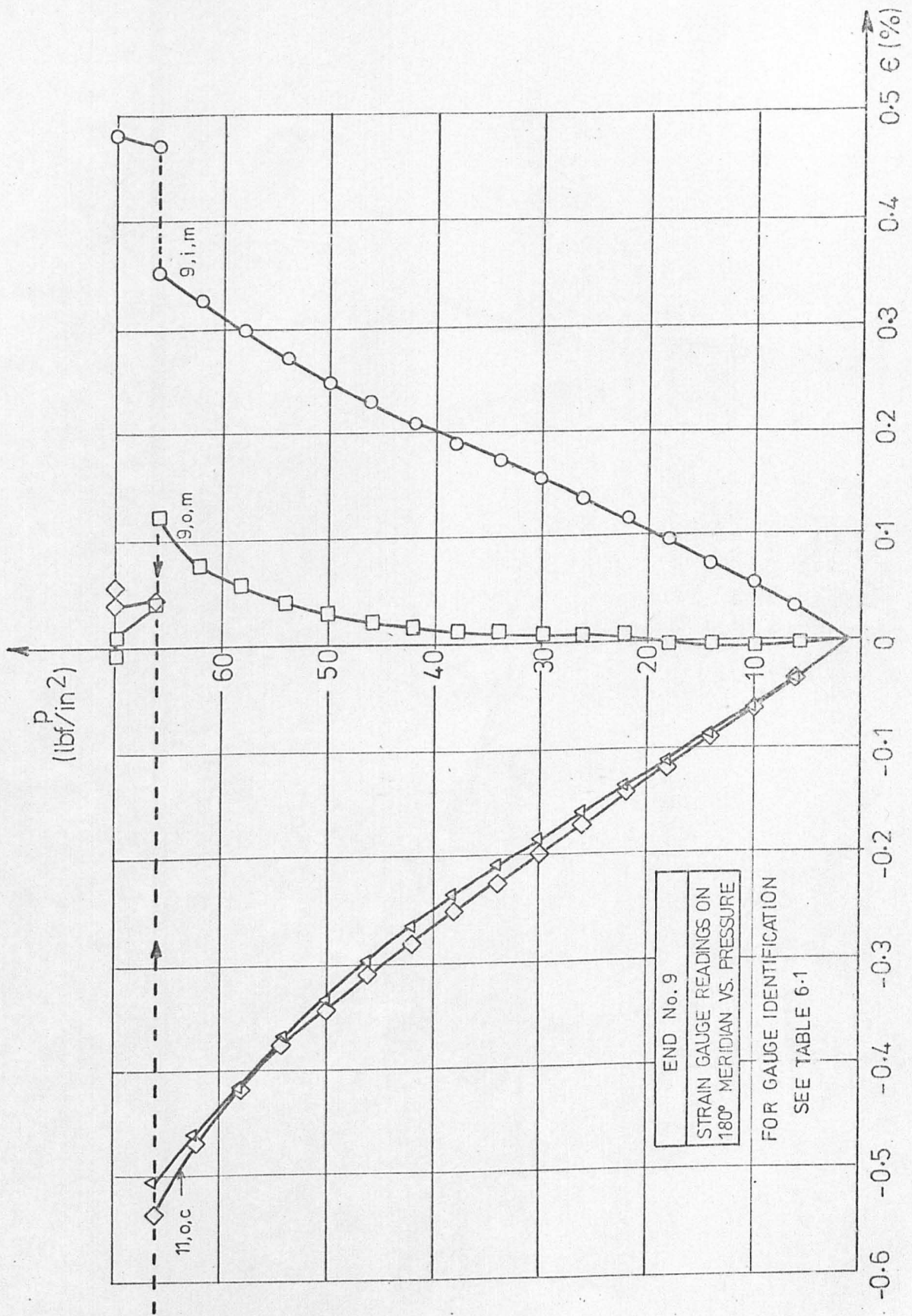


FIG.7.6

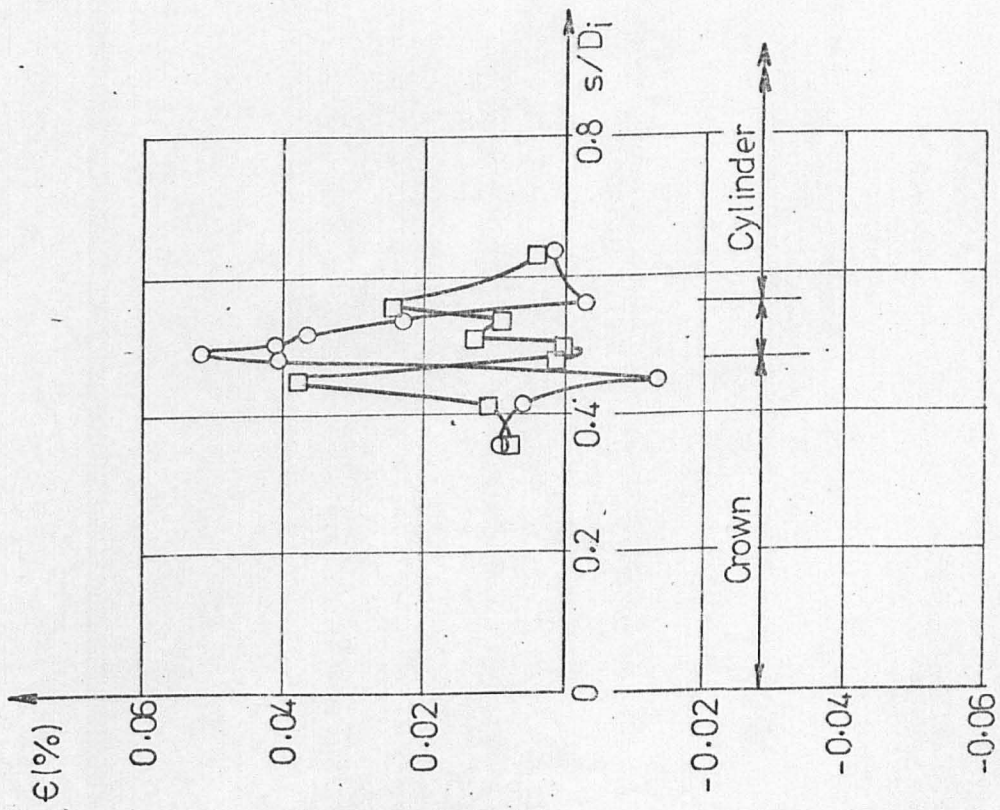
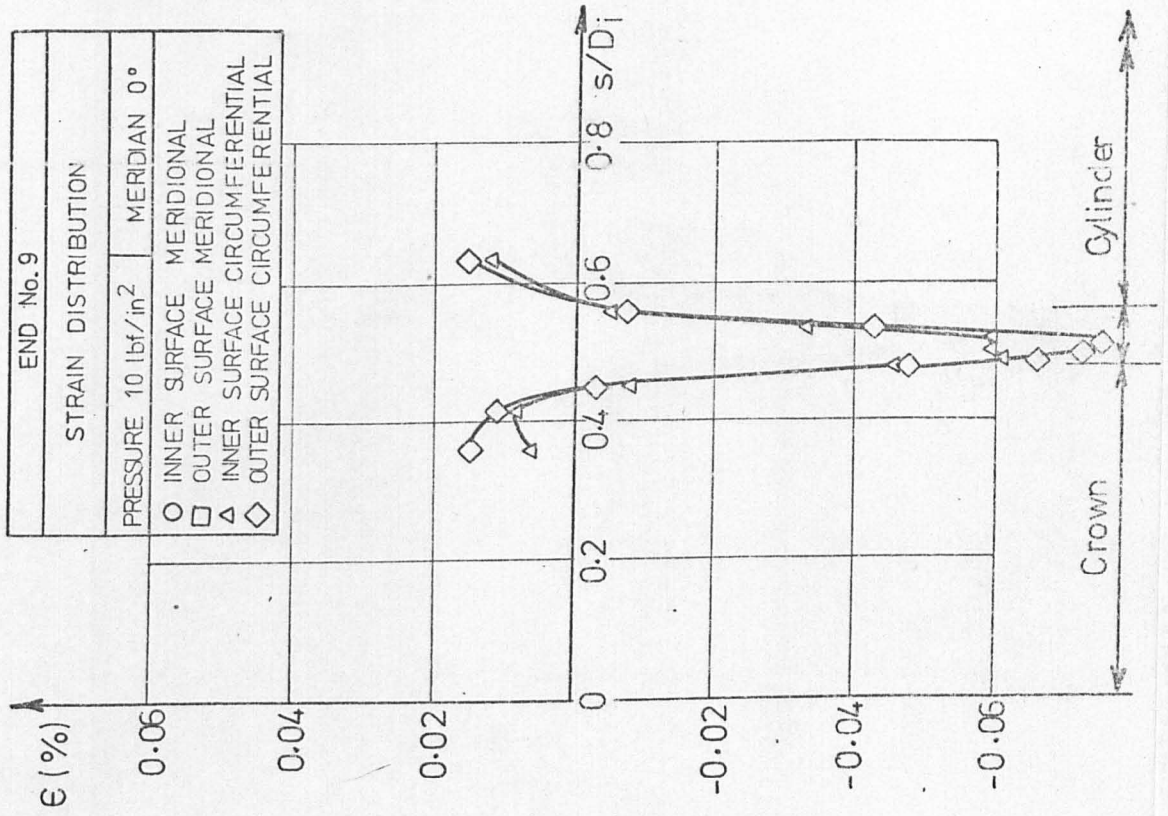


FIG. 7.7



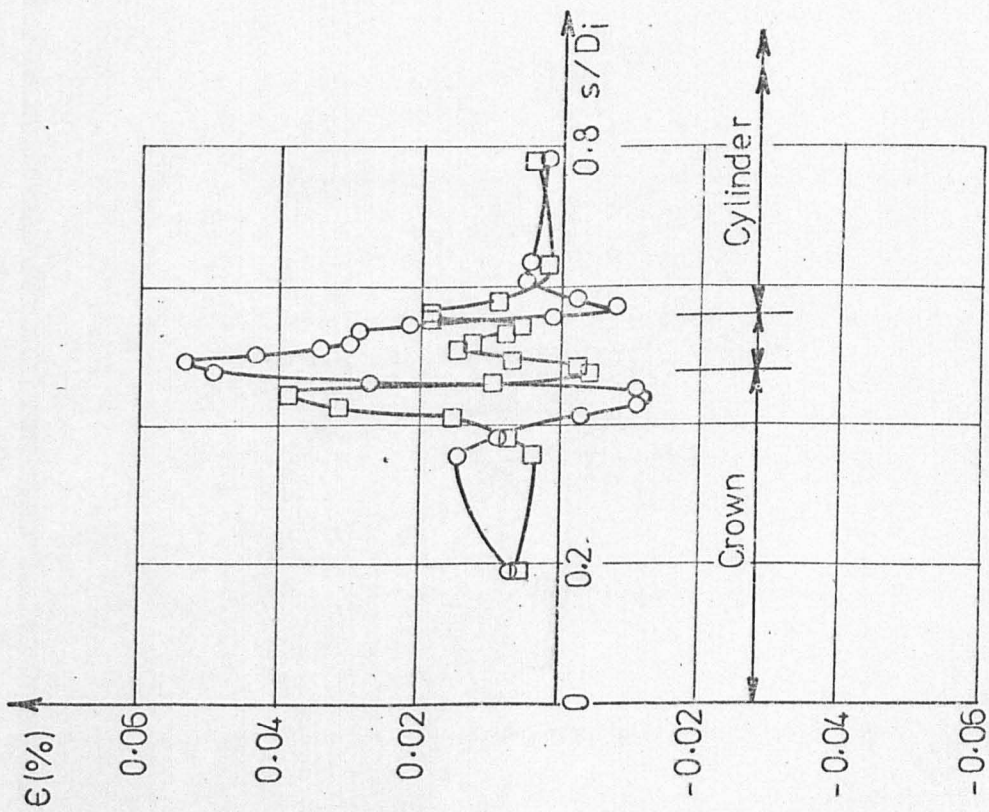
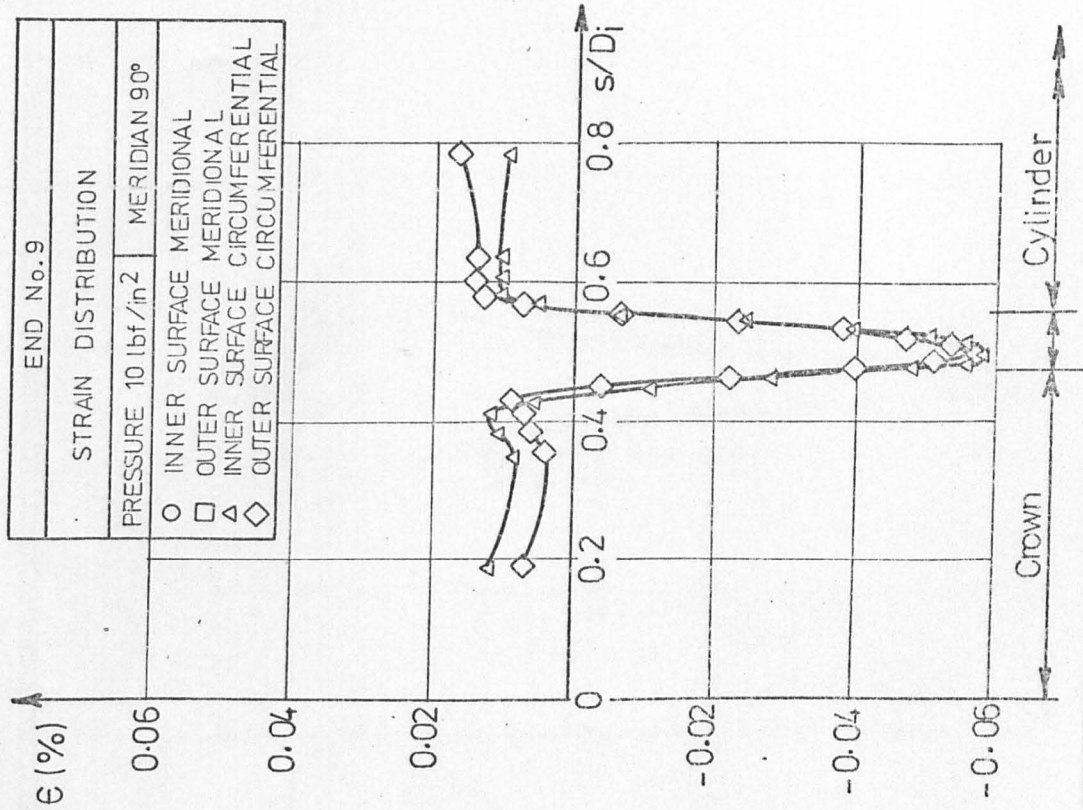


FIG. 7-8

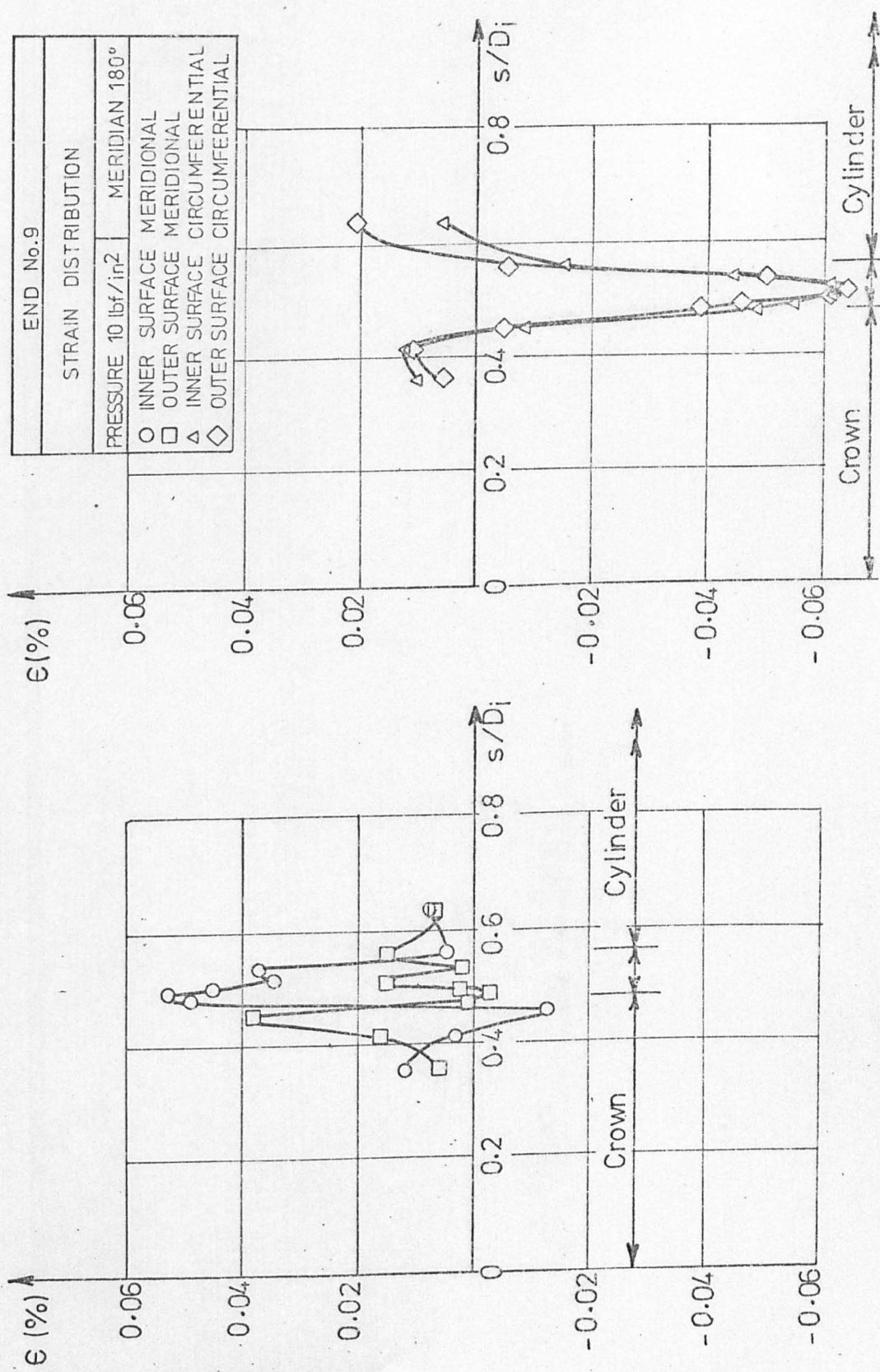


FIG. 7.9

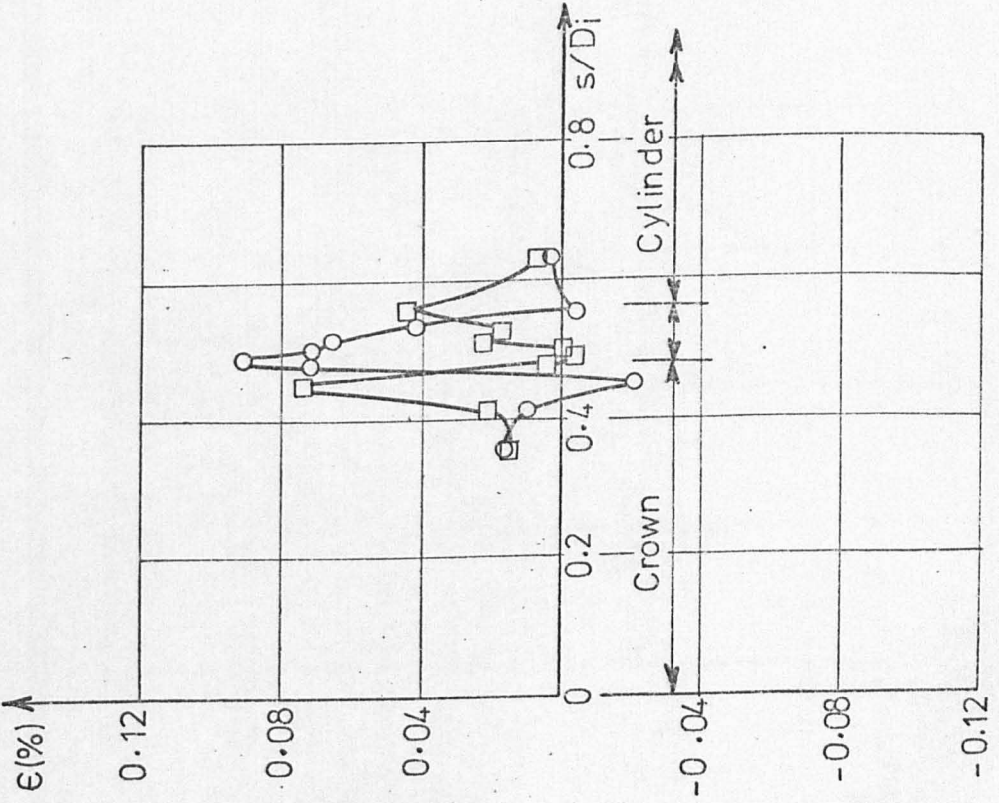
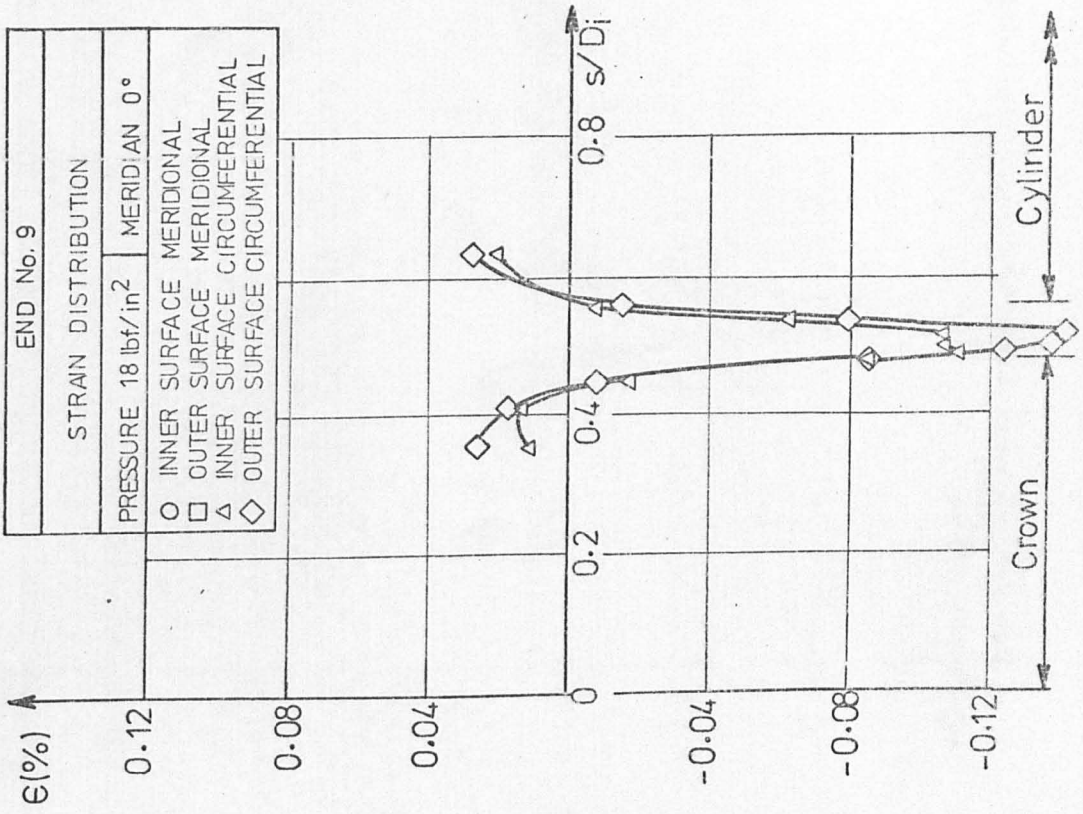


FIG. 7.10

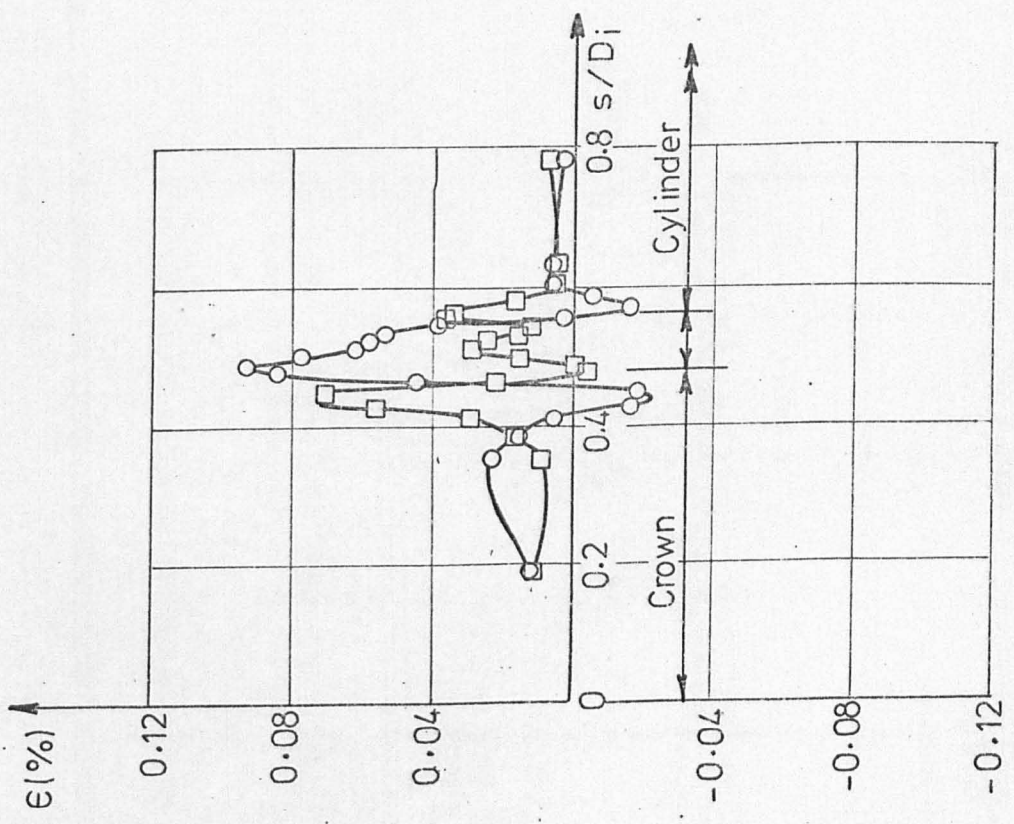
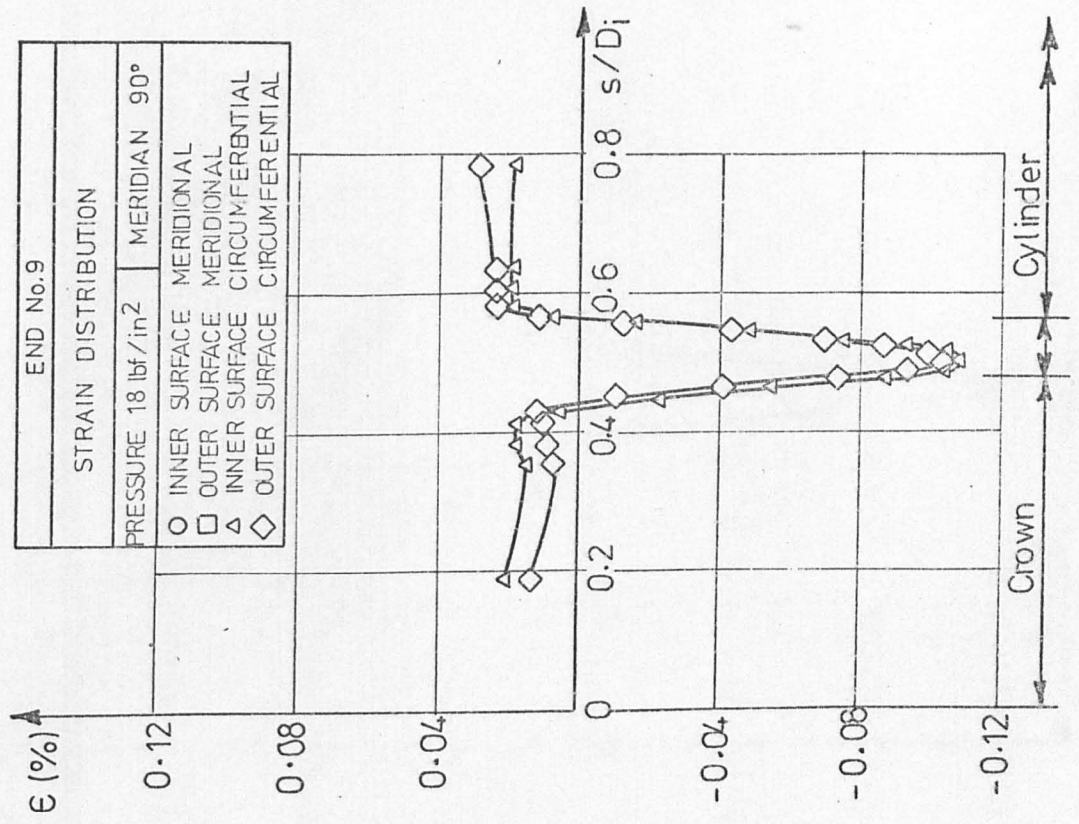


FIG. 7-11

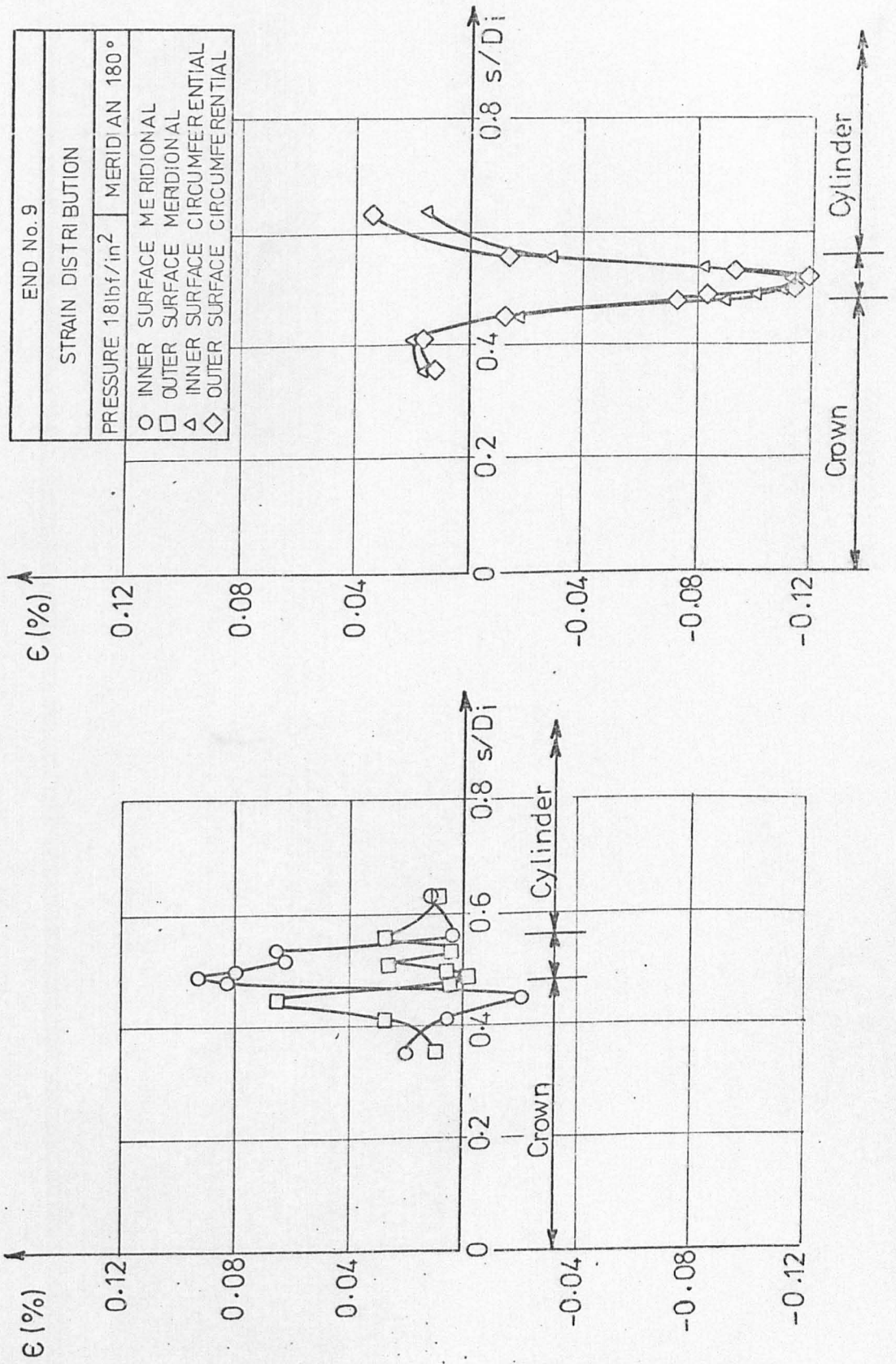


FIG. 7.12

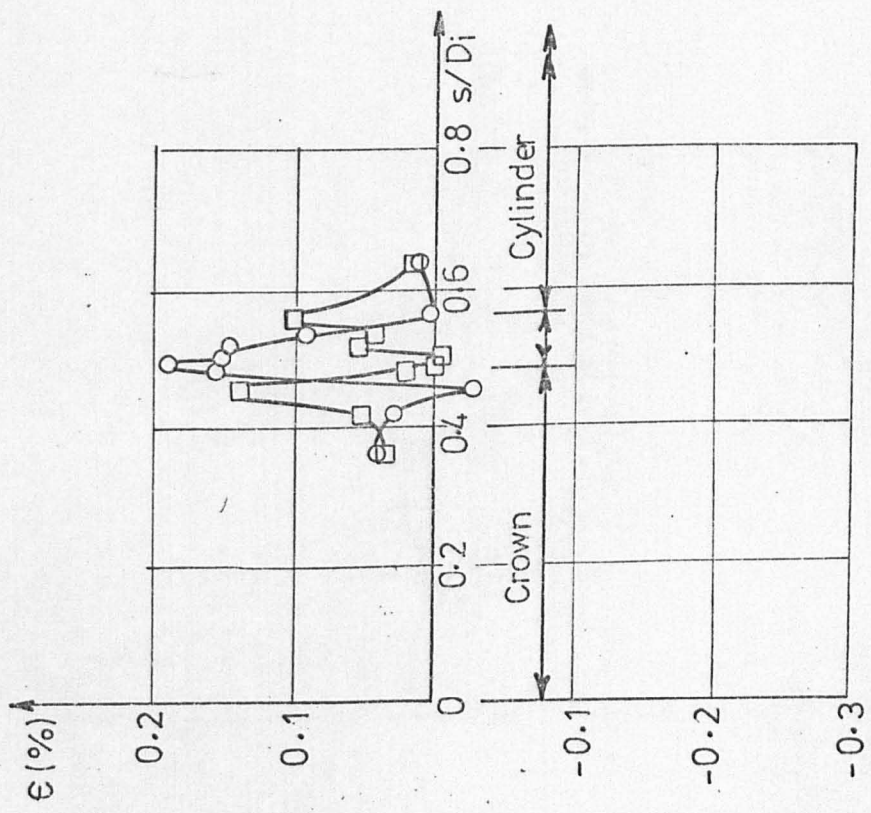
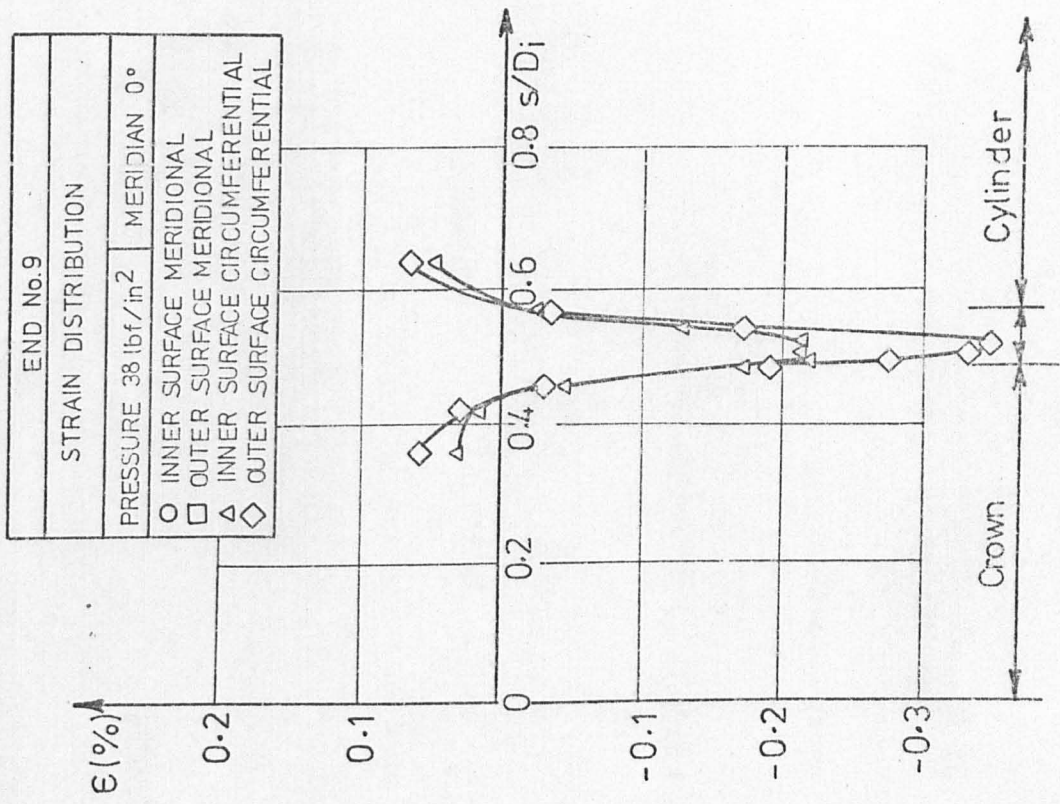


FIG. 7-13

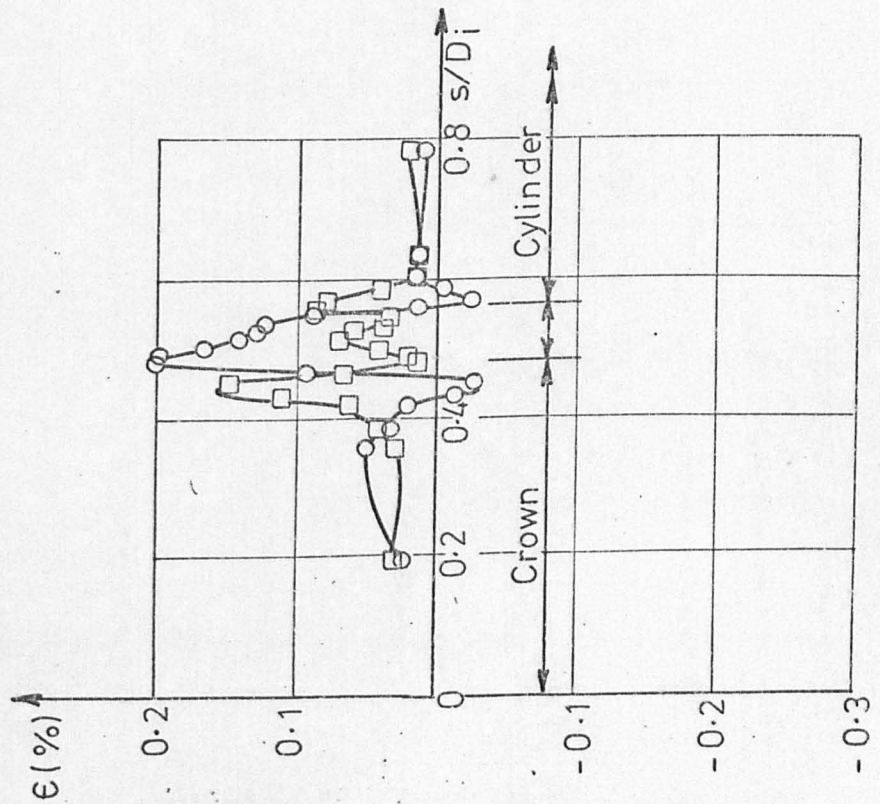
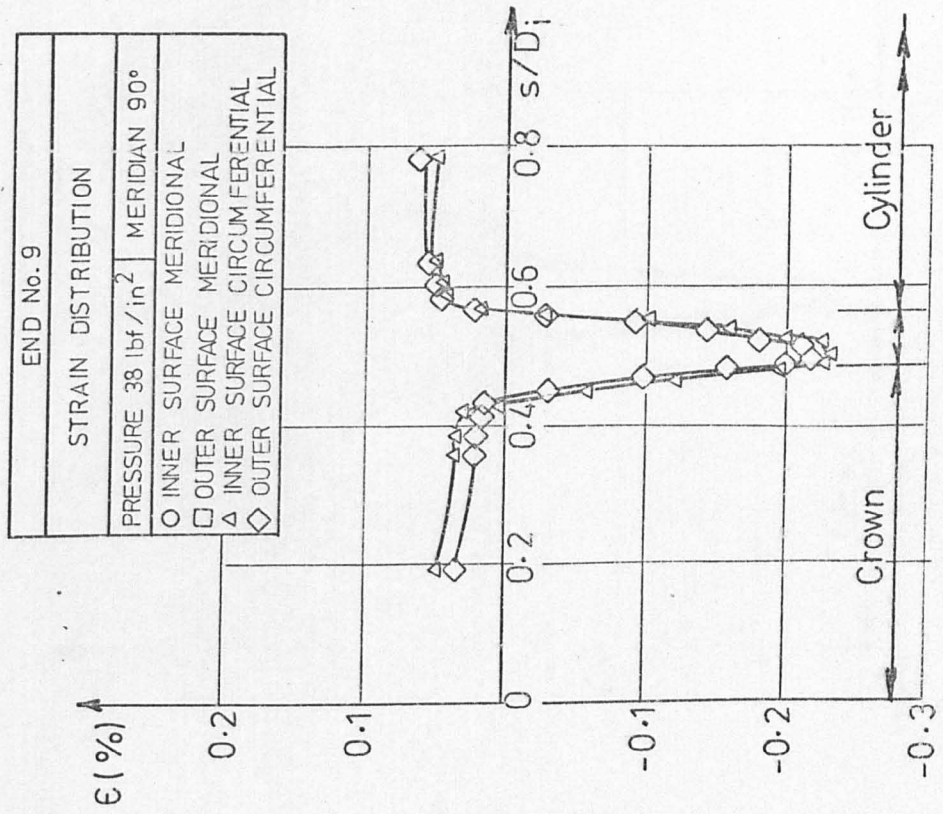


FIG. 7-14

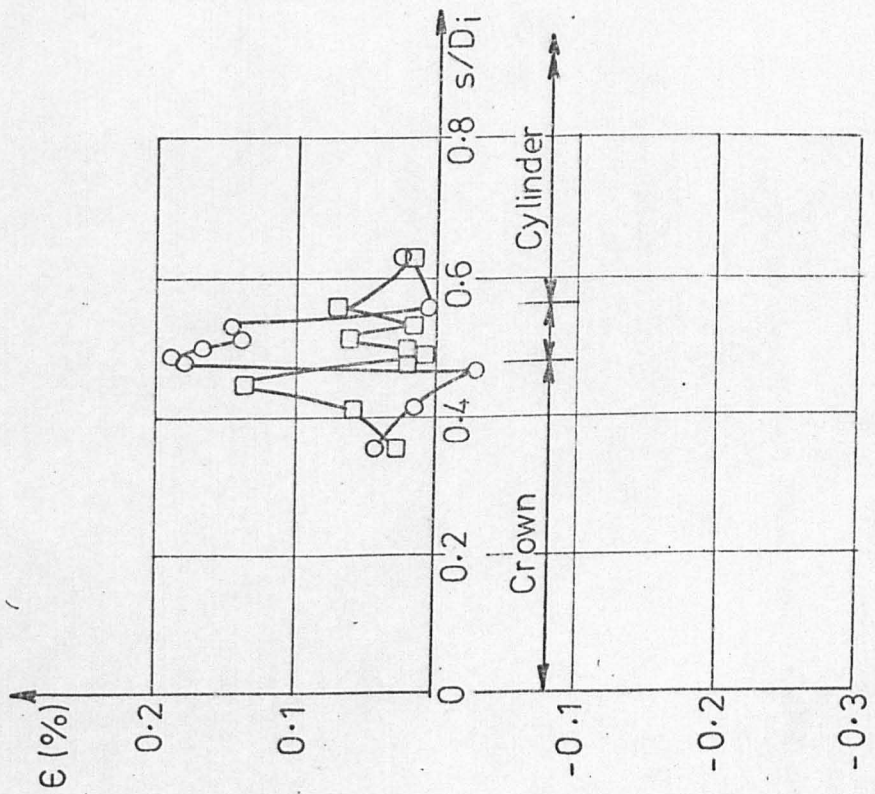
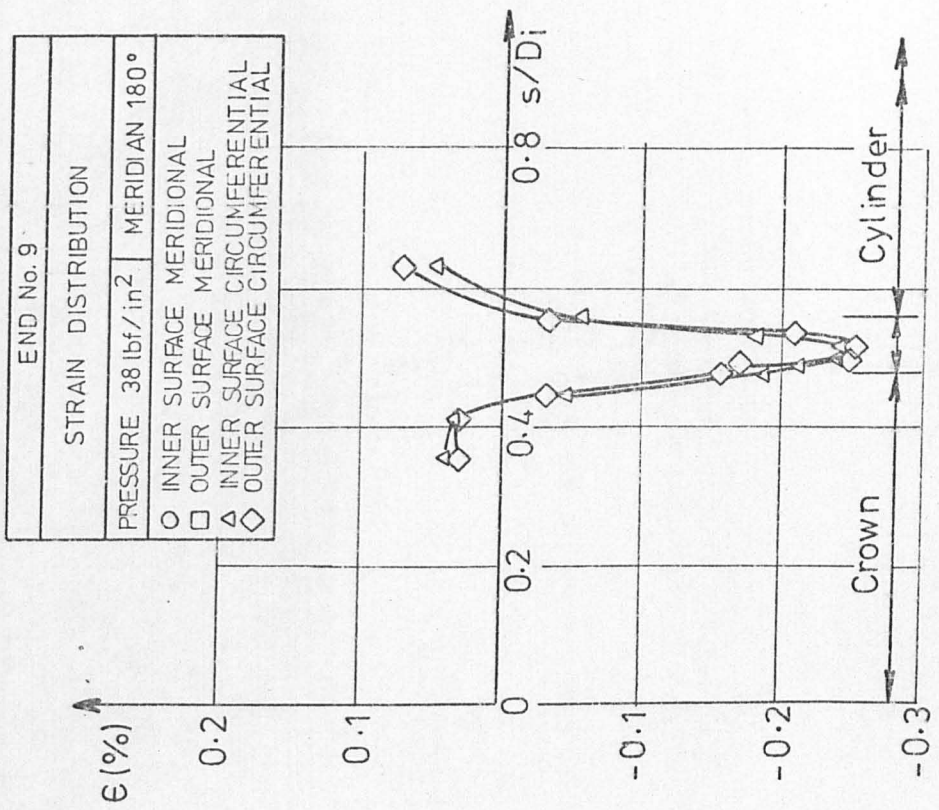


FIG. 7-15



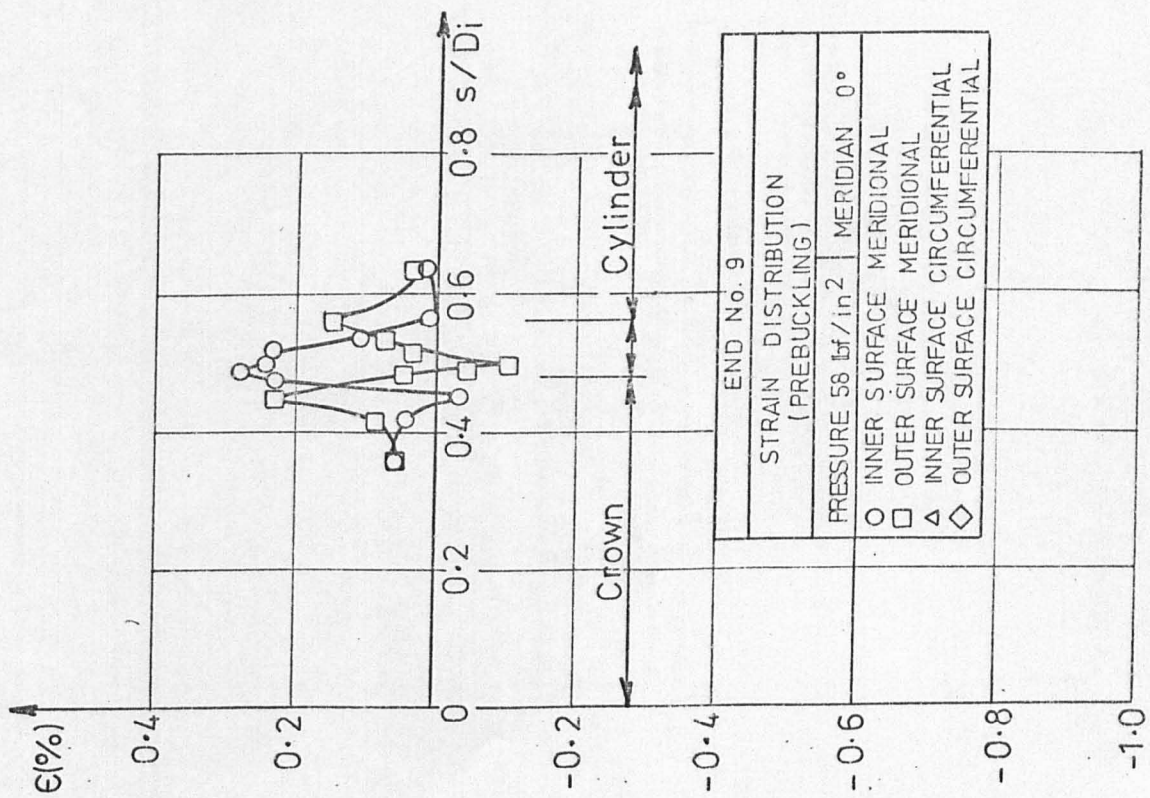
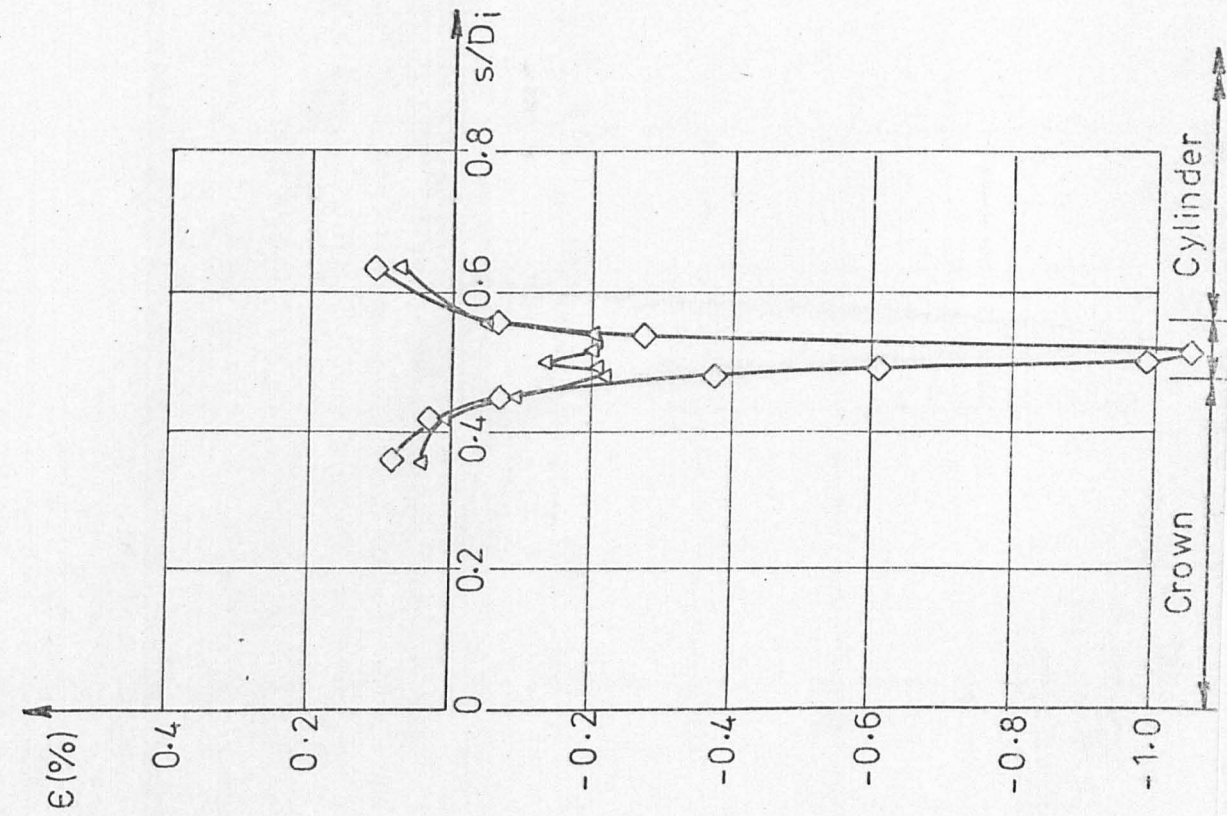


FIG. 7.16

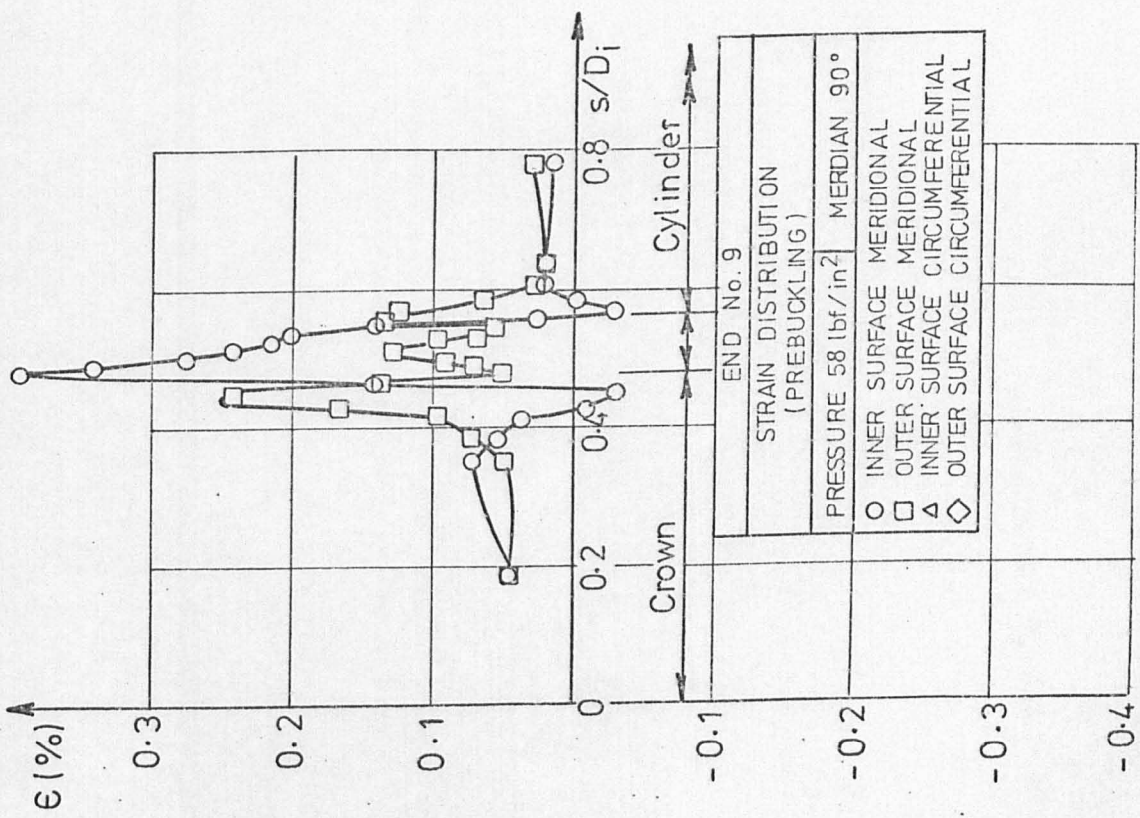
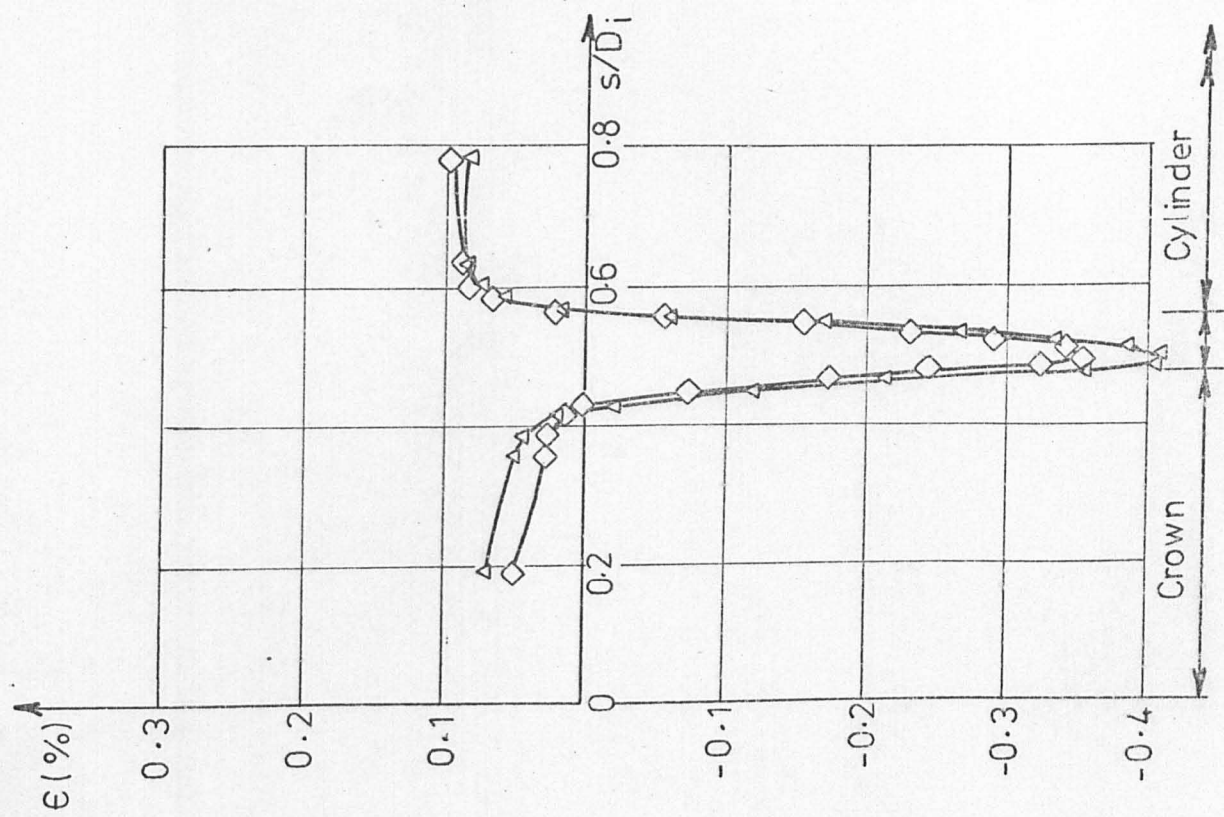


FIG. 7.17

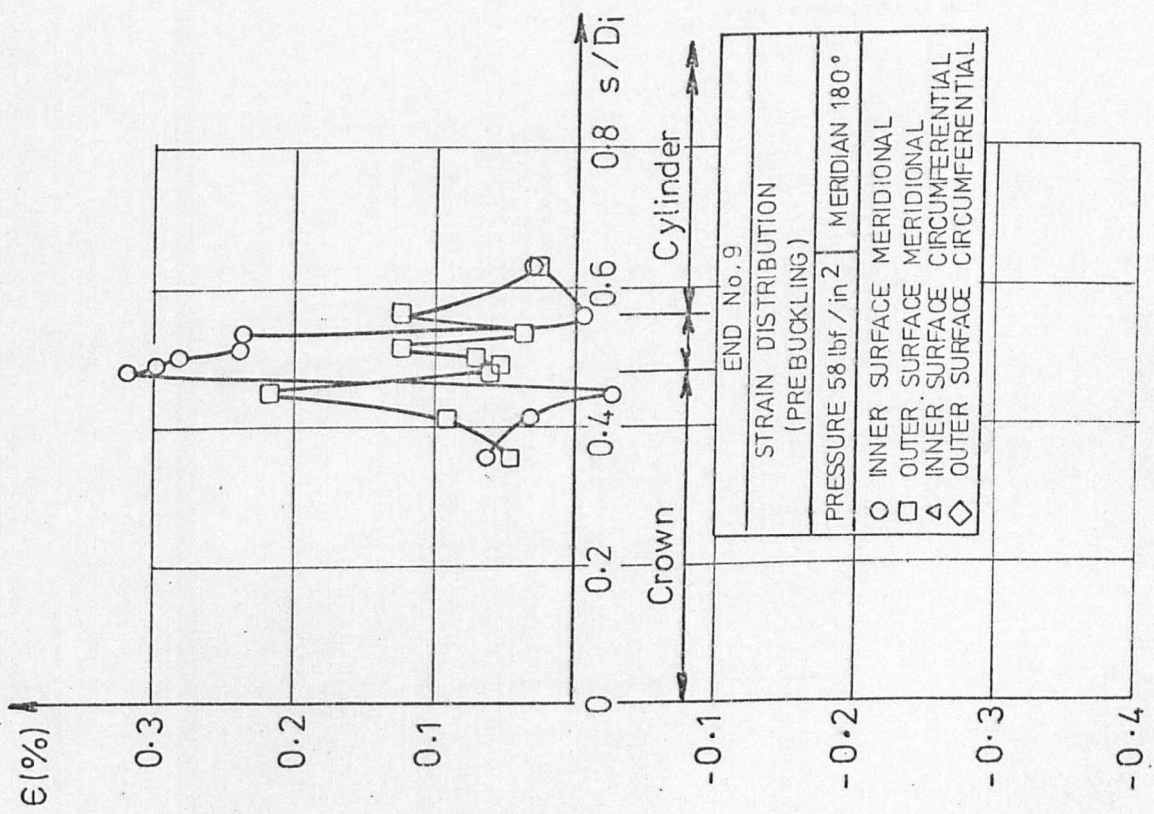
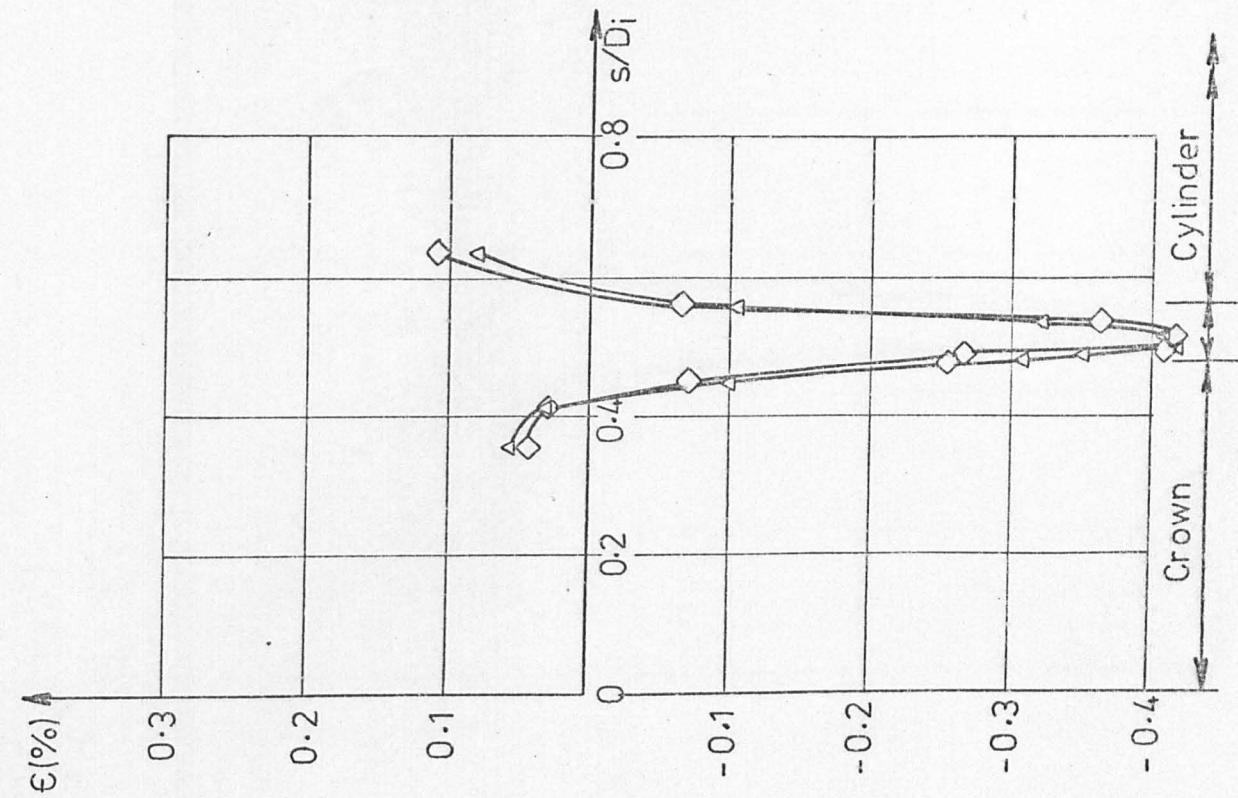


FIG. 7.18

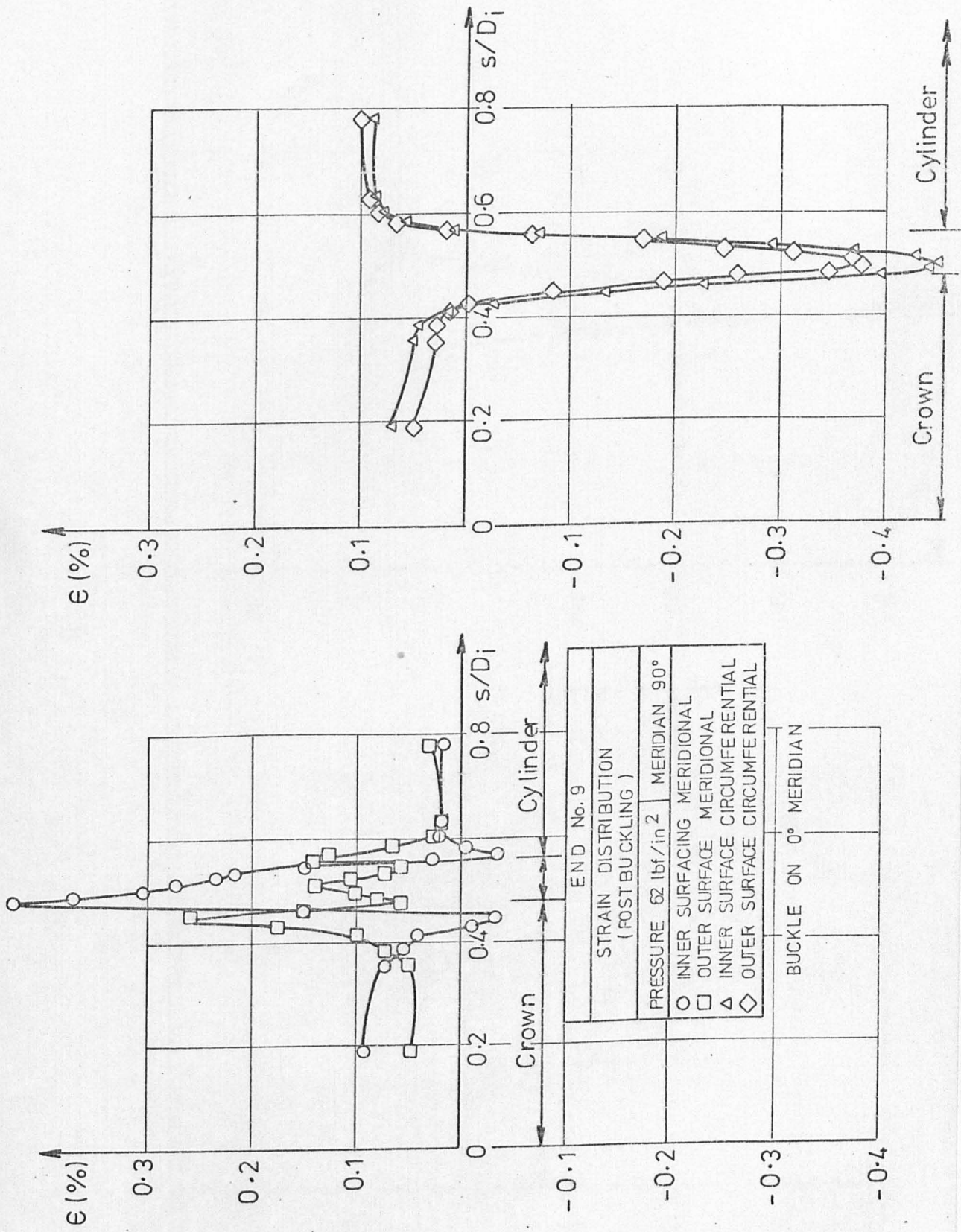
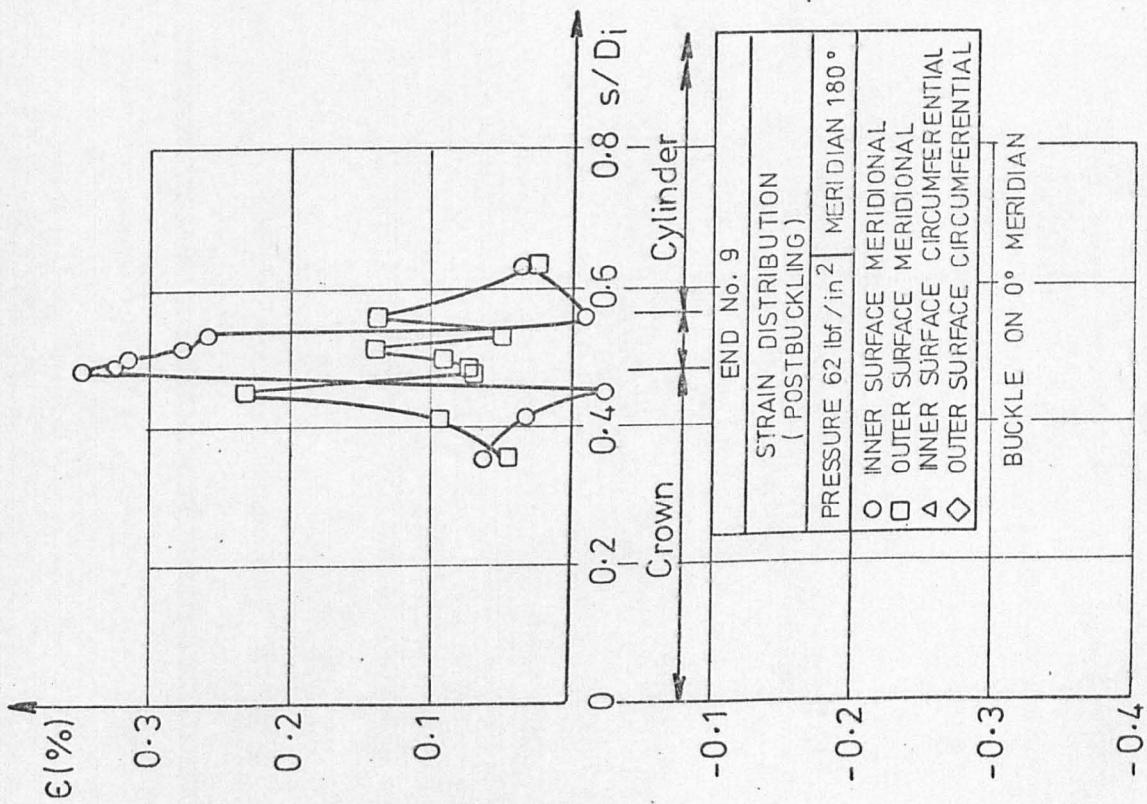
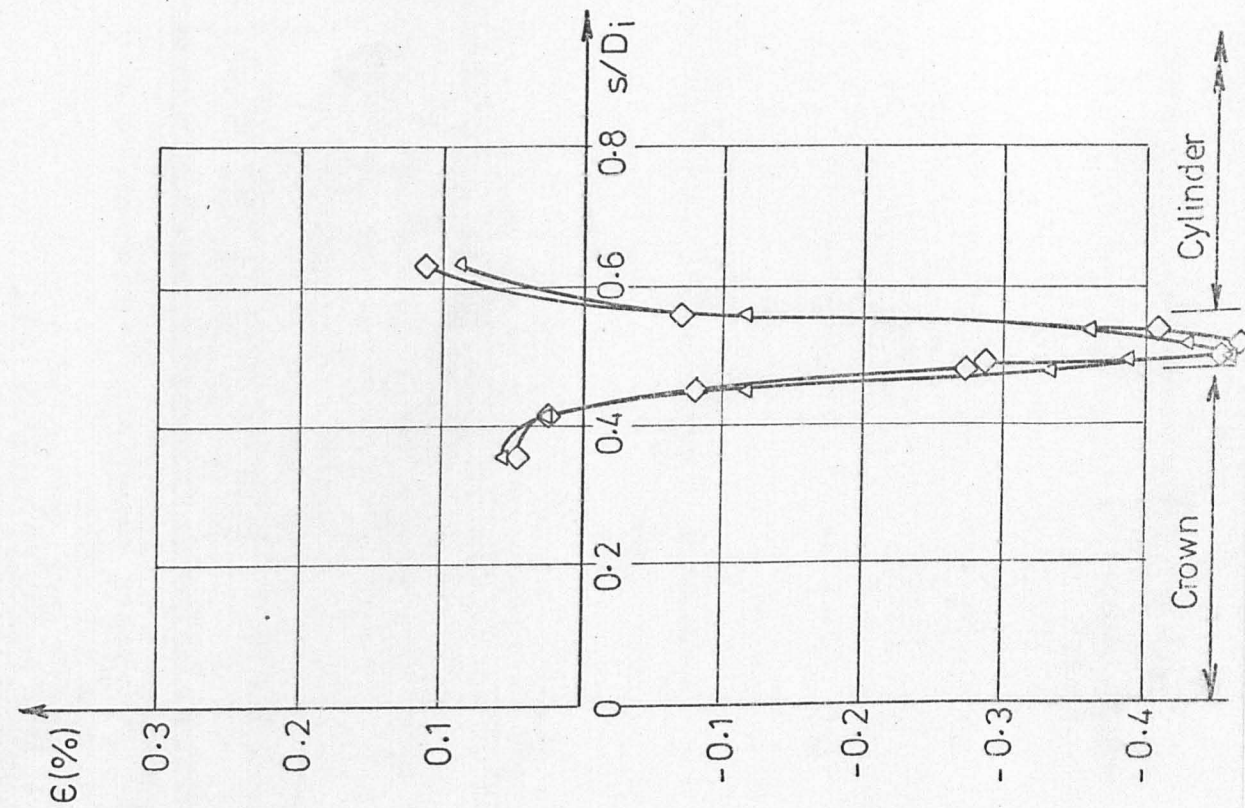


FIG. 7-19



END No. 9	
STRAIN DISTRIBUTION (POSTBUCKLING)	
PRESSURE 62 lbf/in <sup>2</sup>	MERIDIAN 180°
○	INNER SURFACE MERIDIONAL
□	OUTER SURFACE MERIDIONAL
△	INNER SURFACE CIRCUMFERENTIAL
◇	OUTER SURFACE CIRCUMFERENTIAL
BUCKLE ON 0° MERIDIAN	

FIG. 7-20

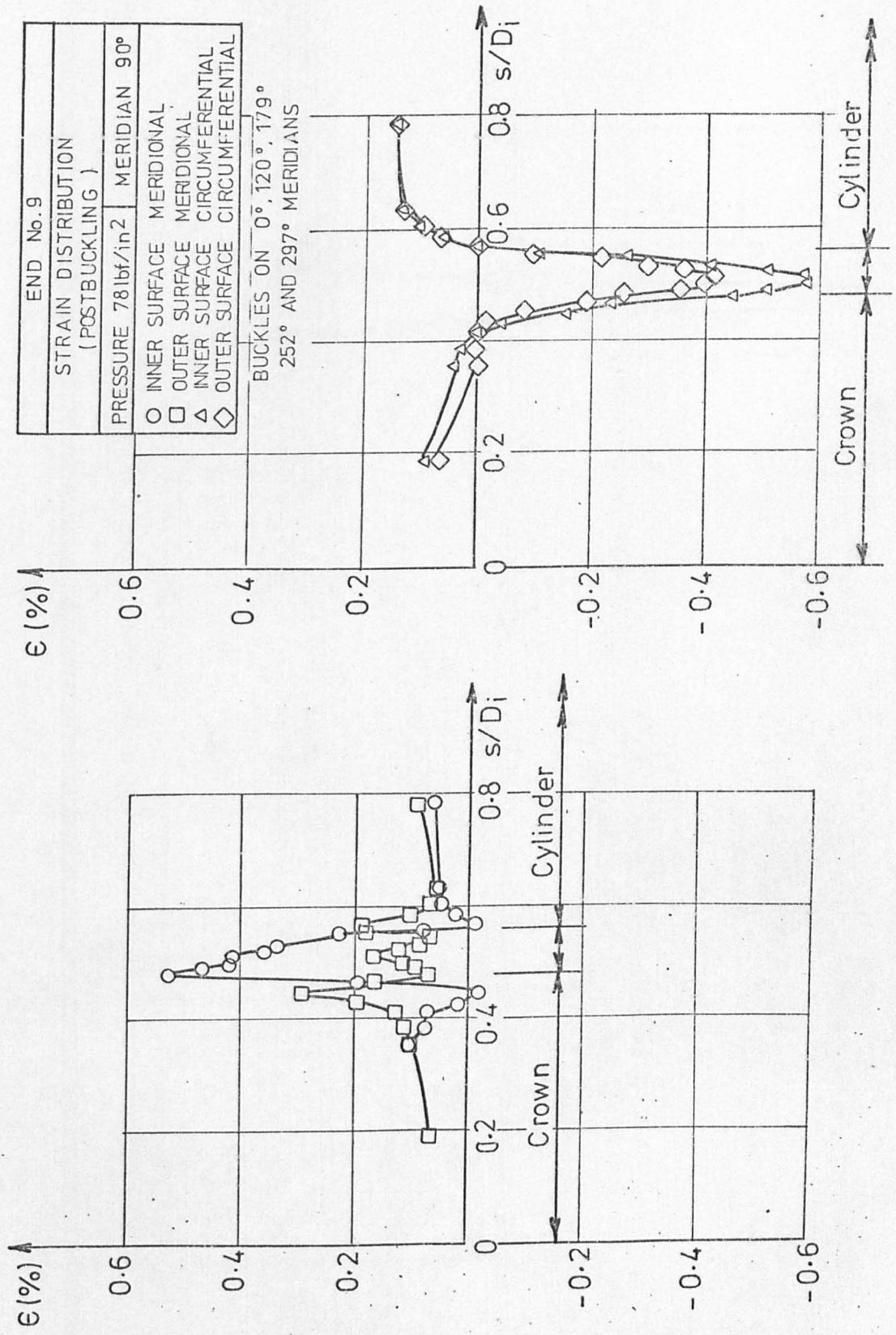
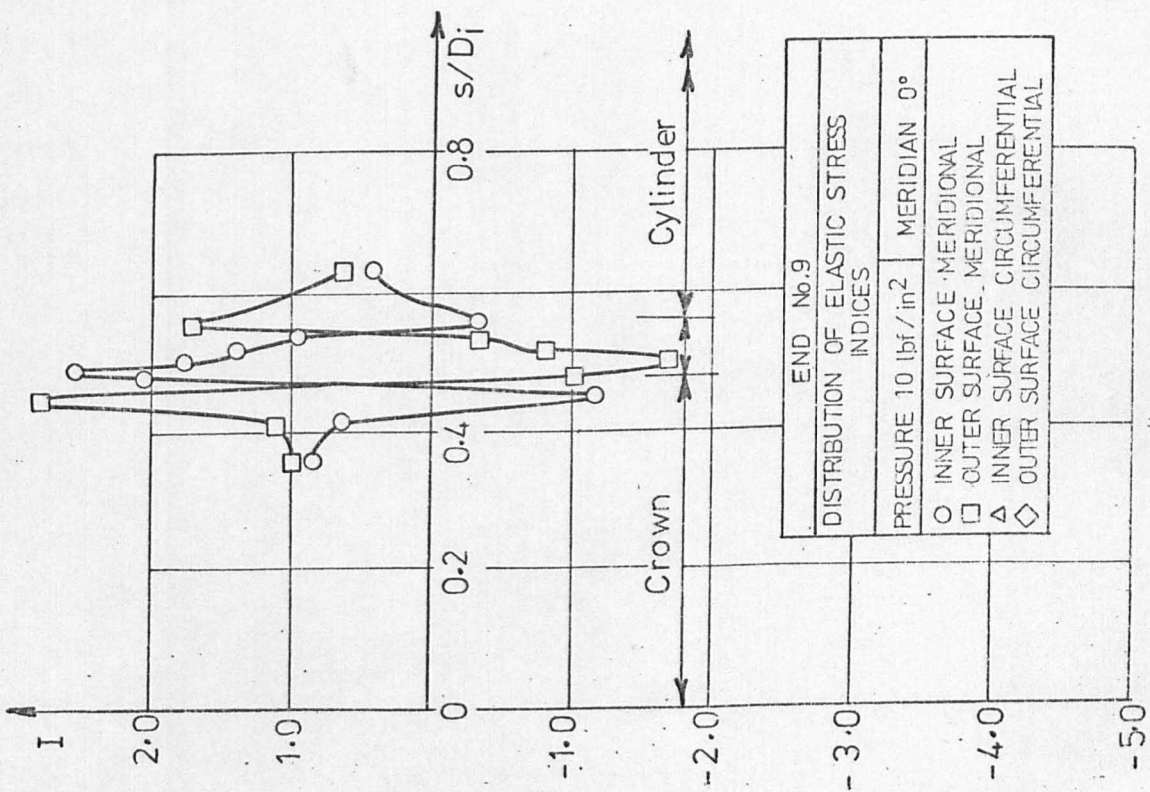
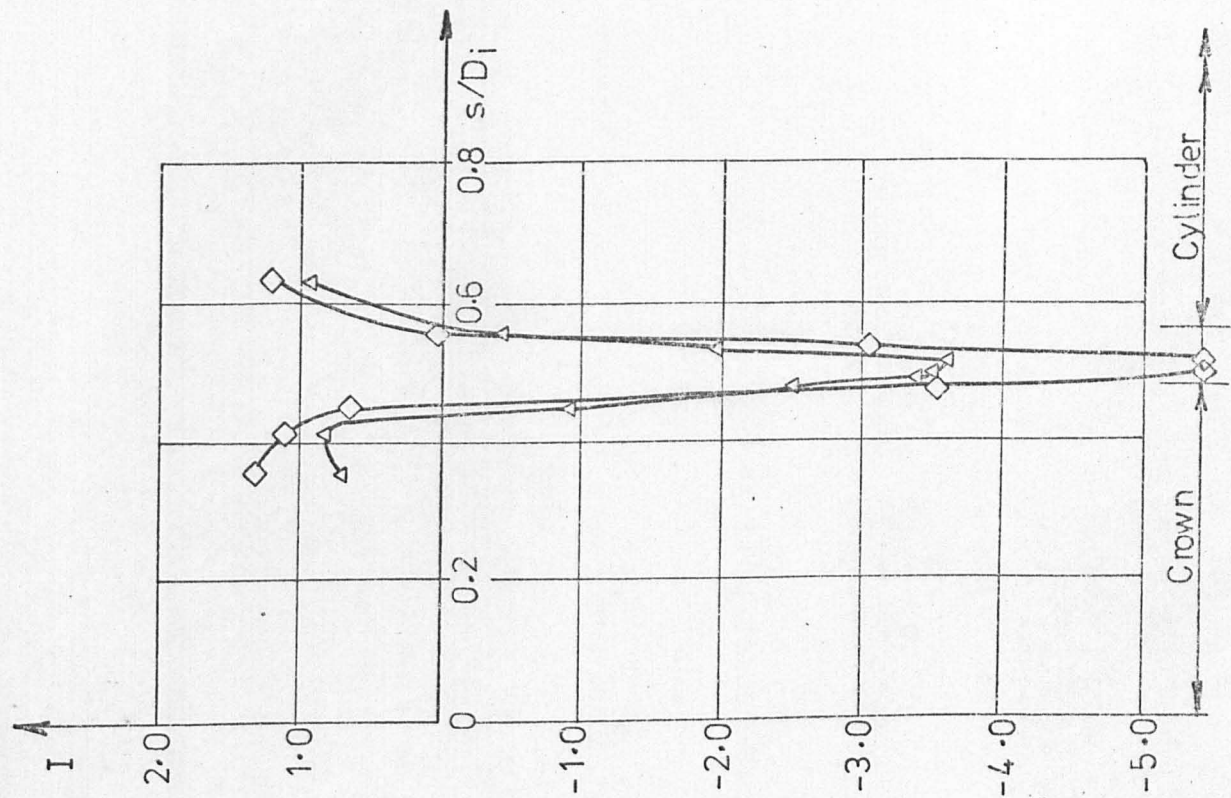


FIG. 7.21



END No.9	
DISTRIBUTION OF ELASTIC STRESS INDICES	
PRESSURE 10 lbf/in <sup>2</sup>	MERIDIAN 0°
○	INNER SURFACE MERIDIONAL
□	OUTER SURFACE MERIDIONAL
△	INNER SURFACE CIRCUMFERENTIAL
◇	OUTER SURFACE CIRCUMFERENTIAL

FIG. 7.22

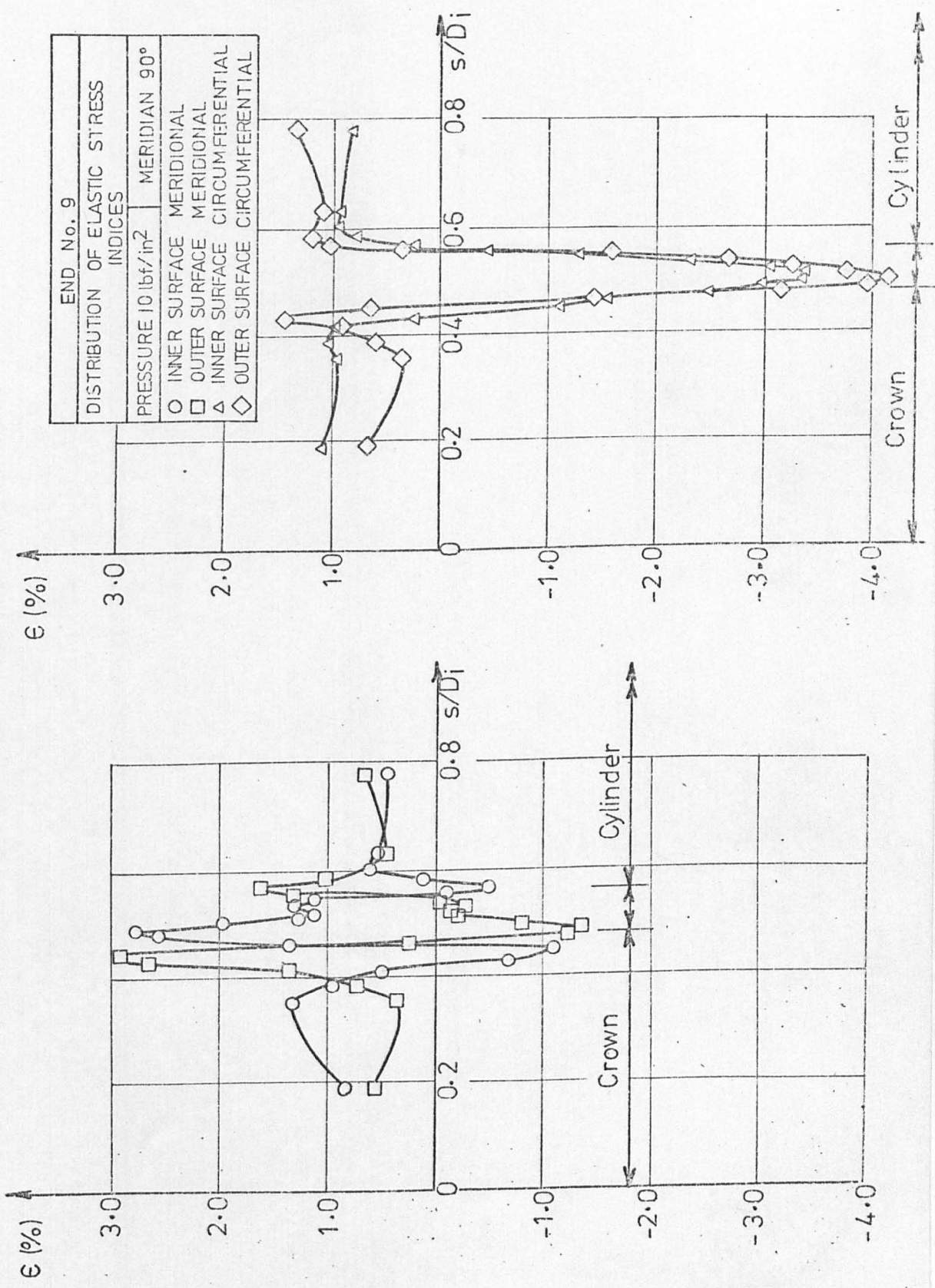


FIG. 7.23



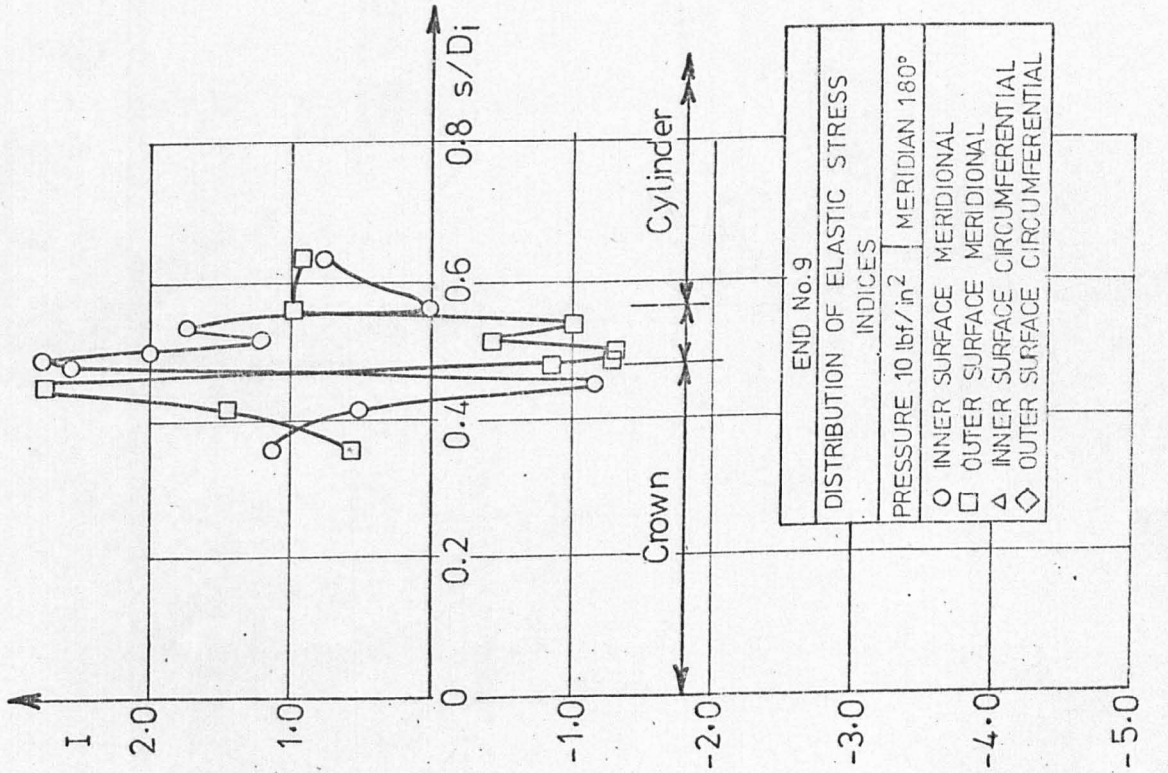
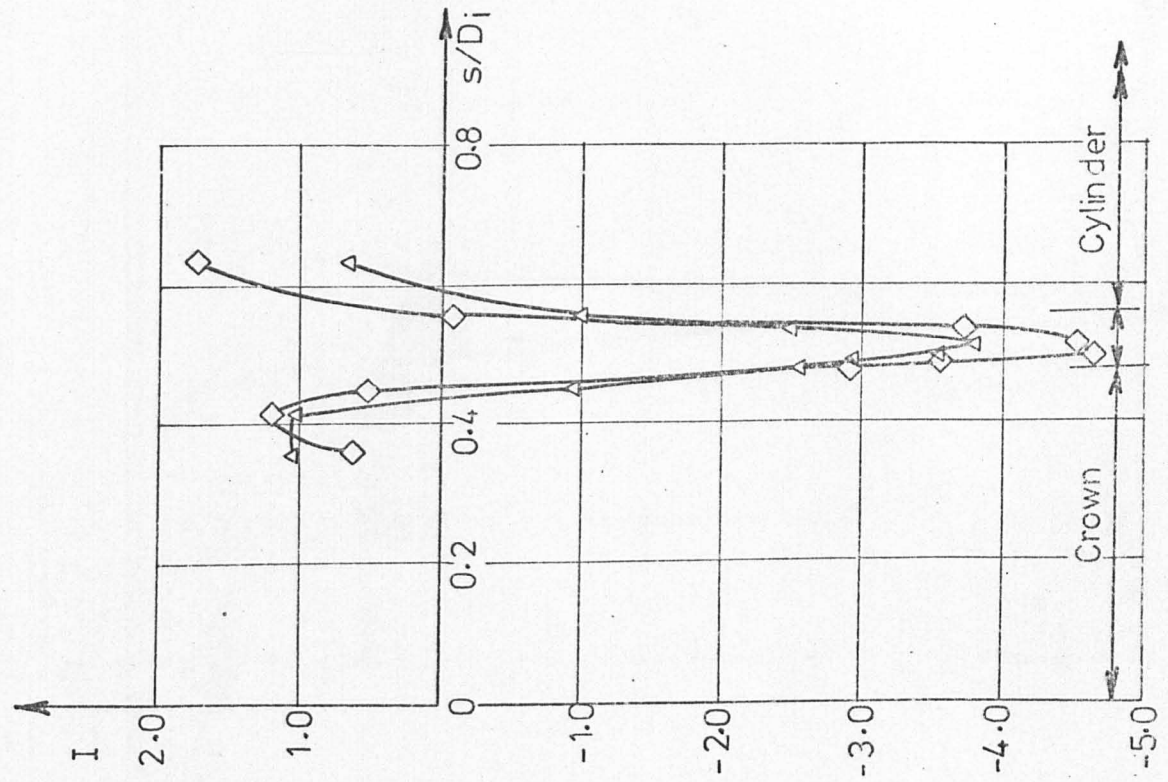


FIG. 7.24

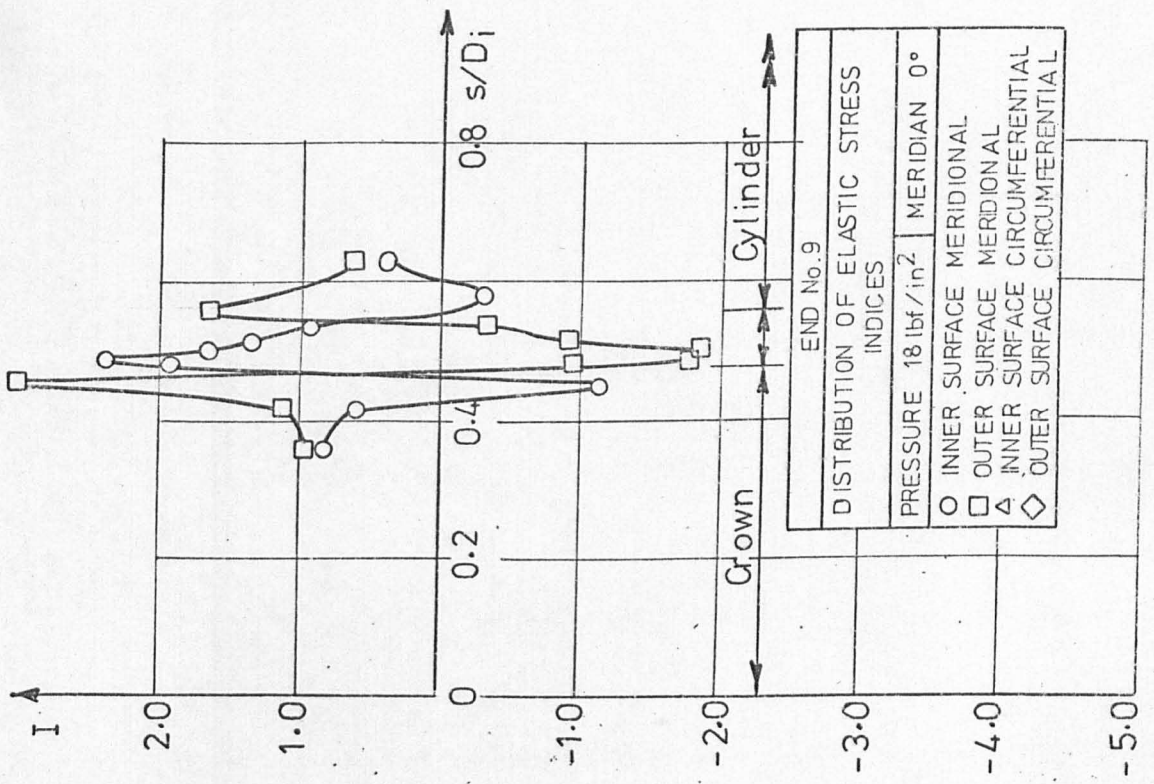
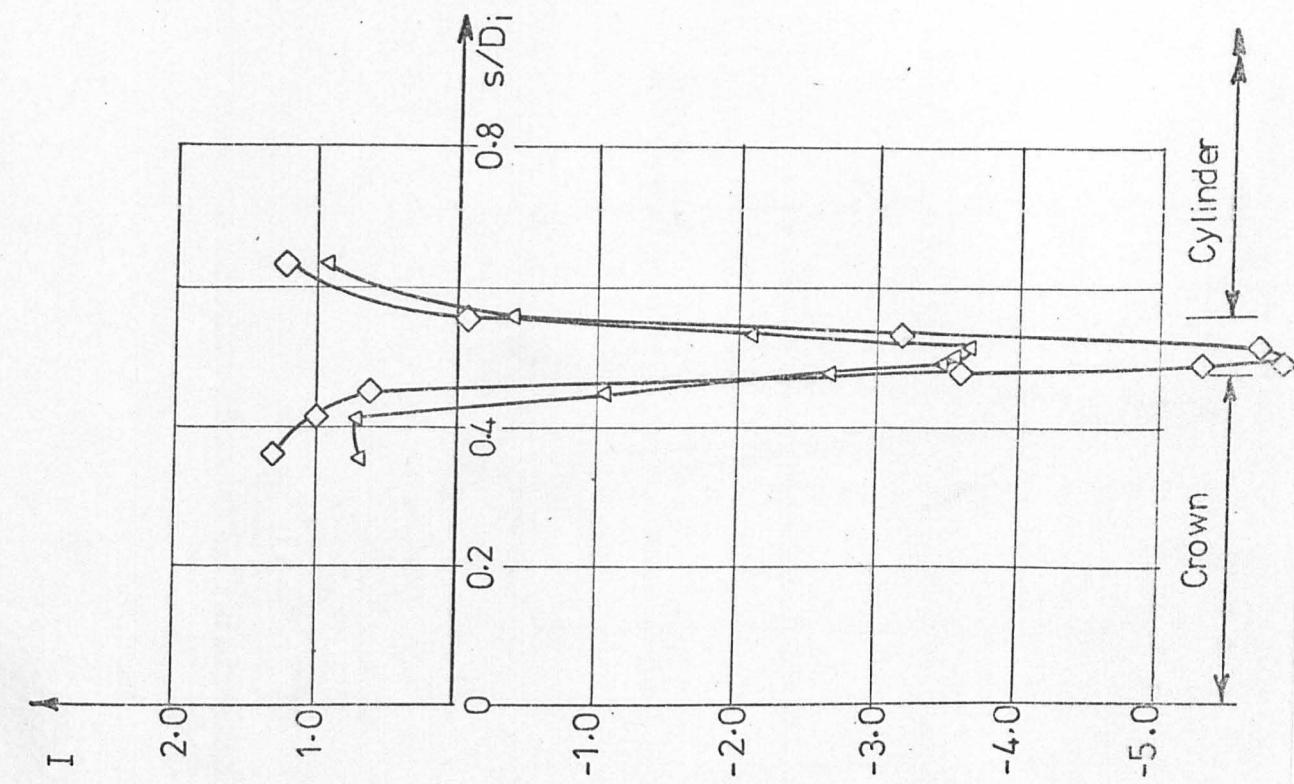


FIG. 7.25

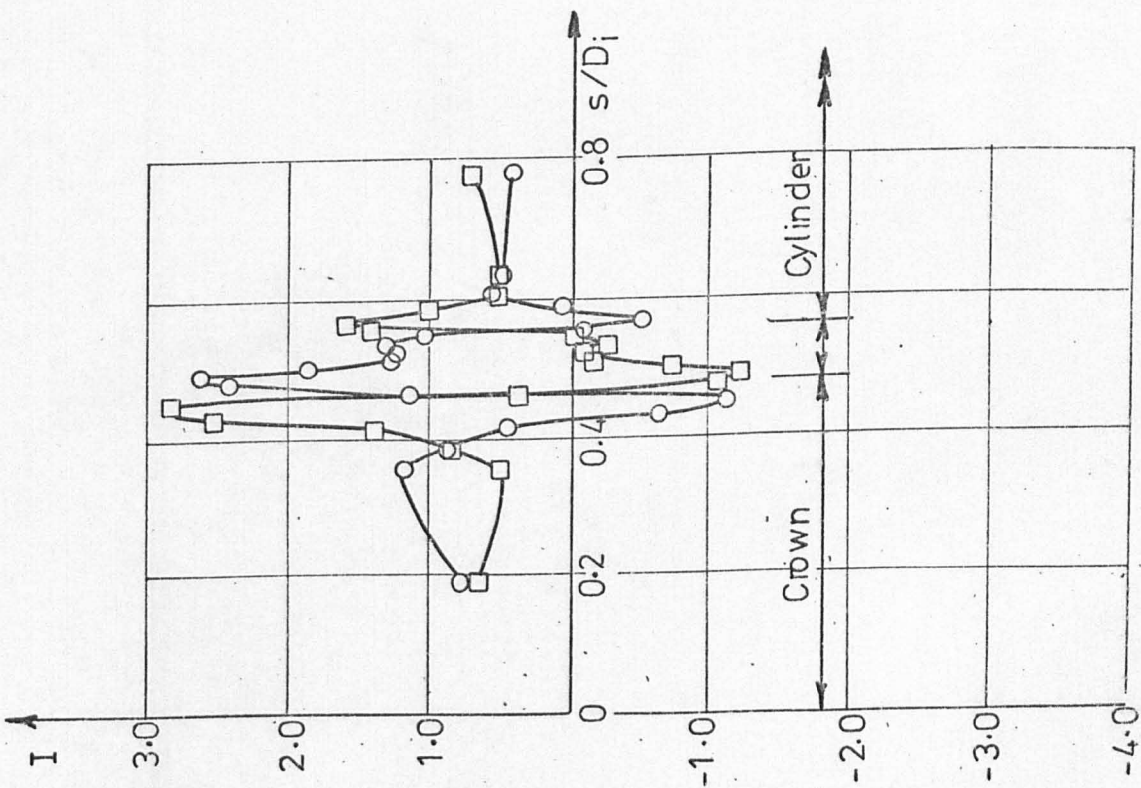
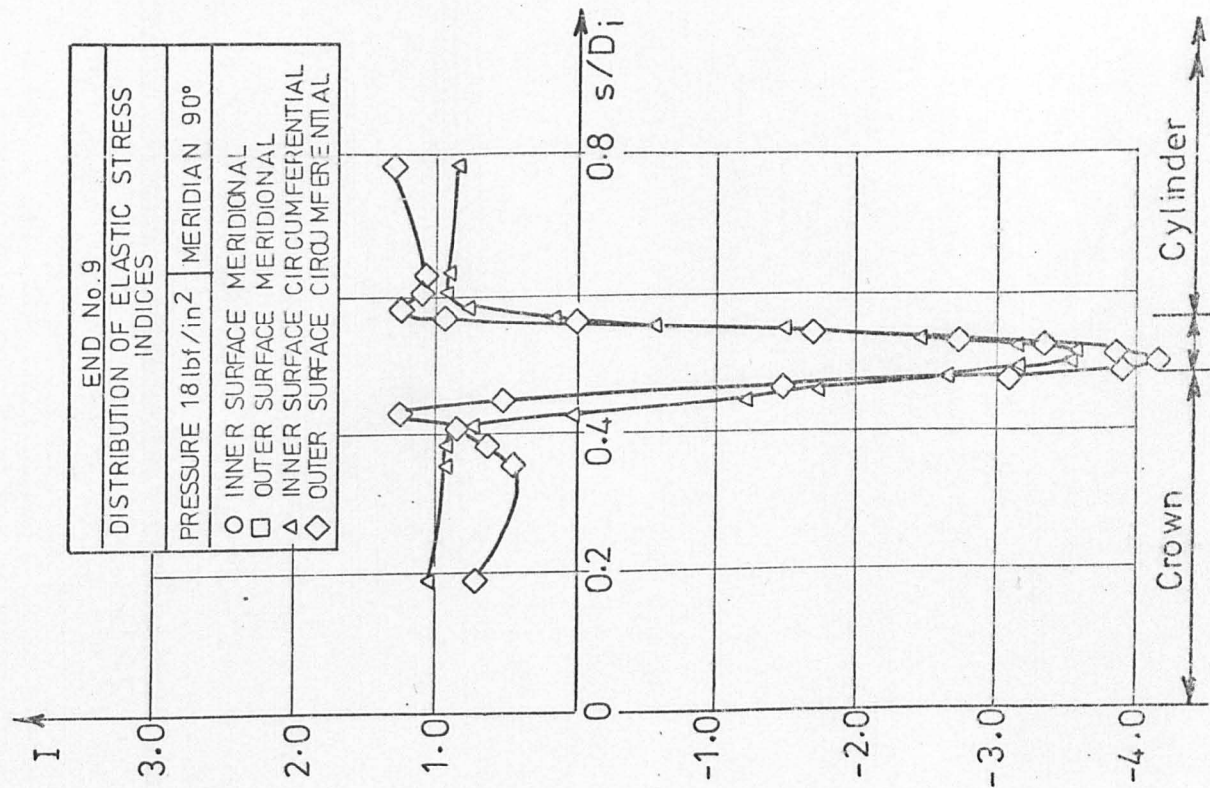
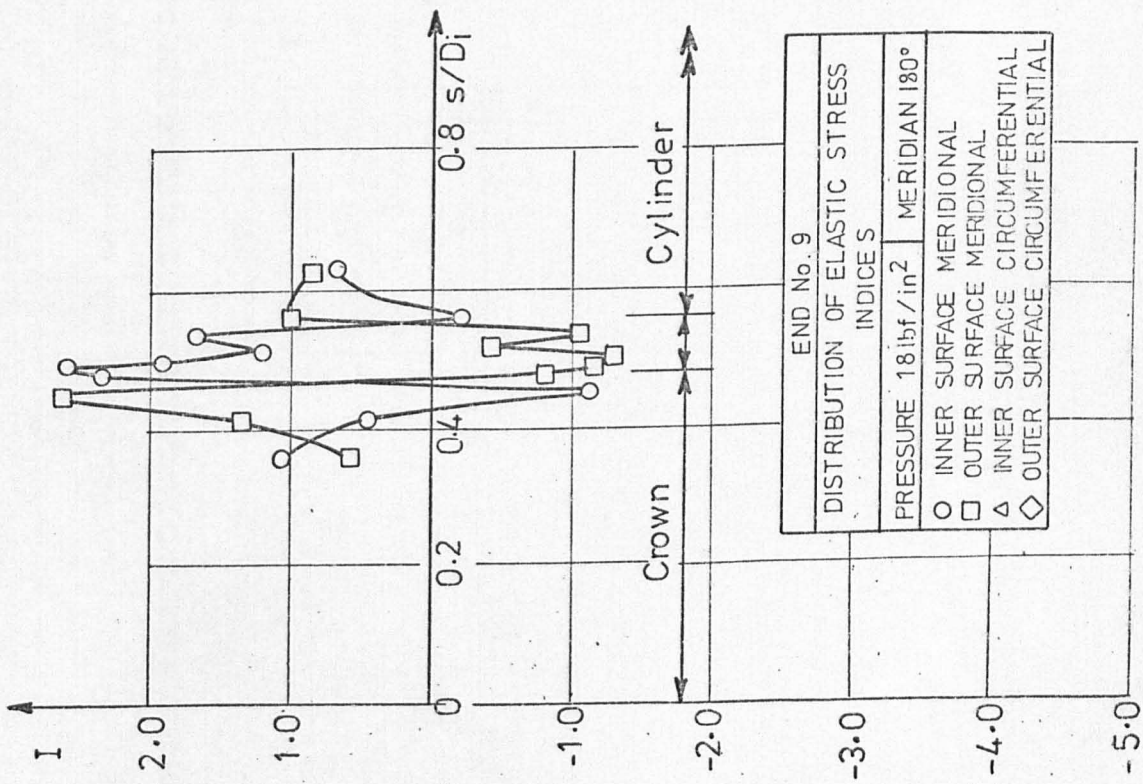
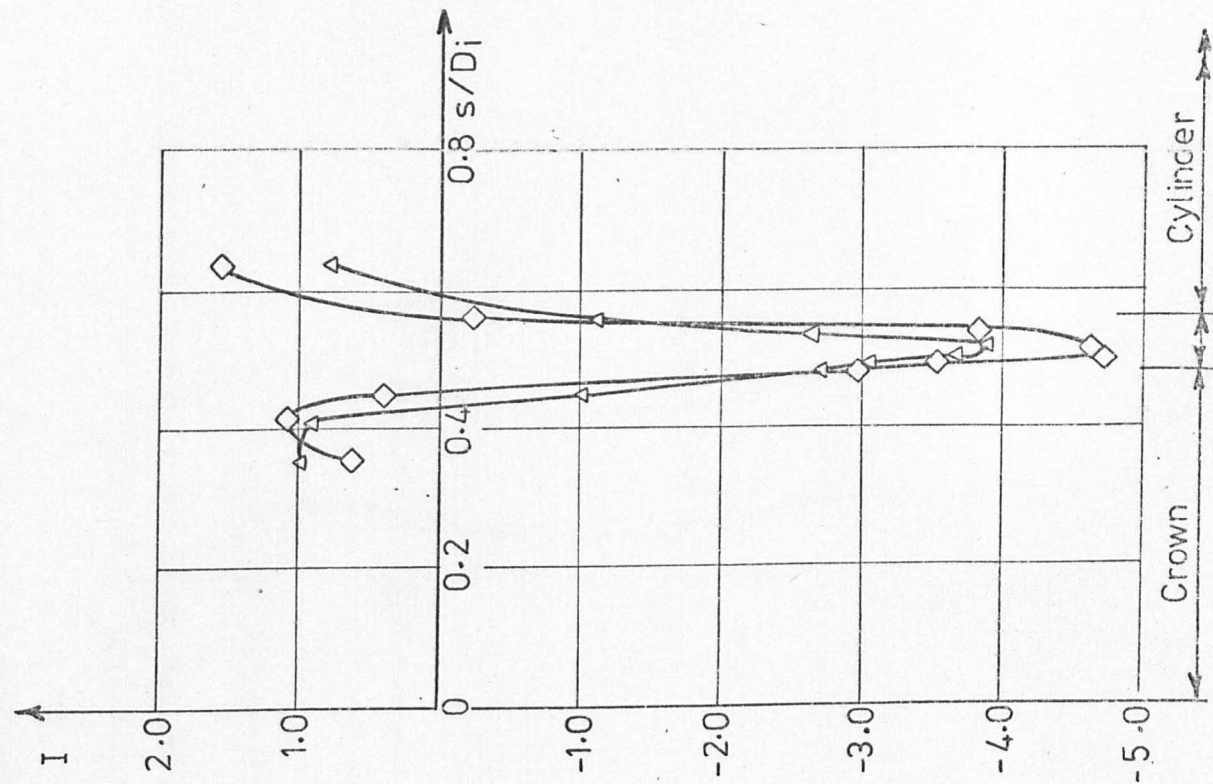


FIG. 7-26



END No. 9	
DISTRIBUTION OF ELASTIC STRESS INDICES	
PRESSURE	MERIDIAN 180°
○	INNER SURFACE MERIDIONAL
□	OUTER SURFACE MERIDIONAL
△	INNER SURFACE CIRCUMFERENTIAL
◇	OUTER SURFACE CIRCUMFERENTIAL

FIG. 7-27

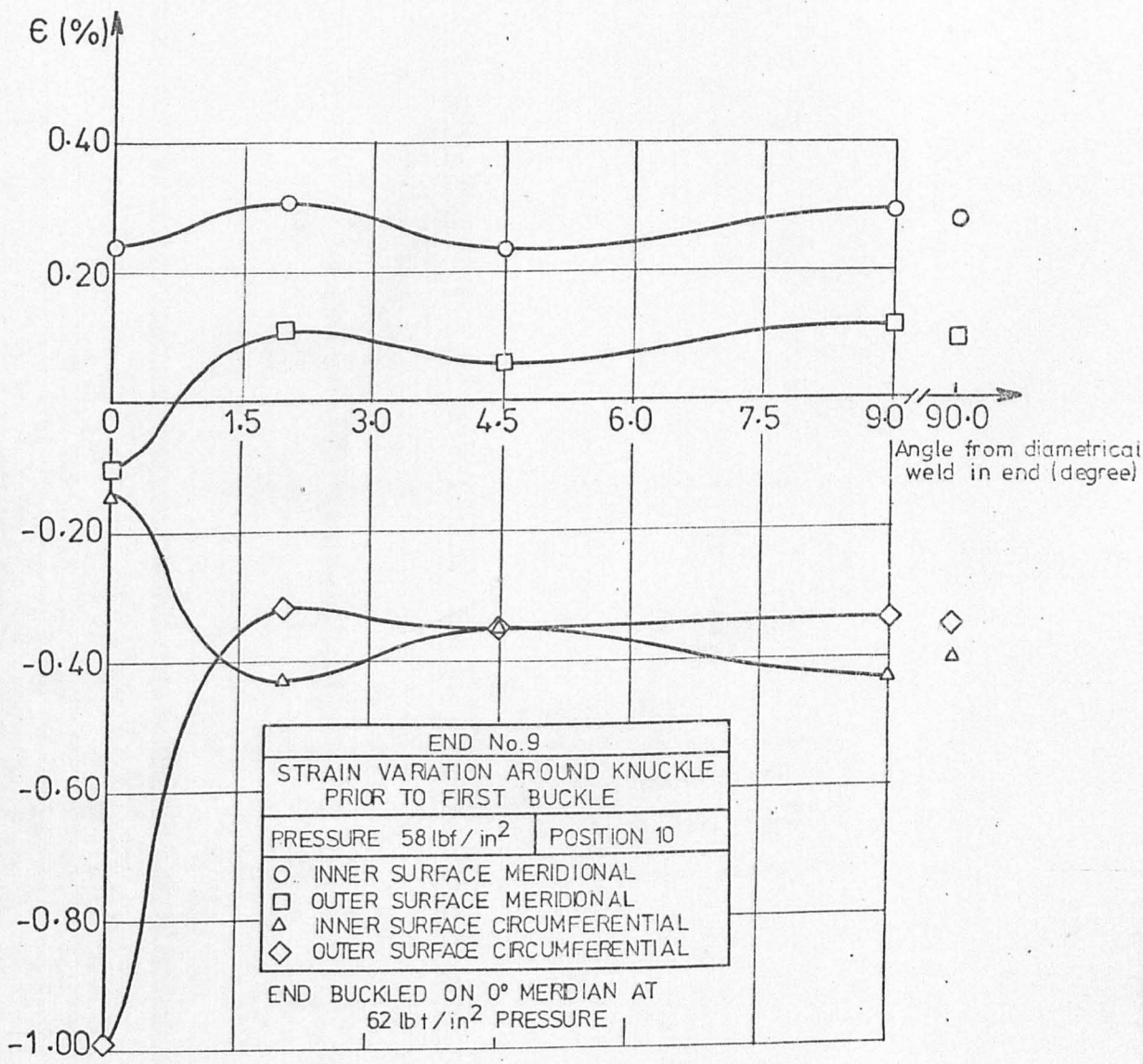


FIG. 7.28

END No. 9  
CREEP STRAIN MEASURED  
BY GAUGE 11,o,c (0°)

FOR GAUGE IDENTIFICATION  
SEE TABLE 6.1

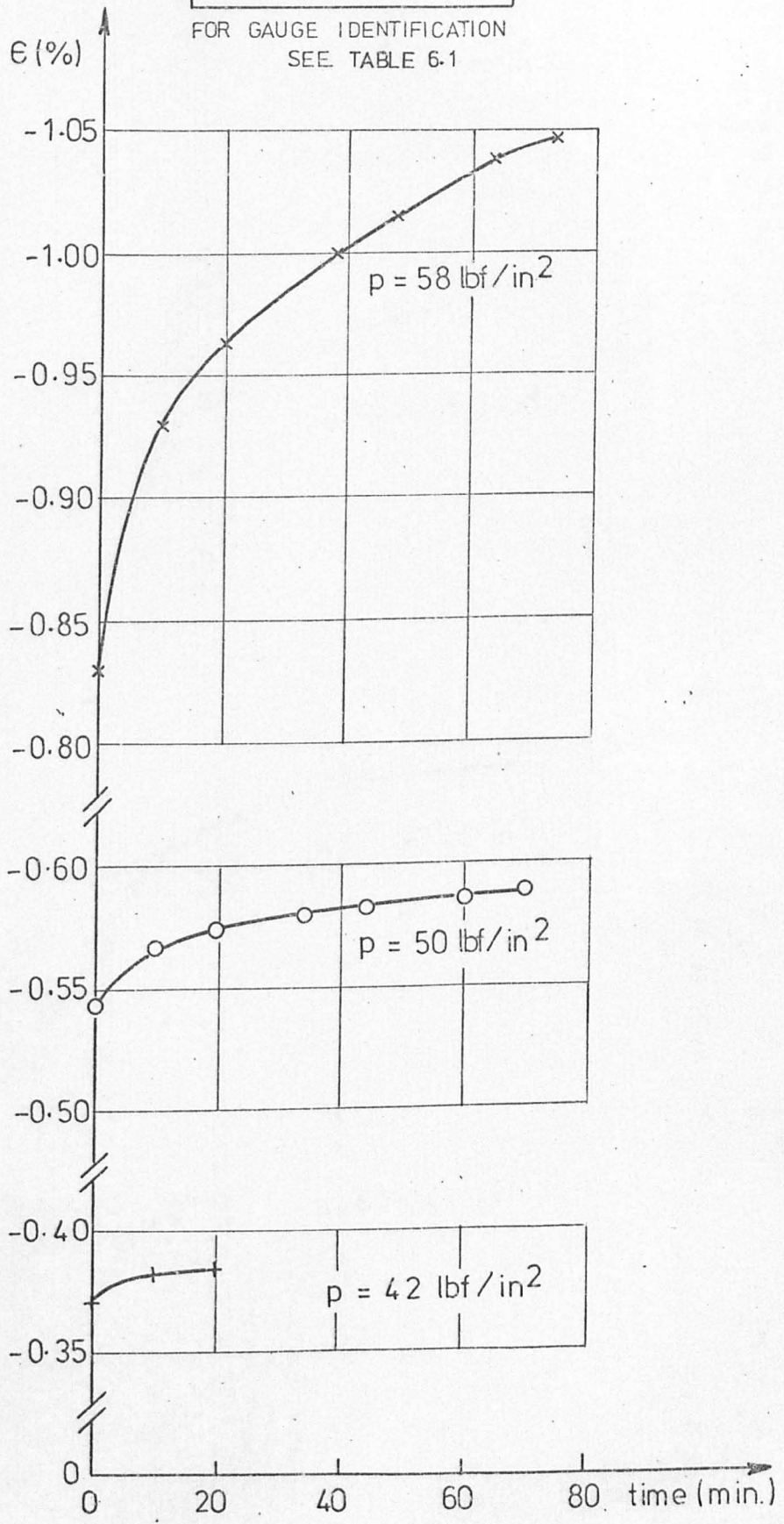


FIG. 7-29

END No. 9  
 CREEP STRAIN MEASURED  
 BY GAUGE 8,i,m (90°)  
 FOR GAUGE IDENTIFICATION  
 SEE TABLE 6.1

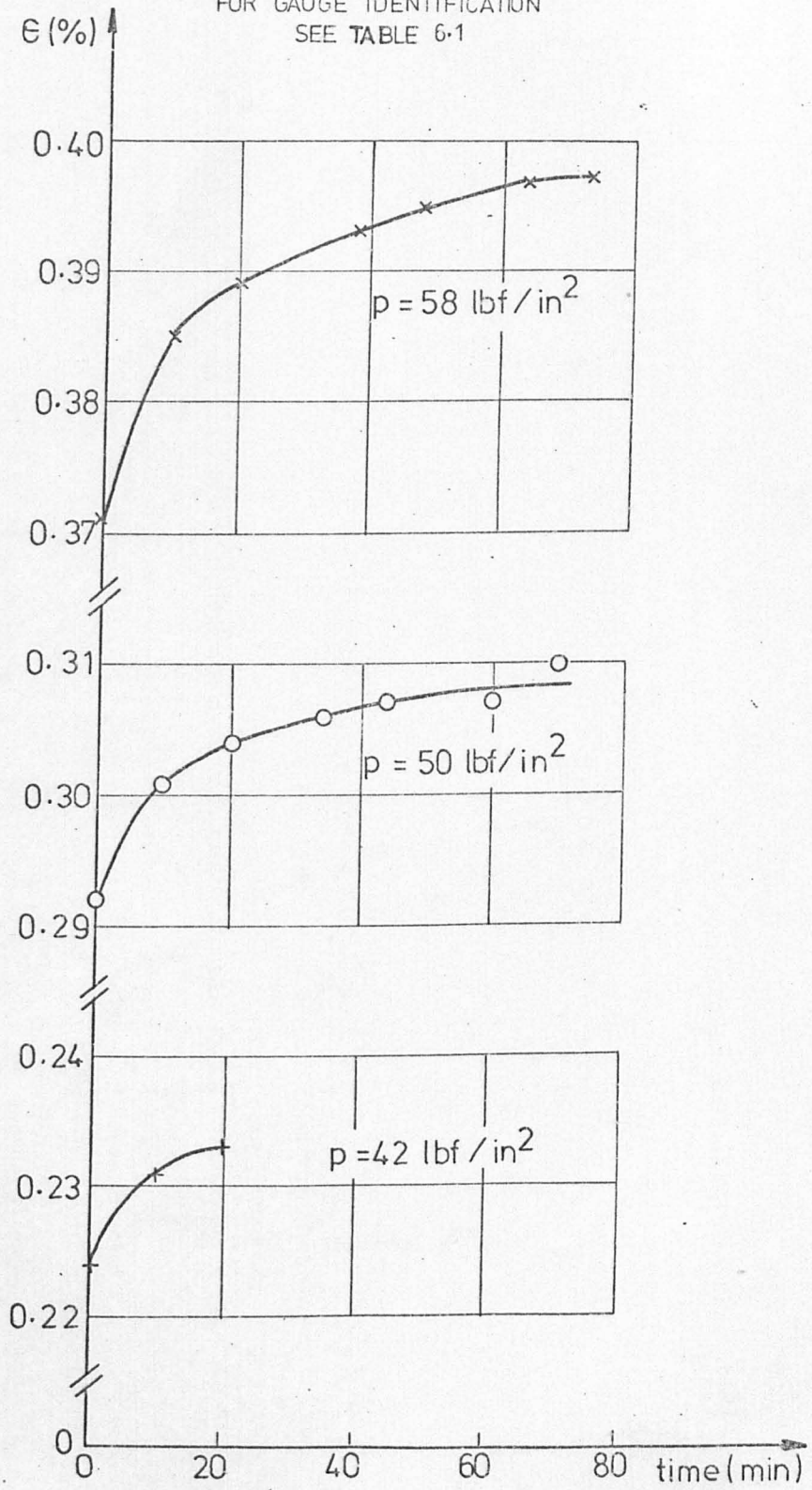


FIG. 7.30

END No. 9  
CREEP STRAIN MEASURED  
BY GAUGE 10,i,c (90°)

FOR GAUGE IDENTIFICATION  
SEE TABLE 6.1

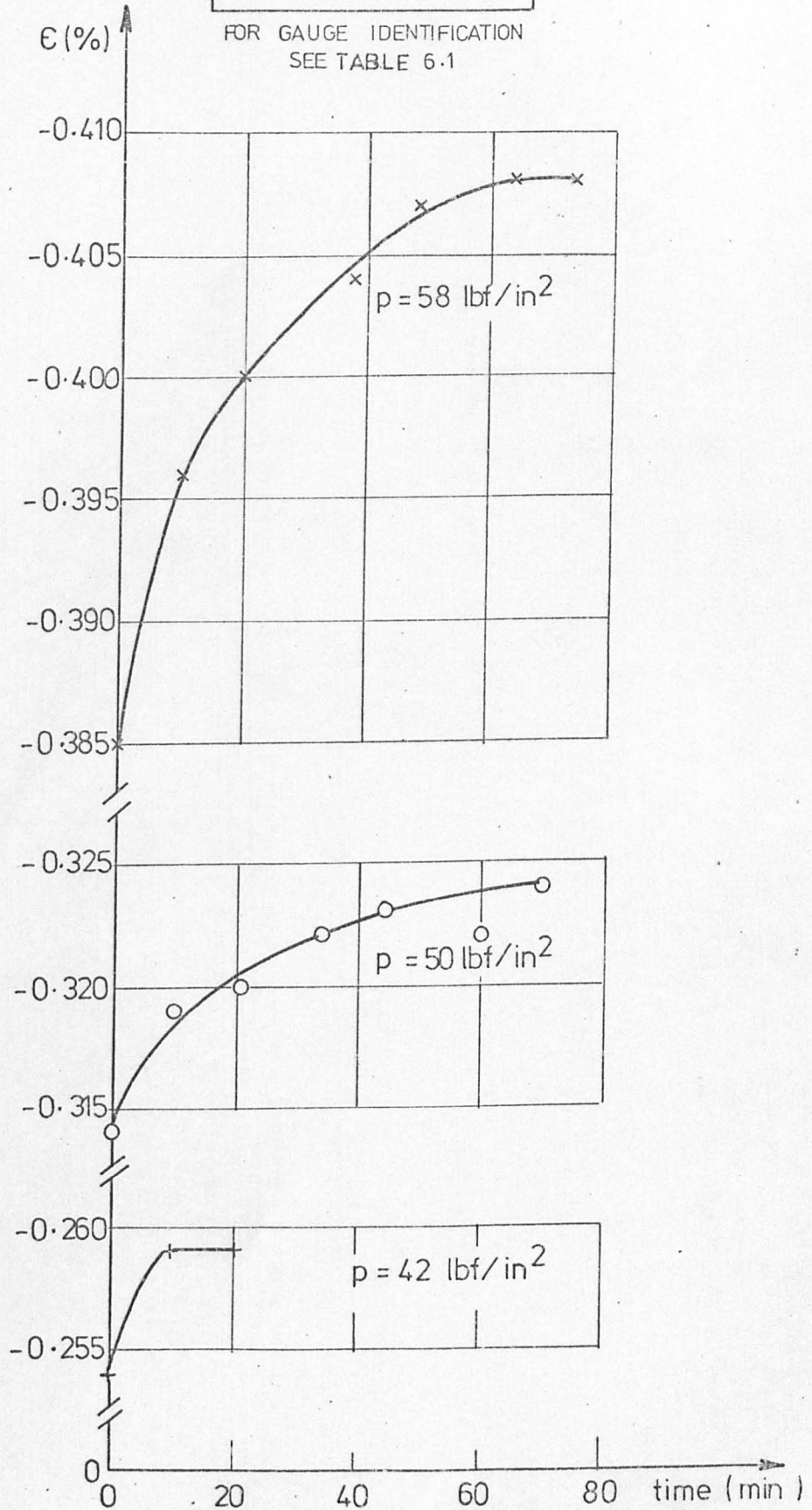


FIG. 7-31



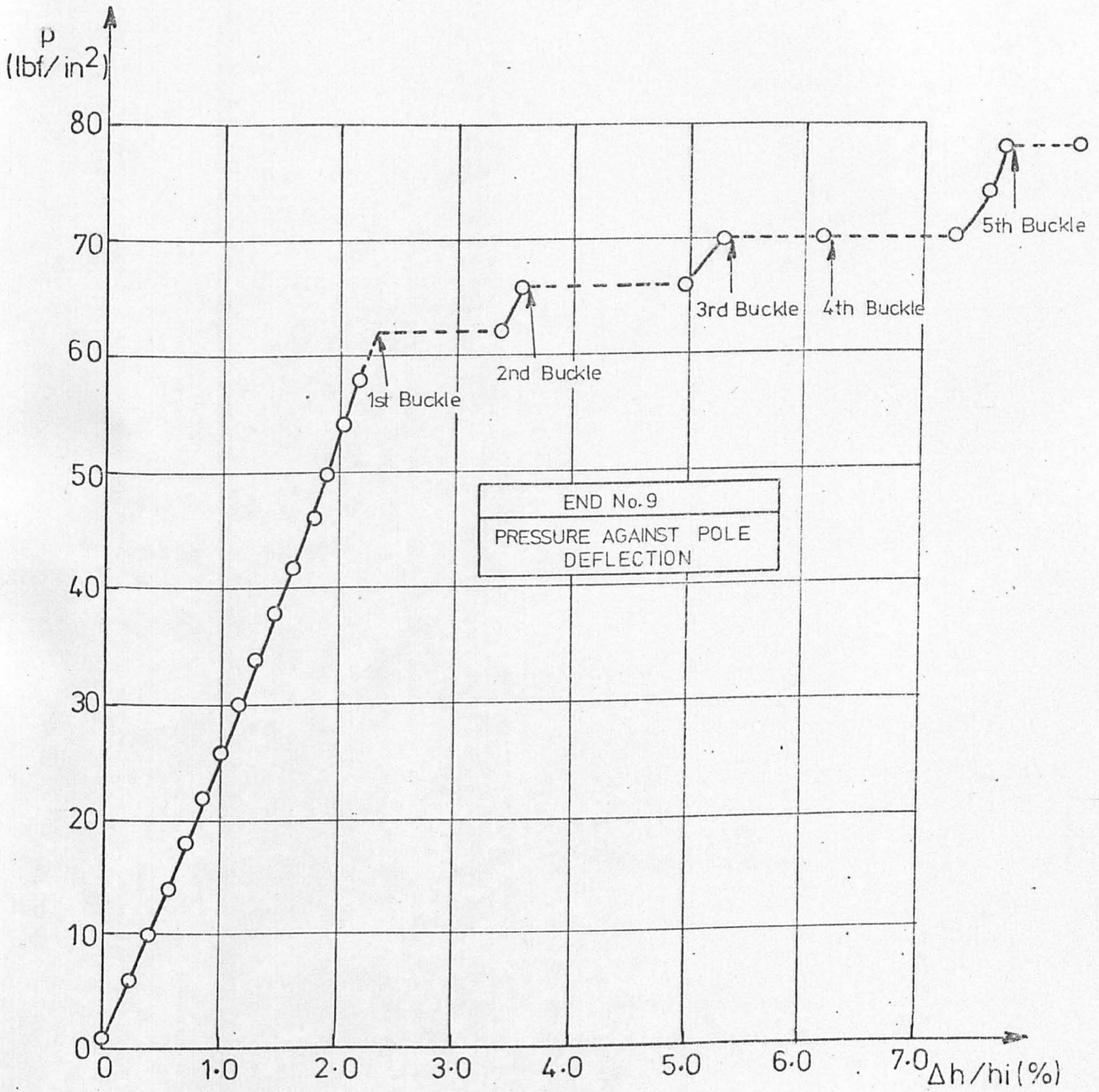


FIG. 7:32

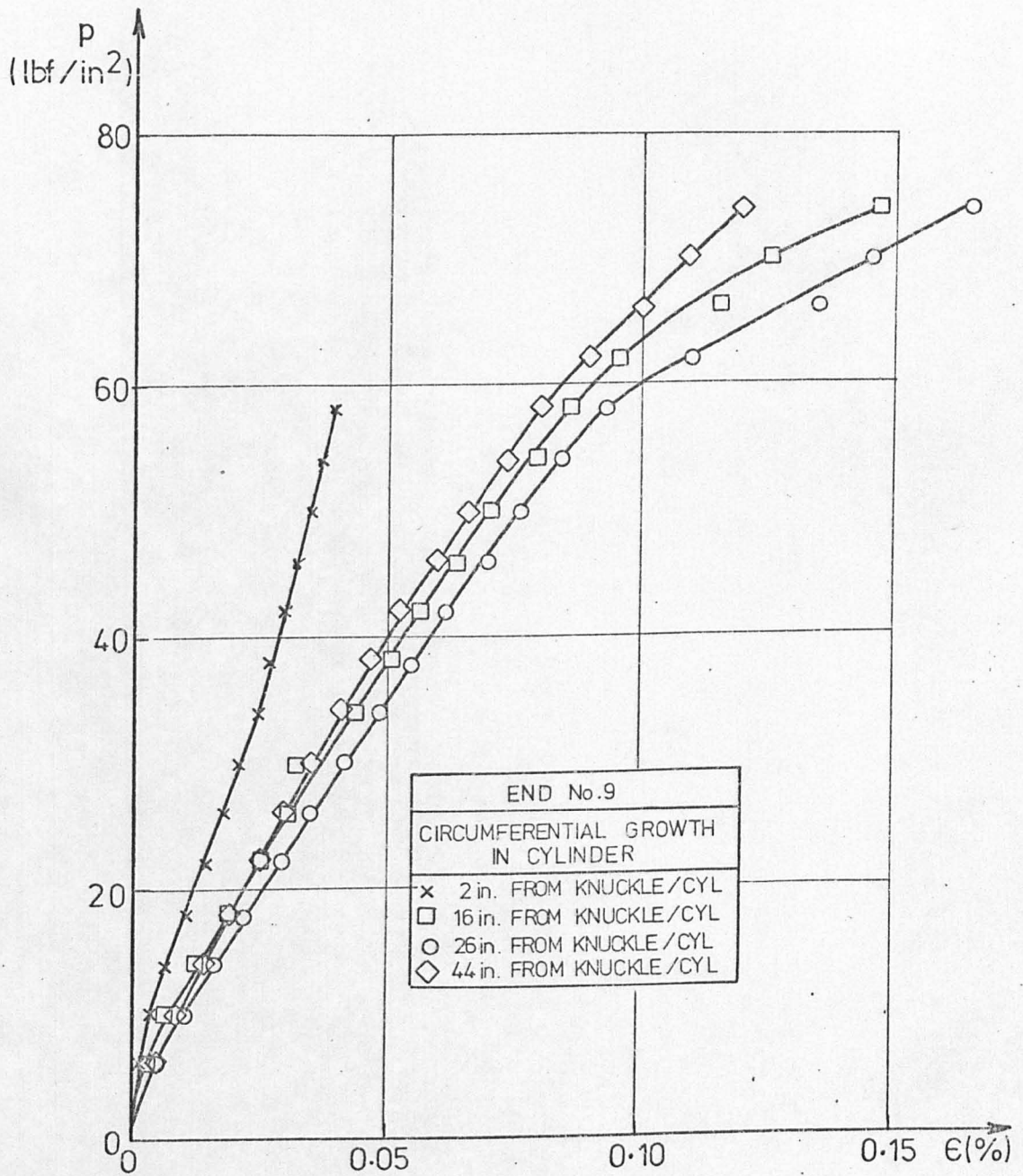


FIG. 7.33

EXAMPLES OF BUCKLES PRODUCED

a) END NO 1 (3rd Buckle)

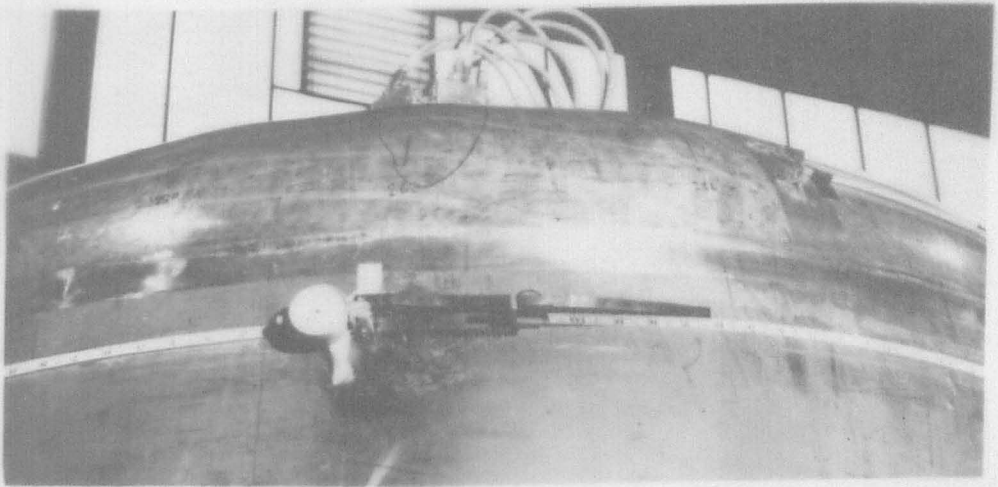
b) END NO 2

c) END NO 3

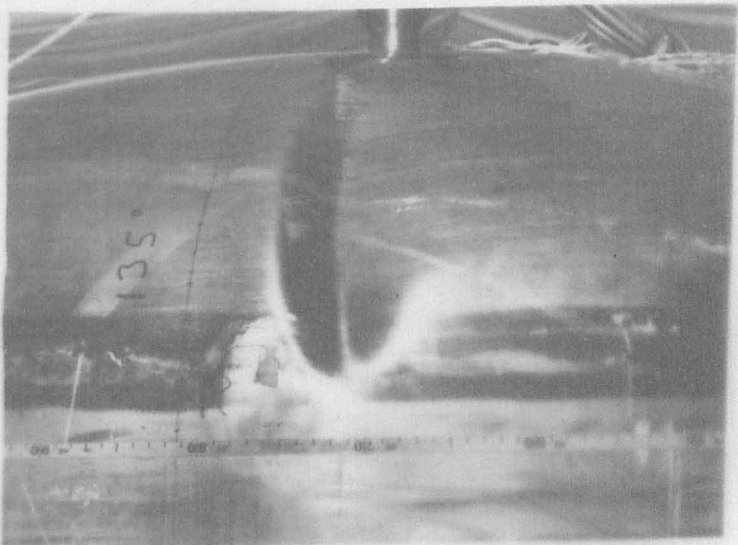
EXAMPLES OF BUCKLES PRODUCED



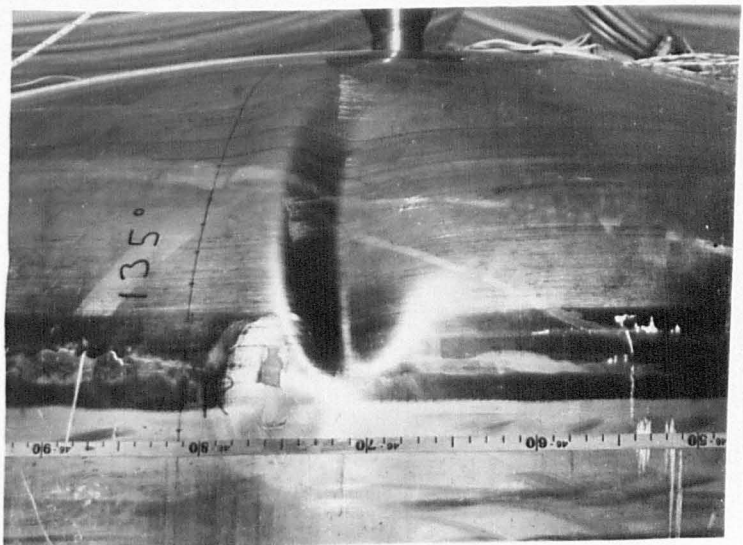
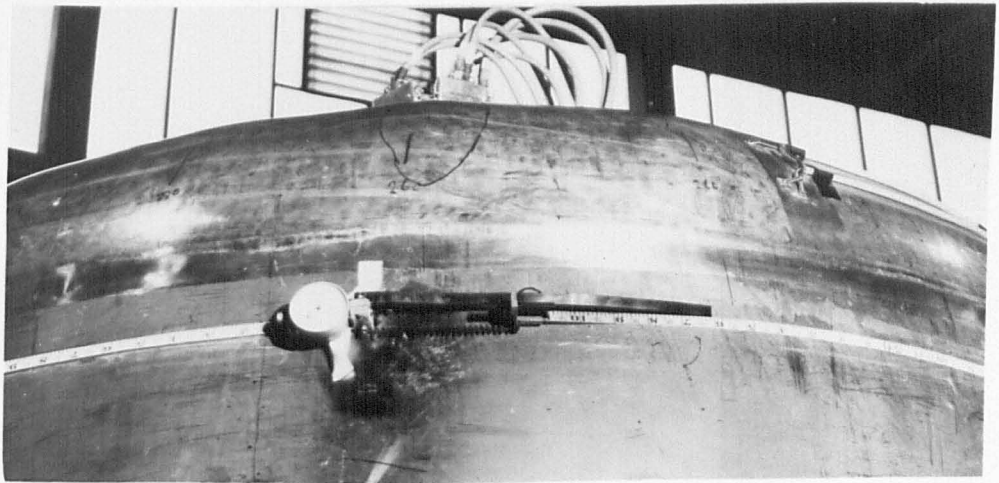
a) END NO 1 (3rd Buckle)



b) END NO 2



c) END NO 3



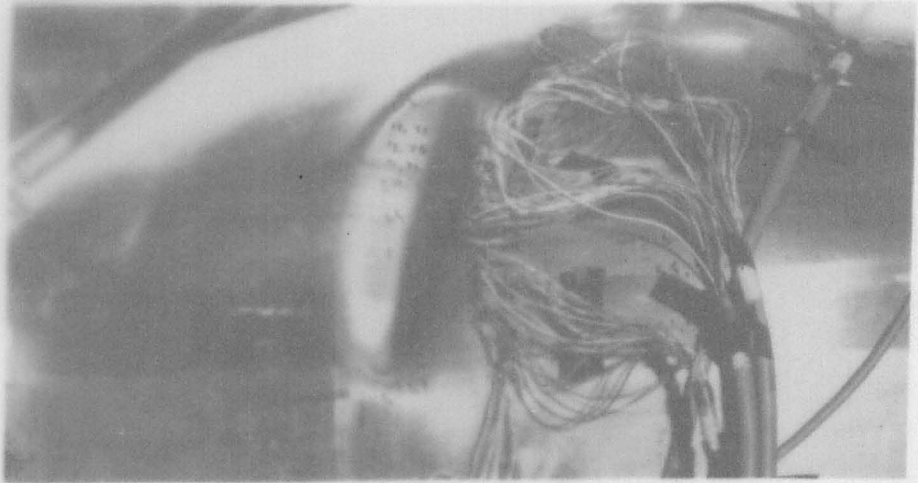
EXAMPLES OF BUCKLES PRODUCED

a) END No 4 (1st Buckle)

b) END No 5

c) END No 6 (2nd + 5th Buckles)

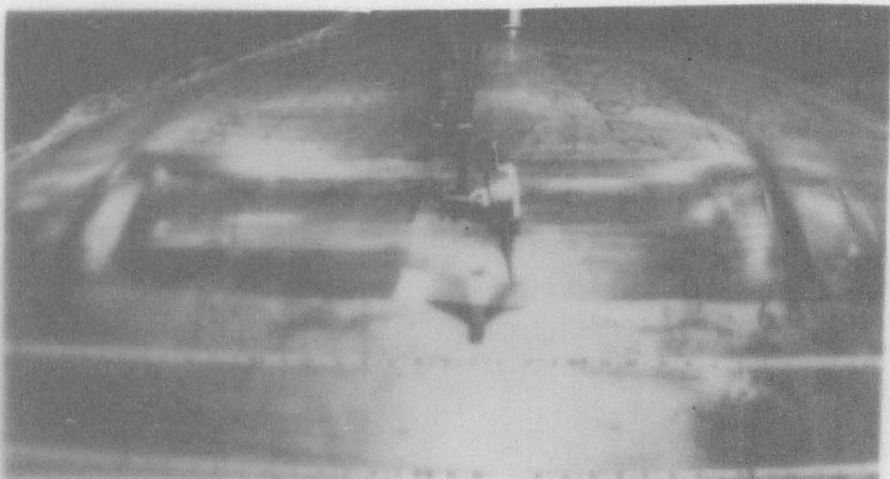
EXAMPLES OF BUCKLES PRODUCED



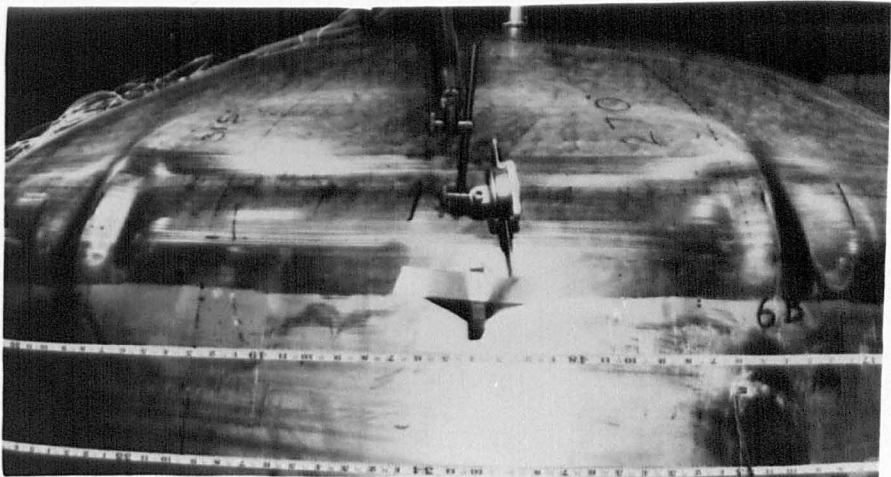
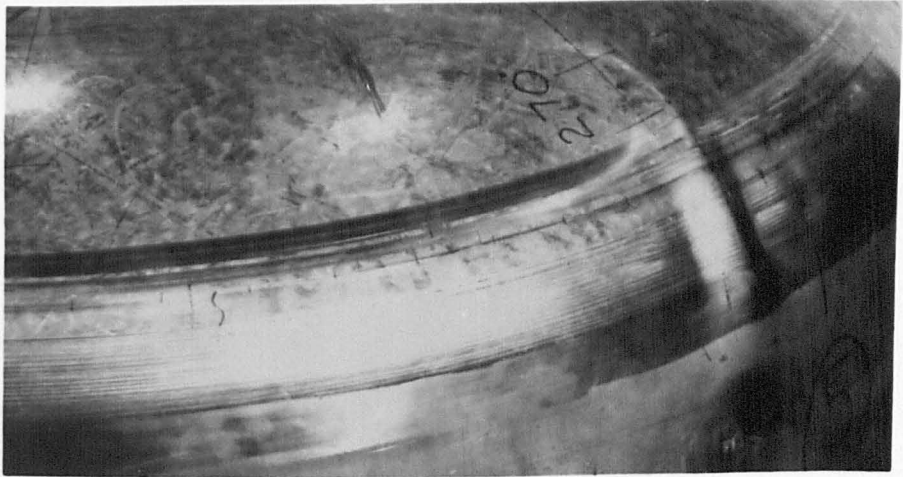
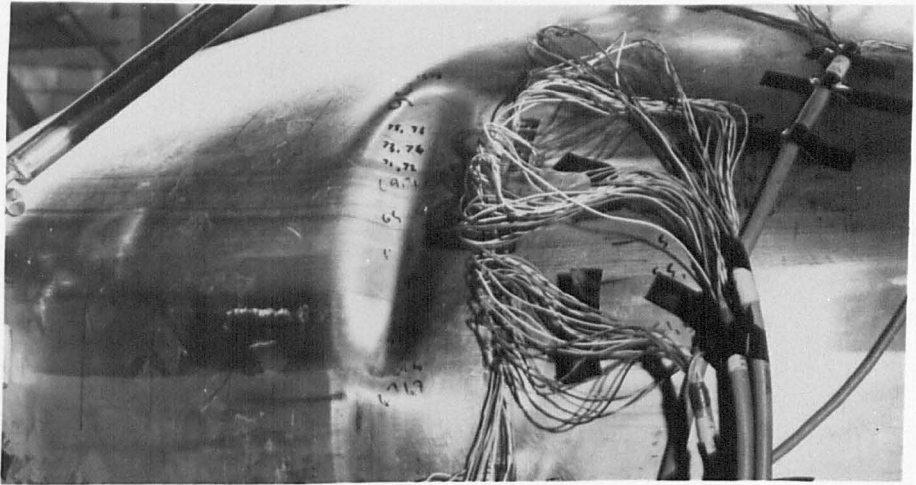
a) END No 4 (1st Buckle)



b) END No 5



c) END No 6 (2nd + 5th Buckles)





EXAMPLES OF BUCKLES PRODUCED

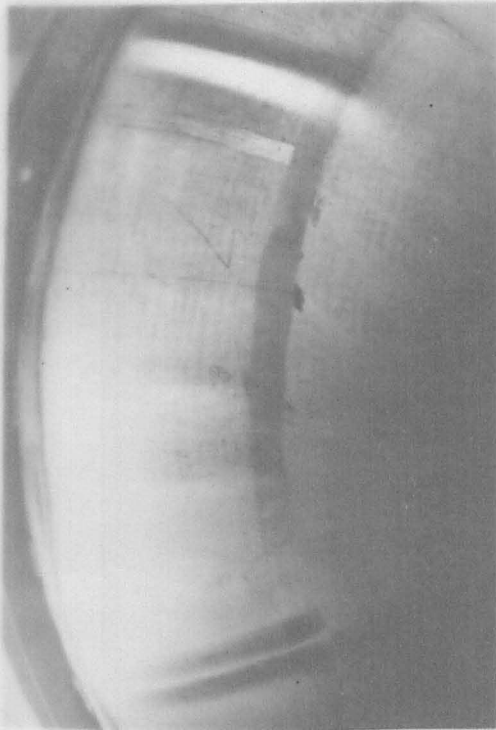
a) END No7  
(3rd - 5th Buckles)

b) END No 8  
(1st Buckle )

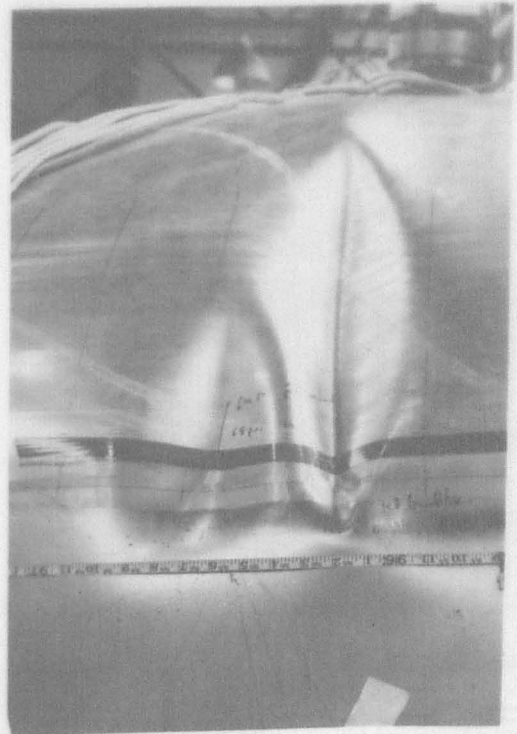
c) END No 9  
( 3rd Buckle)

d) END No 10  
(2nd Buckle)

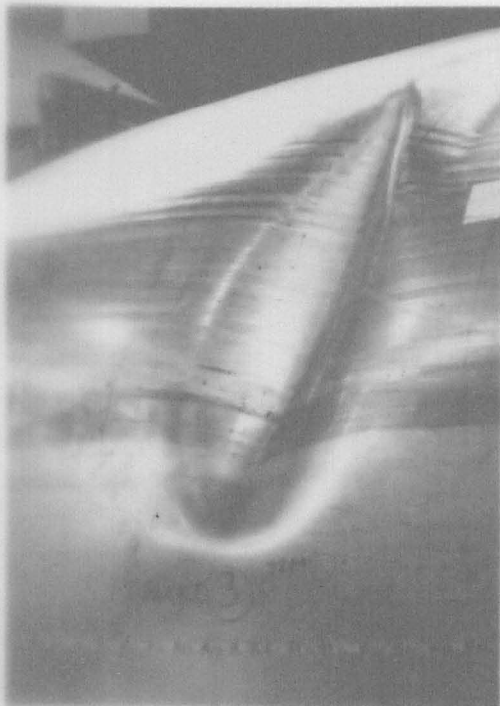
EXAMPLES OF BUCKLES PRODUCED



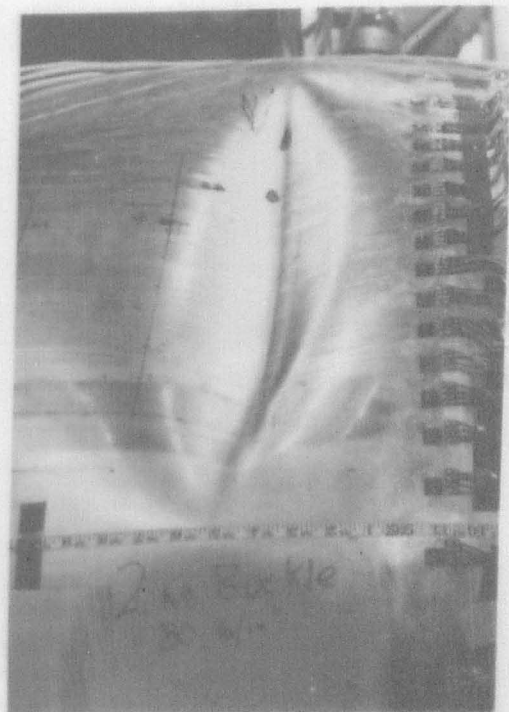
a) END No 7  
(3rd - 5th Buckles)



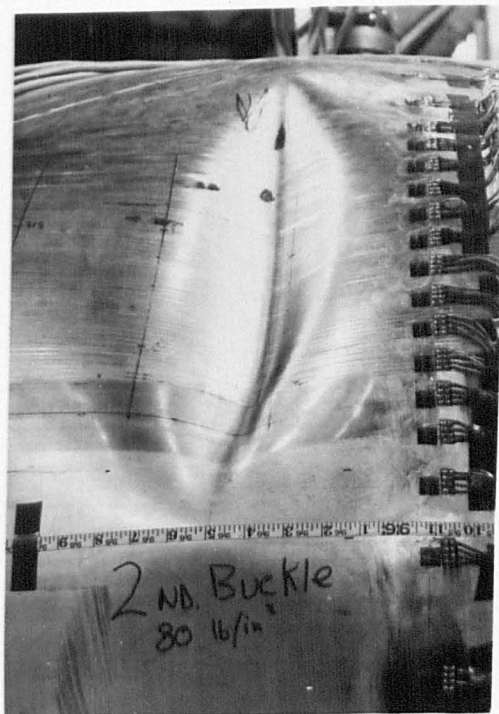
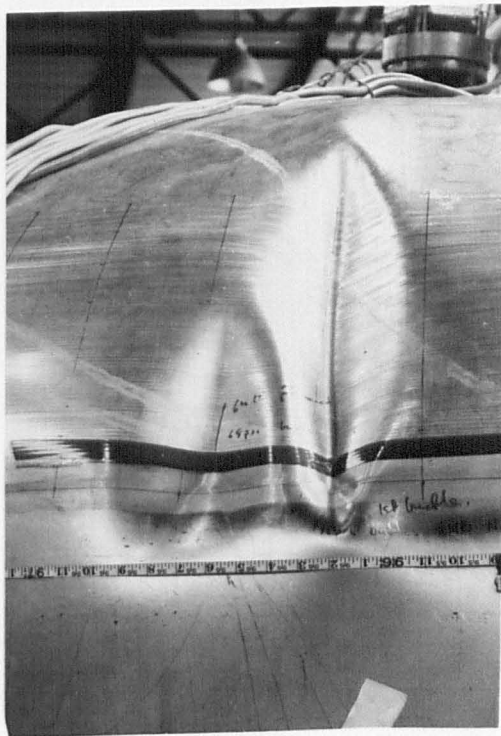
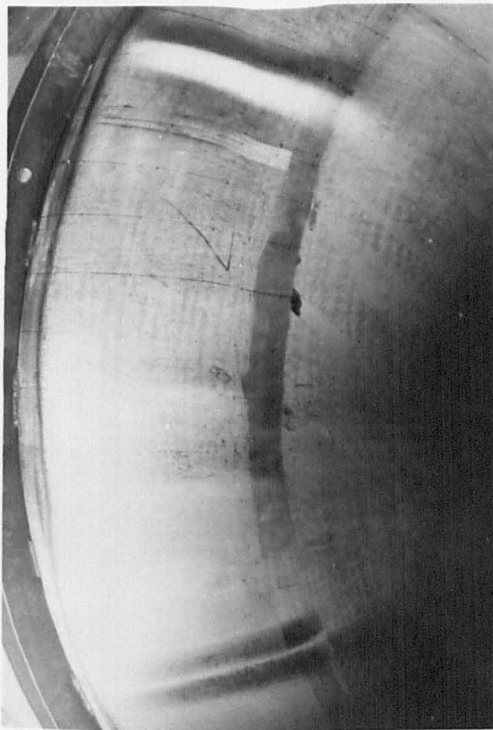
b) END No 8  
(1st Buckle)



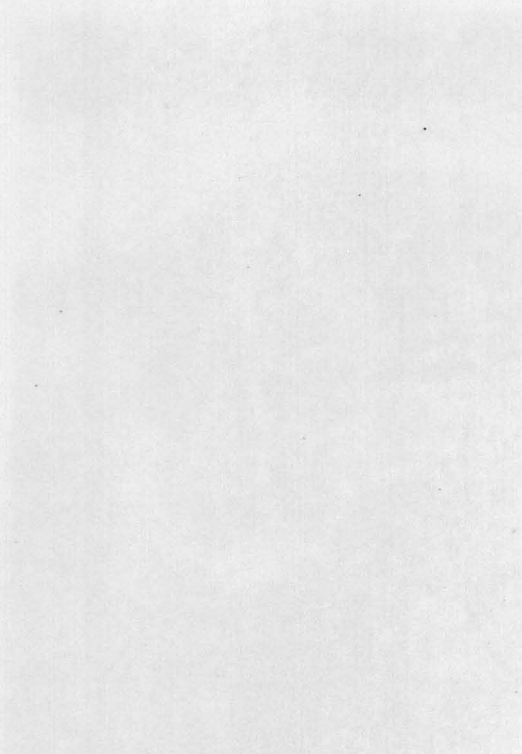
c) END No 9  
(3rd Buckle)



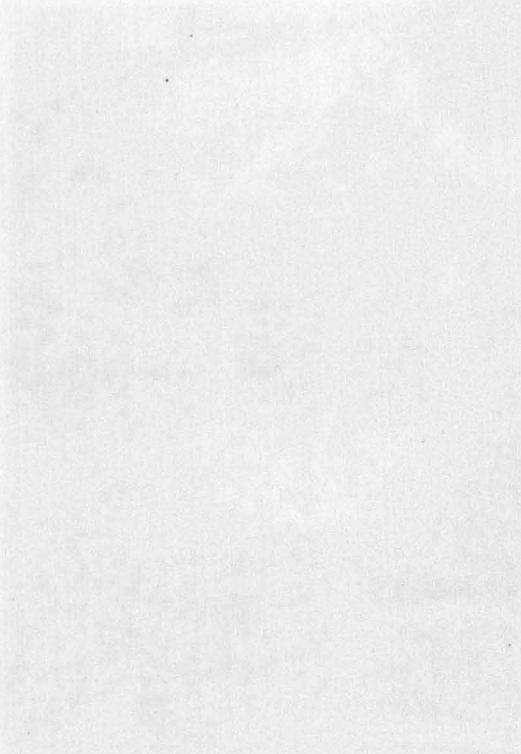
d) END No 10  
(2nd Buckle)



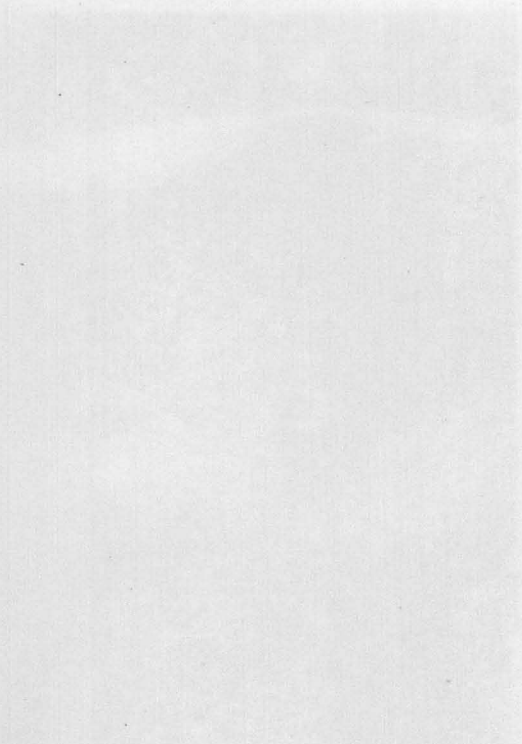
EXAMPLES OF BUCKLES PRODUCED



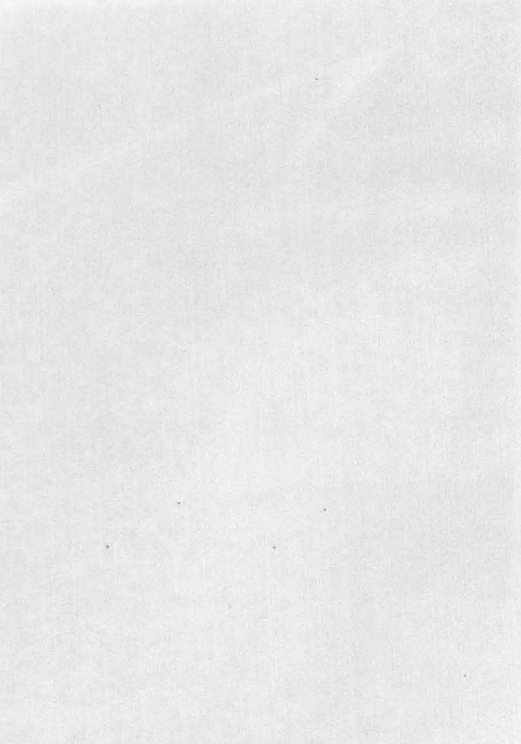
a) END No 11  
( 4th Buckle)



b) END No 12  
(4th Buckle)

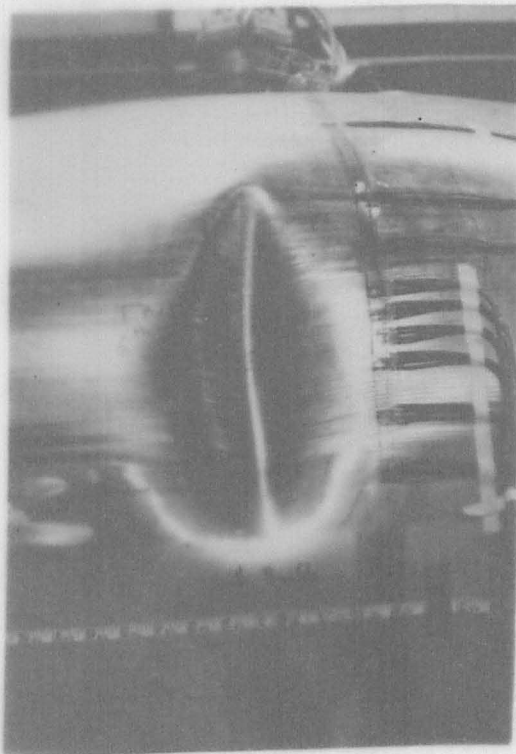


c) END No 13  
(1st Buckle)

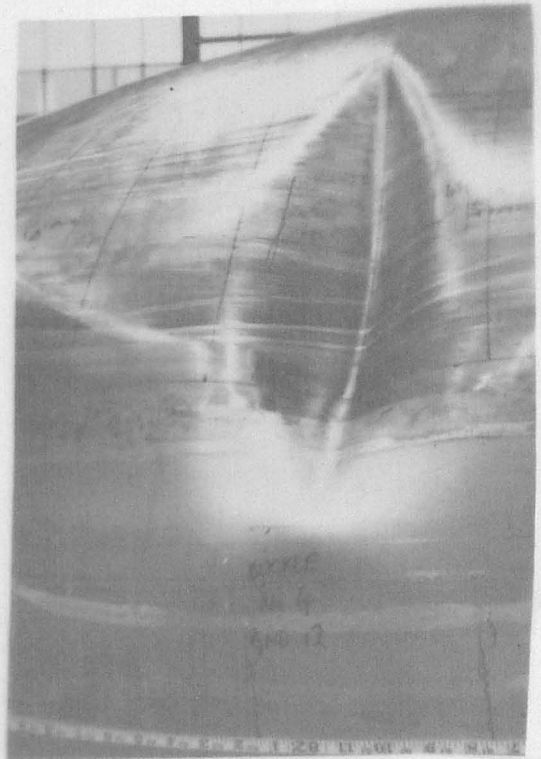


d) END No 13  
( 5th Buckle)

EXAMPLES OF BUCKLES PRODUCED



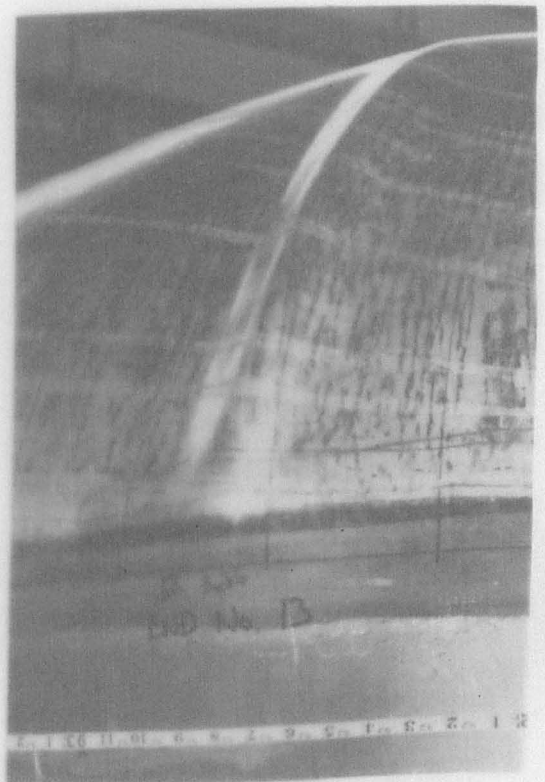
a) END No 11  
(4th Buckle)



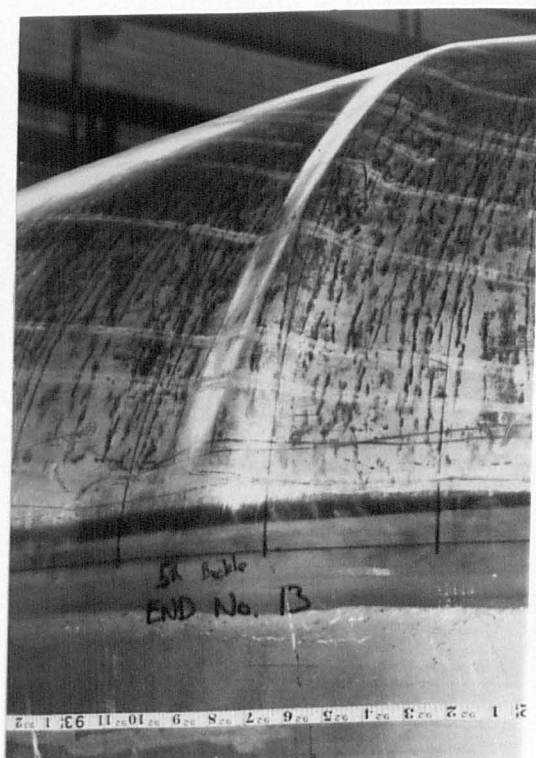
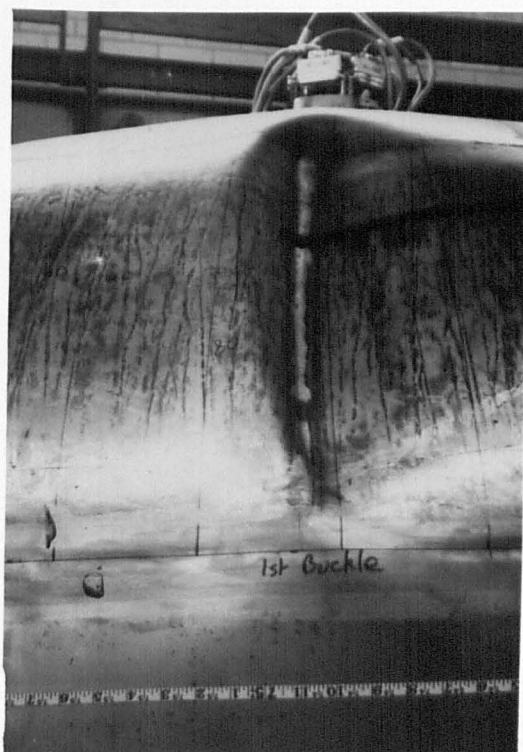
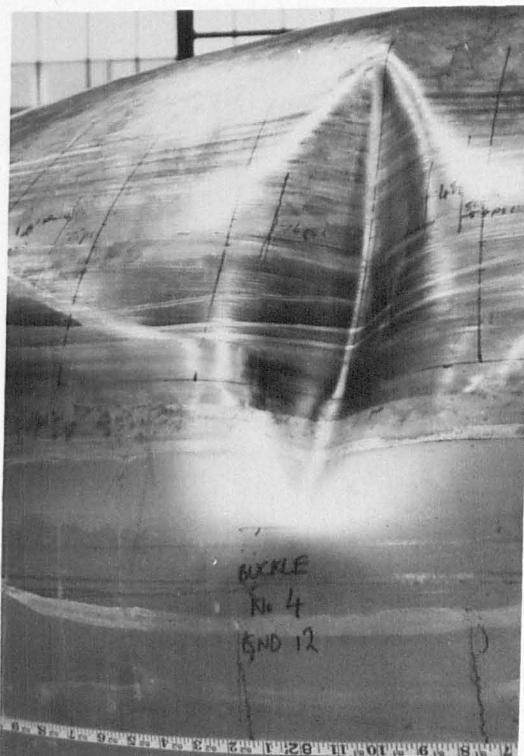
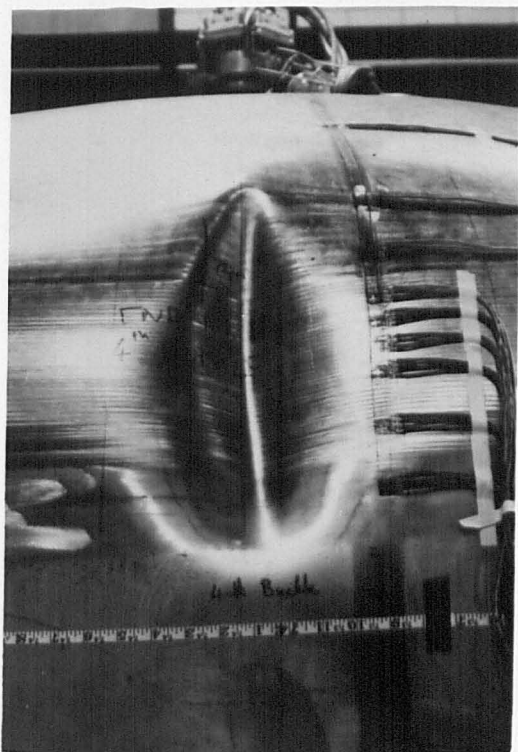
b) END No 12  
(4th Buckle)



c) END No 13  
(1st Buckle)



d) END No 13  
(5th Buckle)



EXAMPLES OF BUCKLES PRODUCED

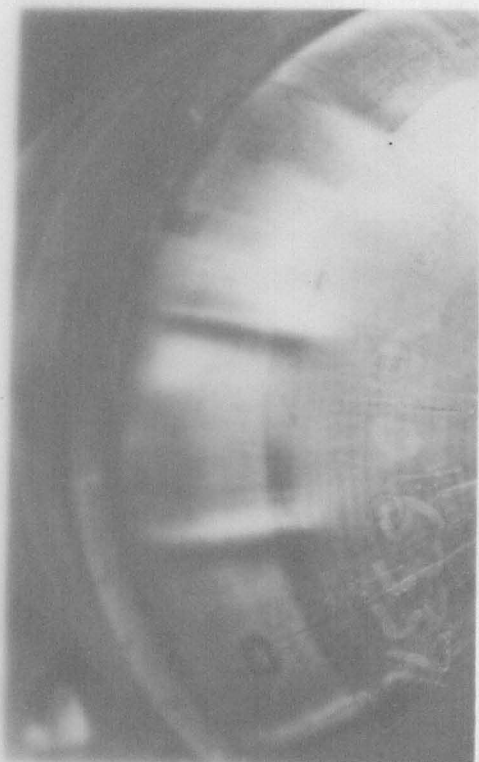
a) END No 14  
(3rd 5th 7th  
9th Buckles)

b) END No 15  
(4th Buckle)

c) END No 16  
(2nd Buckle)

d) END No 17  
(5th Buckle)

EXAMPLES OF BUCKLES PRODUCED



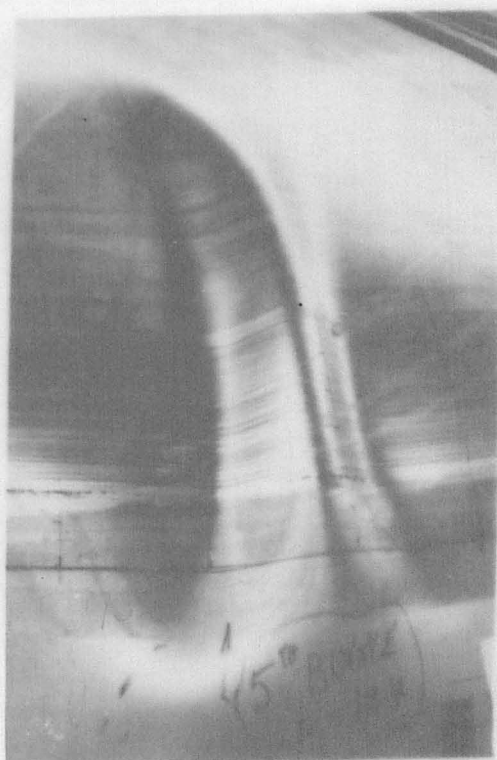
a) END No 14  
(3rd 5th 7th  
9th Buckles)



b) END No 15  
(4th Buckle)

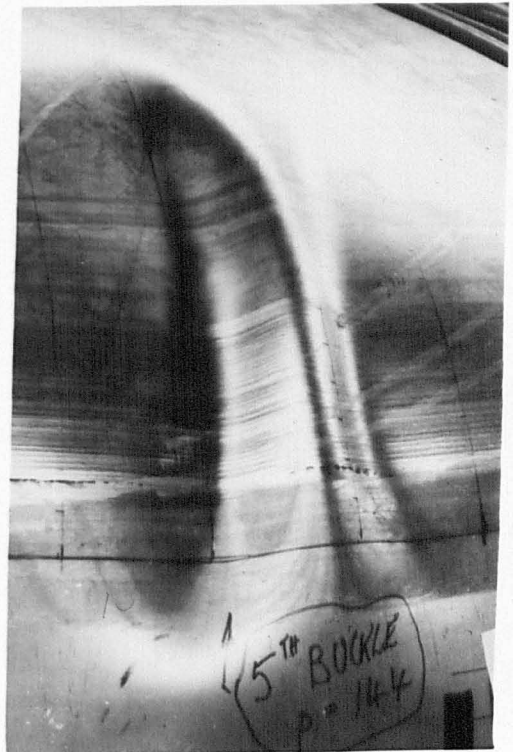
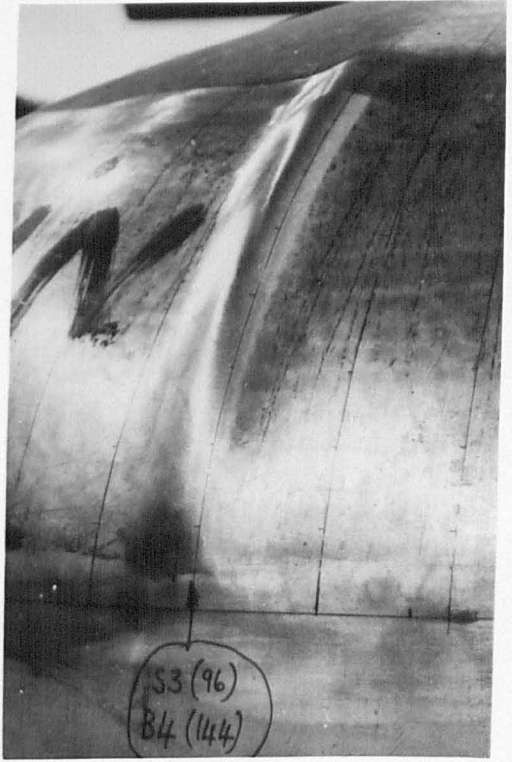


c) END No 16  
(2nd Buckle)



d) END No 17  
(5th Buckle)





## CHAPTER 8

### DISCUSSION

#### 8.1 Individual ends

The first part of this chapter deals with the behaviour of individual test ends and discusses in detail any anomalies or defects peculiar to a particular end. For each end a test history diagram is presented giving a clear and concise visual representation of the pressure loading applied.

##### 8.1.1 End No.1 ( $t_e/D_i = 0.00237$ , $r_i/D_i = 0.167$ , $R_i/D_i = 1.0$ )

The thickness distribution for this end (Fig. A1.1.1) is, in many respects, typical for the crown and segment method of manufacture. The thickness in the crown is reasonably uniform with a tendency for thickening to occur in the region of the knuckle/crown junction. The knuckle panels show slight thinning towards the centre. At the knuckle/cylinder junction the thickness drops abruptly due to the use of a thinner gauge material in the cylinder. The weld dressing at the crown/knuckle and knuckle/cylinder junction has resulted in some undercutting which is particularly severe at the latter position.

The curvature along a meridian (Fig. A1.1.2) deviates significantly from the nominal. In the crown the measured curvature oscillates about the nominal ( $0.0185 \text{ in}^{-1}$ ) with values ranging from  $0.01 \text{ in}^{-1}$  to  $0.031 \text{ in}^{-1}$ . A rapid increase in curvature is observed as the knuckle is approached. However at the knuckle/cylinder junction a sudden drop occurs due to the undercutting at the weld. There are some variations around the knuckle and a pronounced negative value occurs at the knuckle/cylinder junction. The curvature then rises to a fairly high value ( $0.031 \text{ in}^{-1}$ ) in the

cylinder but falls to nearly zero some 7 in into the cylinder. This indicates that the cylinder has been "drawn in" to fit a slightly smaller end thus producing a sizable positive curvature. The measured curvature depends, to an extent, on the gauge length of the measuring device, a long gauge length tending to "smooth out" real variations and a short one registering trivial detail. The possible error in curvature in the knuckle due to reading errors for the gauge used is indicated in the curvature figure for each end. The corresponding error in curvature in the crown is  $0.0004 \text{ in}^{-1}$  for this end. With these values a change of 2.2% could be detected in the crown curvature and 3.3% in the knuckle.

The maximum strain on the outer surface of the knuckle is circumferential and compressive (gauge 8, o, c, Fig. A1.1.3) and starts to become non-linear at a pressure of about  $70 \text{ lbf/in}^2$ . The cylinder hoop strain (gauge 17, o, c) is also shown to be non-linear at higher pressures. The strain gauges were monitored only during the test with end 4 and therefore no strains were obtained for pressures above  $172 \text{ lbf/in}^2$ .

The peak elastic hoop stress index on the outer surface of the knuckle was approximately -1.0 (Fig. A1.1.4). This low value is associated with the relatively large knuckle radius ratio ( $r_i/D_i = 0.167$ ). However the compressive stresses were sufficiently high to cause the end to eventually fail by buckling at a pressure of  $280 \text{ lbf/in}^2$  (Table 7.4). The meridional stress indices clearly illustrate the tendency of the knuckle to "open" under internal pressure. Bending stresses exist towards each end of the knuckle producing minimum peak stress values on the outer surface in these regions. No strain gauges were attached to the interior of this end. It was used as a base for testing each 54 in diameter end.

The four buckles produced (Table 7.4) occurred silently at a pressure of  $280 \text{ lbf/in}^2$  during the test with end 5. The buckles took the form of outward bulges elongated in the meridional direction. A typical buckle

was 10 in long, 3.5 in wide and about 0.25 in high. These rather shallow buckles occurred after the onset of large deformations in both the end and cylinder. The shape and thickness used for this end are clearly approaching the limits at which buckling will occur. Further details about the buckles are given in Table 7.4. A photograph of a typical buckle is shown in Fig. 7.34a.

Details of the test history are explained in Fig. 8.1a.

#### 8.1.2 End No.2 ( $t_e/D_i = 0.00237$ , $r_i/D_i = 0.167$ , $R_i/D_i = 1.0$ )

This end was nominally identical to the previous end (including cylinder details) thus allowing a direct comparison to be made.

The thickness distribution (Fig. A1.2.1) is generally similar to that obtained for end 1. Undercutting is again evident at both the knuckle/crown and knuckle/cylinder welds.

The wide variations in curvature are shown in Fig. A1.2.2. The curvature variations in the end however are considerably greater than in end 1. In the crown the curvature approaches zero at one point indicating a flat area on the end. The relatively high curvature immediately before the knuckle/cylinder junction is notable. A negative value again occurs at this junction due to undercutting at the weld. The curvature in the cylinder adjacent to the weld is low suggesting that the diameters of the cylinder and end are close.

Fig. A1.2.3 shows the variation in strain with pressure for individual strain gauges. Maximum hoop knuckle strains on both the inner and outer surfaces are compressive (gauges 10, o,c, and 9, i,c,), the latter being larger throughout the pressure range for the meridian shown. However above about  $120 \text{ lbf/in}^2$  both hoop strains are exceeded by the peak outer surface meridional strain. (It is important to note at this point that the knuckle region develops into a series of flats or bulges

around its circumference at a pressure far below the first buckling pressure. As a result the strain readings around the vessel vary depending on where the strain gauges are situated circumferentially). The figure also shows that at about  $182 \text{ lbf/in}^2$  the cylinder has developed a permanent hoop strain of 0.1% (gauge 20, i,c). This feature is also clearly illustrated in Fig. A1.2.4 where very large cylinder hoop strains are shown to exist at  $218 \text{ lbf/in}^2$  pressure. The effect of these large deformations in the cylinder on buckling is complex. The increase in diameter at the knuckle/cylinder junction will tend to relieve the compressive hoop strains in the knuckle thus increasing the critical pressure. However the rotation of the knuckle at the junction may well have the effect of facilitating the development of buckles. Appreciable cold creep effects were first noticed at a pressure of  $100 \text{ lbf/in}^2$ .

The distribution of elastic stress indices (Fig. A1.2.5) shows the high compressive hoop knuckle stresses occurring on both surfaces of the knuckle. The peak outer surface hoop stress, the maximum occurring, has an index value of -1.21, the corresponding value on end 1 being -1.0. Towards the knuckle/cylinder junction a second, but lower peak value occurs for the outer surface hoop stress distribution. This did not occur on end 1 but the existence of a saddle point is indicated at the same position (Fig. A1.1.4). The opening of the knuckle under internal pressure is shown by the meridional stress distribution. Again large bending stresses exist in the knuckle at the junctions with the crown and cylinder. The high meridional stress value on the inner surface of the crown must be attributed to the significant changes in curvature (Fig. A1.2.2) in the crown.

The test history of this end is shown in Fig. 8.1b. A partial buckle, formed at a pressure of  $278 \text{ lbf/in}^2$ , did not develop any further although a pressure of nearly  $300 \text{ lbf/in}^2$  was applied. The buckle was

about 8 in long, 3.5 in wide and 0.1 in high and took the form of an outward bulge. About ten other less prominent bulges were also present spaced around the circumference of the knuckle. As four far more prominent buckles were present on the nominally identical base end, end 2 was reloaded three more times up to the maximum test pressure after the end of the increasing pressure testing. (The base end had experienced about 5 pressure cycles of increasing magnitude during tests with the other ends). However no further buckle development occurred. A photograph of the buckle is shown in Fig. 7.34b.

### 8.1.3 End No.3 ( $t_e/D_i = 0.00237$ , $r_i/D_i = 0.111$ , $R_i/D_i = 1.0$ )

The thickness variation along a meridian (Fig. A1.3.1) is typical of the thinning which occurs with the pressed and spun method of manufacture. The crown thickness is reasonably uniform. There is a rapid decrease in thickness throughout the knuckle starting at the junction with the crown. The spinning/rolling process produces a series of distinct circumferential grooves on the exterior surface of the knuckle. On this vessel the grooving is severe resulting in the oscillatory nature of the thickness variation over most of the knuckle. Again there is a distinct indication of undercutting in the region of the knuckle/cylinder weld.

Around the pole the curvature variation in the crown (Fig. A1.3.2) is similar to that for a crown and segment end, oscillating about the nominal value. There is however a significant increase in curvature as the knuckle/crown junction is approached. In this region the curvature becomes negative (i.e. the centre of curvature is outside the vessel). This is a common feature on pressed and spun ends and is clearly visible on some ends. The knuckle curvature reaches maximum values near the junctions with the crown and cylinder. The minimum curvature occurring towards the centre of the knuckle is also frequently found in this type

of end. There is a rapid decrease in curvature towards zero near the cylinder indicating little mismatch in diameters between the end and cylinder.

The plot of individual strains with pressure (Fig. A1.3.3) shows clearly the high level of hoop strain on both surfaces of the knuckle (gauges 9, o,c and 9, i,c). However the maximum strain throughout the pressure test is the meridional strain on the inner surface (gauge 9, i,m). The compressive outer surface meridional strain illustrated (gauge 8, o,m) reaches a maximum strain of  $-0.055\%$  at a pressure of  $140 \text{ lbf/in}^2$ , and thereafter decreases steadily. This behaviour is due to the changing shape of the knuckle. As a result of the reduction in curvature of the knuckle the compressive bending strains increase less rapidly than the direct meridional strains, which are tensile, and these become dominant at higher pressures. The cylinder strain graph (gauge 21, o,c) indicates a  $0.1\%$  proof pressure of about  $170 \text{ lbf/in}^2$ . This feature is also clearly shown in the post yield strain distribution (Fig. A1.3.4). Appreciable cold creep effects first occurred at  $100 \text{ lbf/in}^2$ .

The elastic stress distribution illustrated in Fig. A1.3.5 shows the maximum stress to be the circumferential compression on the outer surface of the knuckle ( $I = -3.05$ ). This feature is in sharp contrast with the stress distribution in thicker ends in which the maximum stress is characteristically the meridional stress on the inner surface of the knuckle. This feature is an important pointer to the possibility of buckling in the end (ref. 6). The hoop stress distribution in the knuckle is characterised by a high compressive mean stress with a relatively small bending stress; the sign of the moment being consistent with the tendency of the knuckle to buckle inwards. In comparison the meridional stress distribution in the knuckle has a high bending component with a small mean stress. The inner surface meridional stress has maximum values

at each end of the knuckle. As the knuckle opens under internal pressure large bending stresses occur in these regions. Corresponding minimum values are present on the outer surface. This twin peak effect is common on ends with relatively "long" knuckles.

The test history is shown in Fig. 8.2a. The single buckle produced occurred after approximately 30 min at  $248 \text{ lbf/in}^2$  (Fig. 7.34c). It consisted of a clearly visible inward "dent" elongated in the meridional direction. The occurrence of the buckle was instantaneous. The buckle was approximately 10.5 in long, 3.5 in wide and 1 in deep. It traversed the arc of the knuckle and extended into the crown and cylinder. Considerable distortions were visible in the area surrounding the buckle and although the buckle occurred inwards the net change in volume of the vessel was an increase (indicated by a sudden drop in pressure). Close examination failed to reveal any incipient buckles in the knuckle.

#### 8.1.4 End No.4 ( $t_e/D_i = 0.00237$ , $r_i/D_i = 0.074$ , $R_i/D_i = 1.0$ )

The knuckle region of this end shows the appreciable thinning associated with the pressed and spun method of manufacture (Fig. A1.4.1). A reduction in thickness of about 25% occurs. However the grooving on the exterior of this end was far less pronounced than for end 3 and therefore the thickness decreased steadily throughout the knuckle. Undercutting is again present at the knuckle/cylinder junction.

The curvature variations in the crown are generally similar to those for end 3 (Fig. A1.4.2). However the knuckle variations are less pronounced, and there is a significant negative value at the knuckle/cylinder junction. The negative curvature in the crown near the knuckle is again present together with the minimum curvature towards the centre of the knuckle. The curvatures at the points measured are distributed fairly evenly about the nominal values.



The pressure - strain curves (Fig. A1.4.3) again show the presence of high compressive hoop strains in the knuckle. The peak outer surface hoop strain (gauge 10, o,c) exceeds that on the inner surface (gauge 12, i,c) throughout the pressure range recorded. However the maximum strain is the meridional strain on the inner surface (gauge 10, i,m). The behaviour of the outer surface meridional strain (gauge 9, o,m) is similar to that for end 3. The maximum strain of  $-0.14\%$  is reached at a pressure of  $118 \text{ lbf/in}^2$ . The strain then decreases until zero is reached at about  $180 \text{ lbf/in}^2$ . Other strain plots show similar non-linear effects. Shape changes are again responsible for this behaviour.

The strain distribution,  $26 \text{ lbf/in}^2$  below the buckling pressure, is shown in Fig. A1.4.4. The outer surface meridional strain has developed a double peak in the lower half of the knuckle, the feature evolving from a "saddle point" at lower pressures. The inner surface hoop strains have formed an unusual distribution at this pressure. This may well be due to the formation of "flats" on the end. The distribution is consistent with with tendency of the knuckle to move inwards. It is interesting to note that the first buckle occurred on a meridian ( $97^\circ$ ) close to these gauges.

The maximum peak stress index (Fig. A1.4.5) is  $-5.0$  and occurs in the hoop direction on the outer surface of the knuckle. This high value is clearly associated with the small knuckle radius and large crown radius. The corresponding value for end 3, an end with a larger knuckle radius, was  $-3.0$ . Only one maximum value occurs in the meridional distribution in the knuckle.

The three buckles produced occurred at  $198 \text{ lbf/in}^2$  over a period of 1.5 min (Table 7.4). The buckles occurred instantaneously and created a considerable amount of noise during their formation. A photograph of the first buckle is shown in Fig. 7.35a. The buckles were generally similar to that described for end 3, in terms of type and dimensions. The end was

the first to be tested and no attempt was made to increase the pressure beyond that at which the three buckles occurred.

The test history is shown in Fig. 8.2b.

8.1.5 End No. 5 ( $t_e/D_i = 0.00237$ ,  $r_i/D_i = 0.074$ ,  $R_i/D_i = 0.833$ )

The thickness distribution, Fig. A1.5.1, again contains all the features of a pressed and spun end. However a thickness variation of 0.006 in is present in the crown. This is larger than previously observed. The grooves on the exterior of the knuckle appear to cause an increase in thickness near the junction with the cylinder. Undercutting is again present at the weld.

The curvature variation in the crown (Fig. A1.5.2) is similar to those for ends 3 and 4. The knuckle curvature only attains the nominal value at the two junctions and the minimum value, which occurs at the centre of the knuckle is only half of the nominal value. A "flat" region was clearly visible on the knuckle. This defect has produced an end which is appreciably different from the nominal near the most highly stressed region, and can be expected to have a significant effect on the test results obtained. The most likely effect is to reduce the peak stress and strain values occurring due to the effectively larger knuckle radius. Positive curvatures in the cylinder, adjacent to the end, indicate that the former has been "drawn in" to accommodate a slightly smaller diameter end.

The pressure-strain curves for individual strain gauges (Fig. A1.5.3) shows many of the features already described for other ends. However in contrast to earlier ends the inner surface hoop strain (gauge 8, i,c) exceeds that occurring on the outer surface (gauge 8, o,c) throughout the pressure range. The maximum strain on the meridian is again the inner surface meridional strain (gauge 8, i,m). A 0.1% permanent hoop strain occurs in the cylinder (see gauge 20, i,c) at a pressure of about 180 lbf/in<sup>2</sup>.

The yielding of the cylinder is also clearly illustrated in the strain distribution graph (Fig. Al.5.4).

The peak elastic stress (Fig. Al.5.5) is the outer surface circumferential stress. The index is -3.16 and the peak occurs in the knuckle near the junction with the crown. The corresponding value for end 4 was -5.0. The effect of reducing the crown radius whilst holding the knuckle radius constant is to reduce the peak elastic stress index. The short knuckle arc of this end has produced large meridional bending stresses in the knuckle.

The single buckle produced was similar in nature to those on ends 1 and 2. The buckle, which formed gradually and silently, appeared as an outward bulge. It was about 7 in long, 3 in wide and 1 in deep. A photograph of the buckle is shown in Fig. 7.35b.

The test history is illustrated in Fig. 8.3a.

#### 8.1.6 End No.6 ( $t_e/D_i = 0.00237$ , $r_i/D_i = 0.074$ , $R_i/D_i = 0.778$ )

This end differed from end 5 in having a smaller nominal crown radius.

The thickness distribution (Fig. Al.6.1) is similar to that for end 5. A thickness variation of 0.009 in was present along the crown portion of the meridian plotted.

The curvature distribution (Fig. Al.6.2) shows the knuckle to be much better formed than that of end 5. There is no negative curvature in the crown near the knuckle/crown junction.

It is interesting to note (Fig. Al.6.3) that the outer surface hoop strain (gauge 10, o,c) exceeds that on the inner surface (gauge 10, i,c). Effects due to geometric changes are again apparent; some of the gauge readings at the higher pressures are affected by the occurrence of buckles near to the gauges.

The peak stress indices (Fig. A1.6.5) are in the main greater than those on end 5 in spite of the nominally smaller crown radius. This peculiarity can only be explained by assuming that the "flat" region observed in the knuckle of end 5 has had a considerable effect on the stress levels occurring in that end. The maximum peak stress in end 6 is again the outer surface hoop stress (Fig. A1.6.5). It has a value of -3.84.

The five buckles formed were similar in every respect to the buckle on end 5. A photograph of the second and fifth buckles is shown in Fig. 7.35c.

The test history is illustrated in Fig. 8.3b.

#### 8.1.7 End No.7 ( $t_e/D_i = 0.00119$ , $r_i/D_i = 0.167$ , $R_i/D_i = 1.0$ )

This end was used as a base for the other 108 in diameter ends. A support ring made from mild steel channel was welded to the cylinder approximately 0.5 in from the knuckle/cylinder weld (Fig. 4.2). The end was therefore effectively built-in at this point and this fact must be borne in mind when considering the results for this end.

The thickness distribution for two meridians are shown in Fig. A1.7.1. The  $0^\circ$  meridian corresponds to a diametrical weld in the crown and the dressing has resulted in rather low thickness values. Although varying in detail the two curves confirm that little thinning occurs in the knuckle of a crown and segment constructed end. Some undercutting is evident at the knuckle/crown junction of the  $0^\circ$  meridian.

The curvature distribution (Fig. A1.7.2) shows many of the features described for the smaller ends (ends 1 and 2). Considerable deviations from the nominal occur in both the crown and knuckle. However the negative curvature observed near the knuckle/crown junction did not occur in the small crown and segment ends. Possible measuring errors in curvature were 3.6% of the nominal value in the knuckle and 2% of the nominal value in the crown.

Gauges were applied only on the outer surface of the knuckle of this end, along a meridional weld (angular reference  $223^{\circ}$ ) and along a meridian through the centre of a knuckle segment (angular reference  $269^{\circ}$ ). They were only monitored during the first pressurisation of the end (i.e. test with end 9).

The pressure-strain curves for the maximum reading circumferential and meridional gauges on the two meridians are shown in Fig. Al.7.3. For pressure levels below that for the first buckle ( $60 \text{ lbf/in}^2$ ) strains on the welded meridian ( $233^{\circ}$ ) exceeded corresponding strains midway along a knuckle segment ( $269^{\circ}$ ). It is notable that the outer surface meridional strains are positive. The effect of buckling on these strains is clearly shown. The second buckle occurred at  $60 \text{ lbf/in}^2$  on the  $240^{\circ}$  meridian. The reductions in circumferential and meridional strains on the  $233^{\circ}$  meridian are a direct result of this buckle. The steps at 68, 72 and  $80 \text{ lbf/in}^2$  are also associated with buckles. The strain distribution along the two gauged meridians  $4 \text{ lbf/in}^2$  below the first buckling pressure is shown in Fig. Al.7.4. The strain distributions for each meridian are similar. The strains on the  $233^{\circ}$  meridian are influenced at this pressure by prebuckling "flats" or "bulges".

The elastic stress index distribution along the gauged meridians are shown in Fig. Al.7.5. The peak outer surface hoop stress indices are -1.83 and -2.70 on the  $269^{\circ}$  and  $233^{\circ}$  meridians respectively. The gauges were some  $5\frac{1}{4}$  inches apart and the peak strain may have been "missed"; nevertheless these differences are considerable. The values may have been influenced by the support ring. However comparisons with end 13, a nominally identical end without a support ring, does not suggest any appreciable effect.

The first buckles occurred at a pressure of  $60 \text{ lbf/in}^2$ , considerably lower than that anticipated (see section 8.1.13). The nine buckles produced on this end occurred silently and took the form of outward bulges

elongated in the meridional direction (Fig. 7.36a). A typical buckle was 22 in long, 4 in wide and 1 in high. The position of each buckle and other details are given in Table 7.4. The test history described in Fig. 8.4a is of course a combination of those for the other 108 in diameter ends.

8.1.8 End No. 8 ( $t_e/D_i = 0.00119$ ,  $r_i/D_i = 0.111$ ,  $R_i/D_i = 1.0$ )

This spun end has the same nominal shape parameters as end 3 but half the thickness to diameter ratio.

The thickness distribution (Fig. A1.8.1) is similar to that described for the smaller spun ends. There is a steady reduction in thickness throughout the knuckle until a minimum thickness of 0.080 in is reached at the knuckle/cylinder junction. This low value is a result of serious undercutting at the weld. Careful inspection revealed that the end was poorly formed. The end had apparently been manufactured slightly oversize and consequently considerable distortions had formed in the region of the knuckle when the end had been welded to the cylinder. The distortions took the form of a series of shallow ripples over a 3 ft. segment of the knuckle, one ripple being particularly pronounced (Approximate depth of the order 0.05 in). The first buckle occurred at this position as a direct consequence of the initial distortion.

The knuckle curvatures vary considerably from the nominal (Fig. A1.8.2). These variations may be associated with the distortions in the knuckle described previously. Negative curvatures are again present in the crown near the junction with the knuckle.

The peak strain in this end is the maximum compressive circumferential strain on the outer surface of the knuckle (gauge 10, o,c,  $0^\circ$  meridian; gauge 9, o,c,  $90^\circ$  meridian) (see Figs. A1.8.3 and A1.8.4). This is at variance with the corresponding 54 in diameter end (end 3) where the maximum strain was the tensile meridional strain on the inner surface.

The end buckled at approximately one third the buckling pressure of end 3. Again non-linearities and discontinuities are apparent in these strain plots.

The strain distributions  $4 \text{ lbf/in}^2$  below the first buckling pressure are shown for the  $0^\circ$  and  $90^\circ$  meridians in Figs. A1.8.5 and A1.8.6. The  $0^\circ$  meridian is coincident with the diametrical weld. The outer surface hoop distribution has a double peak on the  $90^\circ$  meridian. The coarser gauge coverage on the  $0^\circ$  meridian revealed only one peak, but a saddle point is clearly present. There is a minor peak in the inner surface circumferential strain along the  $0^\circ$  meridian. The reading at this position is from gauge 9, i,c in Fig. A1.8.3. The plot for this gauge is conspicuously non-linear and it is considered probable that the minor peak was caused by a local manufacturing distortion along the weld. The meridional strains along the two meridians differ significantly.

The elastic stress index distributions for the  $0^\circ$  and  $90^\circ$  meridians are shown in Figs A1.8.7 and A1.8.8. The largest stress index, on both meridians, is the outer surface circumferential value. Values of -3.8 and -2.8 are present on the  $0^\circ$  and  $90^\circ$  meridians respectively. The outer surface hoop stress distributions have double peaks. In general the peak stress indices are higher on the weld. The meridional distributions have peak values near the knuckle/crown and knuckle/cylinder junctions.

The first buckle was produced in the region of manufacturing distortion previously described. At  $66 \text{ lbf/in}^2$  a small "buckle" occurred in the knuckle near the junction with the cylinder at the position of the most severe "ripple". This was followed, at  $70 \text{ lbf/in}^2$ , by the first full buckle (in the same position). A photograph of this buckle is shown in Fig. 7.36b. The folding of the knuckle material during buckling caused a leak at the knuckle/cylinder weld adjacent to the buckle. The leak became worse as the test proceeded and eventually had to be repaired. It is doubtful if the first buckle would have occurred at  $70 \text{ lbf/in}^2$  in the

absence of the manufacturing distortion.

Four additional buckles were produced as the pressure was increased to 94 lbf/in<sup>2</sup>. The buckles occurred suddenly and created considerable noise and vibration. The buckles were inward buckles, similar to those obtained on ends 3 and 4. A typical buckle was 22 in long, 8 in wide and just over 2 in deep. It traversed the knuckle arc (arc length 13.5 in) and extended into the crown and cylinder.

The test history is shown in Fig. 8.4b.

#### 8.1.9 End No. 9 ( $t_e/D_i = 0.00119$ , $r_i/D_i = 0.074$ , $R_i/D_i = 1.0$ )

The more extensive set of graphs for this end are presented in Chapter 7. The thickness distribution along the 90° meridian, shown in Fig. 7.1, again illustrates the thinning which occurs during manufacture. However the thinning in the knuckle is less severe than that on earlier spun ends (e.g. Fig. A1.8.1). The secondary peak thickness midway through the knuckle is not unique to this end (see Fig. A1.3.1). Considerable undercutting has occurred at the knuckle/cylinder weld.

The curvature distributions on the 45° and 180° meridians, shown in Figs. 7.2 and 7.3 respectively, are generally similar to those previously described for other ends. Both meridians have a region of negative curvature in the crown near the junction with the knuckle and the 180° meridian (coincident with a diametrical weld) shows negative curvatures in the cylinder.

Figs. 7.4, 7.5 and 7.6 show pressure-strain plots for individual strain gauges on the three gauged meridians. On the 0° meridian the outer surface hoop strain, the maximum strain, increases throughout the pressure range (gauge 11, o,c). The corresponding inner surface strain (gauge 10, i,c) reaches a maximum value of -0.25% at 50 lbf/in<sup>2</sup> and then decreases at higher pressures. The behaviour of these two gauges is clearly consistent with the tendency of the knuckle to move inwards at the



position under consideration. The fold line of the first buckle was coincident with the  $0^\circ$  meridian and occurred at  $62 \text{ lbf/in}^2$ . For the  $90^\circ$  meridian the inner surface hoop strain (gauge 10, i,c) exceeds that on the outer surface (gauge 10, o,c). The maximum inner surface meridional strain (gauge 8,i,m) is greater on this meridian than the other gauged meridians. Corresponding strain values vary considerably around the circumference of the knuckle at the higher pressures. The strain changes on the  $90^\circ$  meridian at  $70 \text{ lbf/in}^2$  were caused by the third buckle. The second buckle occurred about 1.5 in from the  $180^\circ$  meridian at  $66 \text{ lbf/in}^2$  (Fig. 7.6). As the buckle formed the outer surface hoop strain (gauge 11, o,c) became tensile and the corresponding inner surface strain (gauge 10, i,c) more compressive.

Strain distributions on the  $0^\circ$ ,  $90^\circ$  and  $180^\circ$  meridians at pressure levels throughout the test are shown in Figs. 7.7 to 7.21. At  $10 \text{ lbf/in}^2$  and  $18 \text{ lbf/in}^2$  the material acts elastically and it can be seen that the distributions on the three meridians are generally similar although the peak hoop strains are higher on the welds ( $0^\circ$  and  $180^\circ$  meridians) than on the  $90^\circ$  meridian. As the pressure is increased the correspondence of the strain distributions for the various meridians deteriorates to a degree depending on the position of the meridian relative to a potential buckle (see for example Figs. 7.16, 7.17 and 7.18).

The elastic stress index distributions for each gauged meridian at pressures of  $10 \text{ lbf/in}^2$  and  $18 \text{ lbf/in}^2$  are shown in Figs. 7.22 to 7.24 and 7.25 to 7.27 respectively. The peak hoop stress indices on the welds exceed those away from welds. The maximum stress index on all meridians is the outer surface circumferential, the value at  $18 \text{ lbf/in}^2$  on the  $0^\circ$  meridian being  $-5.8$  (Fig. 7.25) and on the  $90^\circ$  meridian  $-4.2$ . (The corresponding value for end 4 (same nominal shape parameters,  $t_e/D_i = 0.00237$ ) was  $-5.0$ ). The peak tensile outer surface meridional stress occurring in the crown is of the same magnitude as the tensile inner

surface meridional stress in the knuckle.

The strain around the knuckle just prior to the first buckle is shown in Fig. 7.28. (Strain gauges were positioned in the knuckle 2.5 in from the knuckle/cylinder junction.) The first buckle occurred on the  $0^\circ$  meridian. It can be seen that the high strain values occurring on the future buckle fall rapidly over a small distance (about 1.5 in).

Figs. 7.29, 7.30 and 7.31 show the amount of cold creep recorded by three strain gauges at three pressure levels. Clearly creep increases rapidly with increasing pressure. Creep effects were first noticed at a pressure of  $34 \text{ lbf/in}^2$ .

The increase in pole deflection with pressure was practically linear up to the first buckling pressure (Fig. 7.32). The cylinder strains at four distances from the knuckle/cylinder junction are shown in Fig. 7.33. Near the junction, the cylinder strains are reduced by the influence of the end closure. The steel bands and support ring cause a reduction in strain at the lower end of the cylinder.

The six buckles produced occurred over a pressure range of 62 to  $78 \text{ lbf/in}^2$  and were similar to those on end 8. A typical buckle was 18 in long, 7 in wide and 2.2 in deep. The first two buckles were coincident with the diametrical weld. A post test inspection revealed the presence of a crack on the fold line of the buckle on the inner surface. The crack, about 1.5 in long, did not result in a leak. A photograph of the third buckle is shown in Fig. 7.36c.

The test history is illustrated in Fig. 8.5a.

8.1.10 End No.10 ( $t_e/D_i = 0.00119$ ,  $r_i/D_i = 0.074$ ,  $R_i/D_i = 0.833$ )

The thickness distribution along the  $90^\circ$  meridian is shown in Fig. A1.10.1. The crown thickness of 0.133 in is reduced by forming to 0.117 in in the knuckle, with a further severe reduction to 0.095 in

at the knuckle/cylinder junction due to weld dressing.

The curvature distribution (Fig. A1.10.2) is similar to those obtained for other spun ends. A region of negative curvature is present near the pole, a manufacturing distortion not previously observed.

On the  $180^\circ$  meridian the hoop strains on both surfaces of the knuckle are virtually identical up to a pressure of  $45 \text{ lbf/in}^2$  (Fig. A1.10.3). Above this pressure the outer surface hoop strain (gauge 9, o,c) increases more rapidly than the inner surface strain (gauge 11, i,c). The latter reaches a maximum value of  $-0.35\%$  at  $70 \text{ lbf/in}^2$  before starting to decrease with increasing pressure. The readings are clearly affected by a buckle, the third, at  $82 \text{ lbf/in}^2$ . The buckle was coincident with the gauged meridian. On the  $90^\circ$  meridian (Fig. A1.10.4) the readings are affected by the second buckle which occurred on the  $96^\circ$  meridian at  $78 \text{ lbf/in}^2$ . Up to that pressure the maximum reading strain gauge on the meridian is the outer surface hoop gauge (gauge 10, o,c). The tensile inner surface meridional strain (gauge 7, i,m), although smaller in magnitude, is less affected by the buckle. As the material folds inwards at the buckle the knuckle hoop stresses at the edge of the buckle become tensile and compressive on the outer and inner surfaces respectively.

The high level of compressive hoop strain present in the knuckle prior to buckling is clearly evident in the strain distribution graphs (Fig. A1.10.5 and A1.10.6). At this pressure ( $70 \text{ lbf/in}^2$ ) the cylinder is still well below its yield pressure of about  $90 \text{ lbf/in}^2$ .

The peak stress indices on the  $180^\circ$  and  $90^\circ$  meridians are  $-4.2$  and  $-4.1$  respectively, both for hoop stresses on the outer surface. (The corresponding stress index on end 9, (with a larger crown radius and smaller end height) away from the weld, was  $-4.2$ .) The stress index distributions are shown in Fig. A1.10.7 and A1.10.8. The  $180^\circ$  meridian is on the diametrical weld. The principal features of the two distributions

match closely. The meridional distributions show the existence of double peak stresses.

The first buckle occurred at  $78 \text{ lbf/in}^2$ , compared with  $62 \text{ lbf/in}^2$  for end 9. Two buckles, the first and third, occurred on the diametrical weld. It is usual for at least one buckle, often one of the first to occur, to be coincident with a weld. Each buckle consisted of an inward fold, elongated in the meridional direction. They were similar to those described for end 8. A typical buckle was 18.5 in long, 6 in wide and 2.2 in deep. A photograph of the second buckle is shown in Fig. 7.36d.

The test history is illustrated in Fig. 8.5b.

8.1.11 End No.11 ( $t_e/D_i = 0.00119$ ,  $r_i/D_i = 0.074$ ,  $R_i/D_i = 0.722$ )

Considerable thinning has occurred in the knuckle during manufacture (Fig. A1.11.1). There is a marked increase in thickness in the crown (about 0.007 in) near the junction with the knuckle. The undercutting at the weld is not as prominent as on other ends.

The curvature distribution (Fig. A1.11.2) is again similar to those for previously described spun ends; no negative crown curvatures were recorded however. The end was well formed with no notable distortions.

The pressure-strain plots of individual strain gauges are shown in Figs. A1.11.3 and A1.11.4 for the  $180^\circ$  and  $90^\circ$  meridians respectively. On the  $180^\circ$  meridian (weld) the maximum strain throughout the test was the outer surface hoop strain (gauge 8, o,c). The compressive inner surface hoop strain (gauge 10, i,c) is greater in magnitude than the tensile inner surface meridional strain (gauge 8, i,m), the former reaching a maximum value of  $-0.43\%$  at  $90 \text{ lbf/in}^2$ . The fourth buckle occurred at  $94 \text{ lbf/in}^2$ , 4 in from the  $180^\circ$  meridian and damaged most of the nearby gauges. On the  $90^\circ$  meridian the inner surface hoop strain exceeds that on the outer surface and is slightly greater in magnitude than the inner

surface meridional strain up to  $78 \text{ lbf/in}^2$ . The "flats" or "ripples" produced on an end prior to buckling have an appreciable effect on the strain readings; the strain gauges on the  $90^\circ$  meridian were situated near the crest of a "ripple". The second buckle, which occurred at  $90 \text{ lbf/in}^2$ , 21 in from the  $90^\circ$  meridian, caused the hoop strains to decrease by over 0.04% strain.

The strain distributions at  $82 \text{ lbf/in}^2$  are shown in Figs. Al.11.5 and Al.11.6. The difference in strain levels on the two meridians is clearly illustrated.

The maximum peak hoop stress index on the  $90^\circ$  meridian (Fig. Al.11.8) is -3.5. This compares with -4.1 and -4.2 for ends 10 and 9 respectively. The effect of reducing the crown radius is a decrease in peak stress index and an increase in first buckling pressure. On the  $180^\circ$  meridian (Fig. Al.11.7) the outer surface hoop stress index is -4.1. Stress index values on the weld tend to be higher than those situated elsewhere on the vessel. The meridional stress distributions show clearly the considerable amount of meridional bending in the knuckle.

The first buckle occurred at a pressure of  $86 \text{ lbf/in}^2$ . In all six buckles were produced as the pressure was increased to  $98 \text{ lbf/in}^2$ . A photograph of the fourth buckle is shown in Fig. 7.37a. Each buckle was similar to those on end 8. A typical buckle was 16 in long, 5.1 in wide and 2 in deep.

The test history is illustrated in Fig. 8.6a.

#### 8.1.12 End No.12 ( $t_e/D_i = 0.00119$ , $r_i/D_i = 0.056$ , $R_i/D_i = 1.0$ )

The thickness distribution is typical of a pressed and spun end (Fig. A.12.1). The minimum thickness measured in the knuckle, excluding the undercutting at the weld, was 0.112 in. The thinning due to rolling is less severe than on most of the other spun ends. The crown is over 0.004 in thicker near the knuckle than elsewhere.

The curvature distribution (Fig. A1.12.2) contains most of the features already described. The region of negative curvature in the crown near the pole could be clearly seen. Distortion had occurred during manufacture. The most notable feature is that the knuckle curvature is considerably less than the nominal. The end, with a nominal knuckle radius of 6 in, had a  $r/D$  ratio of 0.056 which is just below the minimum allowed by some of the codes. The actual knuckle radius was about 8 in.

The variations of individual strains with pressure are shown in Figs. A1.12.3 and A1.12.4 for the  $0^\circ$  and  $90^\circ$  meridians respectively. On the  $0^\circ$  meridian (the diametrical weld in the end) the peak hoop strains on both surfaces of the knuckle are similar in magnitude up to the occurrence, on the  $2^\circ$  meridian at  $70 \text{ lbf/in}^2$ , of the third buckle. On the  $90^\circ$  meridian the two peak hoop strains are coincident up to about  $37 \text{ lbf/in}^2$ . Above this pressure however the inner surface hoop strain increases more rapidly until the occurrence of the second buckle at  $70 \text{ lbf/in}^2$  on the  $92^\circ$  meridian. The hoop gauge readings are clearly influenced by the proximity of the buckle.

The strain distributions  $4 \text{ lbf/in}^2$  below the first buckling pressure are shown in Figs. A1.12.5 and A1.12.6. A rapid increase in the inner surface hoop strain on the  $90^\circ$  meridian is clearly illustrated.

The maximum peak elastic stress index is again that occurring in the hoop direction on the outer surface (Figs. A1.12.7 and A1.12.8). Values of -5.5 and -4.7 were obtained on the  $0^\circ$  and  $90^\circ$  meridians respectively at a pressure of  $14 \text{ lbf/in}^2$ . (End 9, which had a nominally larger knuckle radius had a corresponding stress index value of -4.2 on the  $90^\circ$  meridian.) The tendency for peak stress values to be higher on the welds is evident again in this end. Only single maximum stress values are present on the meridional stress index distribution in the knuckle.

The first buckle occurred after 4 minutes at a pressure of 66 lbf/in<sup>2</sup>, a higher value than expected. This must be attributed to the unintentionally large knuckle radius. The buckles were similar to those produced on ends 8, 9 etc. They occurred instantaneously and created considerable noise and vibration. They were typically 18.5 in long, 6 in wide and 2.5 in deep. A photograph of a typical buckle, the fourth, is shown in Fig. 7.37b. The fifth buckle occurred on the 180° meridian and produced a crack about 0.25 in long which resulted in a leak from the vessel. This necessitated the termination of the test.

The test history is shown in Fig. 8.6b.

#### 8.1.13 End No. 13 ( $t_e/D_i = 0.00119$ , $r_i/D_i = 0.167$ , $R_i/D_i = 1.0$ )

This end, a crown and segment end with a knuckle radius of 18 in, was nominally identical in shape to end 7. However, whilst end 7 was built-in 0.5 in from the knuckle/cylinder junction, this vessel had a 4 ft length of cylinder welded to it.

The thickness distribution clearly reflects the method of manufacture, with negligible thinning occurring in the knuckle (Fig. A1.13.1). The crown is thickest near the junction with the knuckle. Slight undercutting is present on the knuckle/crown and knuckle/cylinder welds.

The curvature distribution (Fig. A1.13.2) illustrates the large variations occurring in both crown and knuckle. At one position a curvature of 0.094 in<sup>-1</sup> was measured in the knuckle, compared with a nominal value of a little over 0.055 in<sup>-1</sup>.

The pressure-strain graphs for corresponding strain gauges along the two gauged meridians (Figs. A1.13.3 and A1.13.4) show considerable differences. The 118° meridian was coincident with a weld between two knuckle panels whilst the 90° meridian was near the centre of a panel. At higher pressures (above 60 lbf/in<sup>2</sup>) the maximum outer surface hoop

strain exceeds that on the inner surface along the  $118^\circ$  meridian. As already mentioned the knuckle region of an end forms a series of "flats" or "ripples" long before the occurrence of the first buckle. The tensile inner surface meridional strain was slightly smaller in magnitude than the outer surface hoop strain throughout the test. The strain readings on the  $118^\circ$  meridian were affected by the occurrence, at  $94 \text{ lbf/in}^2$ , of the fourth buckle. On the  $90^\circ$  meridian (Fig. A1.13.4) the maximum hoop strain occurred on the inner surface (gauge 9, i,c). However the inner surface meridional strain (gauge 9, i,m) was of similar magnitude and was the maximum strain above  $78 \text{ lbf/in}^2$ . The  $90^\circ$  meridian was probably situated near the crest of a ripple. The strain readings on this meridian were also affected by the fourth buckle. Gauge 20, i,c, situated in the cylinder, shows the 0.1% proof pressure to be nearly  $90 \text{ lbf/in}^2$ .

The strain distributions for the  $118^\circ$  and  $90^\circ$  meridians, shown in Figs. A1.13.5 and A1.13.6, illustrate the differences in strain levels just prior to the first buckling pressure. On the  $118^\circ$  meridian the hoop distributions have double peaks on both surfaces. The corresponding curves for the  $90^\circ$  meridian have only single peaks but a saddle point is present on the outer surface distribution.

The maximum peak stress index on each meridian was the outer surface circumferential index (Figs A1.13.7 and A1.13.8). Values of -2.3 and -1.8 were observed on the  $118^\circ$  and  $90^\circ$  meridians respectively. (End 7, nominally identical in shape, had corresponding hoop stress indices of -2.7 and -1.8. This suggests that the effect of restraining the cylinder near the knuckle is negligible.) The meridional distributions have double peaks, a typical feature on an end with a long knuckle arc.

This end was unique in that two different types of buckle were produced. The first two were of the type observed on ends 3, 4 and 8 etc. although they created less noise (the first buckle is shown in Fig. 7.37c).



The two buckles formed instantaneously and took the form of inward dents elongated in the meridional direction. The remaining three buckles were similar to those formed on ends 1, 2, 5, 6 and 7, i.e. elongated outward bulges. A photograph of the fifth buckle is shown in Fig. 7.37d. Prior to the formation of these buckles the ripples, formed earlier in the test, became more distinct and took the form of slight bulges; at a particular pressure one of these bulges would become unstable and develop without noise into a full buckle over a period of a few seconds. These buckles consisted of outward bulges elongated in the meridional direction. It is thought that the outward type of buckle may in fact be two inward type buckles side by side, the bulge being the interface between the buckles. This end first buckled at  $82 \text{ lbf/in}^2$  compared with  $60 \text{ lbf/in}^2$  for the nominally identical end 7. The difference is a possible consequence of the hoop ring. It can be argued that the support ring, by preventing any growth or rotation at the rim of the end, increases the compressive hoop stresses in the knuckle thus lowering the buckling pressure. However the base for the 81 in diameter ends (end 14) did not buckle at a lower pressure than that for the similar end (end 15).

The test history for this end is illustrated in Fig. 8.7a.

8.1.14 End No.14 ( $t_e/D_i = 0.00158$ ,  $r_i/D_i = 0.167$ ,  $R_i/D_i = 1.0$ )

This end was used as a base for ends 15, 16 and 17. It was nominally identical to end 15 in shape and thickness but had a support ring welded to its cylinder 0.5 in from the knuckle/cylinder junction. The end was 81 in in diameter and was formed by the crown and segment method of manufacture.

Except for an unusually pronounced undercut of 0.020 in at the knuckle/cylinder weld, the thickness distribution (Fig. A1.14.1) is typical of that to be found in a crown and segment end.

The curvature irregularities (Fig. A1.14.2) were of a similar order to those found previously in ends of this type. No negative values were

recorded. A notable feature was the high peak in the knuckle curvature just inside the knuckle/crown junction - a similar peak was found in ends 13 and 15.

The pressure-strain graphs for the  $325^{\circ}$  and  $0^{\circ}$  meridians are shown in Figs. A1.14.3 and A1.14.4 respectively. (Note that these plots have different strain scales.) The  $325^{\circ}$  meridian was coincident with the weld between two knuckle panels whilst the  $0^{\circ}$  meridian was situated towards the centre of a panel. On the  $325^{\circ}$  meridian the inner surface hoop strain (gauge 8, i,c) was greater than the outer surface value (gauge 9, o,c). Above  $84 \text{ lbf/in}^2$  the inner surface hoop strain increased rapidly whilst that on the outer surface reached a maximum of  $-0.30\%$  at  $114 \text{ lbf/in}^2$ . The fourth buckle eventually occurred on the nearby  $336^{\circ}$  meridian at a pressure of  $138 \text{ lbf/in}^2$ . Up to  $102 \text{ lbf/in}^2$  the maximum strain on the meridian was the tensile inner surface meridional. The strain readings on this base end were only taken during the test with end 16 (first pressurisation) i.e. up to  $120 \text{ lbf/in}^2$ .

On the  $0^{\circ}$  meridian the outer surface hoop strain (gauge 9, o,c) exceeds that on the inner surface (gauge 9, i,c) throughout the test. However the maximum strain was the inner surface meridional (gauge 9, i,m).

The strain distributions illustrate again the wide variation in strain levels on different meridians (Fig. A1.14.5 and A1.14.6). In spite of the large compressive hoop strains on the inner surface of the  $325^{\circ}$  meridian a buckle did not develop at this position.

The largest peak stress index is again the outer surface circumferential value. Values of  $-2.2$  and  $-2.3$  were obtained on the  $0^{\circ}$  and  $325^{\circ}$  meridians respectively (Figs. A1.14.8 and A1.14.7). The meridional distributions show a "double" peak in the knuckle near the crown.

The first buckle occurred at  $120 \text{ lbf/in}^2$  during the test with end 17. The buckles were the same type as those on end 7, taking the form of

outward bulges elongated in the meridional direction. A typical buckle traversed the knuckle arc and extended about 4 in into the crown. In all nine buckles were produced, the last at a pressure of 190 lbf/in<sup>2</sup>. The buckles occurred gradually and silently and were spaced around the circumference of the end. Details are given in table 7.4. When the pressure was subsequently increased to 240 lbf/in<sup>2</sup> during the test with end 15 no further buckles were obtained. The 3rd, 5th, 7th and 9th buckles produced on this end are shown in Fig. 7.38a.

The test history of this end, described in Fig. 8.7b, is a combination of those for the other 81 in diameter ends.

#### 8.1.15 End No.15 ( $t_e/D_i = 0.00158$ , $r_i/D_i = 0.167$ , $R_i/D_i = 1.0$ )

This end had the same shape parameters and thickness ratio as end 14. However in contrast to end 14, a 35.5 in length of cylinder was welded to the end.

The thickness distribution, illustrated in Fig. A1.15.1, showed no major departures from that expected for a crown and segment end. The slight reduction in thickness towards the centre of the knuckle has been observed on other ends (e.g. ends 1 and 2).

The curvature distribution (Fig. A1.15.2), with a peak value in the knuckle at both junctions, is more similar to that of the 108 in diameter crown and segment end (Fig. A1.13.2) than the other 81 in diameter crown and segment end (Fig. A1.14.2). The mean crown curvature is somewhat greater than the nominal value; the variations in the knuckle curvature are considerable.

Pressure-strain plots from gauges along a welded meridian (86°) and an unwelded meridian (338°) are shown in Figs. A1.15.3 and A1.15.4 respectively. The inner surface meridional strain (gauge 8, i,m) is the greatest in both cases, though the position of the peak moves slightly (gauge 9, i,m) at the higher pressures along the welded meridian. The

largest compressive hoop strains occur on the inner surface along both meridians.

The strain distributions (Figs. A1.15.5 and A1.15.6) also show the maximum strain on both gauged meridians to be the inner surface meridional. On the  $86^\circ$  meridian (weld) the inner surface hoop strain exceeds that on the outer surface by about 0.13% strain. This suggests that the gauges are situated near the crest of a prebuckle ripple. This was confirmed by the formation of the first buckle on the  $87^\circ$  meridian at a pressure of  $107 \text{ lbf/in}^2$ .

The distribution of elastic stress indices on the two gauged meridians are shown in Figs A1.15.7 and A1.15.8. The outer surface hoop stress indices were the greatest; values of -2.1 and -2.3 were obtained for the  $86^\circ$  and  $338^\circ$  meridians respectively. It is apparent from comparisons with end 14 that the support ring on that end had a negligible effect on the peak hoop stresses.

The nine buckles produced on this end were similar in form to those occurring on the other crown and segment ends. They consisted of outward bulges elongated in the meridional direction. A photograph of the fourth buckle is shown in Fig. 7.38b. However the buckles developed more slowly than those previously observed. For example the seventh buckle occurred at a pressure of  $161 \text{ lbf/in}^2$  over a period of nearly 24 hours.

It was notable that considerable pressure increases were required for the development of the later buckles, even though the incipient ripples may have been apparent for some time, and that the later buckles were smaller than the earlier ones.

The test history is shown in Figs. 8.8 and 8.9a.

8.1.16 End No.16 ( $t_e/D_i = 0.00158$ ,  $r_i/D_i = 0.074$ ,  $R_i/D_i = 1.0$ )

The thickness (Fig. A1.16.1) in this spun end shows an abrupt

reduction in the knuckle near the junction with the crown and considerable undercutting due to weld dressing at the knuckle/cylinder junction. However the minimum thickness on the meridian of about 0.115 in (excluding undercutting) is not low.

The curvature distribution (Fig. A1.16.2) shows minor concavities in both crown and cylinder. The average knuckle curvature is somewhat smaller than the nominal. This will tend to produce lower stresses and possibly a higher buckling pressure than anticipated.

The pressure-strain plots for individual strain gauges (Figs. A1.16.3 and A1.16.4) show very considerable differences between gauges on the  $0^\circ$  and  $90^\circ$  meridians. (Note that these plots have different strain scales.) On the  $0^\circ$  meridian (coincident with the diametrical weld) the maximum strain up to the occurrence of the second buckle (at  $101 \text{ lbf/in}^2$ ) was the outer surface circumferential strain (gauge 8, o,c), suggesting that the meridian was near the trough of a prebuckle ripple. The peak tensile inner surface meridional strain (gauge 8, i,m) is slightly greater in magnitude than the peak compressive inner surface hoop strain (gauge 11, i,c), the former being less affected by buckling. The gauges were still operative after the second buckle at  $101 \text{ lbf/in}^2$  but the pressure-strain plots show major discontinuities at this pressure.

On the  $90^\circ$  meridian the inner surface meridional and circumferential strains (gauges 9, i,m and 9, i,c respectively) were similar in magnitude. In contrast with the  $0^\circ$  meridian, the maximum hoop compression on the inner surface (gauge 9, i,c) was greater than that on the outer surface (gauge 9, o,c). The meridian is probably situated near the crest of a ripple. Gauge 20,o,c shows that up to a pressure of  $119 \text{ lbf/in}^2$  the cylinder material has not attained 0.1% permanent strain.

The strain distributions  $12 \text{ lbf/in}^2$  below the first buckling pressure of  $95 \text{ lbf/in}^2$  are shown in Figs. A1.16.5 and A1.16.6. The differences in both hoop and meridional strains along the two meridians

are again apparent.

The largest elastic peak stress index on each meridian is the outer surface circumferential index (Fig. A1.16.7 and A1.16.8). The value on the weld is -5.8 compared with -4.2 on the  $90^\circ$  meridian.

The six buckles produced on this end were of the type described for end 8. A typical buckle was 14 in long, 5 in wide and 1.8 in deep and extended into the crown and cylinder. A photograph of the second buckle is shown in Fig. 7.38c.

The test history is shown in Fig. 8.9b.

#### 8.1.17 End No.17 ( $t_e/D_i = 0.00158$ , $r_i/D_i = 0.074$ , $R_i/D_i = 1.0$ )

This pressed and spun end contains all the main features usually associated with this type of end.

The thickness distribution (Fig. A1.17.1) clearly shows the thinning which has occurred in the knuckle due to rolling, together with some undercutting at the knuckle/cylinder weld.

The meridional curvature (Fig. A1.17.2) again shows significant deviations from the nominal, and is in most respects closely similar to that for end 16 (Fig. A1.16.2). As for end 16 the effective knuckle curvature is smaller than that intended.

The pressure-strain curves for individual gauges (Figs. A1.17.3 and A1.17.4) show the outer surface hoop strain (gauge 10, o,c) to be the maximum on both of the gauged meridians ( $0^\circ$  weld,  $90^\circ$  no weld). However the tensile inner surface meridional strain (gauges 10, i,m and 9, i,m) is only slightly smaller in magnitude. Corresponding peak strains on the two meridians are of similar magnitude at lower pressures (below  $60 \text{ lbf/in}^2$ ). At higher pressures the strains on the  $0^\circ$  meridian increase more rapidly. This is due to the onset of yield in the weld region and also the close proximity of the eventual first buckle.

The strain distributions, 12 lbf/in<sup>2</sup> below the first buckling pressure of 107 lbf/in<sup>2</sup> (Figs. A1.17.5 and A1.17.6), also show that the peak strains on the 0° meridian are considerably greater than those on the 90° meridian at higher pressures. It is interesting to note that the first buckle occurred on the 3° meridian.

The distributions of elastic stress indices (Figs. A1.17.7 and A1.17.8) are similar for the two gauged meridians. The outer surface hoop stress indices (the greatest along each meridian) are -4.7 and -4.2 on the 0° and 90° meridians respectively.

The eight buckles were produced at pressure levels from 107 lbf/in<sup>2</sup> to 171 lbf/in<sup>2</sup>. They were similar to those observed on ends 8, 9, 16 etc. A typical buckle was 13 in long, 4.5 in wide and 1.2 in deep. A photograph of the fifth buckle is shown in Fig. 7.38d.

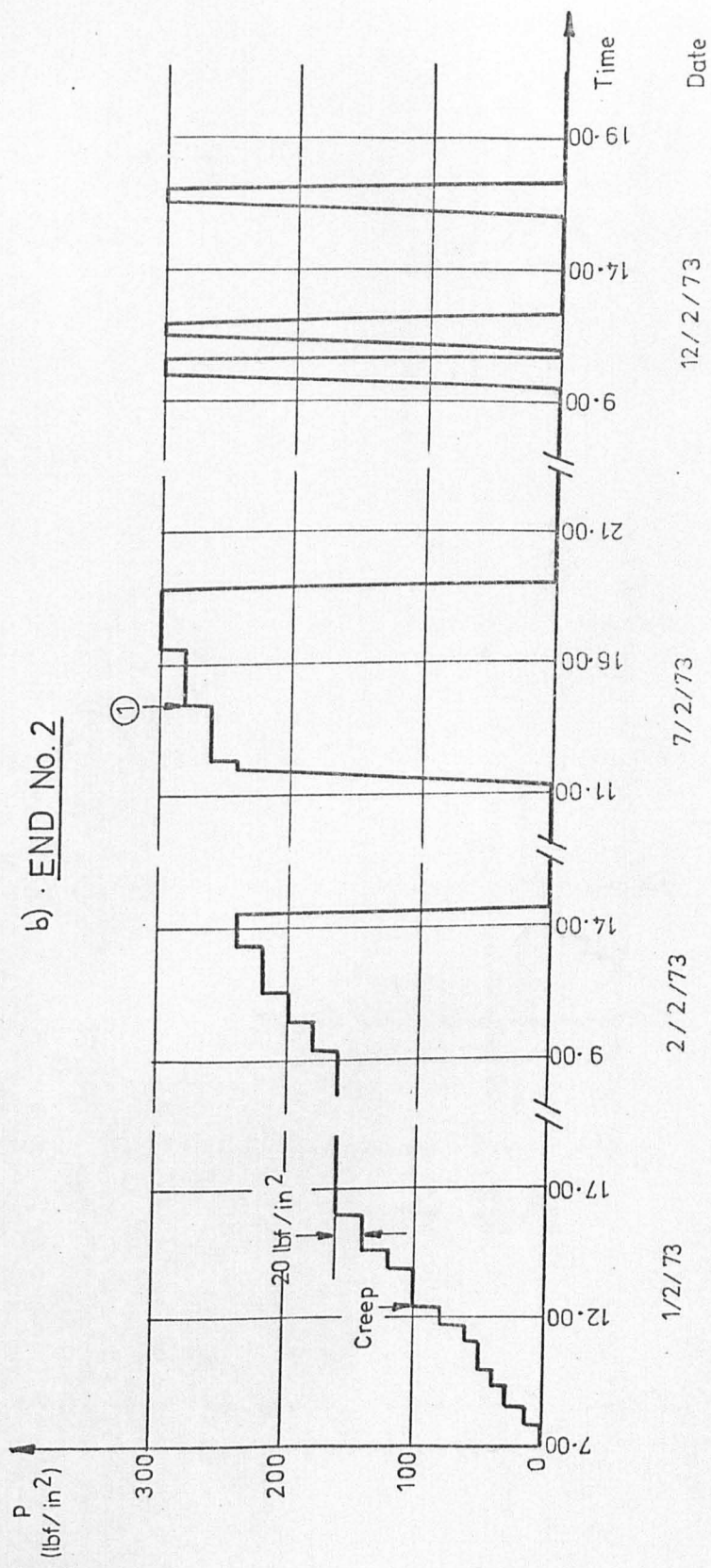
The test history is illustrated in Fig. 8.10.

a) END No. 1

THE TEST HISTORY FOR THIS END IS A COMBINATION OF THOSE FOR THE OTHER 54 in. DIAMETER ENDS IN THE ORDER 4, 3, 5, 6 AND 2. HOWEVER THE PRESSURE AT THE KNUCKLE / CYLINDER JUNCTION WAS 2.0 lbf/in<sup>2</sup> GREATER THAN THAT IN THE OTHER ENDS.

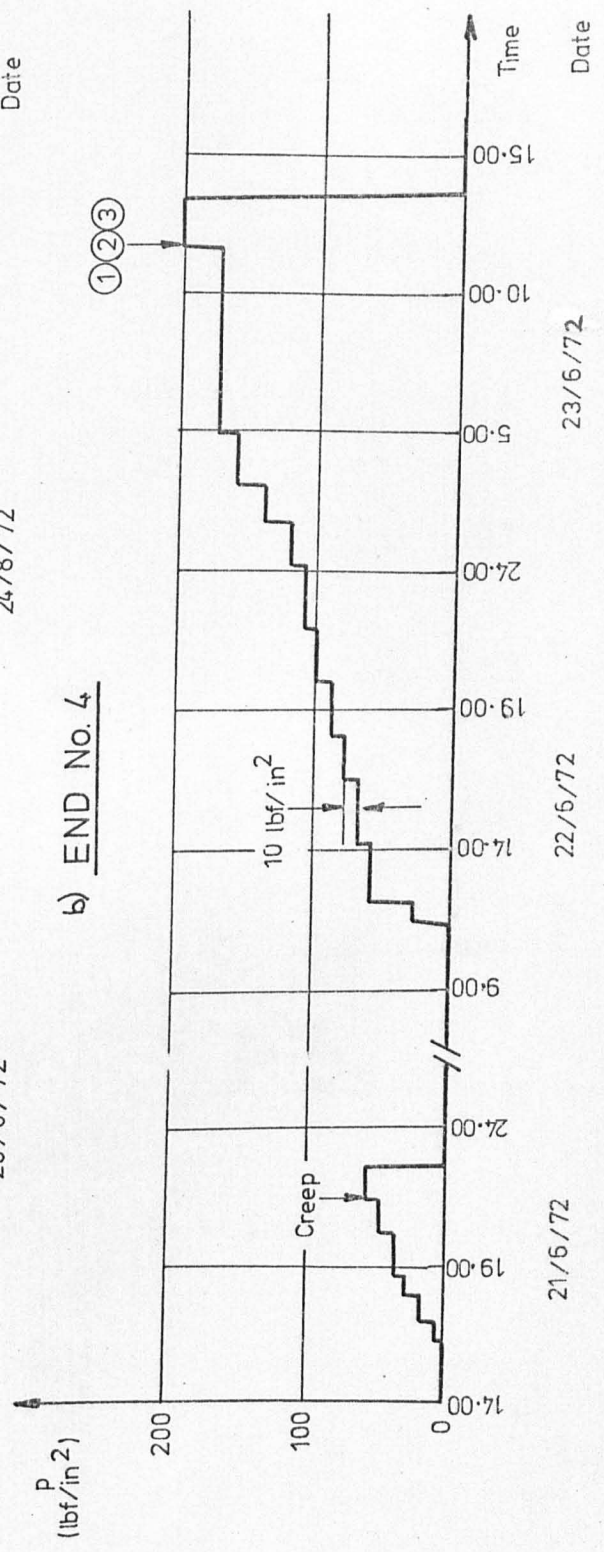
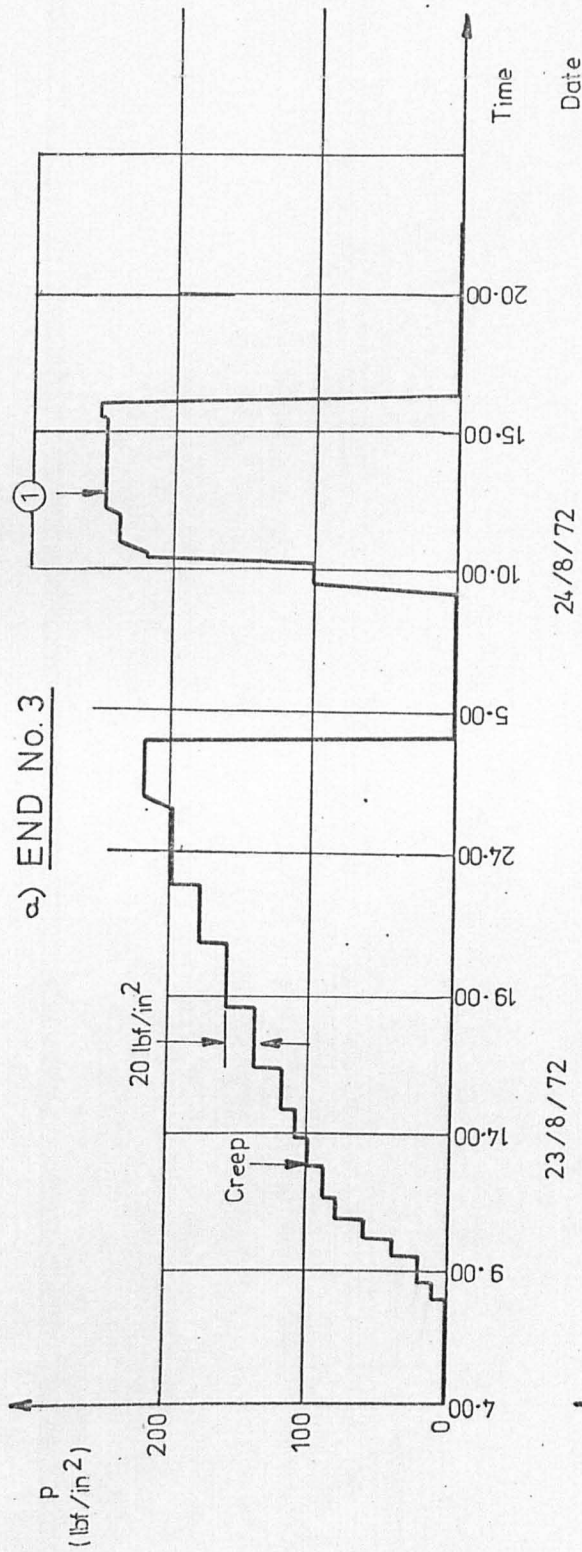
THE BUCKLES IN THE END OCCURRED AT 280 lbf/in<sup>2</sup> DURING THE TEST WITH END 5. CREEP EFFECTS WERE FIRST NOTICED AT A PRESSURE OF 140 lbf/in<sup>2</sup>

b) END No. 2

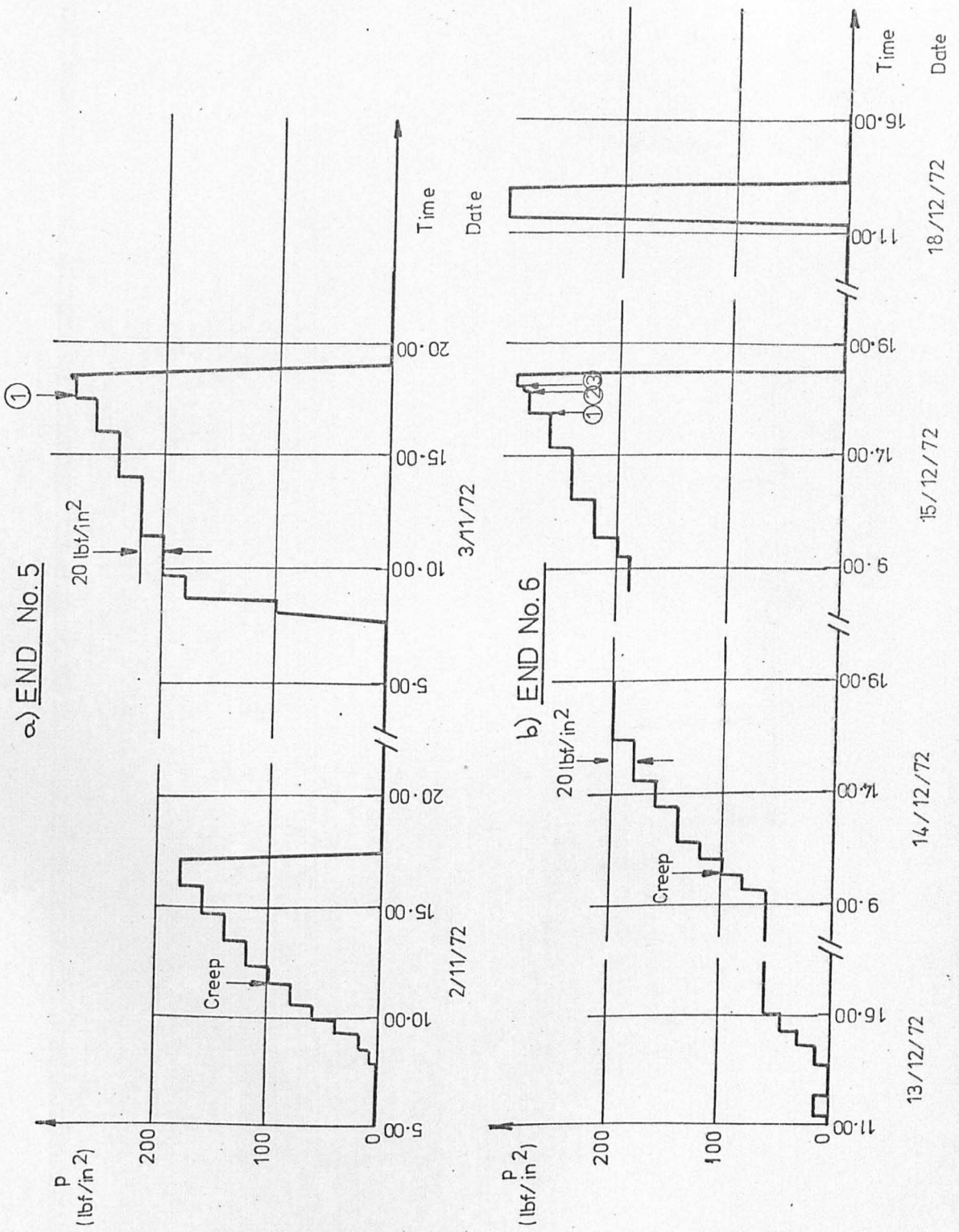


TEST HISTORY DIAGRAMS





TEST HISTORY DIAGRAMS



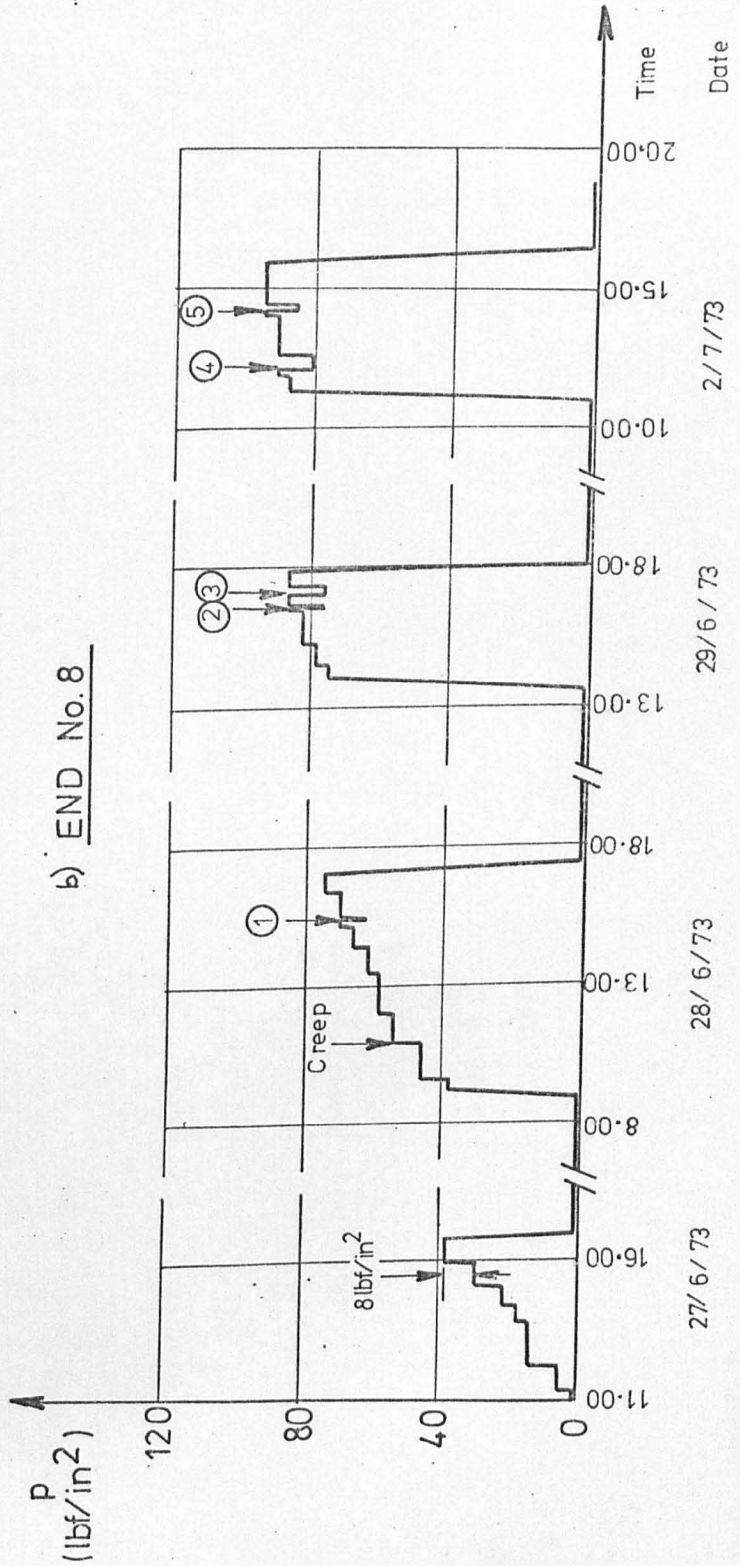
TEST HISTORY DIAGRAMS

a) END No.7

THE TEST HISTORY FOR THIS END IS A COMBINATION OF THOSE FOR THE OTHER 108 IN DIAMETER ENDS IN THE ORDER 9, 8, 10, 11, 12 AND 13. HOWEVER THE PRESSURE AT THE KNUCKLE/ CYLINDER JUNCTION WAS 2.2 lbf/in<sup>2</sup> GREATER THAN THAT IN THE OTHER ENDS

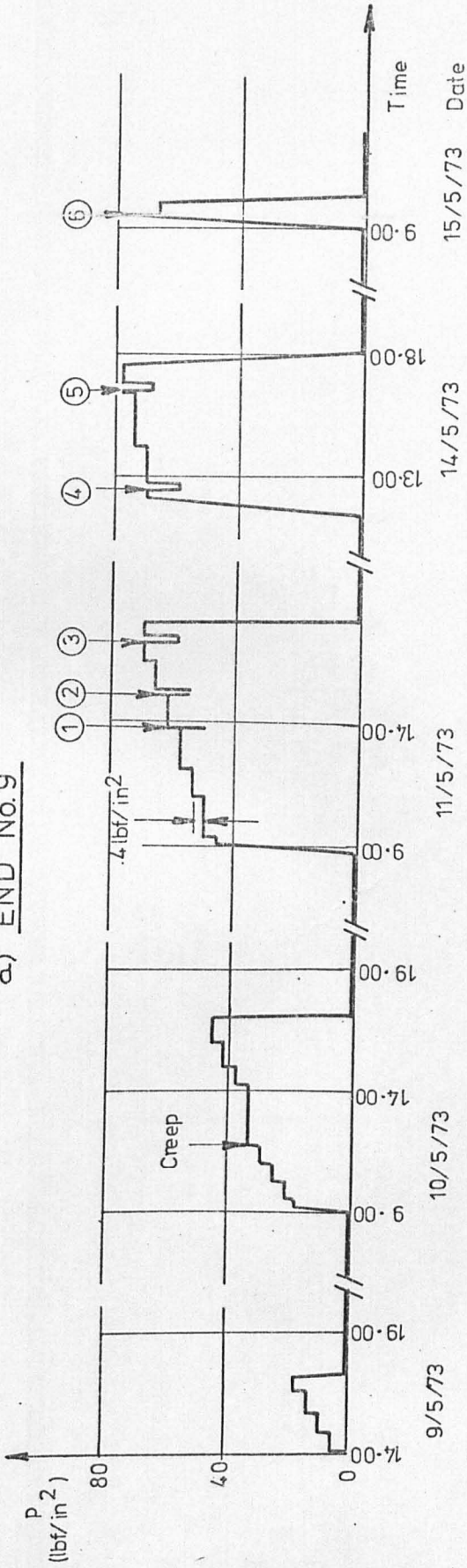
THE BUCKLES IN THE END OCCURRED AT PRESSURE LEVELS BETWEEN 60 AND 92 lbf/in<sup>2</sup> DURING THE TESTS WITH ENDS 9 AND 8. CREEP EFFECTS WERE FIRST NOTICED AT A PRESSURE OF 44 lbf/in<sup>2</sup>

b) END No.8

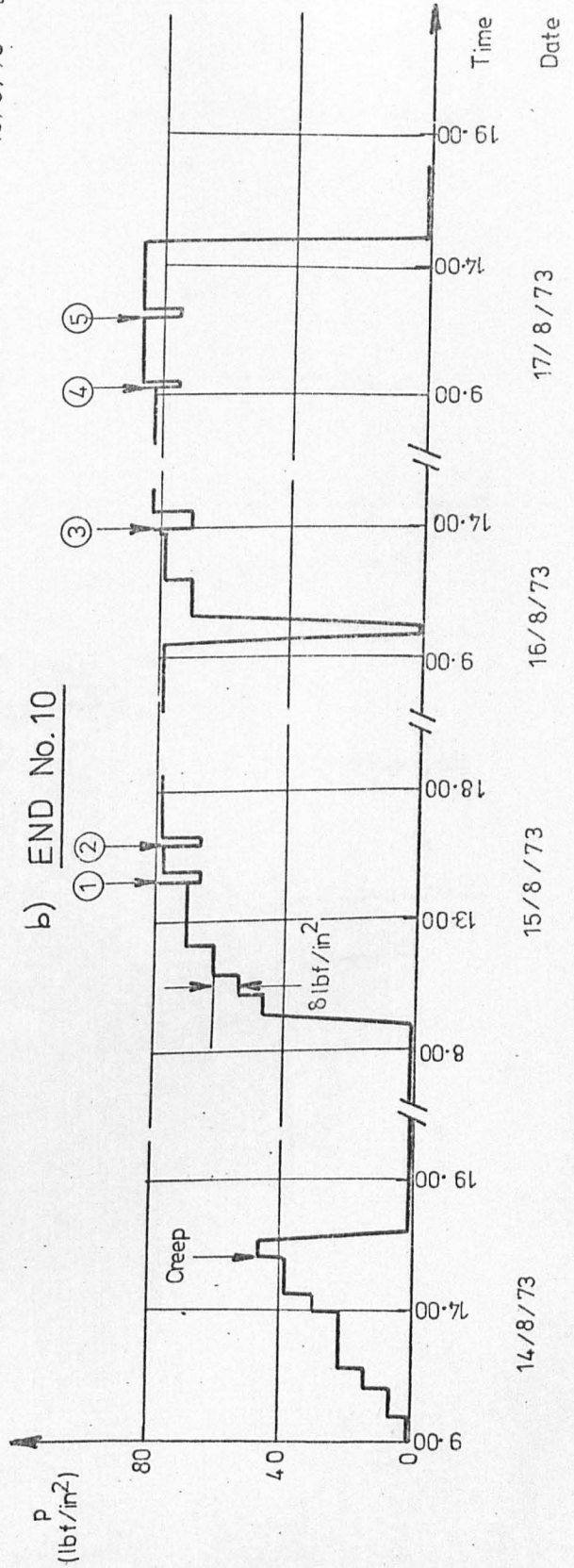


TEST HISTORY DIAGRAMS

a) END No.9



b) END No.10



TEST HISTORY DIAGRAMS

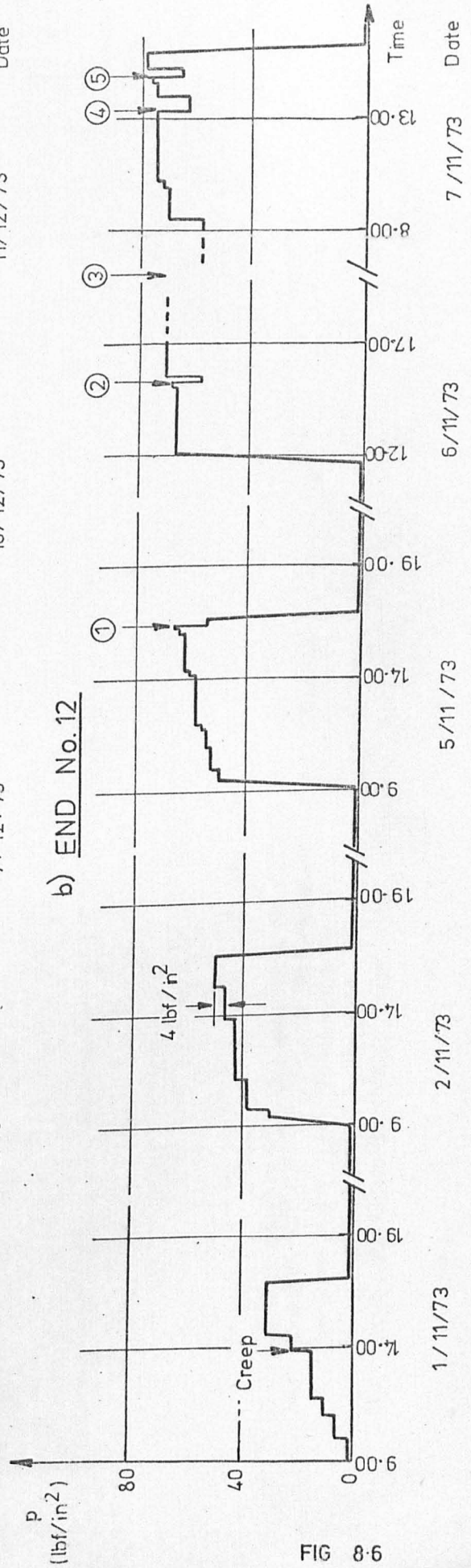
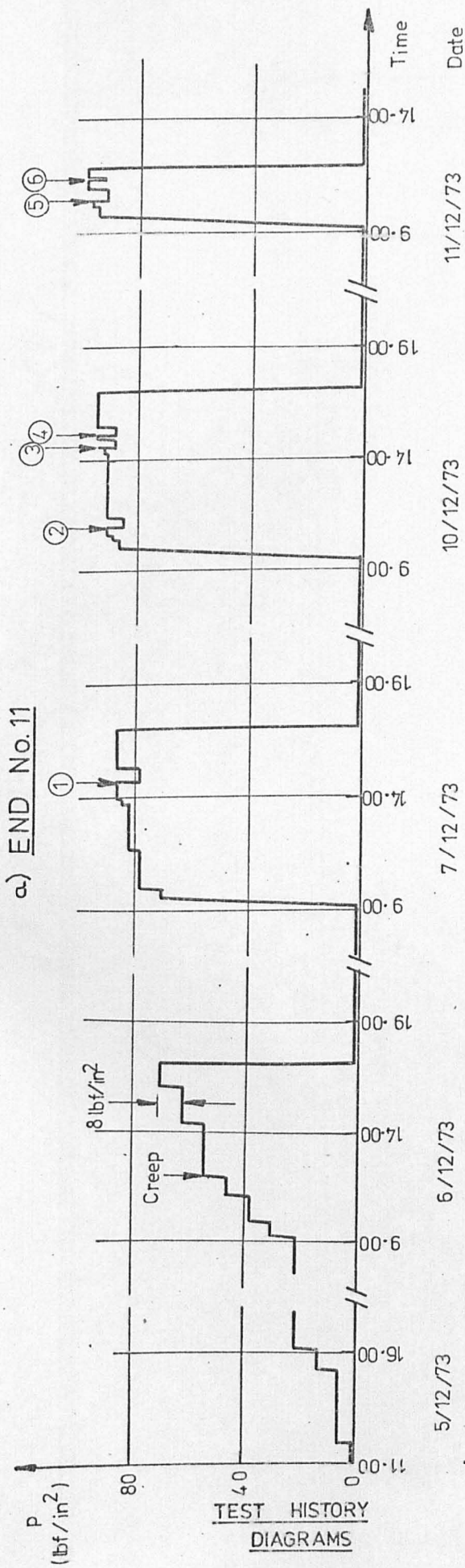
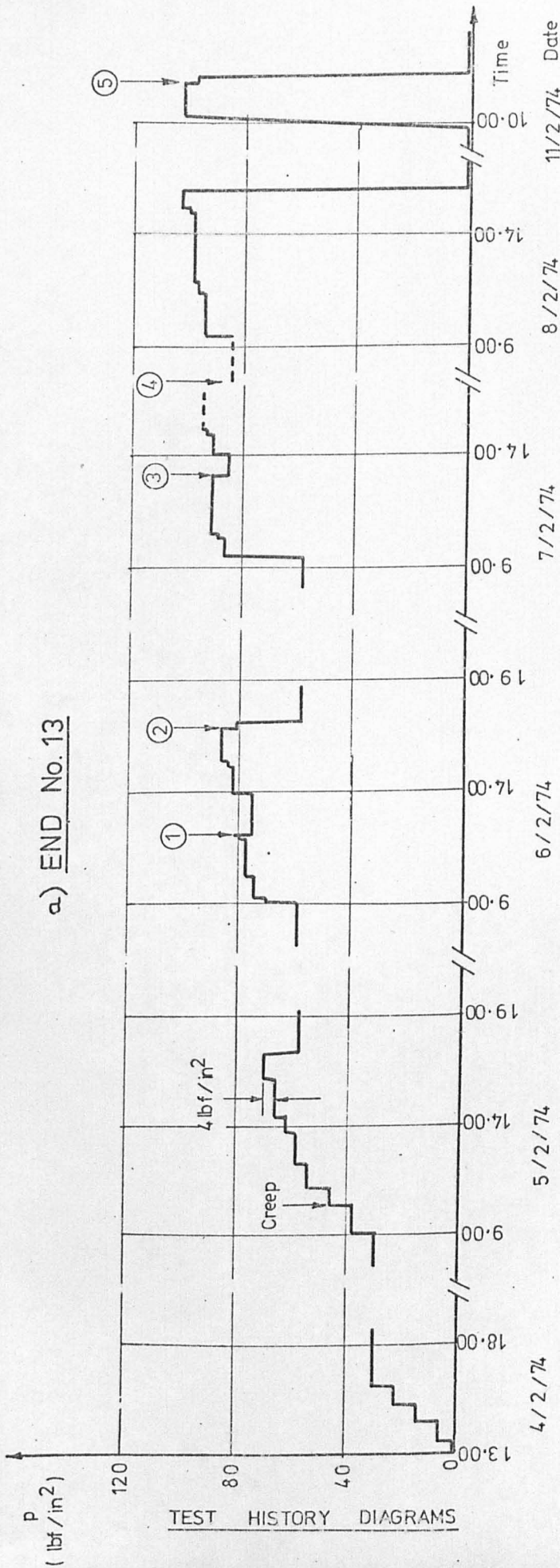


FIG 8-6



TEST HISTORY DIAGRAMS

THE TEST HISTORY FOR THIS END IS A COMBINATION OF THOSE FOR THE OTHER 81 in. DIAMETER ENDS IN THE ORDER 16, 17 AND 15. HOWEVER THE PRESSURE AT THE KNUCKLE / CYLINDER JUNCTION WAS 1.6 lbf/in<sup>2</sup> GREATER THAN THAT IN THE OTHER ENDS.

THE BUCKLES IN THE END OCCURRED AT PRESSURE LEVELS BETWEEN 120 AND 190 lbf/in<sup>2</sup> DURING THE TEST WITH END 17. CREEP EFFECTS WERE FIRST NOTICED AT A PRESSURE OF 72 lbf/in<sup>2</sup>.

END No. 15

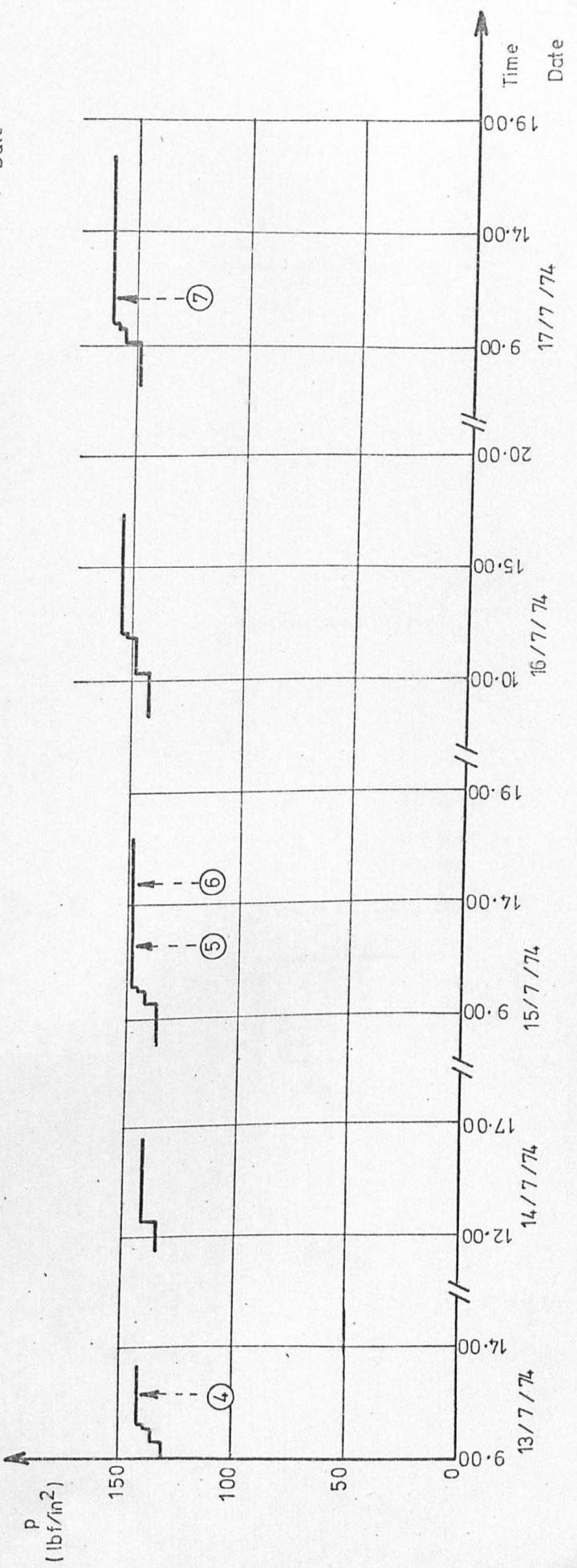
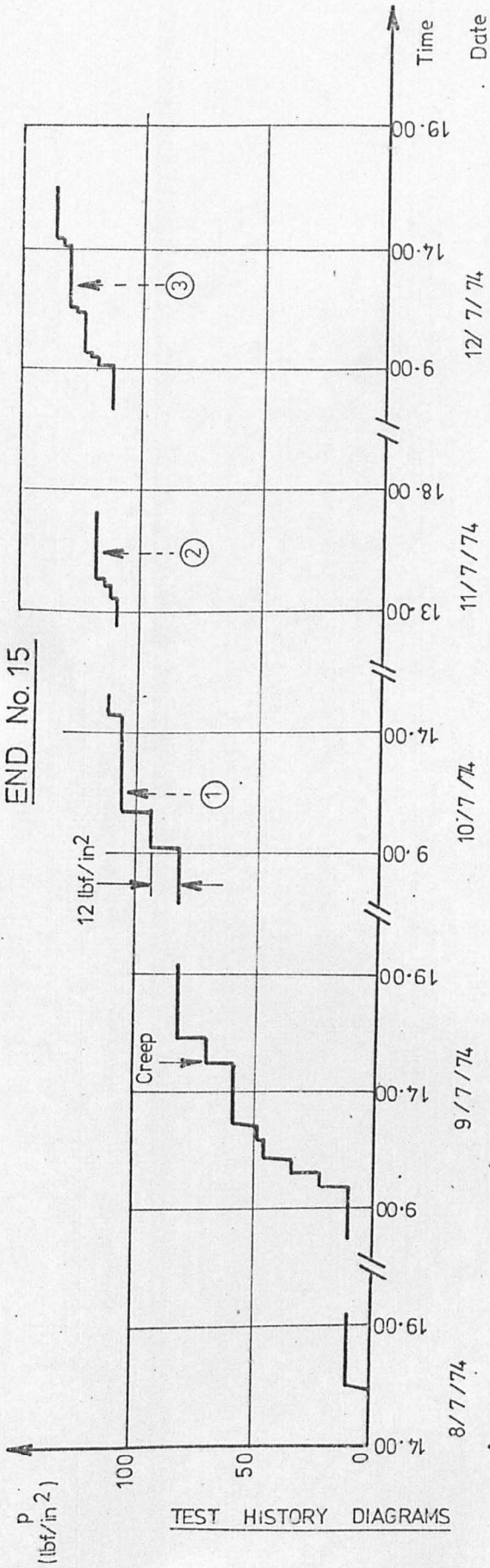
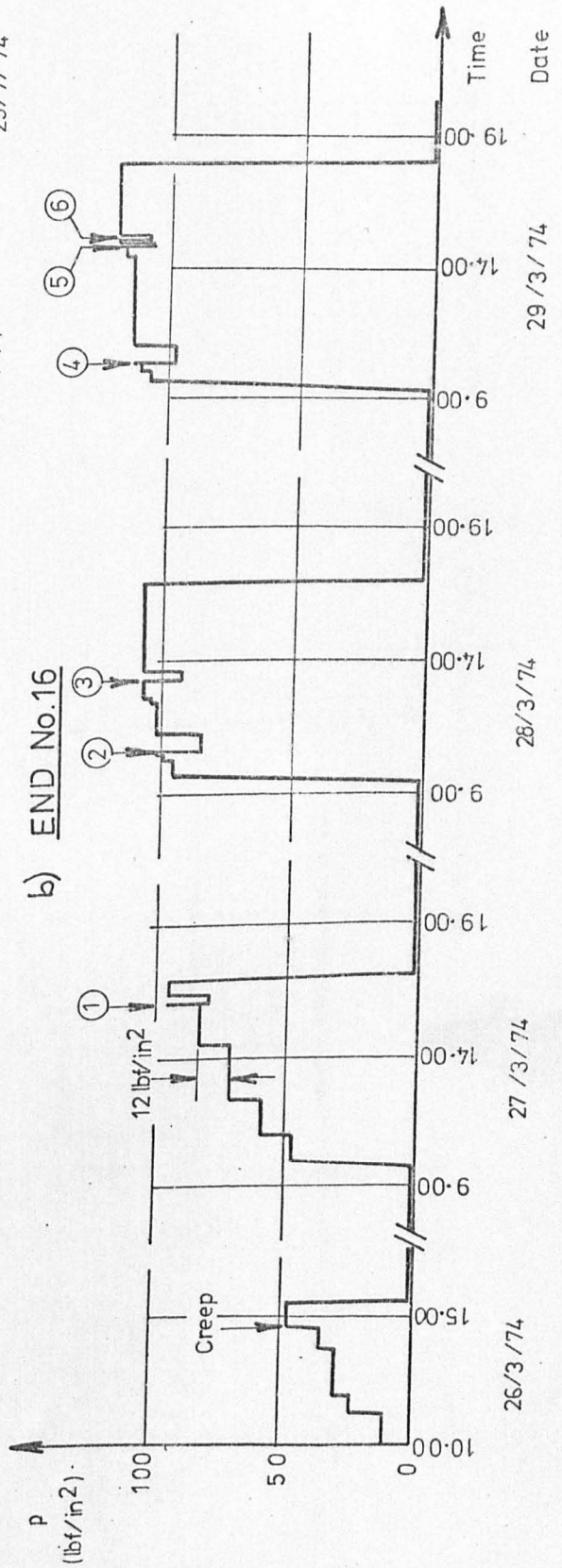
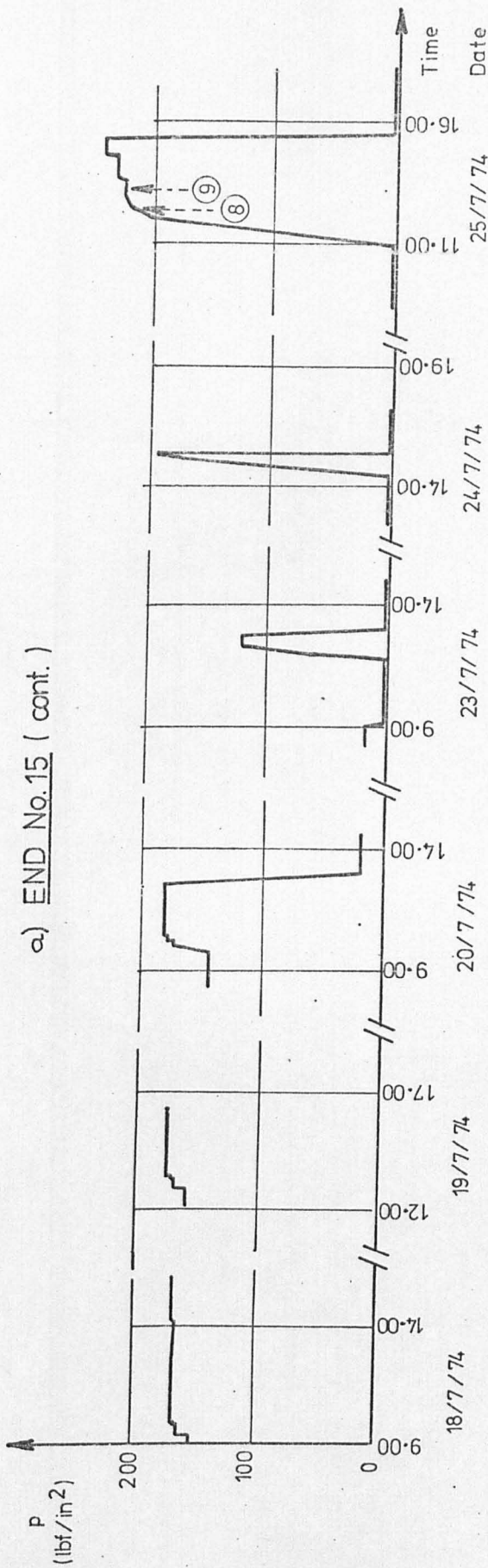


FIG 8-8



TEST HISTORY DIAGRAMS



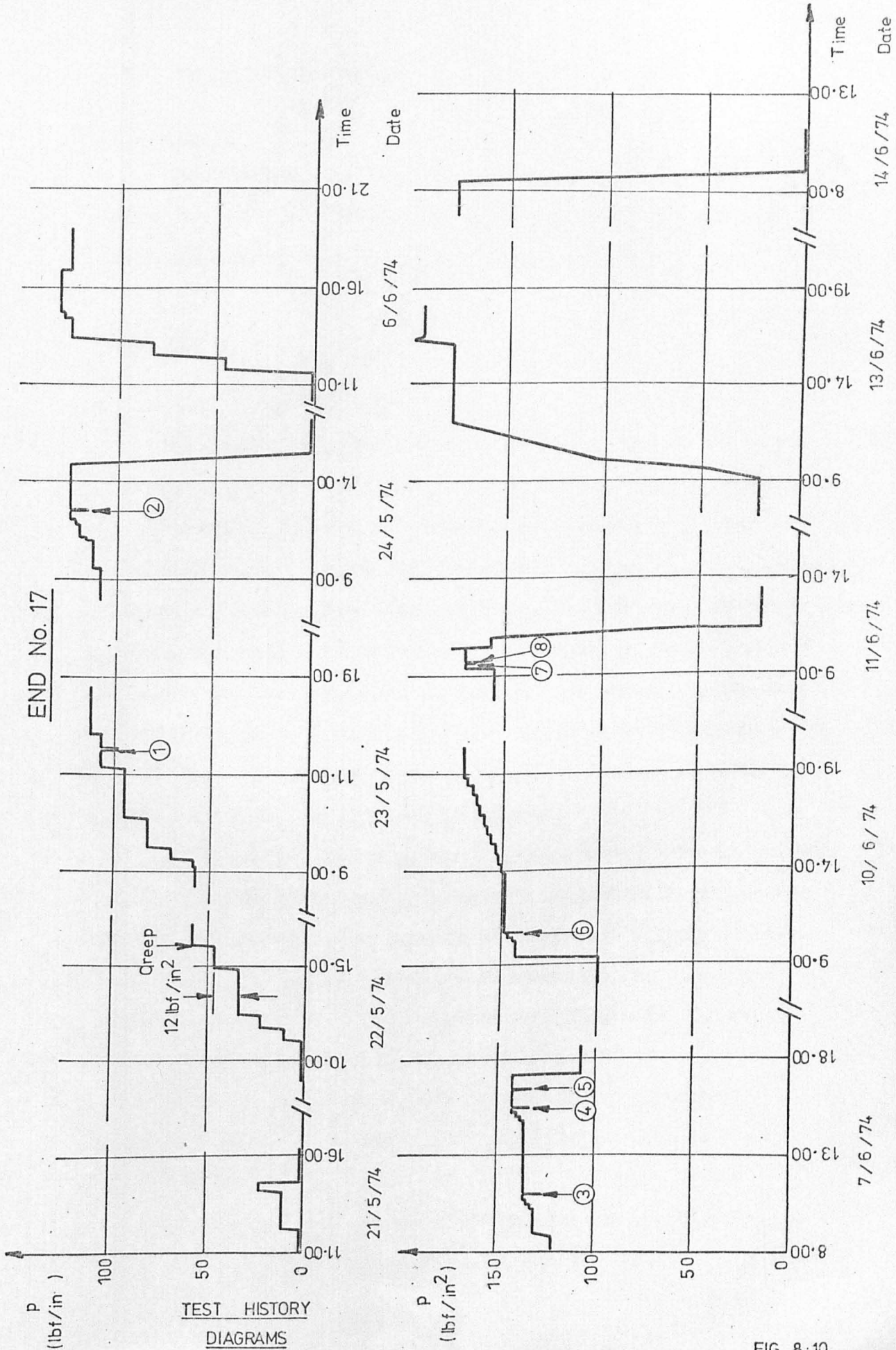


FIG 8-10

## 8.2 Shape/Thickness Defects

### 8.2.1 General

Detailed features of individual ends have been discussed in section 8.1. The main general trends are summarised in the following sections and the effects on end behaviour are mentioned.

### 8.2.2 Thickness

#### 8.2.2.1 Pressed and Spun Ends

1. Considerable thinning occurs in the knuckle region, due to the cold forming process. Some ends (for example No.4) exhibit a reasonably uniform reduction in thickness between the knuckle/crown and knuckle/cylinder junctions. Others (for example No.5) exhibit thickness reductions which are far from uniform. The magnitude and distribution of the thinning depend on the skill and consistency of workmanship of the operator and on the knuckle radius and diameter of the end. The effect is probably also material dependant. Reductions in thickness of up to 25% may occur. It has not been possible to draw any useful generalisations about the dependence of the thinning on end dimensions.
2. Considerable undercutting may be present at the welds in most ends. This is a consequence of weld dressing and will clearly be operator-dependant. It is not always possible to distinguish thinning due to dressing from that due to forming but it would seem that 0.020 in is a reasonable estimate of the maximum reduction. In general the quality of the finished welds in the test ends was good.
3. Except for weld dressing effects, only small variations in thickness occur in the cylinder; a typical range of variation (end No.12) is  $\pm 0.002$  in.
4. The reduction in thickness in the knuckle will result in higher stresses for a given pressure and a weaker section. The buckling pressure

will therefore be reduced. However since the maximum stresses occur near the knuckle/crown junction where the thinning is usually slight the effect will be less significant.

5. On ends with a diametrical weld it is usual for at least one buckle, often one of the first to be produced, to occur on or near the weld. The effect is clearly associated with weld dressing. In a particular case (end No.16) the first buckle occurred on a weld at a pressure of  $95 \text{ lbf/in}^2$ ; a pressure increase of  $6 \text{ lbf/in}^2$  was required before a buckle formed in the unwelded material. In one case, however, (end No.8) the welded meridians survived without a buckle throughout the test.

#### 8.2.2.2 Crown and Segment ends

1. Compared with that in spun ends, the thinning produced by this method of manufacture is very small (about  $0.003 \text{ in}$ ).
2. Undercutting at the welds is also present in these ends. The meridional welds, with the associated undercutting, provide ideal sites for the formation of buckles. This is clearly confirmed by the fact that at least one buckle on each end occurred on or near a weld. Again however, there were welded meridians on which buckles did not occur.

#### 8.2.3 Curvature

1. In both crown and knuckle the curvature varies significantly from the meridional nominal. Again the effect is particularly operator-dependant and tends to be specific to each end. The crown curvature may rise to twice the nominal value (e.g. end No.11) and often becomes negative immediately before the knuckle/crown junction. The knuckle curvature can be nearly twice (end No.15) or half (end No.5) the nominal value over limited knuckle arc lengths. In spun ends there is often a reduction in curvature at the centre of the knuckle.

2. Some minor curvature anomalies occur in the cylinder and in many cases (e.g. end No. 6) a negative value is found near to the knuckle junction. These effects are associated with radial mismatch between cylinder and end, and weld dressing at the junction.

3. The curvature reductions recorded at welds are "superficial" and are probably more realistically seen as local thickness reductions.

4. No simple generalisations can be made on the magnitude and distribution of these curvature "errors" nor on their effect on the buckling pressure. Wide variations occur from end to end and would probably be found in nominally identical ends. There will be a correspondingly high "scatter" in experimental results and a reasonable "factor of safety" will be required in any design applications.

### 8.3 Material Properties

#### 8.3.1 Test procedure

In order to assist in the interpretation of the results obtained from the test ends, the properties of the material used were studied.

It was known (ref. 24) that considerable work-hardening occurred during the manufacture of the ends and an attempt was made to determine the properties for varying degrees of work-hardening.

Sample strips, approximately 7 in long by 1 in wide, were produced from off-cuts of the original plate material of end No. 5. In every case the length of the strip was perpendicular to the rolling direction of the original plate. After taking hardness measurements the samples were reduced in thickness by passing them through a rolling machine. (This was done at room temperature with no subsequent heat treatment.) The reduction in thickness was varied up to a maximum 0.038 in so that the range of reductions found in pressed and spun ends was covered. Some of the samples were rolled longitudinally (i.e. with the length of the strip

parallel to the rolling direction); the remainder were rolled across the width. This was done in an attempt to determine whether the direction of rolling had any effect on the property changes. The hardness of each rolled specimen was measured using a Vickers hardness testing machine.

Tensile test specimens were produced from the rolled samples to BS 18 : Part 2 : 1971 (ref. 40). The gauge length was 2 in and the width 0.5 in. The thickness and width of the specimens were carefully measured with a micrometer and high elongation strain gauges (TML Type (YL-5)) were bonded to each side. The specimens were then loaded in an Instron tensile test machine. The rate of extension was generally maintained at 0.01 in/min during the elastic growth of the material, but in order to keep the duration of the test to an acceptable level the rate was increased to 0.1 in/min after the onset of plasticity.

The two strain gauges on each specimen were incorporated into opposite arms of a Wheatstone bridge circuit and the voltage changes recorded using a digital volt meter. This eliminated errors in strain reading caused by bending. Gauge readings were taken at typically 1 min intervals until the gauges became detached from the specimens at higher strains. A pen record of end-grip movement against load was produced automatically as the test proceeded. A test was concluded when the specimen fractured.

### 8.3.2 Stress-strain characteristics.

The stress-strain curves for two of the tensile test specimens are shown in Fig. 8.11. Specimen 1 was in the original plate condition and thus represents the unworked state of the material at the start of the manufacture of an end. The 0.2% proof stress measured on this specimen was 22 tonf/in<sup>2</sup>; the manufacturer's minimum value is 19 tonf/in<sup>2</sup>. (The manufacturer's guaranteed minimum properties are given in section 3.1.3.)

The onset of non-linearity (i.e. the proportional limit) was detected at 6 tonf/in<sup>2</sup>. Very rapid strain increases occur above a stress level of 24 tonf/in<sup>2</sup>.

Specimen 2 had been reduced in thickness by 0.038 in before testing. The curve first departs from the linear at a stress of about 23 tonf/in<sup>2</sup>. The 0.2% proof stress is 63 tonf/in<sup>2</sup>, nearly three times that obtained on the unworked material, and 14 tonf/in<sup>2</sup> greater than the original ultimate tensile strength. Above a stress level of 65 tonf/in<sup>2</sup> very rapid increases in strain occur.

### 8.3.3 Overall results

A graph of the increase in Vickers hardness number ( $\Delta H_v$ ) against the reduction in thickness for each tensile test specimen is shown in Fig. 8.12. The scatter of the experimental points is relatively small. Thus an estimate of the change in hardness can be determined from the change in thickness and vice versa.

Fig. 8.13a shows the variation of the proportional limit with hardness ( $H_v$ ). There is a wide scattering of experimental points for Vickers hardness values above 300. Great difficulty was experienced in obtaining an accurate value of the proportional limit and the wide scatter was anticipated. Figs. 8.13b to 8.15a show plots of proof stress against Vickers hardness values. Up to 0.1% proof stress there is a large scatter in the experimental points. This is due in part to the steepness of the stress-strain curve, a small variation in intercept position on the curve producing a significantly different stress. However the 0.2% proof stress can be determined more accurately as the stress-strain curve becomes flatter. This is reflected in Fig. 8.15a. All the proof stresses tend to increase with hardness. The relationship appears to be approximately linear for the 0.2% proof stress. In general however the rate of change

of proof stress tends to increase with increasing hardness.

Fig. 8.15b shows the relationship between ultimate tensile strength and hardness for the tensile test specimens. Increases in U.T.S. of 24 tonf/in<sup>2</sup> (i.e. 50%) occur as the Vickers hardness number changes from 200 to 370.

## 8.4 Residual stresses

### 8.4.1 General

The strain and stress distributions discussed in section 8.1 resulted from the application of internal pressure alone. It was considered likely that residual stresses, produced during the manufacture of the ends, would have an appreciable effect on the post-yield and buckling behaviour. (It is not usual practice to stress relieve such ends after manufacture due to large post-heat-treatment deformations (ref. 24).)

The level of residual strain present in the knuckle region of some of the ends prior to the pressure test was measured. This involved considerable work on the end before testing and was not followed as a standard procedure for all ends.

### 8.4.2 Procedure

TML type (FCA-2-17) strain gauges (90° pairs, gauge length 2 mm) were attached to the knuckle at corresponding positions on inner and outer surfaces along one meridian. The positions chosen (i.e. distances from pole) were the same as those used for the pressure test strain gauges. After taking initial readings of the strain gauges a strip of material about 1 in wide, containing all the gauges was cut from the end by means of a hacksaw. Once removed the strip was cut into small pieces just larger than the attached rosettes.

Throughout the cutting operation great care was exercised to ensure that the gauges were not damaged either physically or by excessive heat. The cutting area was continuously cooled by means of a jet of compressed air. Short cutting periods with frequent pauses also assisted in keeping the specimens cool.

After the individual gauge pieces had been cut out the strain gauges were again read and a strain change calculated. Corresponding elastic stresses were derived.

To ensure that the cutting operation had no significant effect on the strain readings, a specimen, identical to those from the knuckle, was cut from a strain free plate of the same material, using the cutting method previously described. The recorded strain change was small, less than 0.005%.

#### 8.4.3 Results

Ends 10, 11 and 13 were studied in this way; the residual stresses and unit forces and moments determined are shown in Figs. 8.16 to 8.18 respectively. End 13 (diameter 108 in) was a crown and segment end, ends 10 and 11 (diameter 108 in) were pressed and spun. Residual stress values obtained by Kemper (ref. 24) on a 65 in diameter end with an 8 in knuckle (pressed and spun construction) are shown in Fig. 8.19.

A notable feature, common to all the spun ends, is the high tensile meridional stress on the outer surface of the knuckle and the corresponding compressive stress on the inner surface. The meridional unit force ( $N_\phi$ ) is small in the knuckle; simple equilibrium considerations show that it would be zero in a perfectly rotationally symmetric end. The consistent negative meridional moments ( $M_\phi$ ) around the centres of the knuckles are evident in Figs. 8.16, 8.17 and 8.19, and it can be seen that in general  $M_\phi$  is greater than  $M_\theta$ .



The circumferential stresses do not show such a consistent trend. However end 11 and Kemper's end have similar levels of hoop residual stresses, tensile on the outer surface and compressive on the inner. (Both ends had 8 in knuckles.) In each of the pressed and spun ends the circumferential force ( $N_{\theta}$ ) is compressive in the knuckle, with the maximum value occurring near the centre of the knuckle arc, and in two of the three cases  $M_{\theta}$  is also negative at this position.

The residual stresses obtained for the crown and segment end (Fig. 8.18) do not show any marked features. However the level of residual stress is generally lower than that associated with the pressed and spun ends. The largest stresses occur near the knuckle/cylinder weld.

In use, the residual stresses are superimposed on the stresses due to the internal pressure. The maximum compressive hoop stress due to pressure tends to occur between the centre of the knuckle and the knuckle/crown junction. The effect of combining the two stress systems is likely to produce a broadening of the band of compression. Figs. 8.20 and 8.21 illustrate the stress levels present in ends 10 and 11 respectively at a pressure of 30 lbf/in<sup>2</sup> when the measured residual stresses and pressure stresses are combined. High compressive hoop stresses are present on both surfaces of the knuckle of end 10. However on end 11 the residual stresses have reduced the outer surface peak hoop stress to a low level whilst greatly increasing the inner surface stress. No clear trend is present, though for end 10 the residual stresses will significantly reduce the first buckling pressure.

The results of hardness tests, made on knuckle material adjacent to the residual stress specimens, are shown in Fig. 8.22. Vickers hardness number is plotted against position. For the spun ends (i.e. Nos. 10, 11 and Kemper's) there are considerable increases in hardness in the knuckle region compared with the Vickers hardness number of 200 for the unworked

material. The increase in hardness for the crown and segment end (i.e. number 13) is appreciably less; a maximum hardness number of about 260 was measured.

#### 8.4.4 Residual stresses predicted from pressure test measurements

The removal of residual strain specimens from an end prior to pressure testing necessitated a repair in the end. Although the repair was successful in each case there was clearly a considerable advantage to be gained in being able to predict pre-test residual stresses without cutting specimens from the end. An attempt was made to do this.

For each position considered the hoop and meridional strains recorded during the pressure test were plotted against pressure. The pressure at which the pressure-strain curves first became non-linear was noted, together with the corresponding hoop and meridional strains. These strain values were used to calculate stresses (assuming elastic conditions) and from these an equivalent uniaxial stress was obtained based on von Mises shear strain energy criterion.

From the plots of the proportional limit against hardness, obtained during material testing (see Fig. 8.13a), a value of limiting elastic stress was determined for the point under consideration. (The hardness values were obtained from the residual strain specimens cut from the vessel.) The difference in the stress values obtained from the material testing and pressure test was taken as an indication of the residual equivalent stress level. The results obtained for end 11 are shown in Fig. 8.23 together with a residual equivalent stress calculated from the pre-test residual strain measurements.

On the inner surface there is reasonably close agreement between the two curves from the knuckle/crown junction to midway around the knuckle arc. The outer surface curves show little agreement.

The analysis assumes that :

- i) residual and pressure stress distributions are rotationally symmetrical
- ii) the yield stress at a given point can be determined from the hardness value,
- iii) the von Mises equivalent stress concept is valid,
- iv) shape changes have no effect on the point at which first departure from the linear occurs during the pressure test,
- v) "layer" residual stresses (i.e. residual stresses that are not relieved in cutting out a portion of the end) are negligible.

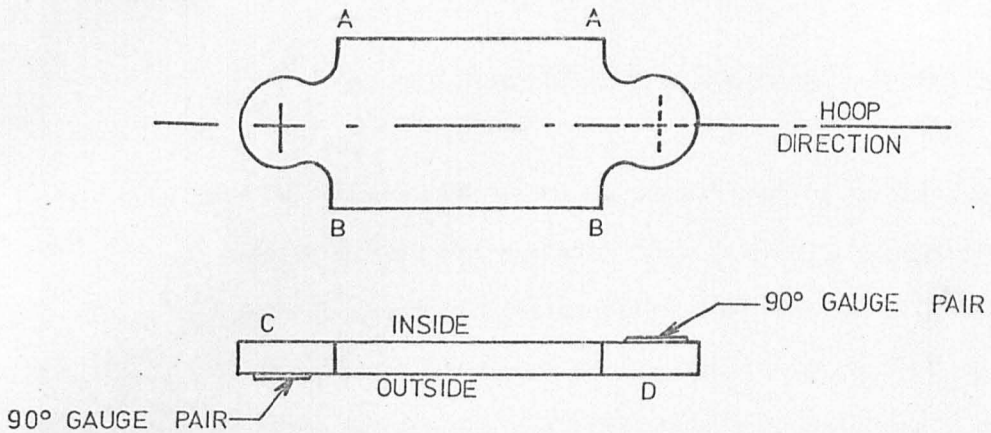
The results indicate that some or all of these assumptions are not fully justified.

#### 8.4.5 Layer residual stresses

It is well known that when a simple beam is subjected to pure bending beyond the yield point and then released, residual stresses remain due to varying levels of yield attained through the thickness of the material during bending. These stresses are designated "layer" stresses. The formation of an end can be considered similar to the bending of a beam beyond the yield point but without the complete removal of the applied moment. The residual stress results described in section 8.4.3 record those stresses which are retained by the structure. Residual stresses of the "layer" type are not necessarily given.

To determine the "layer" stress level a "jig-saw" piece shaped specimen (see Fig. 8.24) was cut from the knuckle of end No. 11.

Strain gauges (TML type (FCA-2-17)) were mounted on opposite sides of the two projecting portions and strain changes were recorded as material was milled progressively, first from face C, then face D. The jig-saw piece was securely clamped across faces AA and BB during these operations. Similar tests on a piece from the original plate confirmed that strain changes produced by the action of the milling cutter alone were small.



LAYER RESIDUAL STRESS SPECIMEN

FIG 8-24

It can be shown from simple plate bending theory that the "layer" residual stresses on the surface from which material is removed are given by :

$$\sigma_{xt} = \frac{-Et}{4(1-\nu^2)} \left( \frac{d\epsilon_x}{dt} + \nu \frac{d\epsilon_y}{dt} \right)$$

$$\sigma_{yt} = \frac{-Et}{4(1-\nu^2)} \left( \frac{d\epsilon_y}{dt} + \nu \frac{d\epsilon_x}{dt} \right)$$

where  $\epsilon_x$  and  $\epsilon_y$  are the strains measured by the gauge on the opposite surface. The equations include both bending and mean stresses.

The results obtained from the test are tabulated below

	Stress (tonf/in <sup>2</sup> )	
	Hoop	Meridional
Inner surface	0.0	3.5
Outer surface	1.0	1.7
Plate material	1.2	0.2

The maximum "layer" stress of  $3.5 \text{ tonf/in}^2$  is small compared with the residual stresses observed previously. (A maximum meridional stress of  $-30 \text{ tonf/in}^2$  was recorded on the inner surface (Fig. 8.17).)

## 8.5 The effect of nominal shape/thickness parameters on end behaviour

### 8.5.1 General

This section covers the effect of variations in the nominal shape and thickness parameters on the elastic, post yield and buckling behaviour of the ends tested. For constant values of two of the three parameters (e.g.  $t_e/D_i$  and  $R_i/D_i$ ) the influence of the third (e.g.  $r_i/D_i$ ) on the stress indices, limit pressures, and first buckling pressures, has been studied.

Throughout this section nominal thicknesses and curvatures have been used, thus enabling the designer to see trends in terms of known quantities (i.e. nominal dimensions). However, the stress indices, limit pressures and first buckling pressures are influenced by the real dimensions and poorly formed ends may thus distort some of the results observed.

### 8.5.2 Elastic behaviour

The dependence of the peak stress indices,  $I_{oc}$  (outer surface circumferential) and  $I_{im}$  (inner surface meridional) on the thickness ratio ( $t_e/D_i$ ) is illustrated in Fig. 8.25. The most notable feature is the lack of consistency among the curves obtained for the three shapes of end. For the ends with  $r_i/D_i$  equal to 0.074 and  $R_i/D_i$  equal to 1.0 there is a reduction in  $I_{im}$  as the thickness ratio is reduced and in  $I_{oc}$  to a ratio of 0.0016, beyond which this index appears to stay constant. This is in contrast with the opinion expressed in ref (6) that peak stress indices increase as the thickness is reduced. However for ends with the same  $r_i/D_i$  ratio but with  $R_i/D_i$  equal to 0.833  $I_{oc}$  increases with reducing

$t_e/D_i$  until a thickness ratio value of about 0.016 is reached. Below this thickness ratio there is a slight reduction in  $I_{oc}$ .  $I_{im}$  for the same ends shows a continuous reduction as the thickness ratio is reduced. For the ends with an  $R_i/D_i$  of 1.0 and  $r_i/D_i$  equal to 0.167 (crown and segment ends) both  $I_{oc}$  and  $I_{im}$  reach maximum values at a  $t_e/D_i$  ratio of about 0.0016. The results produced from this study suggest that there is no simple correlation between the peak stress indices and the nominal thickness to diameter ratio.

The effect on the peak stress indices  $I_{oc}$  and  $I_{im}$  of varying the knuckle radius is shown in Fig. 8.26. The main trend is that the peak stress indices decrease as the knuckle radius is increased. The ends with small knuckle radii experience a large amount of distortion in the knuckle region as the end deforms and thus large stress indices are produced. The lack of consistency previously noted regarding the effect of  $t_e/D_i$  on the stress indices is again clearly illustrated in Fig. 8.26. The curves of both  $I_{oc}$  and  $I_{im}$  against  $r_i/D_i$  show that for two sets of ends tested with  $R_i/D_i$  ratios of 1.0 and  $t_e/D_i$  ratios of 0.00237 and 0.00119 a cross-over point occurs at a  $r_i/D_i$  value of about 0.12. Below this value the thicker ends have higher peak stress indices and above it the thinner ones.

The effect of varying the crown radius ratio ( $R_i/D_i$ ) on the peak stress indices  $I_{oc}$  and  $I_{im}$ , illustrated in Fig. 8.27, does not appear to be consistent over the range of ends tested. For ends with an  $r_i/D_i$  ratio of 0.074 and a  $t_e/D_i$  ratio of 0.00119 or 0.00158  $I_{oc}$  remains practically unchanged as  $R_i/D_i$  decreases from 1.0 to 0.83, but thereafter decreases.  $I_{im}$  decreases as  $R_i/D_i$  decreases in these ends. The deeper end produced by reducing the crown radius is closer in shape to a hemisphere. The distortion in the knuckle will therefore be smaller thus producing lower stress indices. However for the ends with  $r_i/D_i$  ratios of 0.074 and  $t_e/D_i$

ratios of 0.00237 the peak stress indices decrease down to an  $R_i/D_i$  ratio of 0.83 but increase as the ratio is reduced below 0.83. The most likely reason for this is that the end with an  $R_i/D_i$  ratio of 0.83 was poorly formed in the knuckle. This may have resulted in lower stress indices than would otherwise have occurred.

### 8.5.3 Post-yield behaviour

The post yield behaviour is discussed in terms of the effect on the limit pressure of varying the shape parameters and thickness ratio. The limit pressures were obtained as follows :

- i) Calculated from the Shield and Drucker curves (ref. 15), assuming the nominal thickness and dimensions.
- ii) The pressure which produced a permanent strain of 0.1% at the position of maximum strain. (This value of permanent strain has been used since limit pressure values for higher permanent strains could not be obtained for a sufficient number of ends.)
- iii) The pressure given by the type of construction described by Sampayo and Turner (ref. 39) using  $\frac{1}{2}$  the slope of the elastic portion of the pressure-strain curve of the maximum strain position. (See notes associated with Table 7.3).

The Shield and Drucker limit pressure decreases approximately linearly with thickness over the range of thicknesses considered (see Fig. 8.28). The experimental limit pressures are less consistent. Those determined by method (ii) generally decrease as the thickness ratio is decreased. However one shape of end, ( $r_i/D_i = 0.074$ ,  $R_i/D_i = 1.0$ ) shows a slight increase in limit pressure as the  $t_e/D_i$  ratio is reduced from 0.00237 to 0.00158. Limit pressures determined by method (iii) showed a similar feature for each shape of end tested. These latter values are lower than those from method (ii)

and for the spun ends are generally closer to the Shield and Drucker values. However for the crown and segment ends ( $r_i/D_i = 0.167$  and  $R_i/D_i = 1.0$ ) the values calculated by method (iii) are less than those from method (i).

There is a general tendency for the limit pressures to increase, as the knuckle radius becomes larger (Fig. 8.29). However for the smaller  $t_e/D_i$  ratios the effect is relatively small and for ends with a  $t_e/D_i$  ratio of 0.00237 and  $R_i/D_i$  ratio of 1.0 the limit pressure determined by method (iii) shows a pronounced maximum at an  $r_i/D_i$  ratio of 0.11.

The reduction in limit pressure with increasing crown radius ratio ( $r_i/D_i$  and  $t_e/D_i$  constant) is shown in Fig. 8.30. For thicker ends the rate of decrease of the experimental limit pressures lessens as the  $R_i/D_i$  ratio is increased.

#### 8.5.4 Buckling behaviour

The effect on the pressure for the first buckle of varying the thickness ratio whilst holding  $r_i/D_i$  and  $R_i/D_i$  constant is shown in Fig. 8.31 (lower graph). There is a rapid decrease in buckling pressure as the thickness ratio is reduced. The buckling pressures for ends with  $t_e/D_i$  equal to 0.00119 are only about 30% of those for ends with  $t_e/D_i$  equal to 0.00237. The buckling pressures for two of the three shapes of end tested are very close. This indicates that the increase in buckling pressure achieved by increasing the  $r_i/D_i$  ratio from 0.074 to 0.167 is about the same as decreasing the  $R_i/D_i$  ratio from 1.0 to 0.83. The theoretical buckling pressures obtained by Thurston and Holston (ref. 10) for a limited coverage of ends have been used to estimate buckling pressures for some of the ends tested; values are shown in Fig. 8.31 above the experimental curves. The pressures were obtained by extrapolation and therefore give only an approximate indication of the theoretical buckling pressures. The predicted buckling pressures are between 2 and 9 times those observed on the production ends.



The increase in buckling pressure with increasing knuckle radius ratio ( $R_i/D_i$  and  $t_e/D_i$  constant) is illustrated in Fig. 8.32. There is an indication that the effect of varying the knuckle radius becomes less significant for lower  $t_e/D_i$  ratios. This indication is confirmed by the Thurston and Holston estimates.

Reducing the crown radius ratio below 1.0 causes an increase in buckling pressure (Fig. 8.33). Again the largest effect was observed for the thicker ends.

## 8.6 Computations

The experimental coverage was supplemented by a small deflection elastic analysis for end No.4. The computations were carried out by A. Goodman of the Berkeley Nuclear Laboratories of the C.E.G.B. using the finite difference program PATAS (ref. 41) a development of the earlier program PVA2 (ref. 42). The use of this program provided an opportunity to test the validity of computations on an important range of end thicknesses. The program is capable of analysing shell structures which have axisymmetric geometry and loading. Elastic, elasto-plastic, creep and large deformation problems can be solved by the program.

For the analysis of the end it was assumed that the material thickness in the knuckle varied linearly around the arc from the nominal end thickness at the knuckle/crown junction, to the nominal cylinder thickness at the knuckle/cylinder junction. The thickness in the crown and cylinder and the geometry of the end were assumed to be nominal. The lower end of the cylinder was considered to be built-in. A Poisson's ratio value of 0.31 was used.

The results of the analysis (ref. 43) are presented in Fig. 8.34 in the form of elastic stress indices. The corresponding experimental results are given in Fig. A1.4.5 of Appendix 1. There is clearly close agreement between the experimental and computed results. A comparison

between the peak stress indices obtained is given in the table below.

	$I_{im}$	$I_{om}$	$I_{ic}$	$I_{oc}$
<u>Computed</u>	3.89	-2.39	-3.36	-4.94
<u>Experimental</u>				
0° meridian	3.62	-2.84	-3.39	-4.79
45° meridian	3.91	-2.17	-3.35	-5.00
90° meridian	3.60	-2.17	-3.62	-4.99

For each index the computed value lies within the range of values obtained from the test. This close agreement between the computed and experimental values confirms the validity of the program when applied to this type of end and indicates that the assumed thickness variations in the knuckle can give accurate results if the actual thickness variations are similar.

As a logical development of the work the analysis of the post-yield behaviour was considered. Such an analysis would have to take account of the following factors :

1. Variation in material properties along a given meridian due to the effects of work hardening.
2. The residual stress level associated with each position on a meridian.
3. The real geometry of the end.
4. The effect of shape changes.

This development would have been of considerable interest in its own right as a computing exercise but was considered to be of only limited value to the study of these ends. The formation of "bumps" around the circumference of the knuckle prior to buckling produces asymmetric strain distributions which the program is not able to predict. It will be appreciated that for some ends this effect is also present when the material is still acting elastically.

## 8.7 Design considerations

The basic design requirement for these ends is a relatively simple, reliable means of predicting the pressure for the first buckle, or a conservative estimate of that pressure. As a first step towards meeting this requirement the experimentally determined critical pressures were compared with limit pressures, obtained from Shield and Drucker's work (ref. 15), and theoretical pressure values obtained from Thurston and Holston's analysis (ref. 10).

The Shield and Drucker limit pressures were obtained by extrapolating the curves presented in ref. 15. Nominal curvatures and thicknesses were used together with an assumed yield stress of 19 tonf/in<sup>2</sup>.

### 8.7.1 Comparison with limit pressures and theoretical buckling pressures

The values of the ratios of the pressure for the first buckle to the limit pressure (i.e.  $p_{CR}/p_{S\&D}$ ) and the theoretical buckling pressure (i.e.  $p_{CR}/p_{TH}$ ) for each end tested are given in Table 8.1.

The values of the first ratio ( $p_{CR}/p_{S\&D}$ ) over the different sets of ends (characterised by nominal thickness ratio and method of manufacture) show a surprising consistency; mean values are given in the table. The number in each set is relatively small and both the mean value and the spread of the values in a set about the mean must be interpreted with caution. Nevertheless it can be seen that there is no "overlap" between corresponding sets made by the two different processes nor between corresponding sets with ( $t_e/D_i$ ) ratios of 0.00237 and 0.00119.

It is relevant that the ends giving the extreme values within a set generally showed significant shape variations from nominal. For example end 8 ( $p_{CR}/p_{S\&D} = 2.1$ ) was visibly distorted during manufacture in the region where the first buckle occurred. The knuckle radius of end 12 ( $p_{CR}/p_{S\&D} = 3.1$ ) was larger than nominal (see Fig. A1.12.2).

The two base ends (ends No. 7 and 14) with support rings welded to the cylinders 0.5 in from the knuckle have not given consistent results. It is apparent that thickness reductions and shape variations have more influence on buckling pressure than the close proximity of a support ring.

From the mean values given in the table, it is evident that the  $P_{CR}/P_{S\&D}$  ratio is smaller for the crown and segment ends than the corresponding pressed and spun ends. It is not obvious whether this is a feature of the different knuckle radius or the different method of manufacture. Also the ratio for the thicker ends is greater than for the thinner ends.

The consistency and trends evident in Table 8.1 must be considered to some degree fortuitous for the following reasons :

- i) the basis of the limit pressure prediction is the onset of "appreciable plastic deformation" in an ideal-elastic-plastic material and not occurrence of instability.
- ii) nominal dimensions were used in deriving the limit pressures.
- iii) an "as-received plate" yield stress of 19 tonf/in<sup>2</sup> was used in deriving the limit pressures. (It appears that if the actual yield stress was used for the pressed and spun ends a ratio close to unity would be obtained.)

Moreover the  $P_{CR}/P_{S\&D}$  ratios given in the table must be considered specific to ends in this material formed by the two methods used, since, in the elastic buckling range  $P_{CR}$  will depend on Young's modulus - and the limit pressure on the yield stress of the material.

Accepting these points, a useful empirical generalisation of the behaviour of ends over the range tested can be given in the form

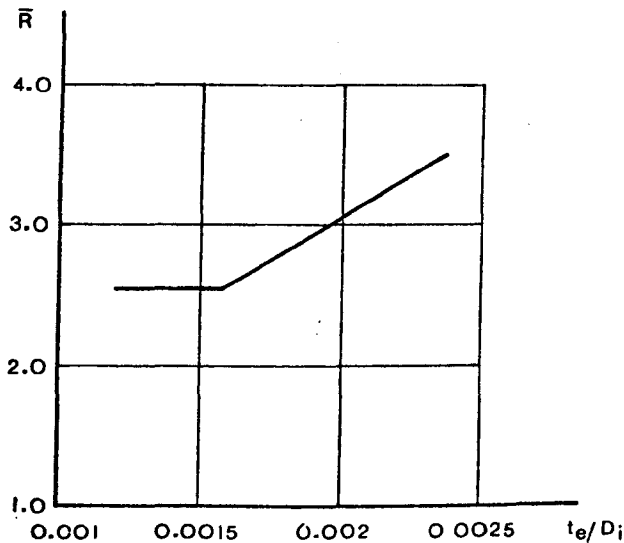
$$P_{CR} = \frac{\bar{R}}{N} P_{S\&D}$$

For the specific thickness ratios studied  $\bar{R}$  is the mean value of the ratio for the pressed and spun ends in Table 8.1, and

$$N = 1 \quad \text{for pressed and spun ends, and}$$

$N = 1.30 + ((1055 t_e/D_i)^{-1} - 0.4)$  for the crown and segment ends.

It is suggested that estimates of  $p_{CR}$  values for similar ends within the thickness ratio range 0.00237 to 0.00119 could be obtained from the above relationship by taking an  $\bar{R}$  value from the graph of Fig. 8.35 and applying the equation for  $N$  over the thickness range.



VARIATION OF  $\bar{R}$  WITH  $t_e/D_i$

FIG. 8.35

There is no similar simple relationship for the critical pressure in terms of the minimum rather than the mean values of the ratio in Table 8.1.

The ratio  $p_{CR}/p_{S\&D}$  has been determined in other investigations; details are given in Table 8.2. Kemper (ref. 24) has presented the ratio for five ends made from high-proof stress stainless steel. The values obtained (1.0 to 1.4) were considerably lower than those for the seventeen test ends. There does not appear to be any marked difference between the ratios obtained for ends produced by different methods. There is some doubt about the method used by Kemper to determine the Shield and Drucker

limit pressures. From ref. 24 it was only possible to determine the value of  $p_{S\&D}$  used for the fourth end. This value ( $24 \text{ lbf/in}^2$ ) was larger than that calculated by the method used in the present study ( $17 \text{ lbf/in}^2$ ). Using a value of  $17 \text{ lbf/in}^2$  the ratio would be increased to 1.9. This value confirms the tendency of the ratio to decrease as the  $t_e/D_i$  ratio is reduced.

Kirk and Gill (ref. 45) have tested some aluminium alloy models (machined from solid). These ends were free from residual stresses and had quite a different form and range of defects. The ratios ( $p_{CR}/p_{S\&D}$ ) for these ends were closer to unity than those obtained for the similar ends in the present study. This is not unexpected as the yield stress value used in calculating the limit pressures for these aluminium ends is closer to the actual value than that used for the stainless steel ends.

The use of the ratio  $p_{CR}/p_{S\&D}$  provides a reasonable means of estimating the buckling pressure of an end.

The ratios of the observed first buckling pressure to the Thurston and Holston buckling pressure (ref. 10) given in Table 8.1 vary from 0.11 to 0.60 and show no regularity or consistency through the different sets. The considerable difficulties of interpolating through the Thurston and Holston data have been mentioned before and must result in an appreciable possible error in the ratio values. Nevertheless it would seem that the Thurston and Holston data provides little assistance in estimating the buckling pressure of an end of the kind studied.

The ratios obtained in other investigations are given in Table 8.2. Kemper's results are of the same order as the present values and are reasonably consistent for the crown and segment ends. However he expresses the view that "the plastic criterion is clearly the one to use for design".

The results of the work of Kirk and Gill on the aluminium models shows some correspondence for the two ends with  $h_i/D_i$  greater than 0.2

(models 4B and 4C) but all the ratios are far from unity.

The model results of Adachi and Benicek (ref. 12) appeared to confirm the validity of the analysis of Thurston and Holston. The analysis cannot be applied with accuracy or even consistency to production ends or a series of metallic models machined from solid. The implication is that the behaviour of an end is markedly dependent on the manufacturing defects.

### 8.7.2 Alternative approaches

The attempt to obtain a relationship between the critical pressure and the end dimensions was pursued by considering the toroidal knuckle as a simple structural element subjected to a buckling load. The first approach was not successful but is outlined here as a precursor to the subsequent treatment.

#### 8.7.2.1 The knuckle as a ring subjected to external pressure

The steps involved were :

- i) The mean compressive hoop stress ( $\bar{\sigma}_\theta$ ) (averaged over the knuckle arc) acting in the knuckle was obtained from simple membrane theory in terms of the internal pressure ( $p$ ) and the nominal end dimensions.
- ii) The external pressure ( $p_o$ ) that would produce the same mean compressive hoop stress in the free knuckle was derived, again using simple membrane theory. Thus a relationship between  $p_o$  and  $p$  was obtained.
- iii) A critical value of  $p_o$  (and hence of  $p$  ( $p_{CR}$ )) was determined from the relationship (ref. 46) for the critical unit load ( $q_{CR}$ ) of a ring subjected to external pressure i.e.

$$q_{CR} (= p_{OCR} r \alpha) = \frac{3EI}{r^2} \quad (8.1)$$

In this expression I is the second moment of area of the knuckle section

$$\left(\frac{r^3 t}{2} \left(\sin \alpha + \alpha - \frac{8}{\alpha} \sin^2 \frac{\alpha}{2}\right) \text{ for a "thin" section};\right.$$

$r_2$  is the effective radius of the knuckle toroid, taken as the circumferential radius of curvature at the centre of the knuckle

$$\left(r + \left(\frac{D}{2} - r\right) \sec \frac{\alpha}{2}\right),$$

The resulting expression was :-

$$P_{CR} = -3E \left(\frac{r}{D}\right)^3 \left(\frac{t_e}{D}\right) \frac{\left[\sin \alpha + \alpha - \frac{8}{\alpha} \sin^2 \frac{\alpha}{2}\right]}{\left[\frac{r}{D} + \left(\frac{1}{2} - \frac{r}{D}\right) \sec \frac{\alpha}{2}\right]^2 \left[\left(\frac{r}{D}\right)^2 \alpha - \left(\frac{1}{2} - \frac{r}{D}\right) \left(\frac{R}{D} - \frac{r}{D}\right) \sin \alpha\right]} \quad (8.2)$$

This expression was evaluated, using nominal dimensions, for each end. The resulting values were invariably low compared with the corresponding experimental value and showed a pronounced dependence on the knuckle radius ratio ( $r/D$ ). (For example, end 1 ( $r_i/D_i = 0.167$ )  $P_{CR} = 75.1 \text{ lbf/in}^2$ ; end 4 ( $r_i/D_i = 0.074$ )  $P_{CR} = 3.1 \text{ lbf/in}^2$ ).

A number of assumptions had been made in deriving equation (8.2) but the over-riding conclusion from this preliminary work was that the  $n = 2$  mode of buckling incorporated in the equation for the critical unit load (equation (8.1)) did not provide a basis for a useful estimate of the experimental buckling pressure.

A particular feature of this preliminary work which was carried over into the subsequent treatment, was the use of the mean compressive hoop stress in the knuckle and its derivation from membrane theory. The Zick and Germain reference (44) was referred to at this stage of the work. Alternatively, the mean compressive hoop stress could have been found directly from the experimental hoop stress index plots, or indirectly from the meridional stress indices as Thurgood (ref. 47) appears to have done. It was considered more useful to retain the simple membrane approach.



### 8.7.2.2 The knuckle as a "column" with a transverse elastic support.

An approach which incorporated a better approximation to the complex buckling mode of the knuckle toroid was required. That proposed by Kirk and Gill (ref. 45) in which the knuckle is treated as a column (or strut), with a transverse elastic support, subjected to a compressive load was used. For such a column, it can be shown (ref. 46) that the critical load P is given by

$$P_{CR} = 2\sqrt{kEI} \quad (8.3)$$

and that the semi-wavelength ( $\frac{\lambda}{2}$ ) of the buckles by

$$\frac{\lambda}{2} = \pi \sqrt[4]{\frac{EI}{k}} \quad (8.4)$$

where k is the stiffness (or modulus) of the elastic "foundation" i.e. the reactive force per unit area for unit transverse displacement. Kirk and Gill (Ref. 45) have produced an approximate expression for k of the form :

$$k = \frac{Et}{1-\nu^2} \left[ \frac{r^2 + 2\nu r r_2 + r_2^2}{r^2 r_2^2} \right] \quad (8.5)$$

Again the membrane theory expression for the mean compressive hoop stress in the knuckle has been used :-

$$\bar{\sigma}_\theta = \frac{p}{rat} \left[ \frac{r^2 \alpha}{2} - \frac{1}{2} \left( \frac{D}{2} - r \right) (R - r) \sin \alpha \right] \quad (8.6)$$

Using equations (8.3) and (8.6) the following expression has been obtained for the critical pressure

$$P_{CR} = \frac{-2ra \sqrt{kEI}}{\left( \frac{r^2 \alpha}{2} - \frac{1}{2} \left( \frac{D}{2} - r \right) (R - r) \sin \alpha \right)} \quad (8.7)$$

where  $I = t_e^3/12(1-\nu^2)$  for a unit width of shell.

With k values from equation (8.5), values of  $p_{CR}$  have been obtained from this equation for all ends tested. They are tabulated in Table 8.3

together with the measured first buckle pressures; the ratios  $p_{CR}$  (experimental)/ $p_{CR}$  (calculated) are also given. In evaluating the equations, values of  $r_i$ ,  $R_i$  and  $D_i$  have been used for  $r$ ,  $R$  and  $D$  respectively.

The calculated critical pressures are considerably greater than the corresponding experimental values. The ratios show some consistency. Average values for each set are given in the table; the relative "spread" within each set about the mean is of the same order as that shown by the  $p_{CR}/p_{S\&D}$  values in Table 8.1. With some caution the mean ratio values and the "spreads" can be commented upon. Again there is no "overlap" in the ranges of ratio values for corresponding sets made by the two different processes. There is a small "overlap" for the pressed and spun ends with  $t_e/D_i = 0.00237$  and  $t_e/D_i = 0.00119$  but the values within the two sets are within 12% of the corresponding mean value. There is an indication of an increase in the ratio with decrease in  $r_i/D_i$  ratio in the pressed and spun ends with  $t_e/D_i$  equal to 0.00119 (see ends 8, 9 and 12) but it must be recalled that values for ends 8 and 12 (the extreme values in the set) were possibly not representative.

The mean ratio is greater for the pressed and spun ends than for the crown and segment ends. It is greater for the thinnest pressed and spun ends than for the thicker ends of this type. The thickness trend for the crown and spun ends is not well defined.

In appraising the figures in Table 8.3 the following points are relevant :-

- i) The calculations give an approximate value for a nominally perfect end; the experimental value will depend to a considerable degree on the severity of the governing defect in the end.
- ii) An approximate value of  $k$  is obtained from equation (8.5), only radial displacement being considered in its derivation.

- iii) The expression for I must be considered approximate.
- iv) The buckling mode assumed (a sinusoidal wave-form) does not appear to be the mode observed. Nevertheless the "width" of the buckles was of the same order of magnitude as that given by equation (8.4) in practically all cases.
- v) The non-uniformity of the hoop stress around the knuckle has been ignored.

The data in Table 8.3 offer a sounder basis for generalisations on end behaviour, particularly for design purposes, than the data in Table 8.1. For example a conservative estimate (i.e. a lower bound) of the critical pressure of ends similar to those tested is obtained from the expressions :-

0.3  $p_{CR}$  for pressed and spun ends.

0.2  $p_{CR}$  for crown and segment ends.

where  $p_{CR}$  is the value obtained from equation 8.7.

Alternatively, with interpolation, an estimate of the buckling pressures for production ends ( $\bar{p}_{CR}$ ) within the thickness ratio range 0.00237 to 0.00119 can be obtained from the relationship :-

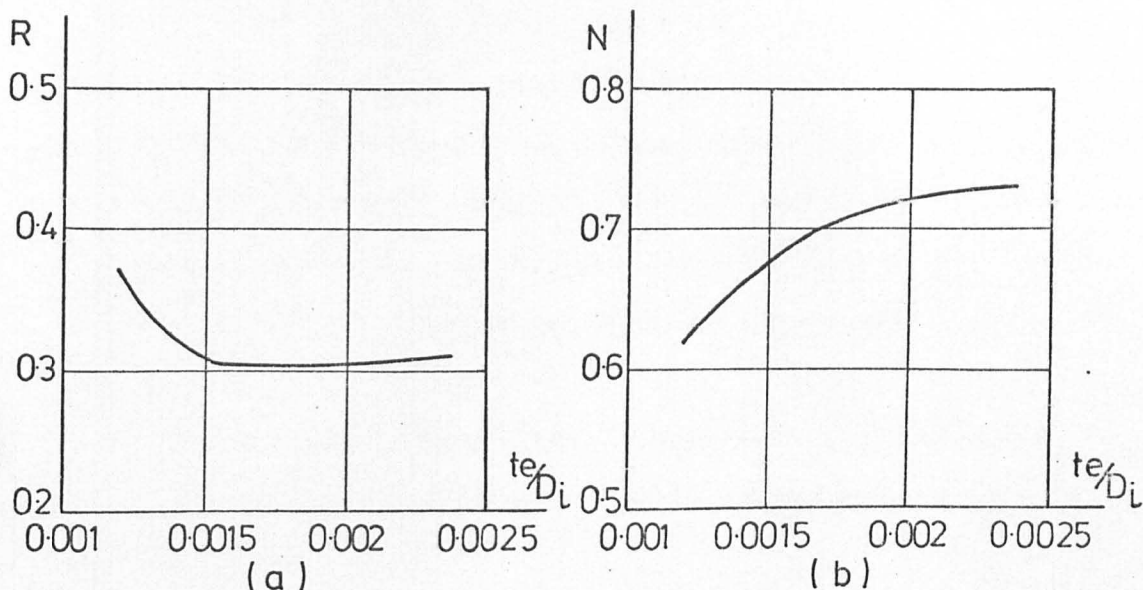
$$\bar{p}_{CR} = R N p_{CR}$$

where R is obtained from Fig. 8.36a for both types of end,

N = 1 for pressed and spun ends, and

N is obtained from Fig. 8.36b for crown and segment ends.

The value of the ratio  $p_{CR}(\text{measured})/p_{CR}(\text{calculated})$  has also been calculated for one end tested by Kemper (ref. 24) (design number 4) and the ends tested by Kirk and Gill (ref. 45). The results are given in the Table 8.4.



DETERMINATION OF R AND N

FIG 8.36

The end tested by Kemper confirms the tendency for the ratio to become larger as the  $t_e/D_i$  ratio is reduced. This pressed and spun end was made from the same material as the seventeen test ends.

The values of the ratio obtained for the Kirk and Gill ends increase as the knuckle radius increases. The possibility of there being a contrary trend in the 108 in diameter stainless steel ends was mentioned previously. This could not be confirmed and it is relevant that the type and severity of the defects in the one set of ends would be quite different from those in the other.

### 8.7.3 Range of buckling pressures

A significant feature of the behaviour of test ends was the occurrence of the buckles over a range of pressure, rather than simultaneously. For example (see Table 7.4) in end No.8 the first buckle occurred at  $70 \text{ lbf/in}^2$  and the fifth at  $94 \text{ lbf/in}^2$ , a pressure increase of 34%; in end No.15 the first buckle occurred at  $107 \text{ lbf/in}^2$  and the ninth at  $219 \text{ lbf/in}^2$ , a pressure increase of 105%.

It is usual for the first five or six buckles to be reasonably uniformly spaced around the circumference of the knuckle and it is probable that these buckles do not influence each other. However subsequent buckles may be affected by the existing buckles. It was notable that the later buckles on the 81 in diameter ends were less "noisy" than the earlier ones; this may be associated with geometry changes.

There is no apparent pattern in the positions of successive buckles, although eventually a more or less regular pattern of buckles is produced.

The pressure at which a buckle occurs, and its position, are clearly dependent on the variety and severity of the defects present. As it is unlikely that two nominally identical ends will have defects of the same severity it is clearly possible for one end to have a lower first buckling pressure than the other.

During manufacture care should be taken to avoid distortions in the knuckle region and thin areas produced by undercutting in the area of welds.

#### 8.7.4 Time-dependence of buckling

The time taken to produce a buckle once a particular pressure level had been reached varied from a few seconds (e.g. first buckle on end No.4) to several hours (e.g. fourth buckle on end No.12). (See also ref. 8) Cold creep effects are clearly responsible for this time-dependence. The material in the knuckle region creeps until a critical condition for the load applied is reached. This suggests that the pressure at which a particular buckle forms is dependent on the length of time for which the pressure is held and it follows that many of the buckles produced on the test ends many have formed at lower pressures if these had been

applied for a very long period of time.

The time-dependence of the buckling must be considered when proof-testing this type of vessel. The test pressure must be held long enough to ensure that no buckling will occur.

#### 8.7.5 Materials

Throughout this project higher proof stress 304 stainless steel has been used for the endstested. However the use of this grade will not increase the strength of an end if elastic buckling is the mode of failure. Therefore for ends with a  $t_e/D_i$  ratio less than about 0.0015 the use of a higher proof stress stainless steel is unlikely to produce any increase in buckling pressure.

For elastic buckling the critical pressure is proportional to the Young's modulus of the material and the results for the thinnest ends can be applied to ends made from other materials if the different imperfections likely to occur are taken into account. However an end of a given shape which fails by elastic buckling when made from stainless steel may fail by plastic buckling or excessive deformation when made from a material with a very low yield stress.

Table 8.1: Ratios of experimental buckling pressure to limit pressure (ref. 15) and theoretical buckling pressure (ref. 10)

End No.	$t_e/D_i$ (nominal)	Pressed and spun		Crown and segment	
		$P_{CR}/P_{S\&D}$	$P_{CR}/P_{TH}$	$P_{CR}/P_{S\&D}$	$P_{CR}/P_{TH}$
1 *	0.00237			2.7	0.13
2	0.00237			2.7	0.13
3	0.00237	3.2	0.22		
4	0.00237	3.3	0.45		
5	0.00237	3.9	—		
6	0.00237	<u>3.6</u>	—	<u>      </u>	
Mean		3.50		2.7	
7 *	0.00119			1.3	0.14
8	0.00119	2.1	0.26		
9	0.00119	2.5	0.39		
10	0.00119	2.6	—		
11	0.00119	2.4	—		
12	0.00119	3.1	0.60		
13	0.00119	<u>      </u>		<u>1.7</u>	0.19
Mean		2.54		1.5	
14 *	0.00158			1.8	0.13
15	0.00158			1.6	0.11
16	0.00158	2.6	0.41		
17	0.00158	<u>2.5</u>	—	<u>      </u>	
Mean		2.55		1.7	

\* Base ends

Table 8.2: Other ratios of experimental buckling pressure to limit pressure (ref.15)  
and theoretical buckling pressure (ref. 10)

Reference	$\frac{t_e}{D_i}$	$\frac{r_i}{D_i}$	$\frac{R_i}{D_i}$	Material	Manufacture	$\frac{P_{CR}}{P_{S\&D}}$	$\frac{P_{CR}}{P_{TH}}$	
<u>Kemper (24)</u>								
1	0.0012	0.16	0.91	High-proof 304 S/S	C & S	1.1	0.23	
2	0.0011	0.163	1.0	High-proof 347 S/S	C & S	1.2	0.21	
3	0.0011	0.166	1.0	High-proof 304 S/S	C & S	1.2	0.22	
4	0.00095	0.063	1.0	High-proof 304 S/S	S	1.4	0.21	
5	0.00081	0.075	1.0	High-proof 304 S/S	S	1.0	0.16	
<u>*Kirk and Gill (45)</u>						<u>LB</u>		
4A	0.00188	0.075	1.0	) Aluminium Alloy ) BS 1476 HE30 WP )	Machined from solid bar	1.1	0.16	
4B	0.00188	0.113	1.0			1.3	1.0	0.28
4C	0.00188	0.169	1.0			1.8	1.5	0.29
						<u>UB</u>		

\* Both lower bound (LB) and upper bound (UB) limit pressures were obtained.



Table 8.3 : Calculated and measured buckling pressures

All pressures are in lbf/in<sup>2</sup>

End No.	$t_e/D_i$ (nominal)	Pressed and Spun			Crown and Segment		
		Critical Pressure		Ratio	Critical Pressure		Ratio
		Calculated	Measured		Calculated	Measured	
1*	0.00237				1225	280	0.229
2	0.00237				1225	278	0.227
3	0.00237	843	248	0.294			
4	0.00237	692	198	0.286			
5	0.00237	812	278	0.343			
6	0.00237	861	278	0.323			
	Mean			0.312			0.228
7*	0.00119				306	60	0.196
8	0.00119	211	70	0.332			
9	0.00119	173	62	0.358			
10	0.00119	203	78	0.384			
11	0.00119	229	86	0.375			
12	0.00119	159	66	0.416			
13	0.00119				306	82	0.268
	Mean			0.373			0.232
14*	0.00158				545	120	0.220
15	0.00158				545	107	0.197
16	0.00158	308	95	0.309			
17	0.00158	361	107	0.297			
	Mean			0.303			0.209

\* Base ends

Table 8.4 Calculated and measured buckling pressures for other ends.

Reference	$\frac{t_e}{D_i}$	$\frac{r_i}{D_i}$	$\frac{R_i}{D_i}$	Critical pressure		Ratio
				calculated	measured	
Kemper (24)						
4	0.00095	0.063	1.0	68.4	32.9	0.481
Kirk & Gill(45)						
4A	0.00188	0.075	1.0	141.9	35.0	0.246
4B	0.00188	0.113	1.0	171.4	54.8	0.320
4C	0.00188	0.169	1.0	245.5	109.9	0.448

All pressures are in lbf/in<sup>2</sup>

STRESS STRAIN CURVES OF  
HIGHER PROOF STRESS 304  
STAINLESS STEEL

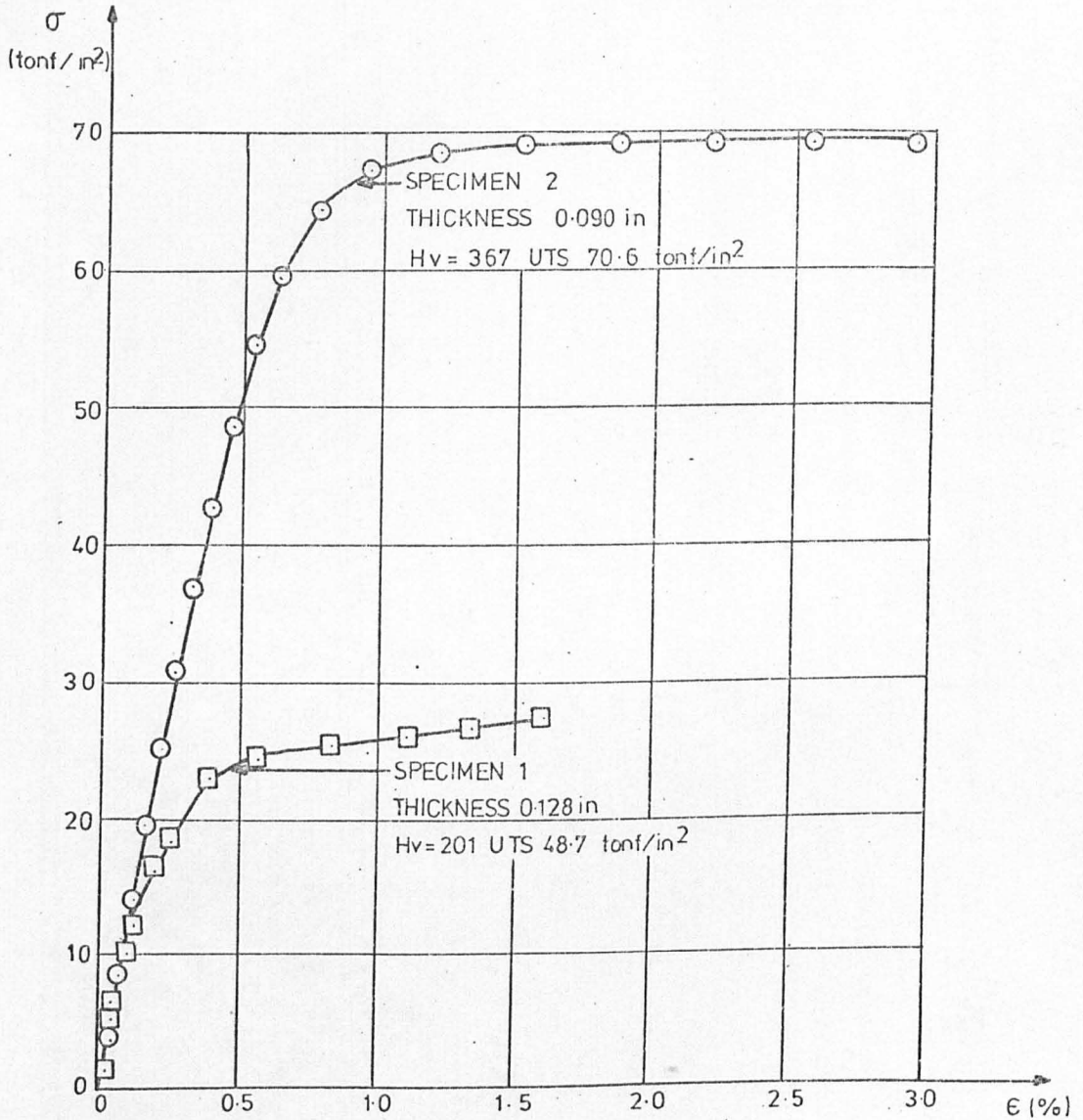


FIG 8-11

CHANGE IN VICKERS HARDNESS NUMBER  
AGAINST REDUCTION IN THICKNESS

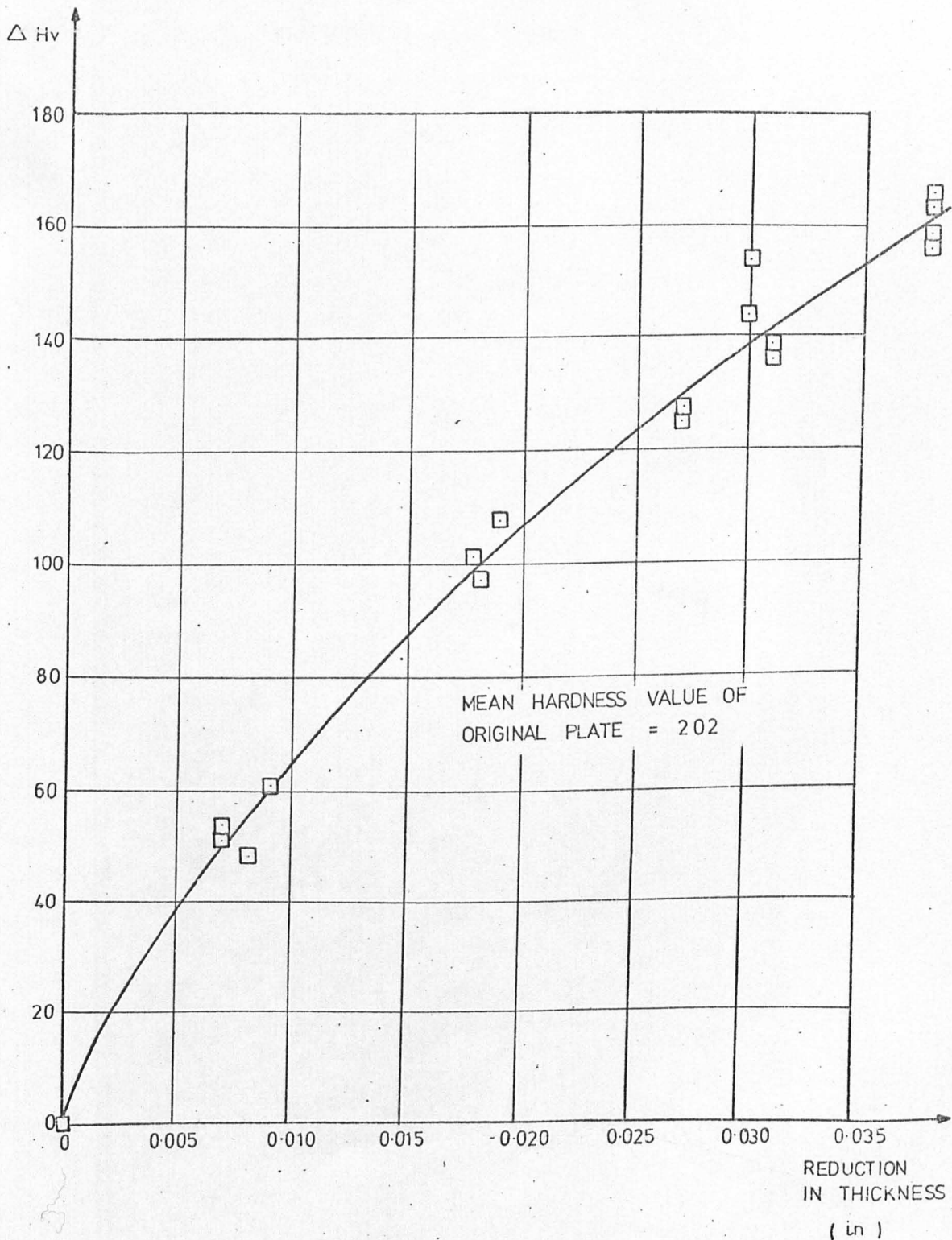
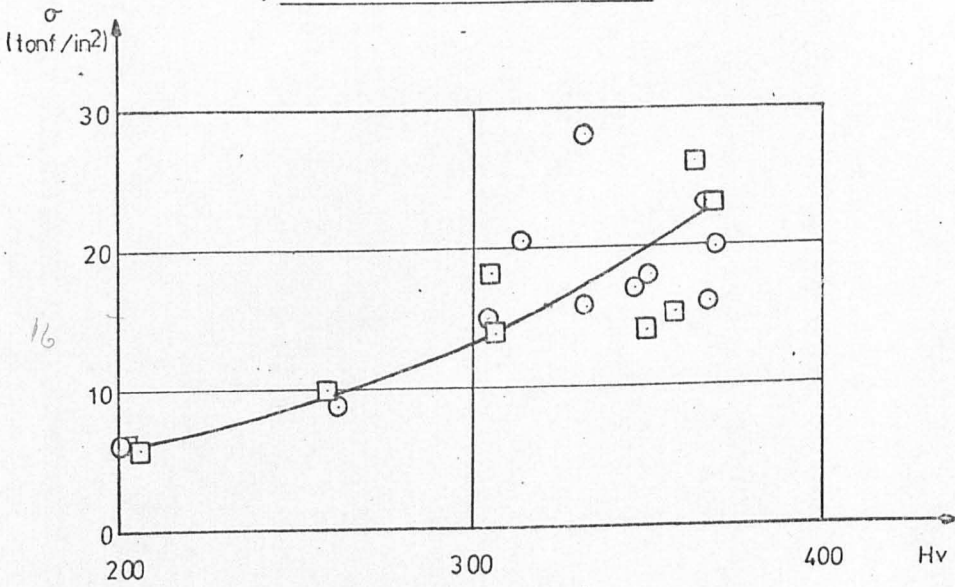
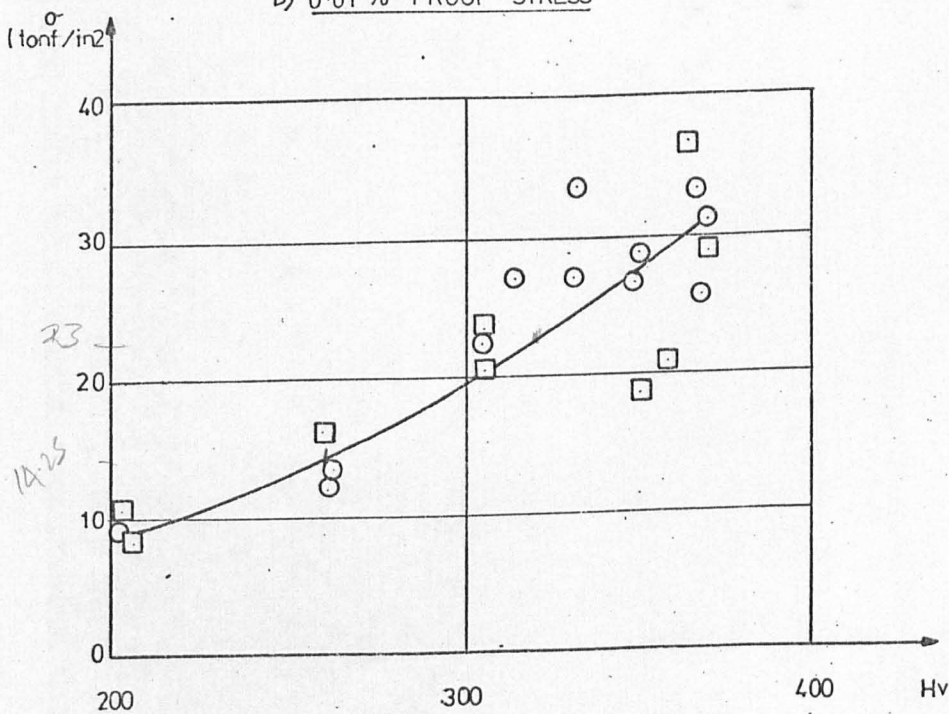


FIG 8-12

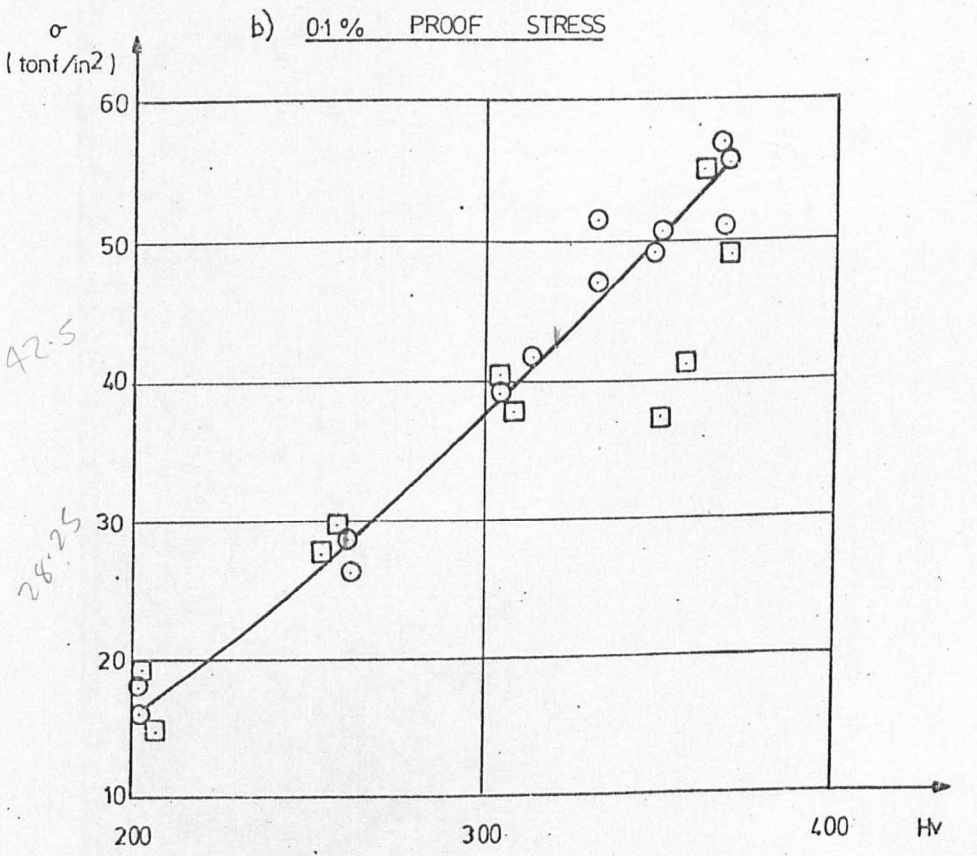
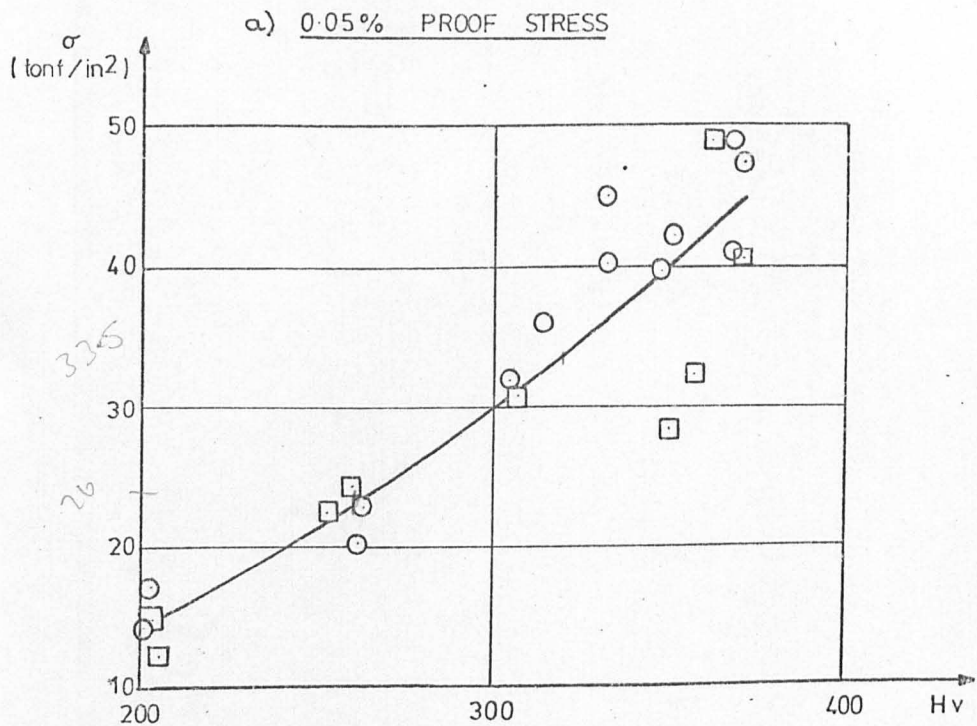
a) PROPORTIONAL LIMIT STRESS



b) 0.01% PROOF STRESS



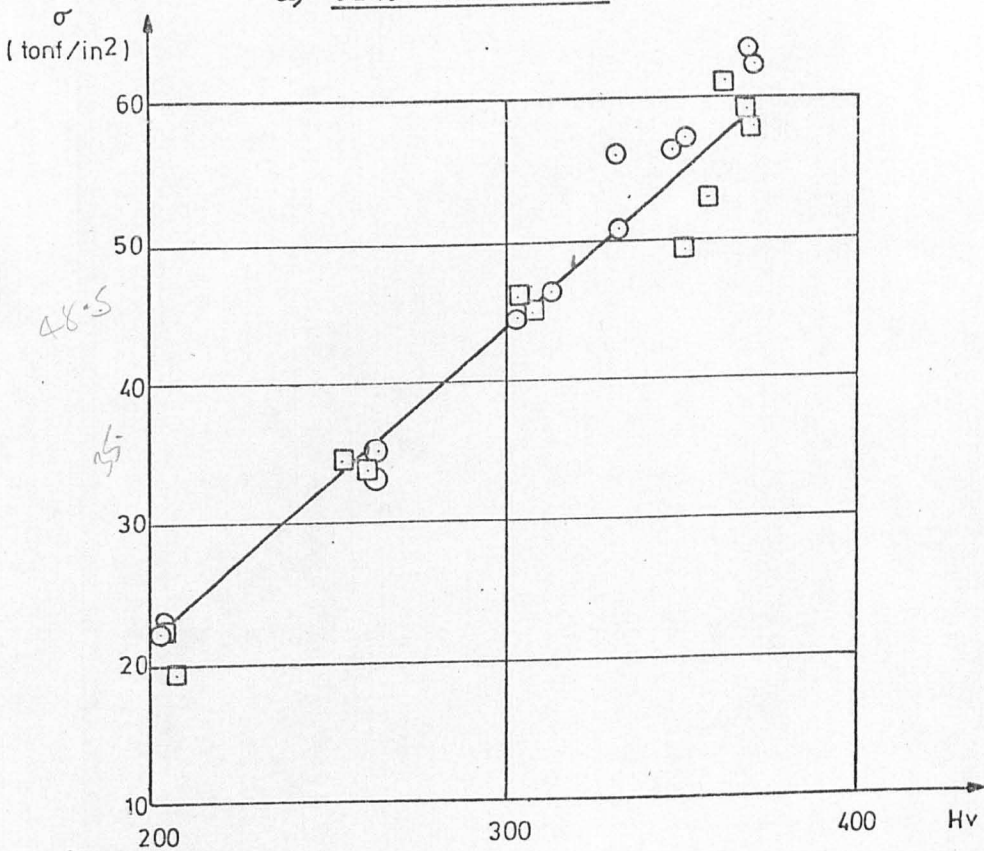
- Specimen rolled along length
- Specimen rolled across width



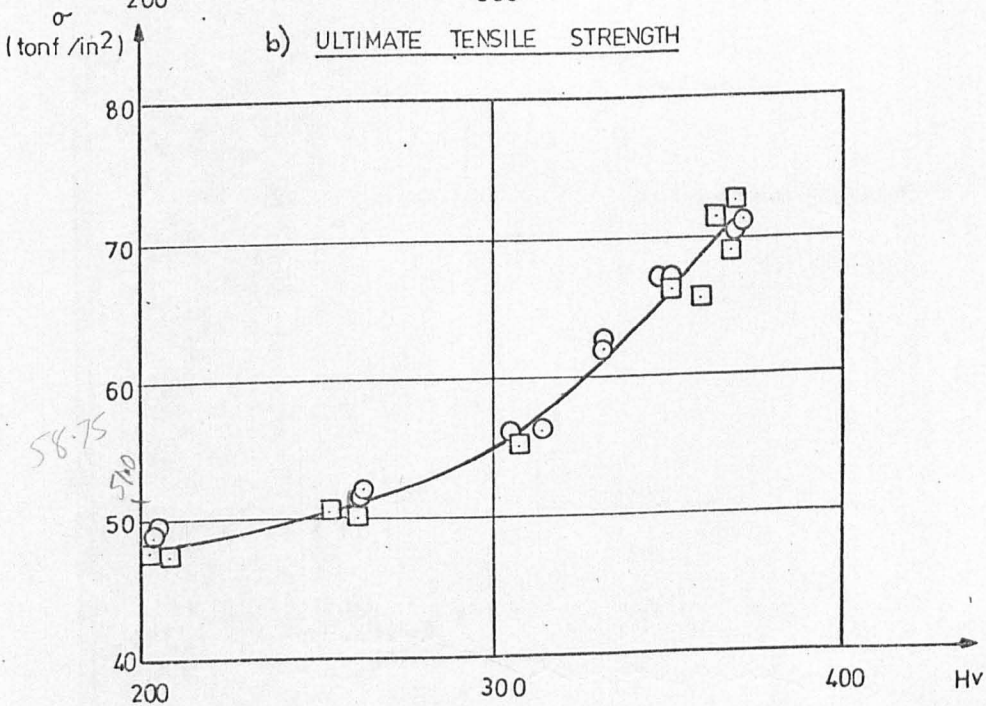
- Specimen rolled along length
- Specimen rolled across width

FIG 8-14

a) 0.2% PROOF STRESS



b) ULTIMATE TENSILE STRENGTH



- Specimen rolled along length
- Specimen rolled across width

FIG 8-15

# RESIDUAL LOADS AND STRESSES FOR END No.10

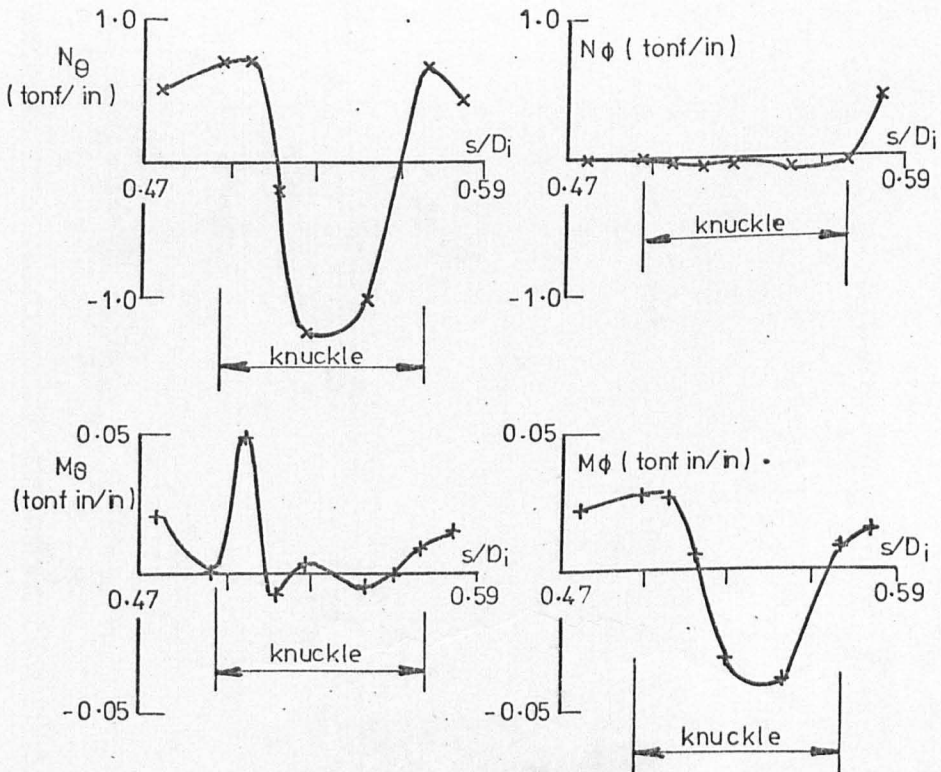
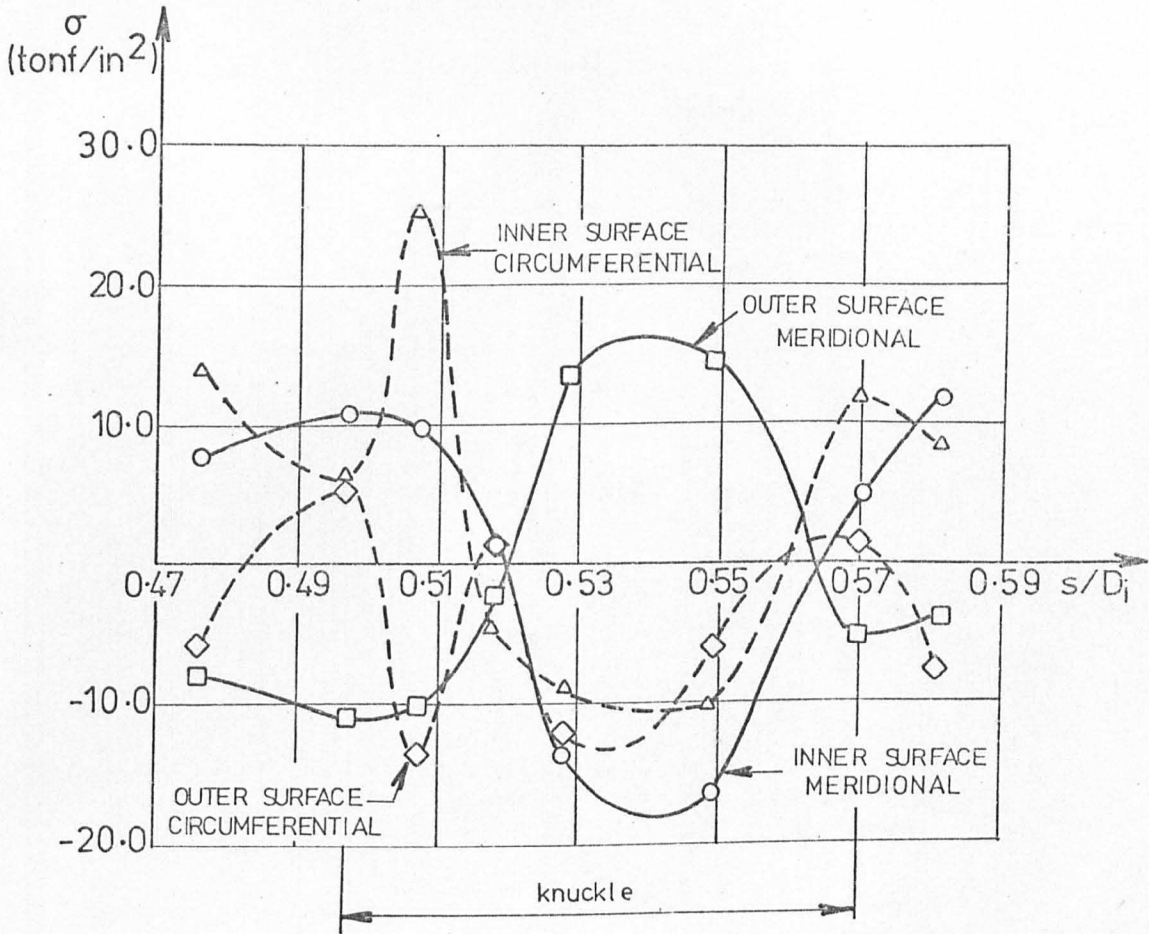


FIG 8-16



RESIDUAL LOADS AND STRESSES  
FOR END No.11

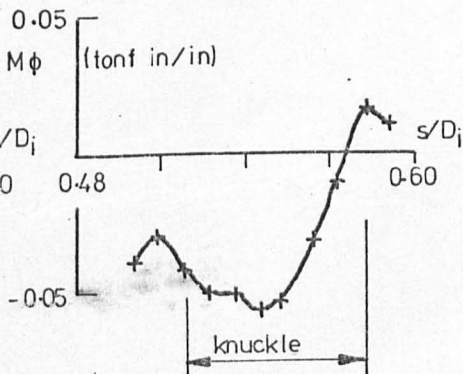
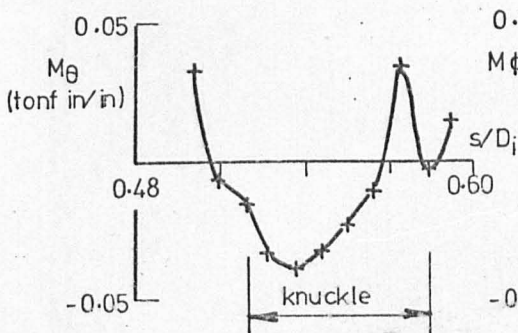
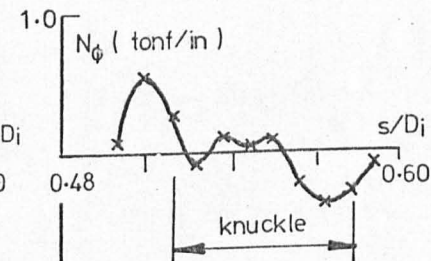
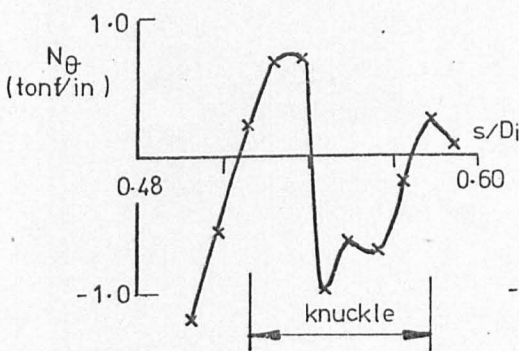
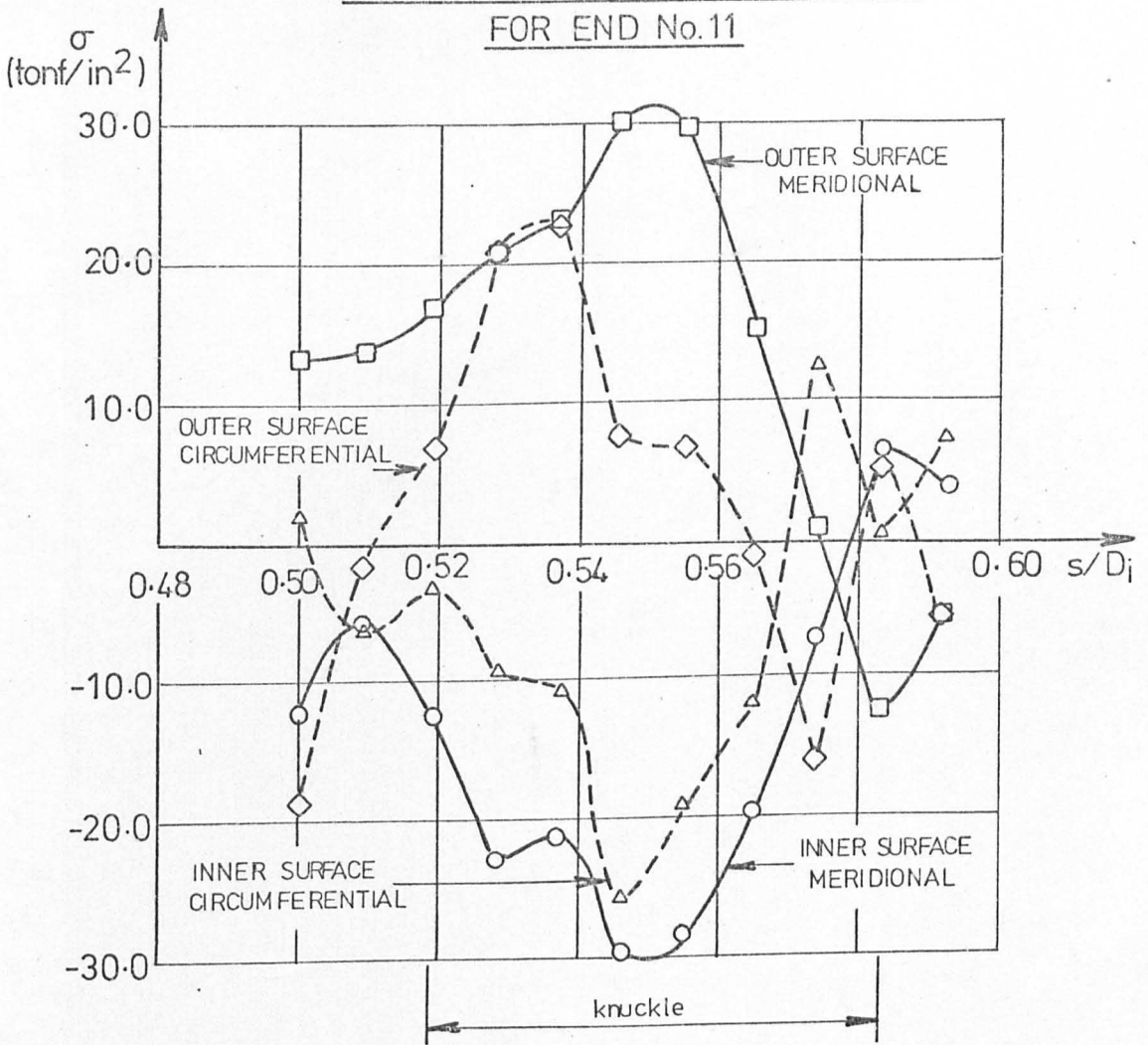


FIG 8-17

RESIDUAL LOADS AND STRESSES FOR END No.13

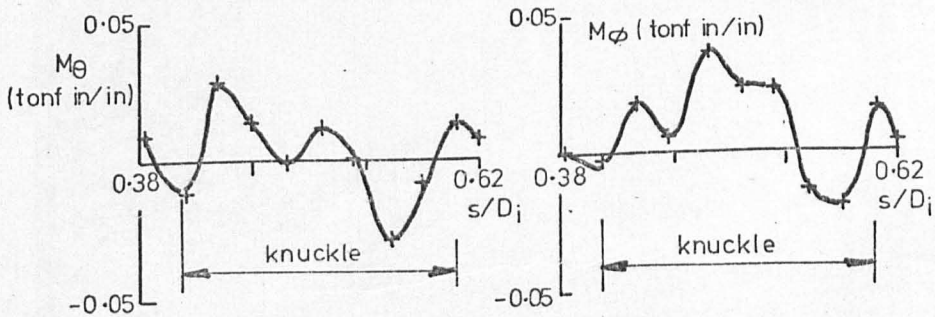
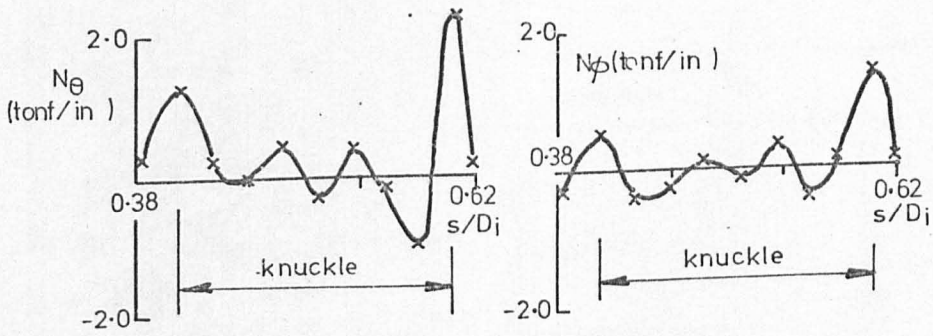
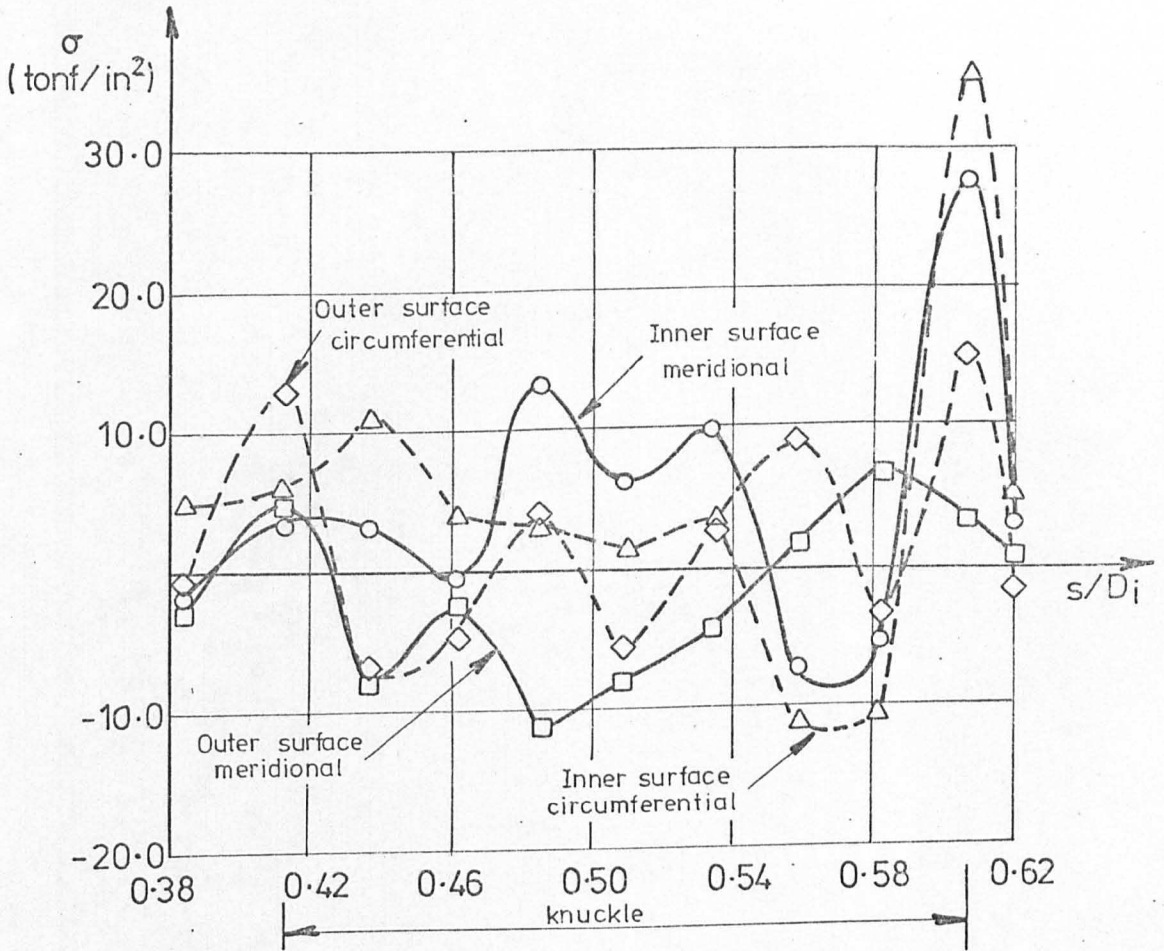


FIG 8-18

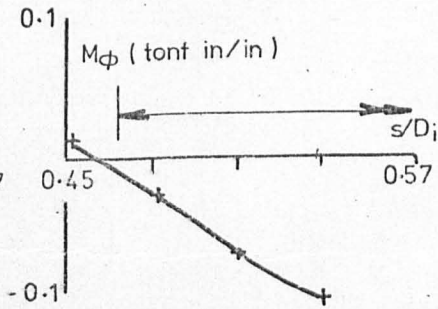
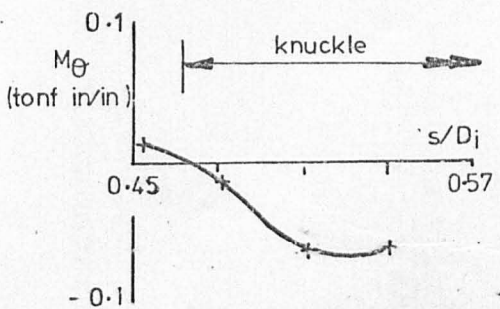
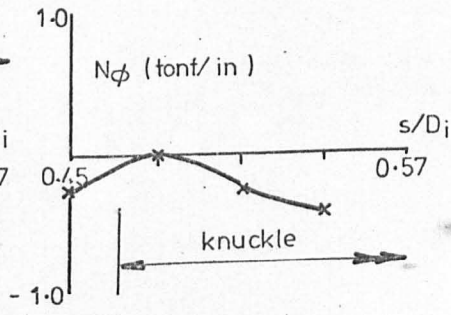
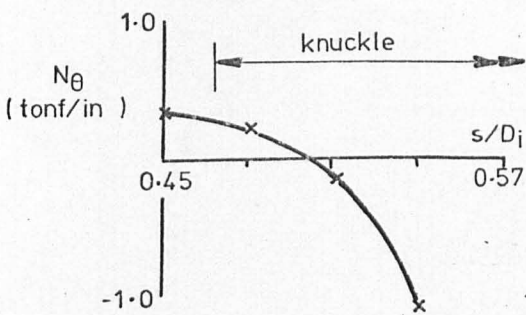
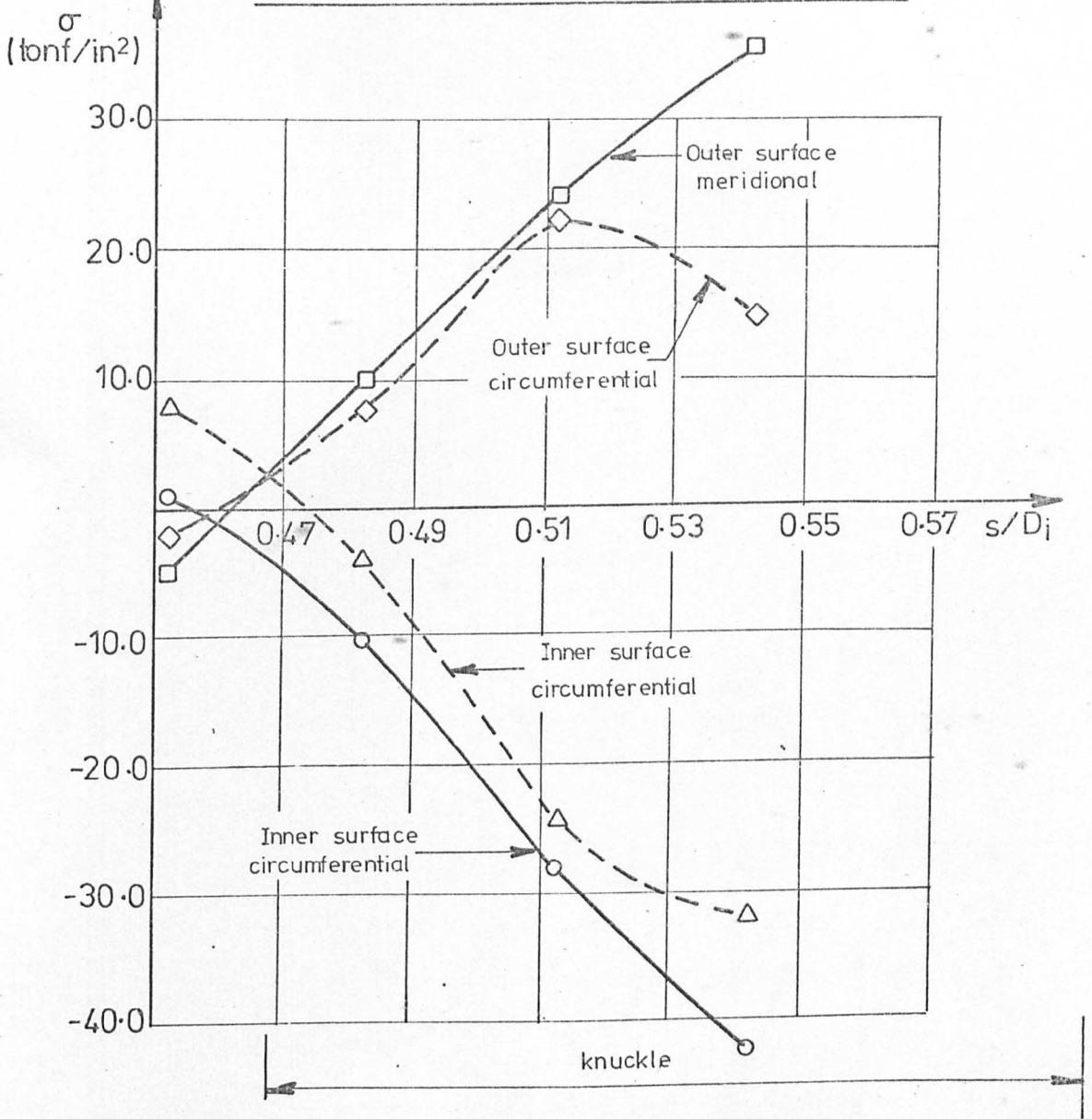


FIG 8-19

COMBINED PRESSURE AND RESIDUAL STRESSES

FOR END No.10

$p = 30 \text{ lbf/in}^2$

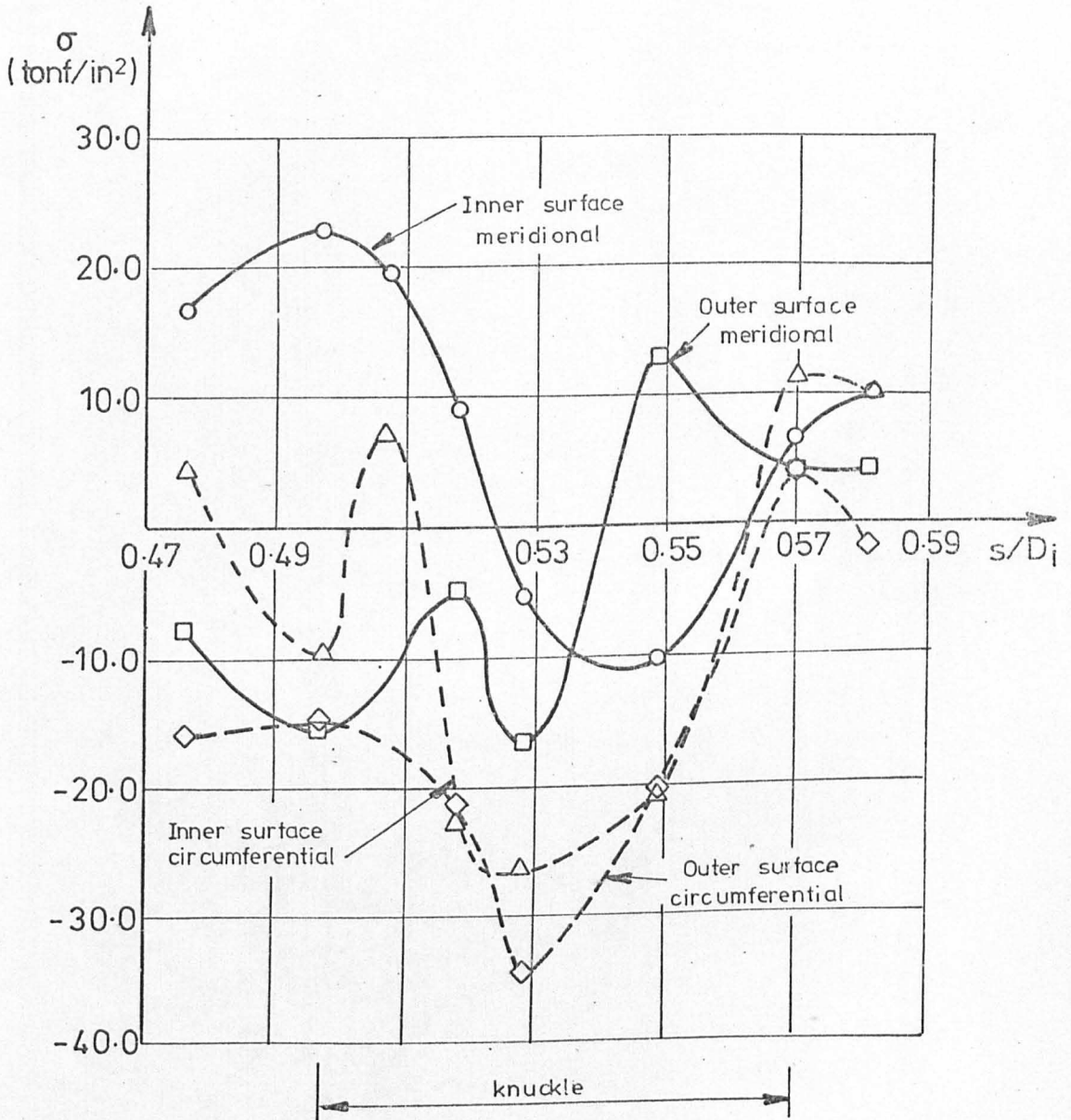


FIG 8-20

COMBINED PRESSURE AND RESIDUAL STRESSES

END No. 11

$p = 30 \text{ lbf/in}^2$

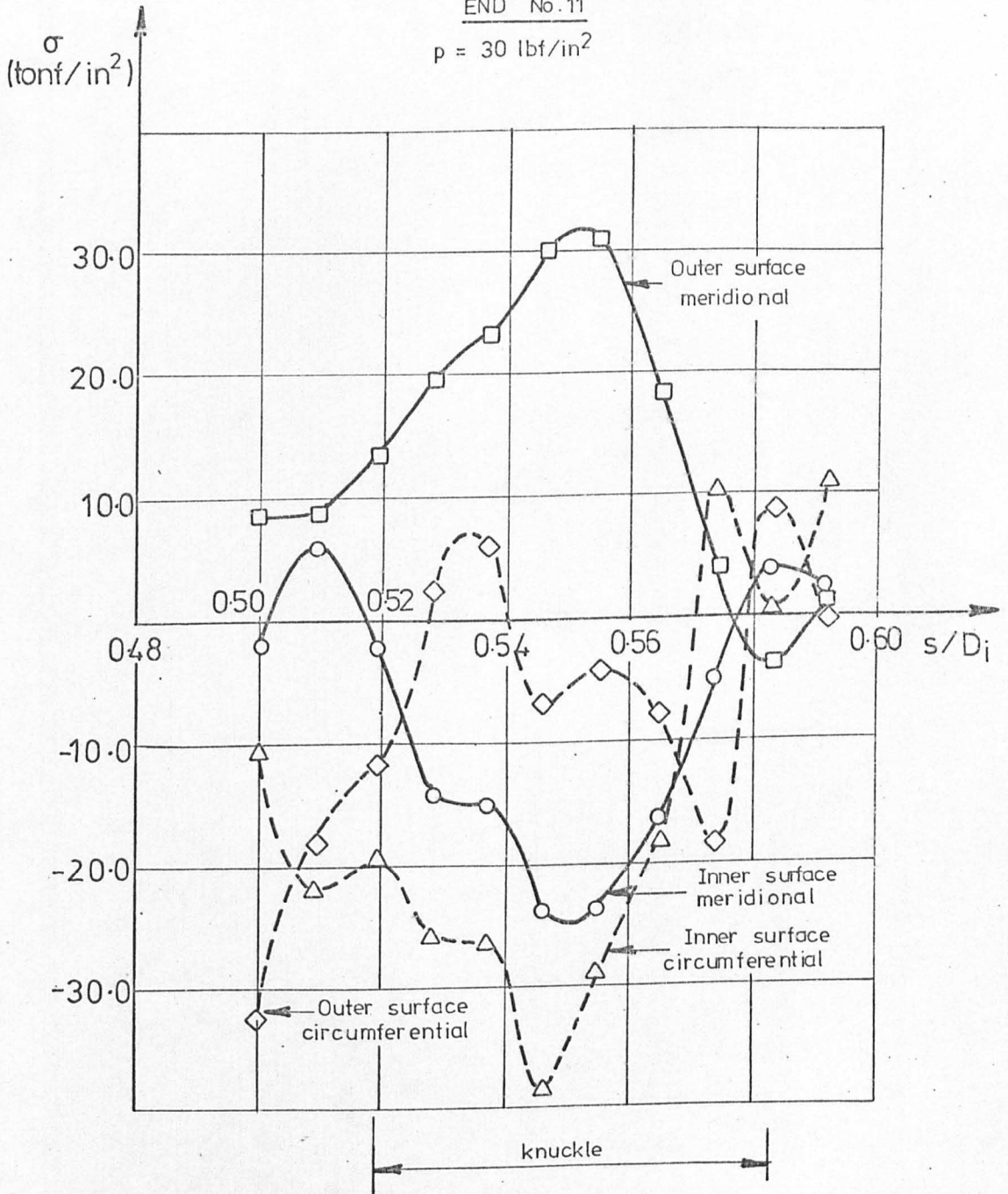


FIG 8-21

SURFACE HARDNESS IN KNUCKLE REGION

(VICKERS HARDNESS NUMBER PLOTTED AGAINST)

POSITION

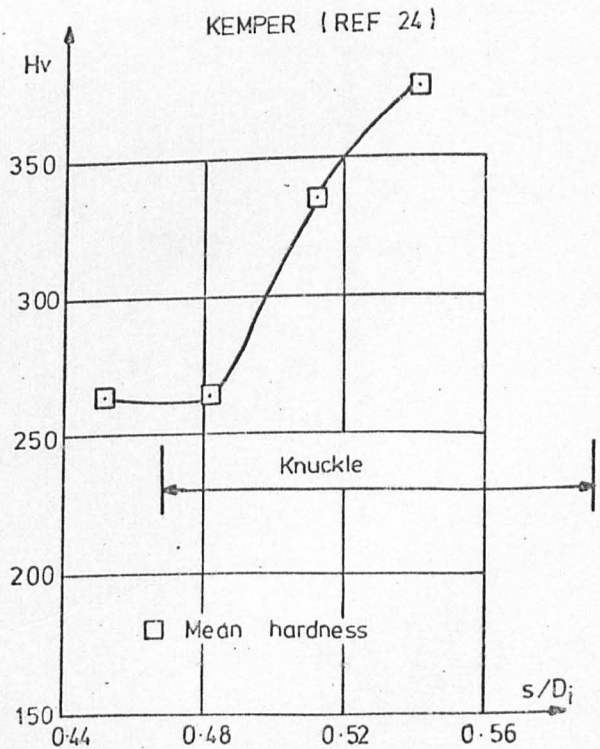
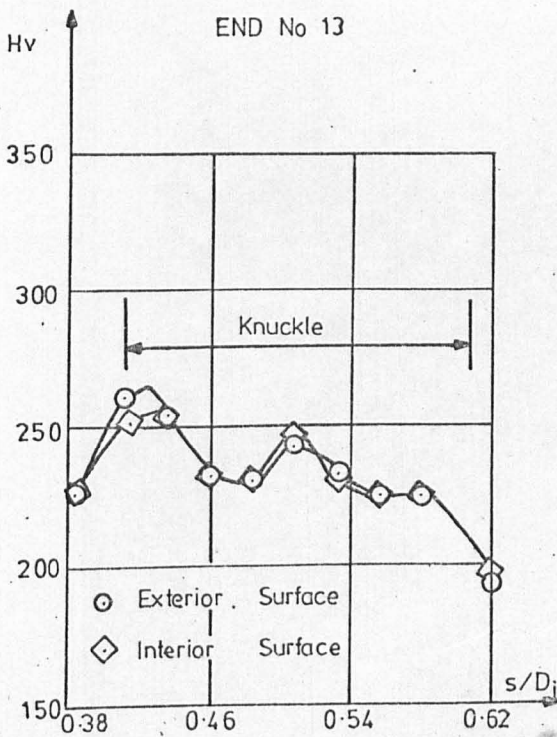
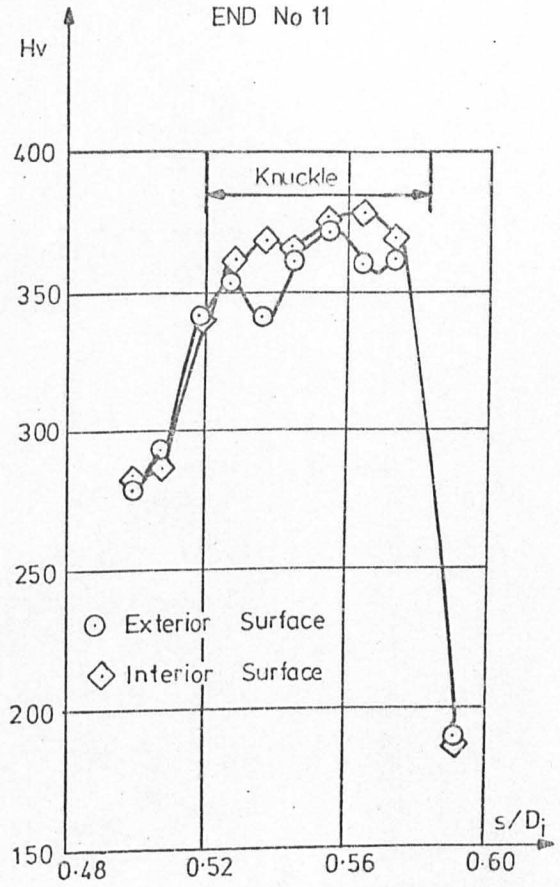
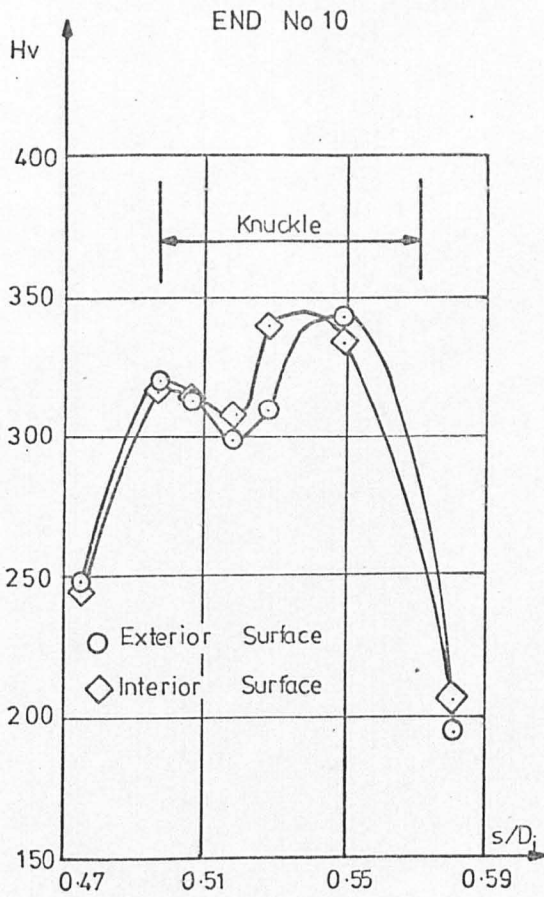


FIG 8-22

DERIVED AND MEASURED EQUIVALENT  
RESIDUAL STRESSES

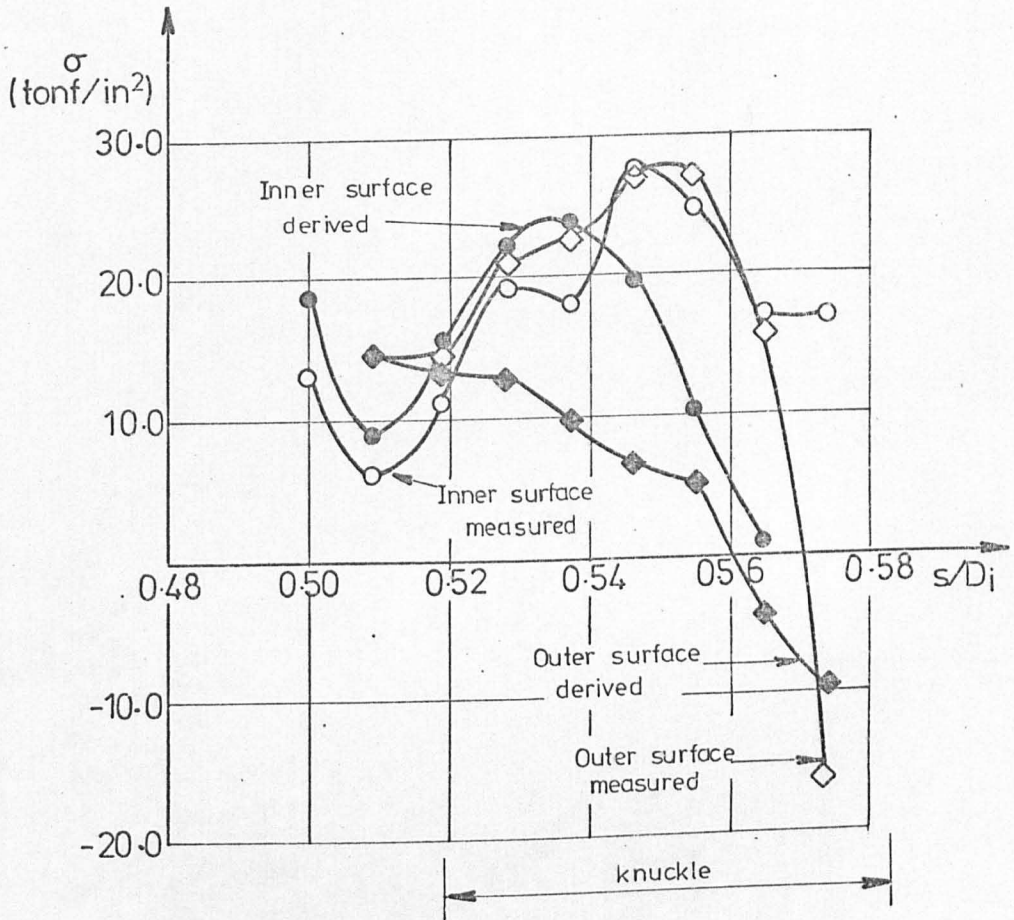


FIG 8-23

THE EFFECT OF THICKNESS ON  
THE PEAK STRESS INDICES

$I_{oc}$  AND  $I_{im}$

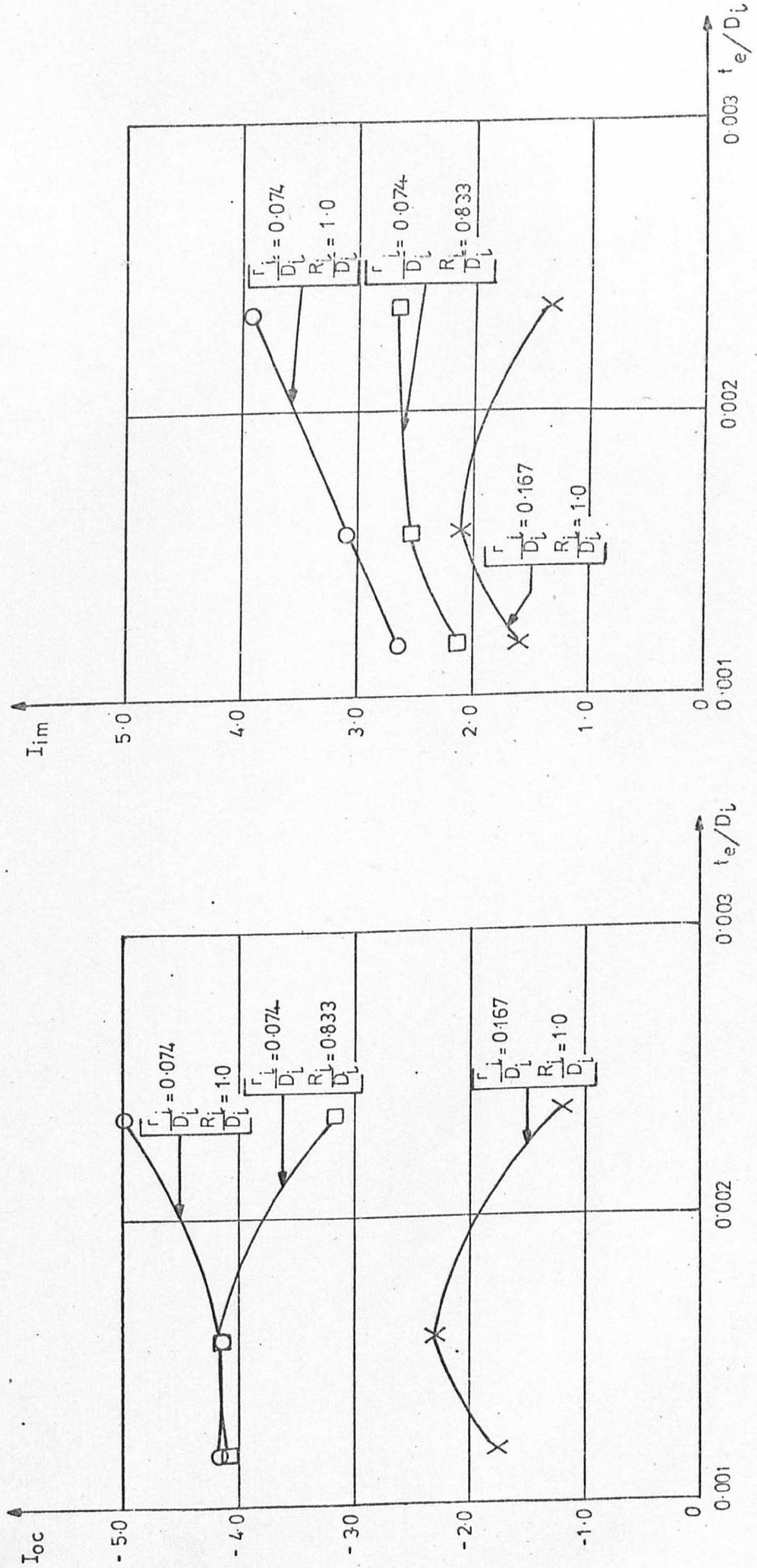


FIG 8.25



THE EFFECT OF KNUCKLE RADIUS  
ON THE PEAK STRESS INDICES

$I_{oc}$  AND  $I_{im}$

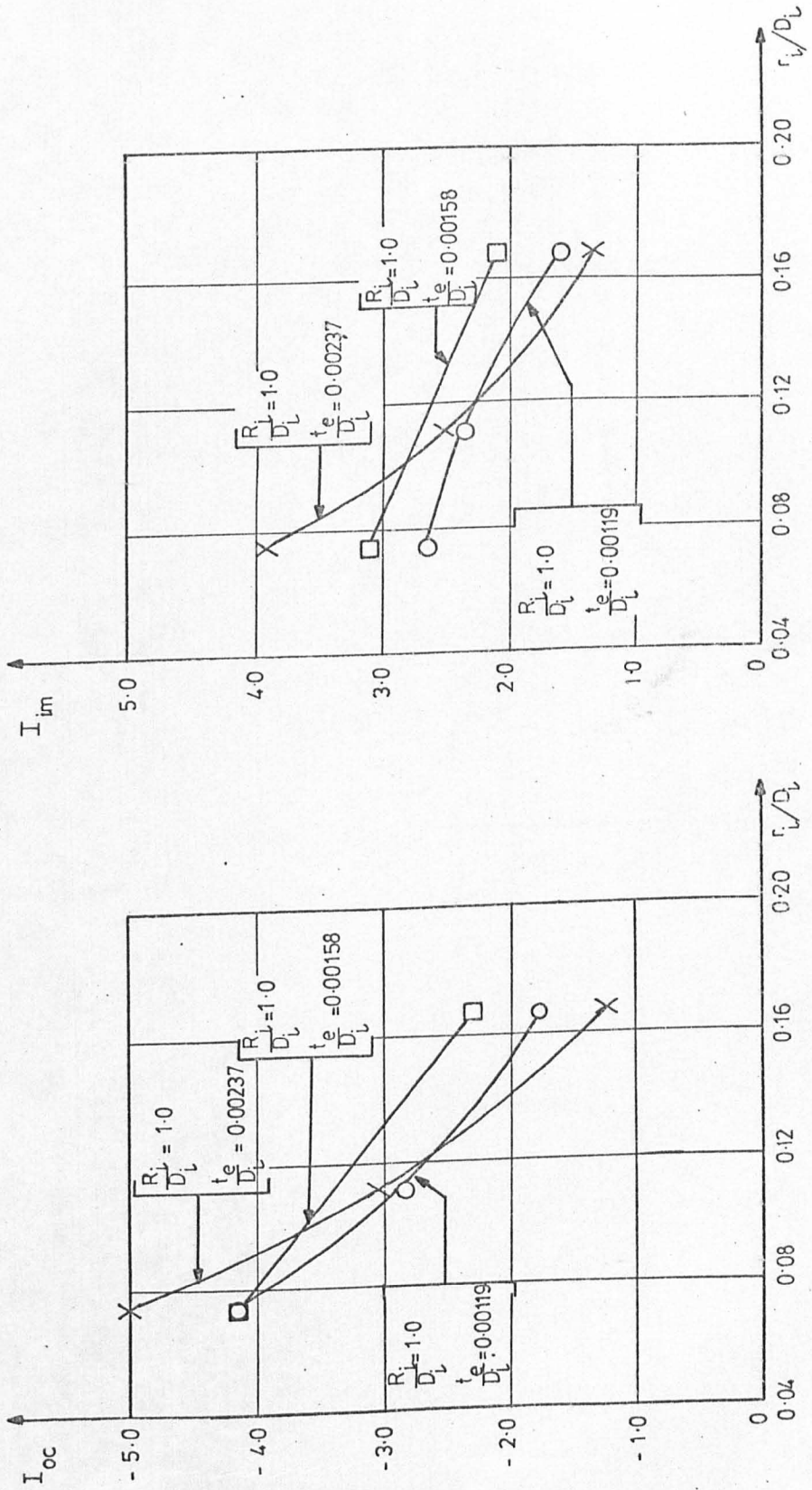


FIG 8-26

THE EFFECT OF CROWN RADIUS  
ON THE PEAK STRESS INDICES

$\frac{I_{oc}}{I_{im}}$  AND  $I_{im}$

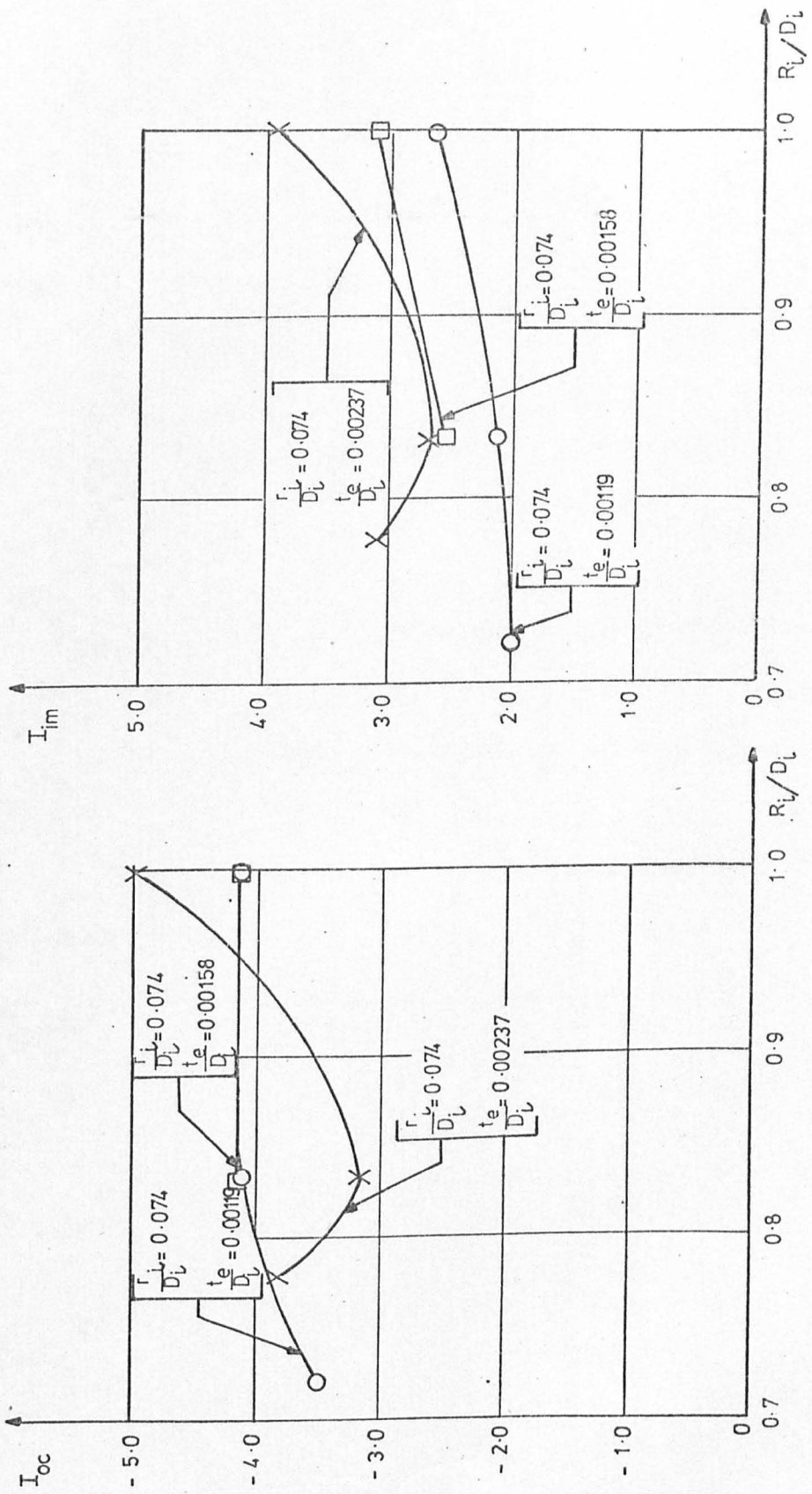


FIG 8-27

THE EFFECT OF THICKNESS ON

LIMIT PRESSURE

○ 0.1% Permanent Strain

X  $\frac{7}{8} \left( \frac{P}{\bar{\epsilon}} \right) e_l$

— From Shield and Drucker curves (ref 15)

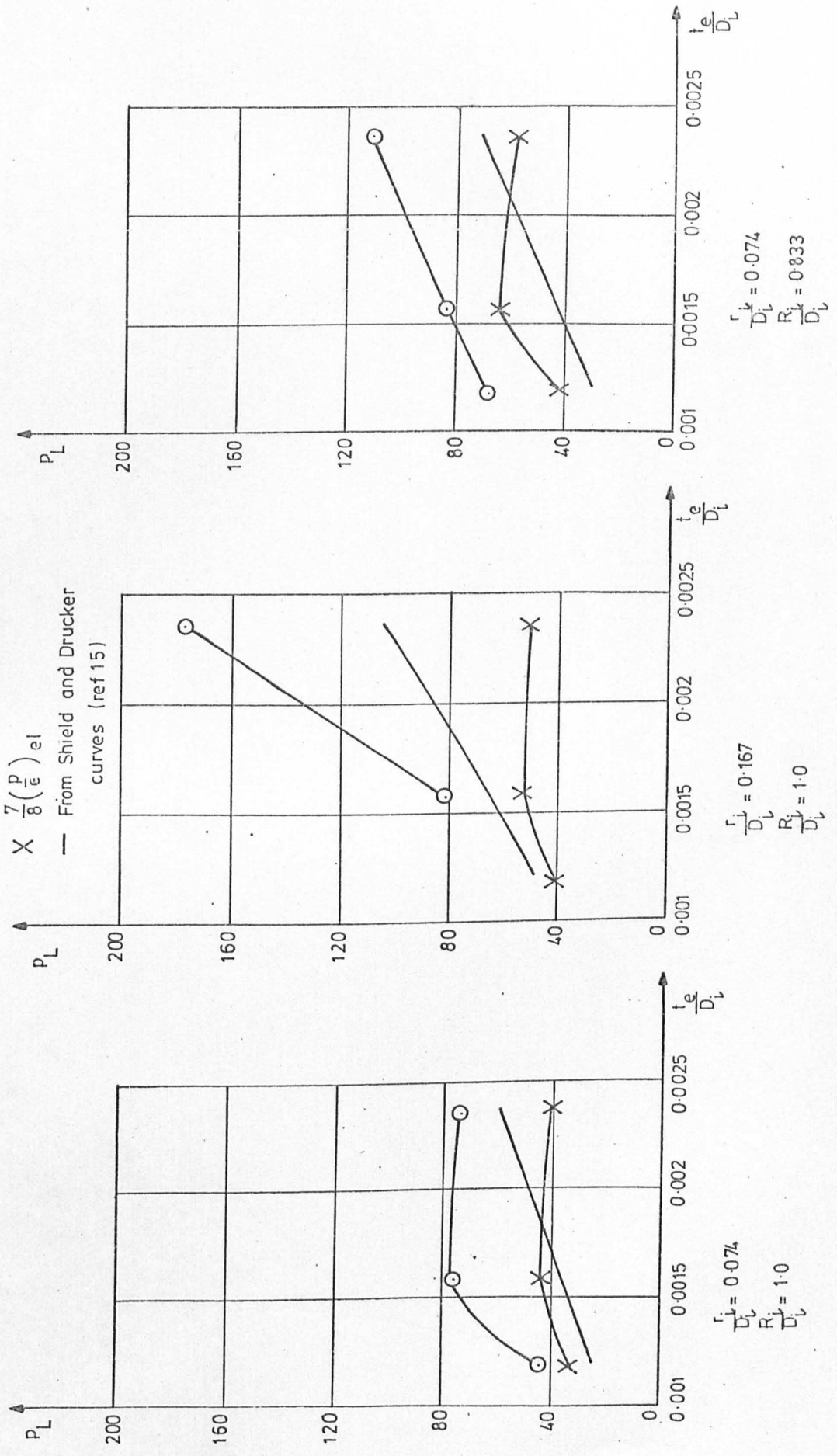


FIG 8-28

THE EFFECT OF KNUCKLE RADIUS

ON LIMIT PRESSURE

○ 0.1% Permanent Strain

X  $\frac{7}{8} (P_e)_{el}$

— From Shield and Drucker curves (ref 15)

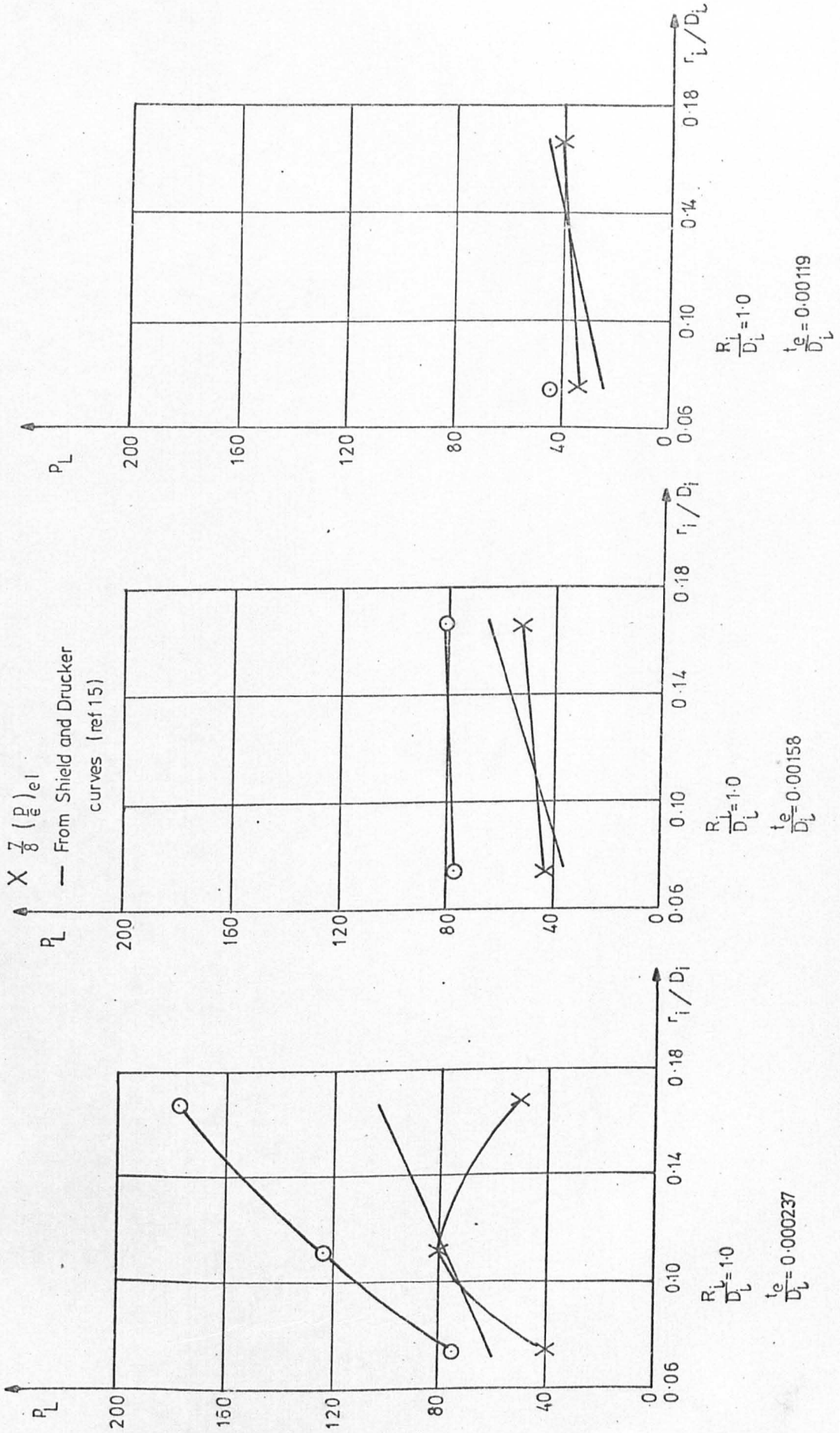


FIG 8-29

THE EFFECT OF CROWN RADIUS

ON LIMIT PRESSURE

○- 0.1% Permanent strain

X  $\frac{7}{8}(\frac{P}{E})_{el}$

— From Shield and Drucker curves (ref-15)

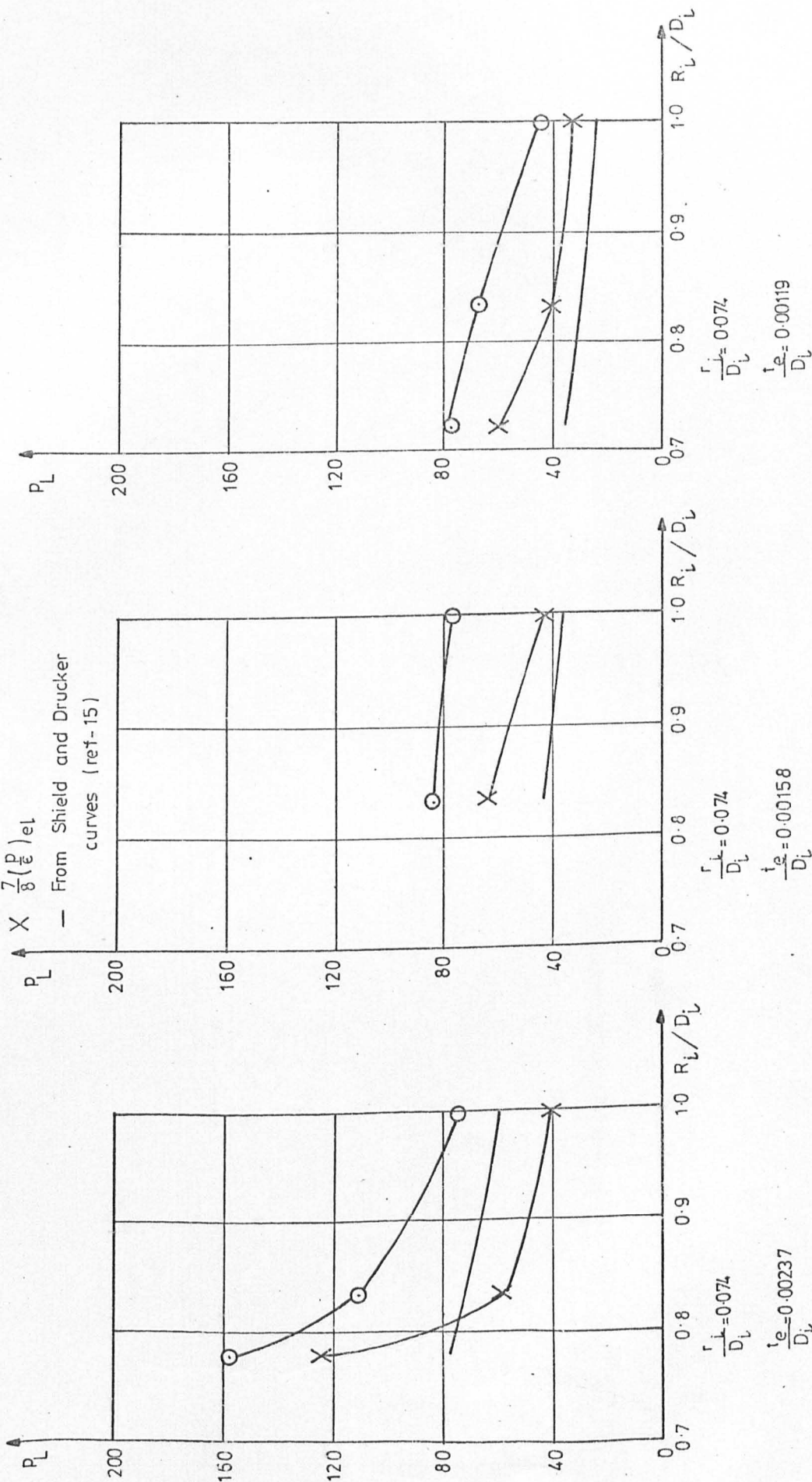


FIG 8-30

THE EFFECT OF THICKNESS  
ON FIRST BUCKLING PRESSURE

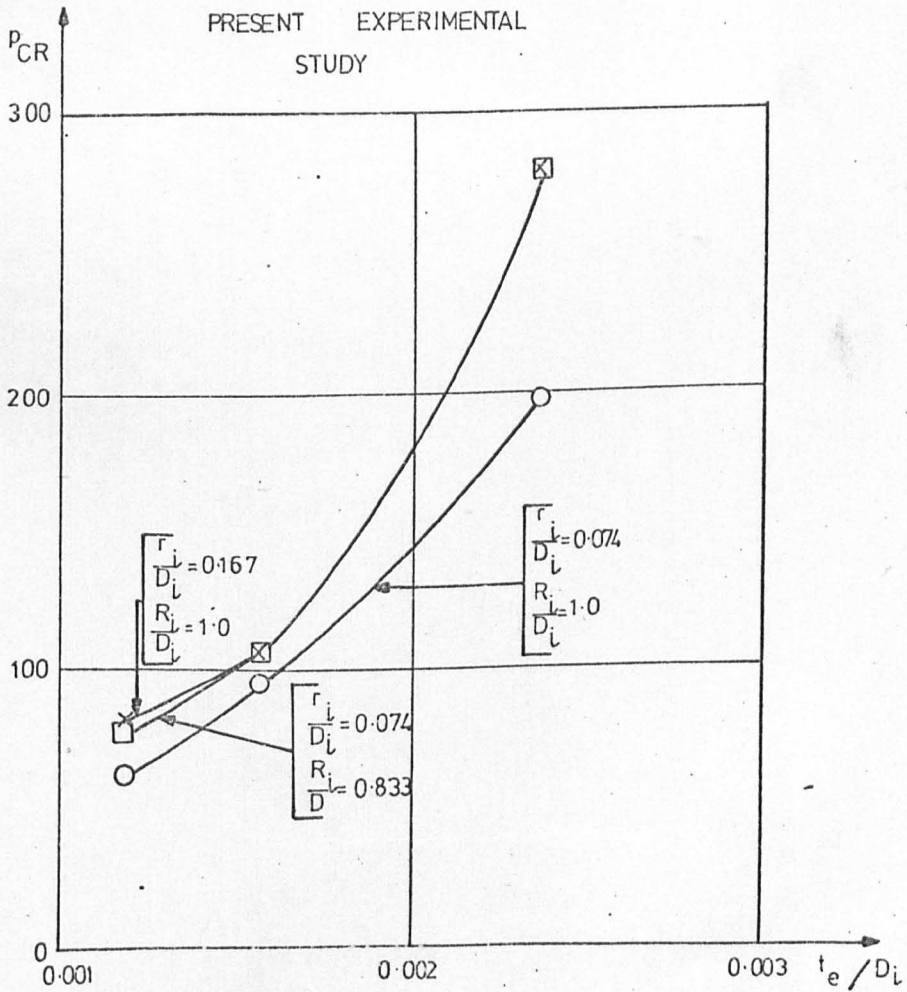
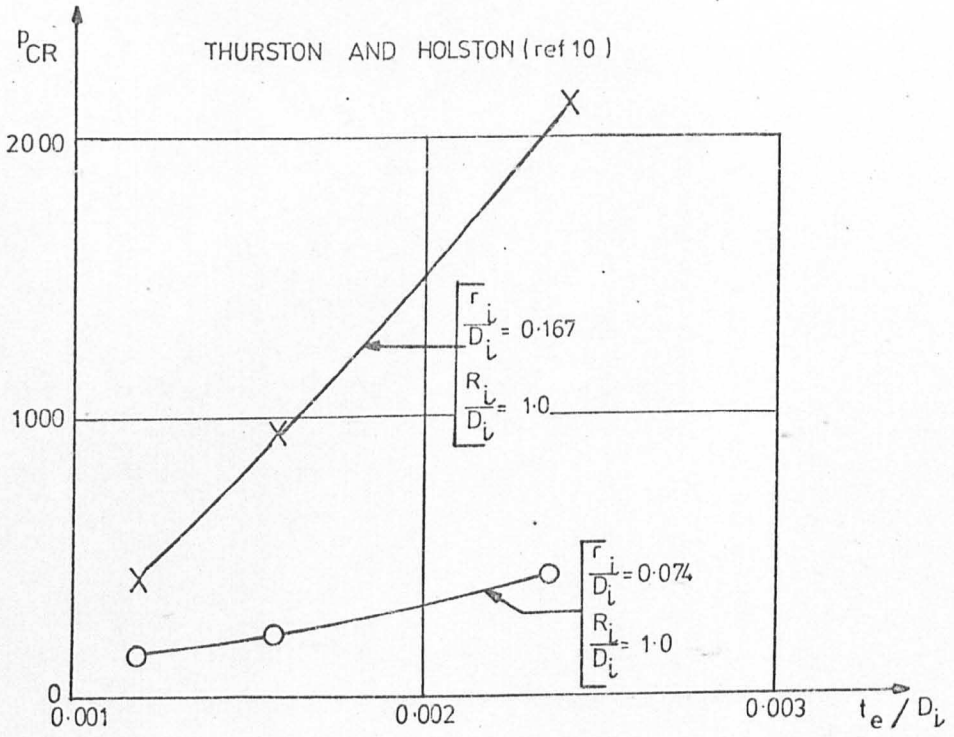


FIG 8-31

THE EFFECT OF KNUCKLE  
RADIUS ON FIRST BUCKLING  
PRESSURE

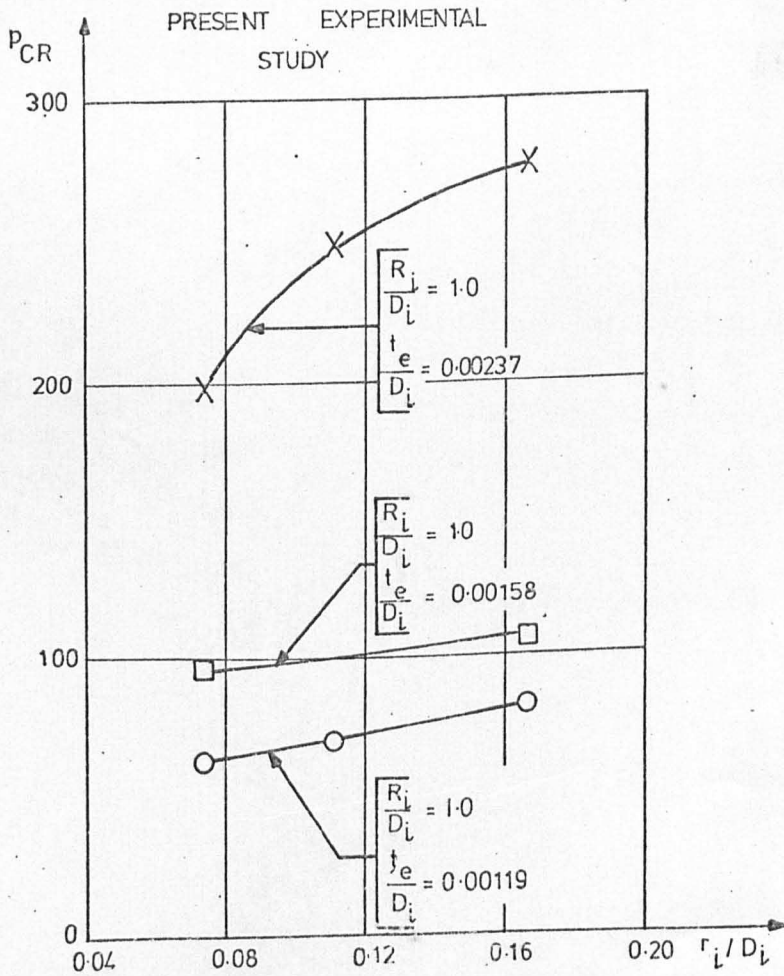
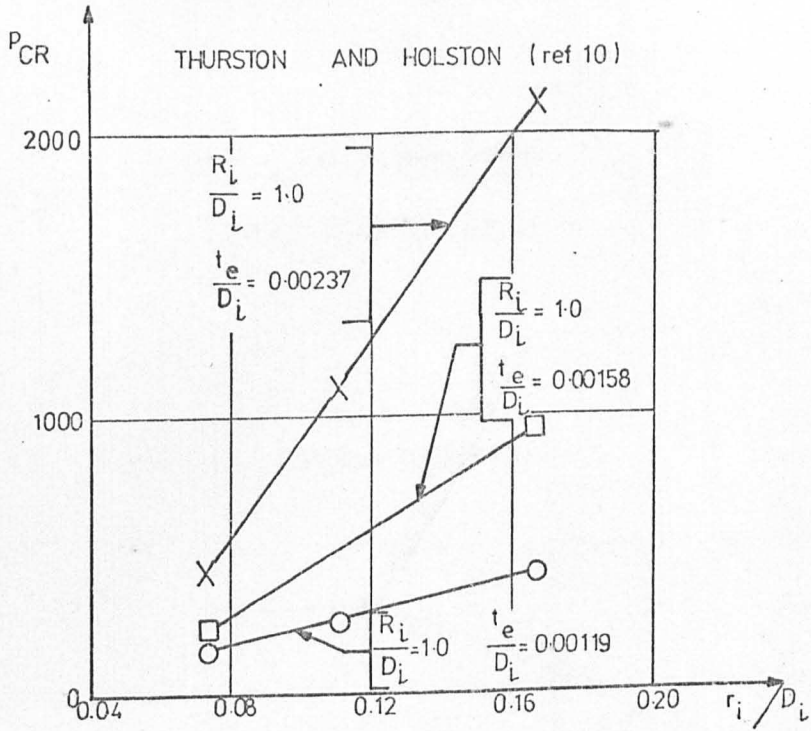


FIG 8-32

THE EFFECT OF CROWN RADIUS  
ON FIRST BUCKLING PRESSURE

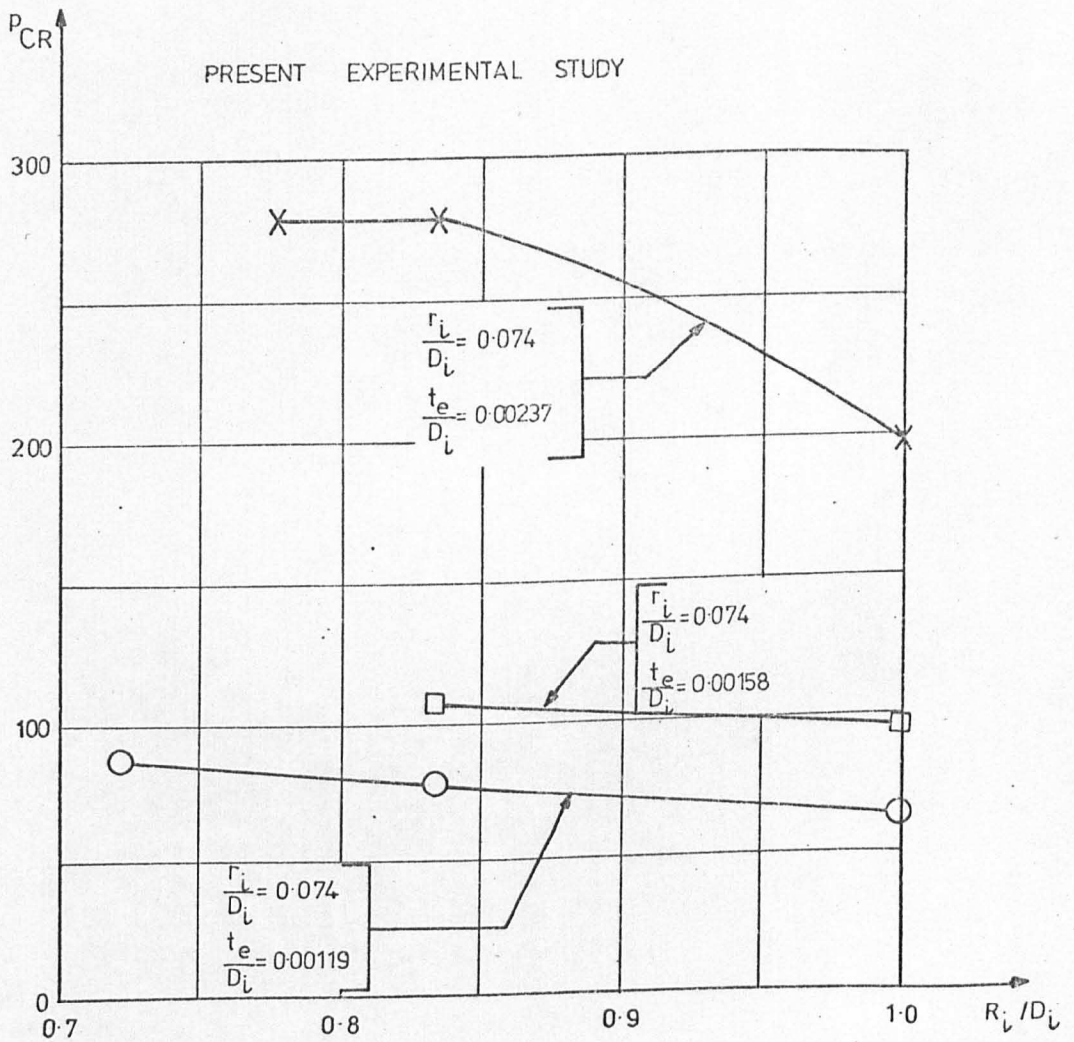


FIG 8-33



END No. 4

DISTRIBUTION OF ELASTIC STRESS INDICES  
COMPUTED BY GOODMAN (REF 43)

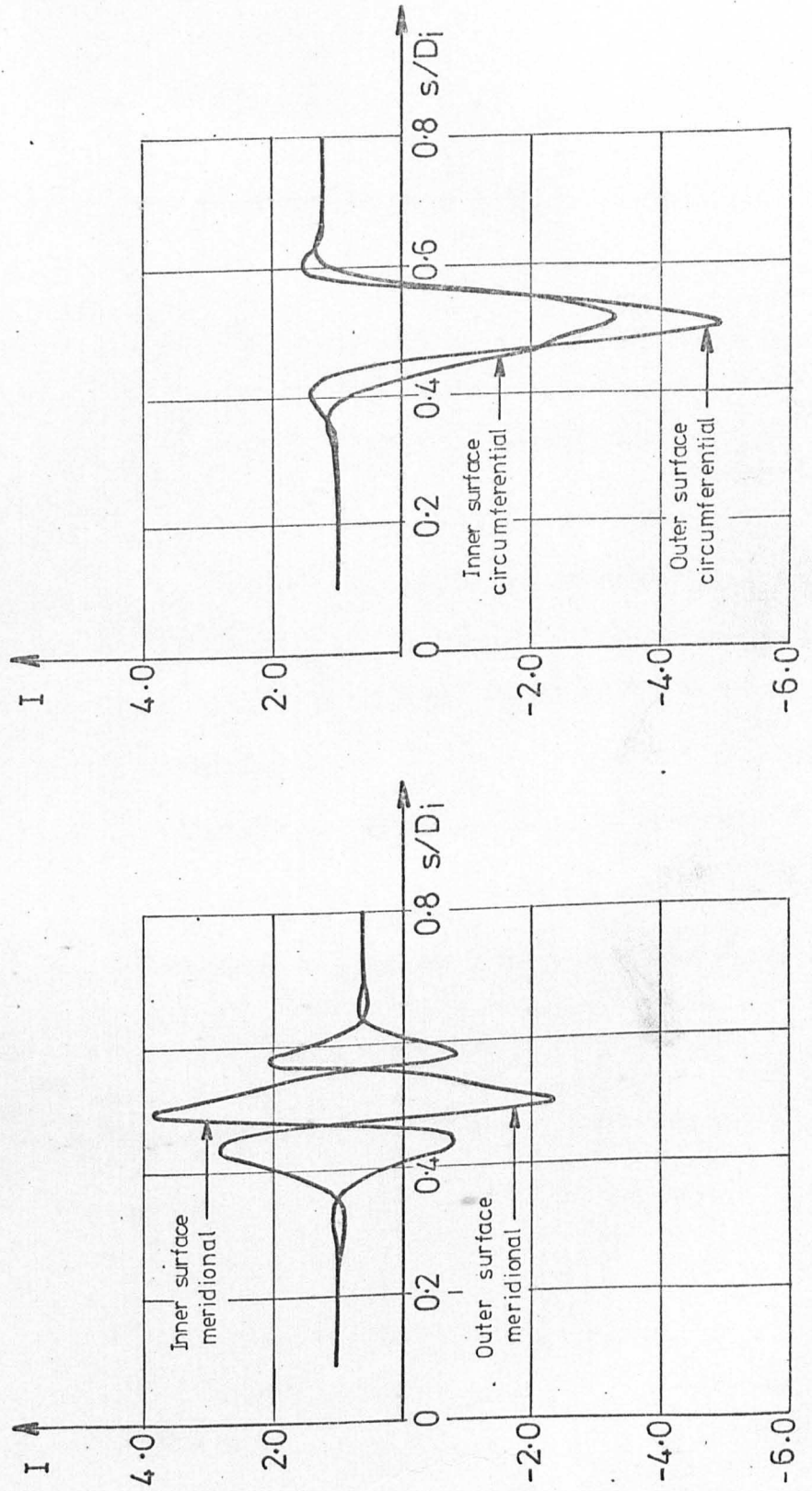


FIG 8-34

CHAPTER 9FUTURE WORK

The main areas in which further study would be worthwhile are listed below.

1. Computation of the elastic and post-yield behaviour of a range of very thin ends, in which real as opposed to nominal dimensions are used and account is taken of residual stresses and varying material properties.
2. A detailed assessment, both theoretical and experimental of the level of residual stresses in typical ends, and their effect on the buckling behaviour. Related material property studies are necessary.
3. A study of the effect of partial vacuums in large very thin vessels.
4. A study of the effect of local loads in large very thin vessels.
5. A limited complementary study using ends in other materials.
6. The formulation of design recommendations to cover this type of end.

CHAPTER 10CONCLUSIONS.

1. The measured shape of a production end may vary considerably from the nominal. Local variations in knuckle curvature from +100% to -50% of nominal have been measured.
2. The thickness of ends manufactured by the pressed and spun method may be 25% less than the nominal value. The corresponding figure for crown and segment ends is about 2%.
3. Considerable undercutting may be present at welds.
4. Manufacturing imperfections may provide ideal sites for the occurrence of buckling. The frequent formation of a buckle at or near to a meridional weld shows the regions of such welds to be particularly susceptible to buckling.
5. High levels of residual stress are present in the knuckle region of production ends, particularly those produced by the pressed and spun method. Values of up to 30 tonf/in<sup>2</sup> have been observed.
6. Work-hardening during forming results in a considerable variation in the material properties of the pressed and spun ends studied. The yield stress may vary by up to a factor of three along a meridian of a typical end.
7. Because the imperfections referred to in 1 - 4 above and the features mentioned in 5 and 6 vary in degree in nominally identical ends, there is likely to be an appreciable variation in the results obtained for such ends.

8. A series of distinct ripples develop in the knuckle region before the occurrence of the first full buckle.
9. Buckling occurs as a result of large compressure hoop stresses on both surfaces of the knuckle.
10. A series of buckles develops in an end at successively higher pressures after the occurrence of the first buckle. The maximum number of buckles produced on an end was nine. On end No.15 these occurred over a pressure range from 107 lbf/in<sup>2</sup> to 219 lbf/in<sup>2</sup>.
11. Two types of buckle were observed. The "snap inwards" type was generally found on the shallower spun ends whilst the deep crown and segment ends tended to form the "gradual outwards" type of buckle. However both types of buckle were observed on both types of end.
12. The dominant geometric parameter affecting the first buckling pressure is the thickness to diameter ratio. A thickness ratio reduction from 0.00237 to 0.00119 results in a critical pressure reduction from 198 lbf/in<sup>2</sup> to 62 lbf/in<sup>2</sup> in a typical case.
13. If the other parameters remain constant, a reduction in the knuckle radius ratio generally results in a reduction in the critical pressure. A knuckle radius ratio reduction from 0.167 to 0.074 results in a critical pressure reduction from 278 lbf/in<sup>2</sup> to 198 lbf/in<sup>2</sup> in a typical case.
14. If other parameters remain constant a reduction in the crown radius ratio generally results in an increase in the critical pressure. A crown radius ratio reduction from 1.0 to 0.722 results in a critical pressure increase from 62 lbf/in<sup>2</sup> to 86 lbf/in<sup>2</sup> in a typical case.

15. Some consistency has been observed between the calculated Shield and Drucker limit pressure and the pressure for the first buckle.
16. The buckling pressures derived from those of Thurston and Holston are several times greater than those observed on production ends. On the ends tested no consistent relationship was apparent between the buckling pressures predicted from the Thurston and Holston work and those measured on the test ends.
17. An approximate treatment in which the knuckle is treated as a column with a transverse elastic support, results in a relationship which gives a reasonably consistent over-estimate of the first buckling pressure for the ends tested.
18. An appreciable time-dependence is observed in the development of buckles.
19. The buckling is not catastrophic though leaks occasionally occur when the buckle is on a weld.
20. Welding an angle or channel ring to the cylinder at the junction with the knuckle does not have an appreciable effect on the first buckling pressure.

## REFERENCES

1. FESSLER, H. and STANLEY, P. "Stresses in torispherical drumheads: a photoelastic investigation", J. Strain Analysis, 1965, 1, 69.
2. GALLETLY, G. D. "Edge influence coefficients for toroidal shells of positive gaussian curvature", J. Eng. Industry, Trans. Am. Soc. Mech. Engrs. 1960, 82, 60.
3. CRISP, R. J. "A computer survey of the behaviour of torispherical drumheads under internal pressure loading", Nuclear Engineering and Design, 1970, 11, 457-476.
4. DRUCKER D. C. and SHIELD, R. T. "Limit analysis of symmetrically loaded thin shells of revolution", J. Appl. Mech., Trans. Am. Soc. Mech. Engrs. 1959, 80, 61-68.
5. FINDLAY, G. E., MOFFAT, D. G. and STANLEY, P. "Torispherical drumheads: a limit-pressure and shakedown investigation", J. Strain Analysis, 1971, 6, 147.
6. FESSLER, H. and STANLEY, P. "Stresses in torispherical drumheads: a critical evaluation", J. Strain Analysis, 1966, 1, 89.
7. GALLETLY, G. D. "Torispherical shells - a caution to designers", J. Eng. Industry, Trans. Am. Soc. Mech. Engrs. 1959, vol.81, series B, no.1, 51-66.
8. MEESTERS, A. G. and SLAAF, C. M. "An investigation on the stress distribution, elastic and plastic deformations in a large, thin-walled dished head of a pressure vessel by means of a hydrostatic test", Slaatsmijnen In Limburg, Report Chem. Constr. Dept. no.88, 1949.
9. FINO, A. and SCHNEIDER, R. W. "Wrinkling of a large thin code head under internal pressure", Welding Research Council Bulletin, No.69, 1961, 11-13.
10. THURSTON, G. A. and HOLSTON, A. A. "Buckling of cylindrical shell end closures by internal pressure", NASA Report CR-540, 1966.
11. KEMPER, M. J. Letter in the Chartered Mechanical Engineer, January 1971.
12. ADACHI, J. and BENICEK, M. "Buckling of torispherical shells under internal pressure", Experimental Mechanics, 1964, 217-222.

- ✓ 13. GALLETLY, G. D. "Influence coefficients and pressure vessel analysis", J. Eng. Industry, Trans. Am. Soc. Mech. Engrs. 1960, 82, 259.
- ✓ 14. SHIELD, R. T. and DRUCKER, D. C. "Limit strength of thin walled pressure vessels with an A.S.M.E. standard torispherical head", Proceedings of the Third U.S. National Congress of Applied Mechanics, 1958, 665-672.
15. SHIELD, R. T. and DRUCKER, D. C. "Design of thin-walled torispherical and toriconical pressure-vessel heads", J. Appl. Mech., Trans. Am. Soc. Mech. Engrs. 1961, 292-297.
16. MESCALL, J. "Stability of thin torispherical shells under uniform internal pressure", NASA Report TN-D-1510, 1962, 671-692.
17. SANDERS, J. L. "Nonlinear theories for thin shells", Quart. Appl. Math. 1963, 21, 21-35.
18. ROTONDO, P. and KRAUS, H. "Buckling of an ellipsoid due to internal pressure", A.S.M.E. paper No. 68-WA/PVP-12, 1968.
19. ESZTERGAR, E. P. and KRAUS, H. "Analysis and design of ellipsoidal pressure vessel heads", J. Eng. Industry, Trans. Am. Soc. Mech. Engrs. 1970, Vol.92, Series B, No.4, 805-817.
20. GERDEEN, J. C. "Use of the computer in the plastic limit analysis of pressure vessels", Proc. of A.S.M.E. Computer Seminar, Dallas, 1968, 37-49.
21. GAJEWSKI, R. R. and LANCE, R. H. "An evaluation of A.S.M.E. ellipsoidal heads", J. Eng. Industry, Trans. Am. Soc. Mech. Engrs. 1969, Vol.91, Series B, No.3, 636-640.
22. JONES, O. "The effects of internal pressure on thin-shell pressure vessel heads", Welding Research Council Bulletin, No.69, 1961, 1-10.
23. STENNET, R. "Gummed up valve causes vessel collapse", Vigilance, The Quart. J. of National Vulcan Engr. Insurance Group, 1970, Vol.2, No.4, 45-46.  
Also abridged version in The Chartered Mechanical Engineer, Oct.1970, 404.

24. KEMPER, M.J. "Buckling of thin dished ends under internal pressure". Presented at a conference on vessels under buckling conditions, 1972 (Institution of Mechanical Engineers, London).
25. British Standard 1500:1958. Fusion welded pressure vessels for use in the chemical, petroleum and allied industries.
26. British Standard 1515: Part 2 Advanced Design and Construction: 1968. Specification for fusion welded pressure vessels for use in the chemical, petroleum and allied industries.
27. British Standard 3915:1965. Specification for carbon and low alloy steel pressure vessels for primary circuits of nuclear reactors.
28. A.S.M.E. Boiler and Pressure Vessel Code Section VIII. Rules for construction of pressure vessels, div. 1, 1971.
- ✓ 29. CLOUD, R.L. "Interpretive report on pressure vessel heads", Welding Research Council Bulletin, No. 119, 1967, 1.
- ✓ 30. LANGER, B.F. "P.V.R.C. Interpretive report of pressure vessel research, Section 1 - design considerations", Welding Research Council Bulletin, No. 95, 1964, 1-53.
- ✓ 31. POPOV, E.P., KHOJASTEH-BAKHT, M. and SHARIFI, P. "Elastic-plastic analysis of some pressure vessel heads", J. Eng. Industry, Trans. Am. Soc. Mech. Engrs., 1970, Vol. 92, 309-316.
- ✓ 32. KRAUS, H. "Elastic stresses in pressure vessel heads", Welding Research Council Bulletin, No. 129, 1968, 1-26.
33. GILL, S.S. Private communication.
34. GALLETLY, G.D. Private communication.
35. BRITISH STEEL CORPORATION "Silver Fox Hi-Proof", Catalogue containing a range of higher proof stress austenitic stainless steel.
36. TUPHOLME, C.B., KEMPER, M.J. and SLATER, D. "High proof strength stainless steels and their fabrication", The Chemical Engineer, 1970, CE 320.



37. WILCOCK, R. and STOTLAND, J.A. "High proof stress austenitic stainless steel," Samuel Fox and Company Ltd. Report, 1967.
38. SAVE, M. "Verification experimentale de l'analyse limite plastique des plaques et des coques en acier doux", Centre de Recherches Scientifiques et Techniques de l'Industrie des Fabrications Metalliques, Brussels, Report No. MT21, 1966.
39. SAMPAYO, V.M. and TURNER C.E. "Computed elastic-plastic behaviour and shakedown of some radial nozzle-on-sphere geometries", Second International Conference on Pressure Vessels Technology, San Antonio, 1973, 331-341.
40. British Standard 18: Part 2: 1971. Methods for tensile testing of metals. Part 2: Steel (general).
41. GOODMAN, A.M. "An interim guide to PATAS: Part 1, elastic and elasto-plastic analysis of shell structures", C.E.G.B. Report, RD/B/N1751, 1970.
42. GOODMAN, A.M. "Users guide to the elastic shell program PVA2", C.E.G.B. Report, RD/B/N1632, 1970.
43. GOODMAN, A.M. Private communication.
44. ZICK, L.P. and ST. GERMAIN, A.R. "Circumferential stresses in pressure vessel shells of revolution", J. Eng. Industry, Trans. Am. Soc. Mech. Engrs., 1963, 201.
45. KIRK, A. and GILL, S.S. "The failure of torispherical ends of pressure vessels due to instability and plastic deformation - an experimental investigation", Internal Report, Div. Struct. Eng., UMLST, Nov. 1974.
46. TIMOSHENKO, S.P. and GERE, J.M. "Theory of elastic stability", 2nd Edition, 1961, McGraw-Hill.
47. THURGOOD, D.A. Communication relating to refs. 1 and 6, J. Strain Analysis, 1966, 1, 448.

## ACKNOWLEDGEMENTS

The author wishes to record his gratitude to:

The Science Research Council, the sponsoring body, for making the work possible.

Professor A. G. Smith, Head of the Mechanical Engineering Department, who provided the facilities.

Dr. P. Stanley, who supervised the work, for his interest, guidance and encouragement.

Mr. D. Cooper, the Project's Experimental Officer, for his invaluable contribution to the experimental work.

Mr. B. Evans and Mr. B. Mynett, Laboratory Technicians, for their assistance with the experimental work.

The staff of the Faculty Workshop, for welding the test vessels.

Mr. A. Goodman of the Central Electricity Generating Board for providing the computer analysis.

Mrs. D. Korner, for her efficient typing.

Miss S. Bowering, for producing the photographs.

Miss C. Davey, for tracing the figures.

His wife Christine, for her invaluable assistance and continuous encouragement.

APPENDIX 1

Thickness and Curvature Variations,  
Pressure-Strain Curves and  
Strain and Stress Index Distributions

END No. 1
THICKNESS VARIATION ALONG 0° MERIDIAN

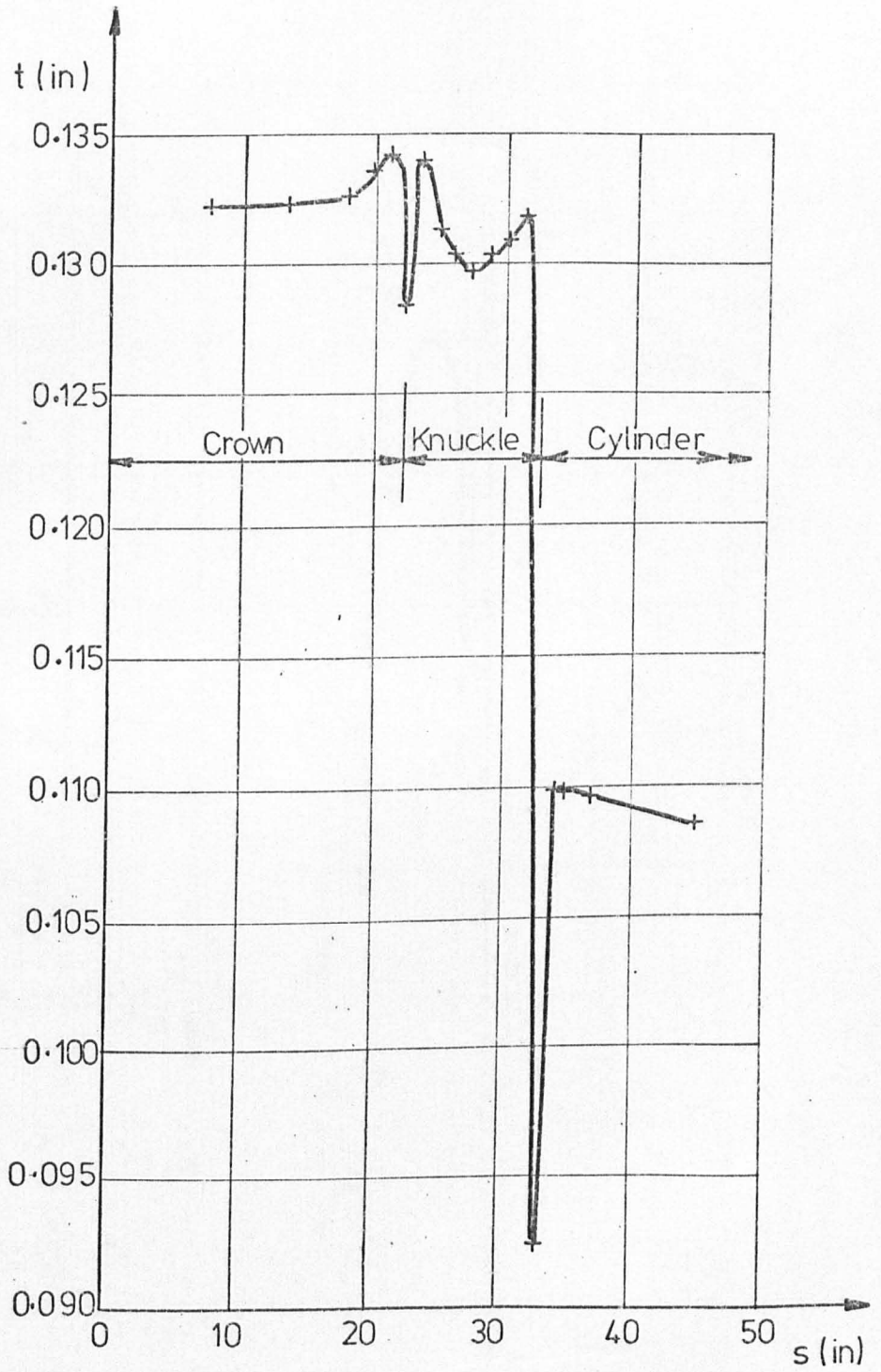


FIG. A1.1.1

END No. 1  
 CURVATURE VARIATION ALONG  
 0° MERIDIAN

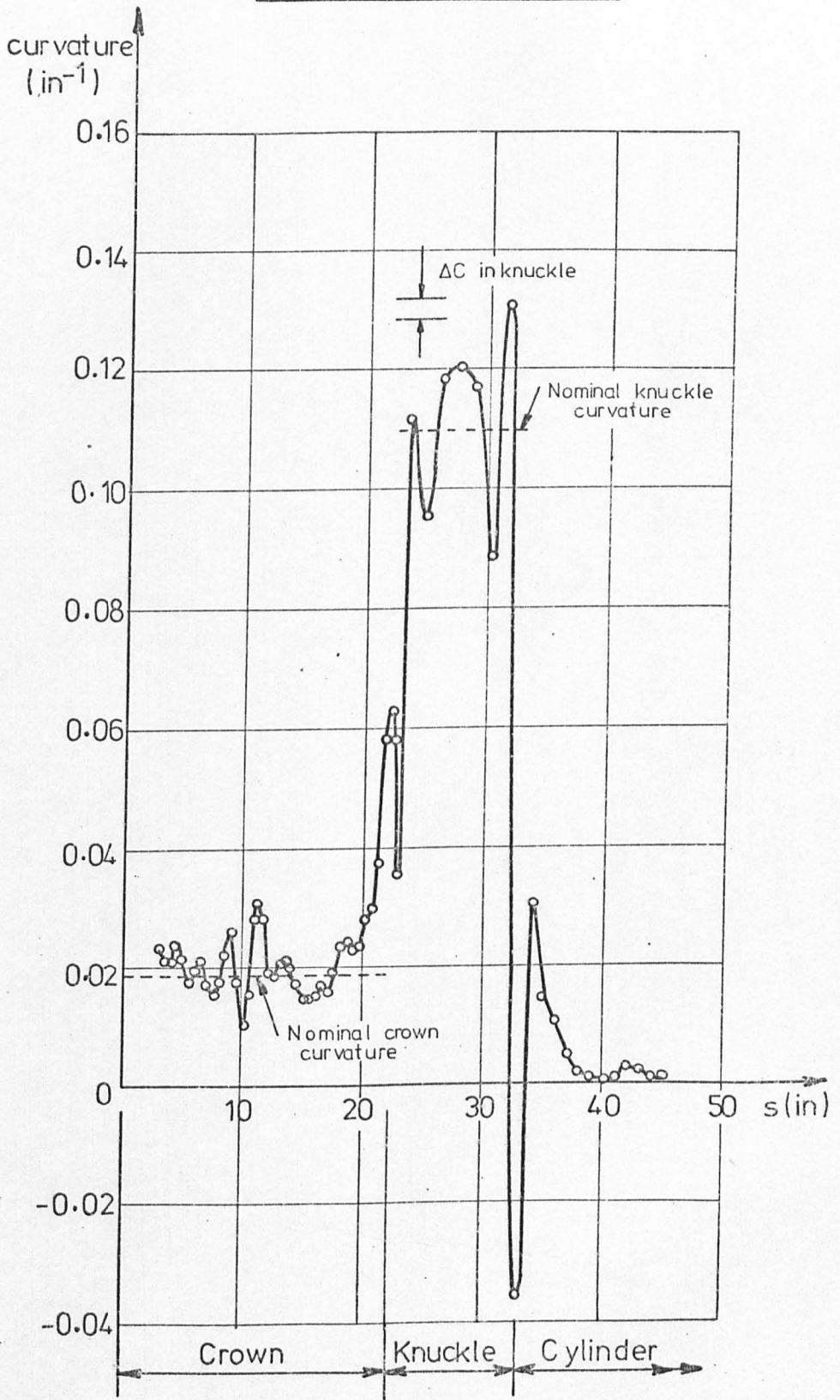


FIG. A1.1.2

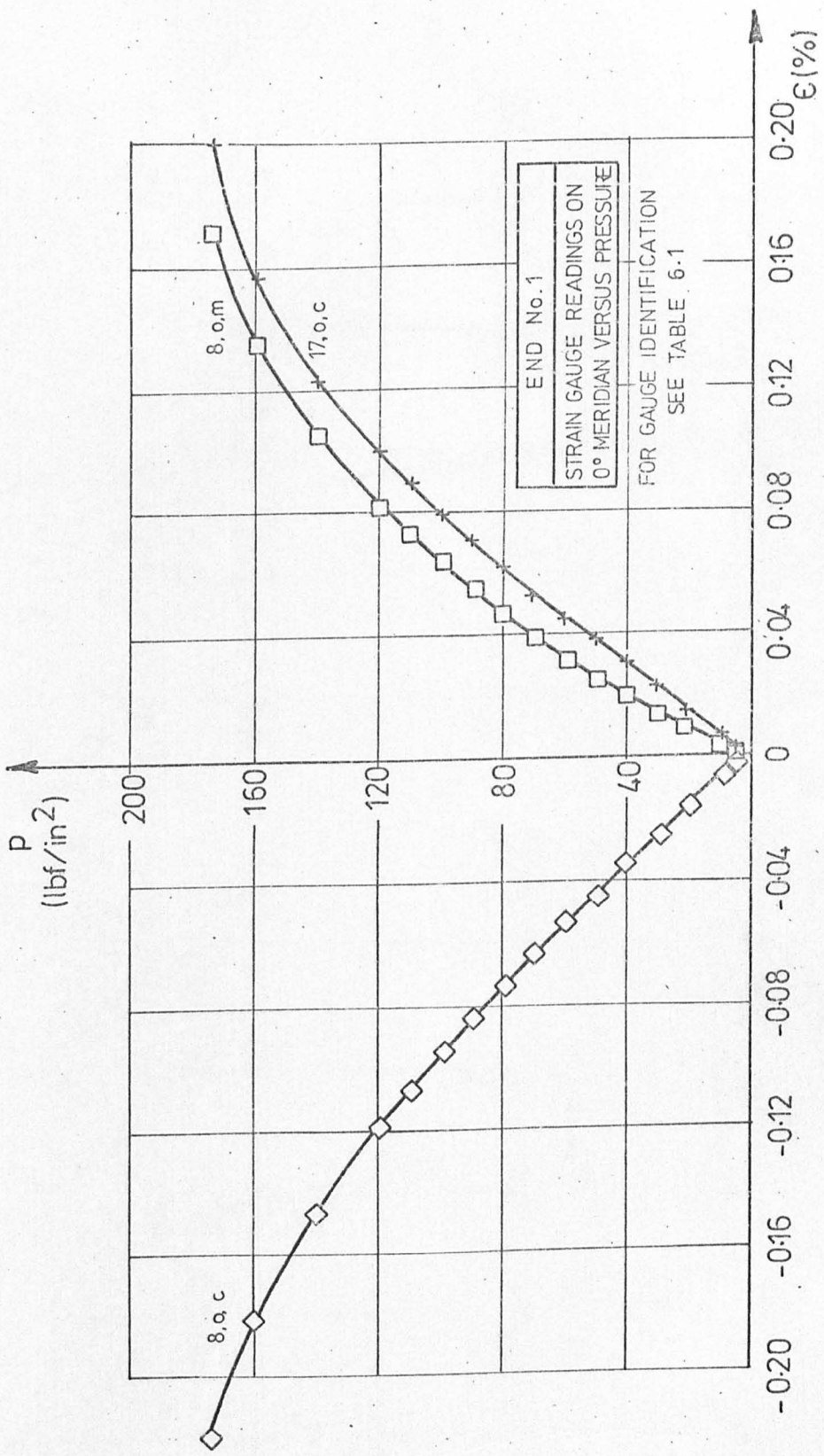


FIG. A1.1.3

END No.1	
DISTRIBUTION OF ELASTIC STRESS INDICES	
PRESSURE 25.3 lbf/in <sup>2</sup>	MERIDIAN 0°
□ OUTER SURFACE MERIDIONAL	
◇ OUTER SURFACE CIRCUMFERENTIAL	

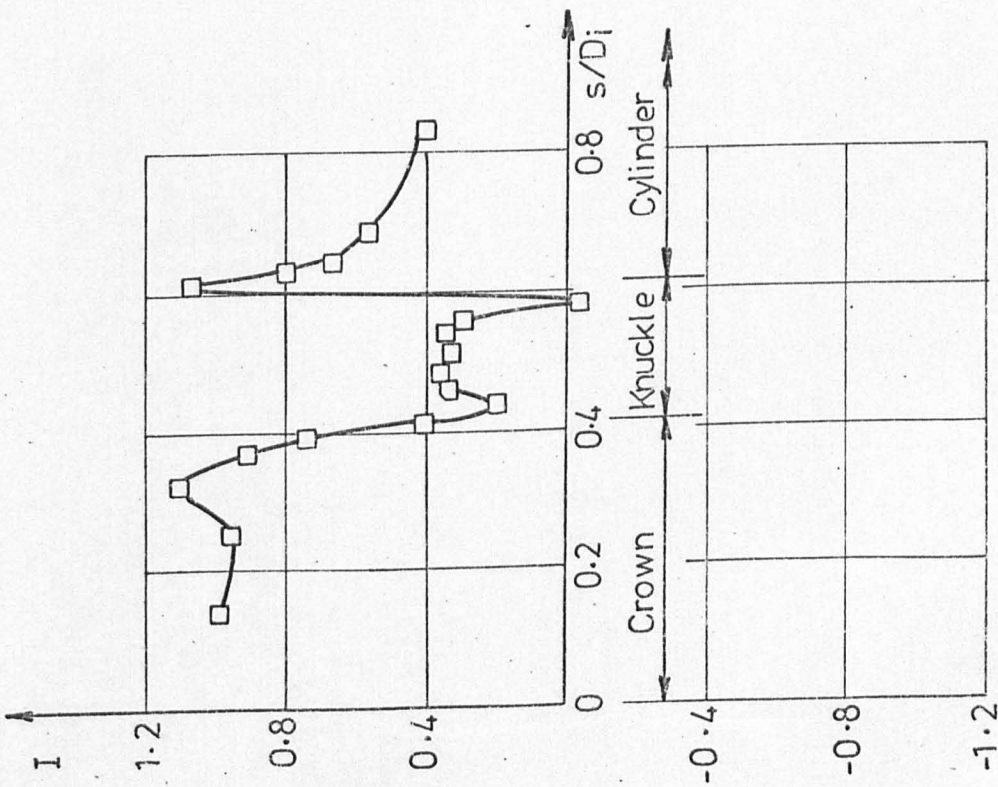
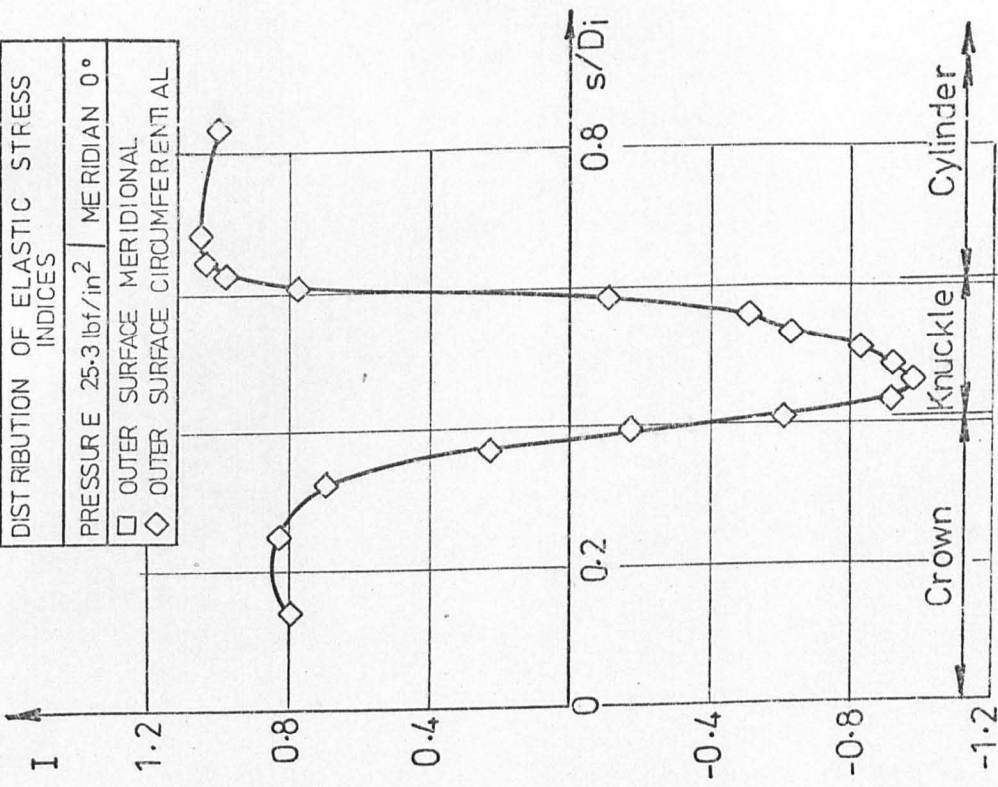


FIG. A1-1-4

END No. 2
THICKNESS VARIATION ALONG 0° MERIDIAN

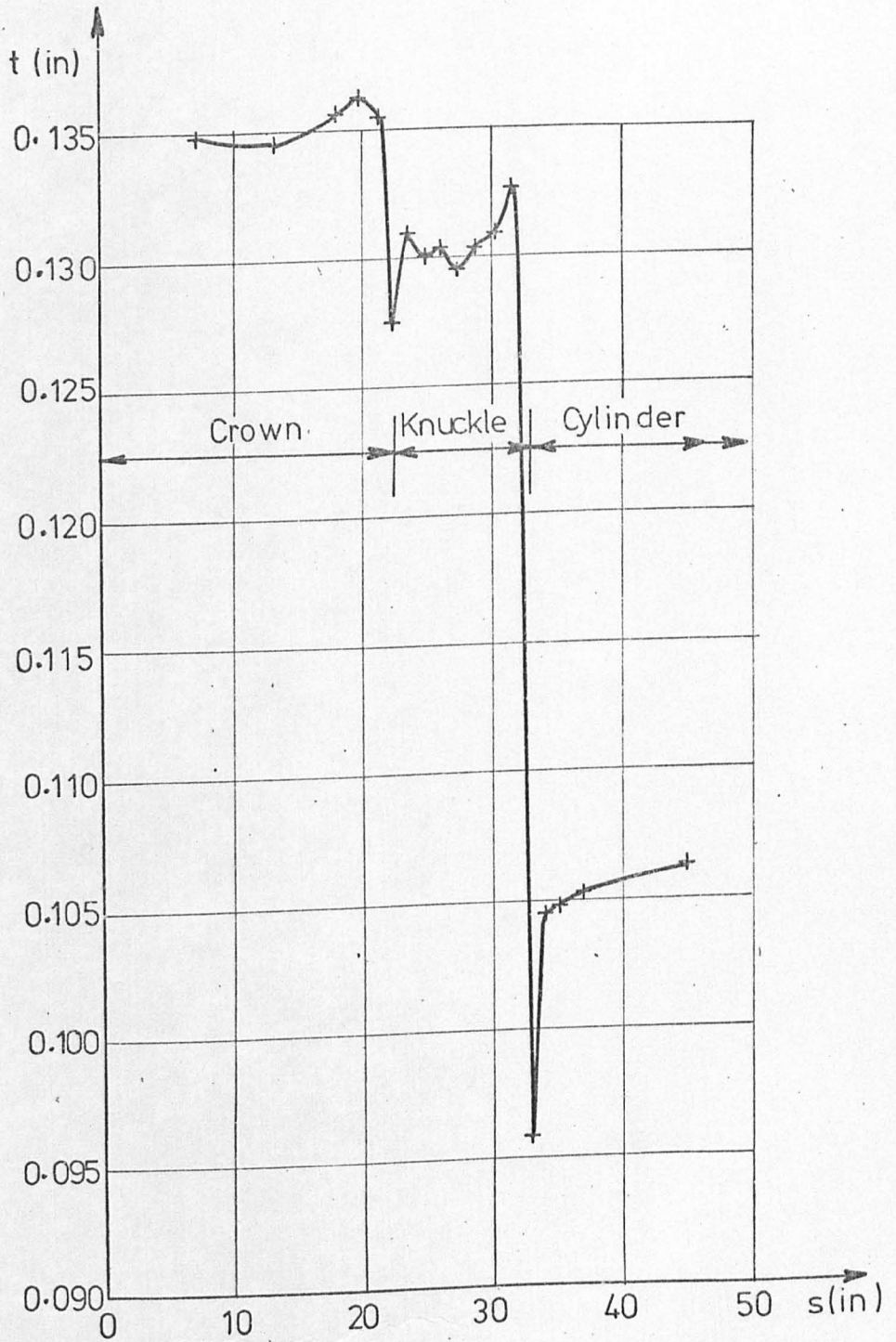


FIG. A1.2.1



END No. 2
CURVATURE VARIATION ALONG 0° MERIDIAN

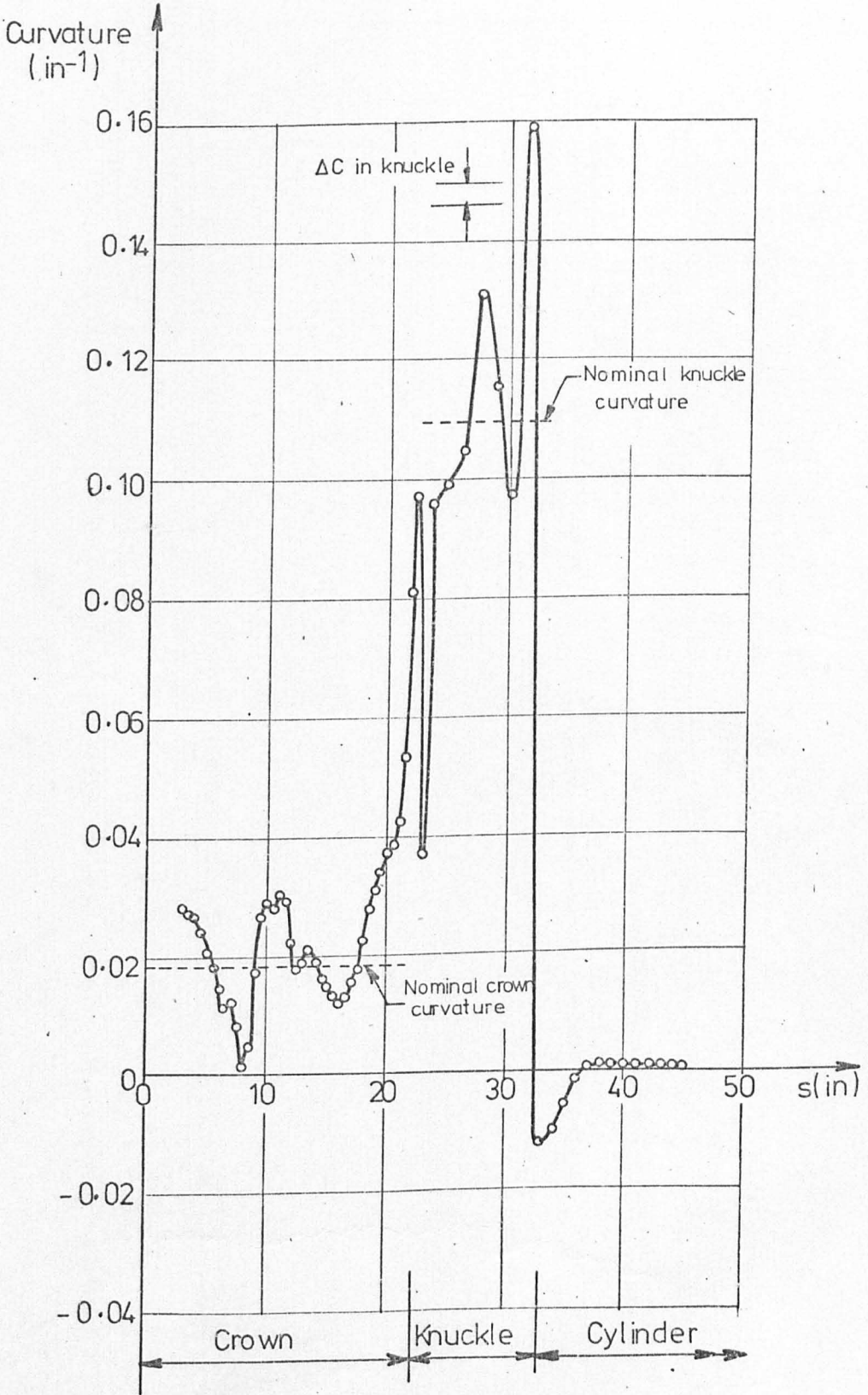


FIG.A1-2-2

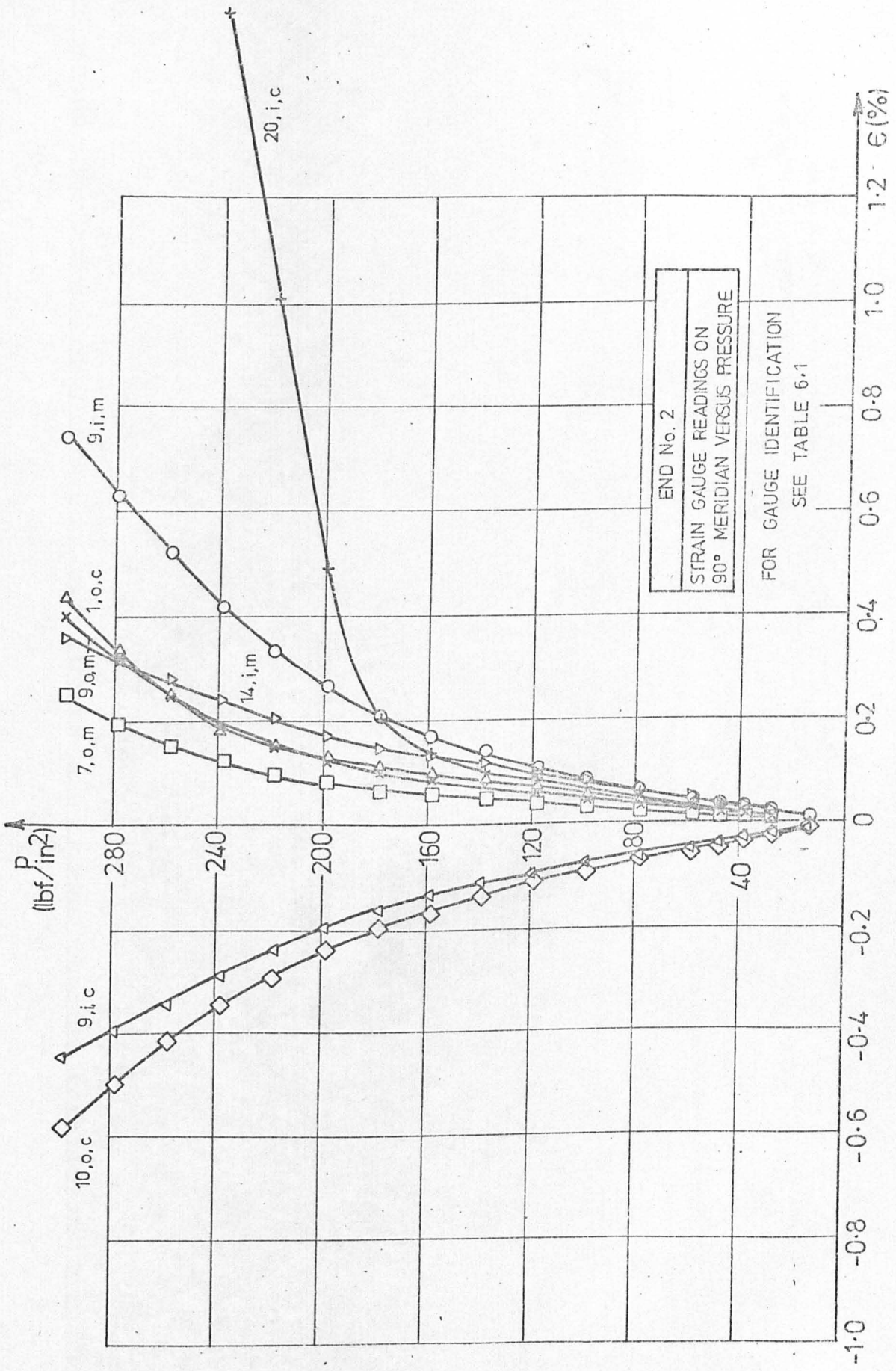
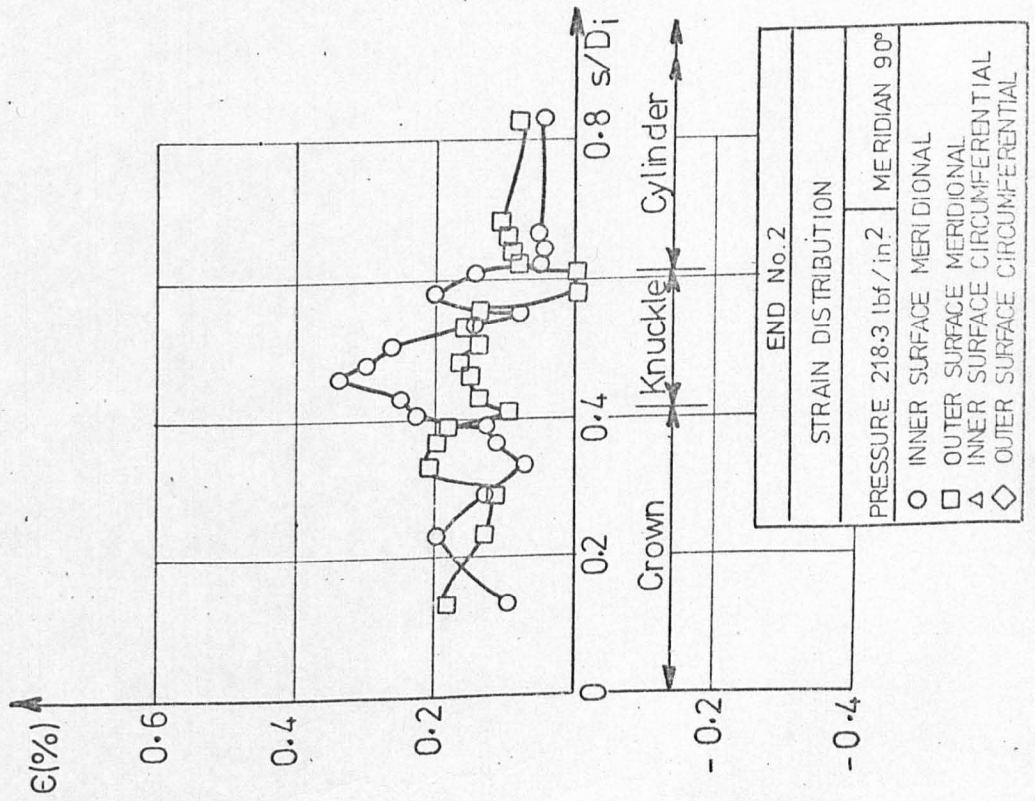
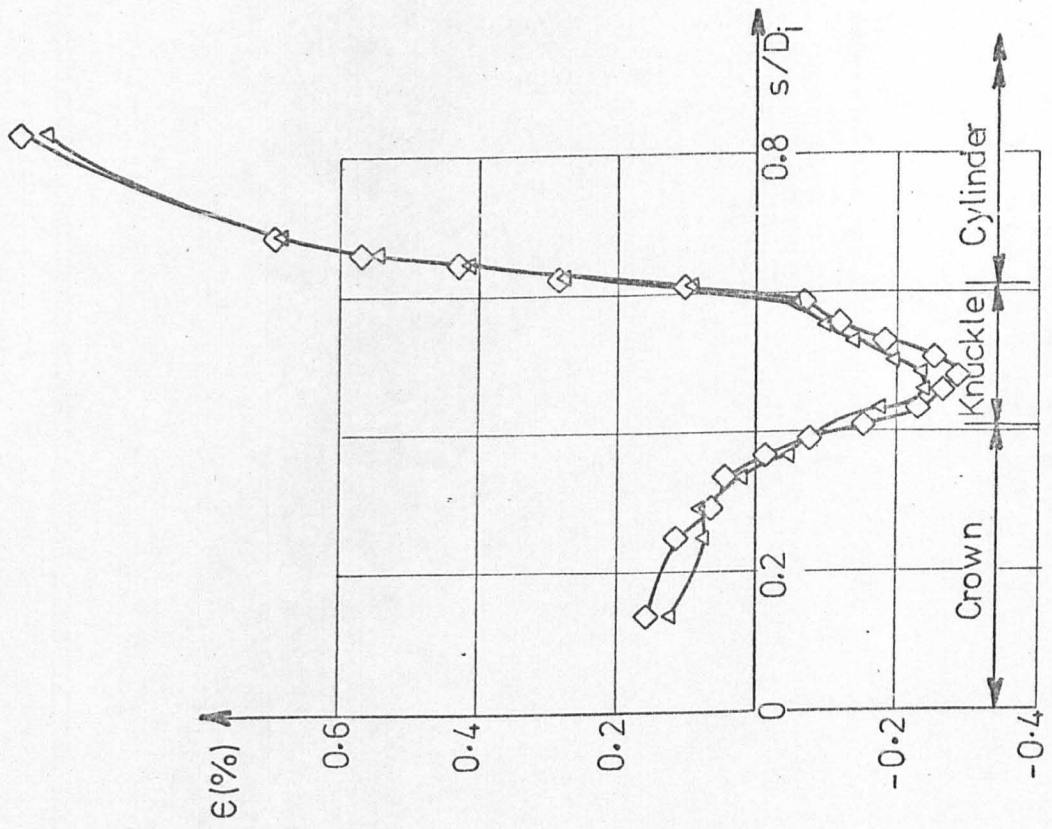


FIG. A1.2.3



END No. 2	
STRAIN DISTRIBUTION	
PRESSURE 218.3 lbf/in <sup>2</sup> MERIDIAN 90°	
○	INNER SURFACE MERIDIONAL
□	OUTER SURFACE MERIDIONAL
△	INNER SURFACE CIRCUMFERENTIAL
◇	OUTER SURFACE CIRCUMFERENTIAL

FIG. A1.2.4

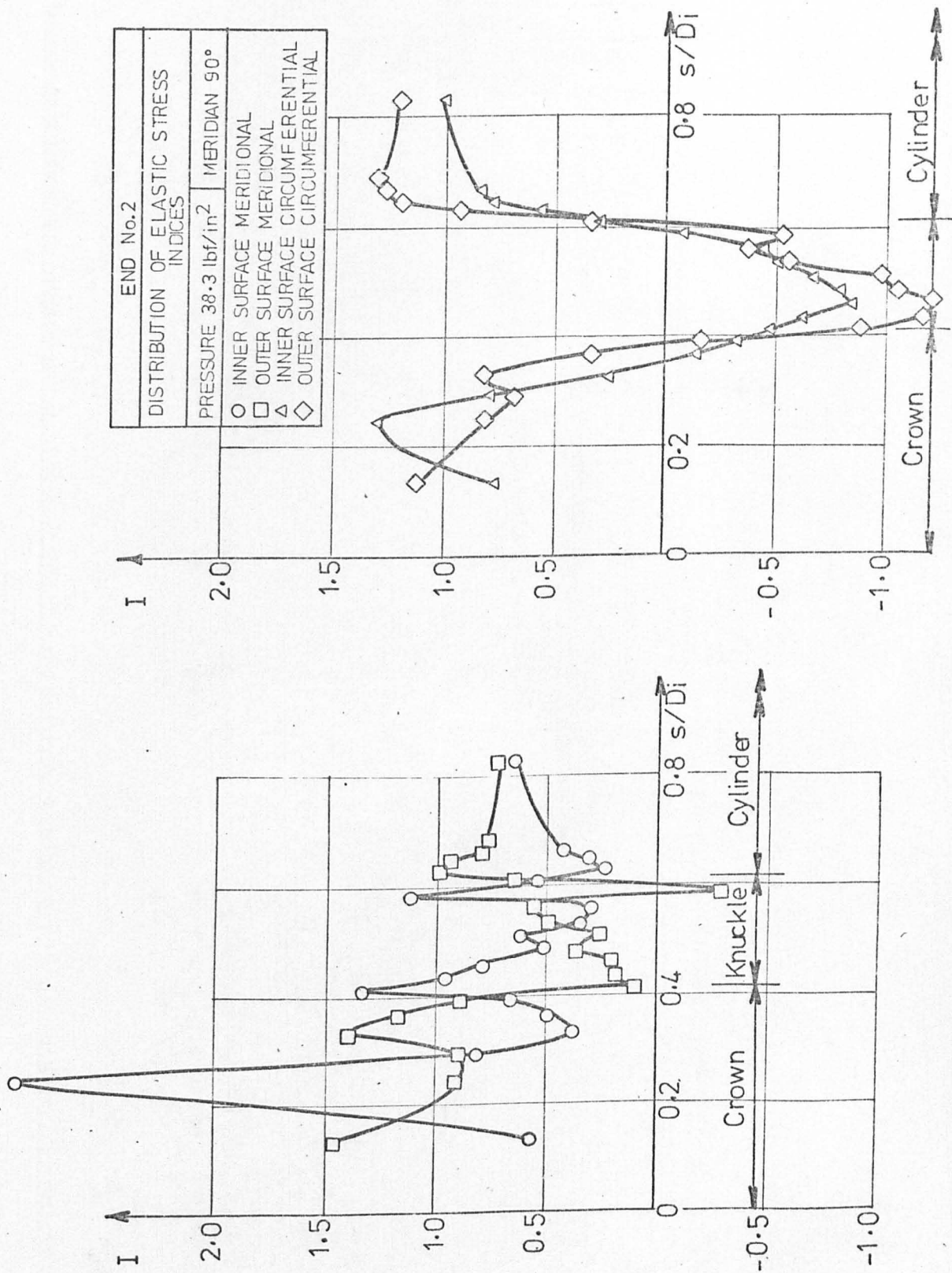


FIG.A1.2.5

END No.3  
THICKNESS VARIATION ALONG  
0° MERIDIAN

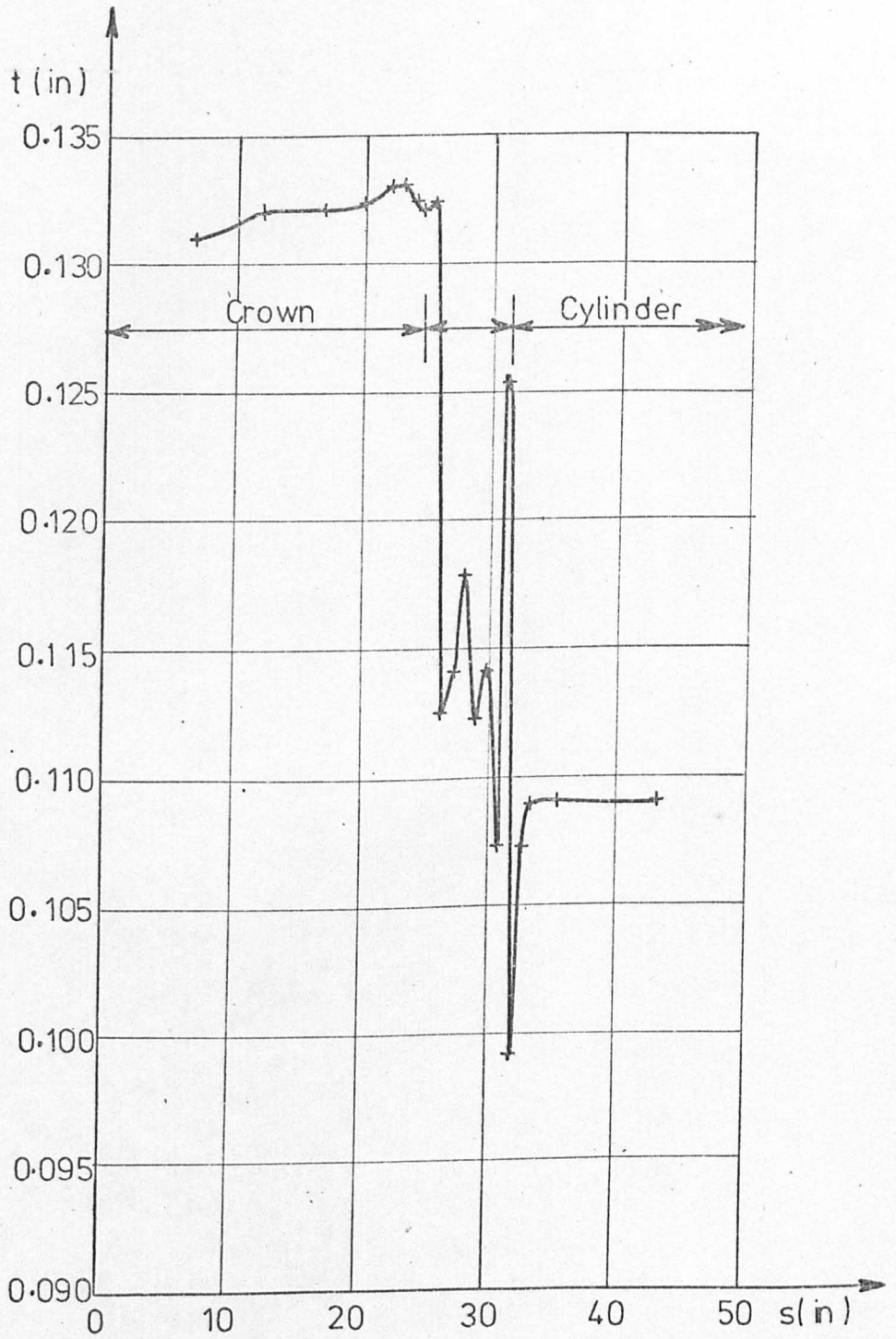


FIG. A1.3-1

END No. 3  
 CURVATURE VARIATION ALONG  
 0° MERIDIAN

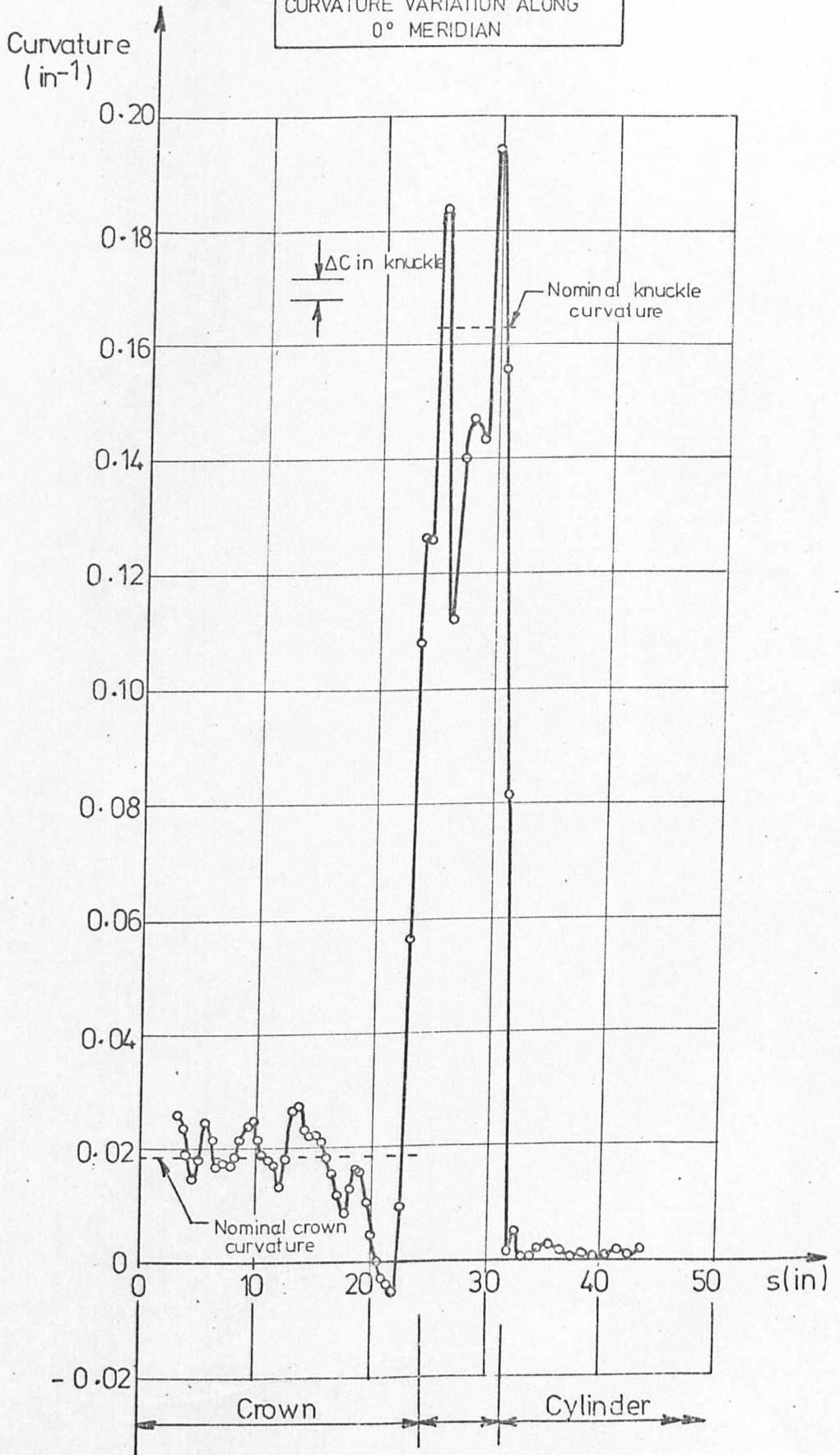


FIG A1.3.2

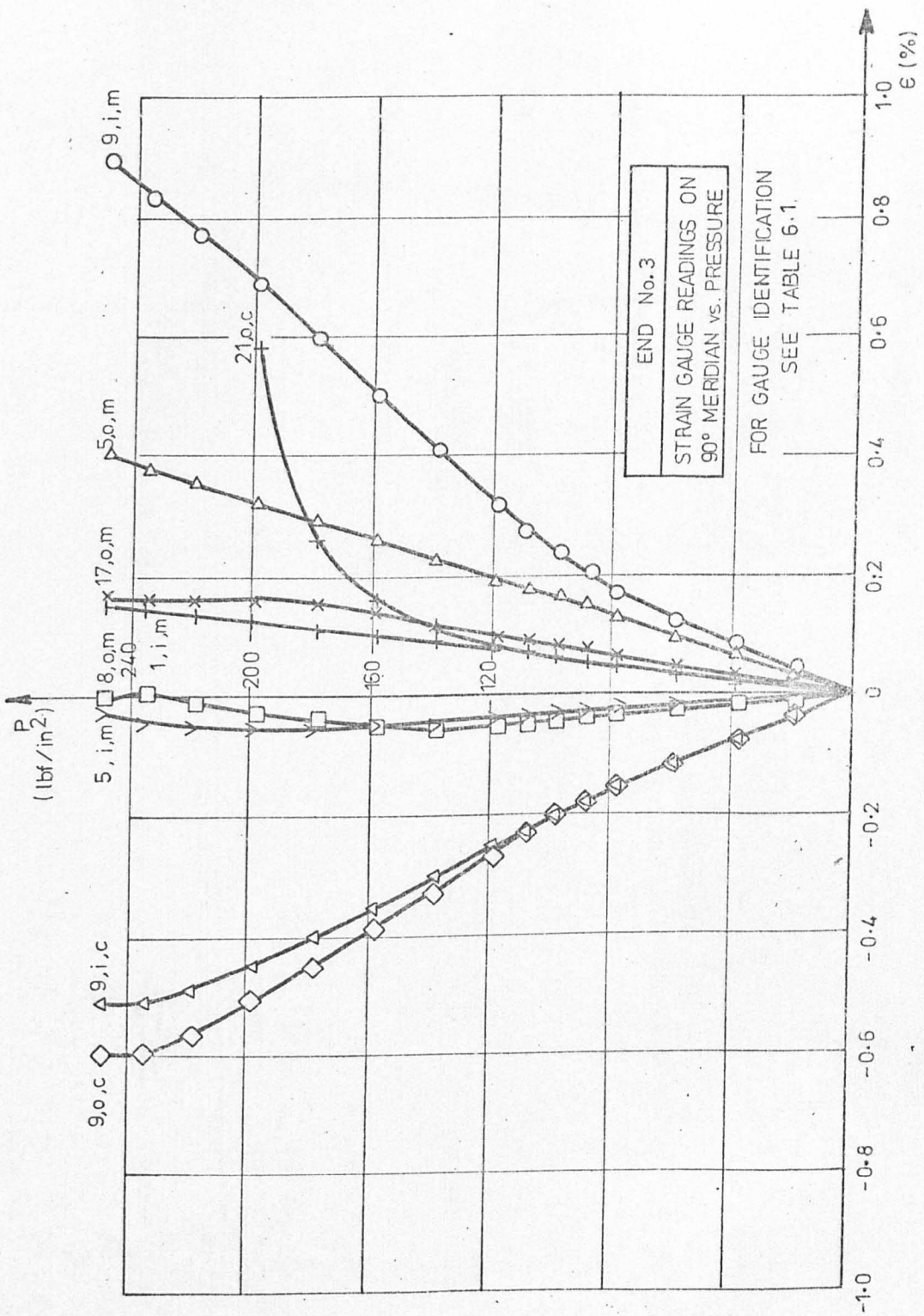


FIG. A1.3.3

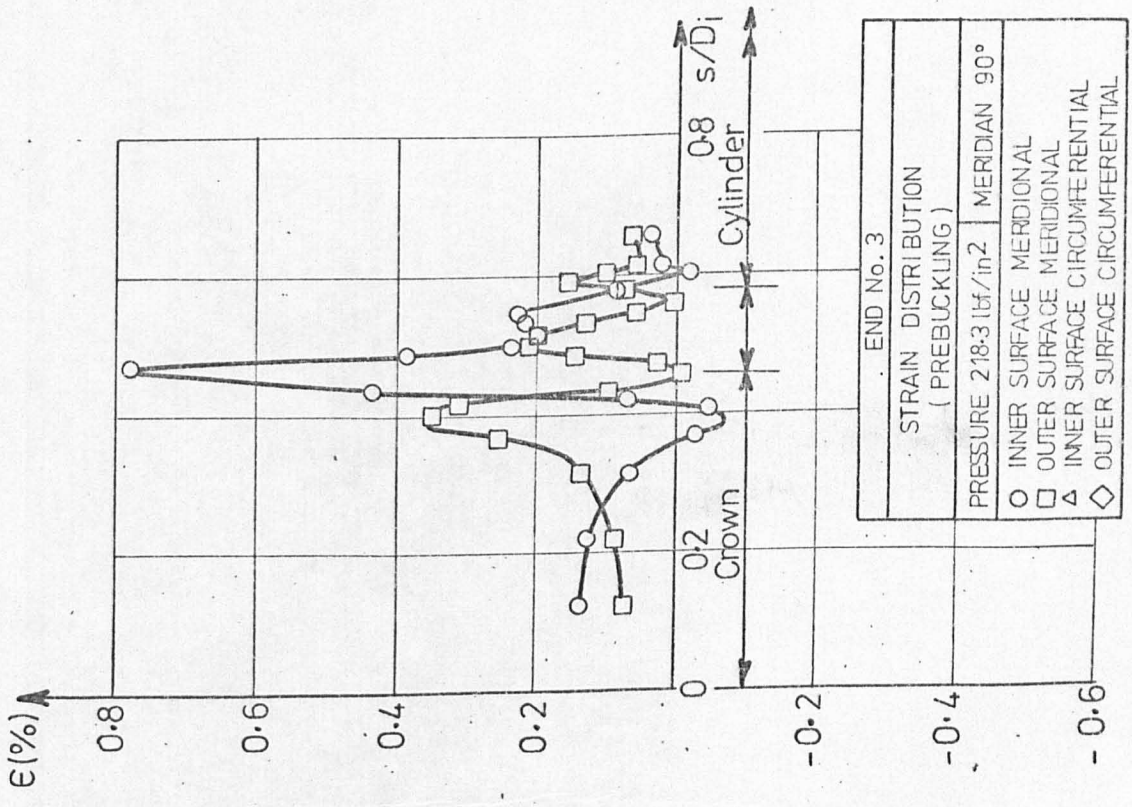
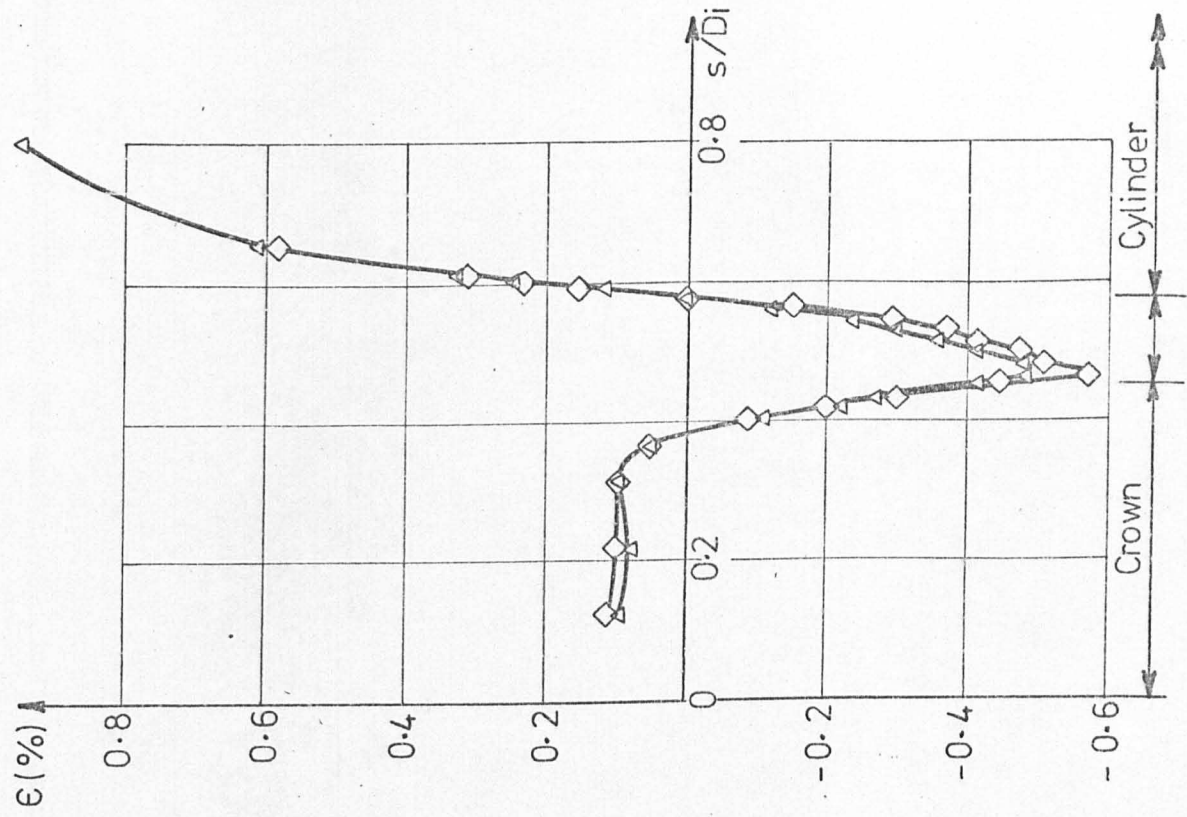


FIG. A1.3.4



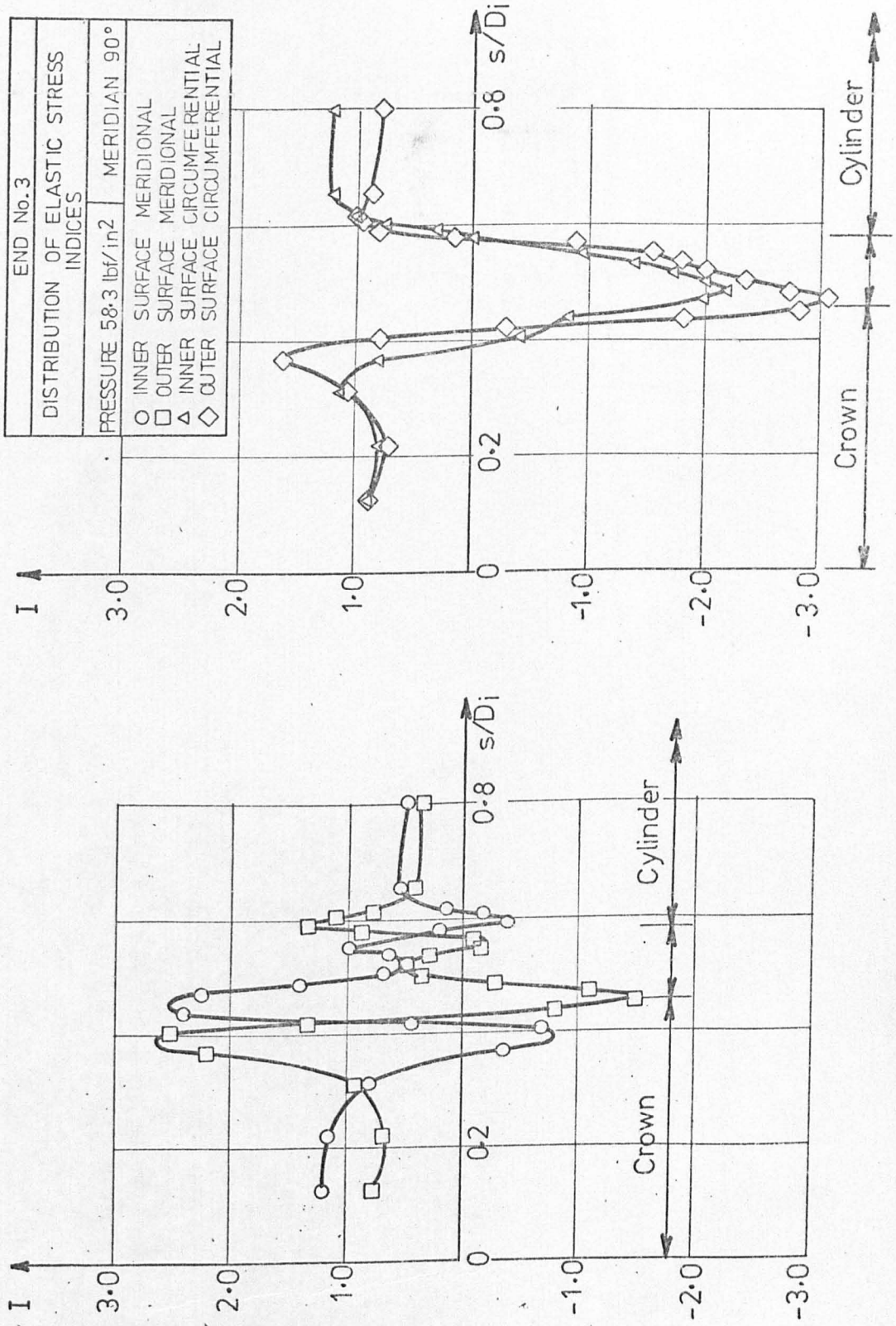


FIG.A1.3.5

END No. 4  
THICKNESS VARIATION ALONG  
0° MERIDIAN

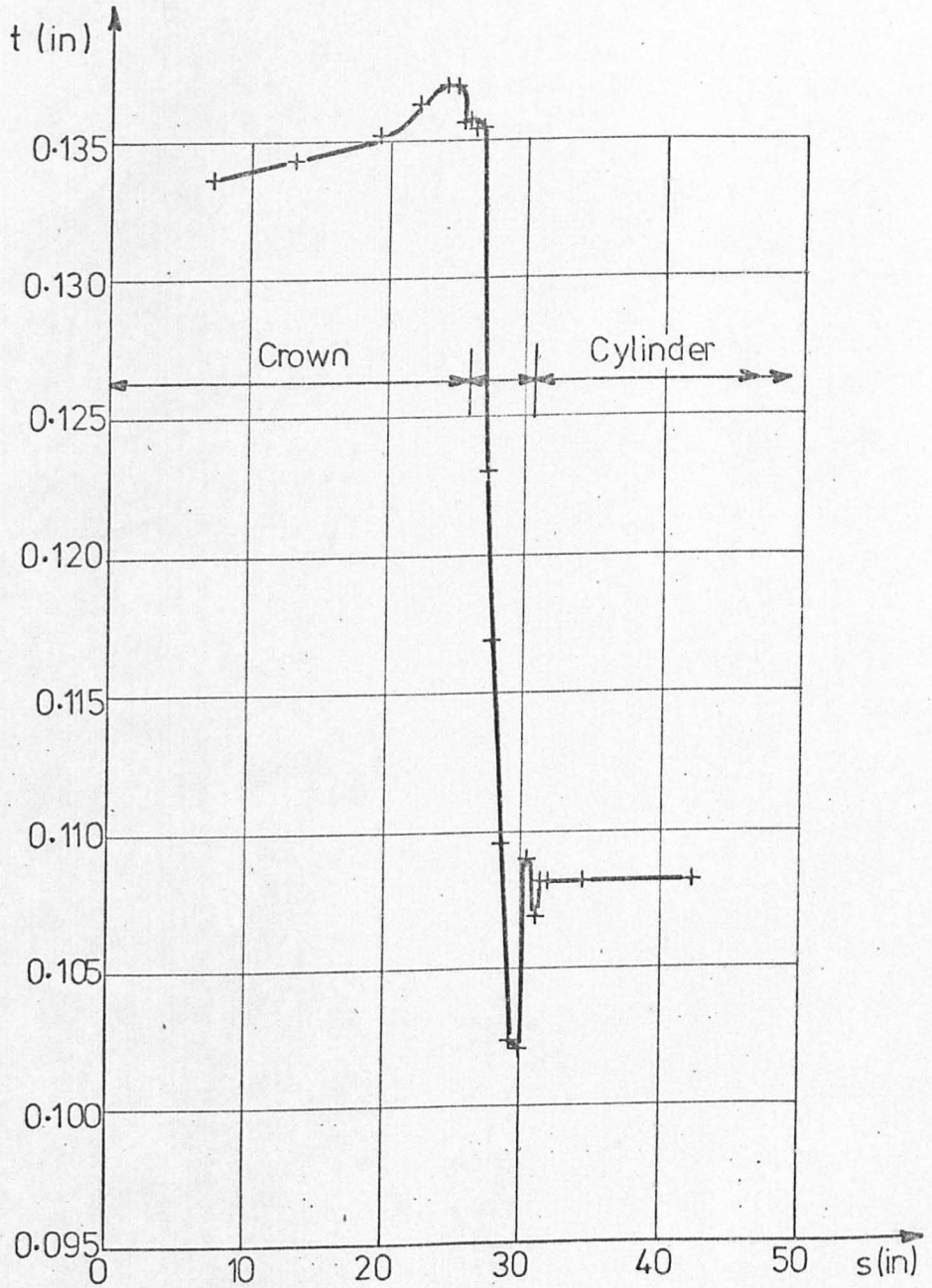


FIG. A1-4.1

END No. 4  
CURVATURE VARIATION ALONG  
0° MERIDIAN

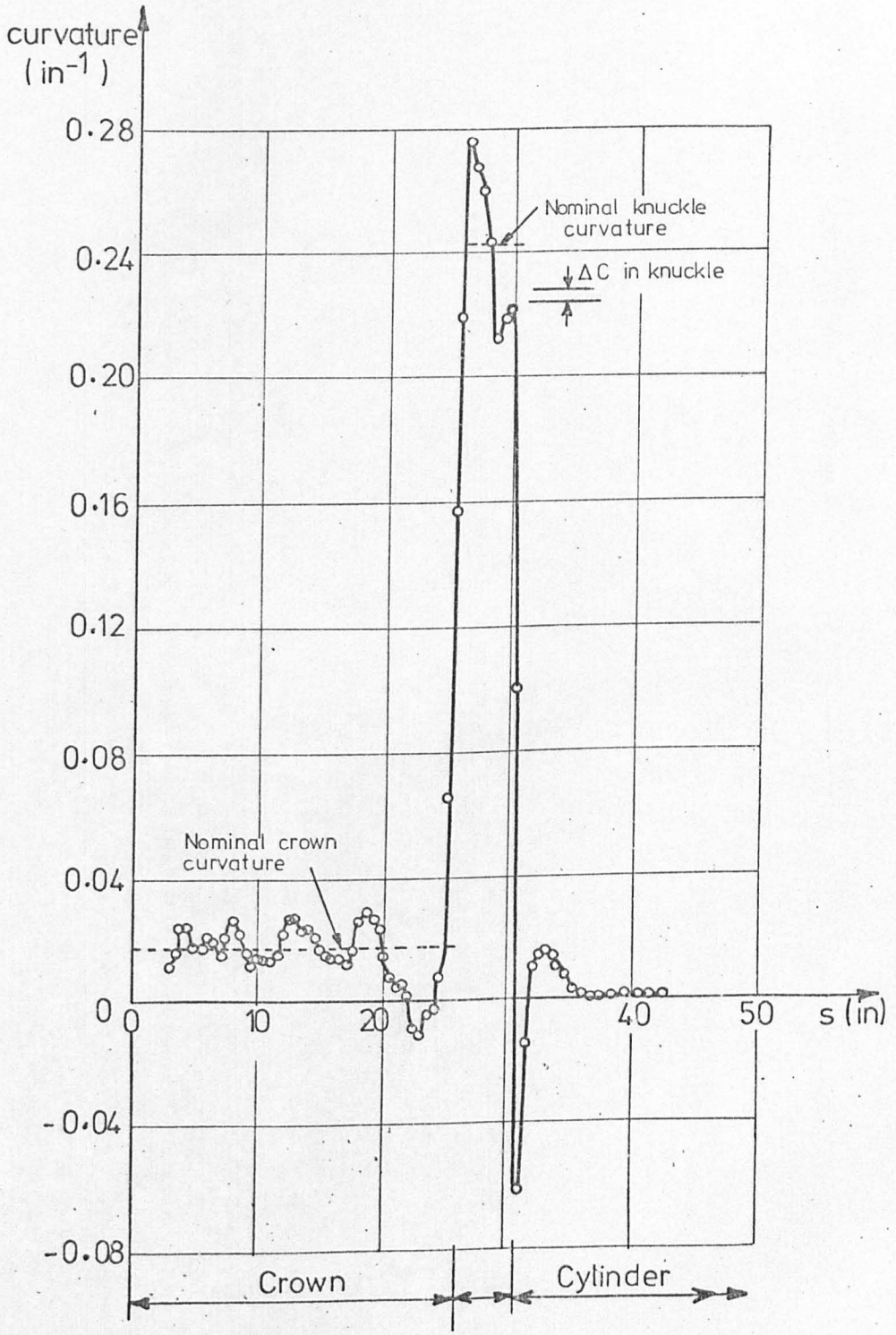


FIG. A1.4.2

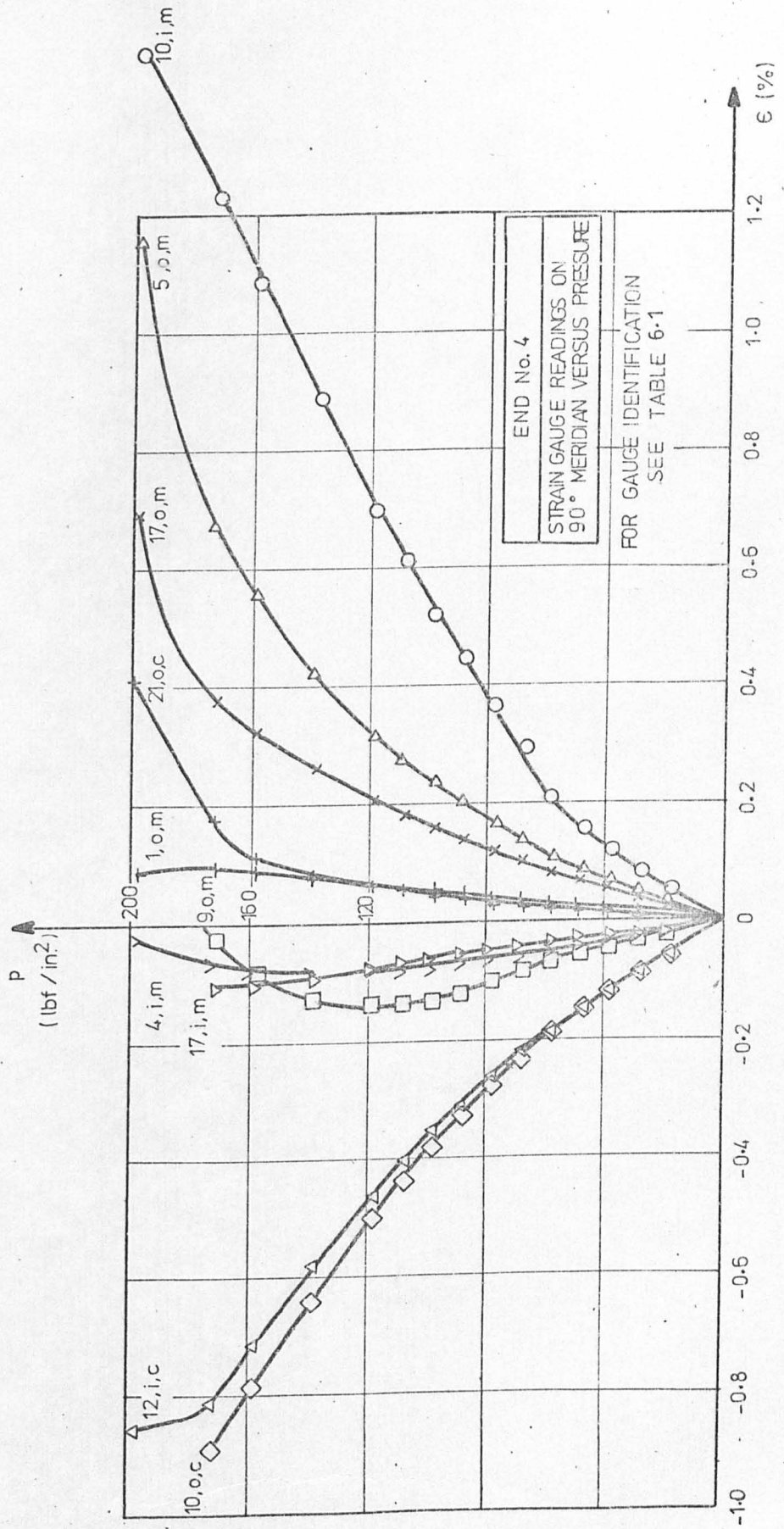


FIG. A1-4.3

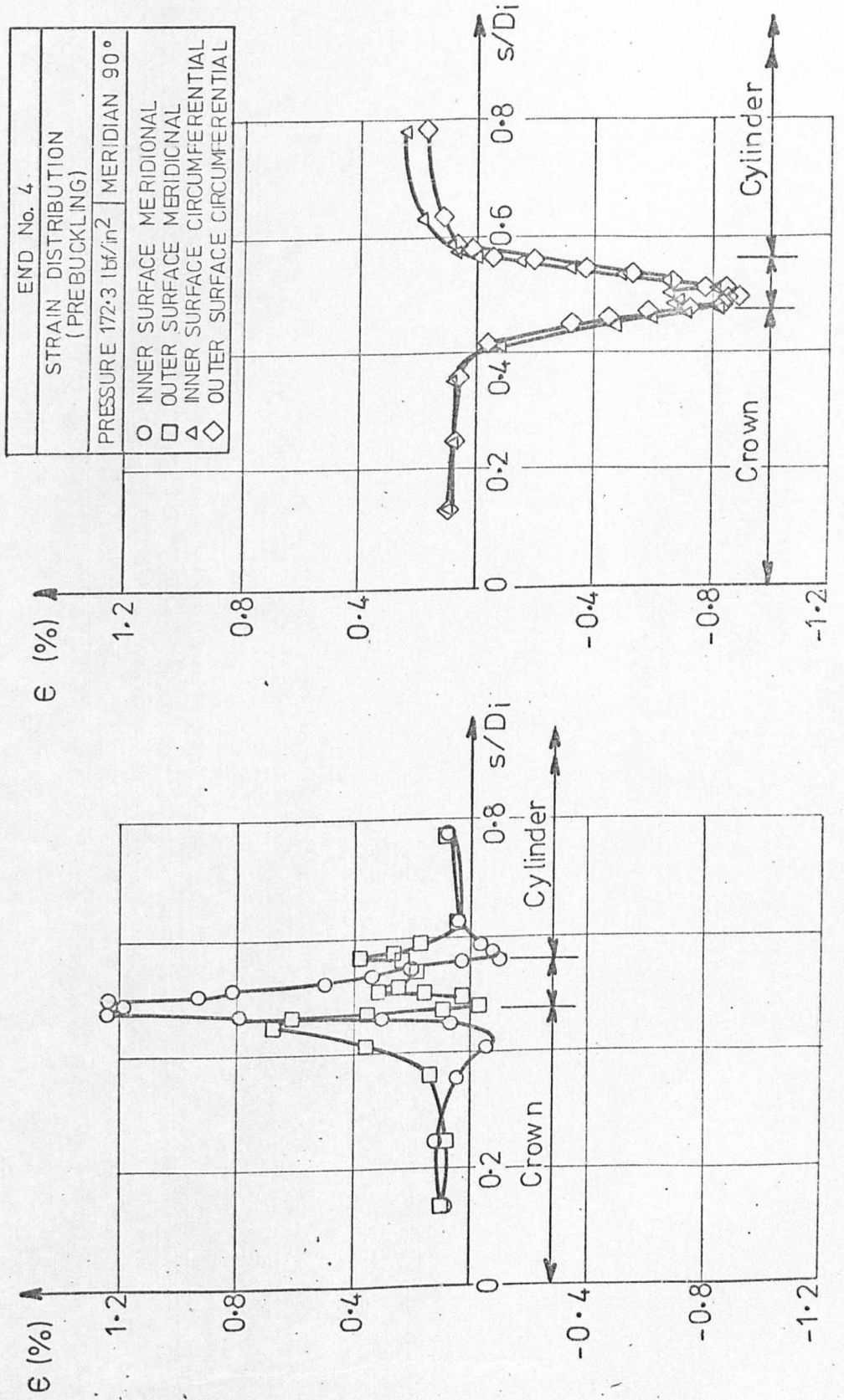


FIG. A1.4.4

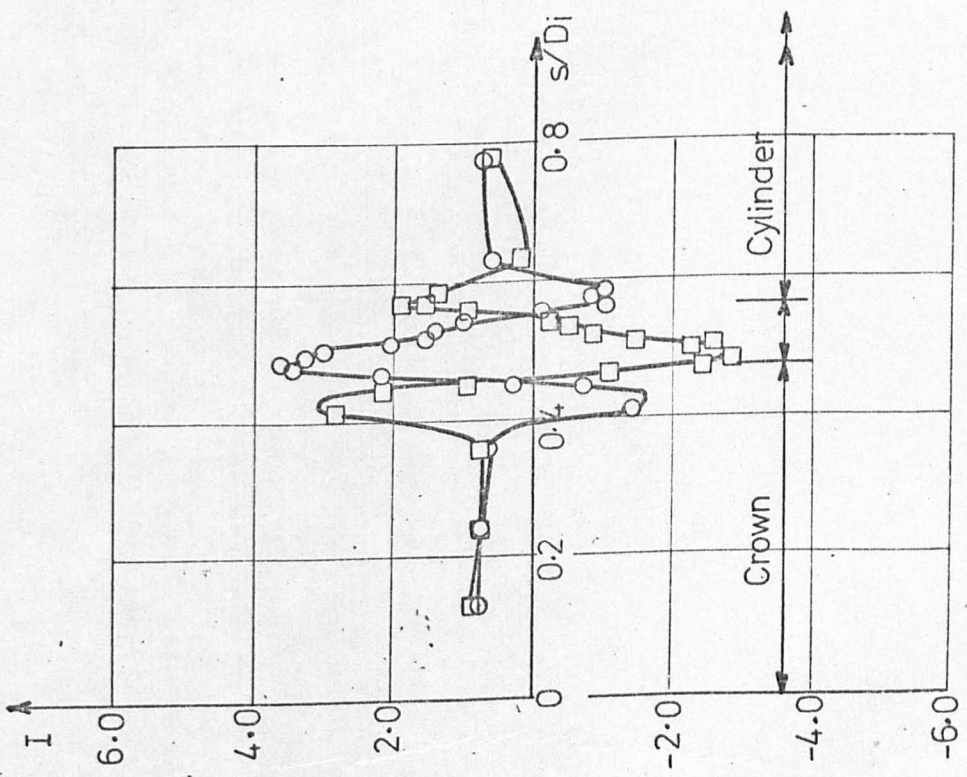
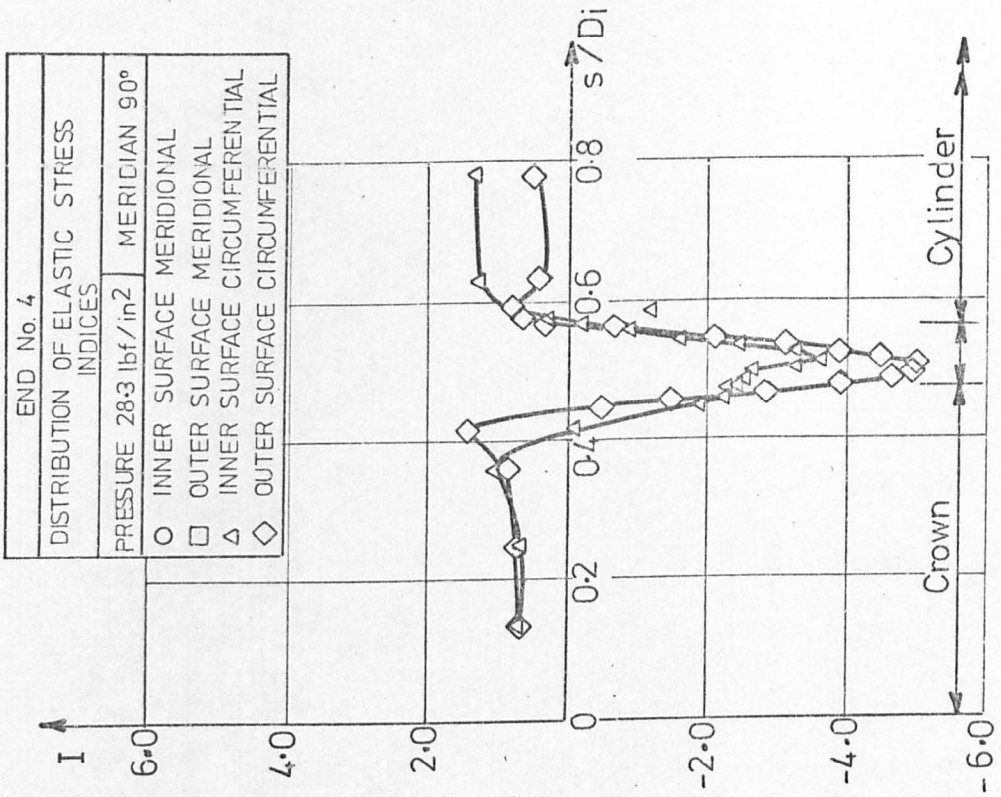


FIG.A1.4.5

END No. 5
THICKNESS VARIATION ALONG 0° MERIDIAN

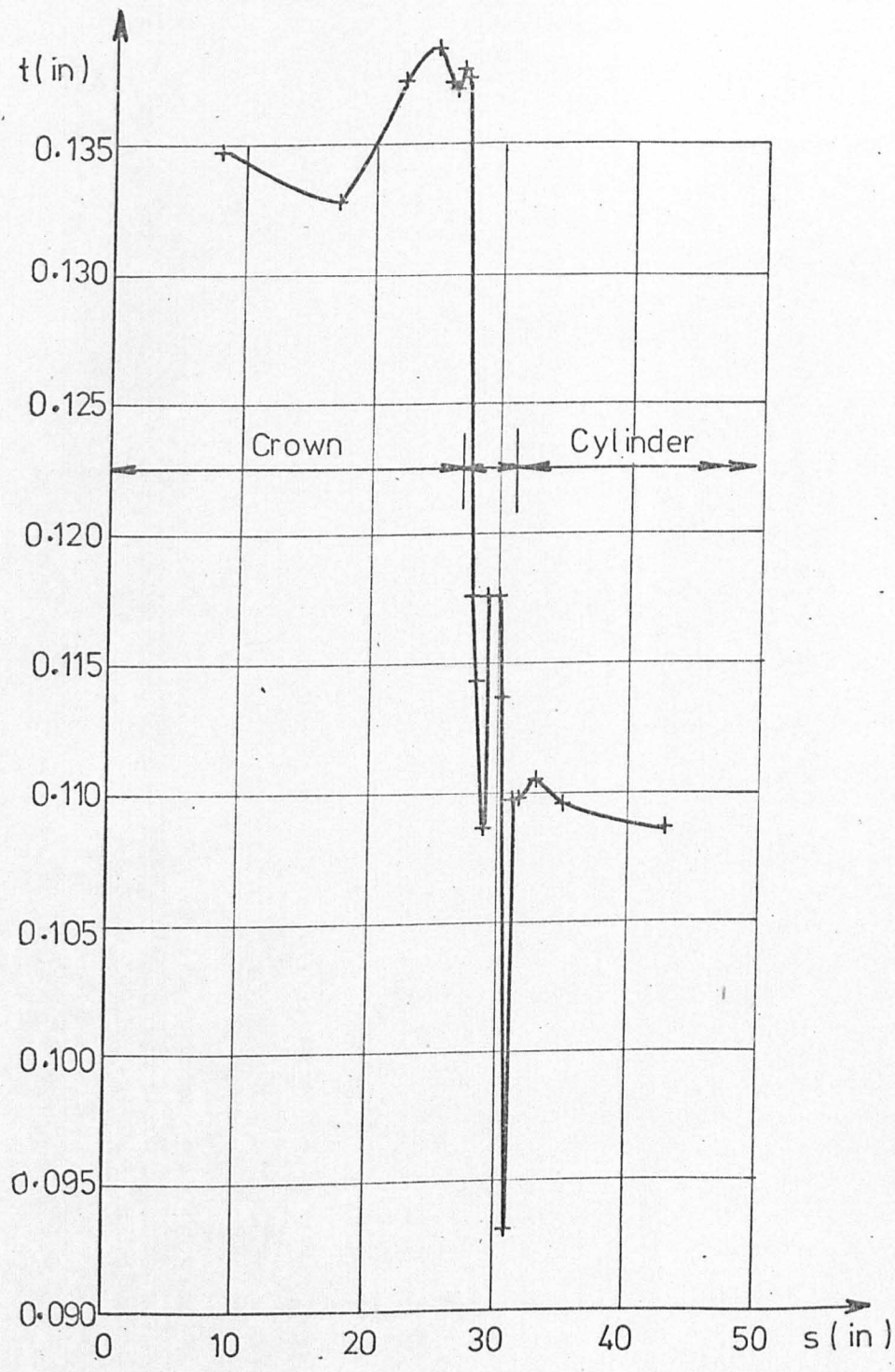


FIG. A1-5.1

END No. 5
CURVATURE VARIATION ALONG 0° MERIDIAN

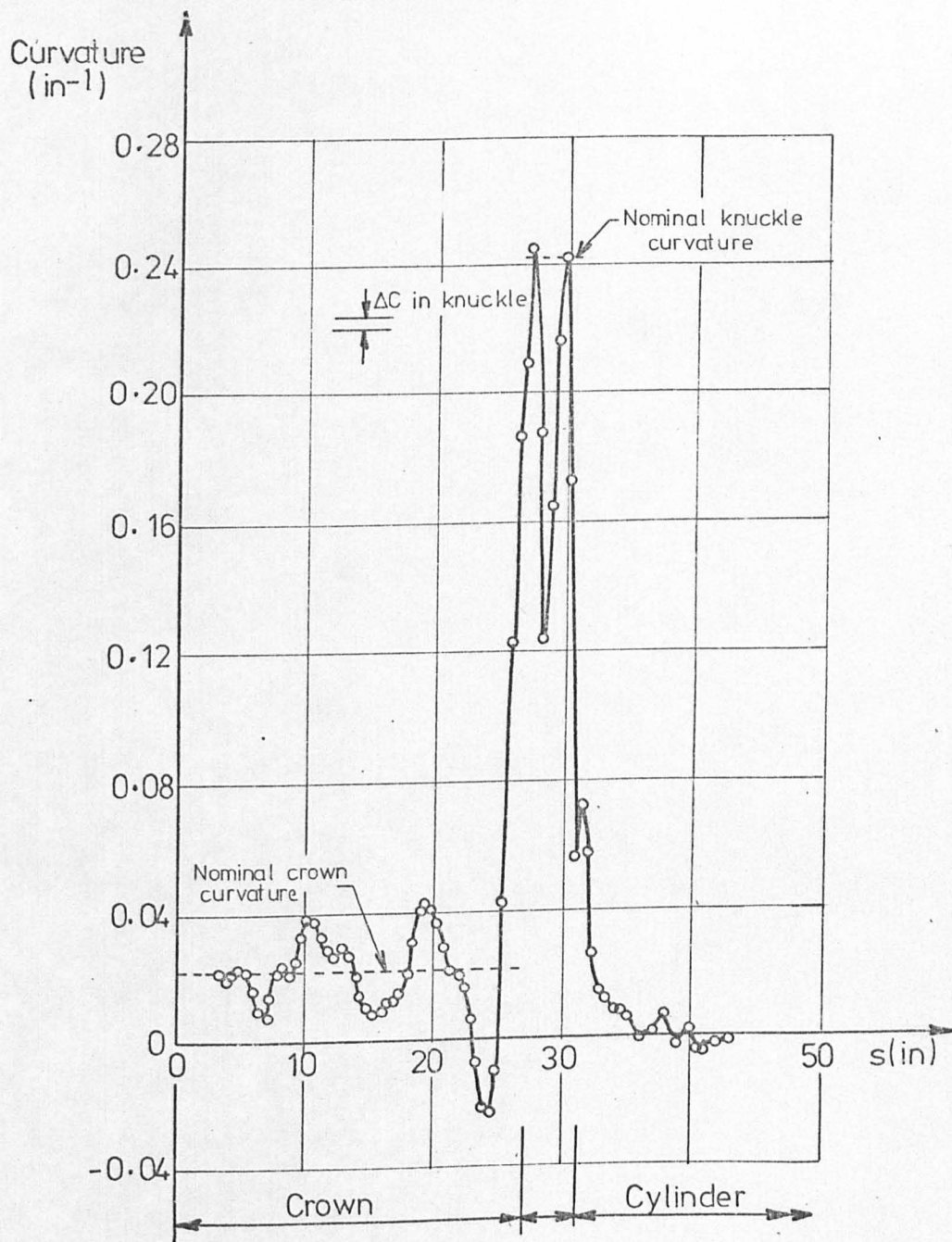


FIG.A1.5.2



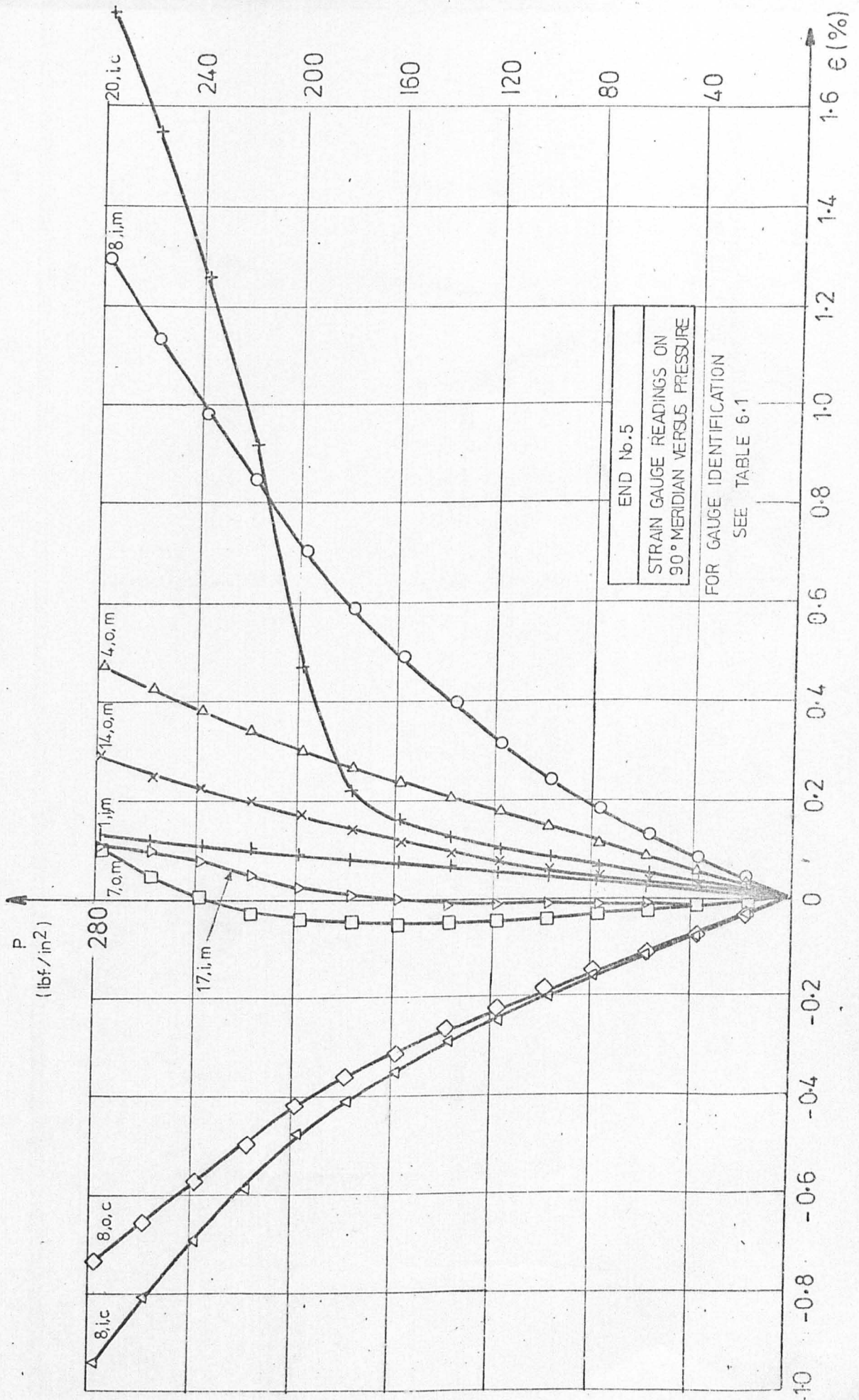
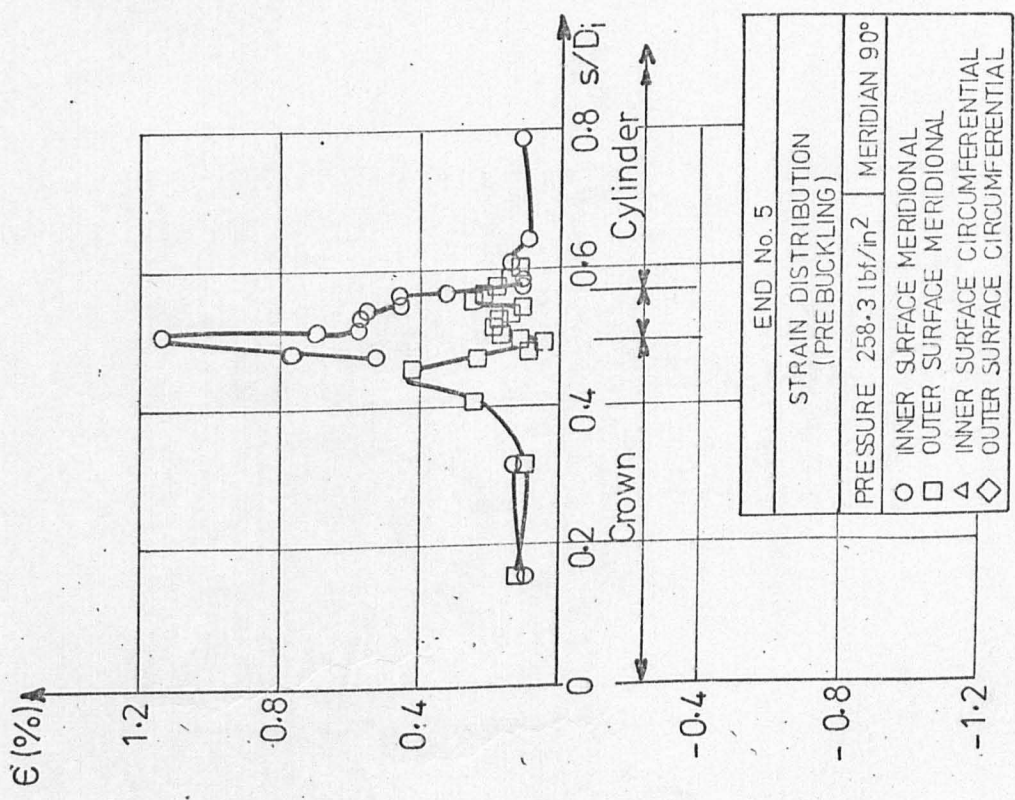
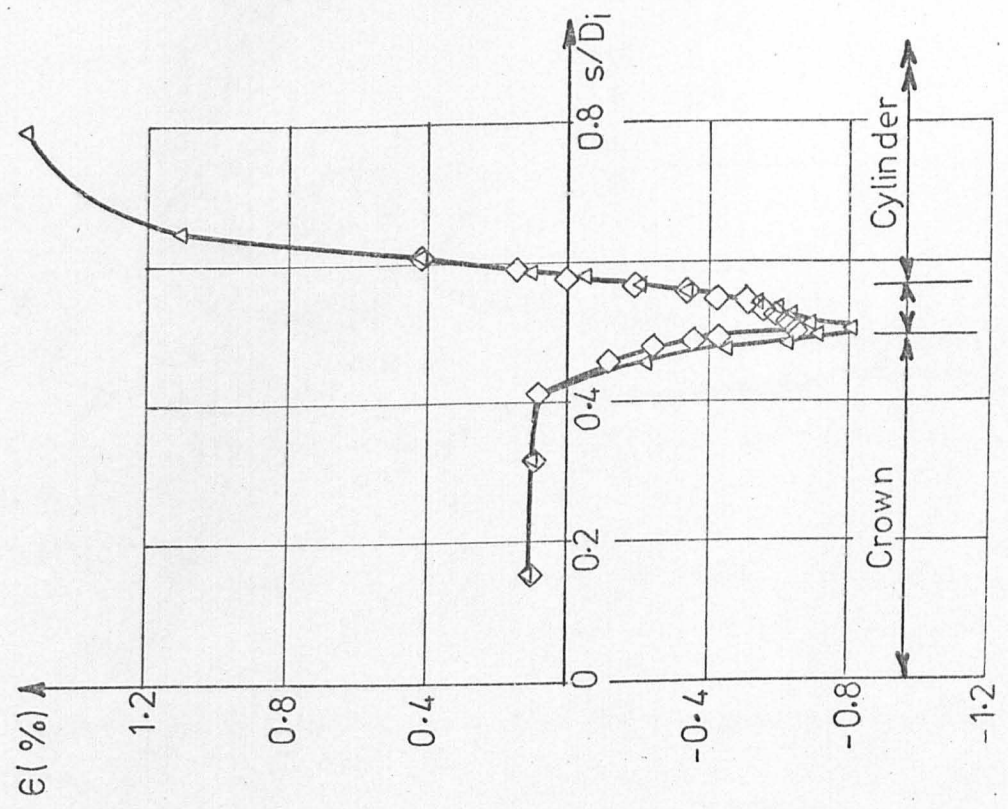


FIG. A1.5.3



END No. 5	
STRAIN DISTRIBUTION (PRE-BUCKLING)	
PRESSURE 258.3 lbf/in <sup>2</sup>	MERIDIAN 90°
○	INNER SURFACE MERIDIONAL
□	OUTER SURFACE MERIDIONAL
△	INNER SURFACE CIRCUMFERENTIAL
◇	OUTER SURFACE CIRCUMFERENTIAL

FIG.A1.5.4

END No. 5	
DISTRIBUTION OF ELASTIC STRESS INDICES	
PRESSURE 38.3 lbf/in <sup>2</sup>	MERIDIAN 90°
○ INNER SURFACE MERIDIONAL	○ INNER SURFACE MERIDIONAL
□ OUTER SURFACE MERIDIONAL	□ OUTER SURFACE MERIDIONAL
△ INNER SURFACE CIRCUMFERENTIAL	△ INNER SURFACE CIRCUMFERENTIAL
◇ OUTER SURFACE CIRCUMFERENTIAL	◇ OUTER SURFACE CIRCUMFERENTIAL

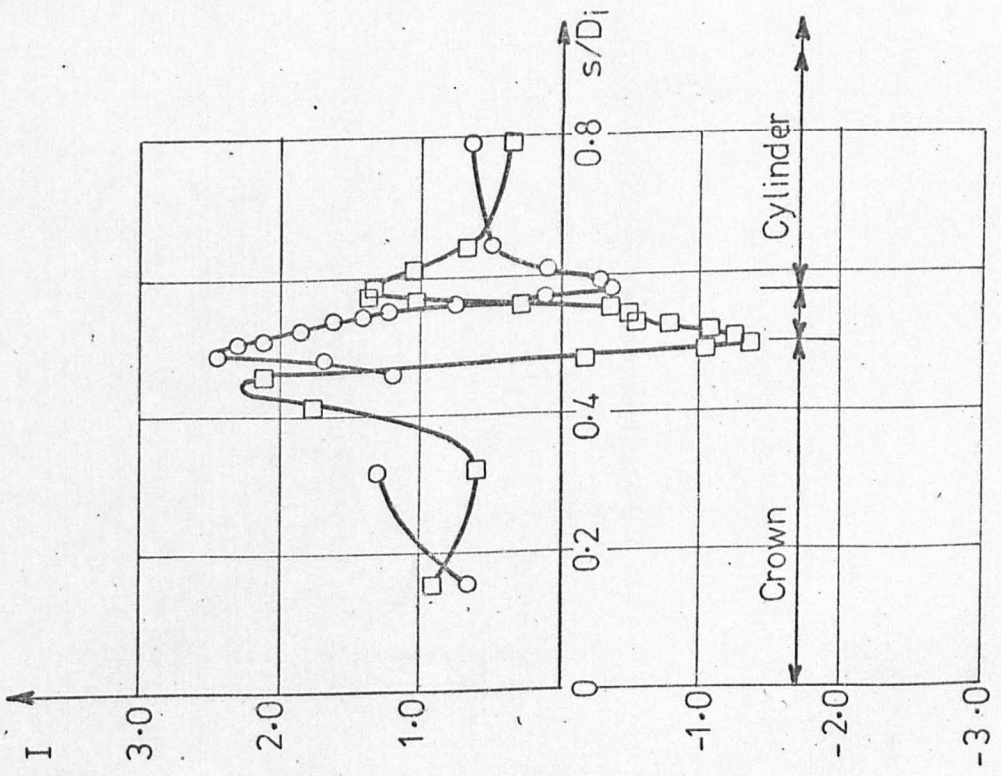
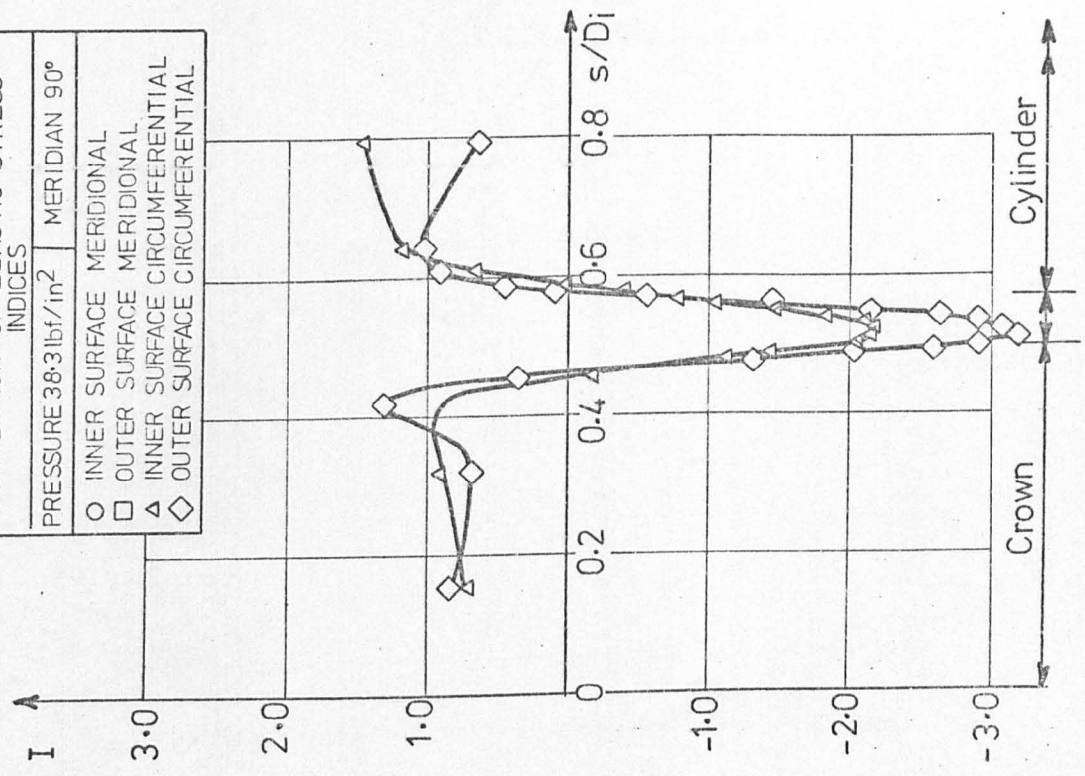


FIG. A1.5.5

END No. 6  
THICKNESS VARIATION ALONG  
0° MERIDIAN

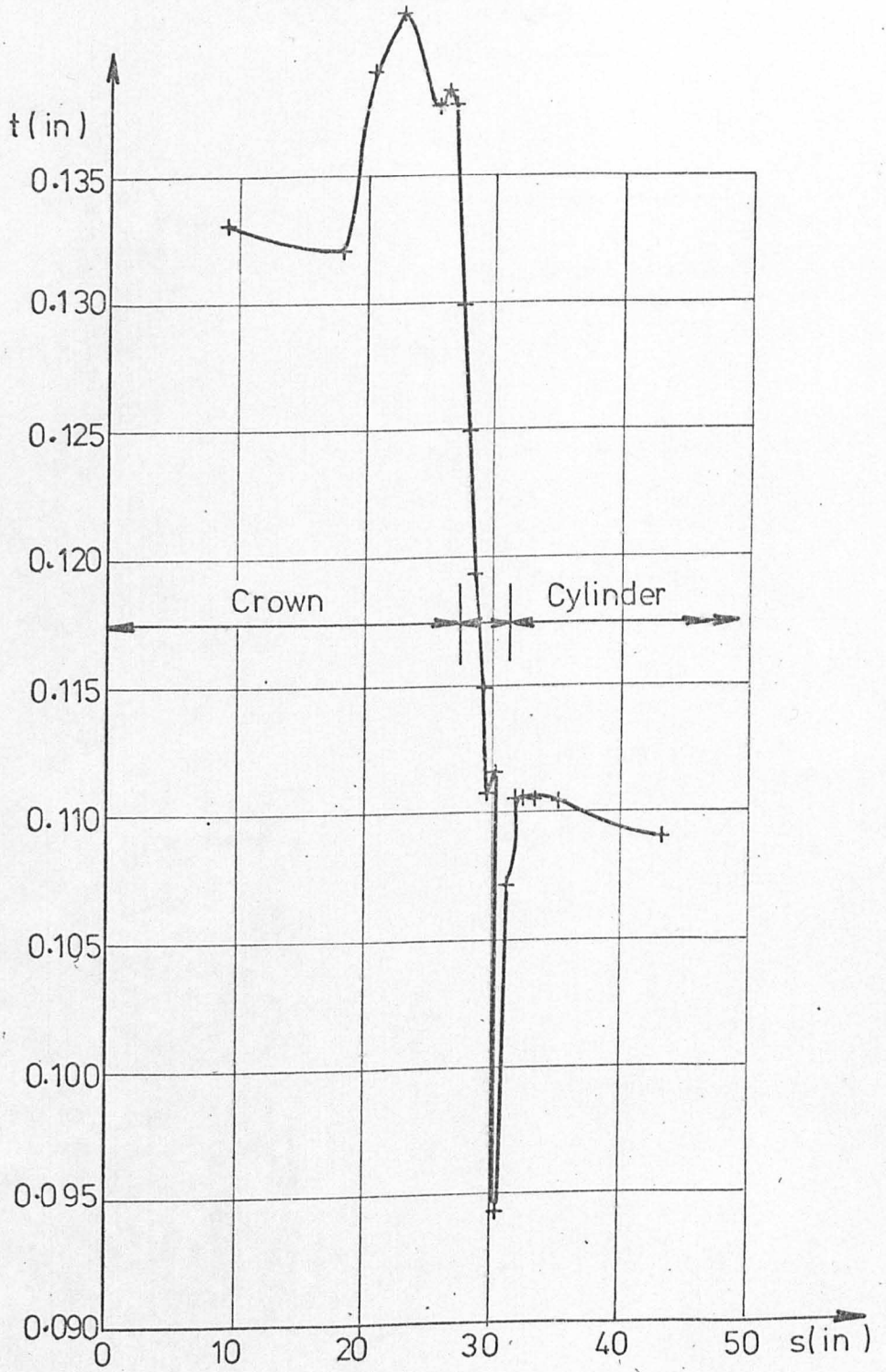


FIG A1.6-1

END No.6
CURVATURE VARIATION ALONG 180° MERIDIAN

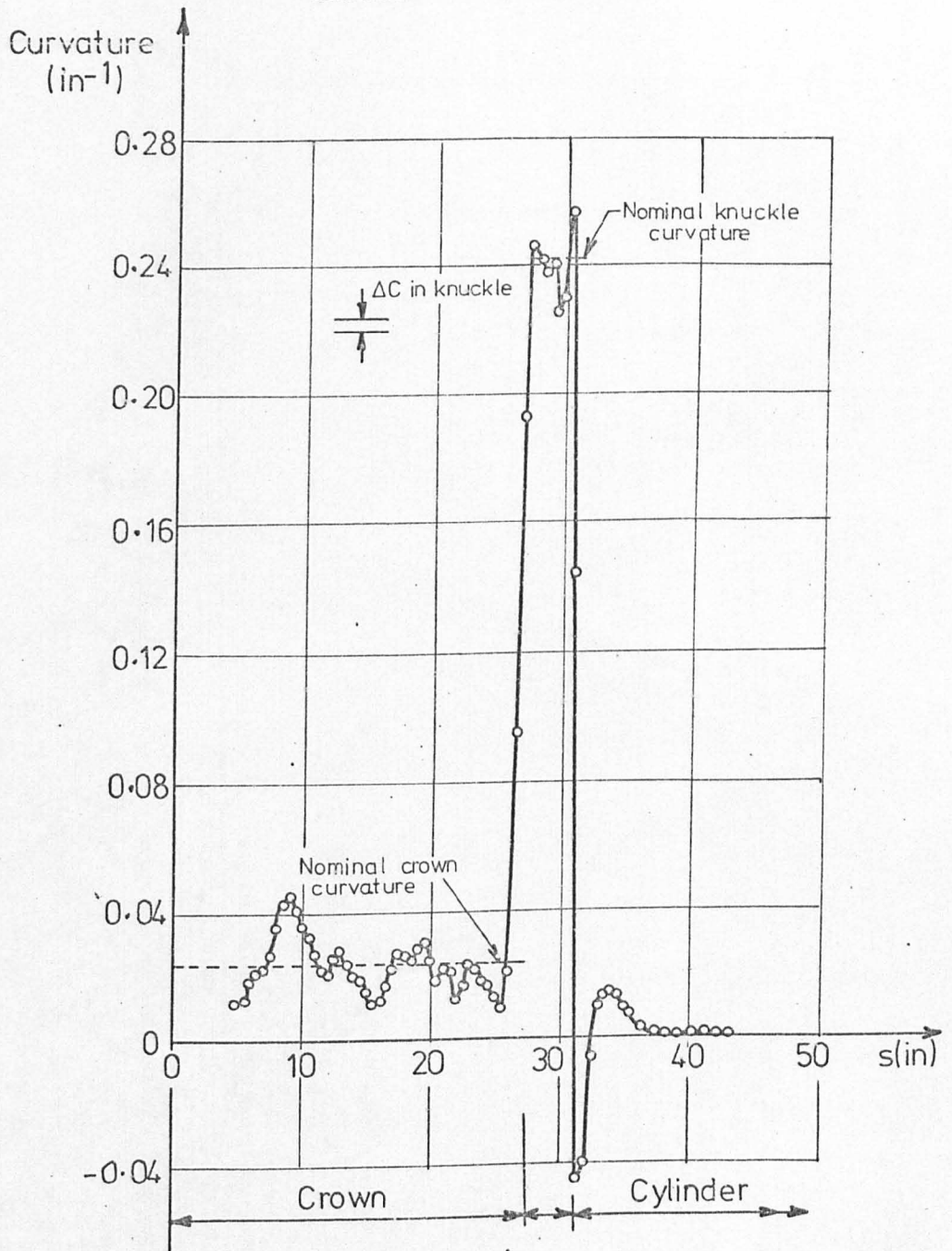


FIG.A1.6.2

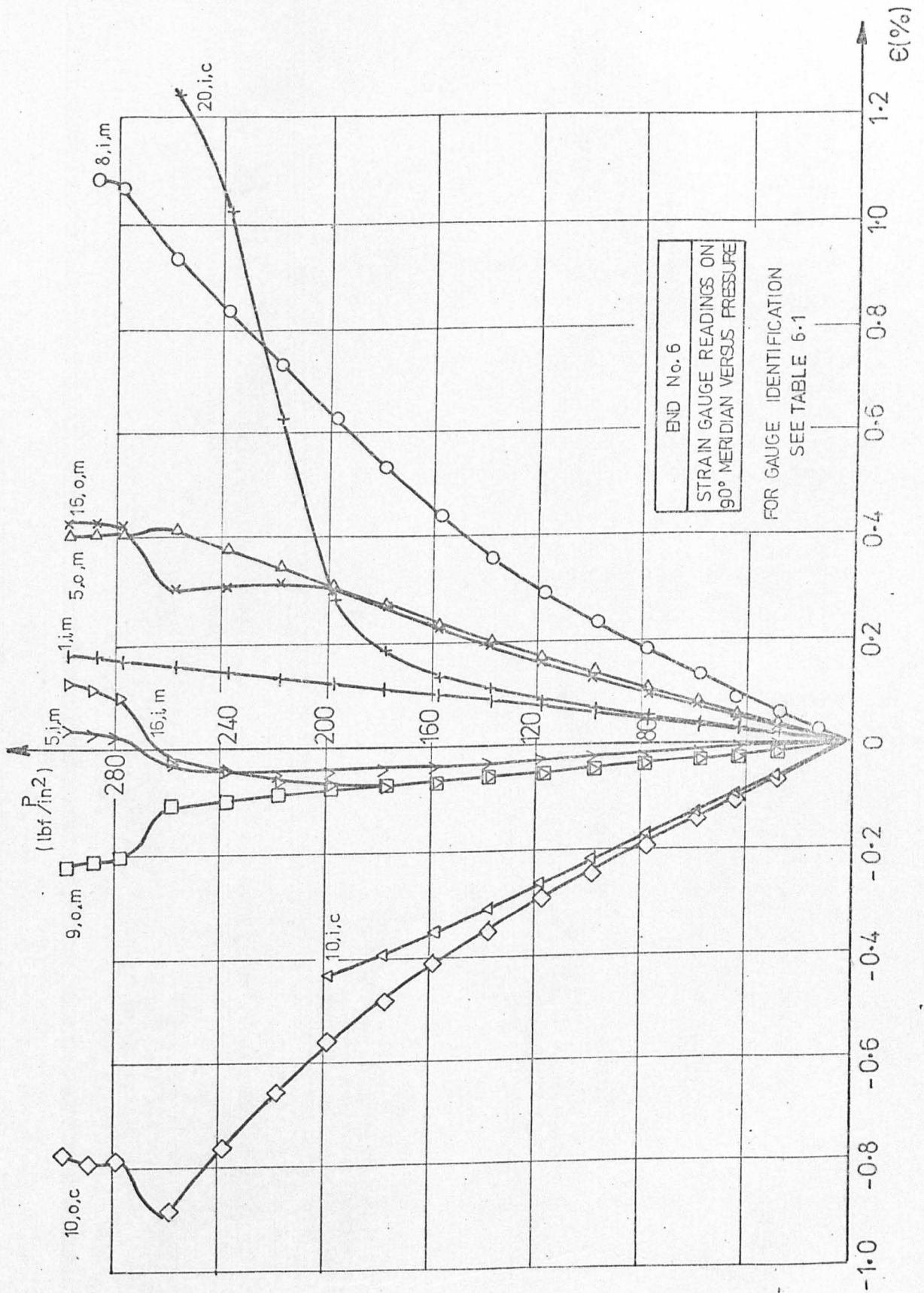


FIG. A1.6.3

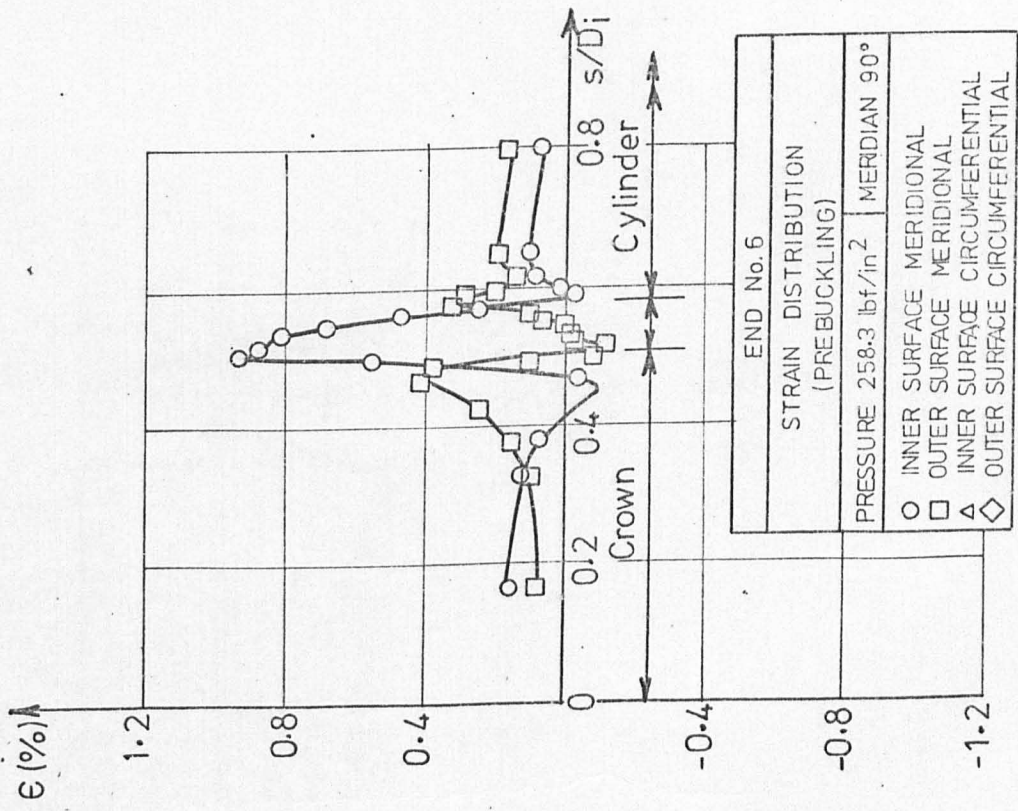
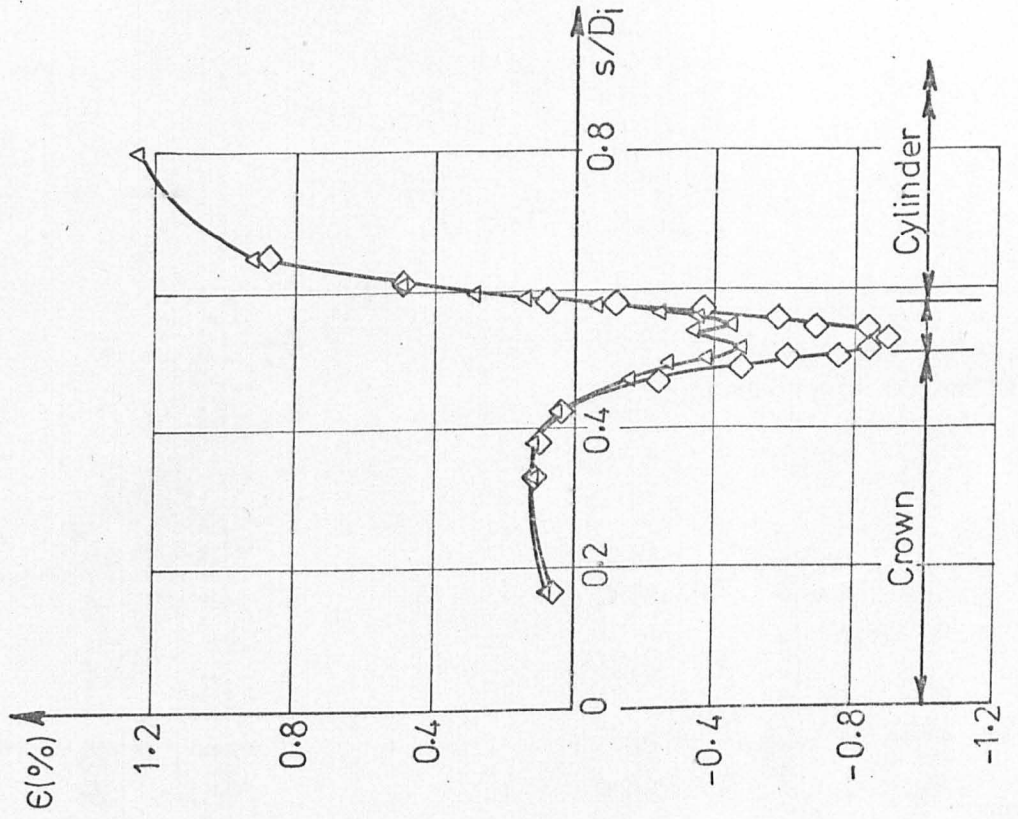


FIG. A1.6.4

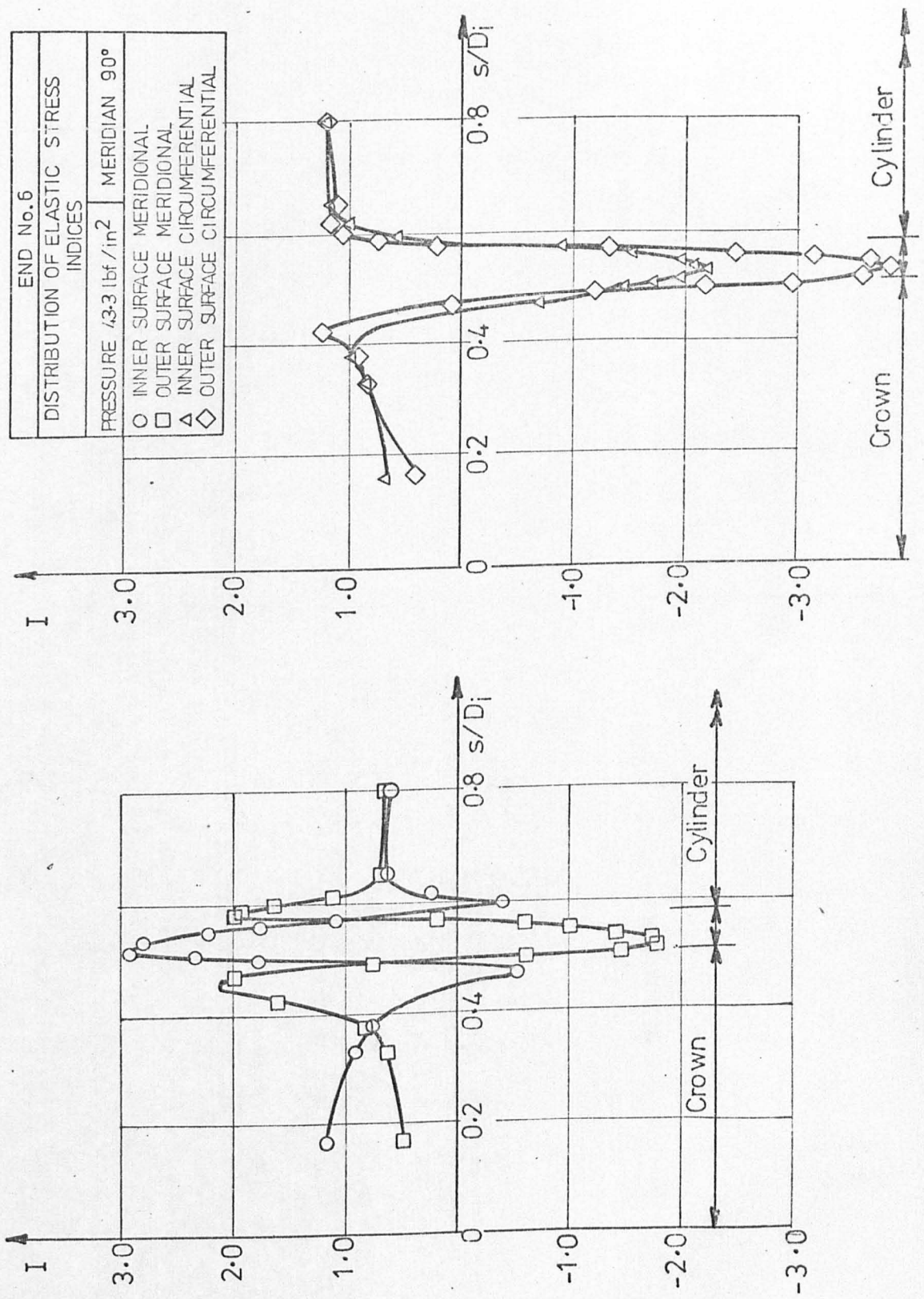


FIG. A1.6.5



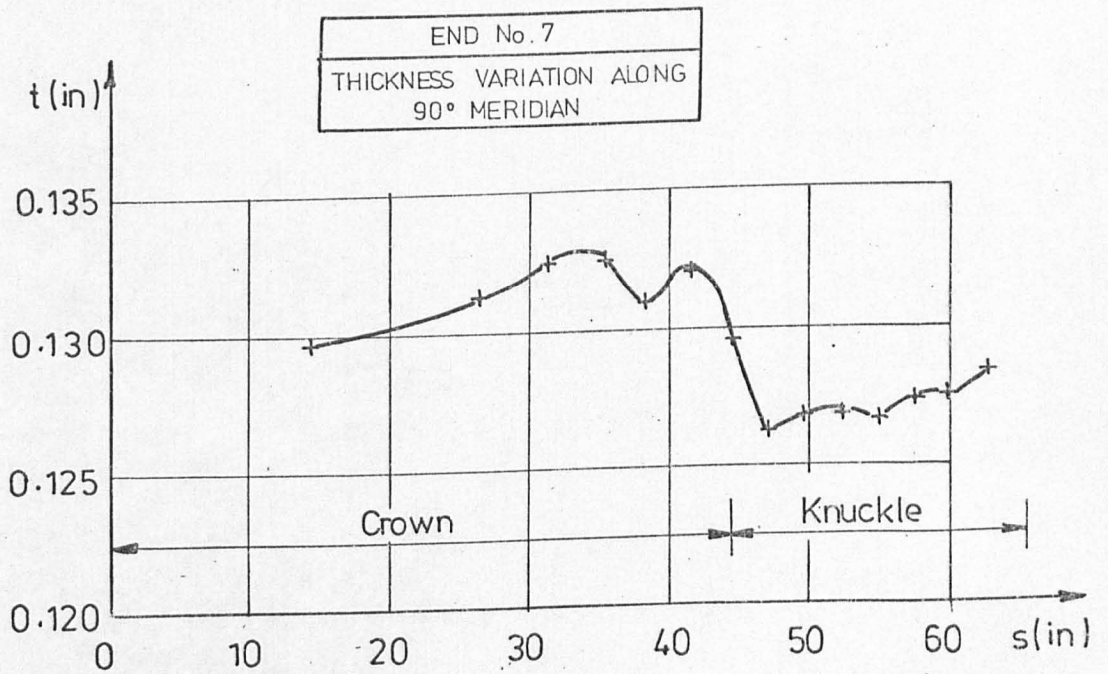
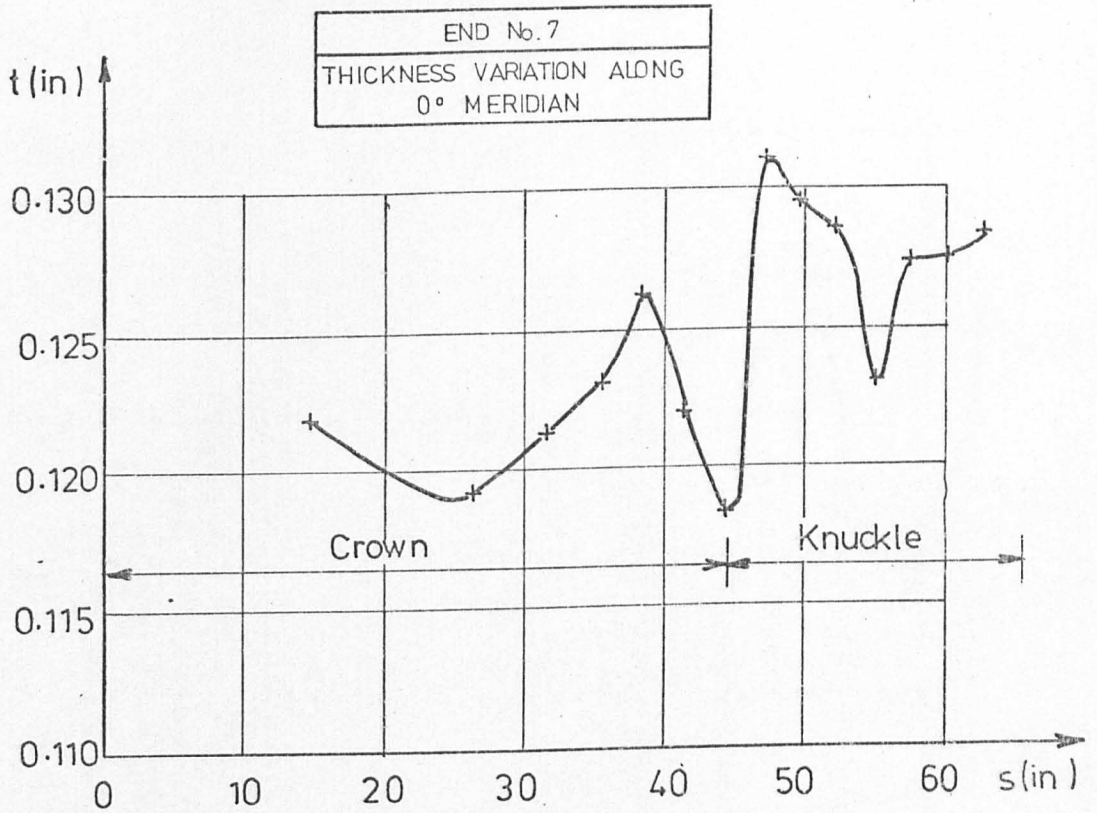


FIG.A1.7.1

END No.7  
 CURVATURE VARIATION ALONG  
 45° MERIDIAN

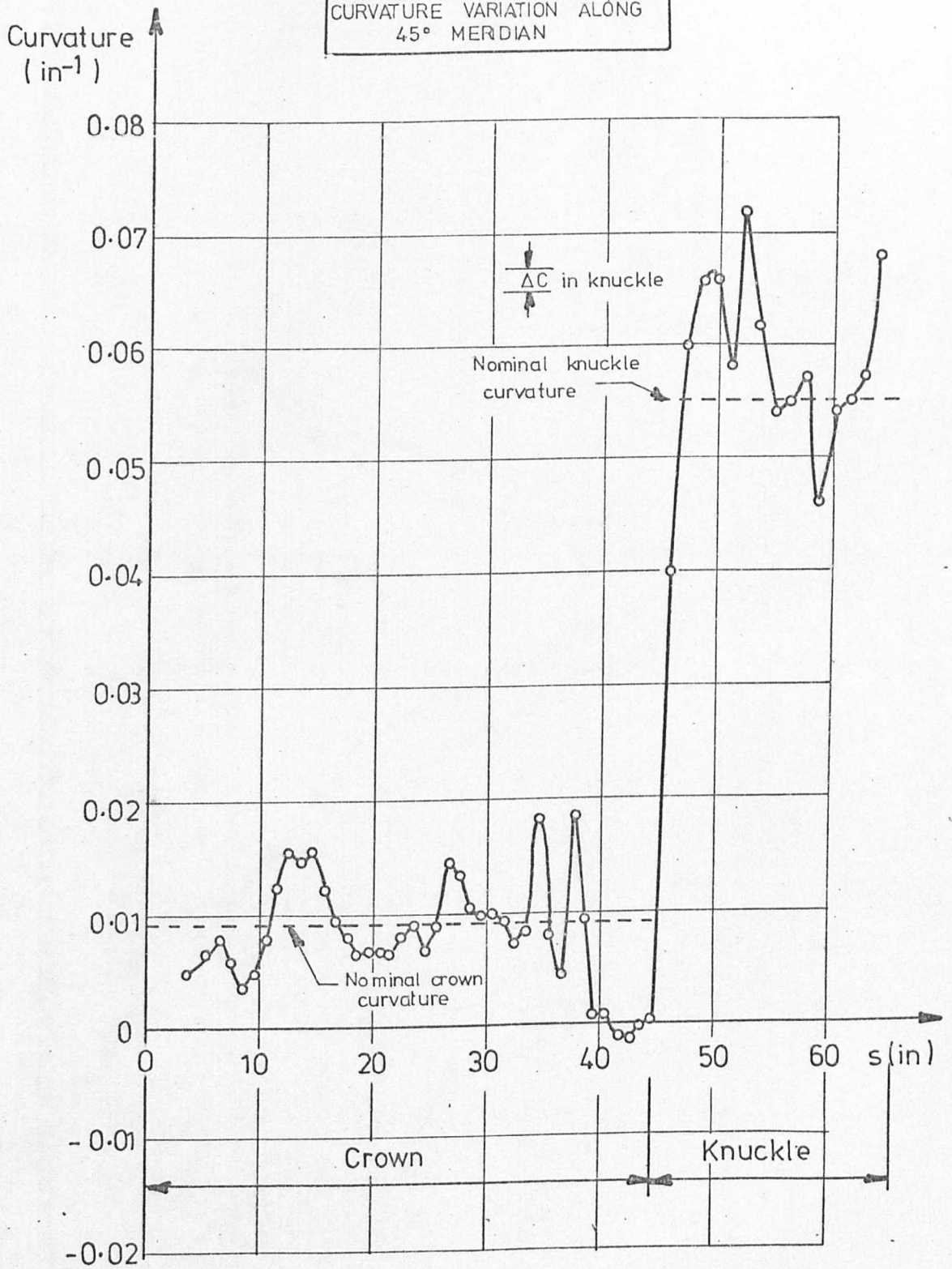


FIG. A1.7-2

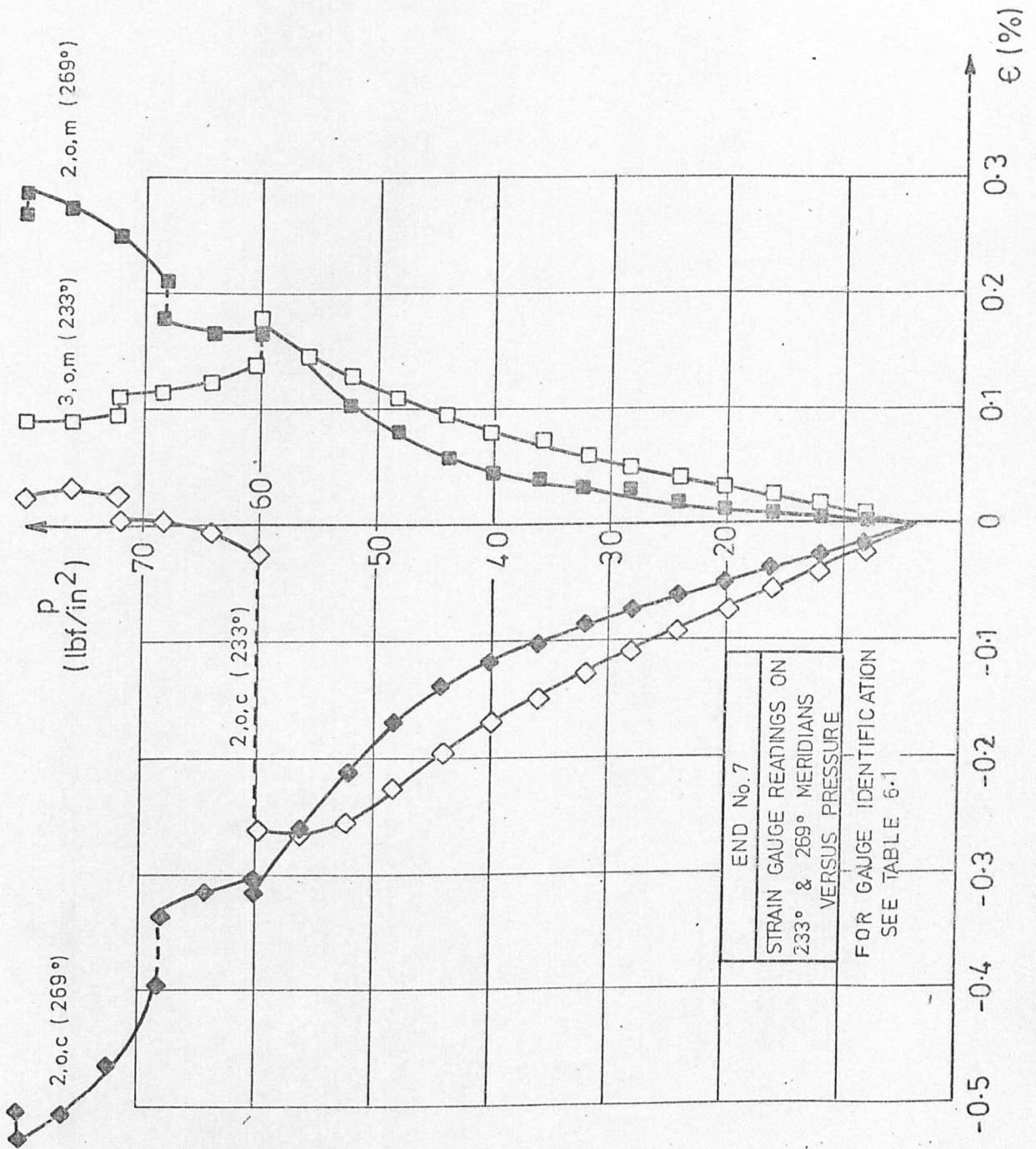
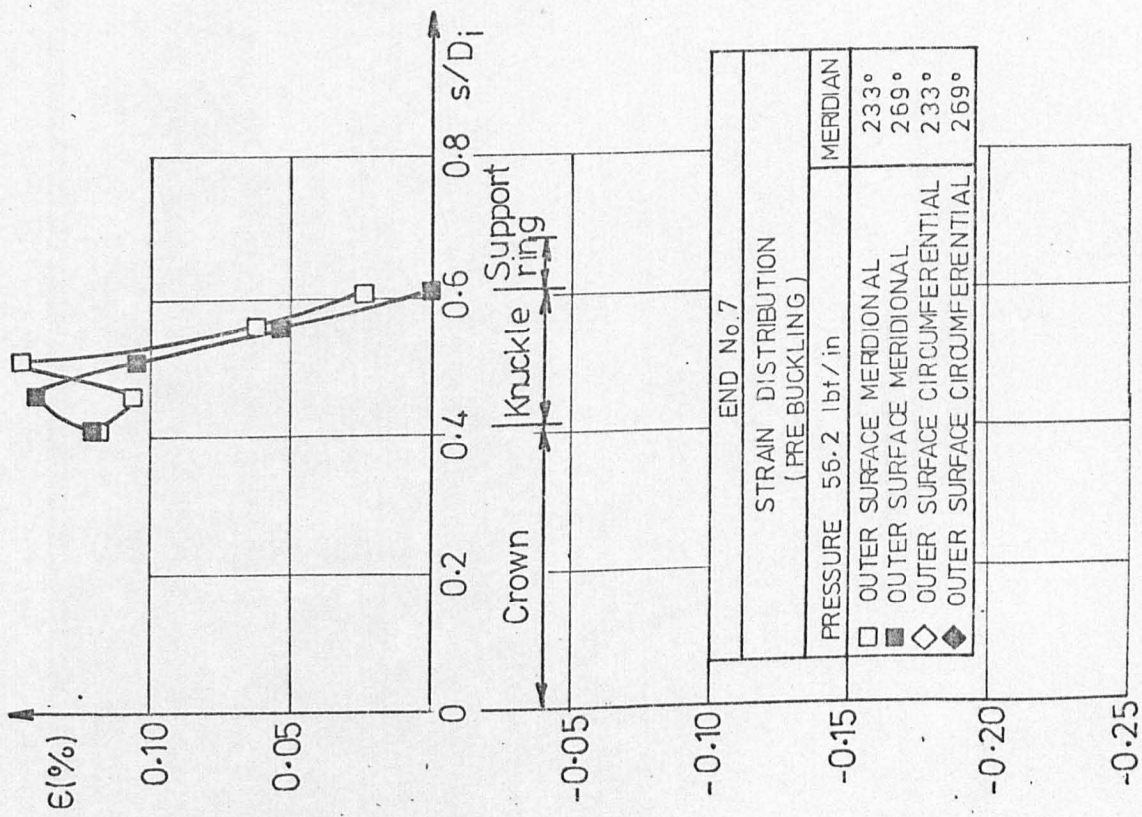
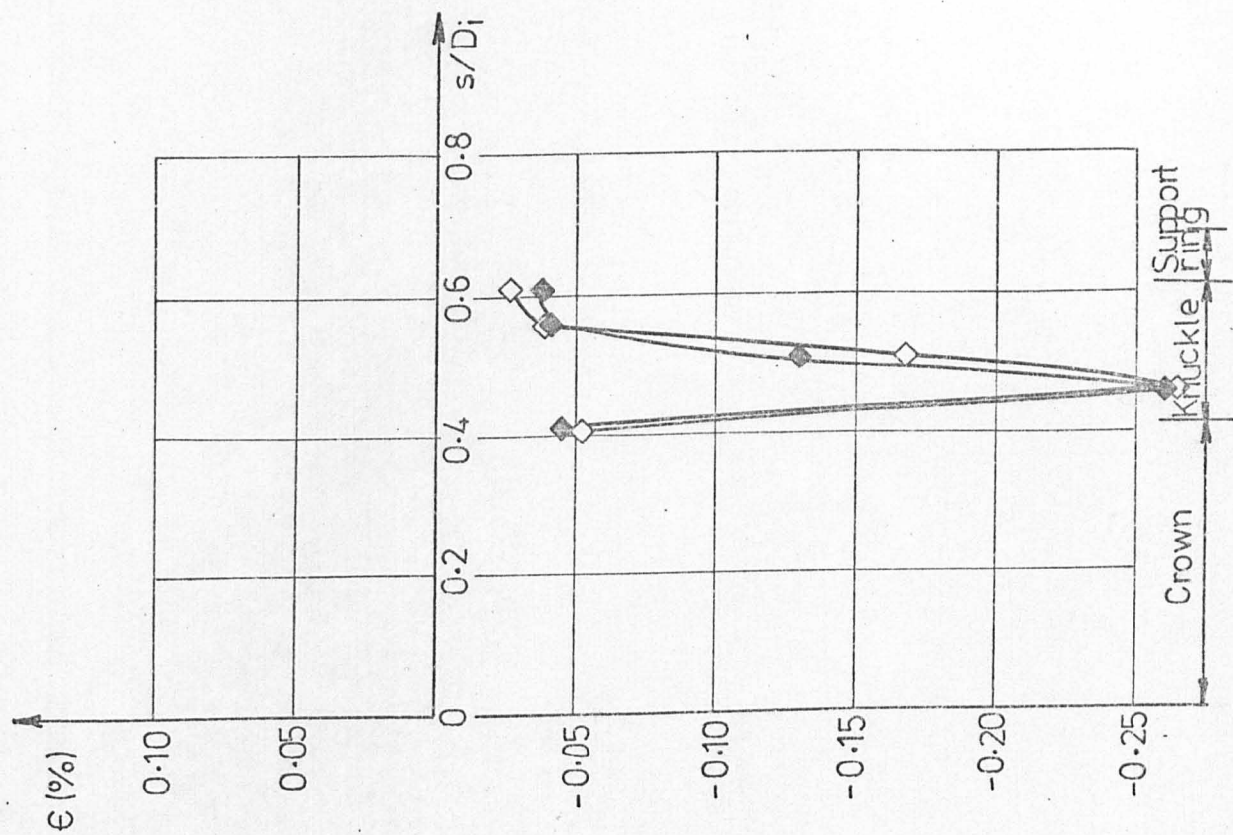
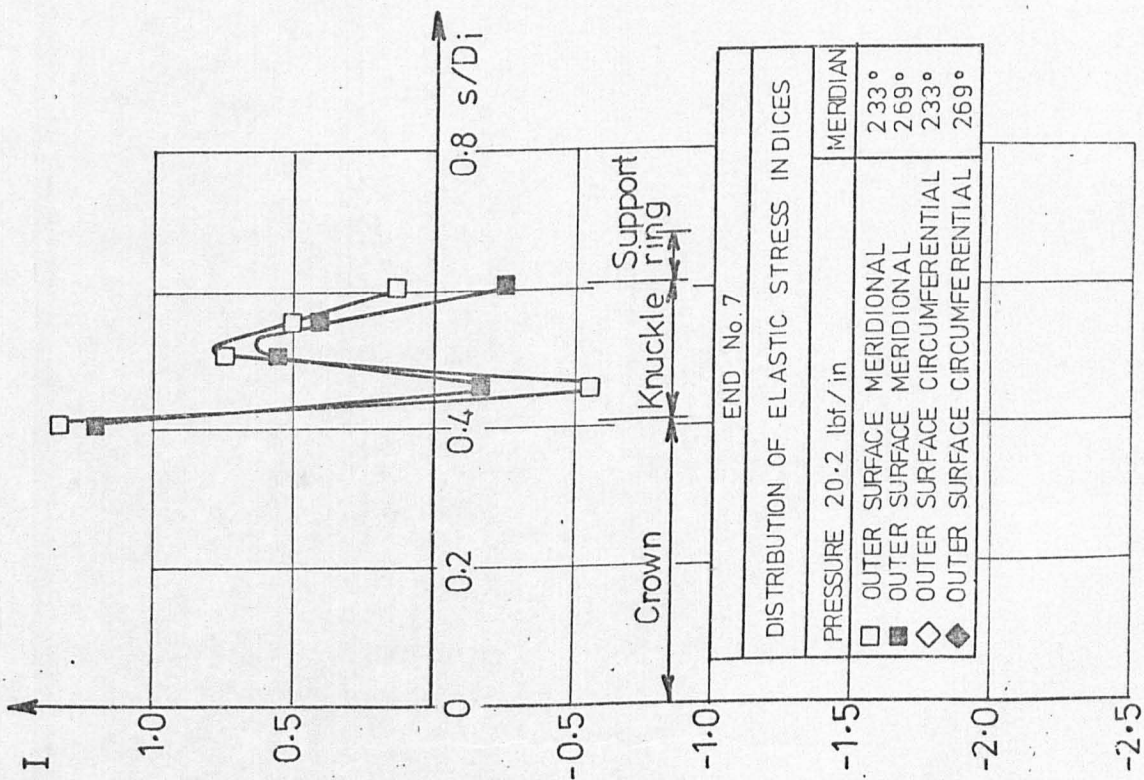
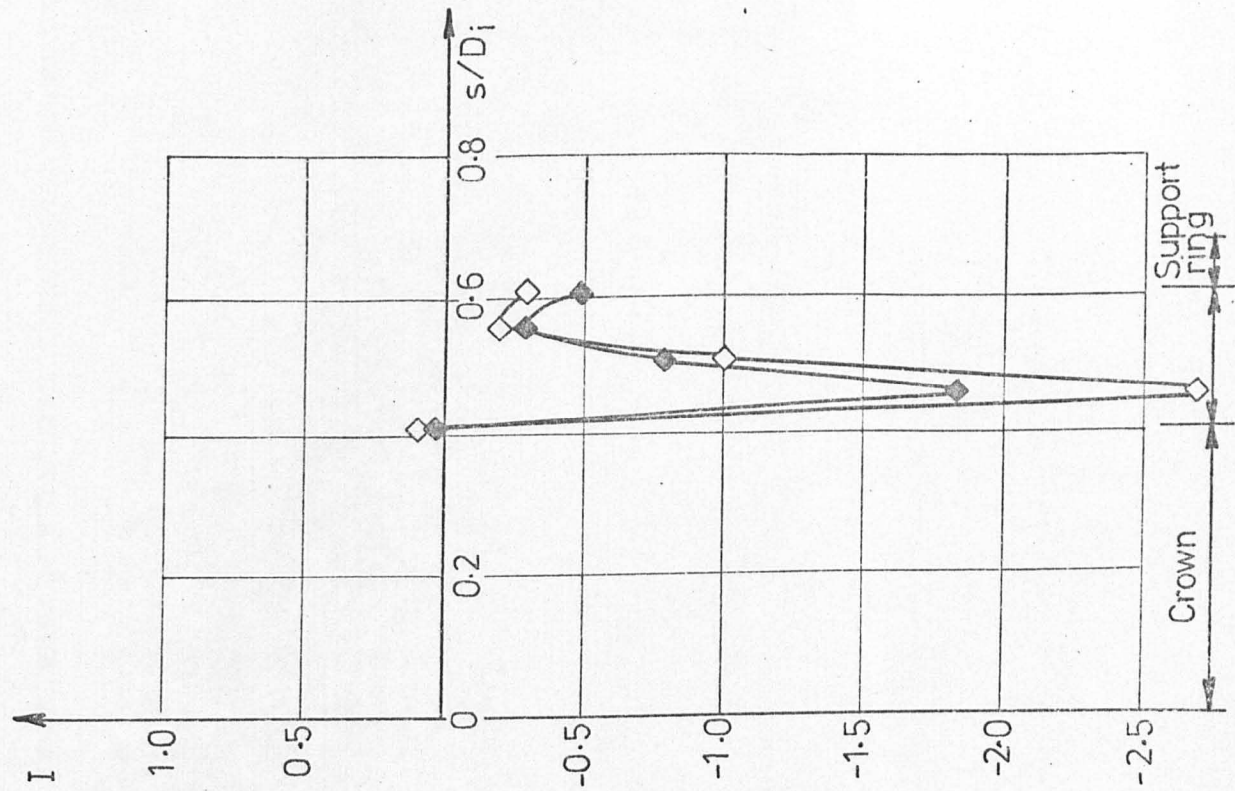


FIG.A1.7.3



END No. 7	
STRAIN DISTRIBUTION (PRE-BUCKLING)	
PRESSURE 56.2 lbt/in	MERIDIAN
□ OUTER SURFACE MERIDIONAL	233°
■ OUTER SURFACE MERIDIONAL	269°
◇ OUTER SURFACE CIRCUMFERENTIAL	233°
◆ OUTER SURFACE CIRCUMFERENTIAL	269°

FIG. A1.7.4



END No. 7

DISTRIBUTION OF ELASTIC STRESS INDICES	
PRESSURE 20.2 lbf/in	MERIDIAN
□	OUTER SURFACE MERIDIONAL 233°
■	OUTER SURFACE MERIDIONAL 269°
◇	OUTER SURFACE CIRCUMFERENTIAL 233°
◆	OUTER SURFACE CIRCUMFERENTIAL 269°

FIG. A1.7.5

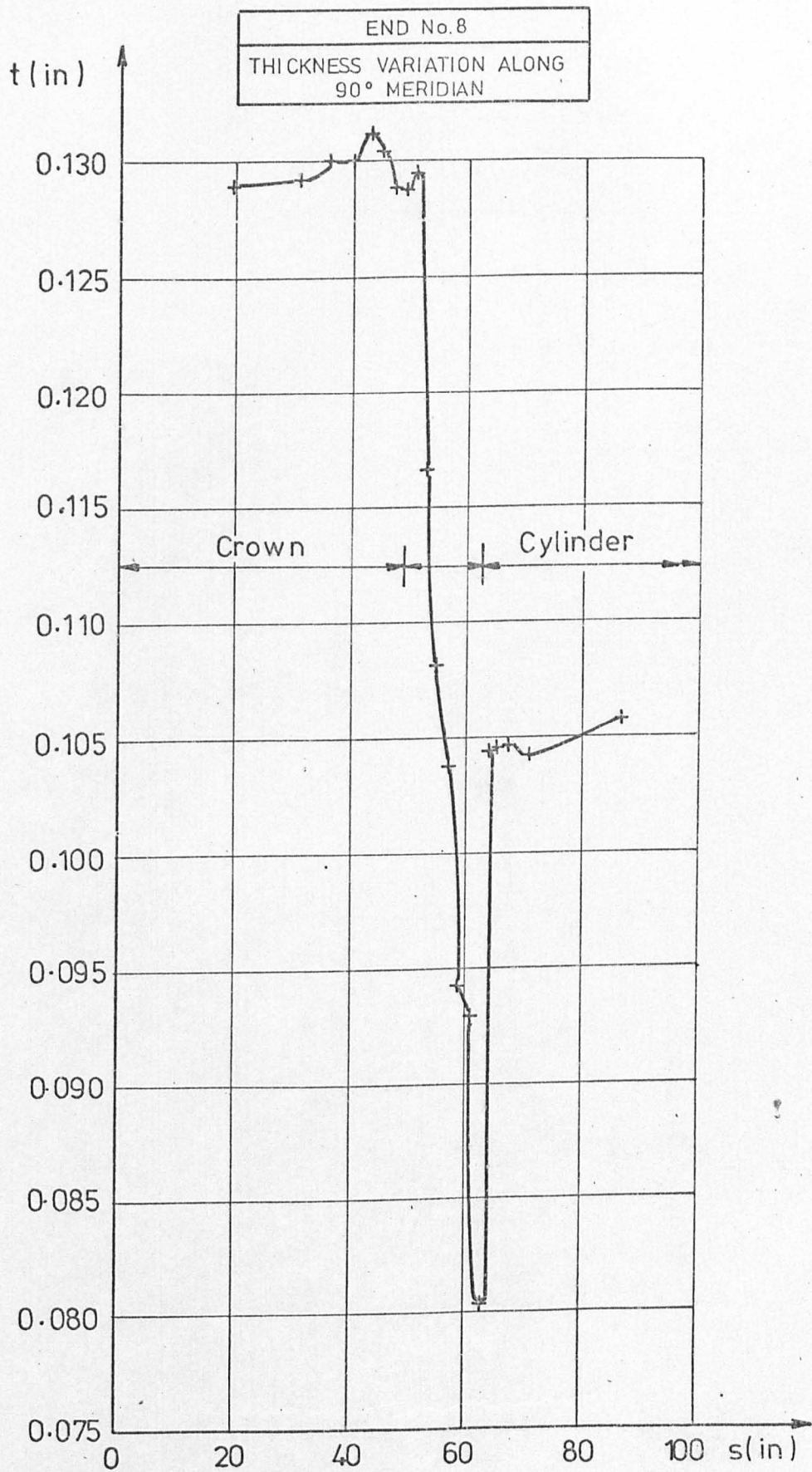


FIG. A1.8.1

END No. 8
CURVATURE VARIATION ALONG 90° MERIDIAN

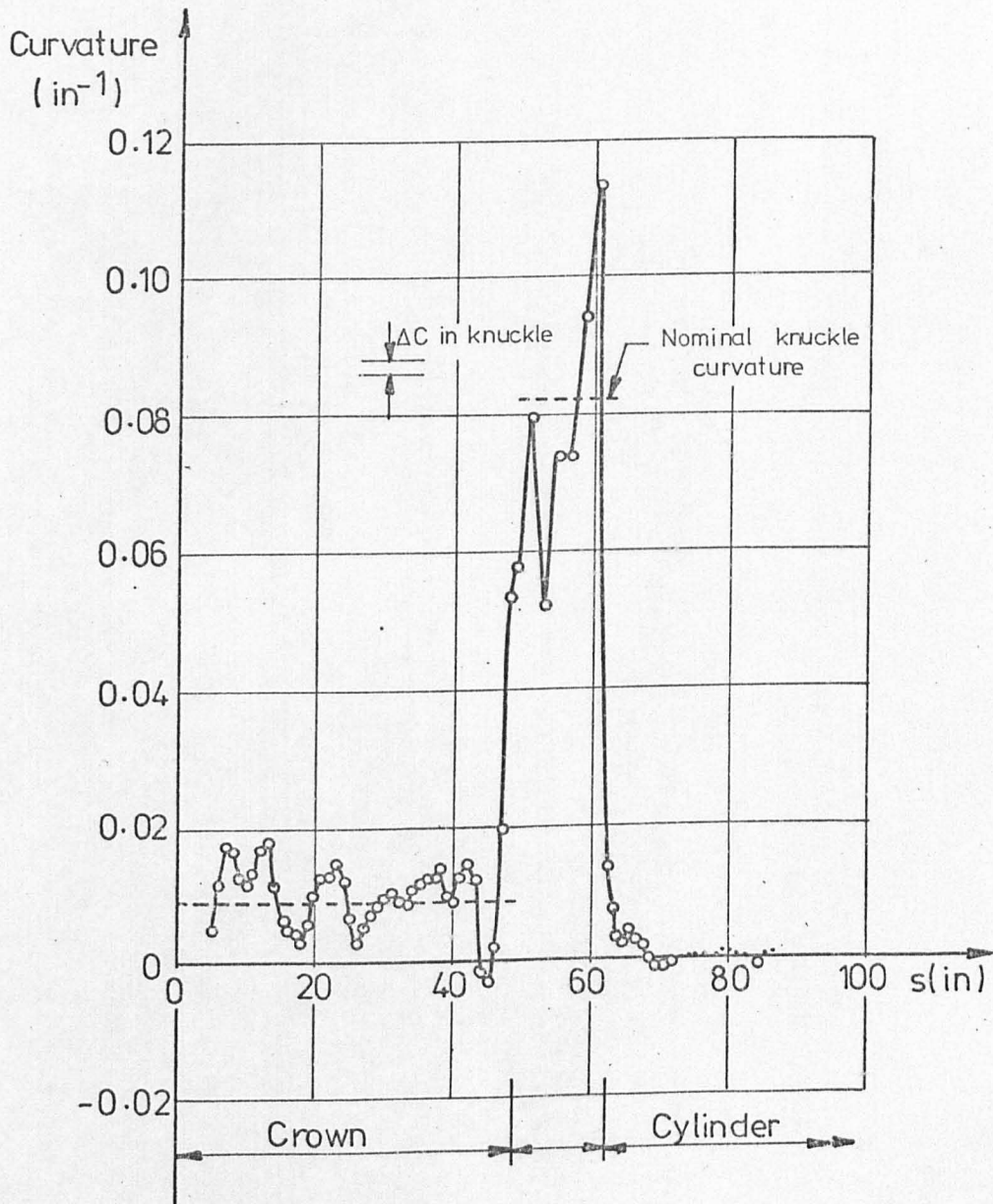


FIG. A1.8-2

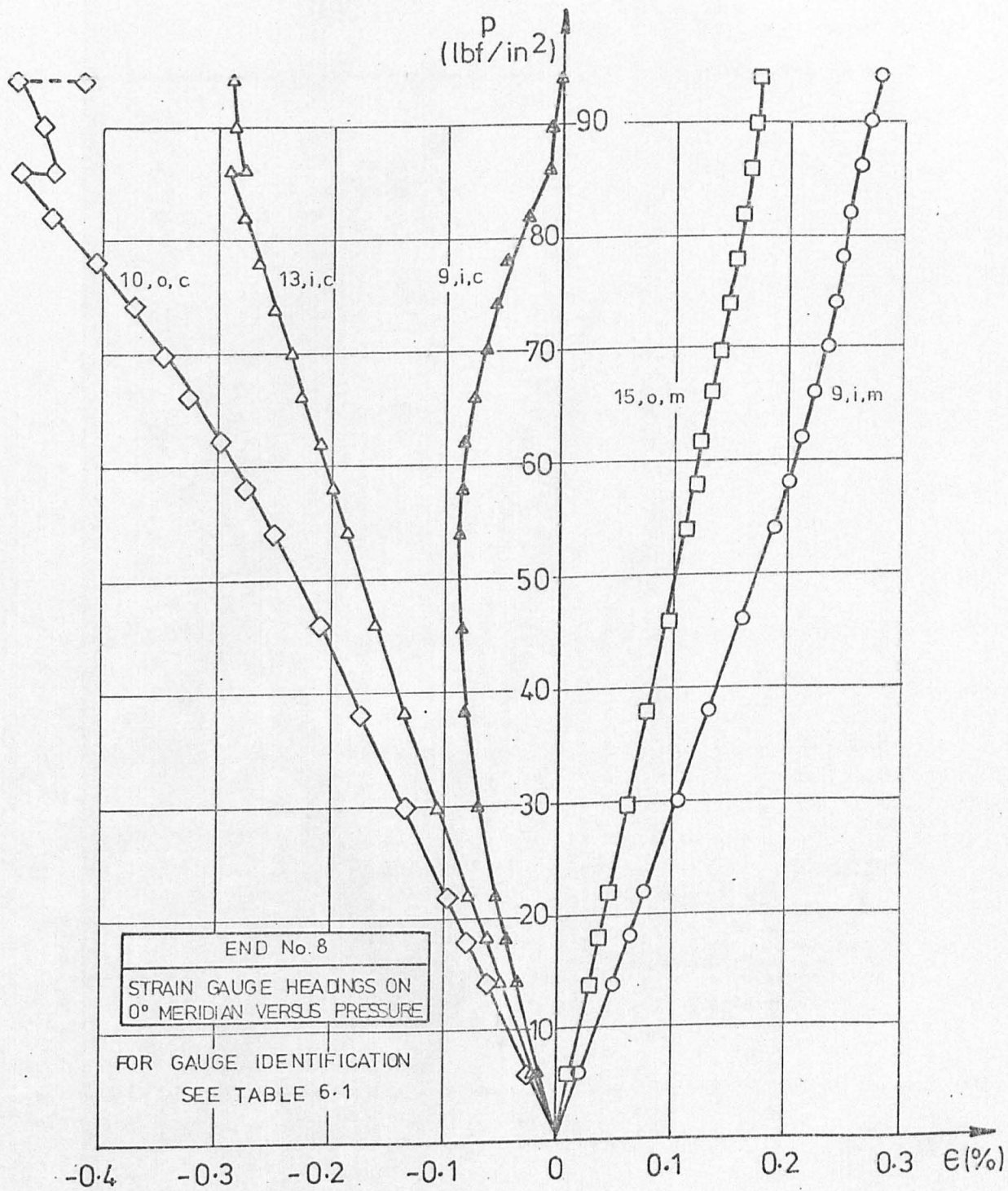


FIG. A1-8.3



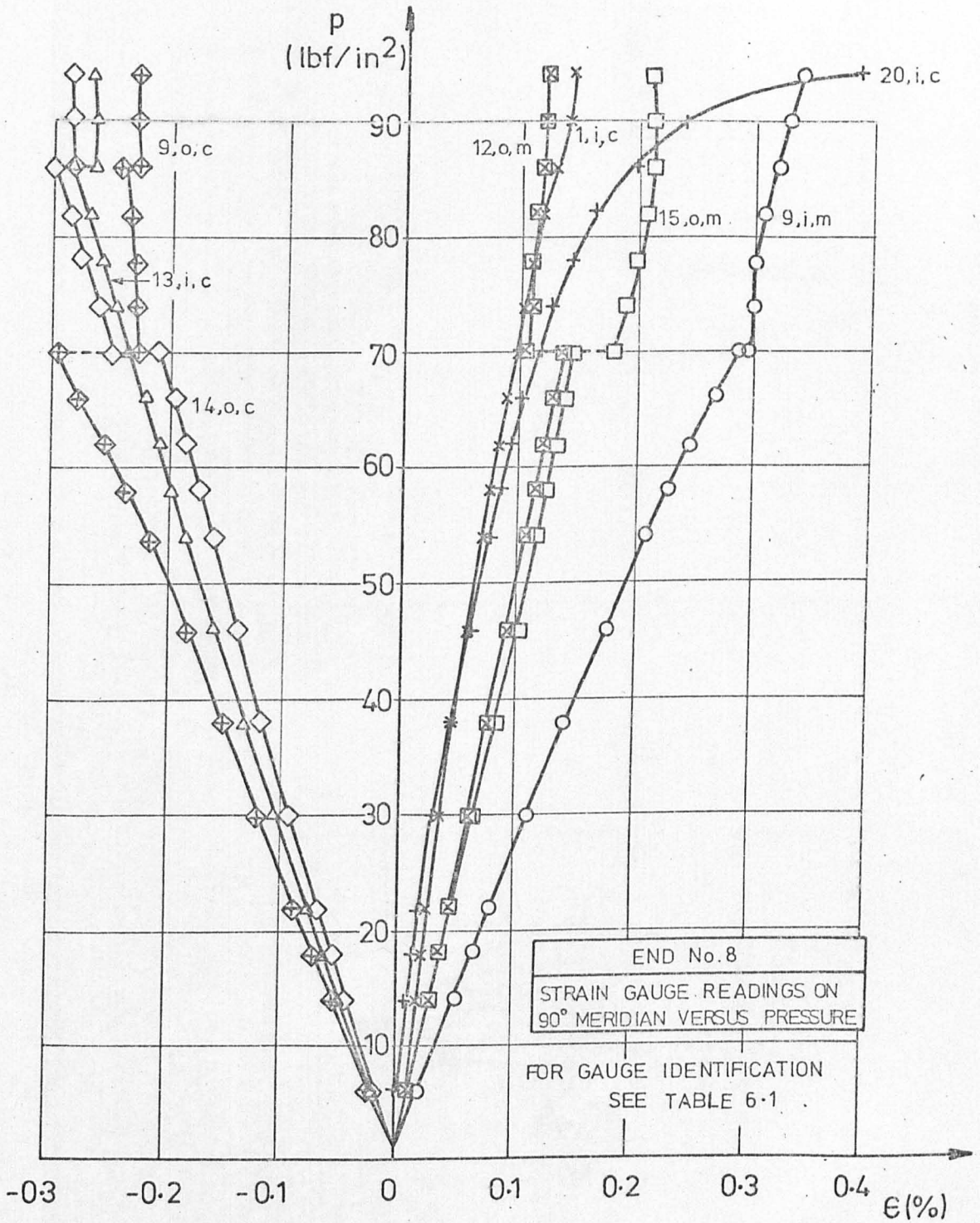


FIG.A1.8.4

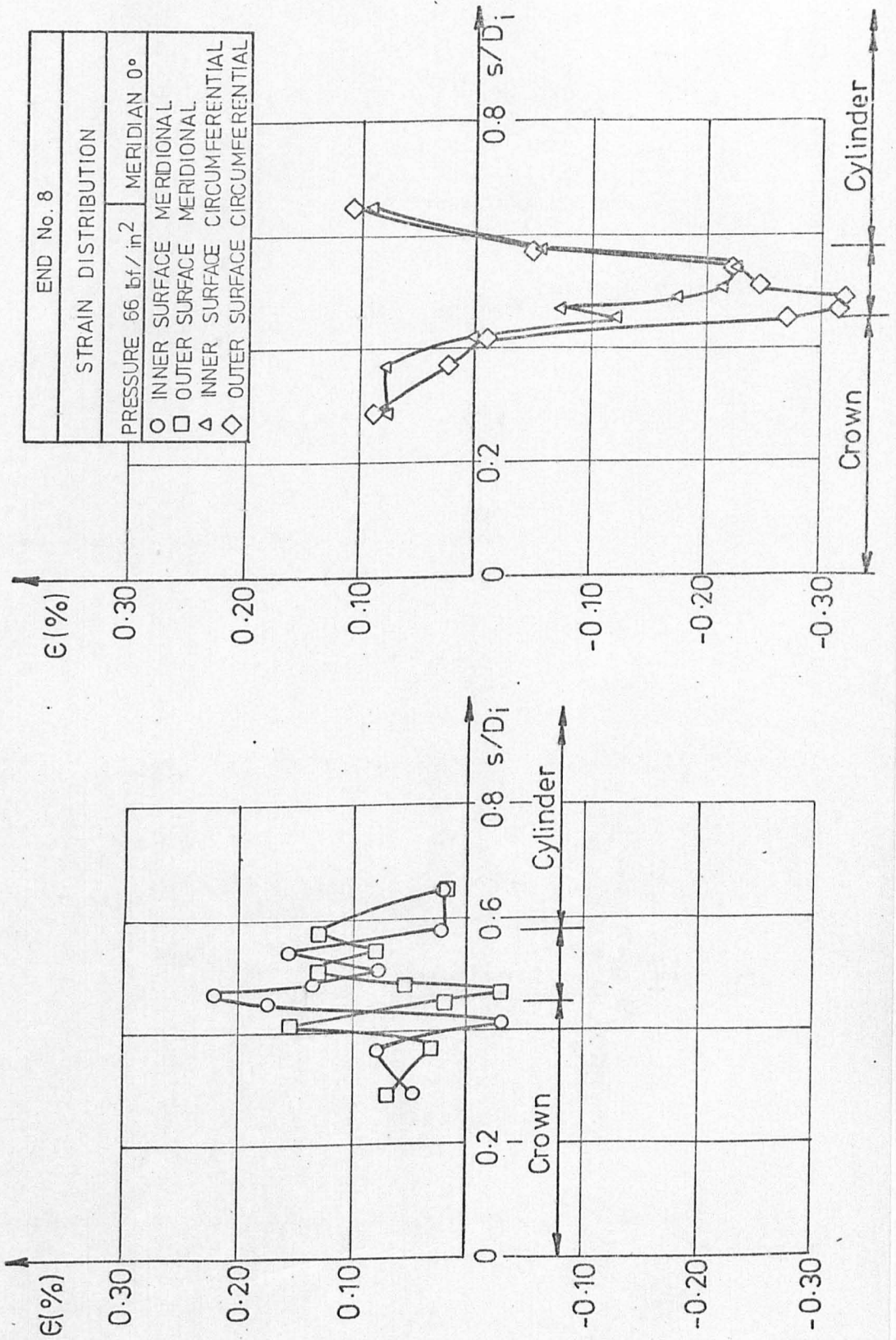


FIG. A1.8.5

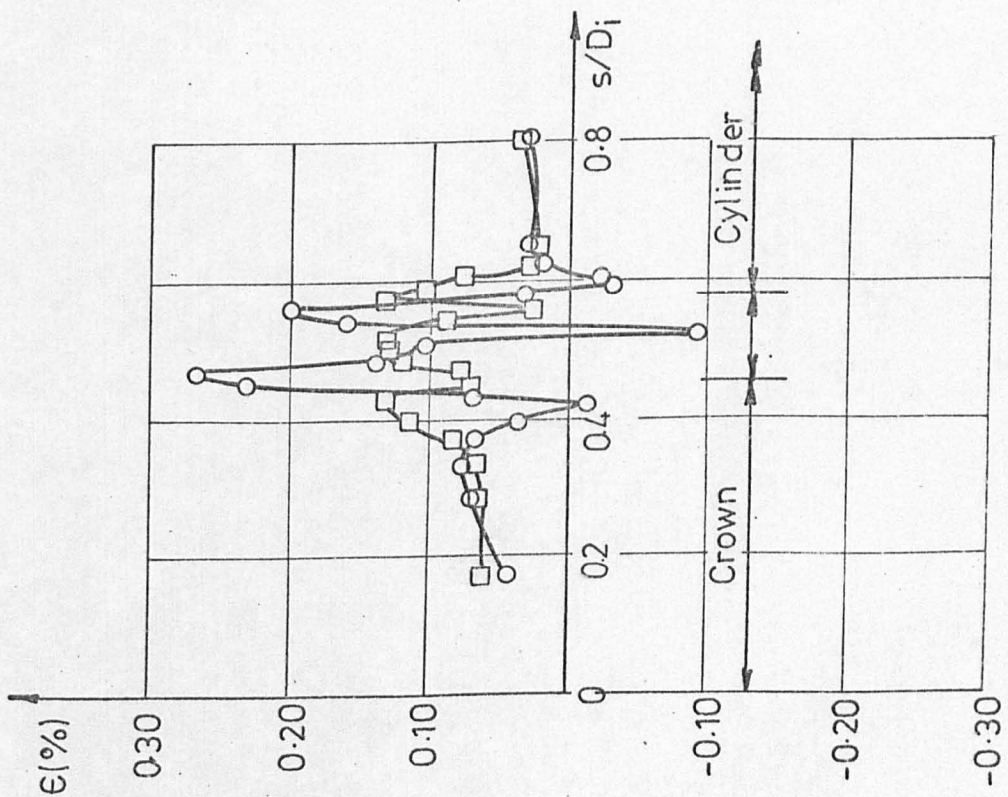
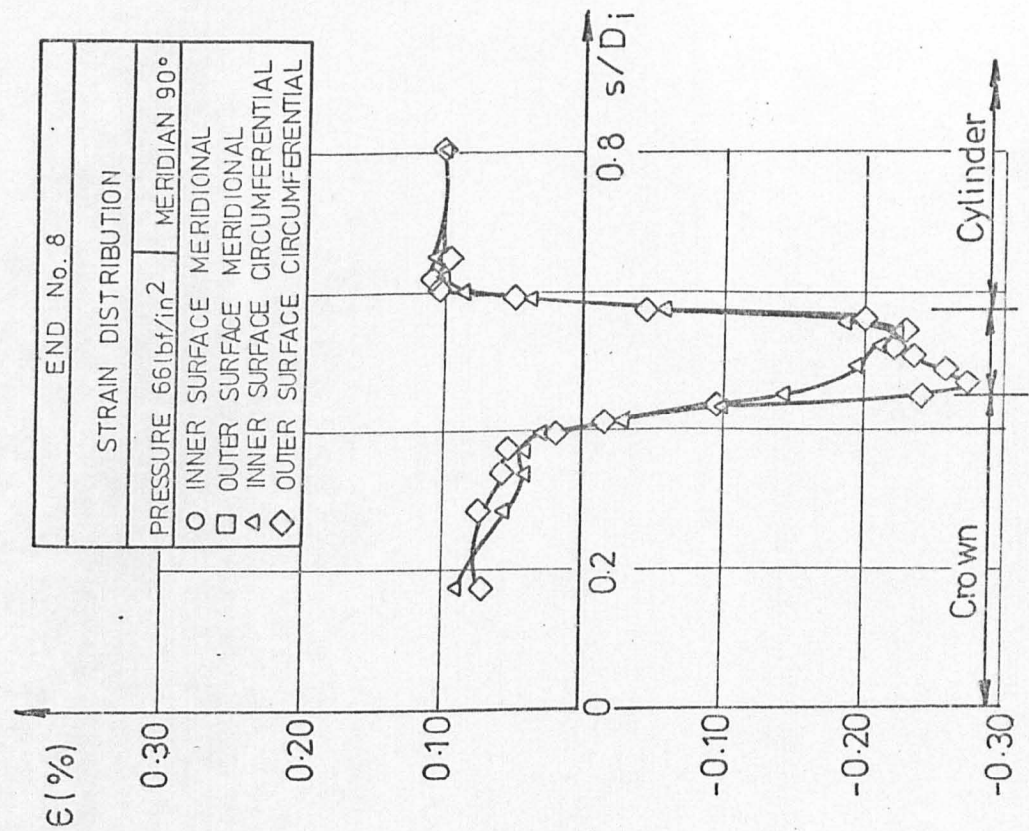


FIG. A1-8-6

END No. 8	
DISTRIBUTION OF ELASTIC STRESS INDICES	
PRESSURE 18 lbf/in <sup>2</sup>	MERIDIAN 0°
○	INNER SURFACE MERIDIONAL
□	OUTER SURFACE MERIDIONAL
△	INNER SURFACE CIRCUMFERENTIAL
◇	OUTER SURFACE CIRCUMFERENTIAL

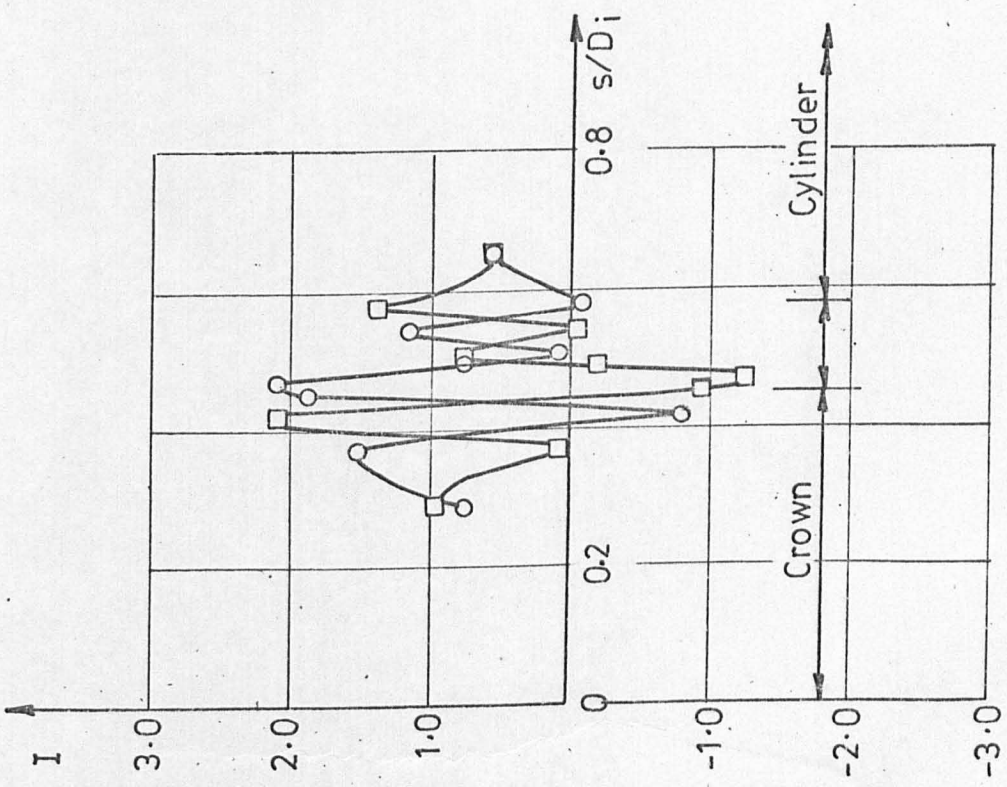
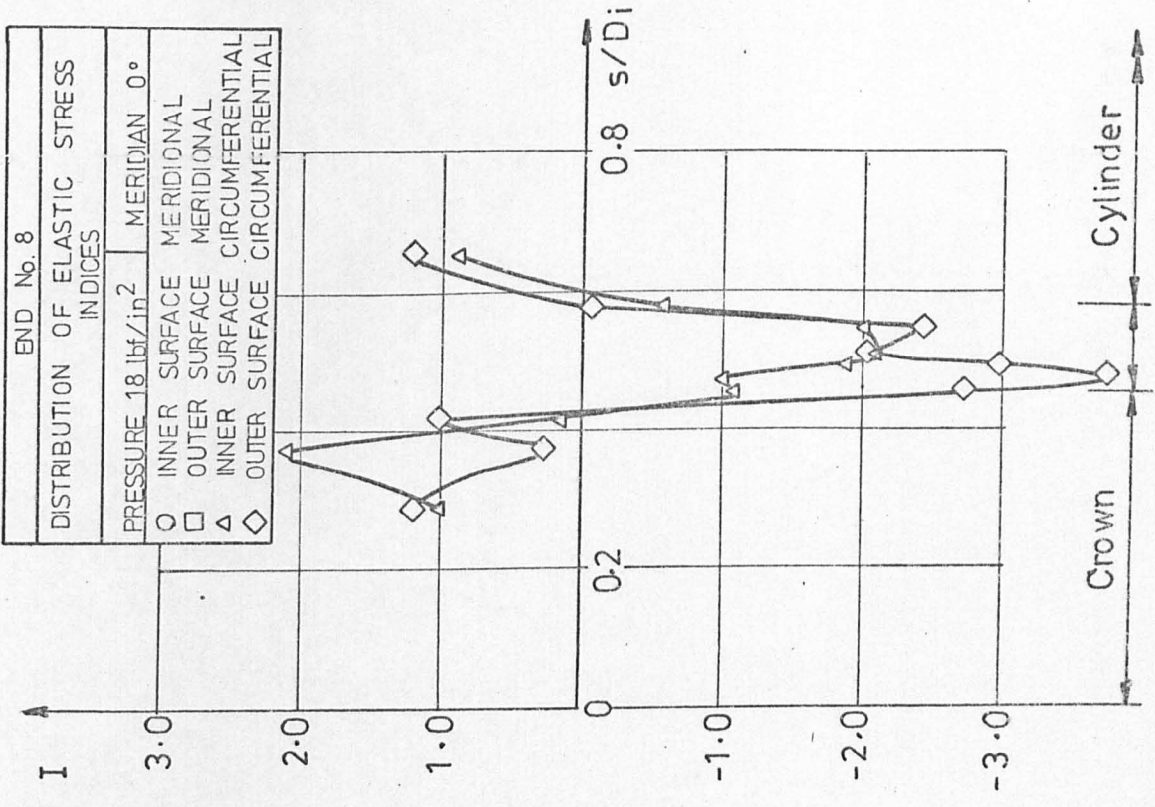


FIG.A1-8-7

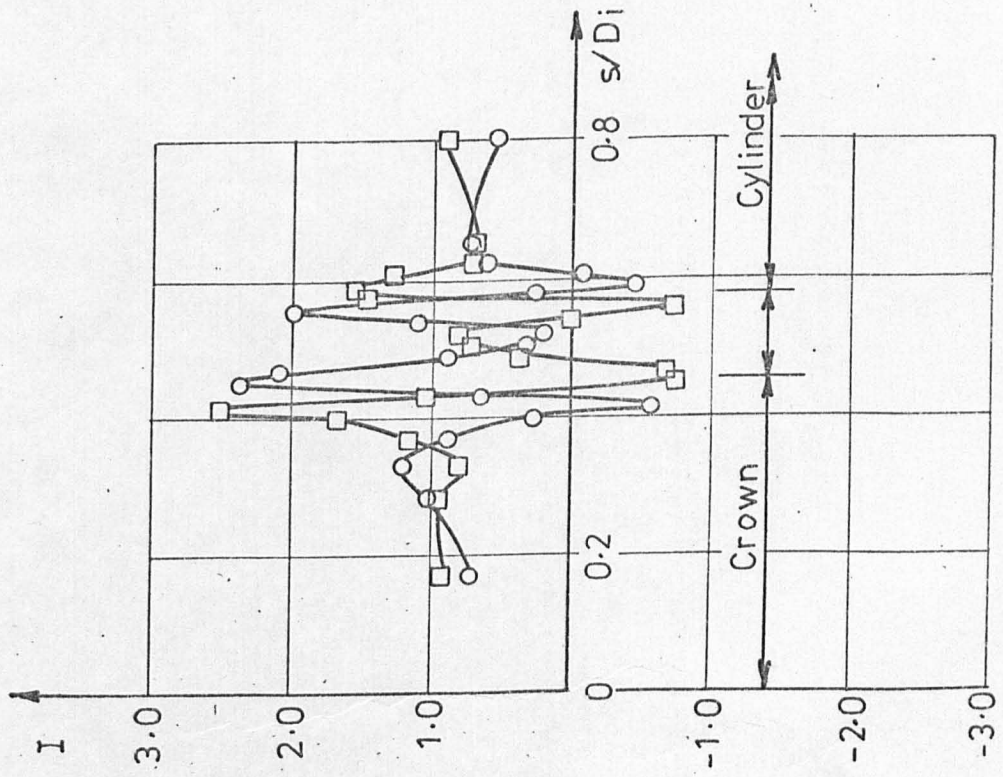
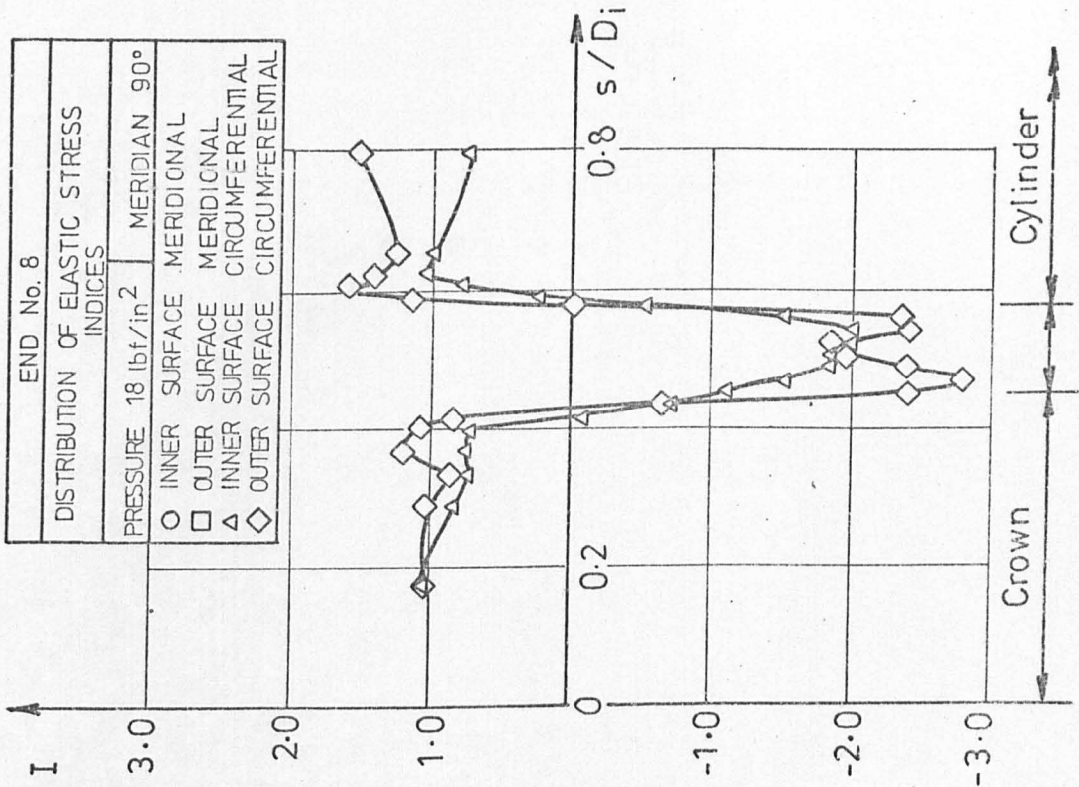


FIG.A1-8-8

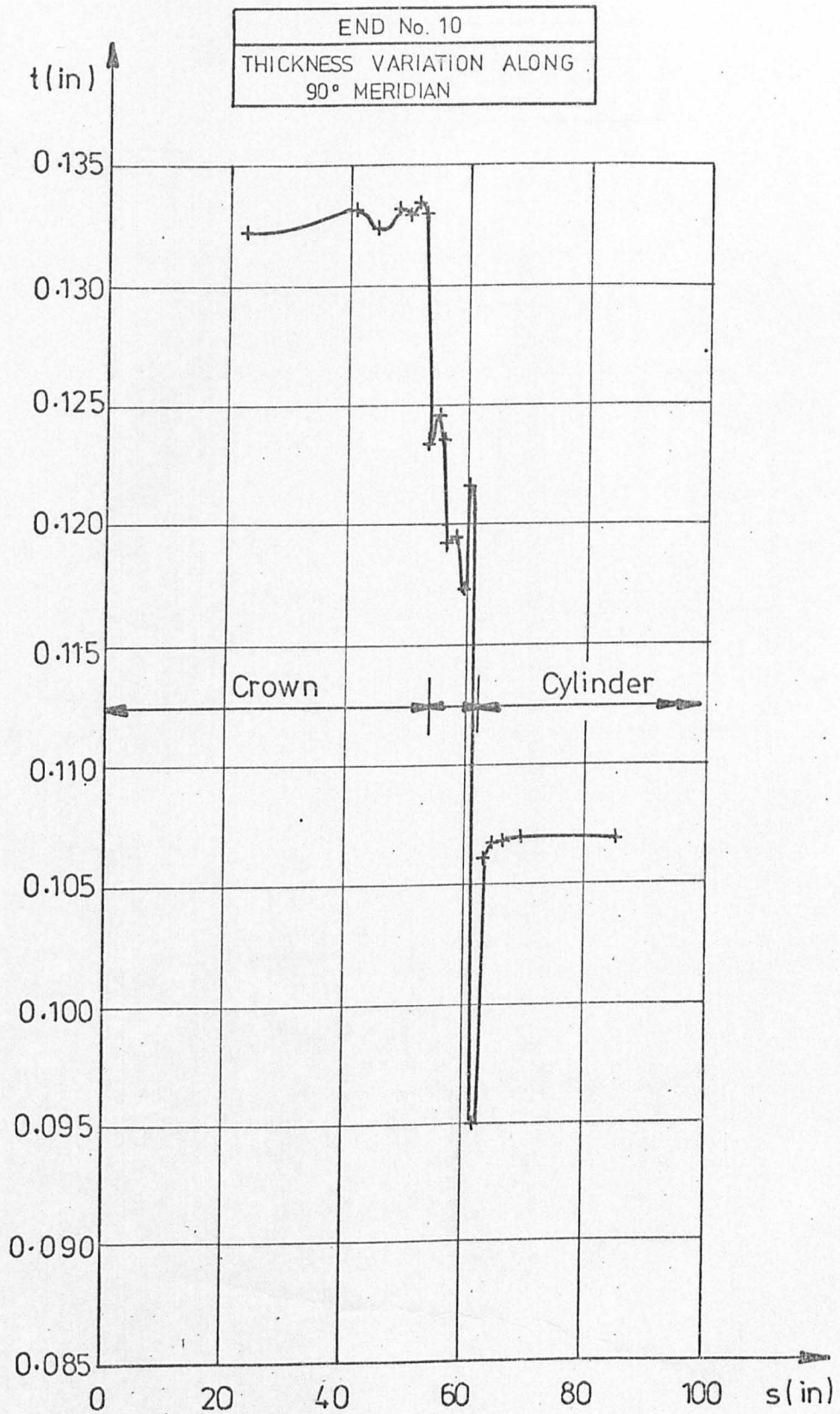


FIG. A1-10-1

END No. 10
CURVATURE VARIATION ALONG 90° MERIDIAN

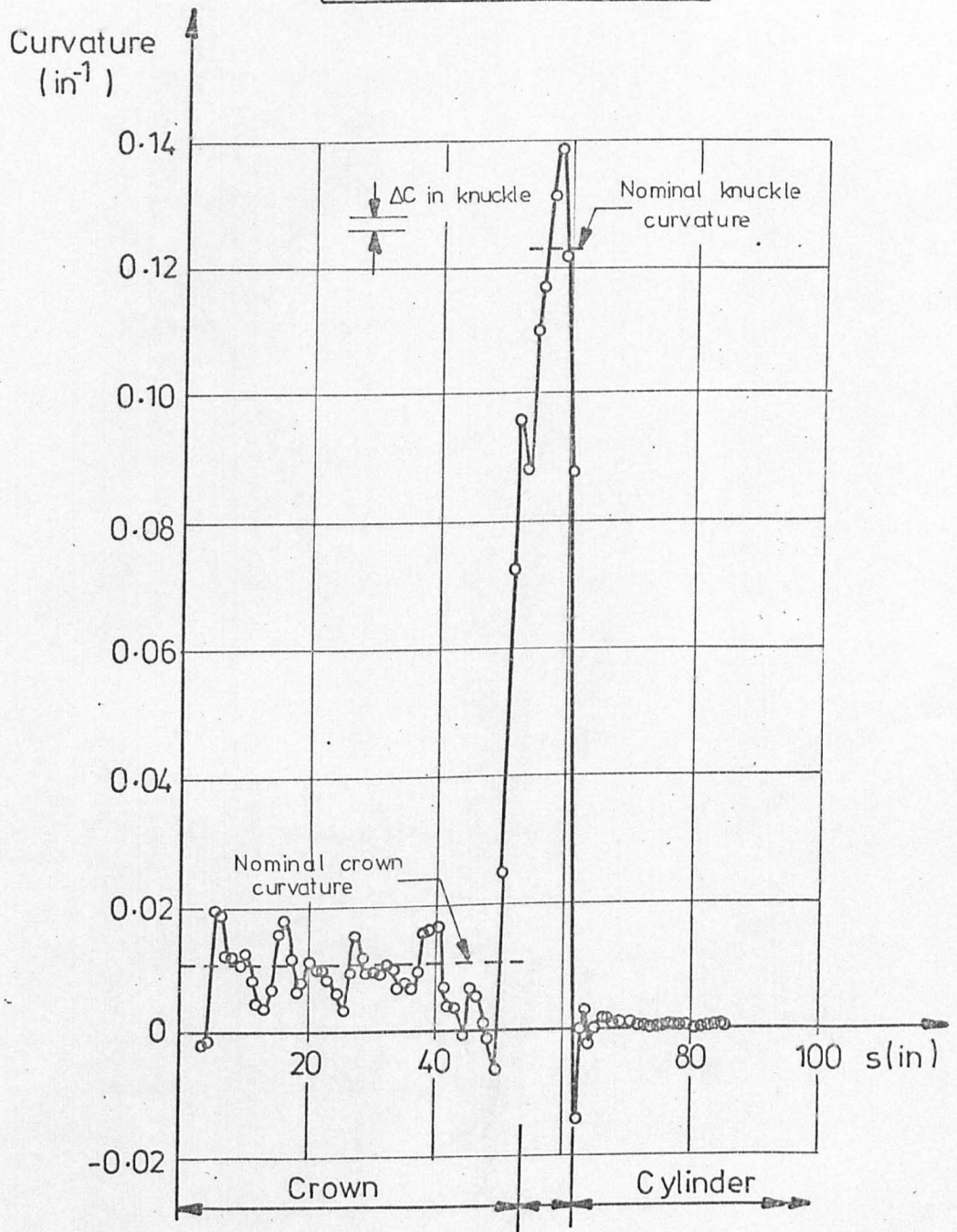


FIG.A1-10.2

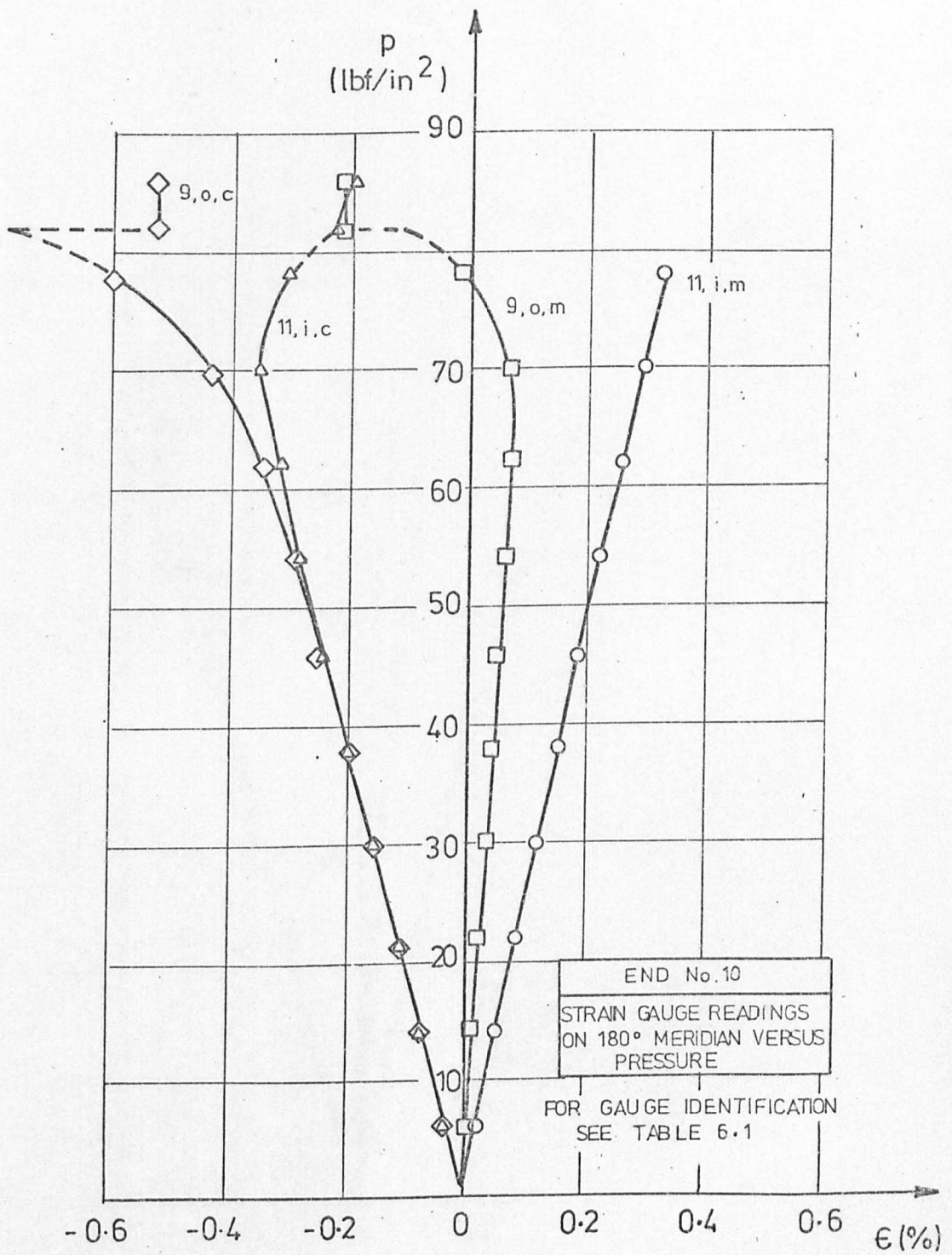
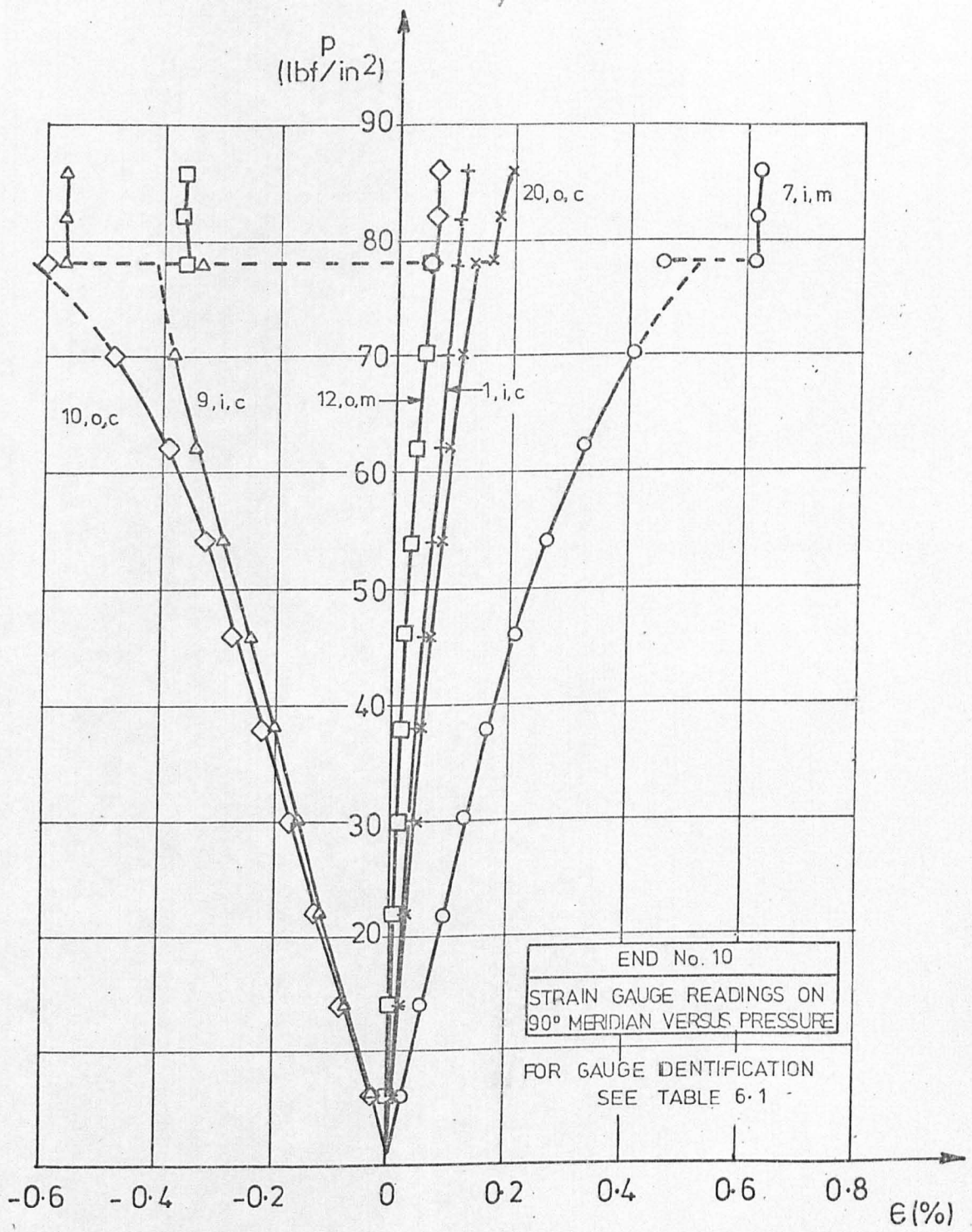


FIG. A1.10.3





END No. 10  
 STRAIN GAUGE READINGS ON  
 90° MERIDIAN VERSUS PRESSURE

FOR GAUGE IDENTIFICATION  
 SEE TABLE 6-1

FIG.A1.10.4

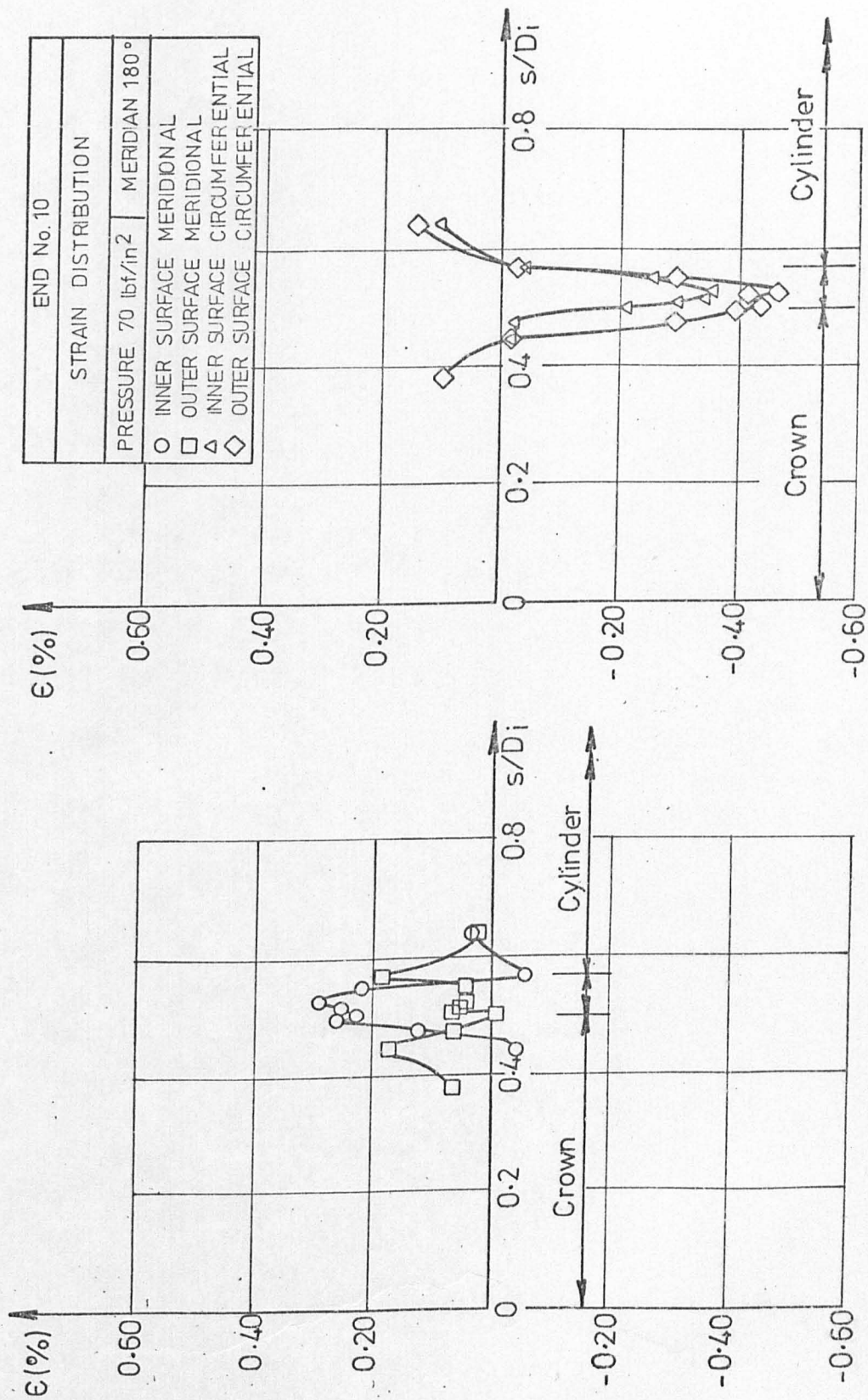


FIG. A1. 10. 5

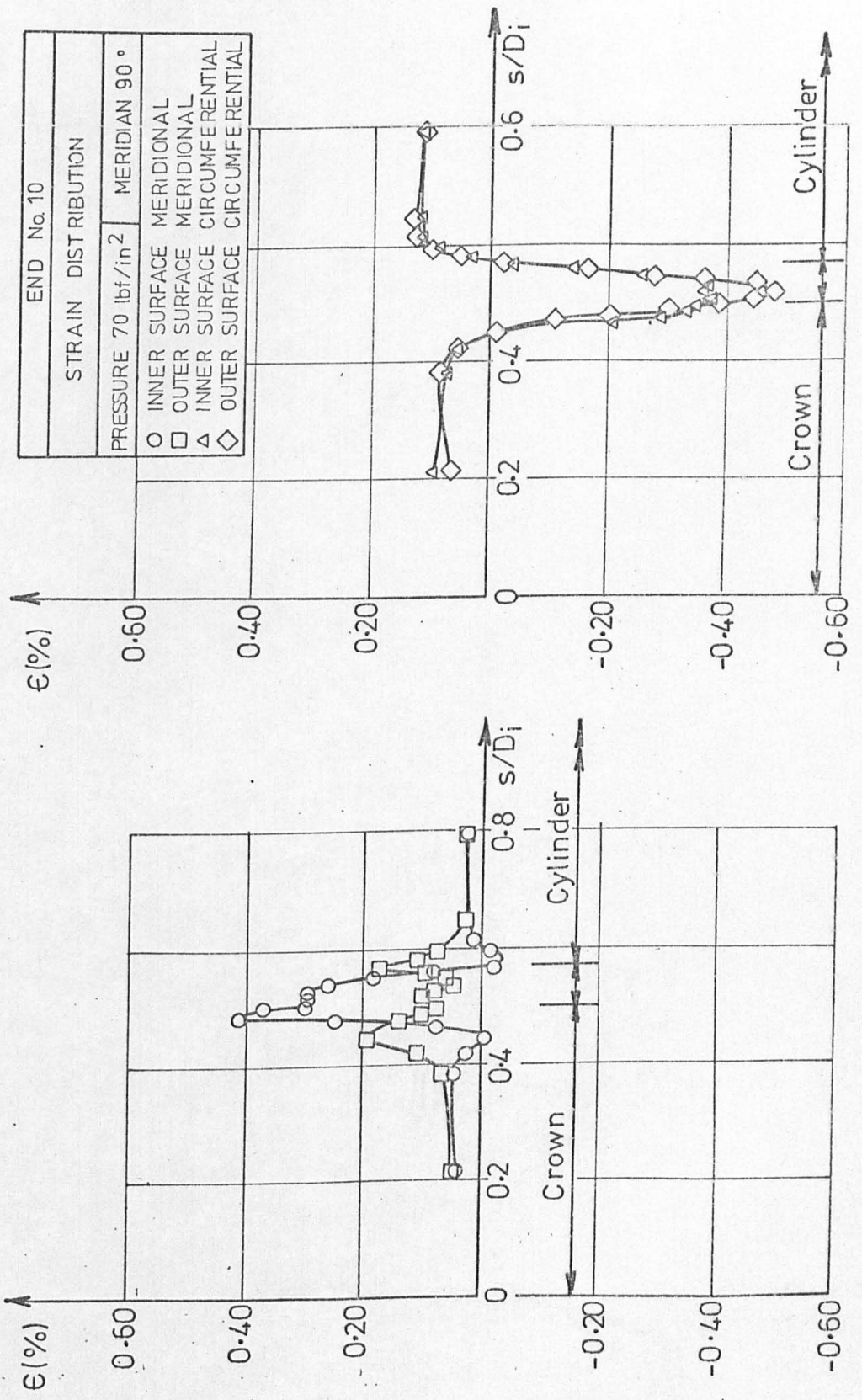


FIG. A1.10.6

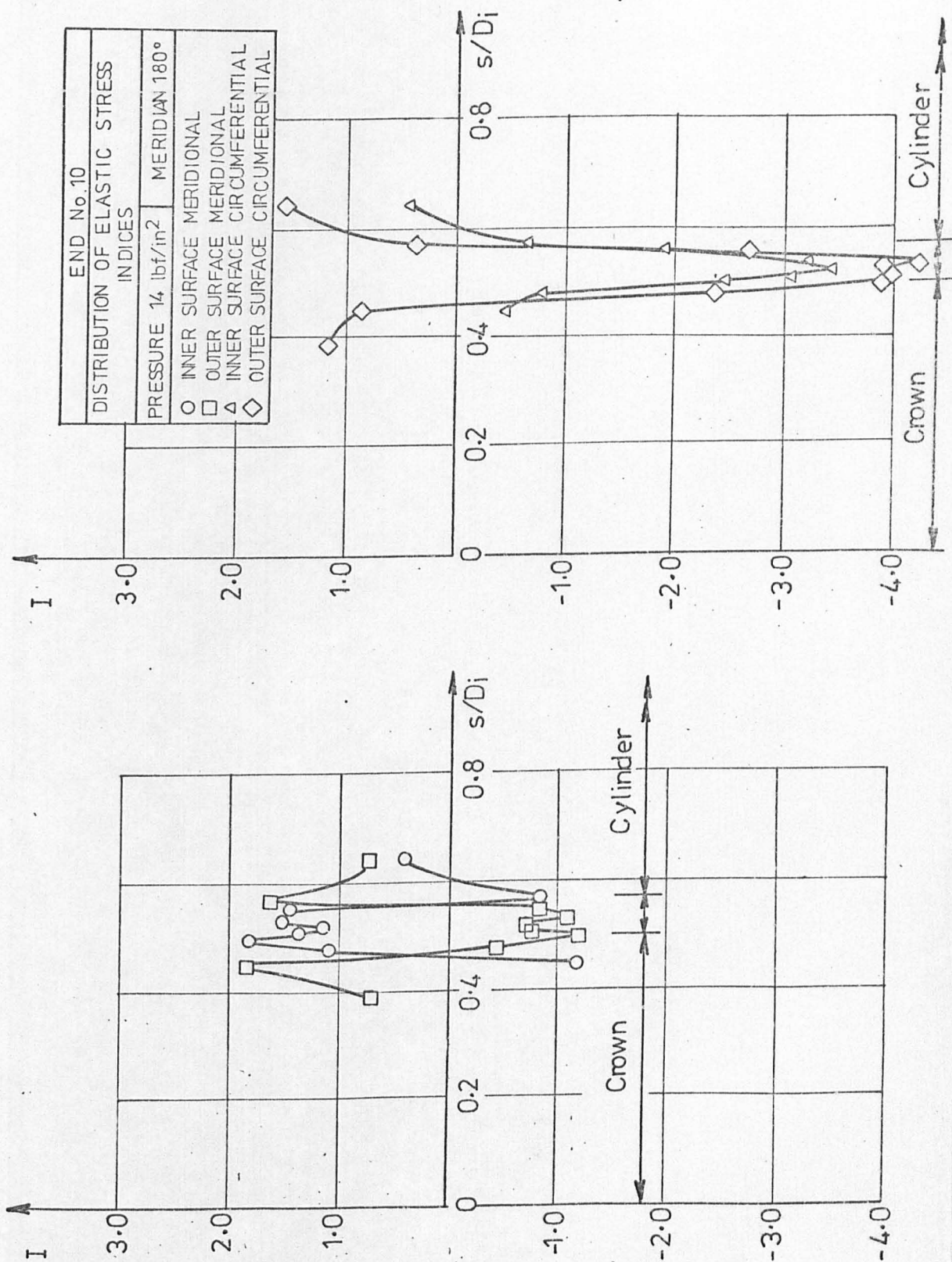


FIG. A1.10-7

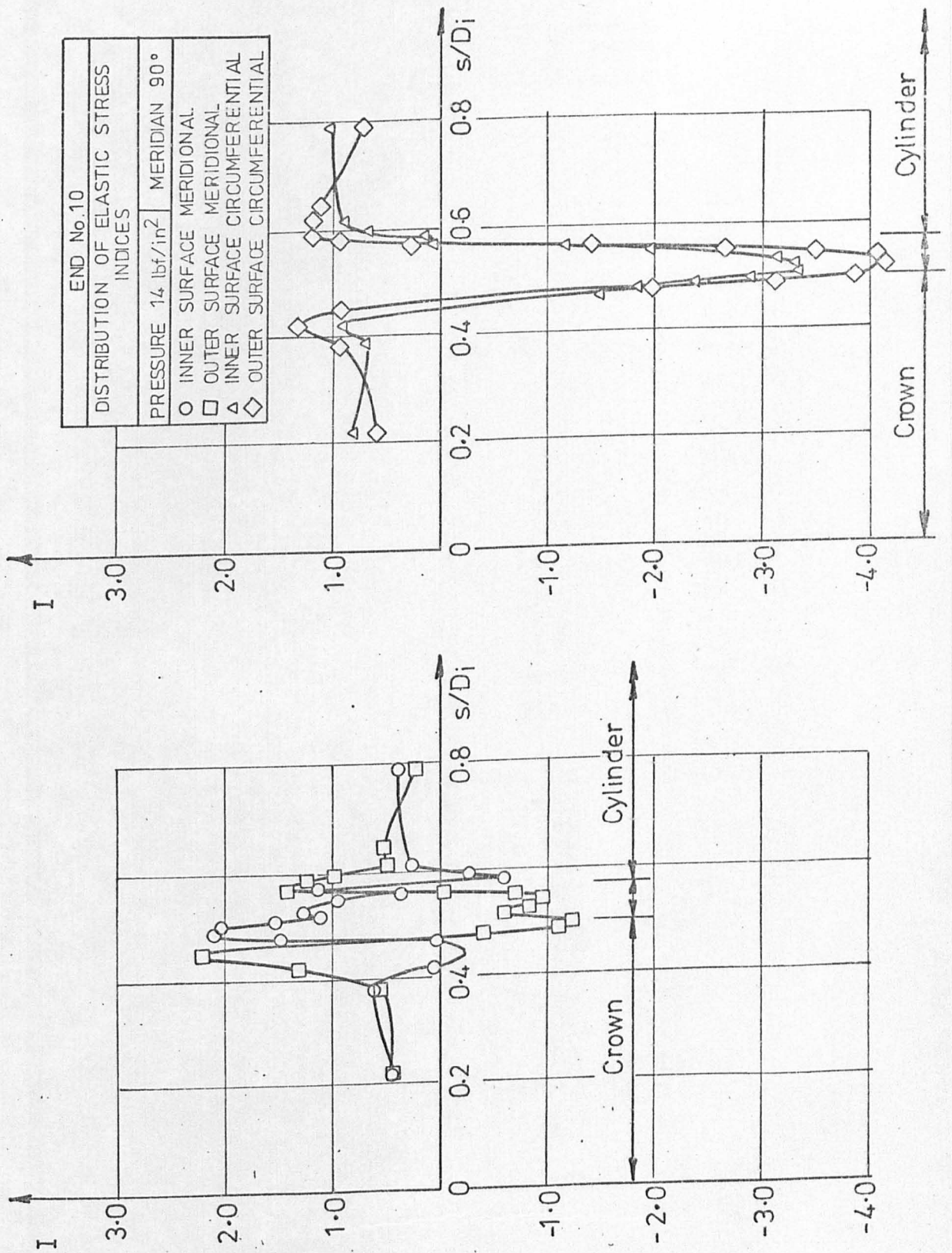


FIG. A1.10.8

END No. 11
THICKNESS VARIATION ALONG 90° MERIDIAN

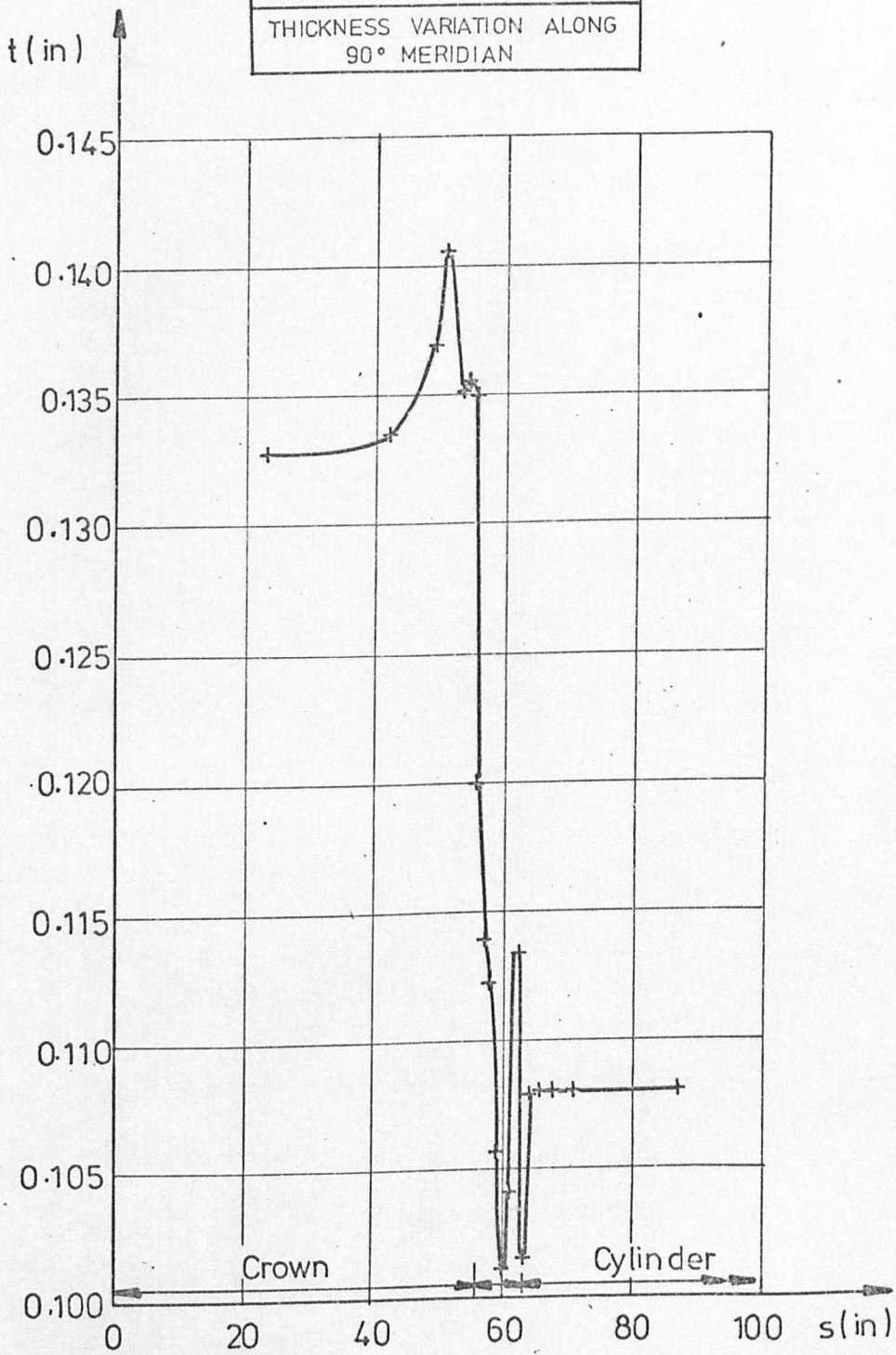


FIG.A1.11.1

END No. 11
CURVATURE VARIATION ALONG 90° MERIDIAN

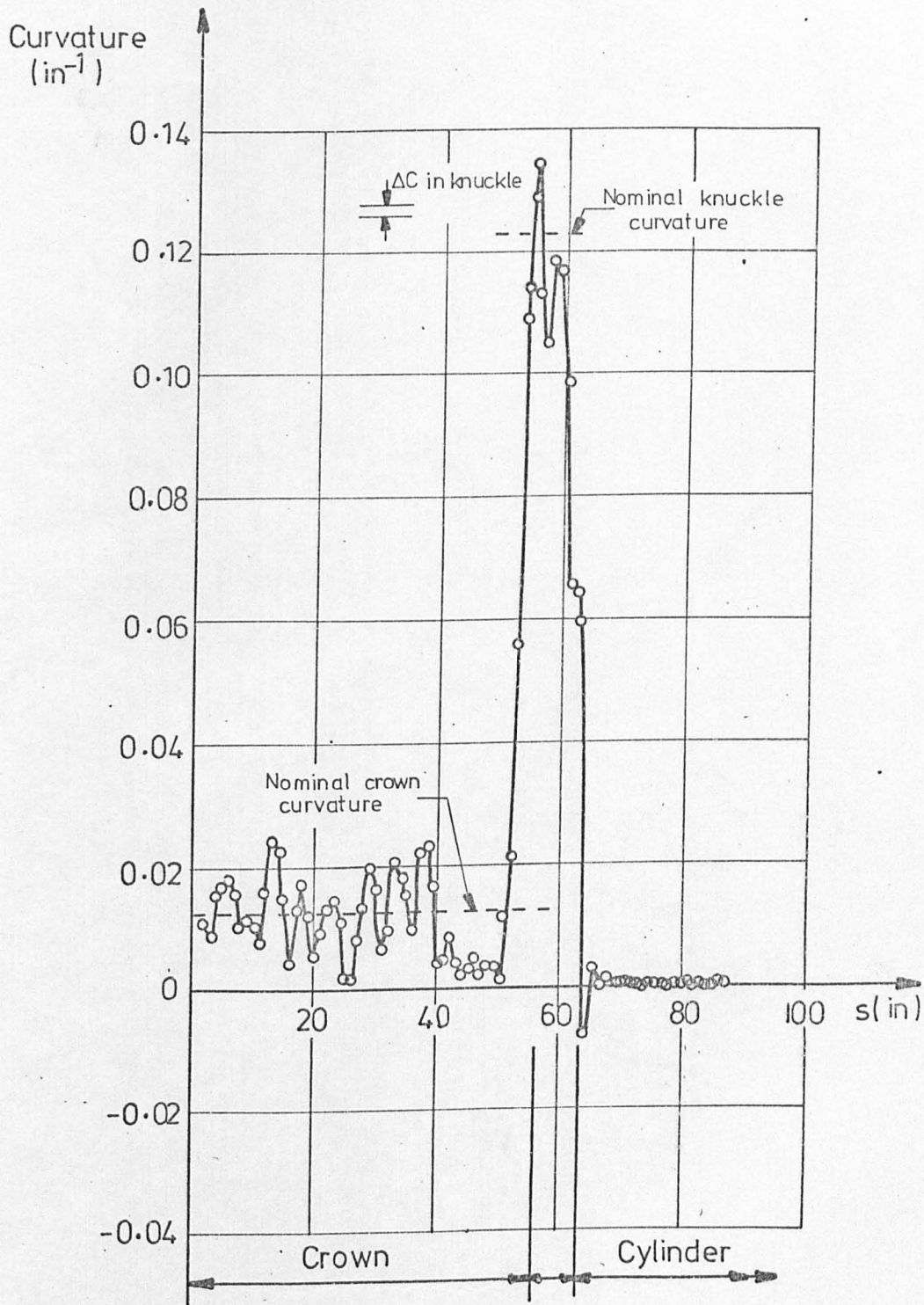


FIG.A1.11.2

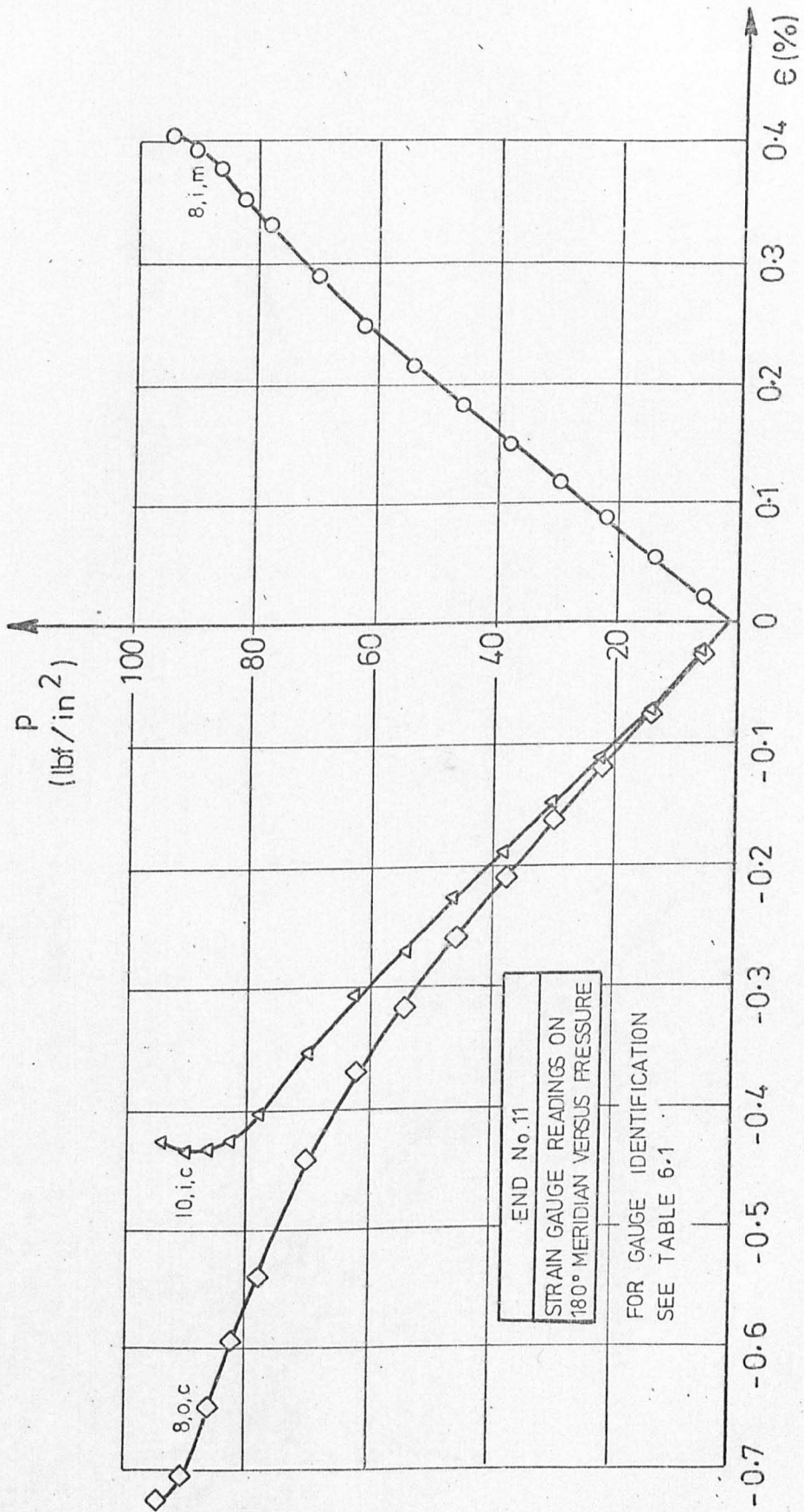


FIG.A1-11.3



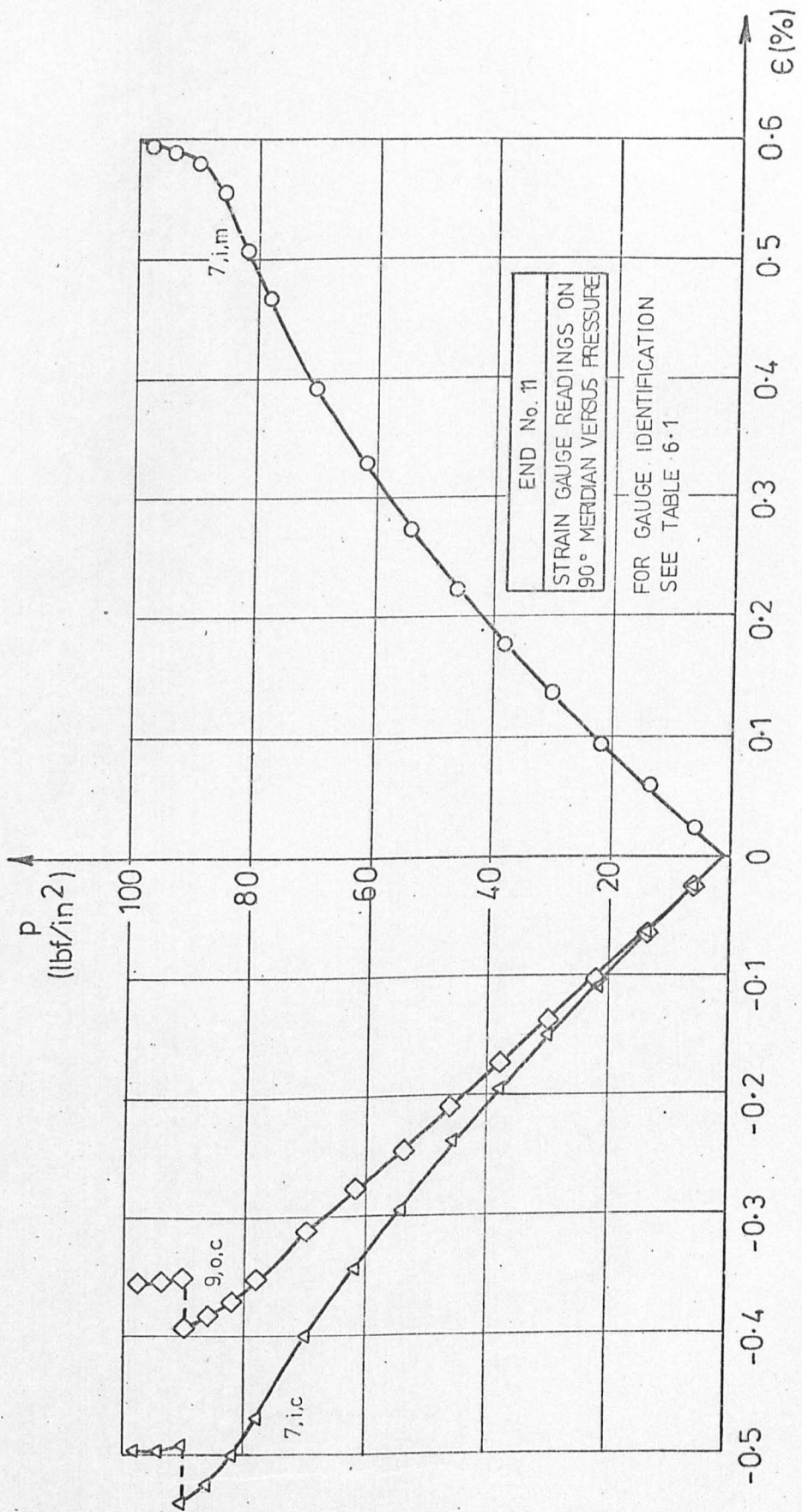


FIG A1.11.4

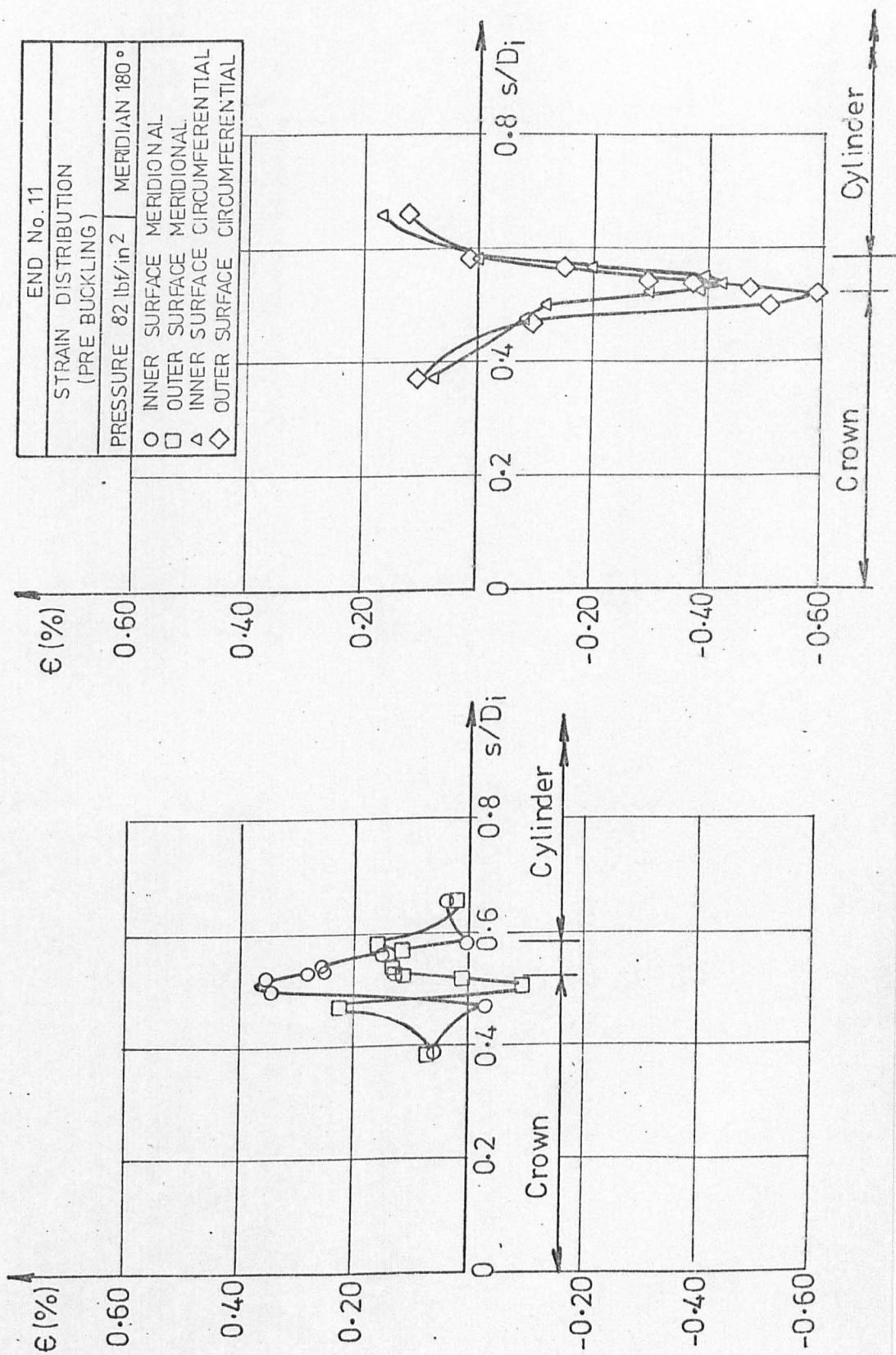


FIG. A1.11.5

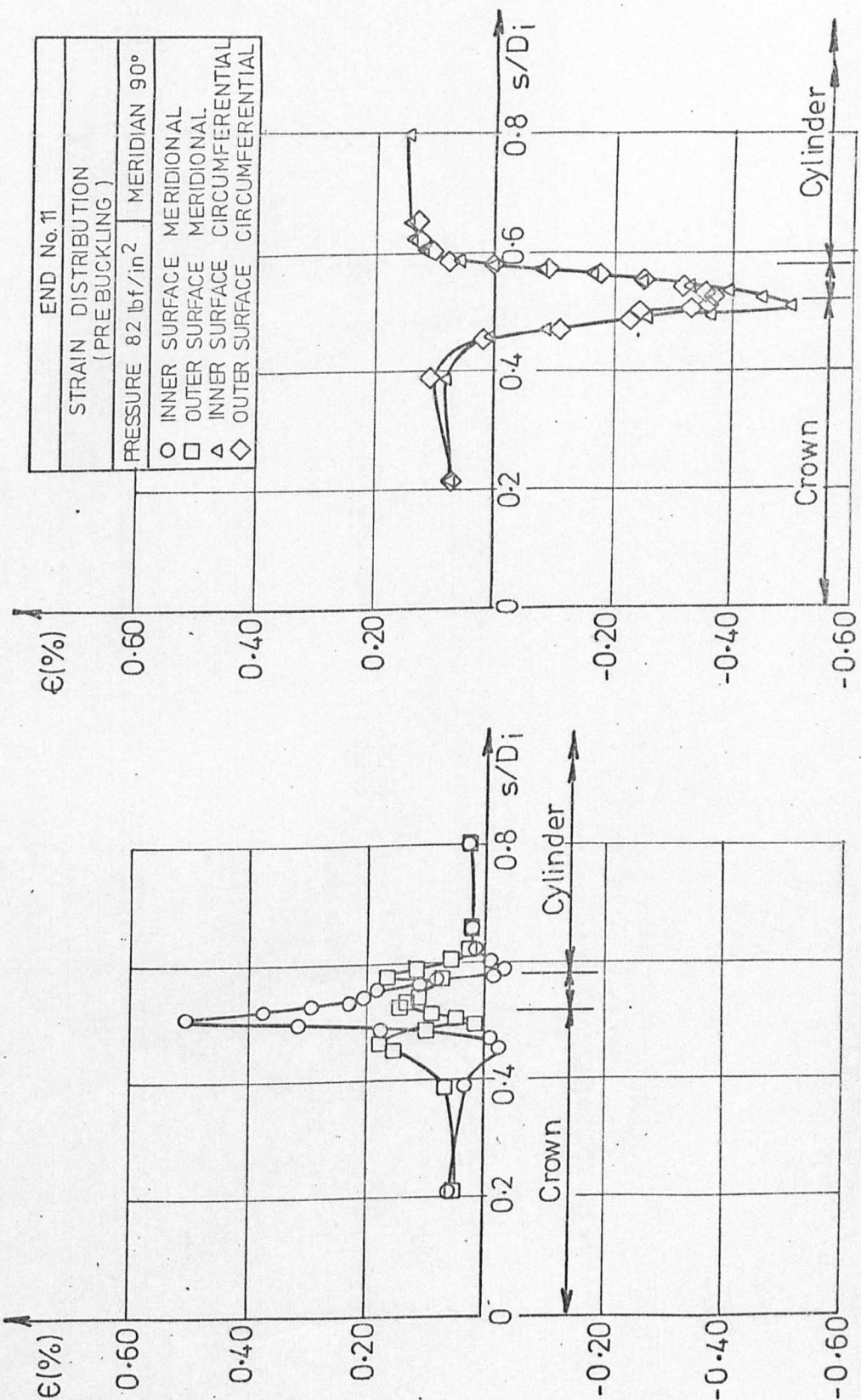
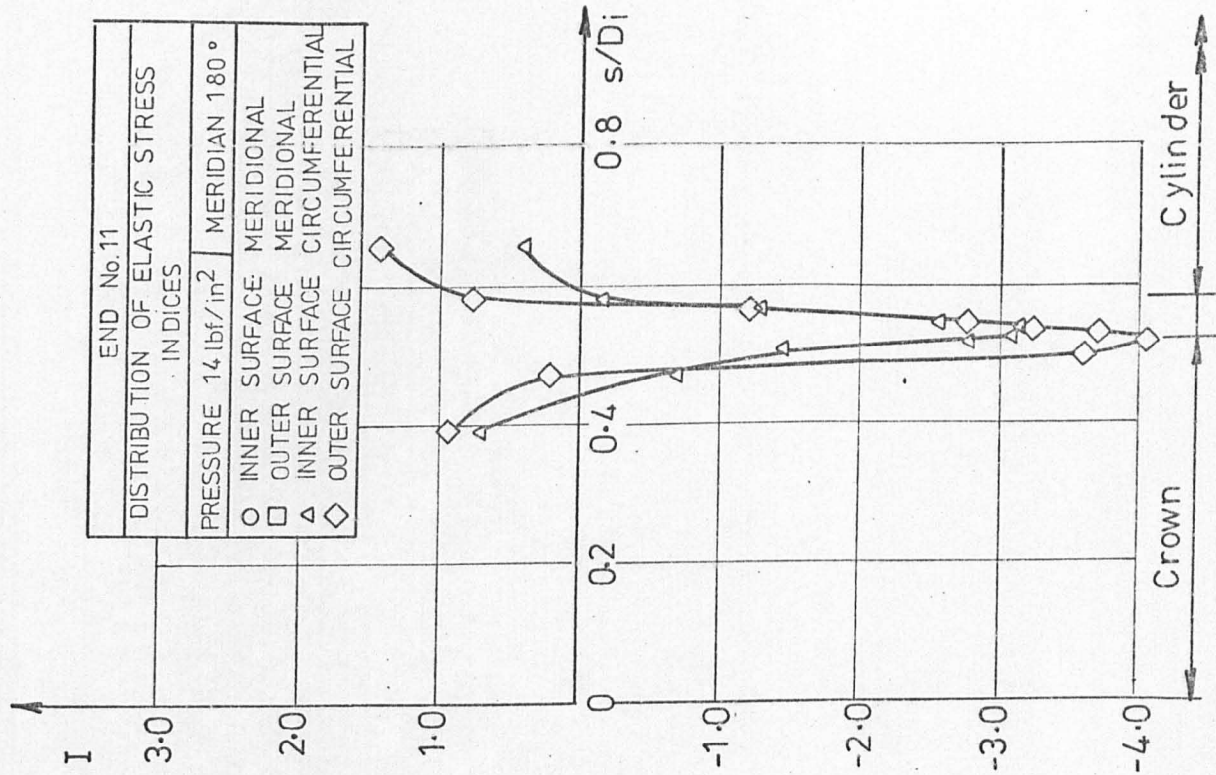
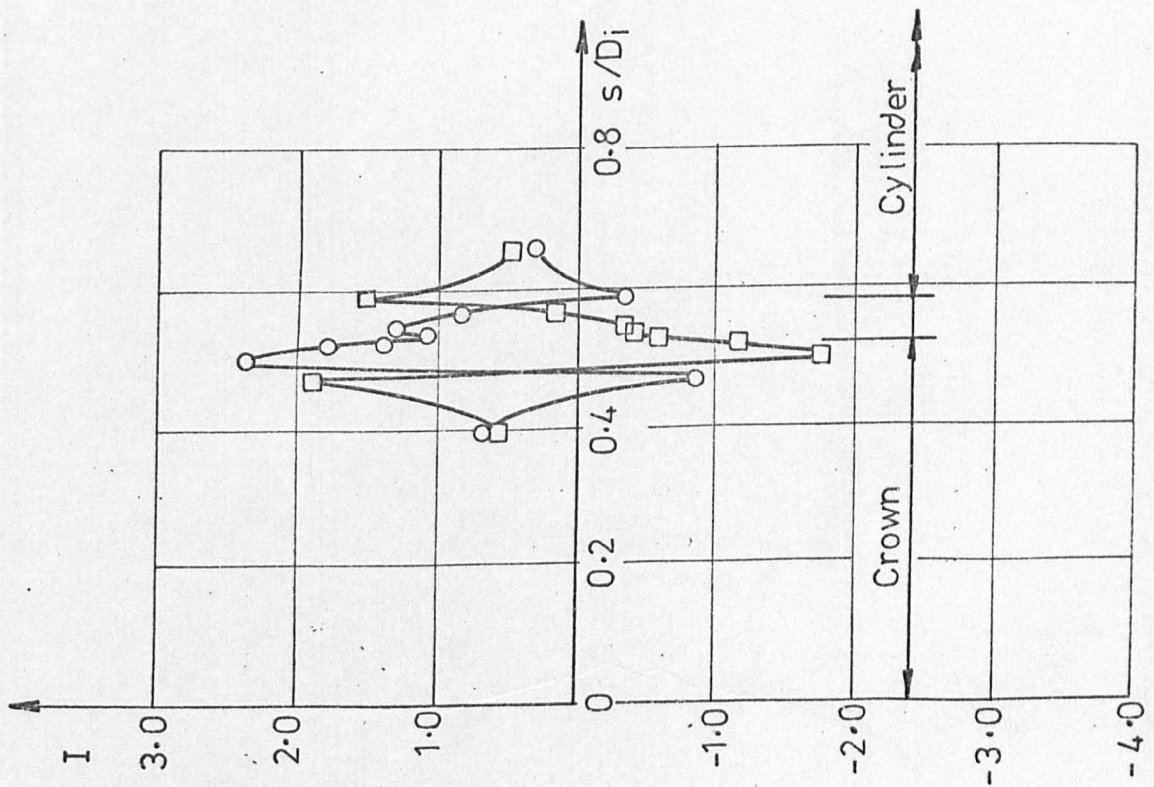


FIG. A1.11.6



END No.11	
DISTRIBUTION OF ELASTIC STRESS INDICES	
PRESSURE 14 lbf/in <sup>2</sup>	MERIDIAN 180°
○	INNER SURFACE MERIDIONAL
□	OUTER SURFACE MERIDIONAL
△	INNER SURFACE CIRCUMFERENTIAL
◇	OUTER SURFACE CIRCUMFERENTIAL

FIG. A1.11.7

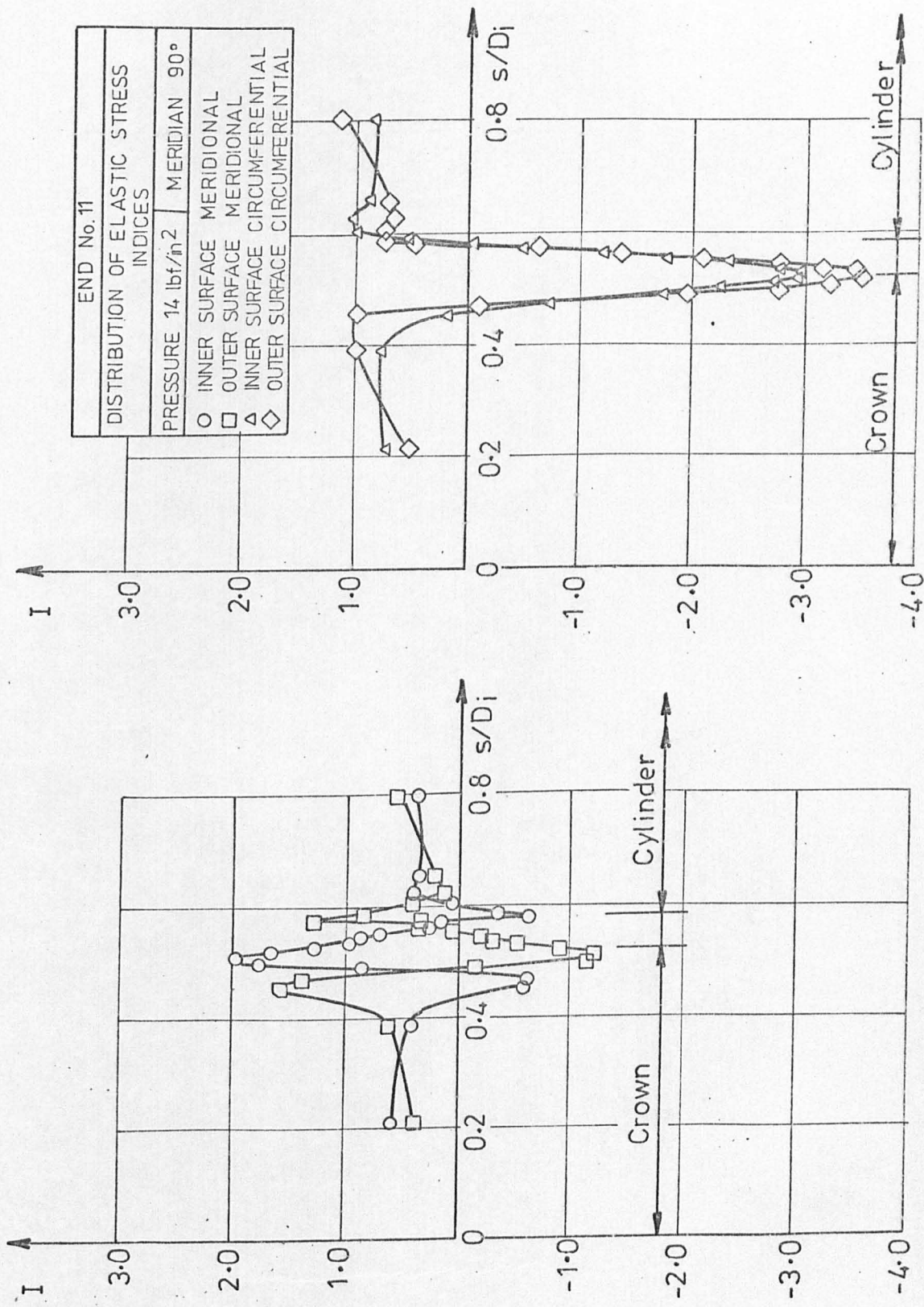


FIG. A1.11.8

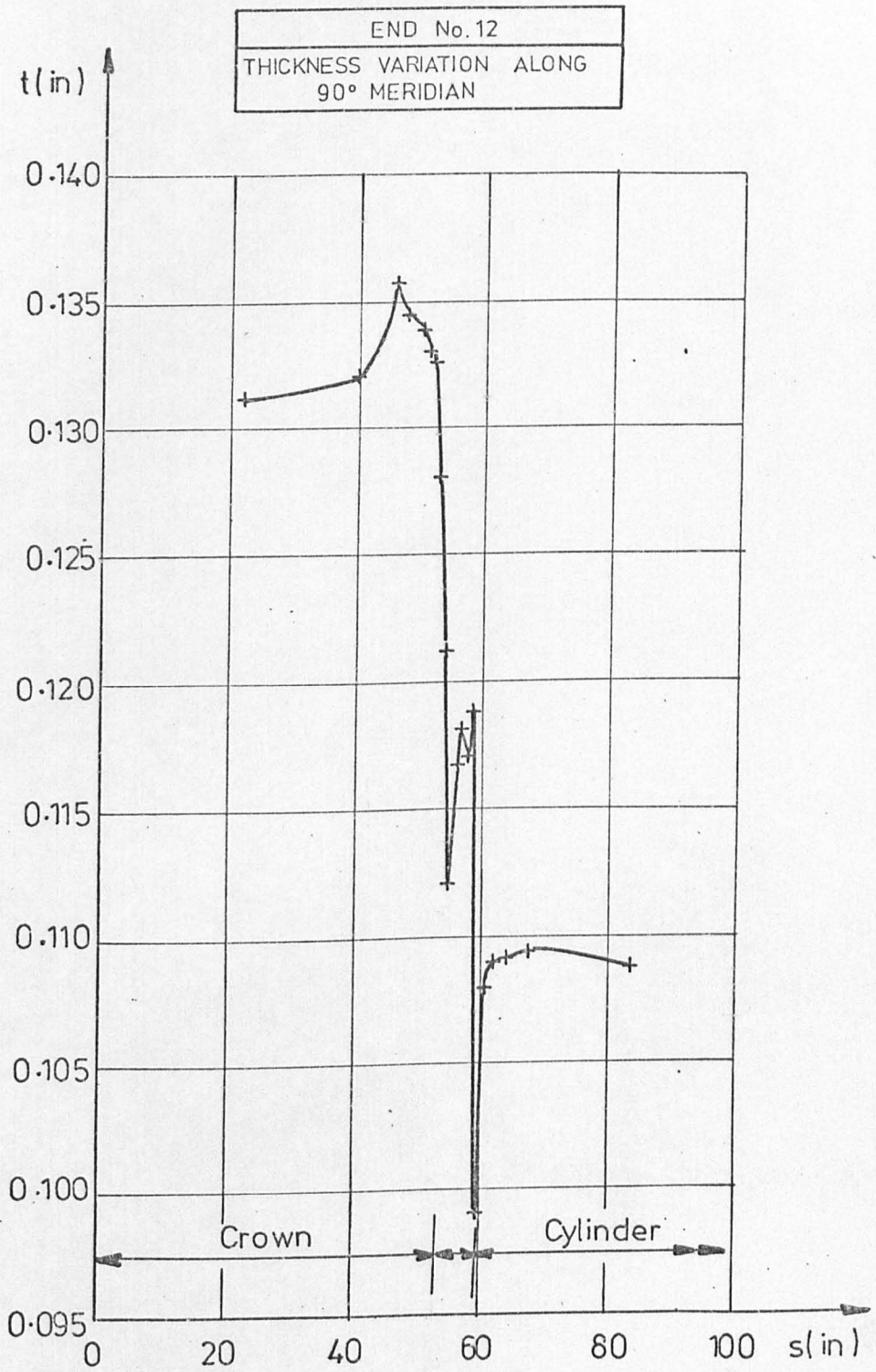


FIG. A1.12.1

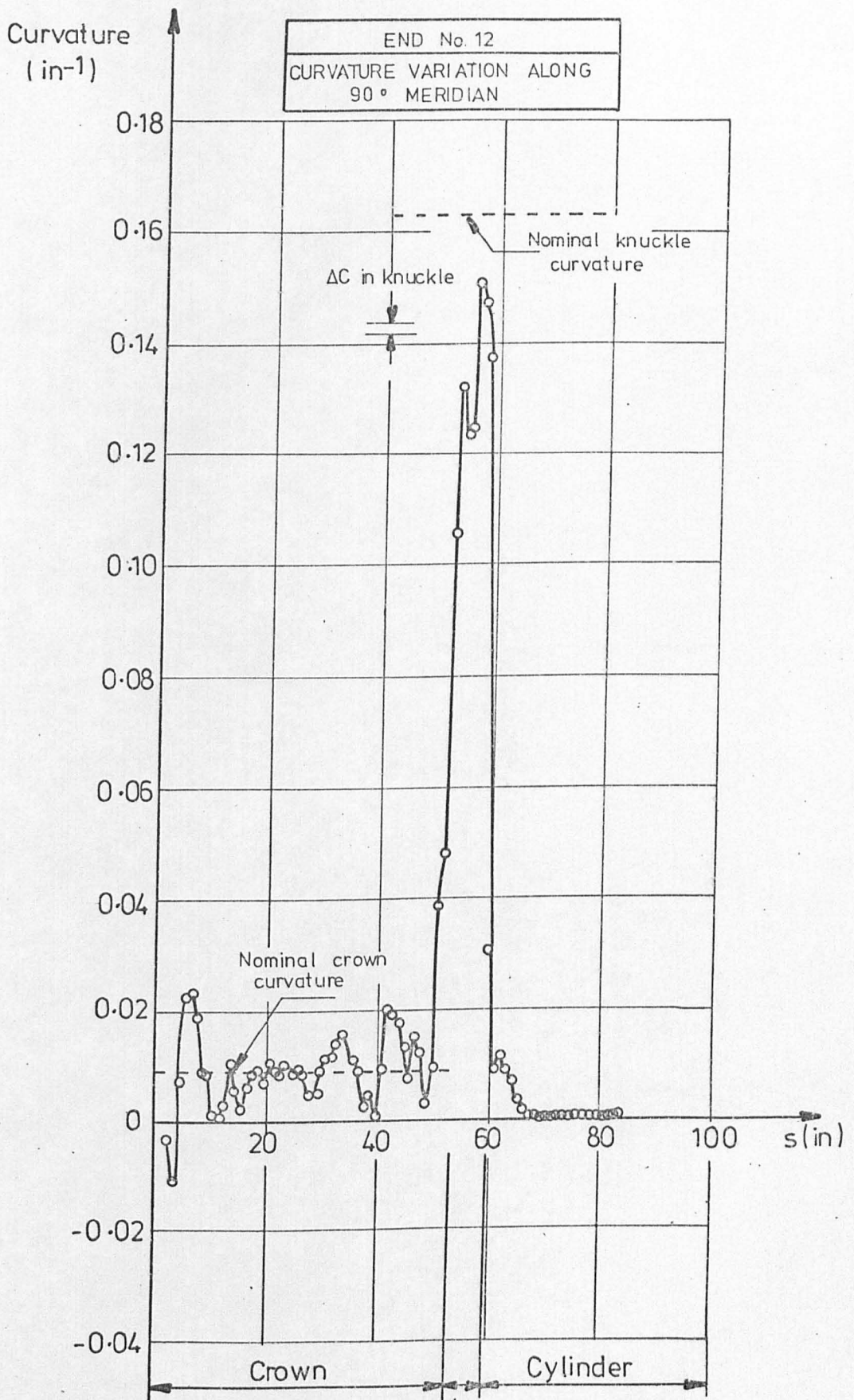
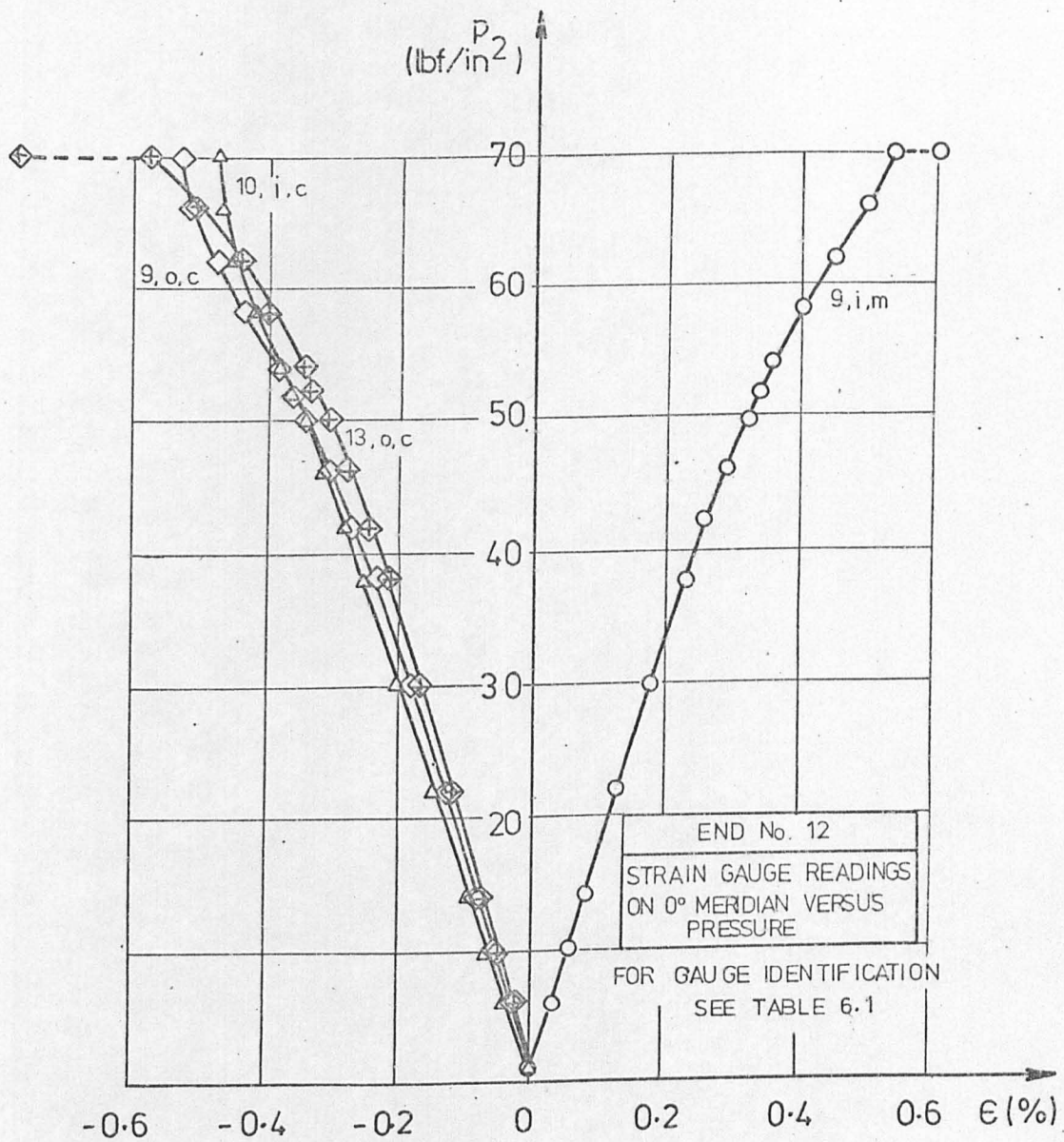


FIG A1.12.2



FIGA1-12.3



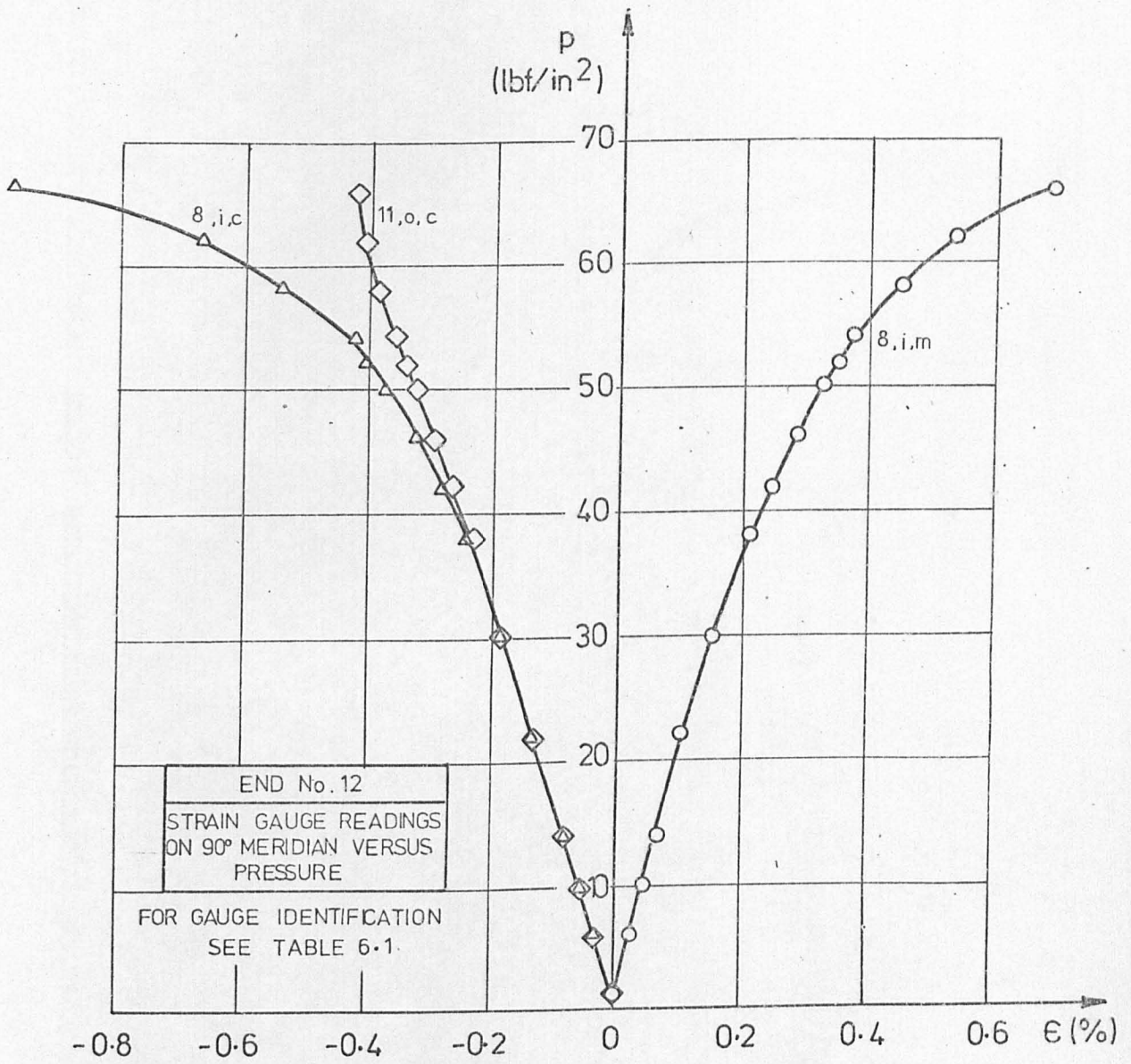


FIG.A1.12.4

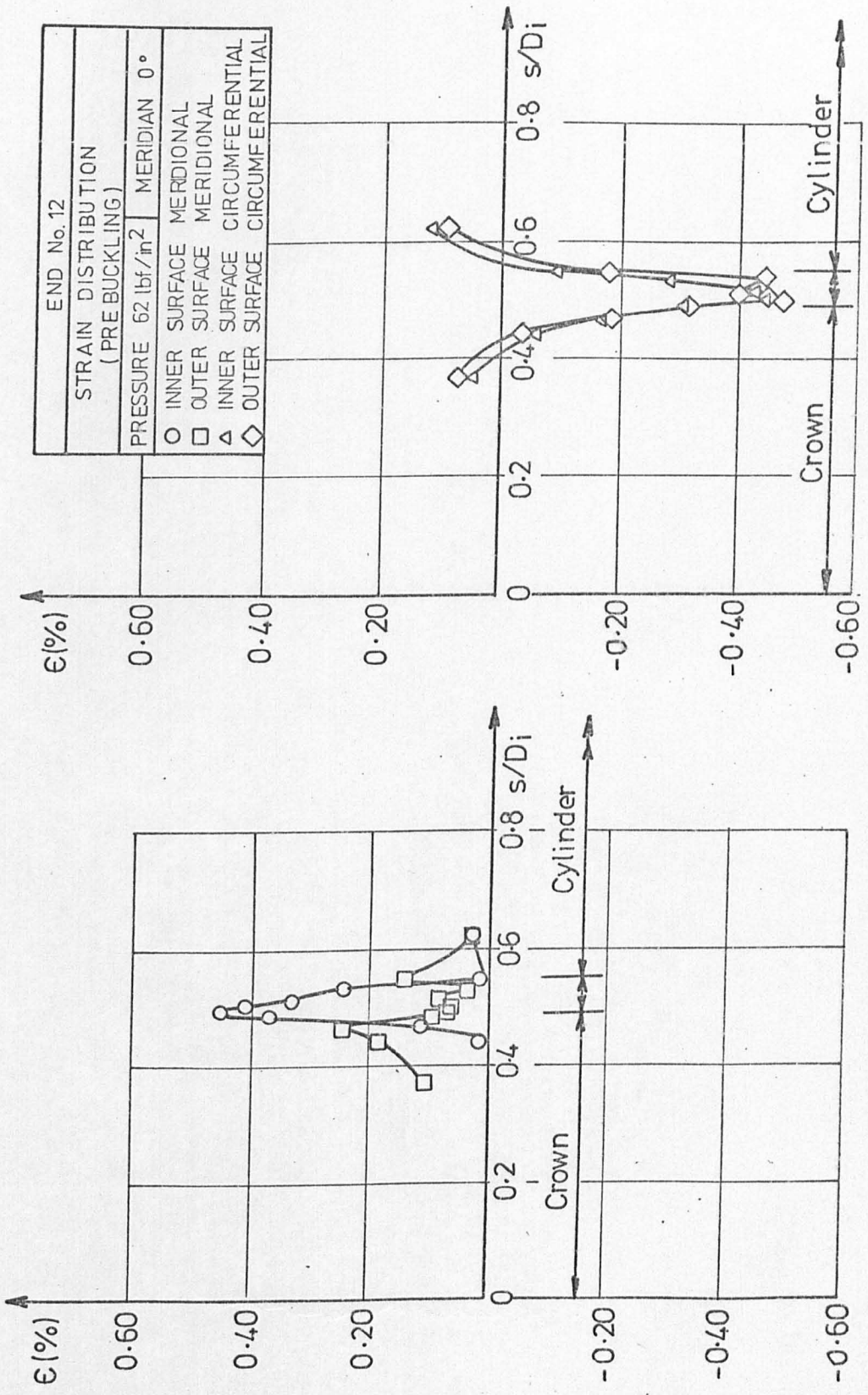
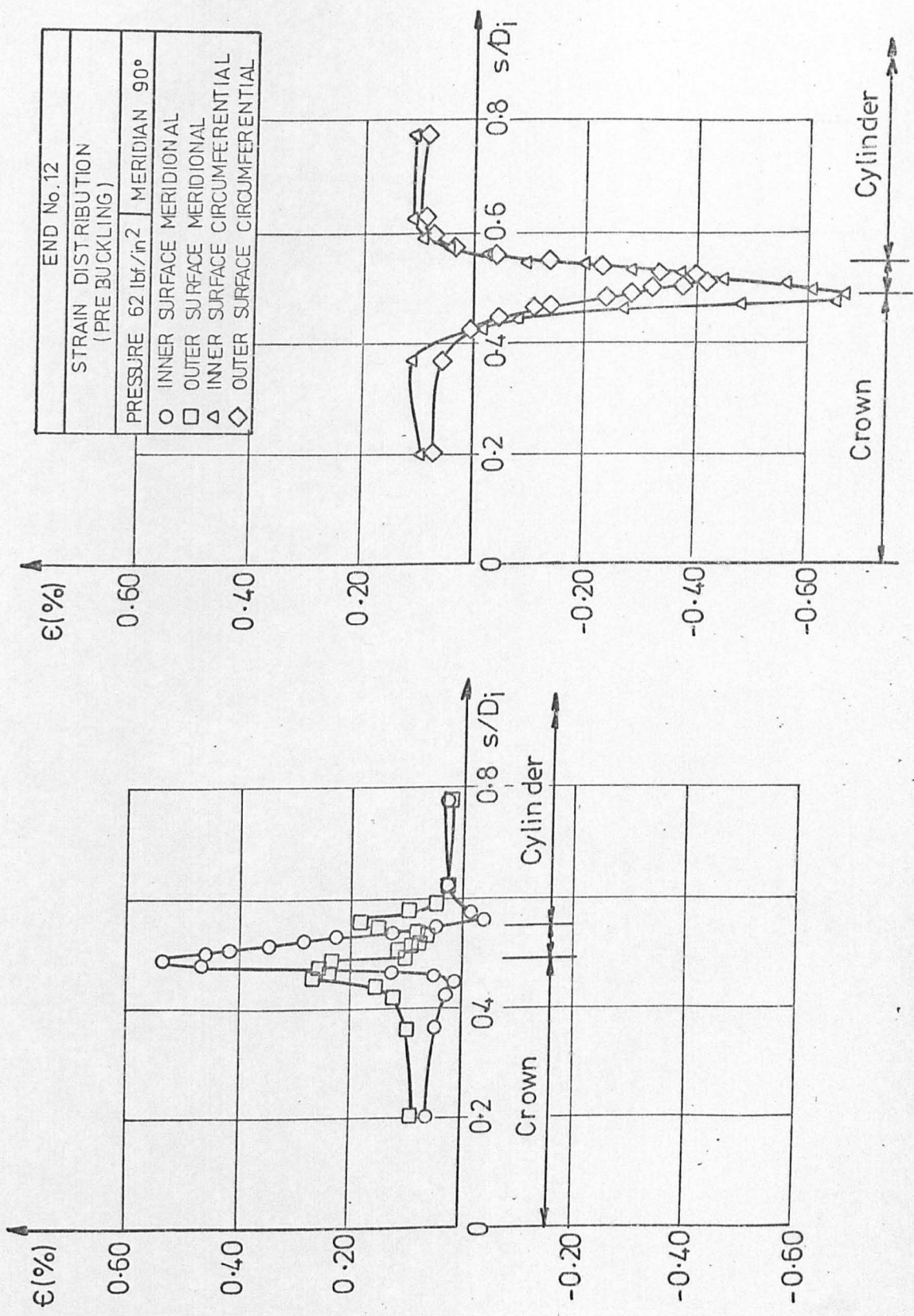
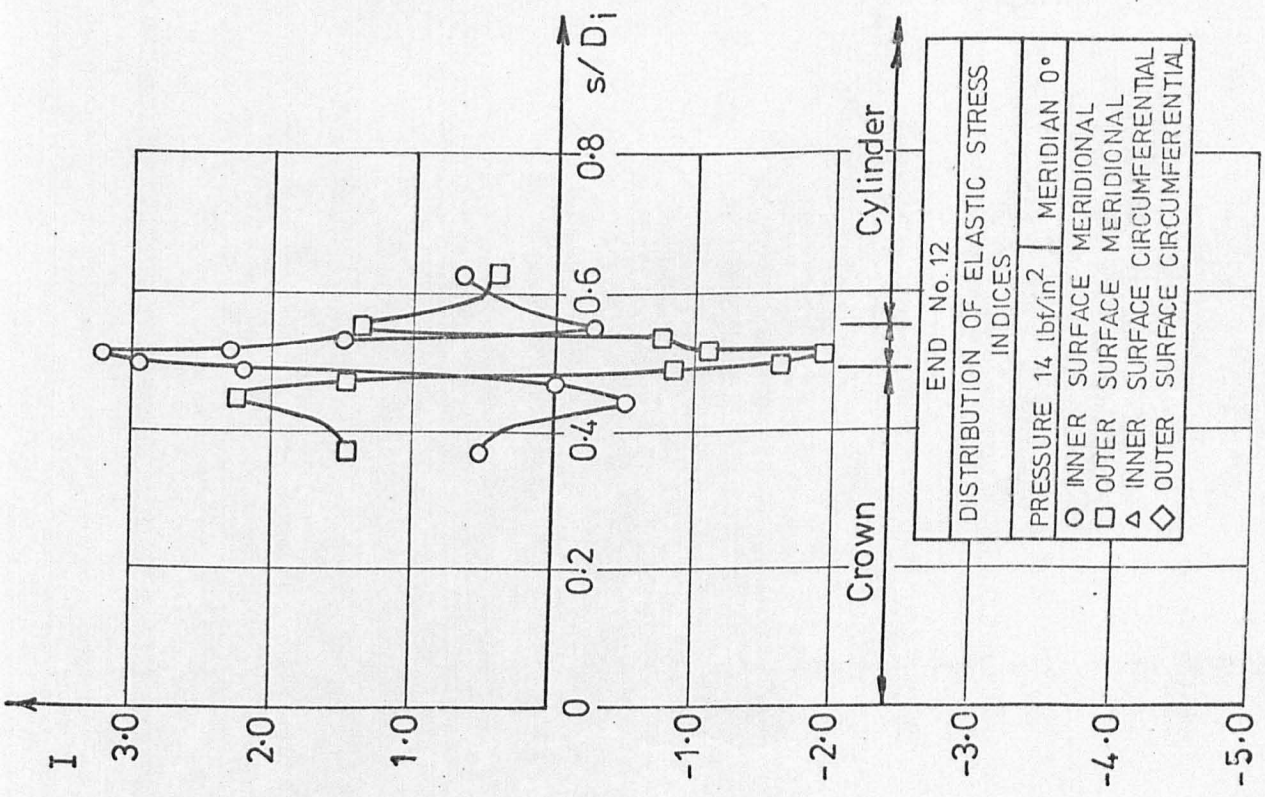
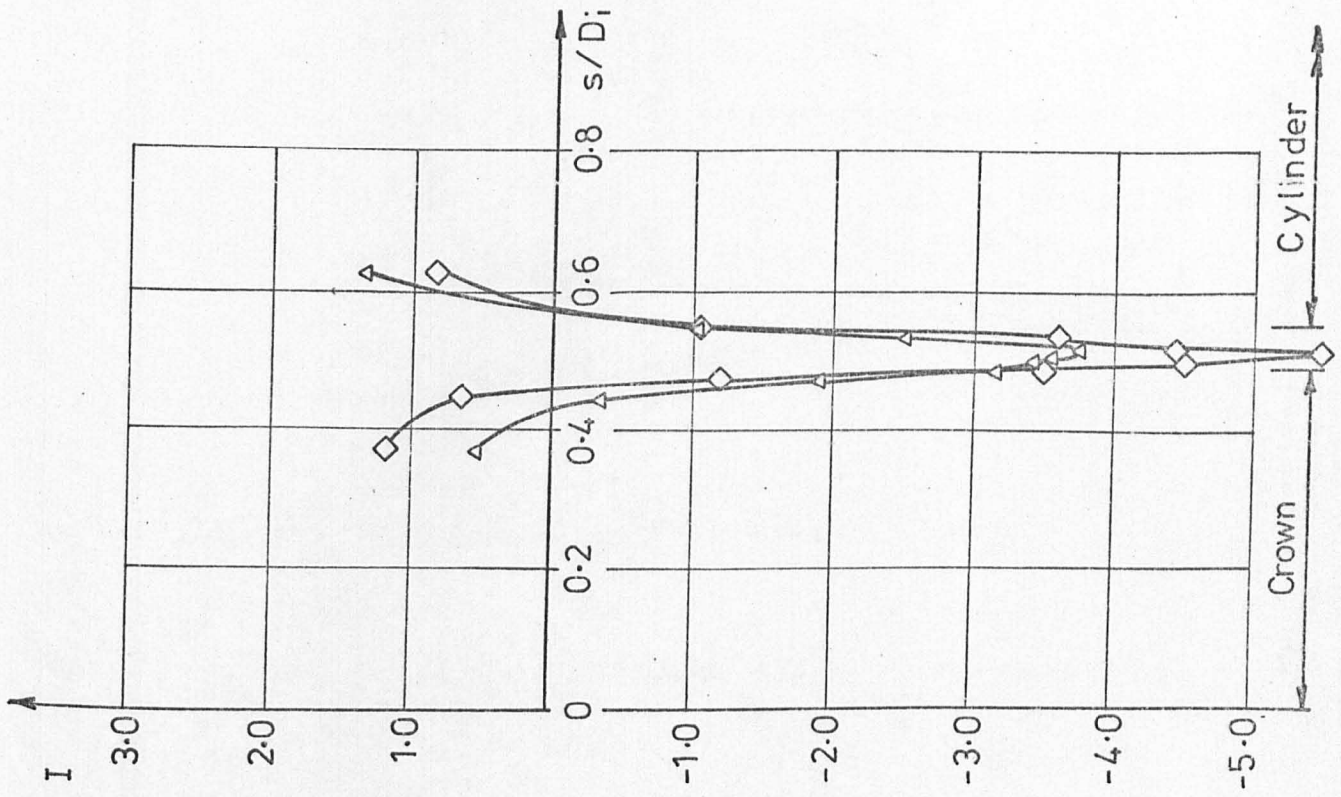


FIG. A1.12.5



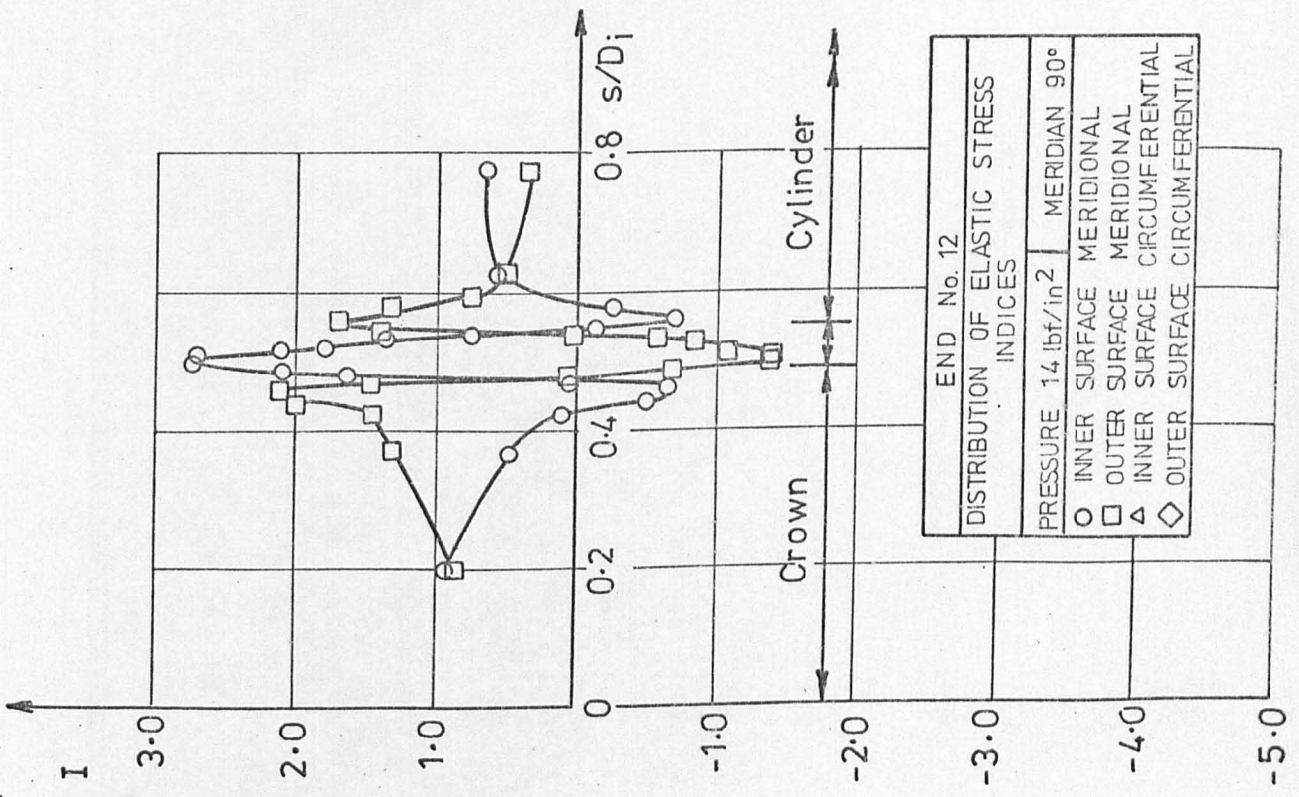
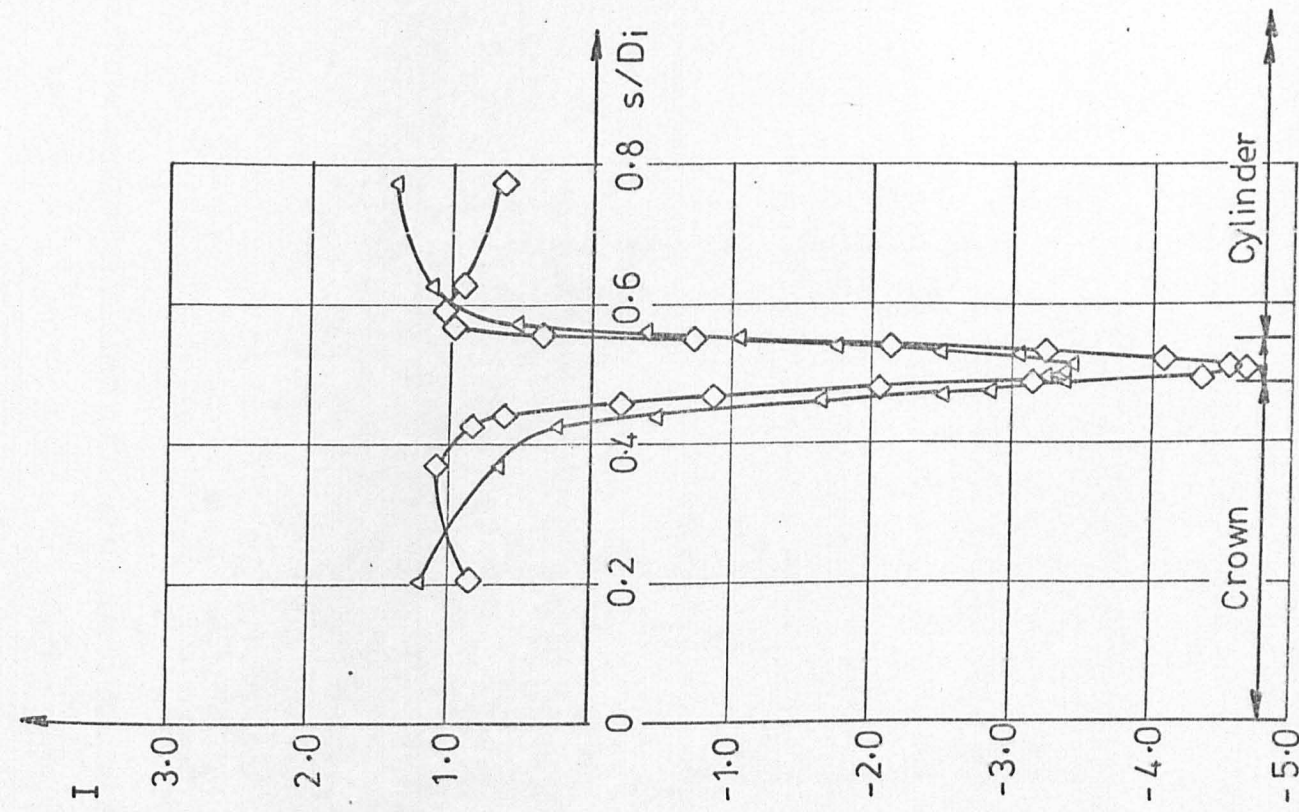
END No. 12	
STRAIN DISTRIBUTION (PRE BUCKLING)	
PRESSURE	62 lbf/in <sup>2</sup> MERIDIAN 90°
○	INNER SURFACE MERIDIONAL
□	OUTER SURFACE MERIDIONAL
△	INNER SURFACE CIRCUMFERENTIAL
◇	OUTER SURFACE CIRCUMFERENTIAL

FIG. A1.12.6



END No.12	
DISTRIBUTION OF ELASTIC STRESS INDICES	
PRESSURE 14 lbf/in <sup>2</sup>	MERIDIAN 0°
○	INNER SURFACE MERIDIONAL
□	OUTER SURFACE MERIDIONAL
△	INNER SURFACE CIRCUMFERENTIAL
◇	OUTER SURFACE CIRCUMFERENTIAL

FIG.A1-12.7



END No. 12	
DISTRIBUTION OF ELASTIC STRESS INDICES	
PRESSURE 14 lbf/in <sup>2</sup>	MERIDIAN 90°
$\circ$ INNER SURFACE	MERIDIONAL
$\square$ OUTER SURFACE	MERIDIONAL
$\triangle$ INNER SURFACE	CIRCUMFERENTIAL
$\diamond$ OUTER SURFACE	CIRCUMFERENTIAL

FIG. A1.12.8

END No. 13
THICKNESS VARIATION ALONG 90° MERIDIAN

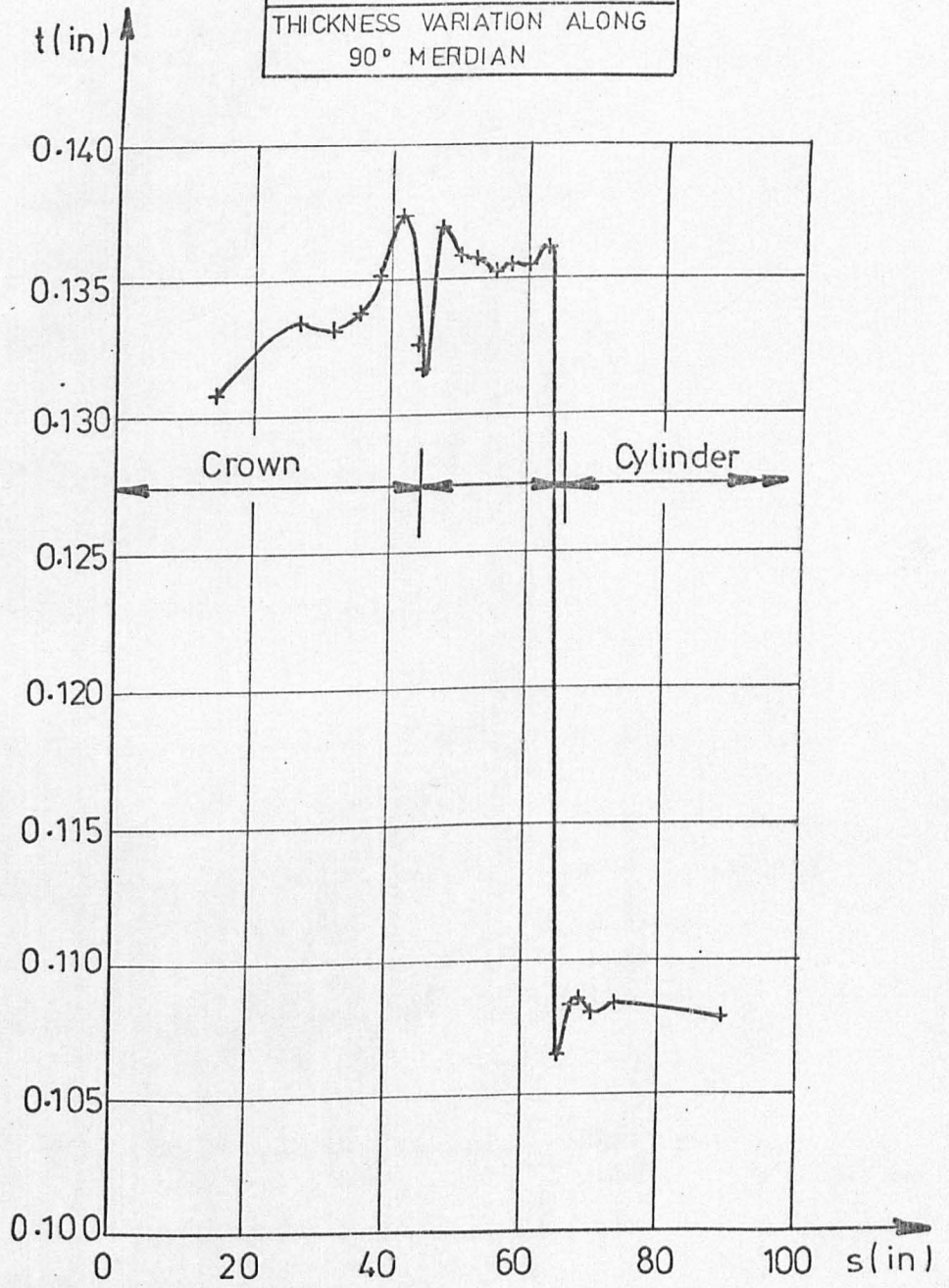
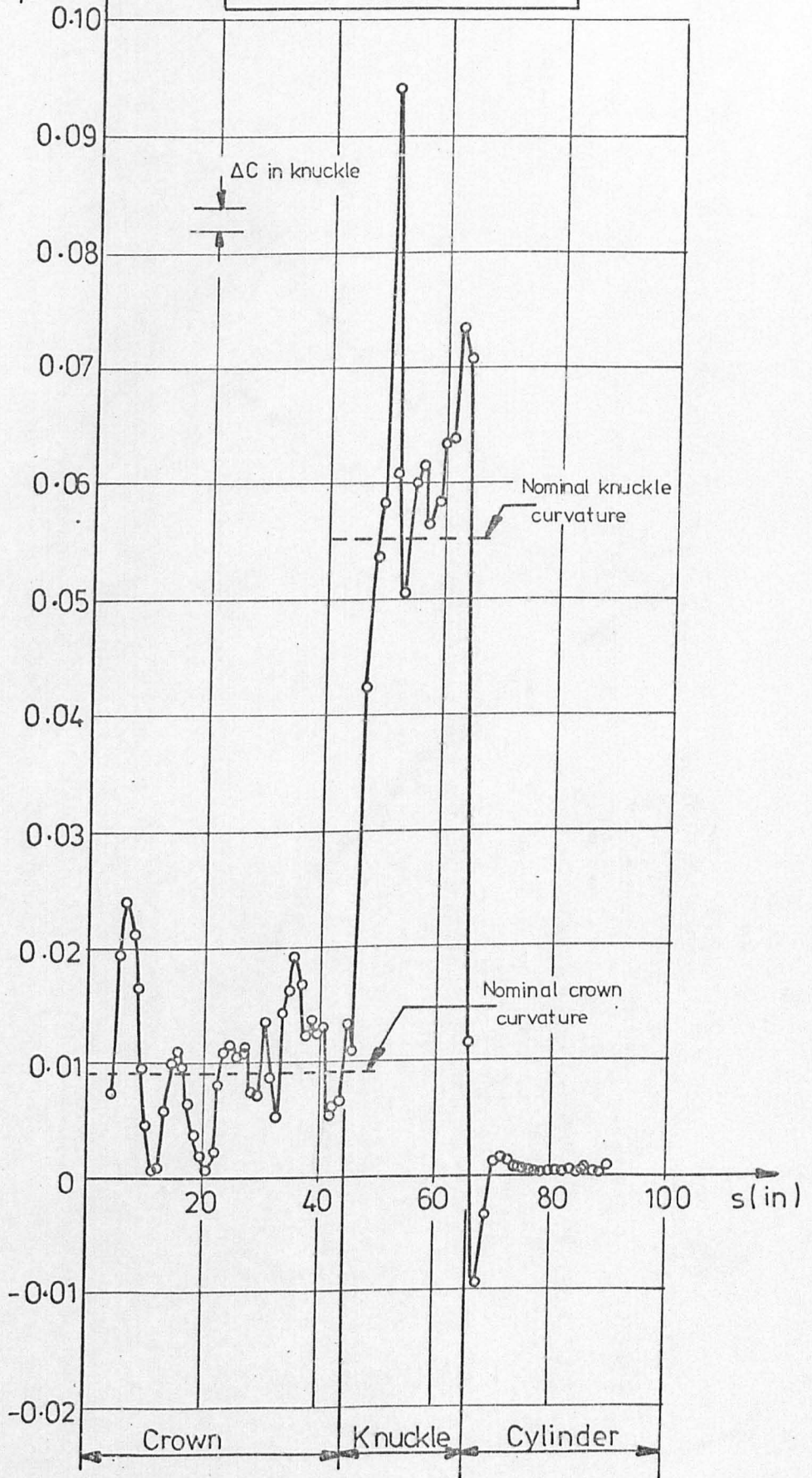


FIG. A1.13.1

Curvature  
(in<sup>-1</sup>)

END No. 13

CURVATURE VARIATION ALONG  
90° MERIDIAN



FIGA1-13. 2

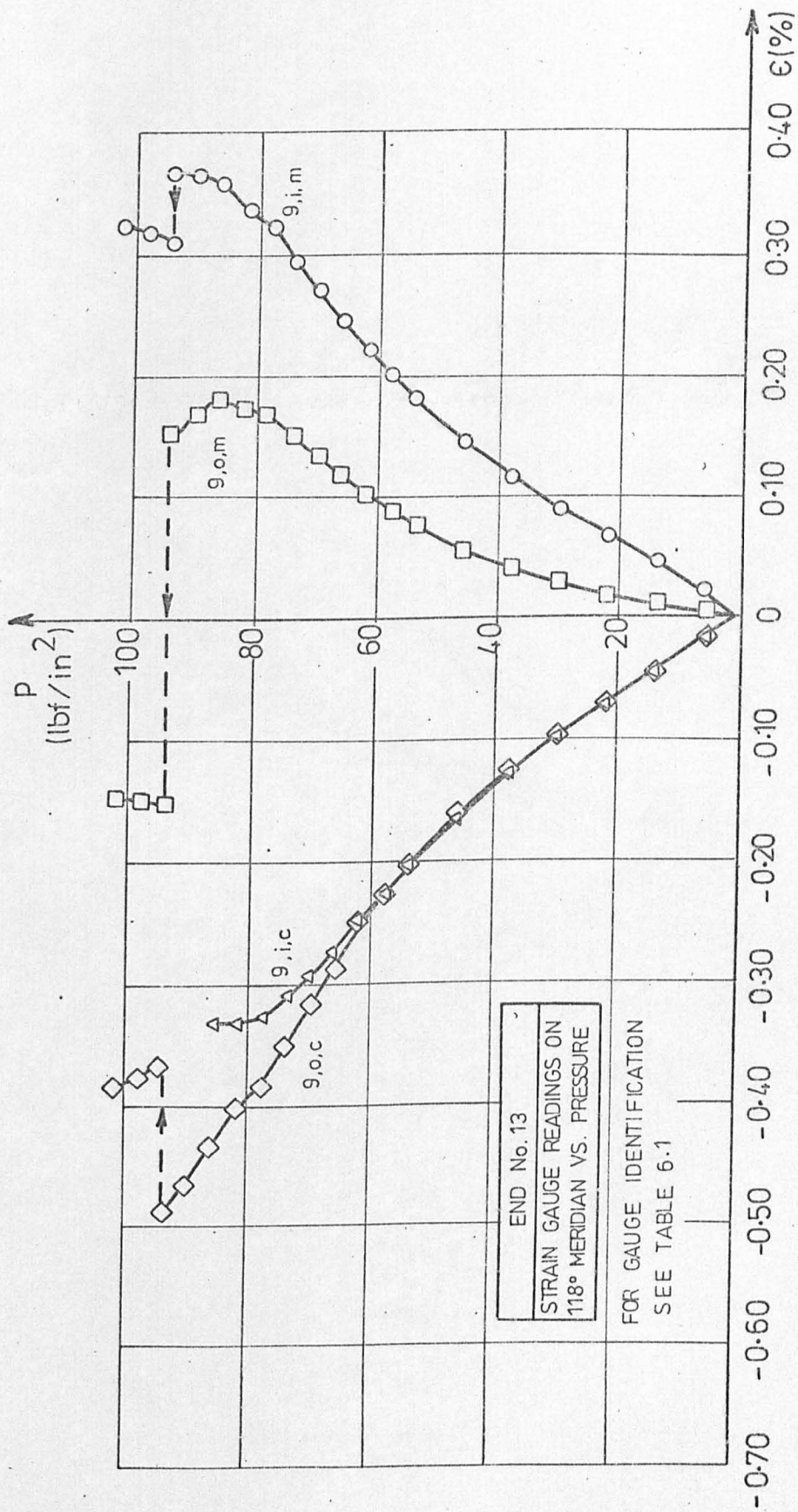


FIG. A1.13.3



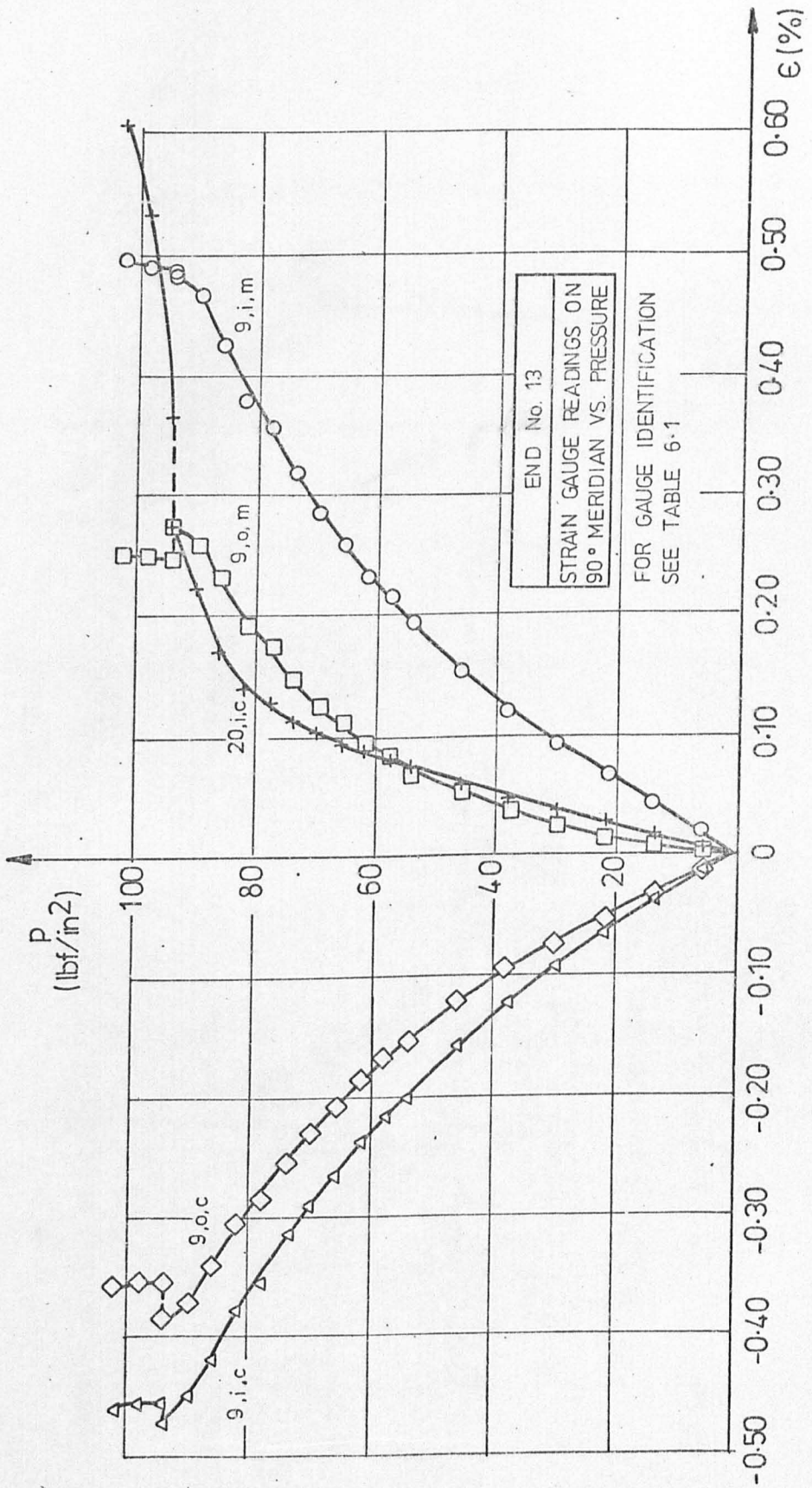


FIG. A1.13.4

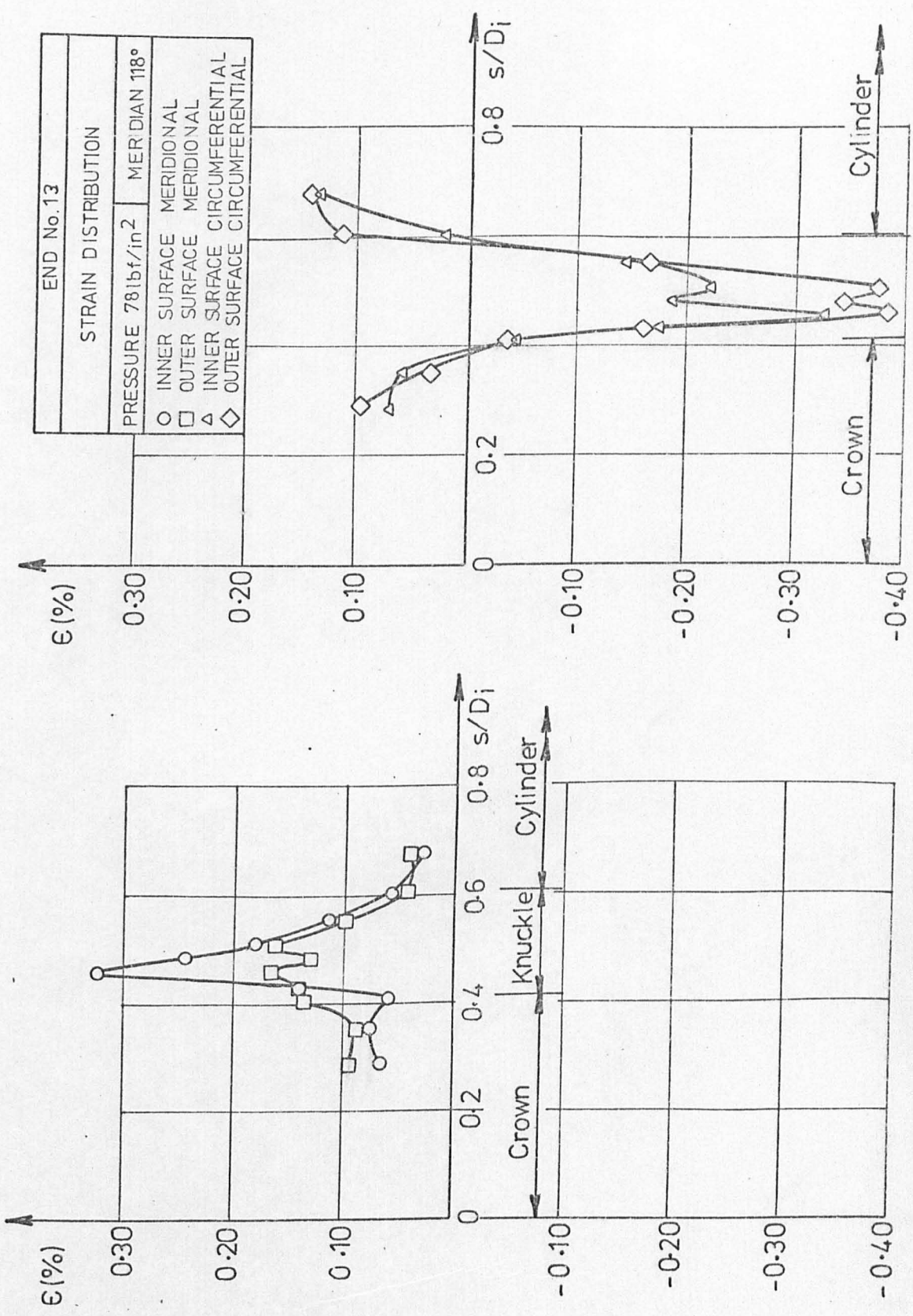


FIG. A1.13.5

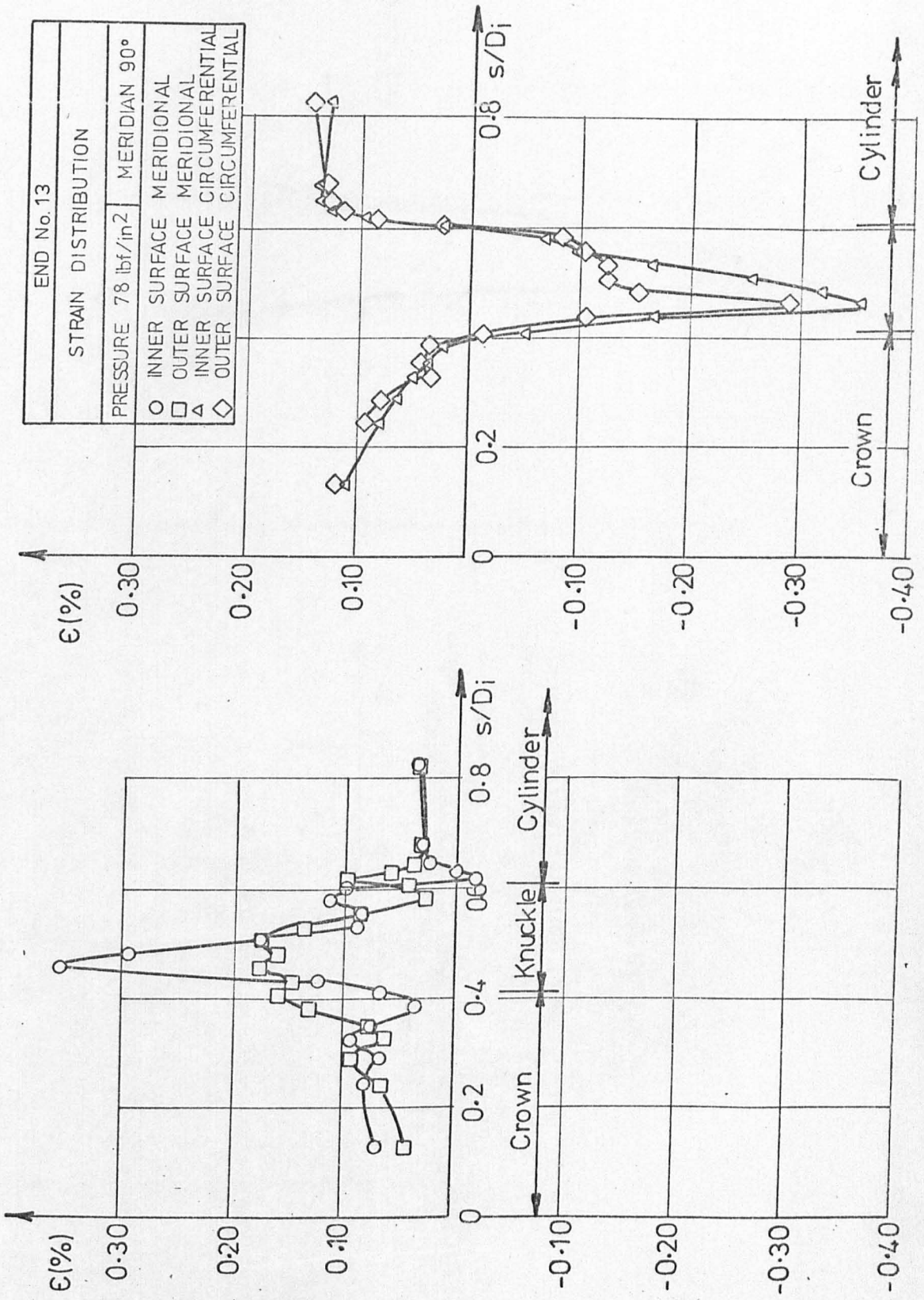
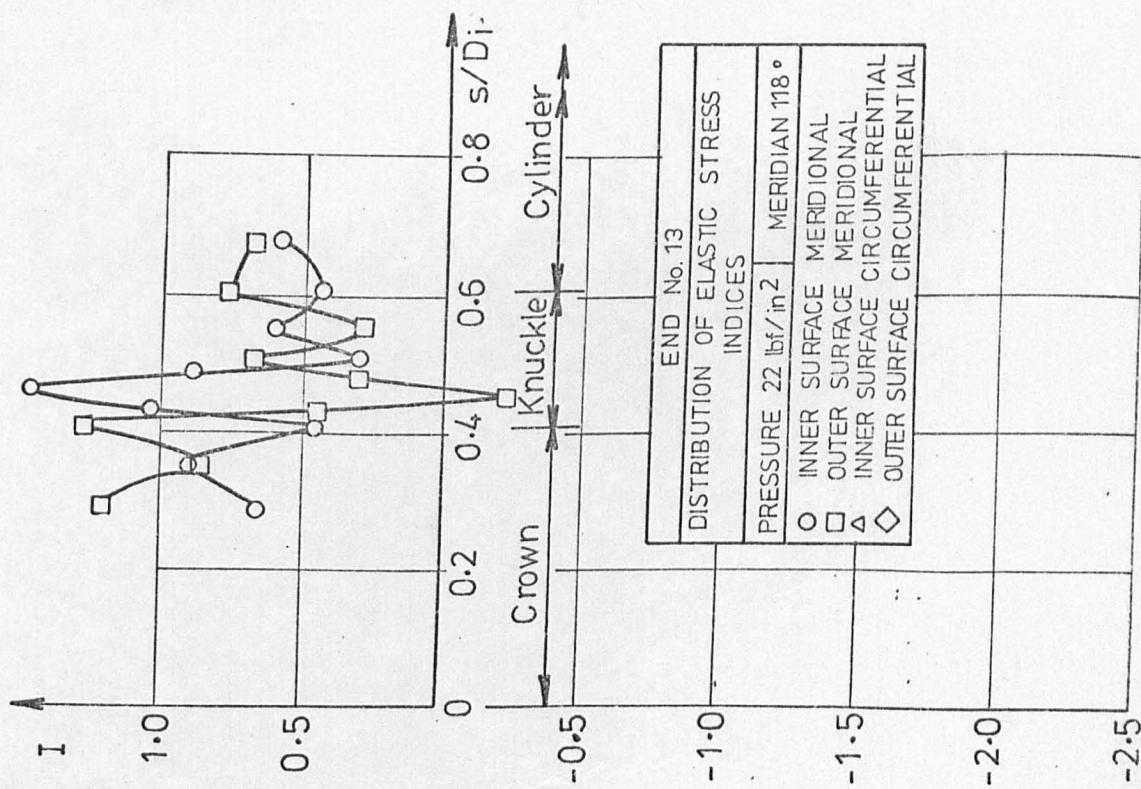
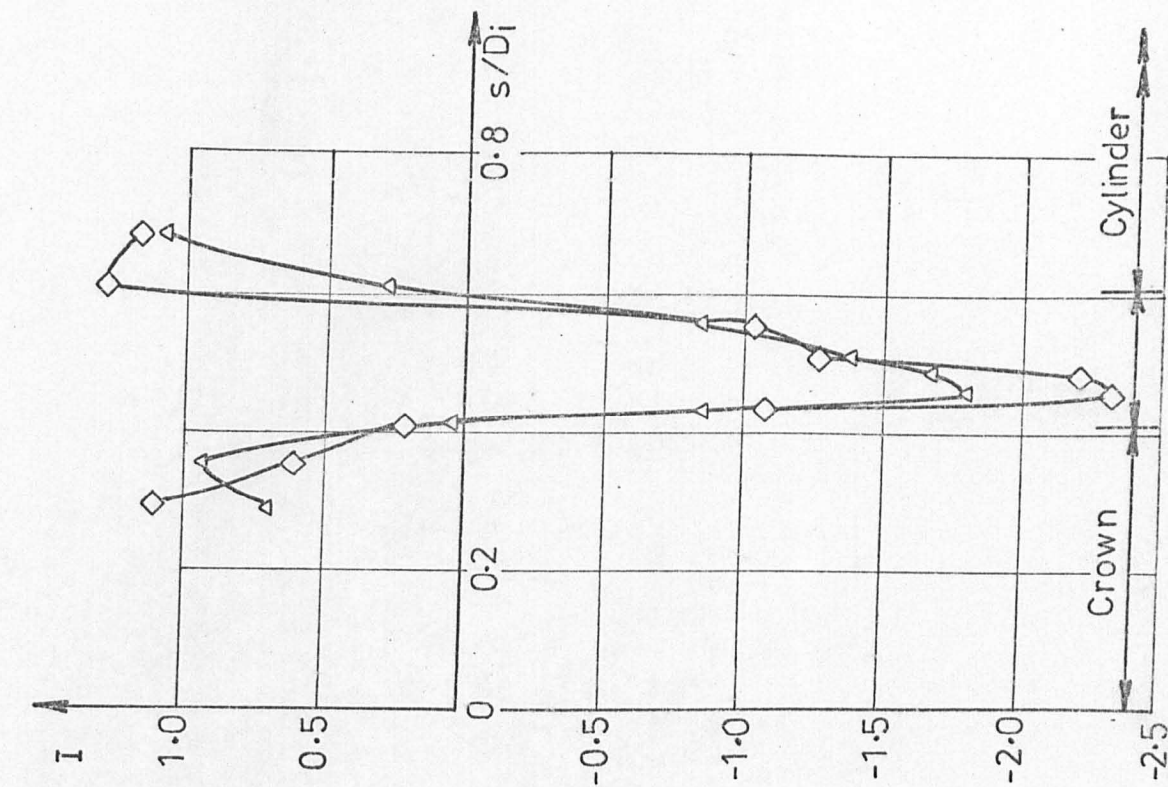


FIG. A1-13.6



END No. 13	
DISTRIBUTION OF ELASTIC STRESS INDICES	
PRESSURE 22 lbf/in <sup>2</sup>	MERIDIAN 118°
○	INNER SURFACE MERIDIONAL
□	OUTER SURFACE MERIDIONAL
△	INNER SURFACE CIRCUMFERENTIAL
◇	OUTER SURFACE CIRCUMFERENTIAL

FIG. A1.13.7

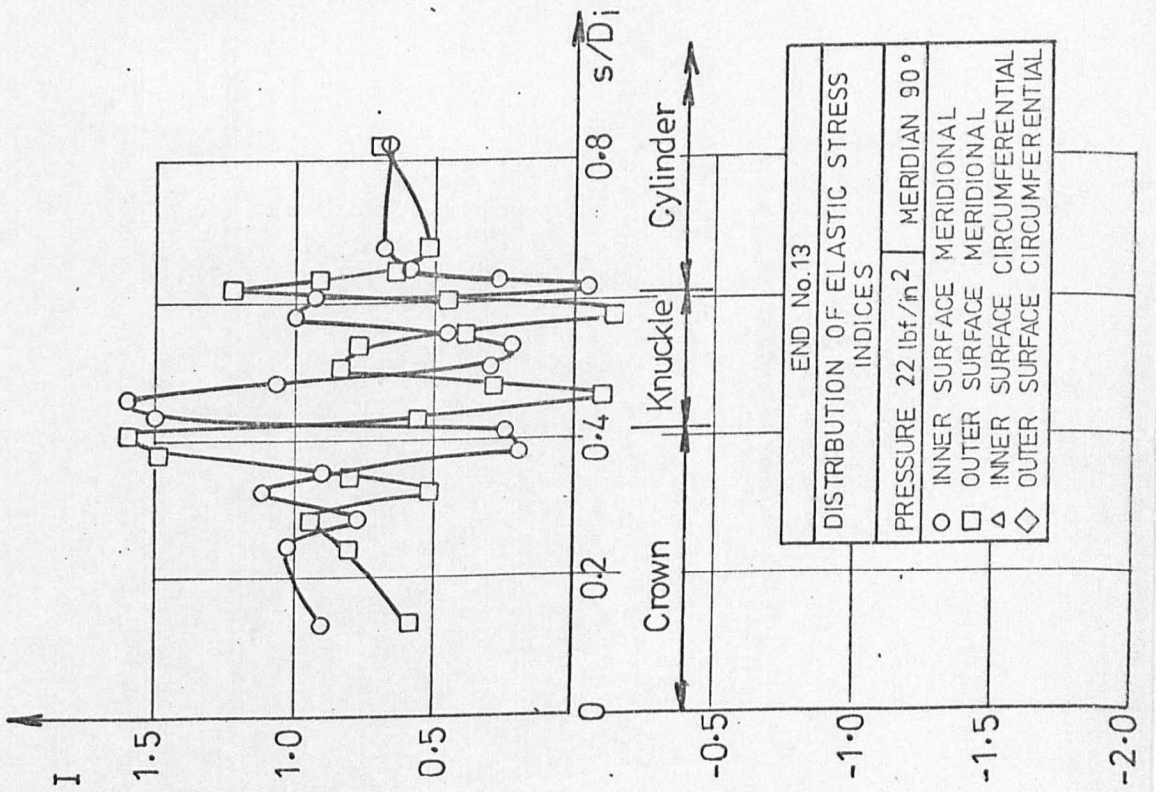
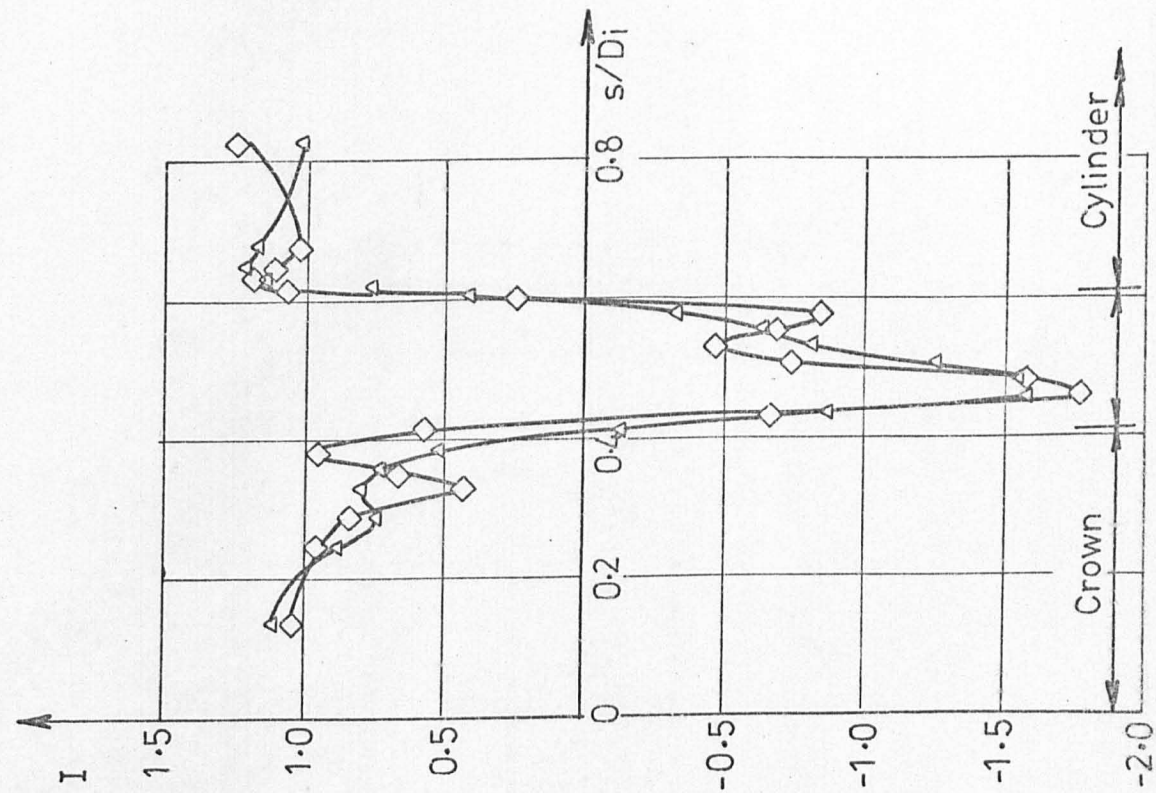


FIG. A1.13.8

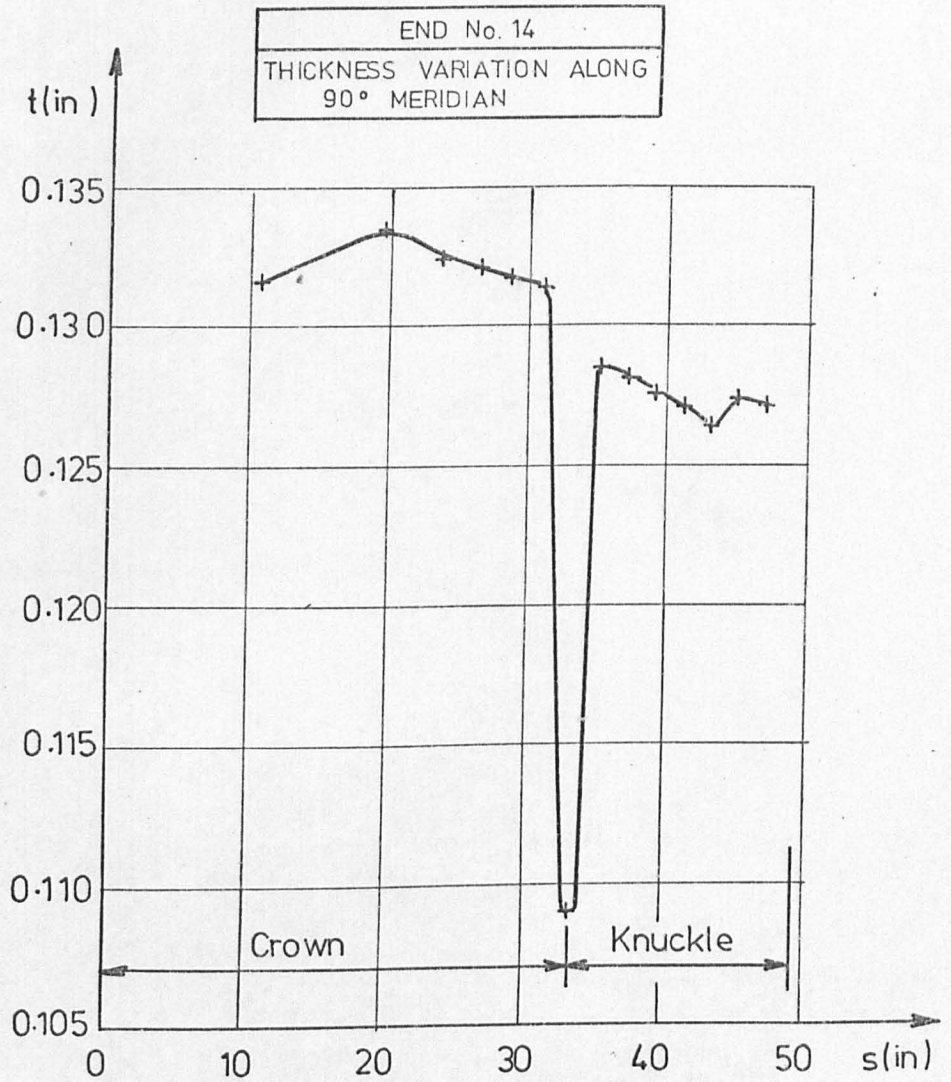


FIG. A1.14.1

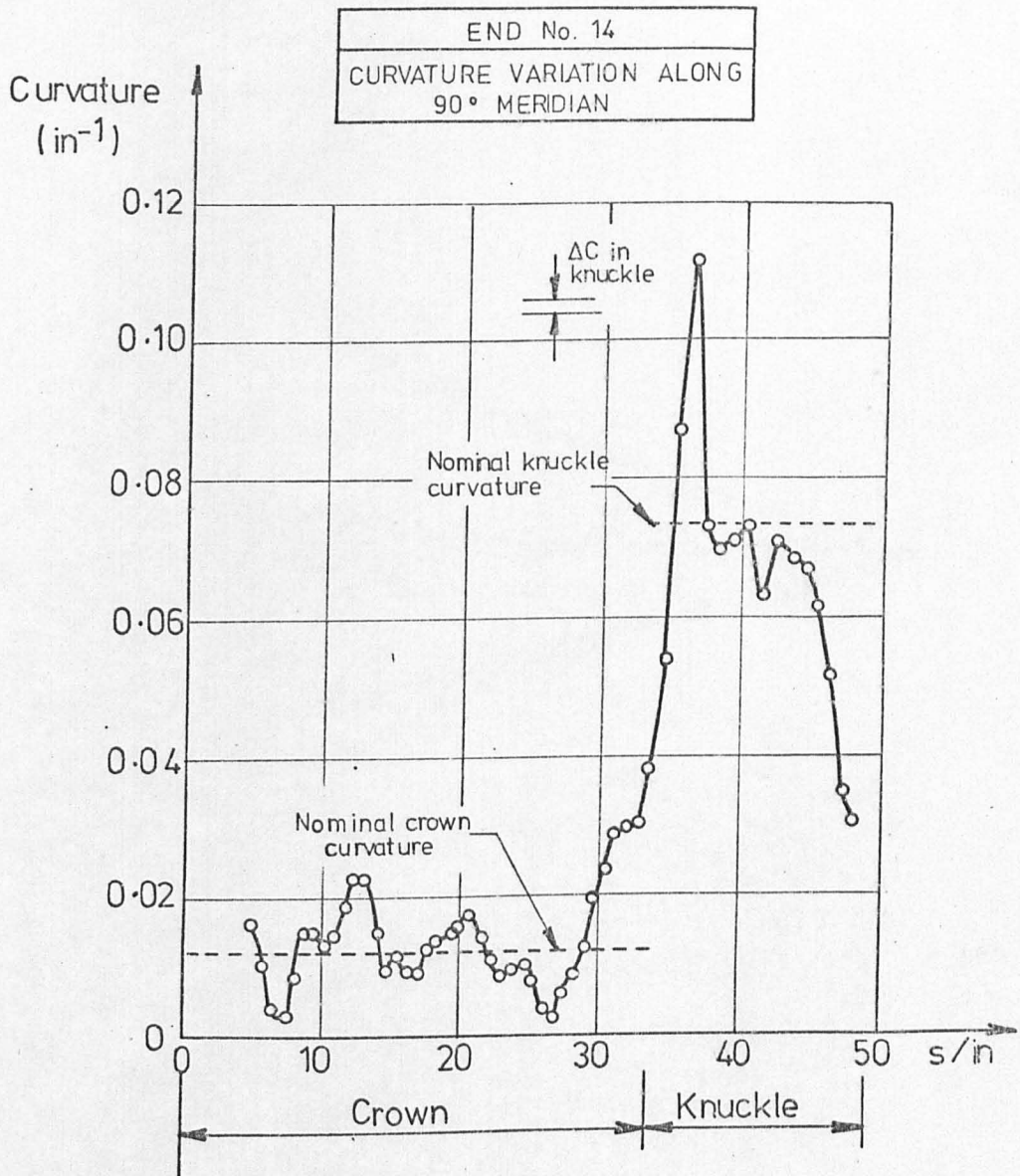


FIG. A1.14.2

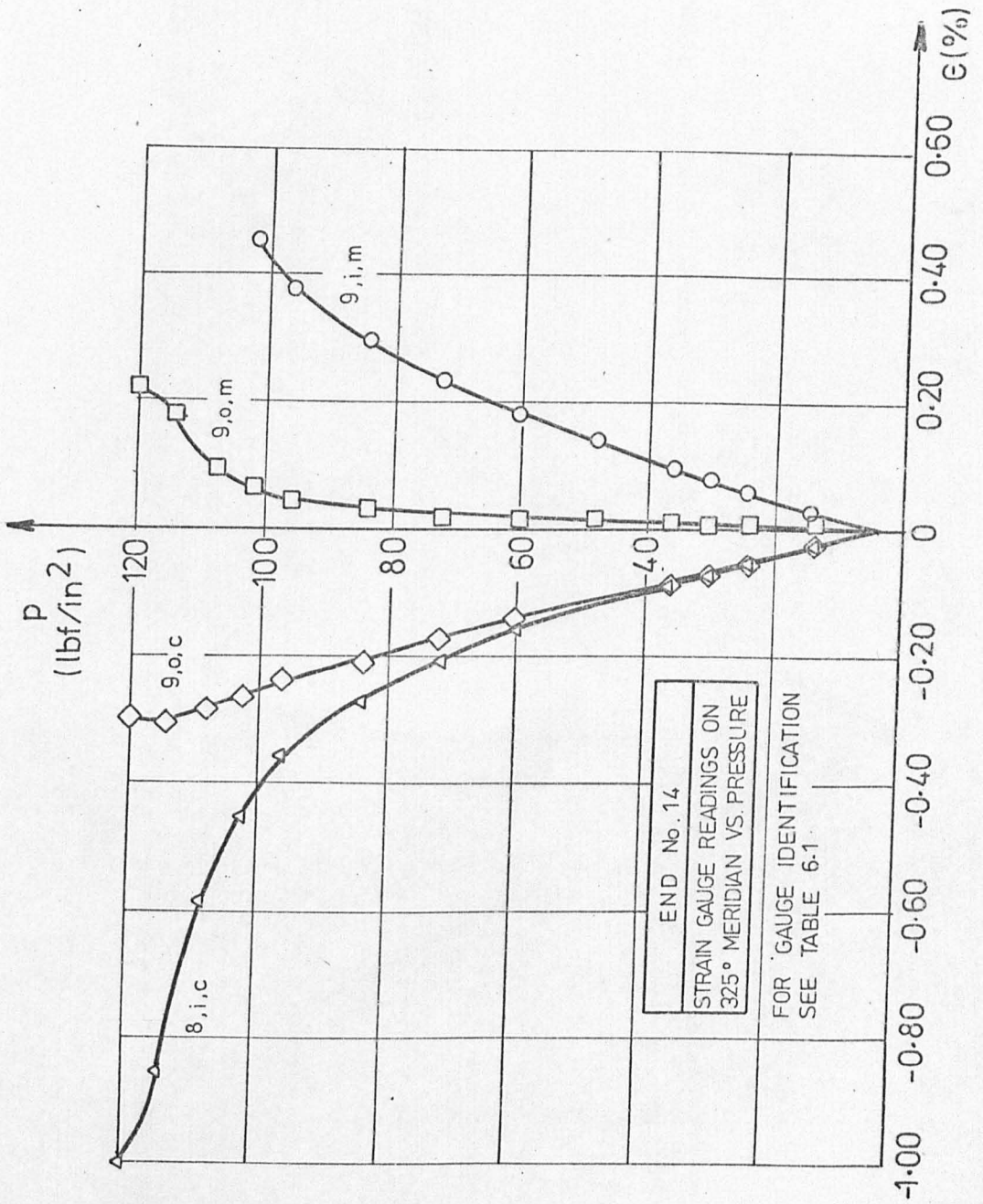


FIG.A1.14.3



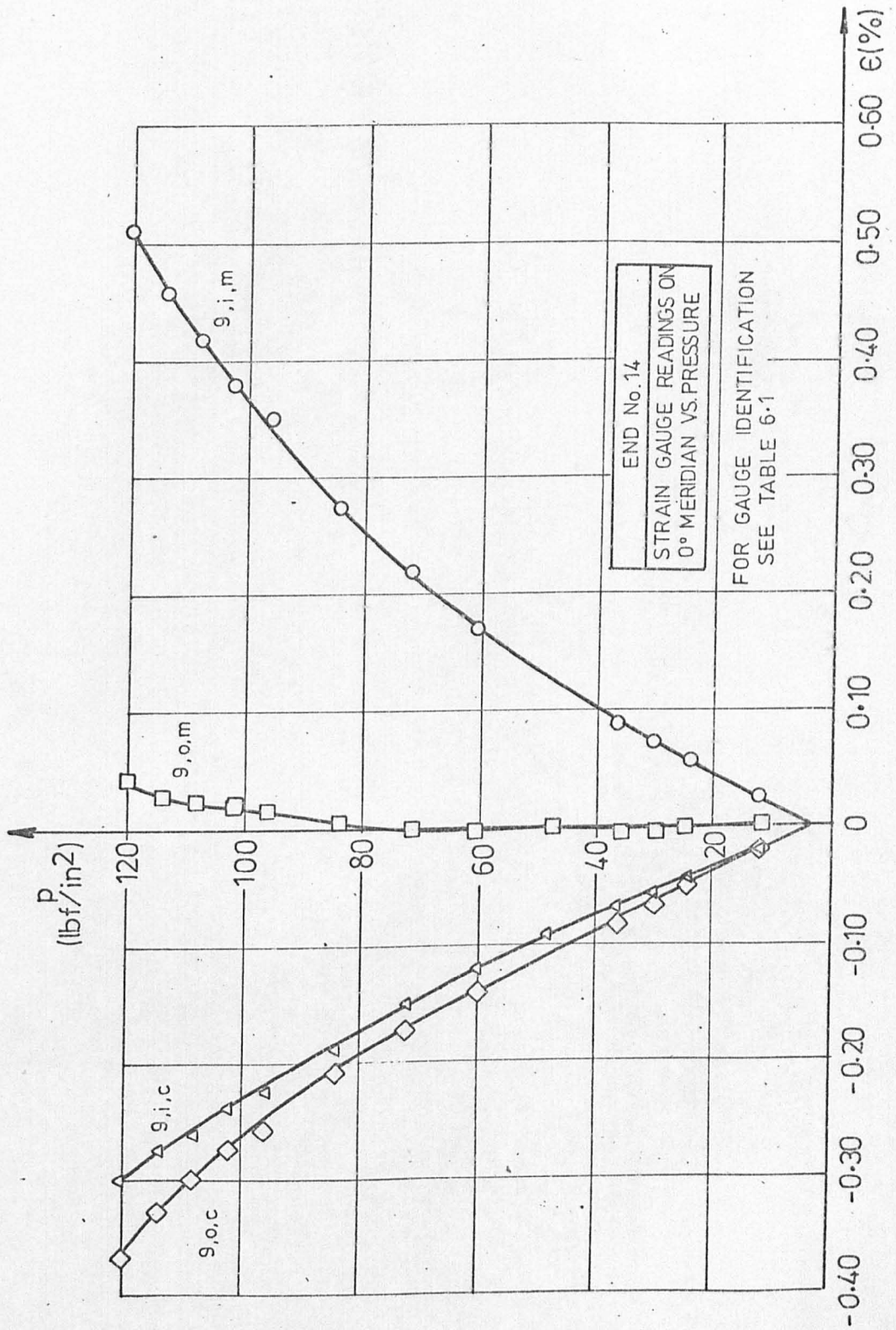


FIG. A1.14.4

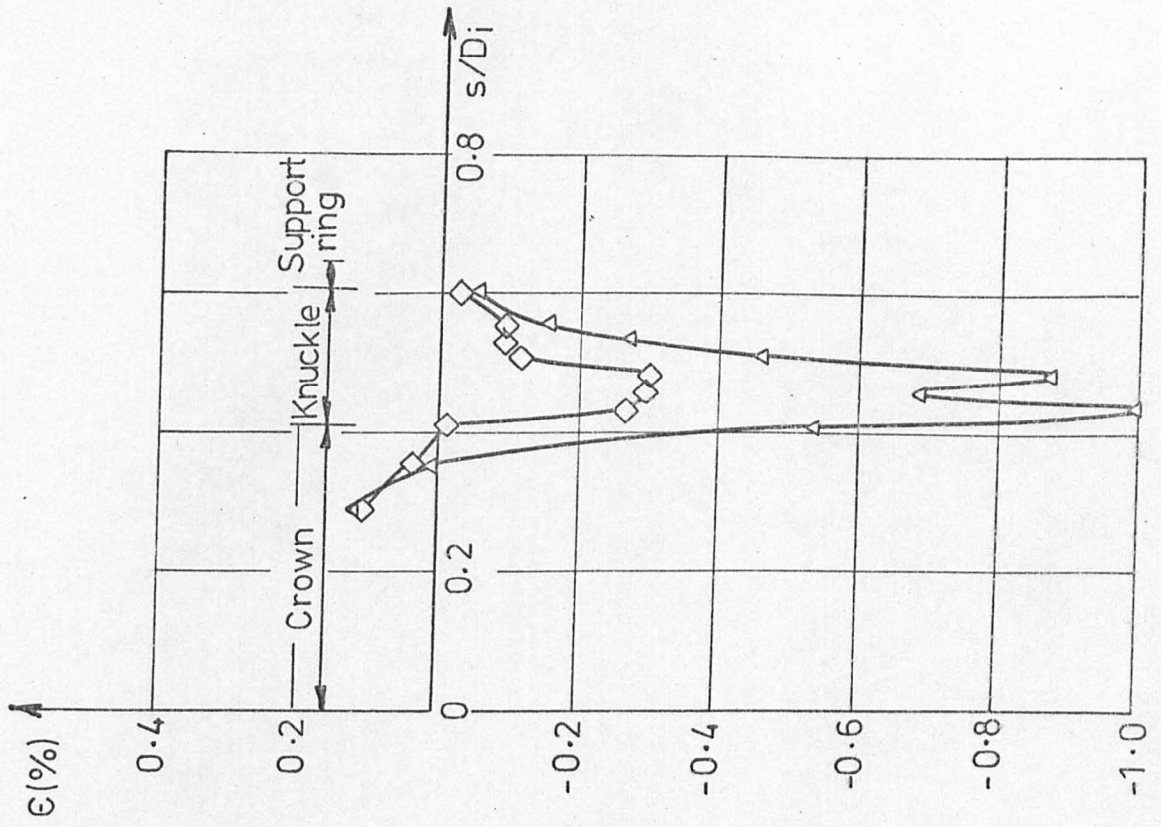
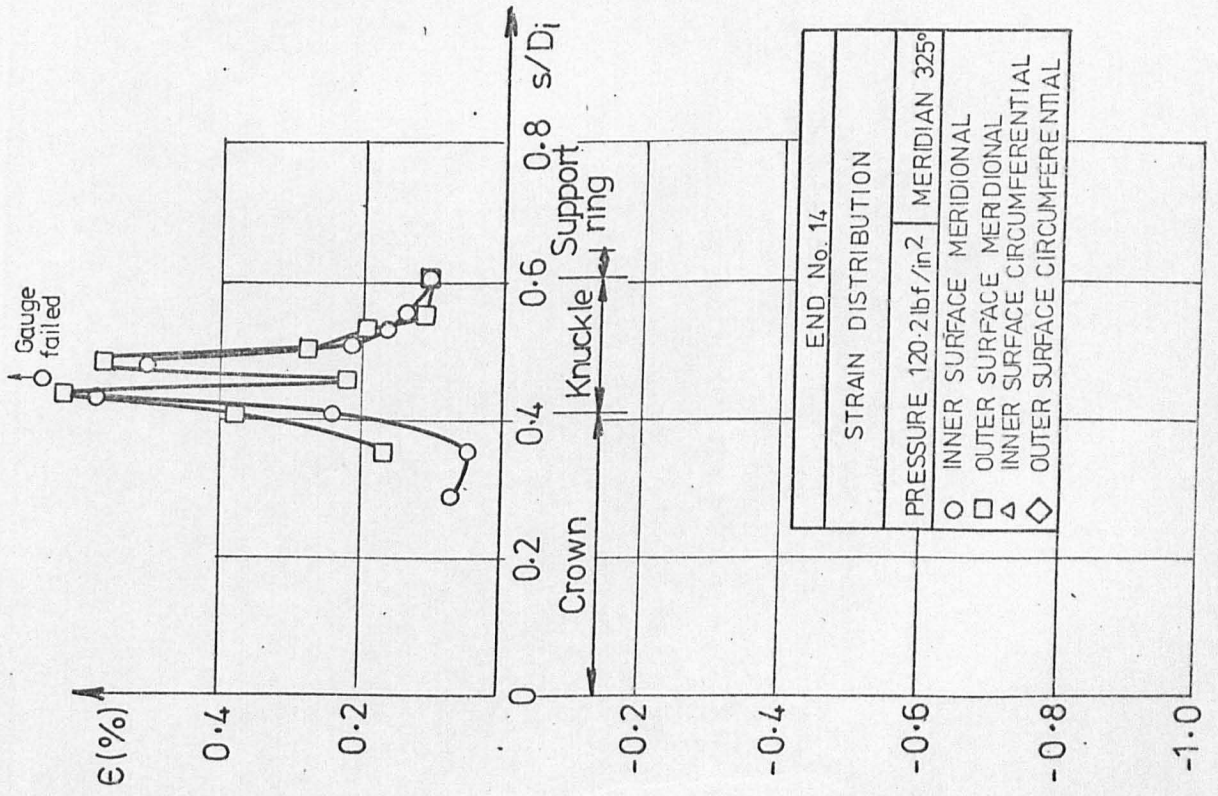


FIG. A1 .14.5

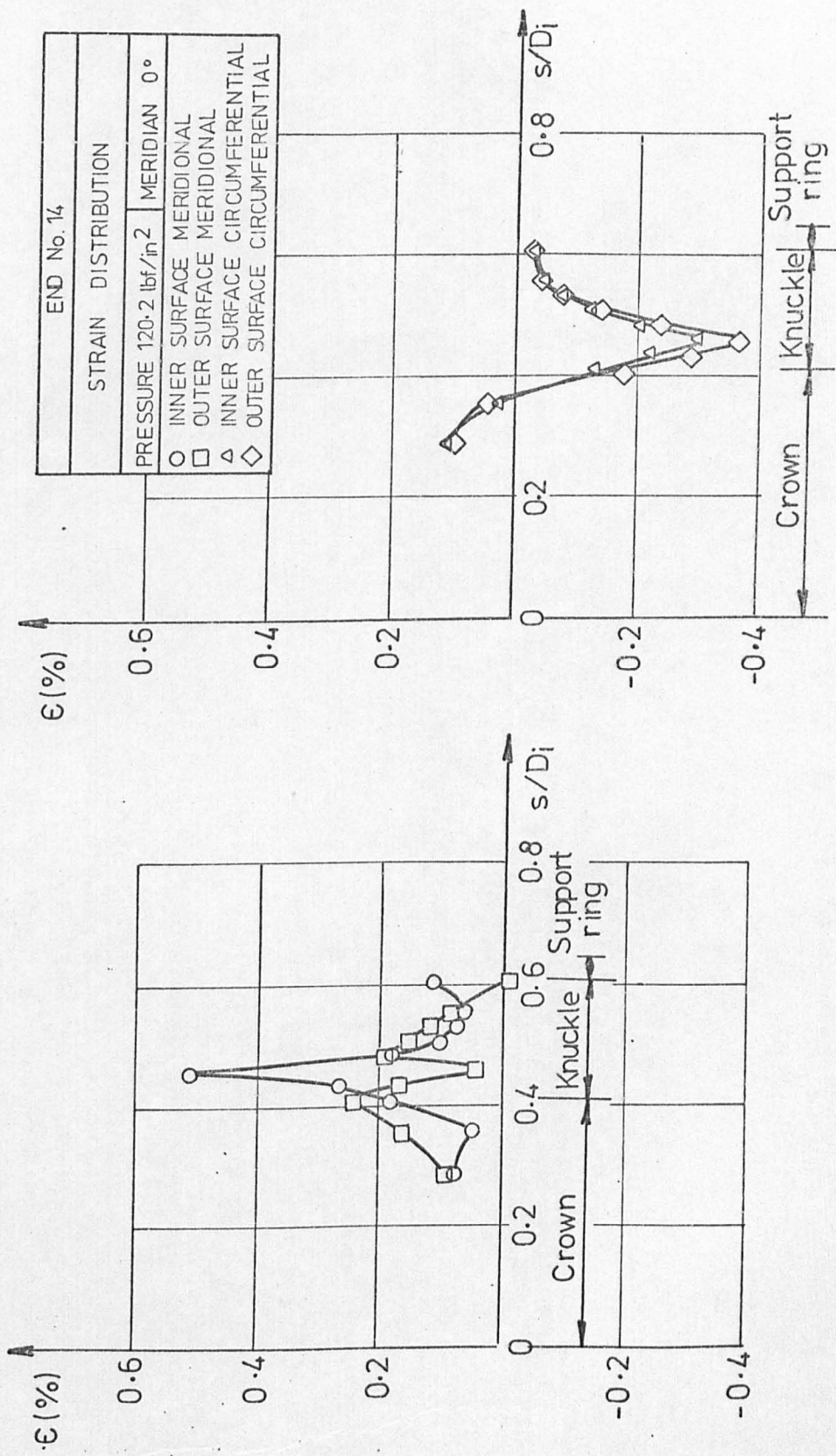


FIG. A1. 14. 6

END No. 14	
DISTRIBUTION OF ELASTIC STRESS INDICES	
PRESSURE 30.2 lbf/in <sup>2</sup>	MERIDIAN 325°
○	INNER SURFACE MERIDIONAL
□	OUTER SURFACE MERIDIONAL
△	INNER SURFACE CIRCUMFERENTIAL
◇	OUTER SURFACE CIRCUMFERENTIAL

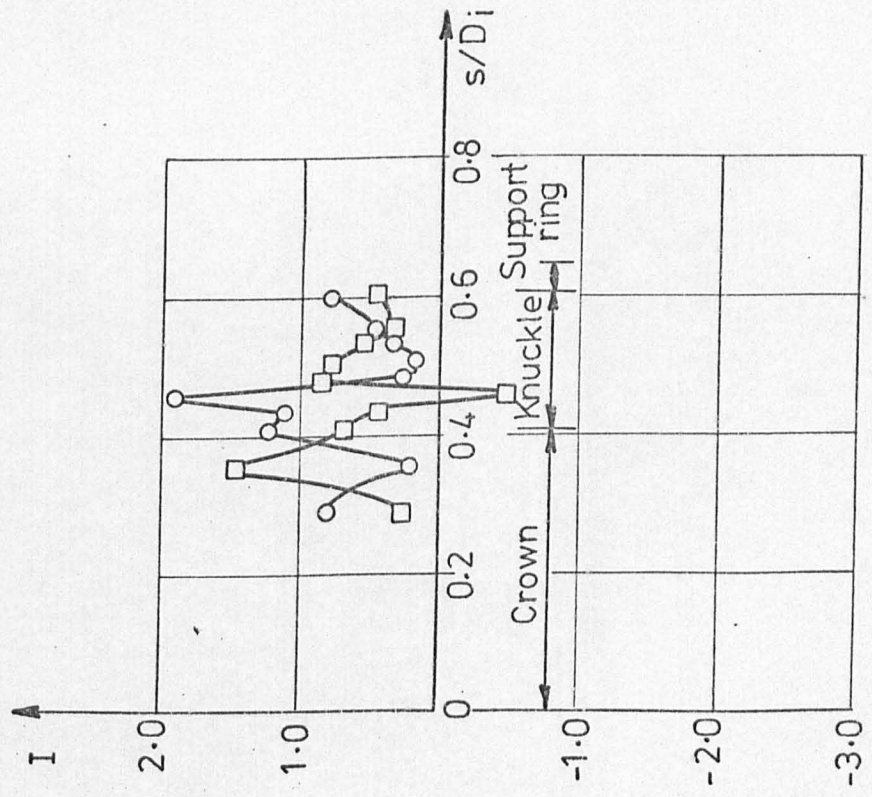
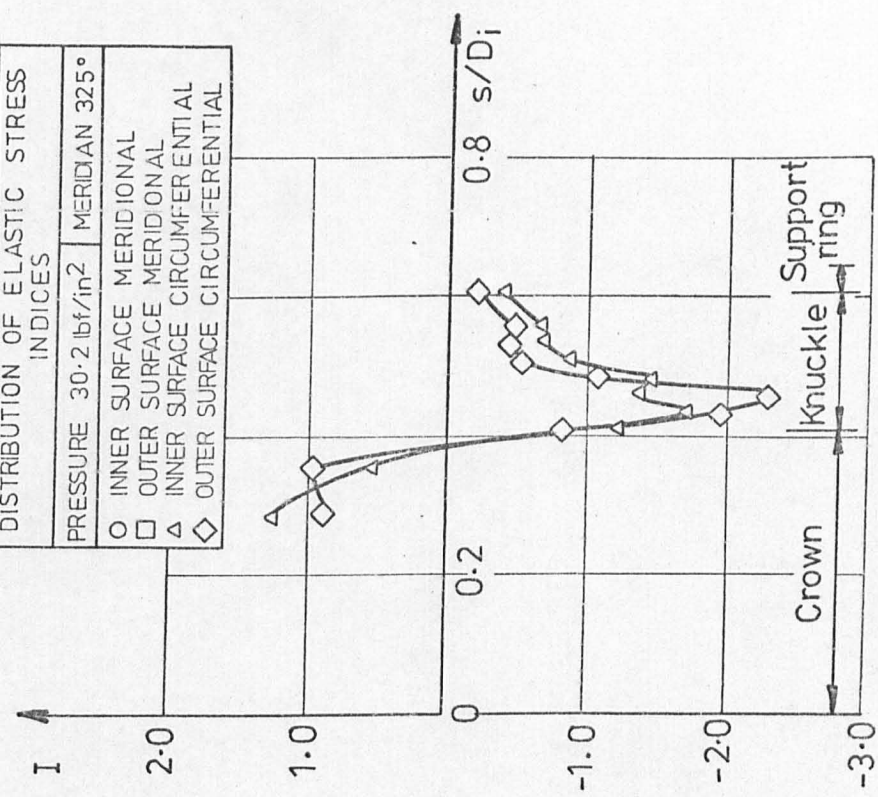


FIG. A1.14.7

END No. 14	
DISTRIBUTION OF ELASTIC STRESS INDICES	
PRESSURE 30.2 lbf/in <sup>2</sup>	MERIDIAN 0°
○	INNER SURFACE MERIDIONAL
□	OUTER SURFACE MERIDIONAL
△	INNER SURFACE CIRCUMFERENTIAL
◇	OUTER SURFACE CIRCUMFERENTIAL

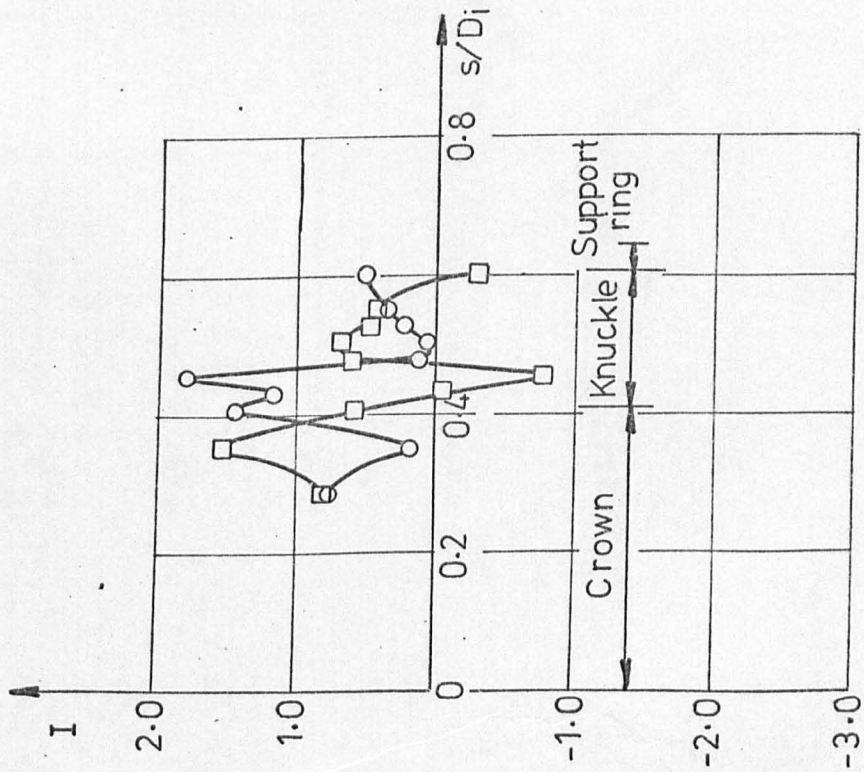
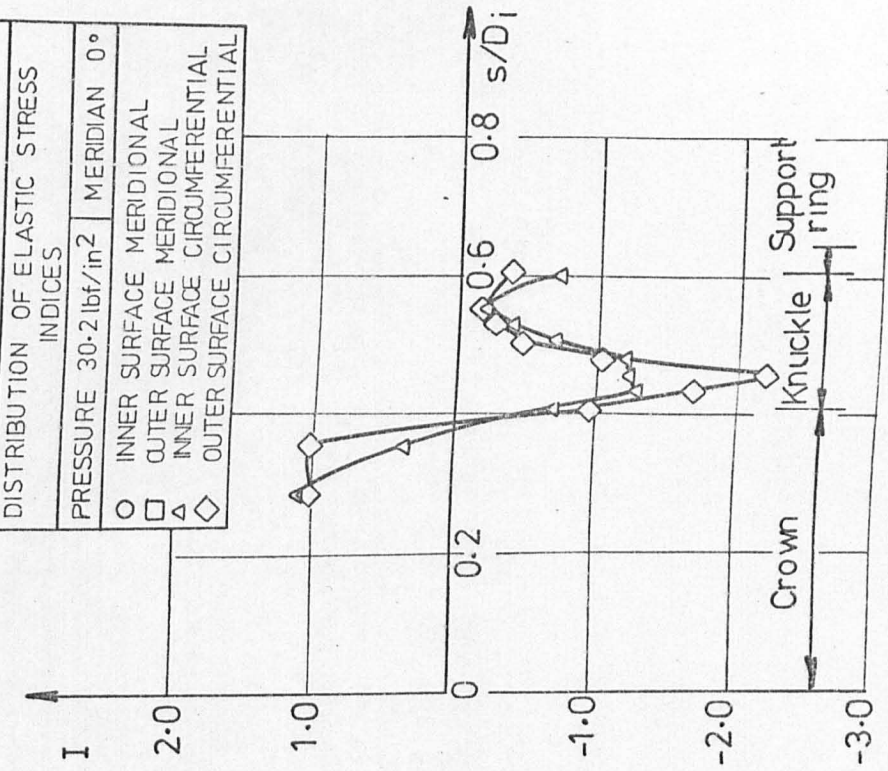


FIG. A1-14.8

END No. 15
THICKNESS VARIATION ALONG 90° MERIDIAN

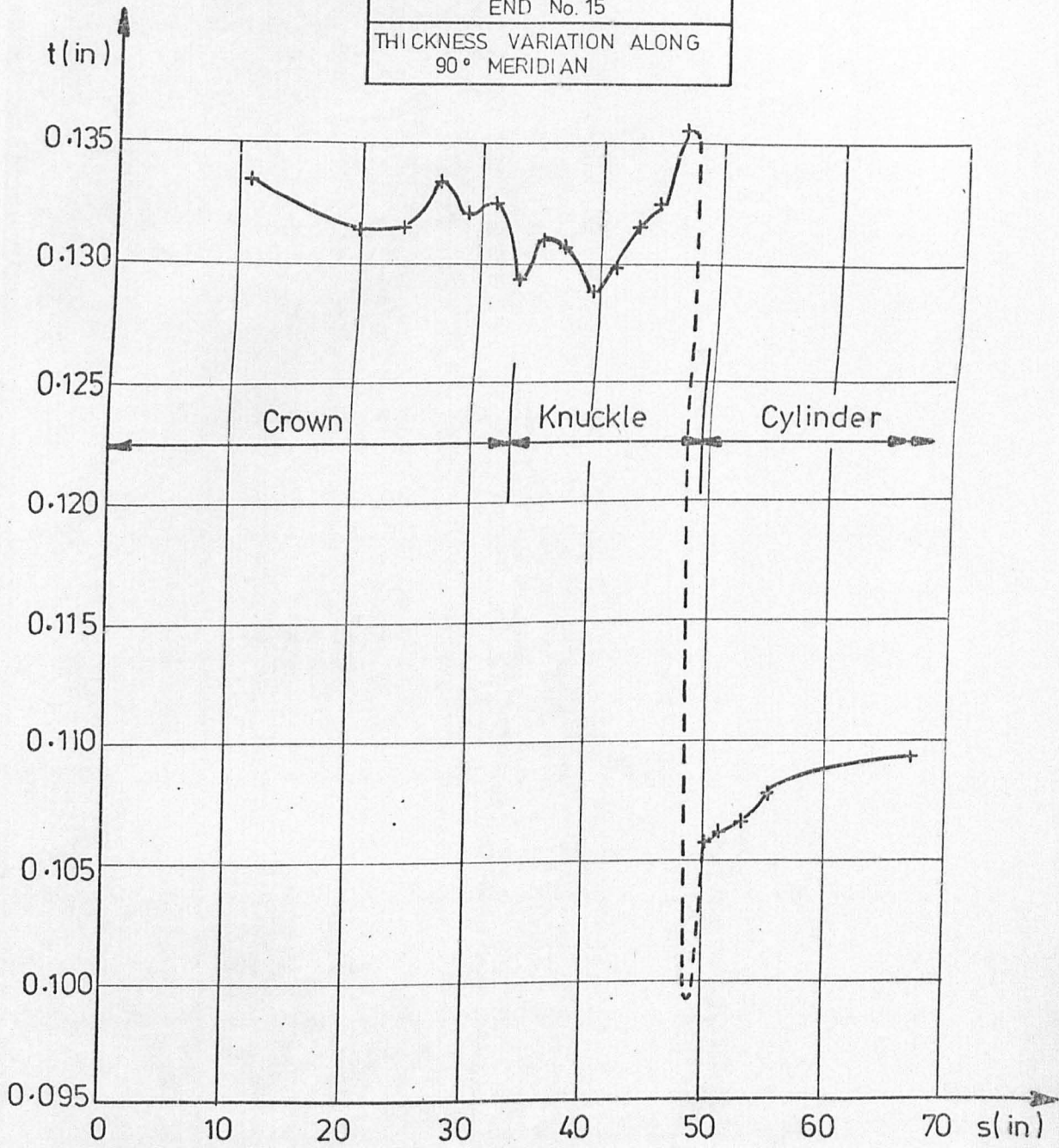


FIG. A1-15.1

END No. 15  
 CURVATURE VARIATION ALONG  
 90° MERIDIAN

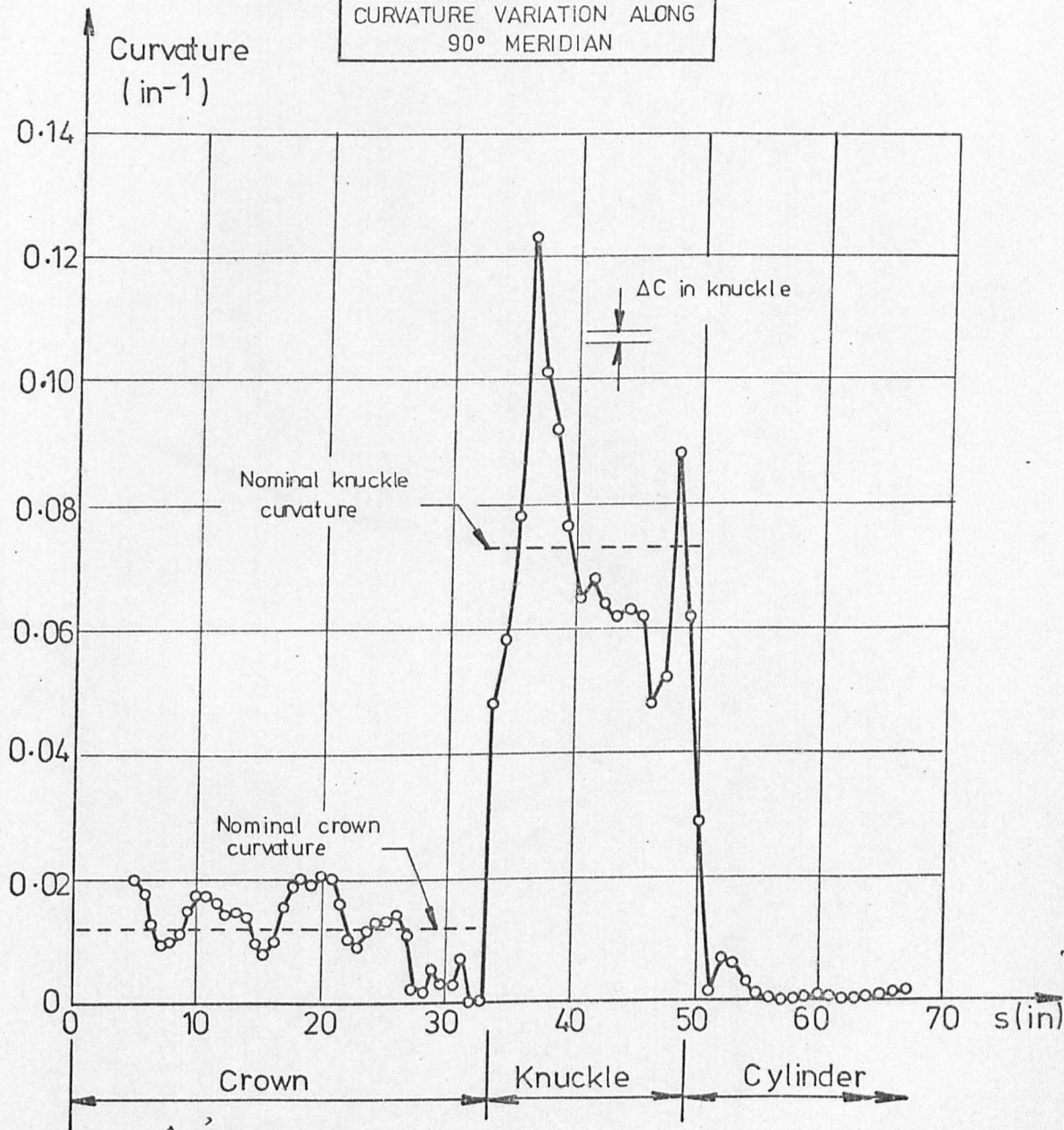


FIG. A1.15-2

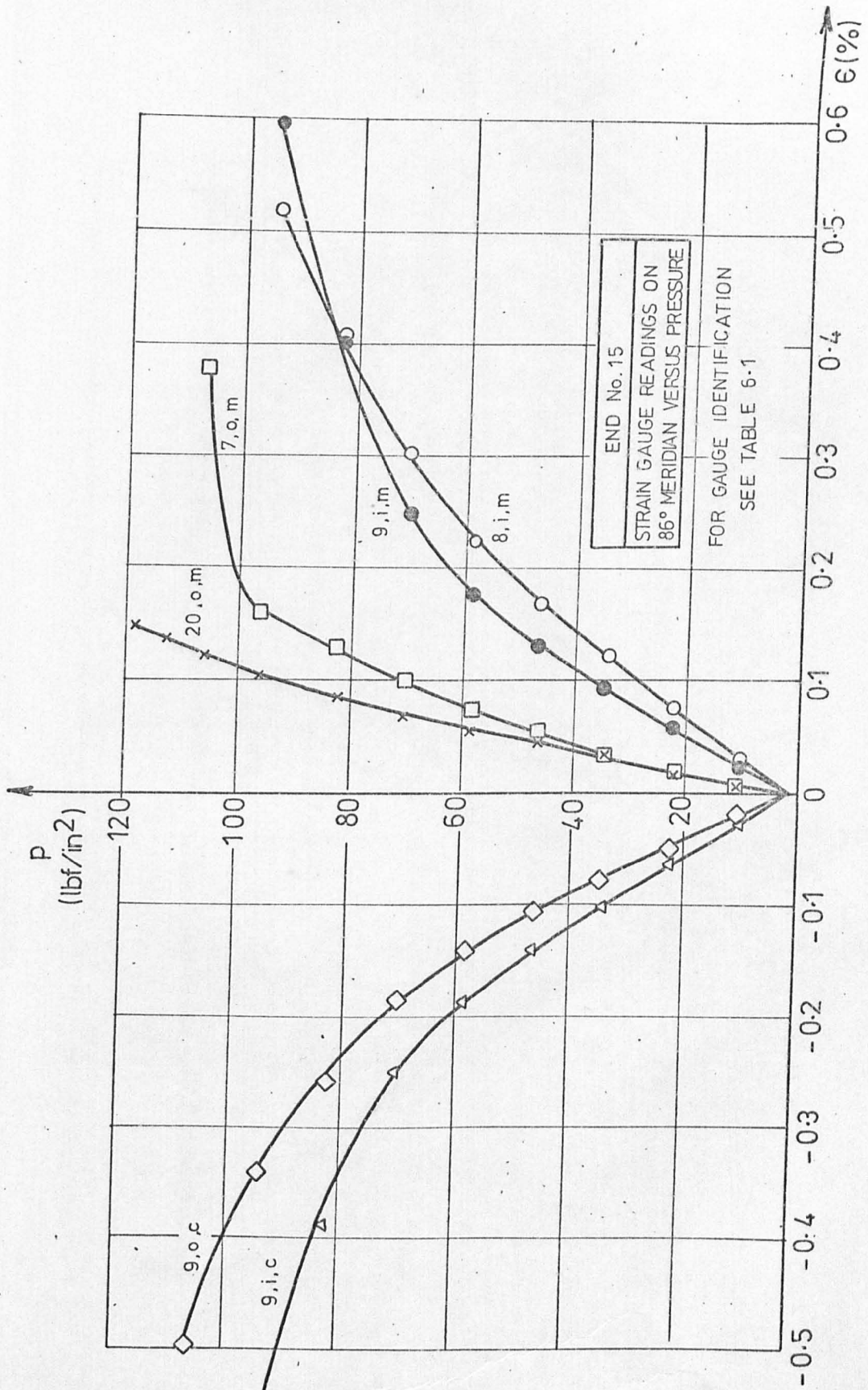


FIG. A1.15.3



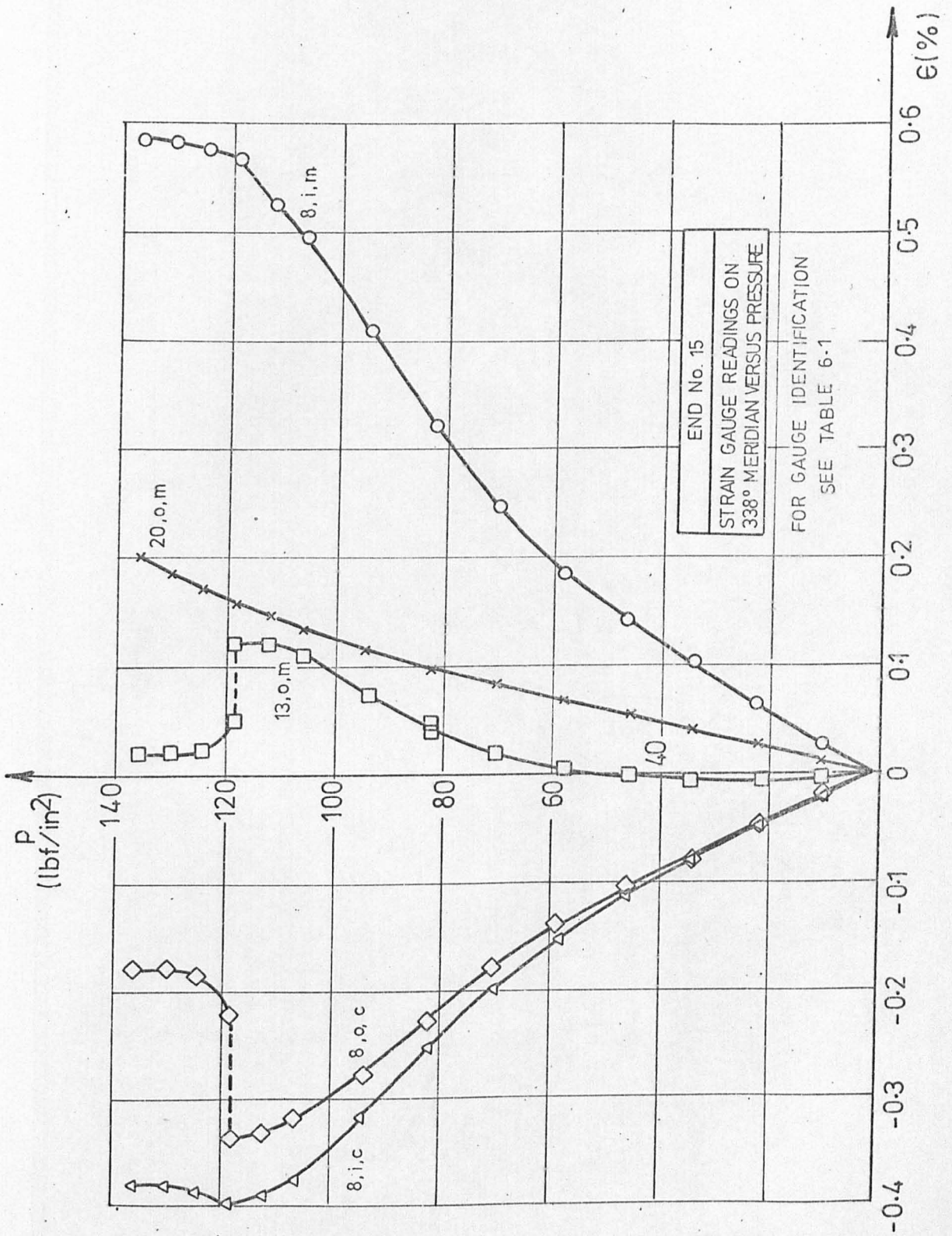


FIG.A1-15.4

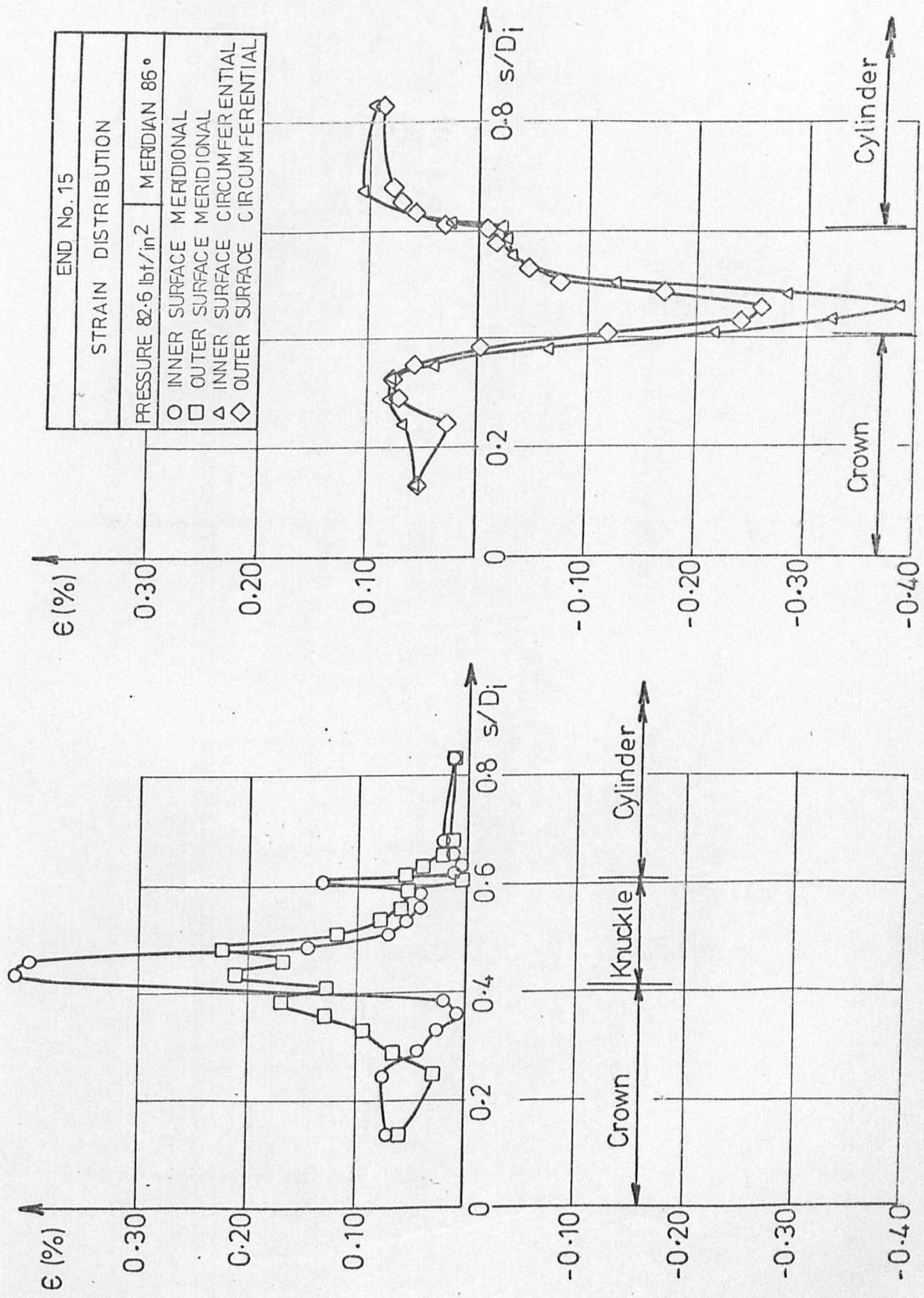


FIG. A1.15.5

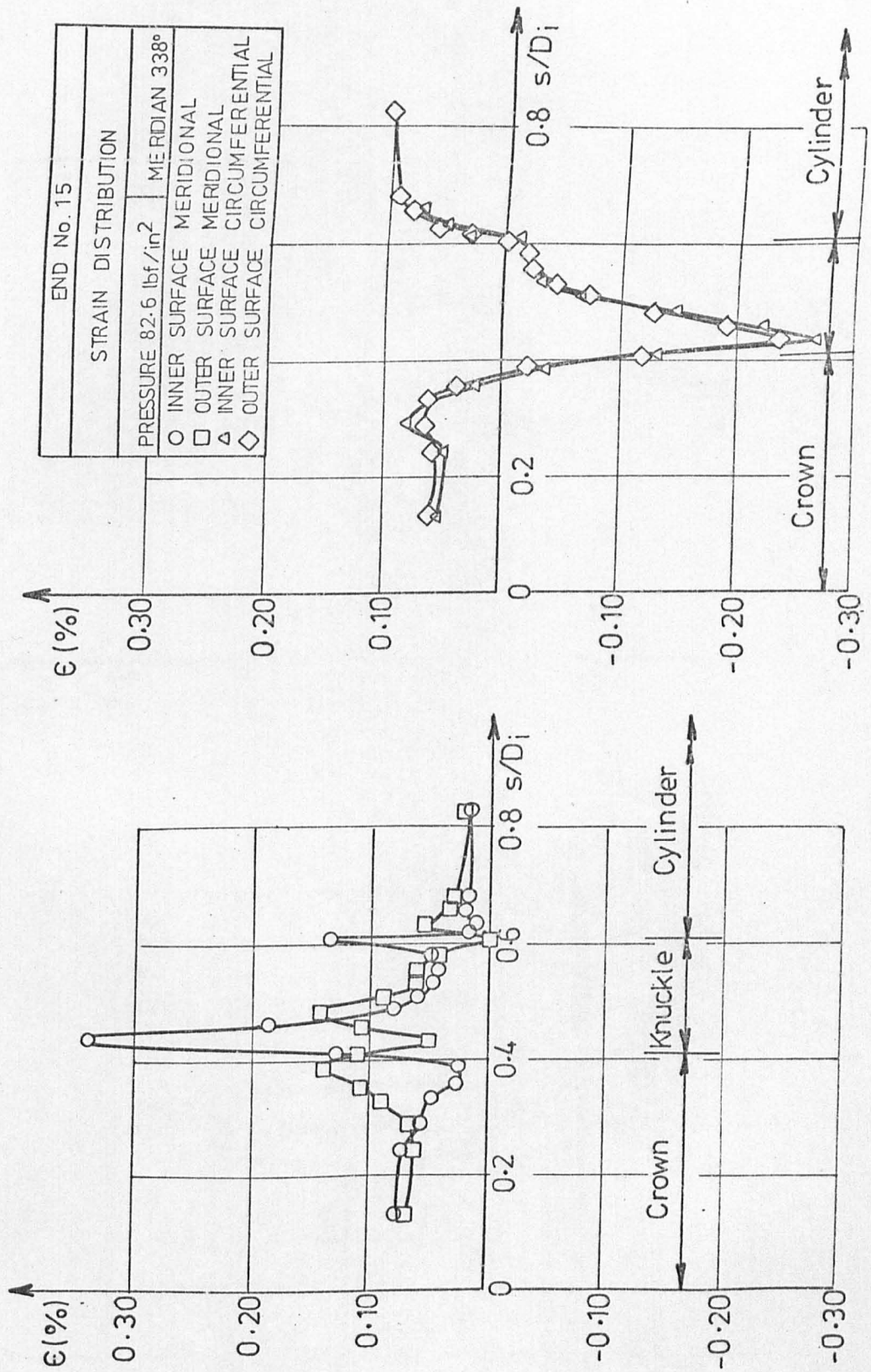


FIG. A1.15.6

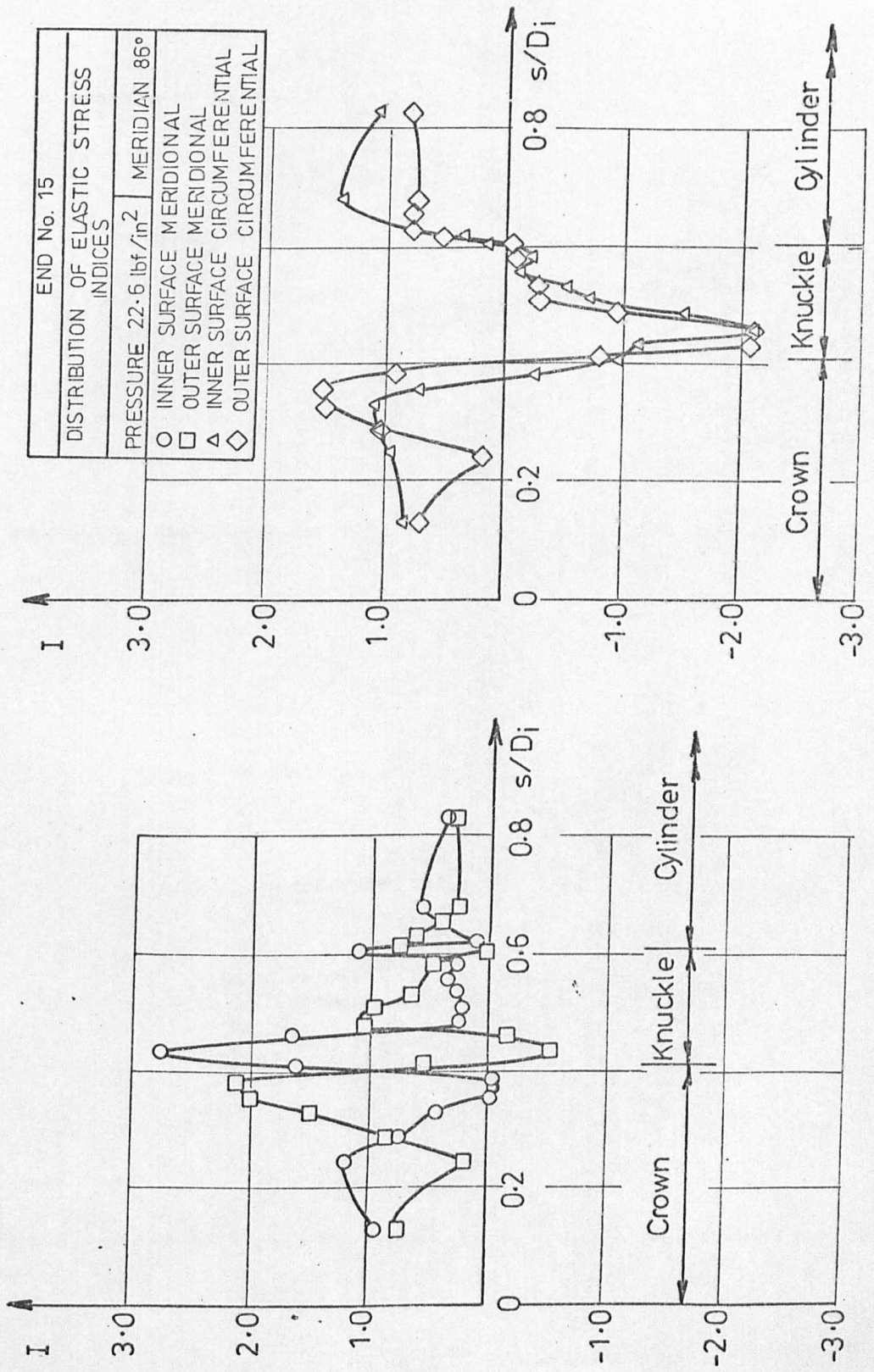


FIG. A1.15.7

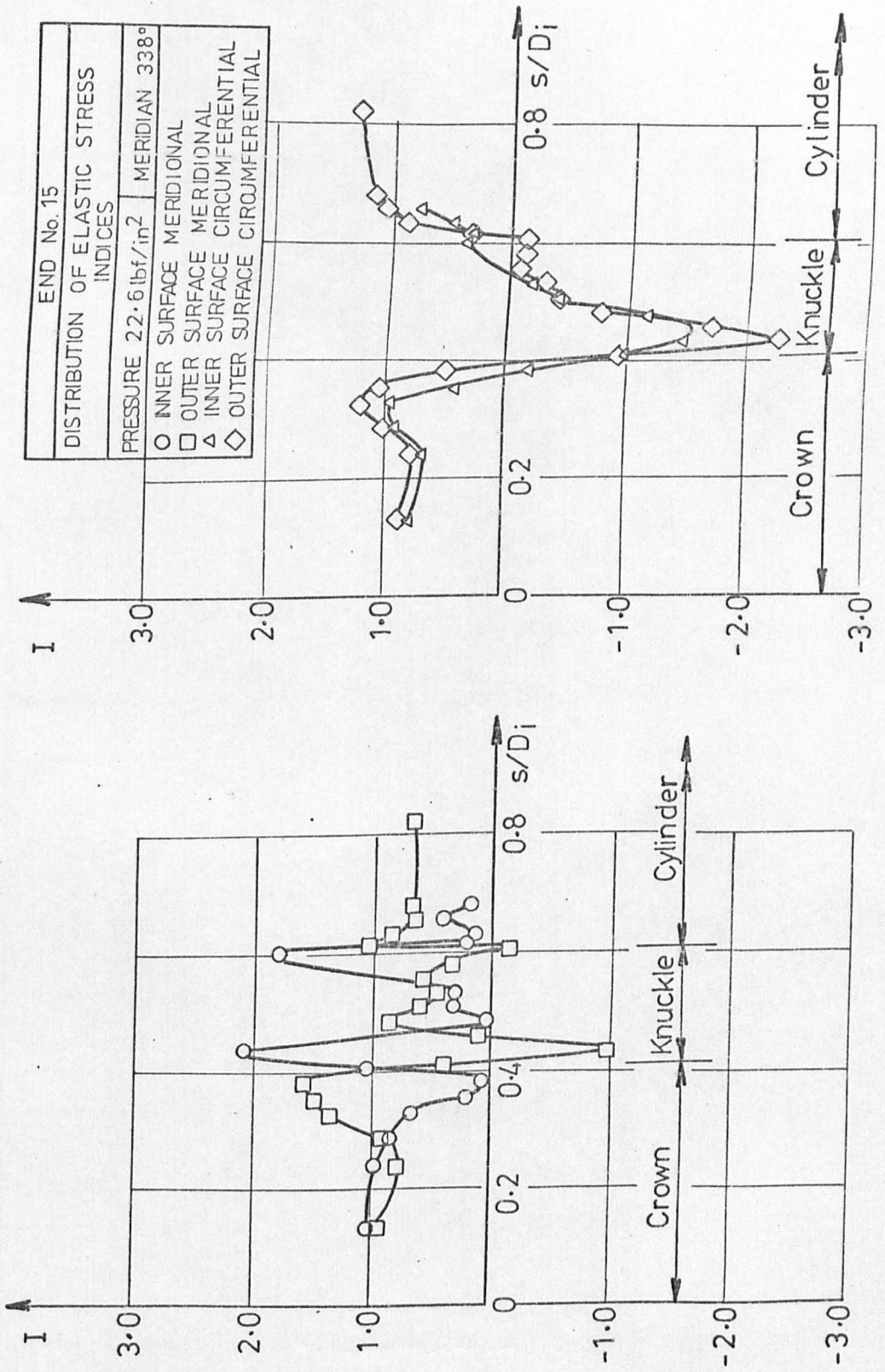


FIG. A1-15-8

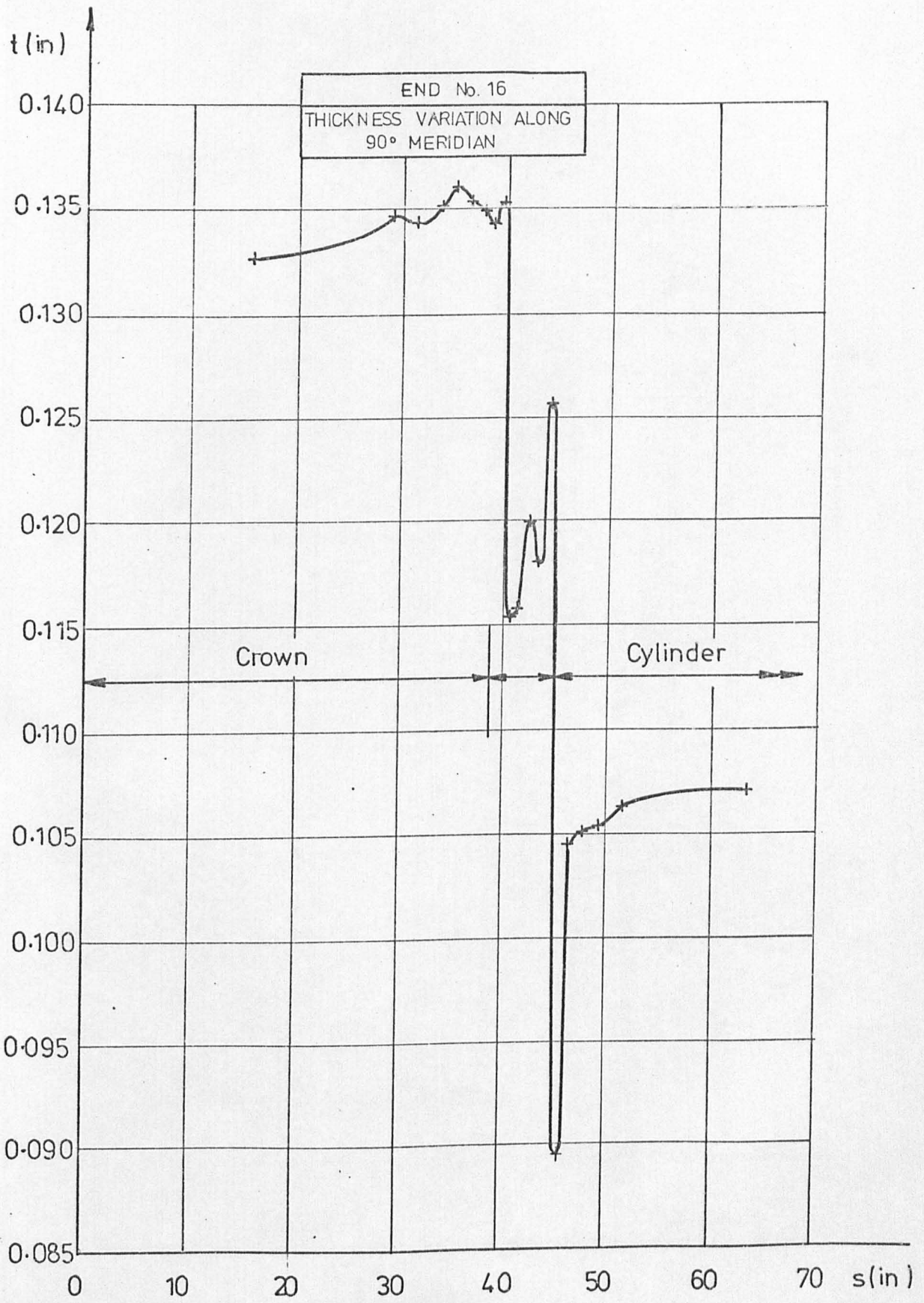


FIG. A1.16.1

END No. 16  
 CURVATURE VARIATION ALONG  
 90° MERIDIAN

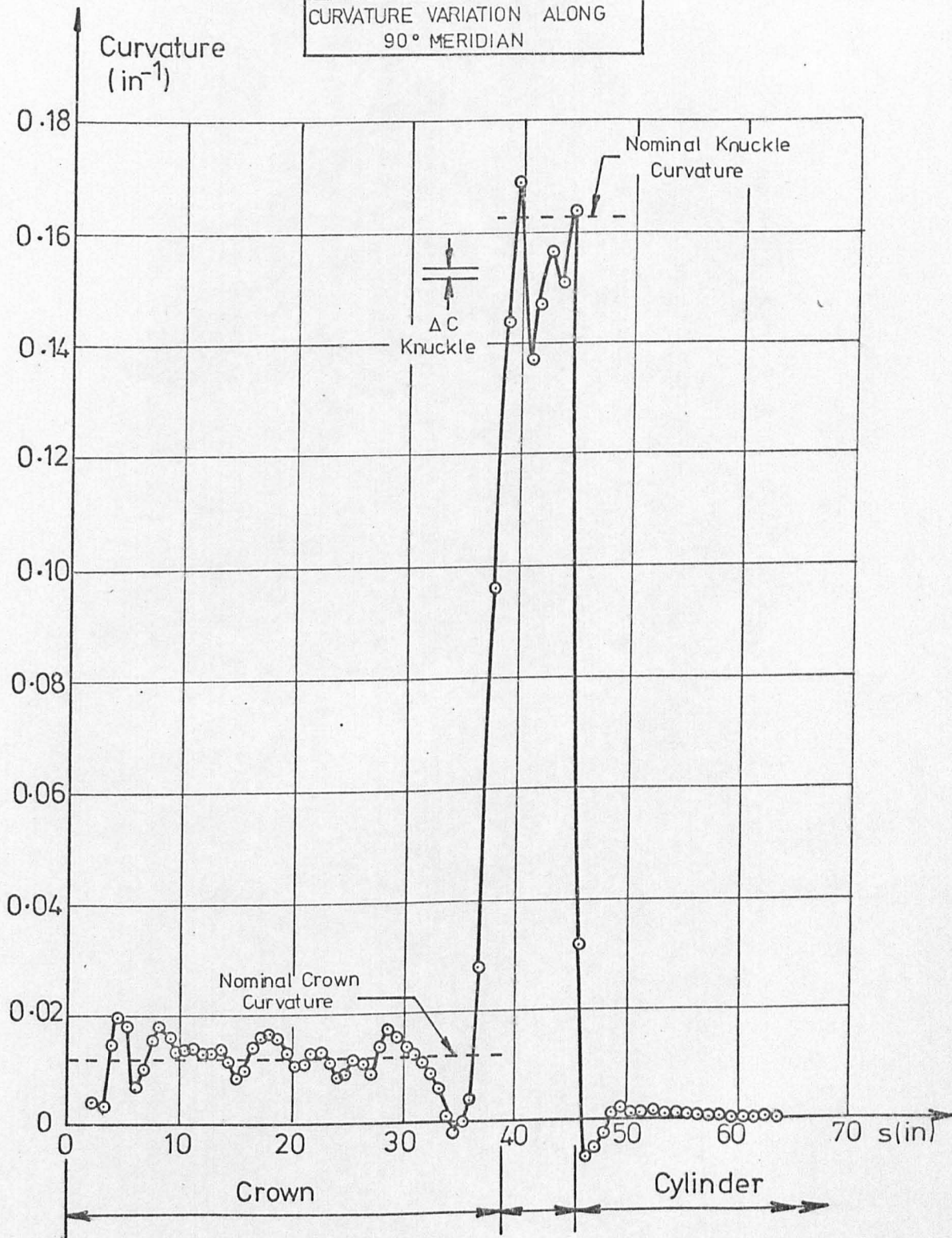


FIG. A1.16.2

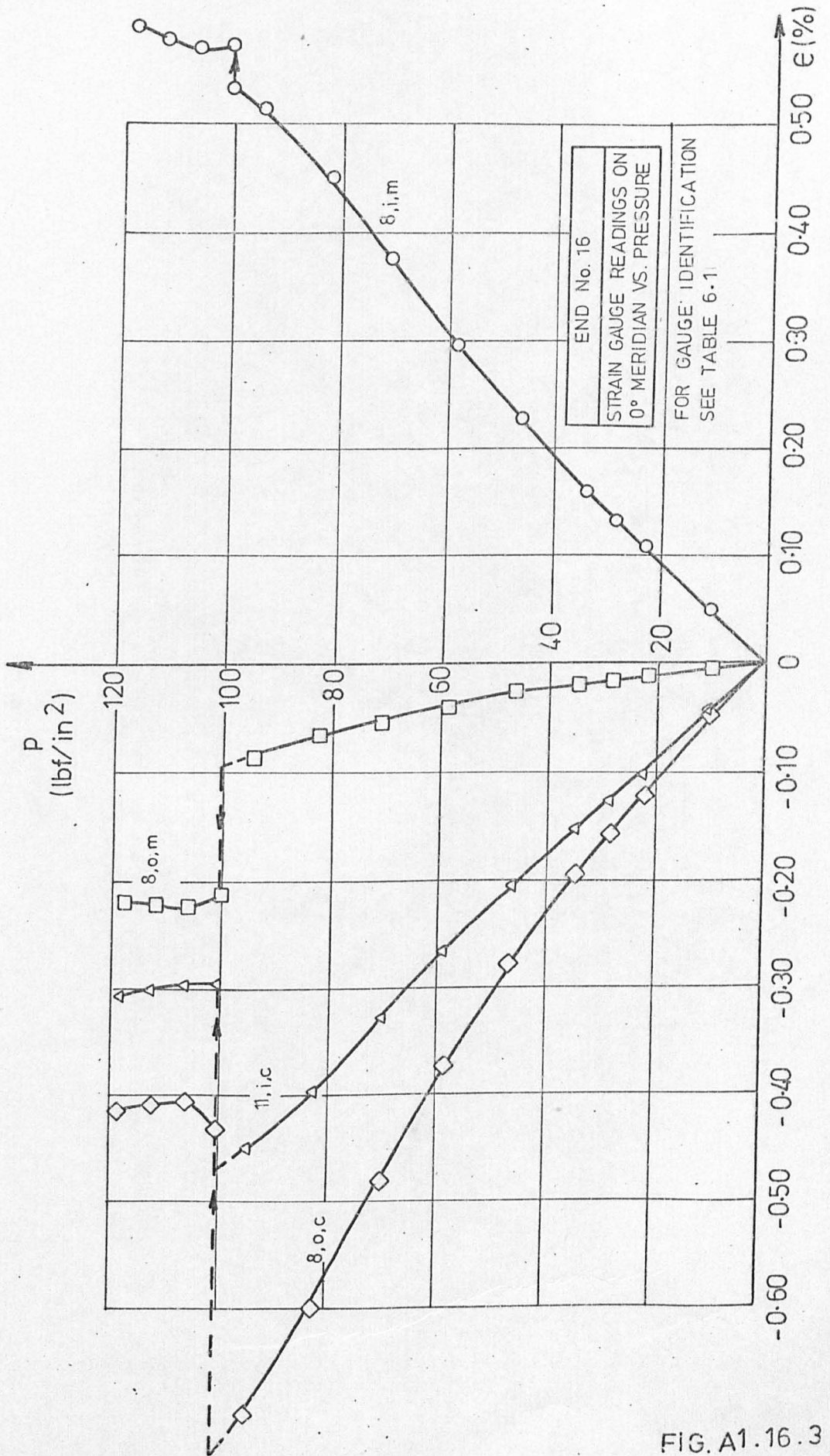


FIG. A1.16.3



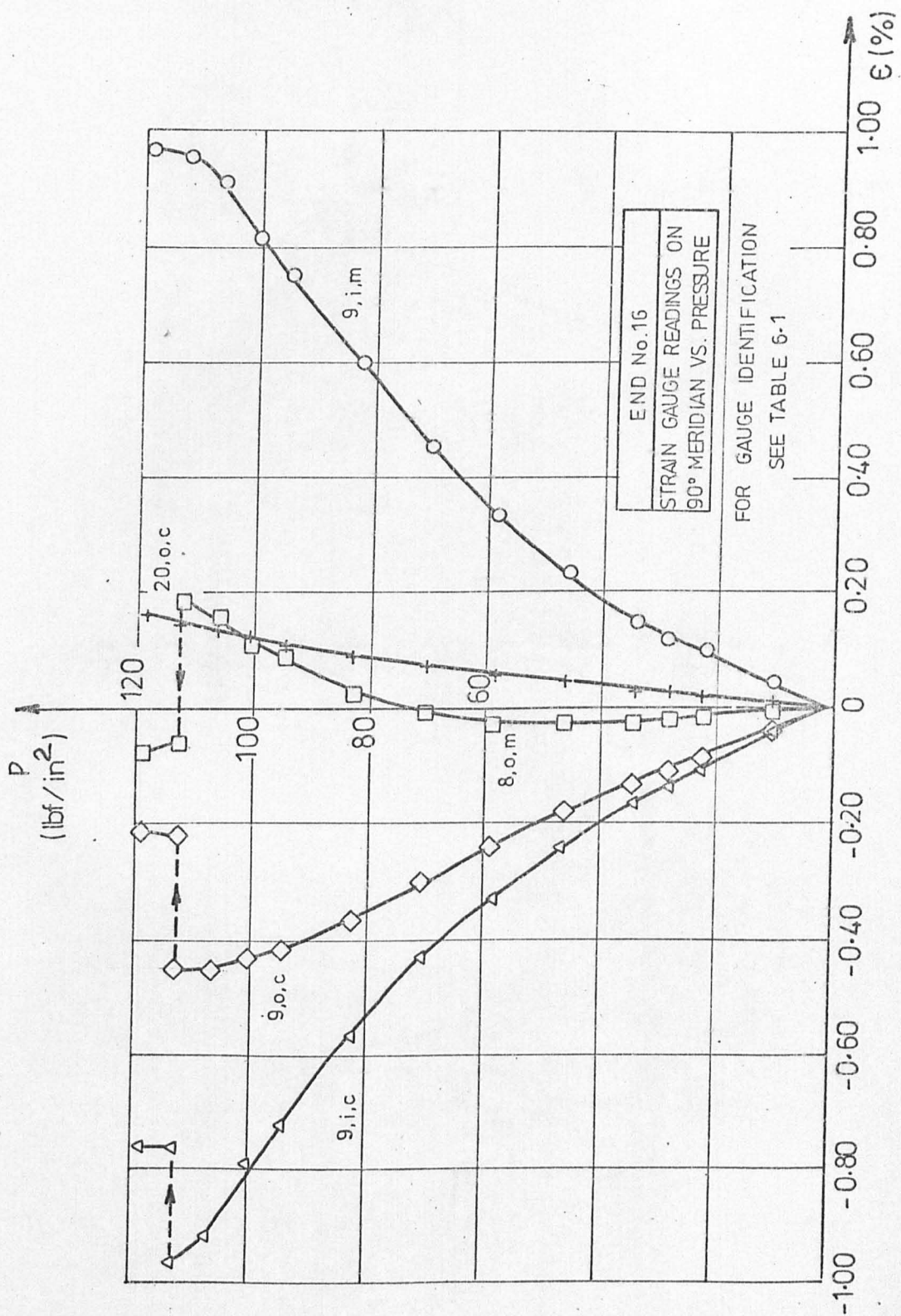


FIG. A1.16.4

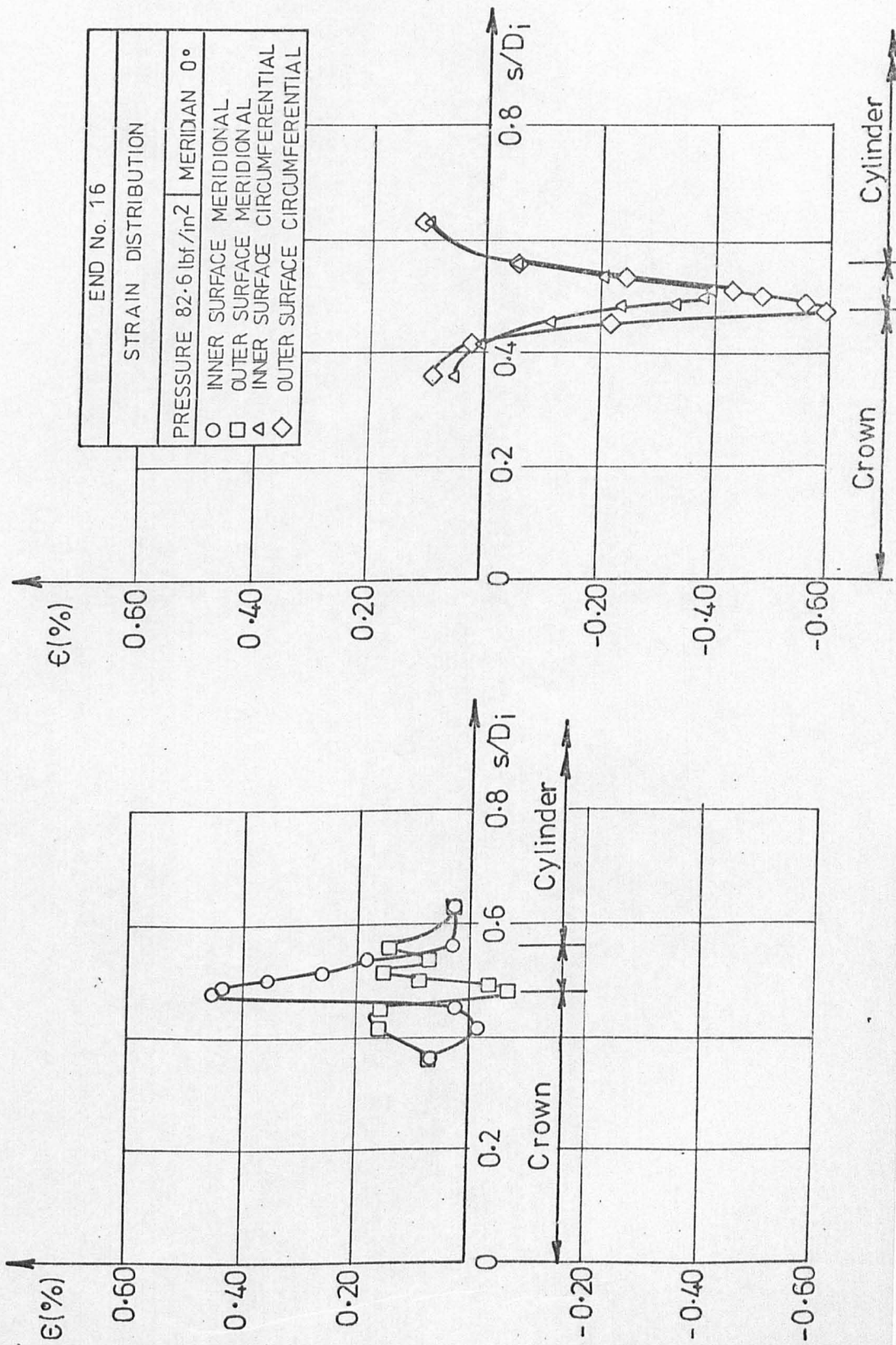


FIG. A1.16.5

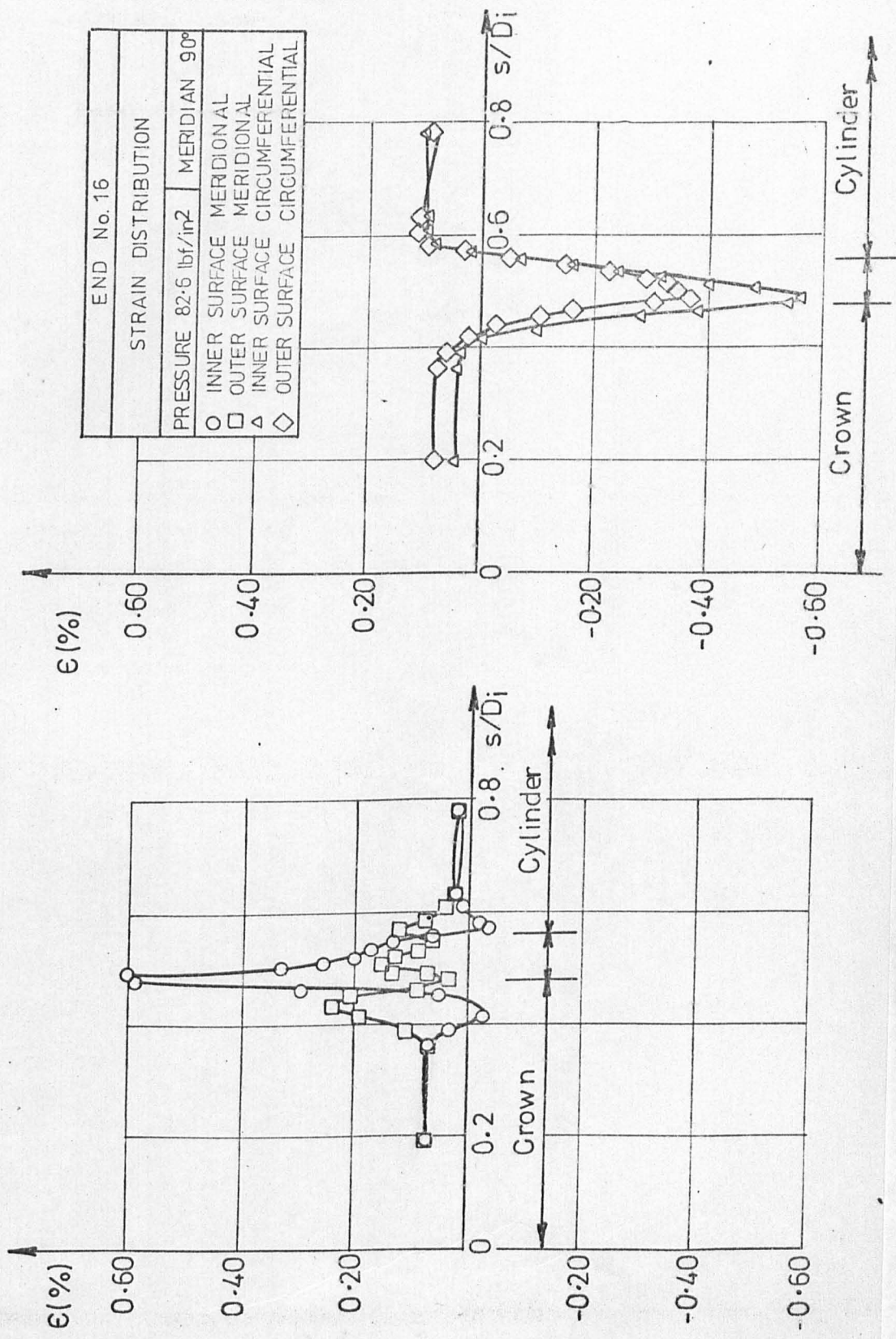


FIG. A1.16.6

END No. 16	
DISTRIBUTION OF ELASTIC STRESS INDICES	
PRESSURE 28.6 lbf/in <sup>2</sup>	MERIDIAN 0°
○	INNER SURFACE MERIDIONAL
□	OUTER SURFACE MERIDIONAL
△	INNER SURFACE CIRCUMFERENTIAL
◇	OUTER SURFACE CIRCUMFERENTIAL

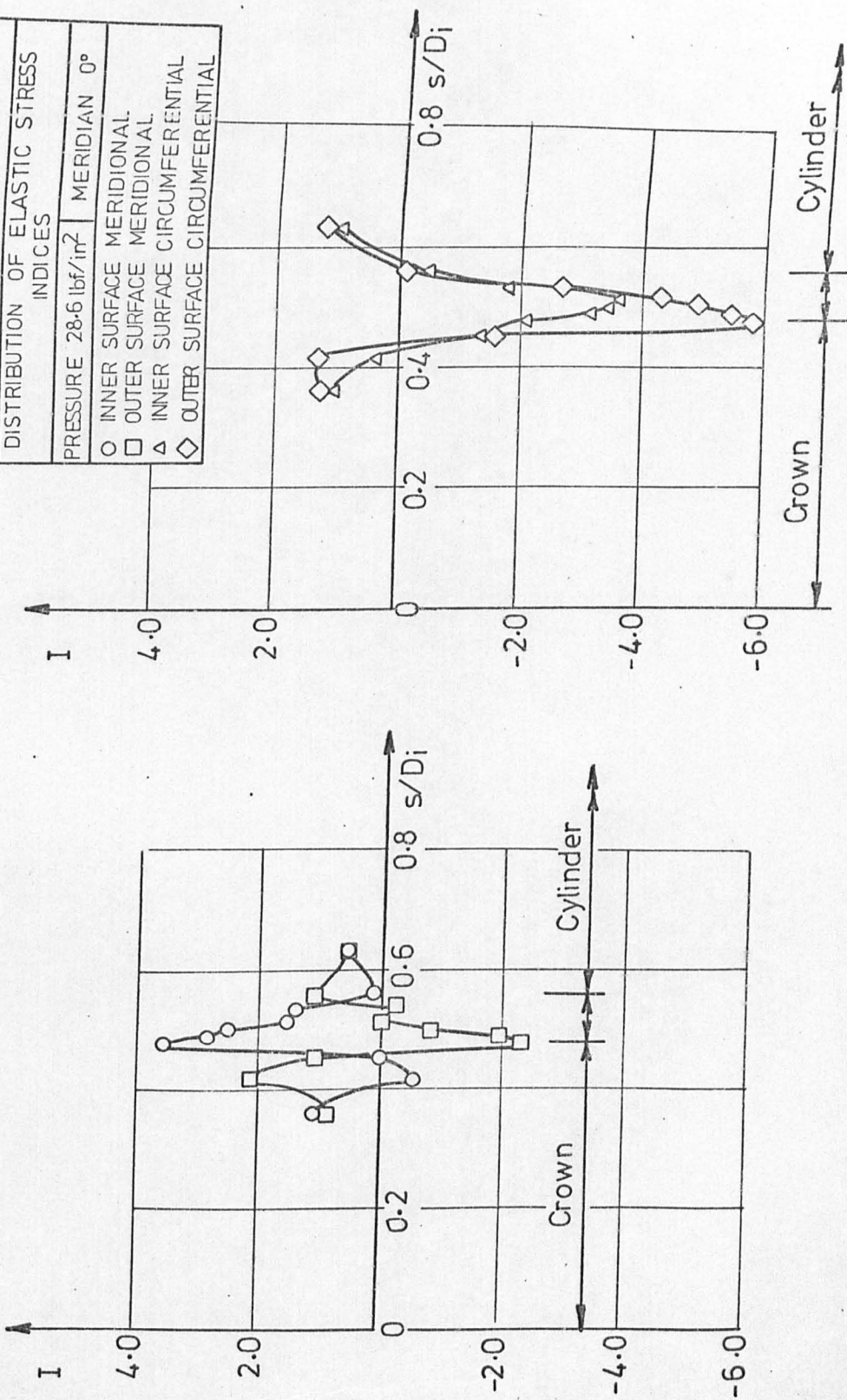


FIG. A1-16.7

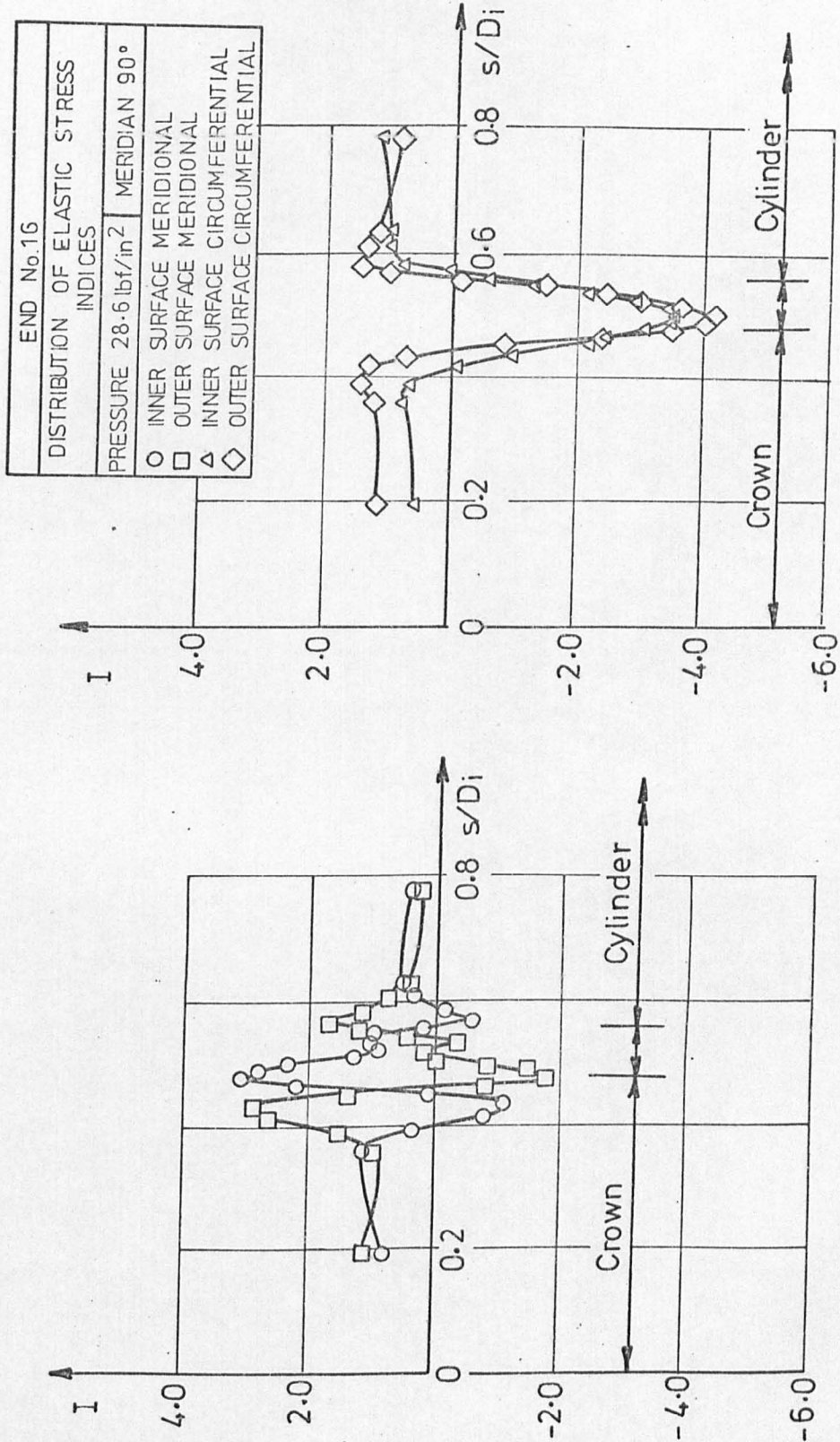


FIG. A1-16-8

END No. 17  
THICKNESS VARIATION ALONG  
90° MERIDIAN

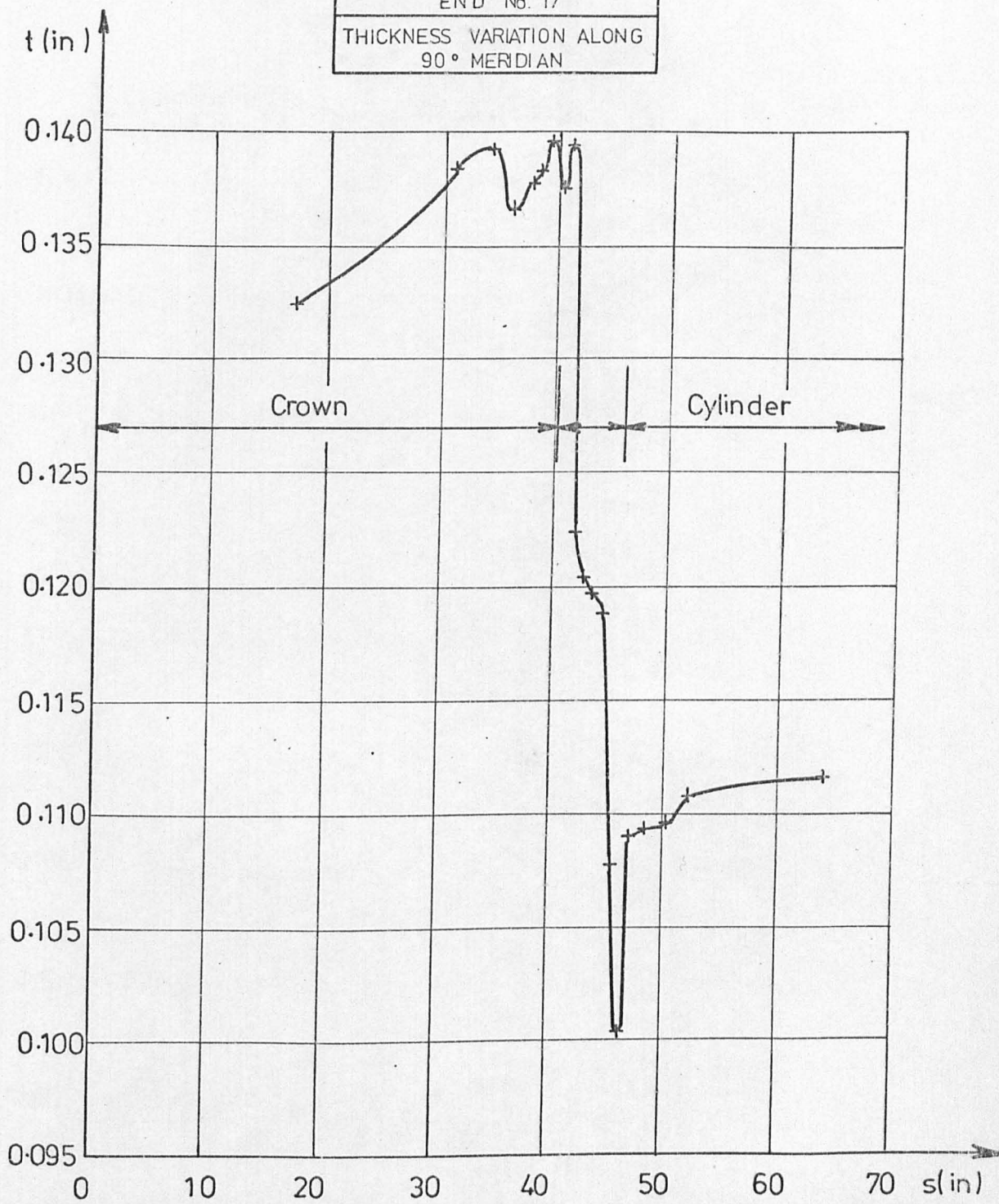


FIG. A1.17.1

END No. 17  
 CURVATURE VARIATION ALONG  
 90° MERIDIAN

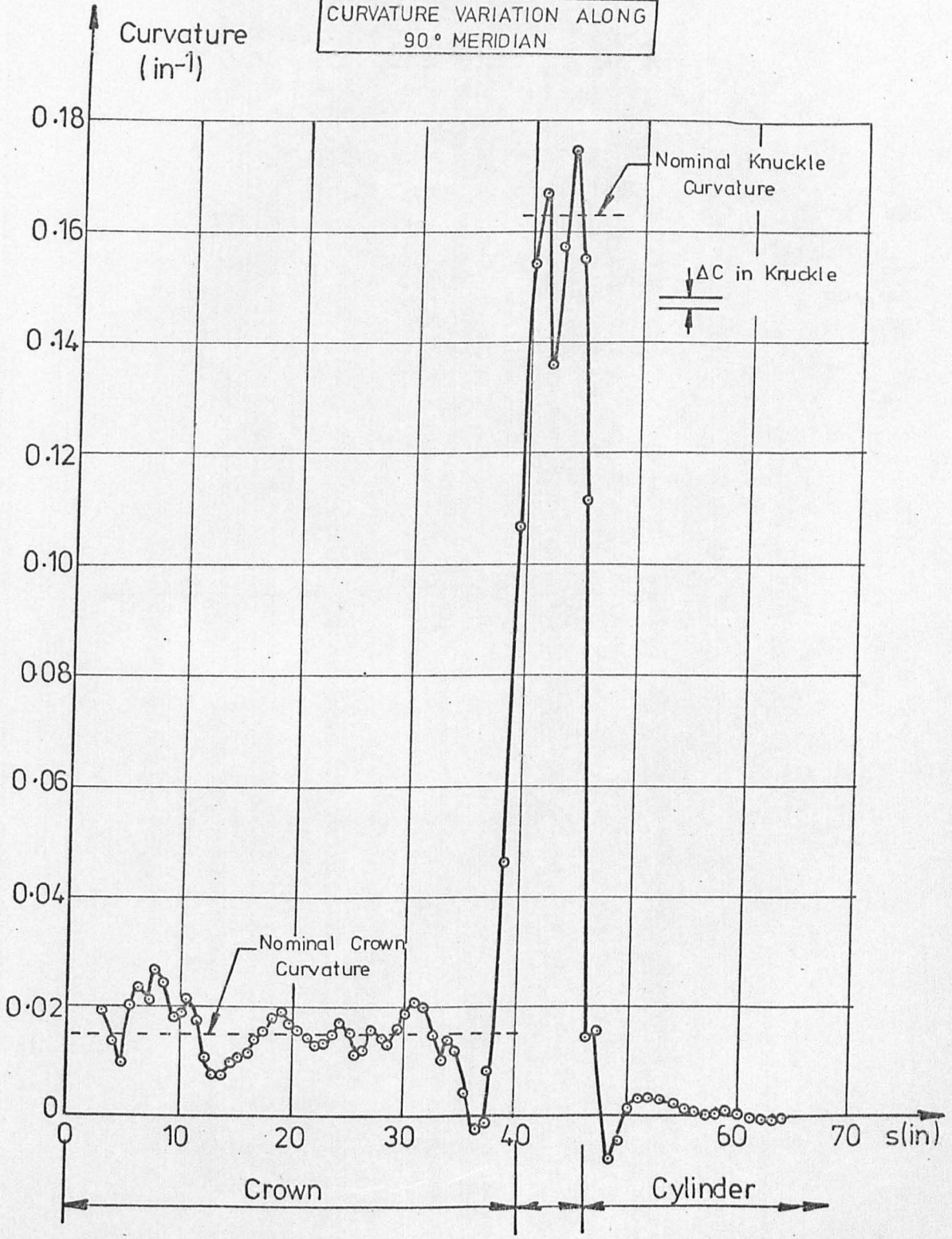


FIG. A1.17.2

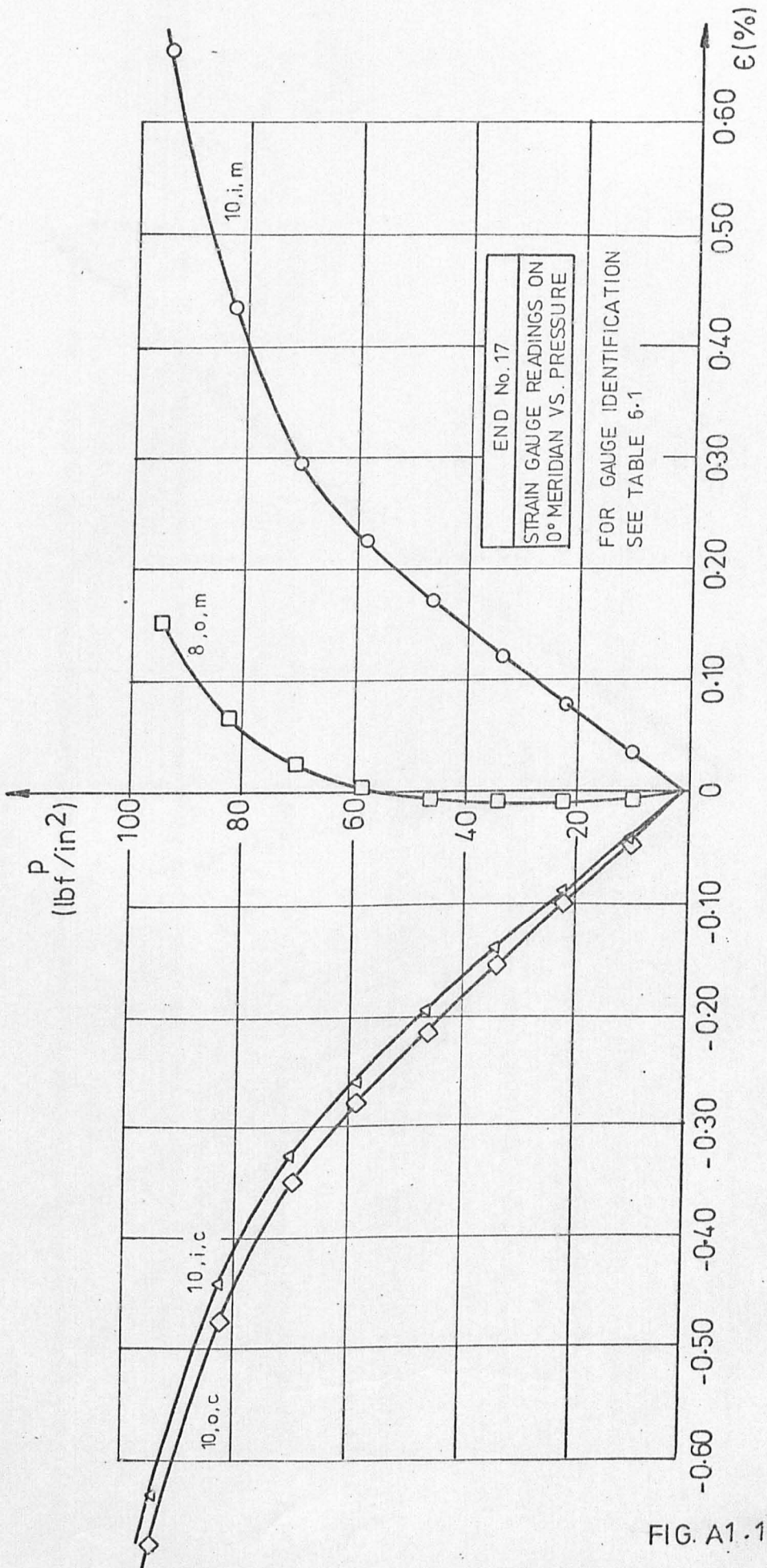


FIG. A1.17-3



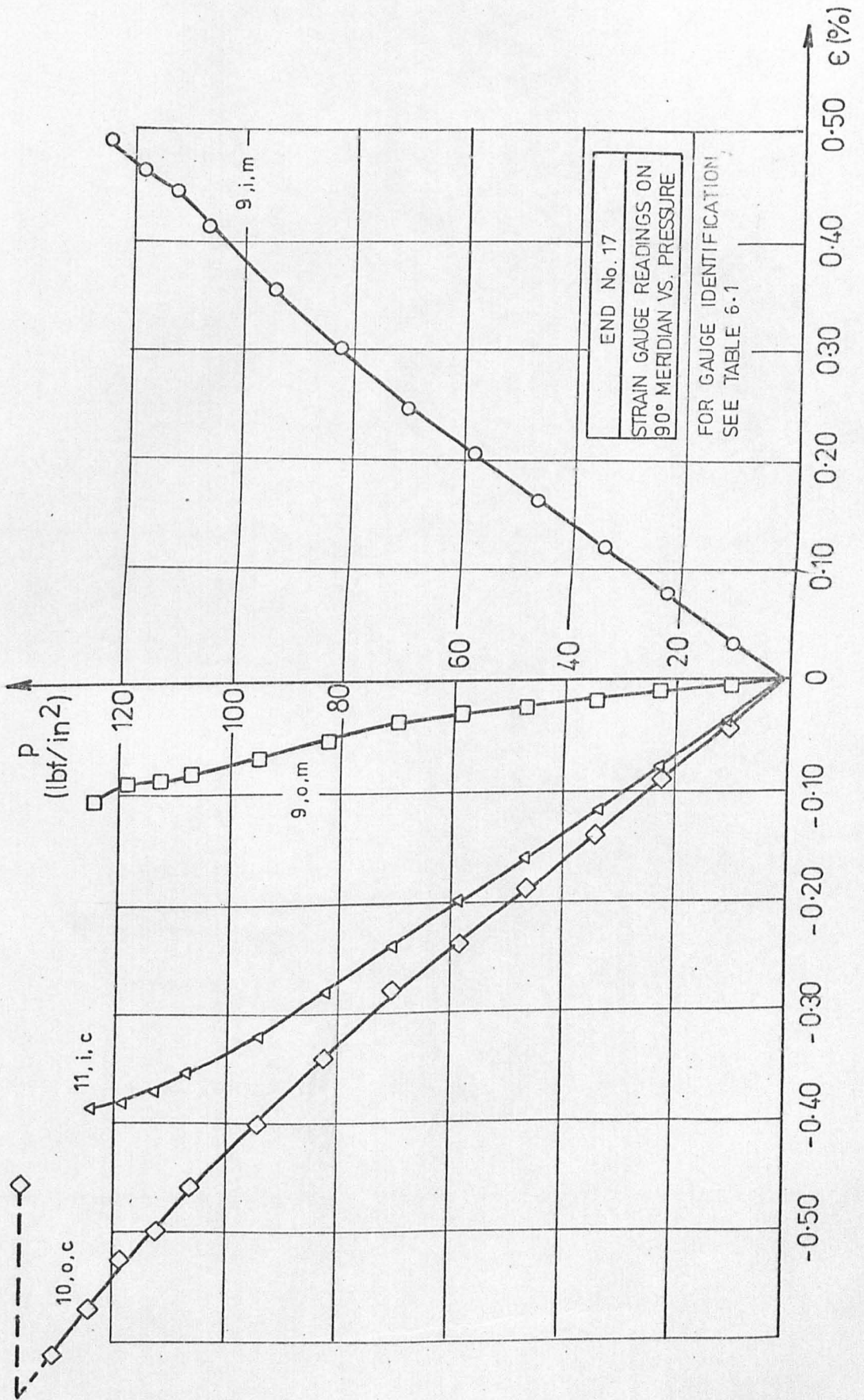


FIG. A1.17-4

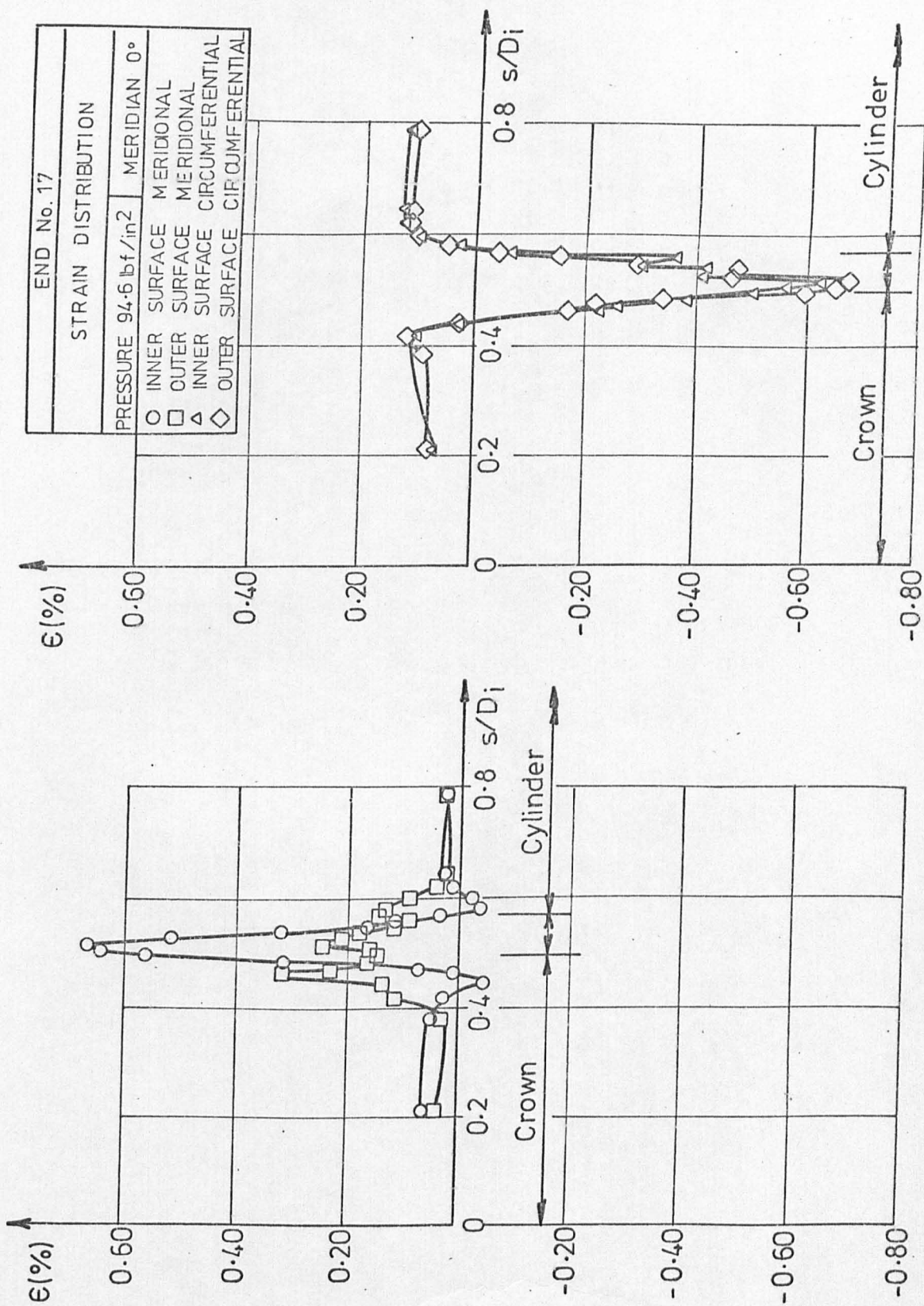


FIG. A1.17-5

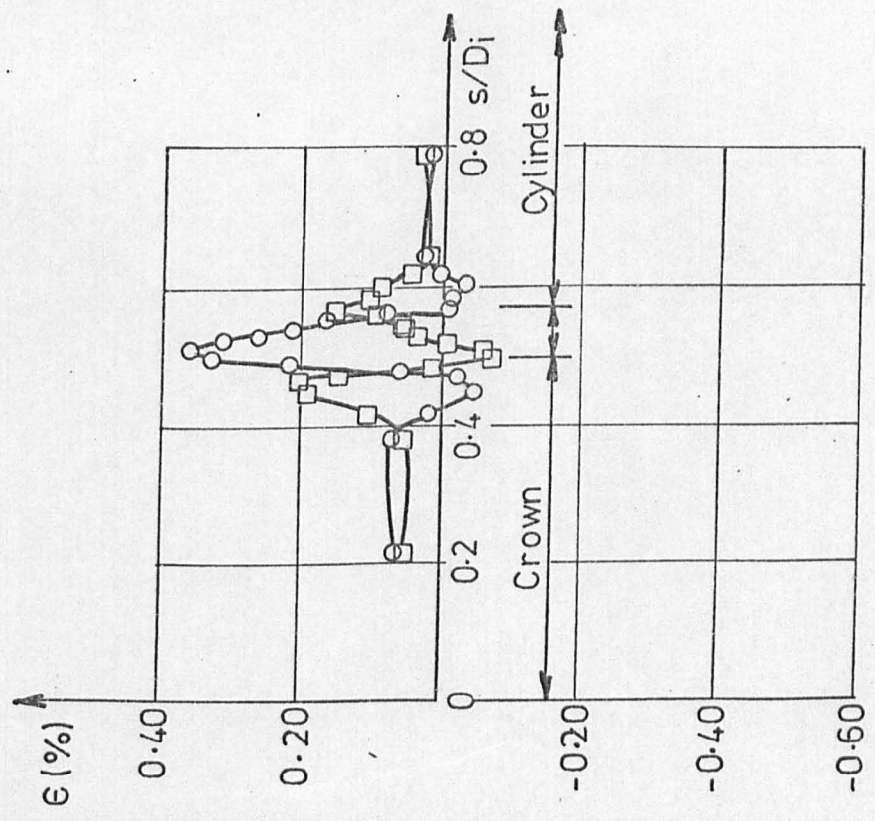
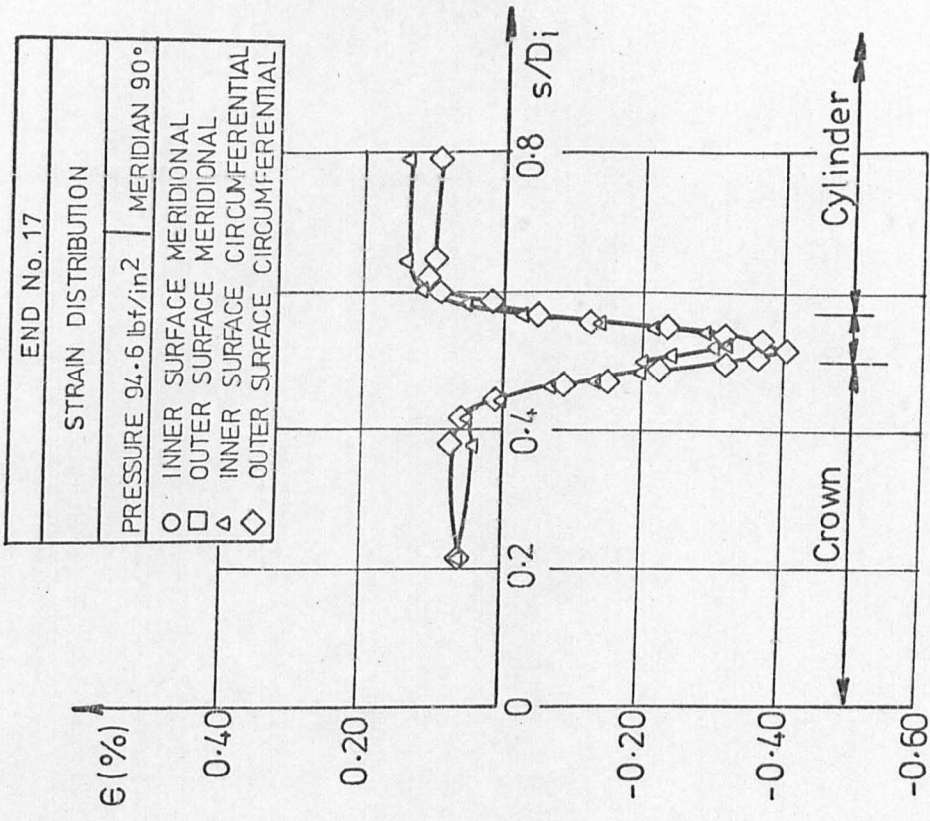


FIG. A1.17.6

END No. 17	
DISTRIBUTION OF ELASTIC STRESS INDICES	
PRESSURE	22.6 lbf/in <sup>2</sup> MERIDIAN 0°
○	INNER SURFACE MERIDIONAL
□	OUTER SURFACE MERIDIONAL
△	INNER SURFACE CIRCUMFERENTIAL
◇	OUTER SURFACE CIRCUMFERENTIAL

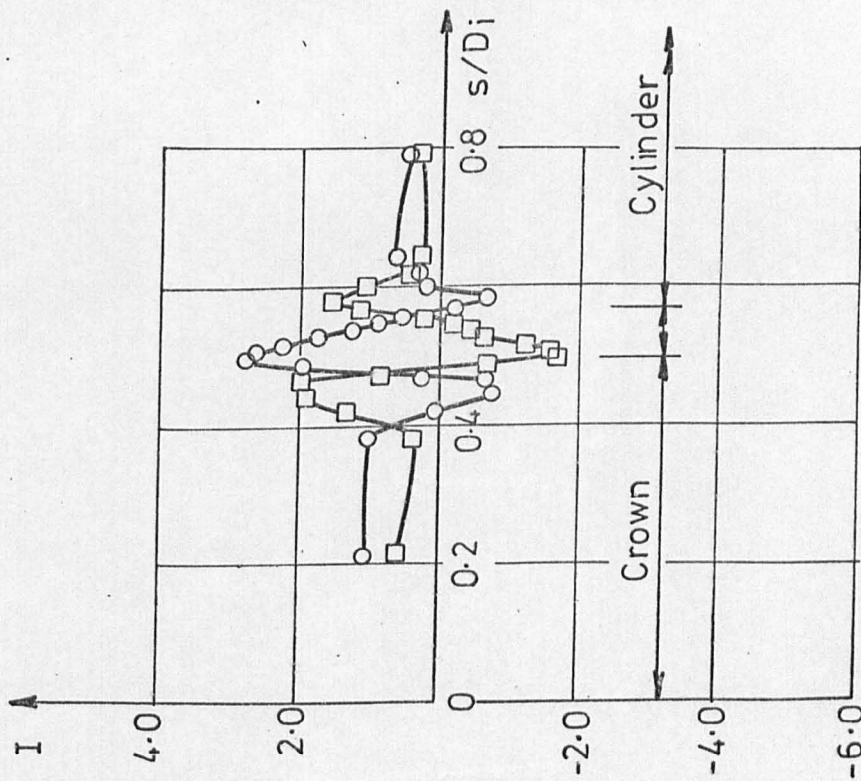
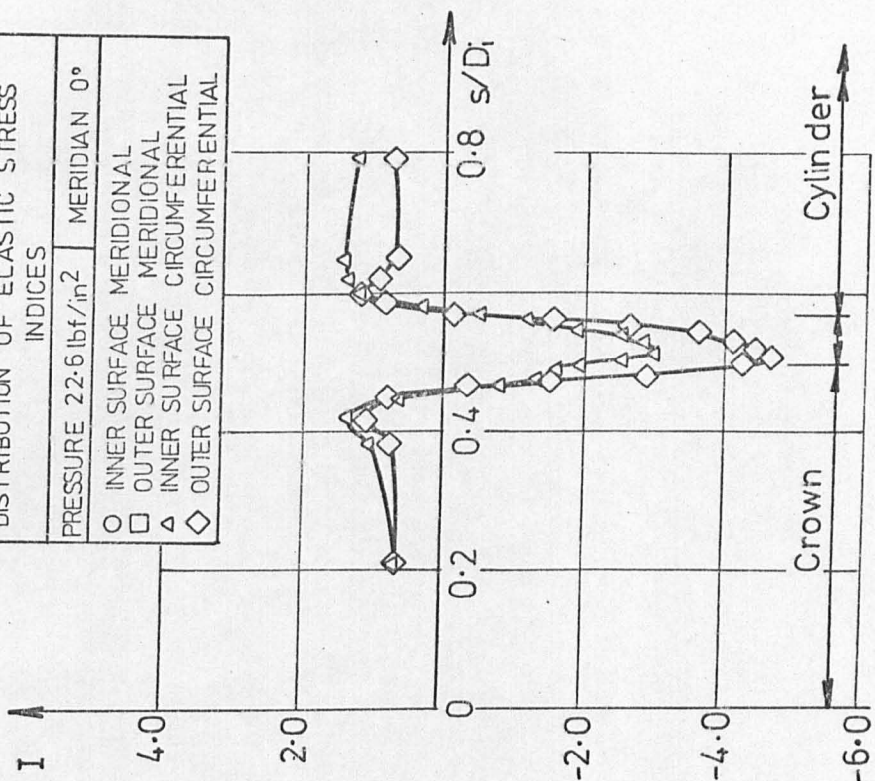


FIG. A1.17.7

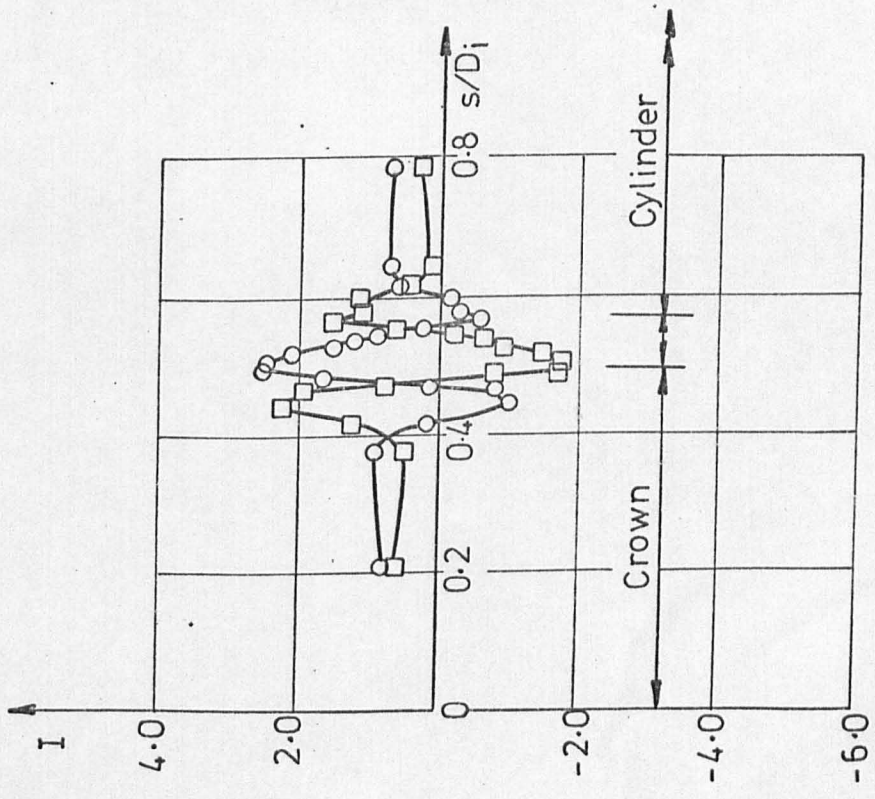
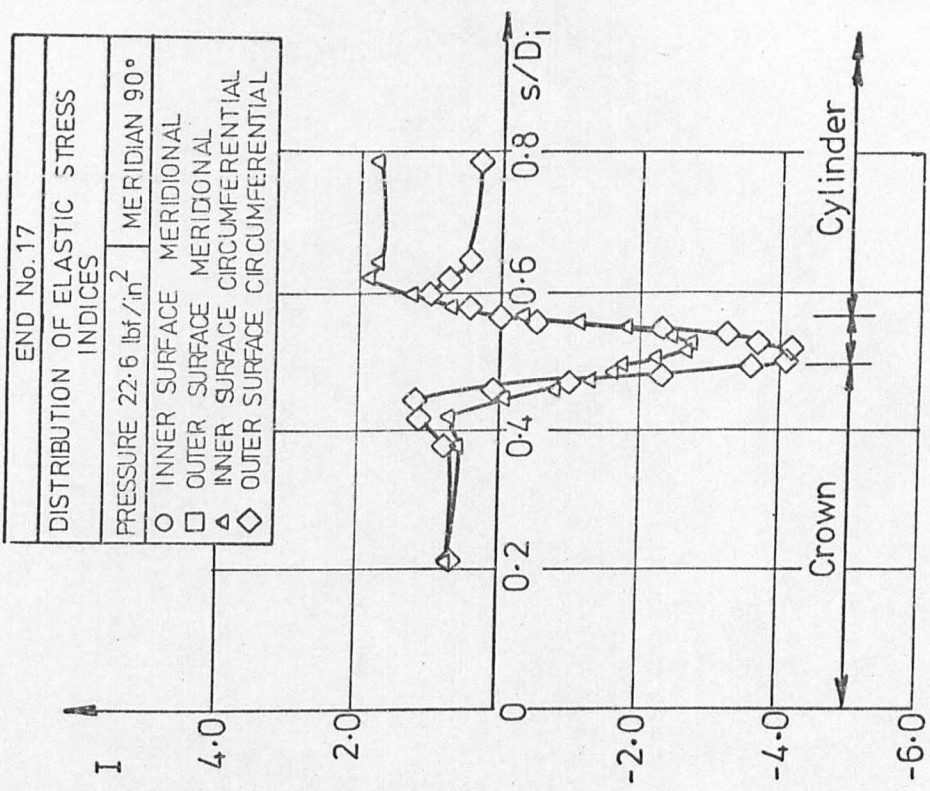


FIG. A1-17.8

APPENDIX 2

Summary Sheets

UNIVERSITY OF NOTTINGHAM

INTERNAL PRESSURE TESTING OF VERY THIN

TORISPHERICAL PRESSURE VESSEL ENDS

SUMMARY SHEET

END NO. 1	DATE June 1972
MATERIAL: HIGH PROOF STRESS 304 AUSTENITIC STAINLESS STEEL	
MANUFACTURE: CROWN AND SEGMENT	
<u>NOMINAL DIMENSIONS AND SHAPE PARAMETERS</u>	
Diameter ( $D_i$ )	= 54.0 in
Knuckle radius ( $r_i$ )	= 9.0 in <span style="float: right;"><math>r_i/D_i = 0.167</math></span>
Crown radius ( $R_i$ )	= 54.0 in <span style="float: right;"><math>R_i/D_i = 1.000</math></span>
End height ( $h_i$ )	= 12.76 in <span style="float: right;"><math>h_i/D_i = 0.236</math></span>
Thickness of end ( $t_e$ )	= 0.128 in <span style="float: right;"><math>t_e/D_i = 0.00237</math></span>
Thickness of cylinder ( $t_c$ )	= 0.104 in <span style="float: right;"><math>t_c/D_i = 0.00193</math></span>
<u>MEASURED THICKNESS OF END</u>	
Minimum thickness at k/cyl.	= 0.093 in
Thickness at centre of knuckle	= 0.132 in
<u>PEAK ELASTIC STRESS INDICES IN KNUCKLE</u> (STRESS $\div pD_i/2t_e$ )	
Inner surface meridional	= -
Outer surface meridional	= 0.20
Inner surface circumferential	= -
Outer surface circumferential	= -1.10
<u>IMPORTANT PRESSURES</u> (lbf/in <sup>2</sup> )	
* Pressure for first yield in cylinder (von Mises)	= 179
+ Pressure for first yield in cylinder (Experimental)	= -
* Pressure for first yield in end (von Mises)	= -
+ Pressure for first yield in end (Experimental)	= -
Limit pressure (Shield and Drucker)	= 104
Elastic buckling pressure (Thurston and Holston)	= 2130
Measured buckling pressure	= 280
Maximum test pressure	= 300
(* Assumed yield stress 18.0 tonf/in <sup>2</sup> )(+ 0.1% proof pressure)	
<u>CIRCUMFERENTIAL STRAINS IN CYLINDER</u>	
At buckling pressure	= -
At maximum test pressure	= -

UNIVERSITY OF NOTTINGHAM

INTERNAL PRESSURE TESTING OF VERY THIN

TORISPHERICAL PRESSURE VESSEL ENDS

SUMMARY SHEET

END NO. 2	DATE February 1973
MATERIAL: HIGH PROOF STRESS 304 AUSTENITIC STAINLESS STEEL	
MANUFACTURE: CROWN AND SEGMENT	
<u>NOMINAL DIMENSIONS AND SHAPE PARAMETERS</u>	
Diameter ( $D_i$ )	= 54.0 in
Knuckle radius ( $r_i$ )	= 9.0 in $r_i/D_i = 0.167$
Crown radius ( $R_i$ )	= 54.0 in $R_i/D_i = 1.000$
End height ( $h_i$ )	= 12.76 in $h_i/D_i = 0.236$
Thickness of end ( $t_e$ )	= 0.128 in $t_e/D_i = 0.00237$
Thickness of cylinder ( $t_c$ )	= 0.104 in $t_c/D_i = 0.00193$
<u>MEASURED THICKNESS OF END</u>	
Minimum thickness at k/cyl.	= 0.092 in
Thickness at centre of knuckle	= 0.131 in
<u>PEAK ELASTIC STRESS INDICES IN KNUCKLE</u> (STRESS $\div pD_i/2t_e$ )	
Inner surface meridional	= 1.33 (1.24 on weld)
Outer surface meridional	= 0.10 (0.30 on weld)
Inner surface circumferential	= -0.88 (-1.70 on weld)
Outer surface circumferential	= -1.21 (-1.29 on weld)
<u>IMPORTANT PRESSURES</u> (lbf/in <sup>2</sup> )	
* Pressure for first yield in cylinder (von Mises)	= 179
+ Pressure for first yield in cylinder (Experimental)	= 182
* Pressure for first yield in end (von Mises)	= 118
+ Pressure for first yield in end (Experimental)	= 178
Limit pressure (Shield and Drucker)	= 104
Elastic buckling pressure (Thurston and Holston)	= 2130
Measured buckling pressure	= 278
Maximim test pressure	= 298
(* Assumed yield stress 18.0 tonf/in <sup>2</sup> ) (+ 0.1% proof pressure)	
<u>CIRCUMFERENTIAL STRAINS IN CYLINDER</u>	
At buckling pressure	= 3.05%
At maximum test pressure	= 3.71%



UNIVERSITY OF NOTTINGHAM

INTERNAL PRESSURE TESTING OF VERY THIN

TORISPHERICAL PRESSURE VESSEL ENDS

SUMMARY SHEET

END NO. 3	DATE August 1972	
MATERIAL: HIGH PROOF STRESS 304 AUSTENITIC STAINLESS STEEL		
MANUFACTURE: PRESSED AND SPUN		
<u>NOMINAL DIMENSIONS AND SHAPE PARAMETERS</u>		
Diameter ( $D_i$ )	= 54.0 in	
Knuckle radius ( $r_i$ )	= 6.0 in	$r_i/D_i = 0.111$
Crown radius ( $R_i$ )	= 54.0 in	$R_i/D_i = 1.000$
End height ( $h_i$ )	= 10.84 in	$h_i/D_i = 0.201$
Thickness of end ( $t_e$ )	= 0.128 in	$t_e/D_i = 0.00237$
Thickness of cylinder ( $t_c$ )	= 0.104 in	$t_c/D_i = 0.00193$
<u>MEASURED THICKNESS OF END</u>		
Minimum thickness at k/cyl.	= 0.098 in	
Thickness at centre of knuckle	= 0.117 in	
<u>PEAK ELASTIC STRESS INDICES IN KNUCKLE</u> (STRESS $\div pD_i/2t_e$ )		
Inner surface meridional	= 2.48	
Outer surface meridional	= -1.51	
Inner surface circumferential	= -2.21	
Outer surface circumferential	= -3.04	
<u>IMPORTANT PRESSURES</u> (lbf/in <sup>2</sup> )		
* Pressure for first yield in cylinder (von Mises)	= 179	
+ Pressure for first yield in cylinder (Experimental)	= 171	
* Pressure for first yield in end (von Mises)	= 52	
+ Pressure for first yield in end (Experimental)	= 124	
Limit pressure (Shield and Drucker)	= 77	
Elastic buckling pressure (Thurston and Holston)	= 1110	
Measured buckling pressure	= 248	
Maximum test pressure	= 253	
(* Assumed yield stress 18.0 tonf/in <sup>2</sup> ) (+ 0.1% proof pressure)		
<u>CIRCUMFERENTIAL STRAINS IN CYLINDER</u>		
At buckling pressure	= 1.52%	
At maximum test pressure	= 2.26%	

UNIVERSITY OF NOTTINGHAM

INTERNAL PRESSURE TESTING OF VERY THIN

TORISPHERICAL PRESSURE VESSEL ENDS

SUMMARY SHEET

END NO. 4	DATE June 1972
MATERIAL: HIGH PROOF STRESS 304 AUSTENITIC STAINLESS STEEL	
MANUFACTURE: PRESSED AND SPUN	
<u>NOMINAL DIMENSIONS AND SHAPE PARAMETERS</u>	
Diameter ( $D_i$ )	= 54.0 in
Knuckle radius ( $r_i$ )	= 4.0 in $r_i/D_i = 0.074$
Crown radius ( $R_i$ )	= 54.0 in $R_i/D_i = 1.000$
End height ( $h_i$ )	= 9.60 in $h_i/D_i = 0.178$
Thickness of end ( $t_e$ )	= 0.128 in $t_e/D_i = 0.00237$
Thickness of cylinder ( $t_c$ )	= 0.104 in $t_c/D_i = 0.00193$
<u>MEASURED THICKNESS OF END</u>	
Minimum thickness at k/cyl	= 0.104 in
Thickness at centre of knuckle	= 0.116 in
<u>PEAK ELASTIC STRESS INDICES IN KNUCKLE</u> (STRESS $\div$ $pD_i/2t_e$ )	
Inner surface meridional	= 3.91
Outer surface meridional	= -2.84
Inner surface circumferential	= -3.62
Outer surface circumferential	= -5.00
<u>IMPORTANT PRESSURES</u> (lb/in <sup>2</sup> )	
* Pressure for first yield in cylinder (von Mises)	= 179
+ Pressure for first yield in cylinder (Experimental)	= 172
* Pressure for first yield in end (von Mises)	= 33
+ Pressure for first yield in end (Experimental)	= 75
Limit pressure (Shield and Drucker)	= 60
Elastic buckling pressure (Thurston and Holston)	= 440
Measured buckling pressure	= 198
Maximum test pressure	= 198
(* Assumed yield stress 18.0 tonf/in <sup>2</sup> ) (+ 0.1% proof pressure)	
<u>CIRCUMFERENTIAL STRAINS IN CYLINDER</u>	
At buckling pressure	= 0.43%
At maximum test pressure	= 0.43%

UNIVERSITY OF NOTTINGHAM

INTERNAL PRESSURE TESTING OF VERY THIN

TORISPHERICAL PRESSURE VESSEL ENDS

SUMMARY SHEET

END NO. 5	DATE November 1972	
MATERIAL: HIGH PROOF STRESS 304 AUSTENITIC STAINLESS STEEL		
MANUFACTURE: PRESSED AND SPUN		
<u>NOMINAL DIMENSIONS AND SHAPE PARAMETERS</u>		
Diameter ( $D_i$ )	= 54.0	
Knuckle radius ( $r_i$ )	= 4.0 in.	$r_i/D_i = 0.074$
Crown radius ( $R_i$ )	= 45.0 in	$R_i/D_i = 0.833$
End height ( $h_i$ )	= 11.06 in	$h_i/D_i = 0.205$
Thickness of end ( $t_e$ )	= 0.128 in	$t_e/D_i = 0.00237$
Thickness of cylinder ( $t_c$ )	= 0.104 in	$t_c/D_i = 0.00193$
<u>MEASURED THICKNESS OF END</u>		
Minimum thickness at k/cyl.	= 0.090 in	
Thickness at centre of knuckle	= 0.107 in	
<u>PEAK ELASTIC STRESS INDICES IN KNUCKLE</u> (STRESS $\div$ $pD_i/2t_e$ )		
Inner surface meridional	= 2.64	
Outer surface meridional	= -1.41	
Inner surface circumferential	= -2.31	
Outer surface circumferential	= -3.16	
<u>IMPORTANT PRESSURES</u> (lbf/in <sup>2</sup> )		
* Pressure for first yield in cylinder (von Mises)	= 179	
+ Pressure for first yield in cylinder (Experimental)	= 181	
* Pressure for first yield in end (von Mises)	= 50	
+ Pressure for first yield in end (Experimental)	= 111	
Limit pressure (Shield and Drucker)	= 72	
Elastic buckling pressure (Thurston and Holston)	= -	
Measured buckling pressure	= 278	
Maximim test pressure	= 283	
(* Assumed yield stress 18.0 tonf/in <sup>2</sup> ) (+ 0.1% proof pressure)		
<u>CIRCUMFERENTIAL STRAINS IN CYLINDER</u>		
At buckling pressure	= 1.87%	
At maximum test pressure	= 2.01%	

UNIVERSITY OF NOTTINGHAM

INTERNAL PRESSURE TESTING OF VERY THIN

TORISPHERICAL PRESSURE VESSEL ENDS

SUMMARY SHEET

END NO. 6	DATE December 1972	
MATERIAL: HIGH PROOF STRESS 304 AUSTENITIC STAINLESS STEEL		
MANUFACTURE: PRESSED AND SPUN		
<u>NOMINAL DIMENSIONS AND SHAPE PARAMETERS</u>		
Diameter ( $D_i$ )	= 54.0 in	
Knuckle radius ( $r_i$ )	= 4.0 in	$r_i/D_i = 0.074$
Crown radius ( $R_i$ )	= 42.0 in	$R_i/D_i = 0.778$
End height ( $h_i$ )	= 11.75 in	$h_i/D_i = 0.218$
Thickness of end ( $t_e$ )	= 0.128 in	$t_e/D_i = 0.00237$
Thickness of cylinder ( $t_c$ )	= 0.104 in	$t_c/D_i = 0.00193$
<u>MEASURED THICKNESS OF END</u>		
Minimum thickness at k/cyl	= 0.095 in	
Thickness at centre of knuckle	= 0.110 in	
<u>PEAK ELASTIC STRESS INDICES IN KNUCKLE</u> (STRESS $\div pD_i/2t_e$ )		
Inner surface meridional	= 3.09	
Outer surface meridional	= -1.89	
Inner surface circumferential	= -2.51	
Outer surface circumferential	= -3.84	
<u>IMPORTANT PRESSURES</u> (lbf/in <sup>2</sup> )		
* Pressure for first yield in cylinder (von Mises)	= 179	
+ Pressure for first yield in cylinder (Experimental)	= 180	
* Pressure for first yield in end (von Mises)	= 41	
+ Pressure for first yield in end (Experimental)	= 158	
Limit pressure (Shield and Drucker)	= 78	
Elastic buckling pressure (Thurston and Holston)	= -	
Measured buckling pressure	= 278	
Maximum test pressure	= 298	
(* Assumed yield stress 18.0 tonf/in <sup>2</sup> ) (+ 0.1% proof pressure)		
<u>CIRCUMFERENTIAL STRAINS IN CYLINDER</u>		
At buckling pressure	= 2.53%	
At maximum test pressure	= 3.23%	

UNIVERSITY OF NOTTINGHAM

INTERNAL PRESSURE TESTING OF VERY THIN

TORISPHERICAL PRESSURE VESSEL ENDS

SUMMARY SHEET

END NO. 7

DATE May 1973

MATERIAL: HIGH PROOF STRESS 304 AUSTENITIC STAINLESS STEEL

MANUFACTURE: CROWN AND SEGMENT

NOMINAL DIMENSIONS AND SHAPE PARAMETERS

Diameter ( $D_i$ )	=	108.0 in		
Knuckle radius ( $r_i$ )	=	18.0 in	$r_i/D_i$ =	0.167
Crown radius ( $R_i$ )	=	108.0 in	$R_i/D_i$ =	1.000
End height ( $h_i$ )	=	25.51 in	$h_i/D_i$ =	0.236
Thickness of end ( $t_e$ )	=	0.128 in	$t_e/D_i$ =	0.00119
Thickness of cylinder ( $t_c$ )	=	0.104 in	$t_c/D_i$ =	0.00096

MEASURED THICKNESS OF END

Minimum thickness at k/cyl	=	-
Thickness at centre of knuckle	=	0.128 in

PEAK ELASTIC STRESS INDICES IN KNUCKLE (STRESS  $\div$   $pD_i/2t_e$ )

Inner surface meridional	=	-
Outer surface meridional	=	-0.16 (-0.55 on weld)
Inner surface circumferential	=	-
Outer surface circumferential	=	-1.83 (-2.70 on weld)

IMPORTANT PRESSURES (lbf/in<sup>2</sup>)

* Pressure for first yield in cylinder (von Mises)	=	-
+ Pressure for first yield in cylinder (Experimental)	=	-
* Pressure for first yield in end (von Mises)	=	-
+ Pressure for first yield in end (Experimental)	=	-
Limit pressure (Shield and Drucker)	=	47
Elastic buckling pressure (Thurston and Holston)	=	430
Measured buckling pressure	=	60
Maximum test pressure	=	104
(* Assumed yield stress 18.0 tonf/in <sup>2</sup> ) (+ 0.1% proof pressure)		

CIRCUMFERENTIAL STRAINS IN CYLINDER

At buckling pressure	=	-
At maximum test pressure	=	-

UNIVERSITY OF NOTTINGHAM

INTERNAL PRESSURE TESTING OF VERY THIN

TORISPHERICAL PRESSURE VESSEL ENDS

SUMMARY SHEET

END NO.        8	DATE        June 1973
MATERIAL: HIGH PROOF STRESS 304 AUSTENITIC STAINLESS STEEL	
MANUFACTURE:    PRESSED AND SPUN	
<u>NOMINAL DIMENSIONS AND SHAPE PARAMETERS</u>	
Diameter        ( $D_i$ )	= 108.0 in
Knuckle radius ( $r_i$ )	= 12.0 in $r_i/D_i = 0.111$
Crown radius    ( $R_i$ )	= 108.0 in $R_i/D_i = 1.000$
End height        ( $h_i$ )	= 21.68 in $h_i/D_i = 0.201$
Thickness of end ( $t_e$ )	= 0.128 in $t_e/D_i = 0.00119$
Thickness of cylinder ( $t_c$ )	= 0.104 in $t_c/D_i = 0.00096$
<u>MEASURED THICKNESS OF END</u>	
Minimum thickness at k/cyl	= 0.078 in
Thickness at centre of knuckle	= 0.105 in (0.099 in on weld)
<u>PEAK ELASTIC STRESS INDICES IN KNUCKLE</u> (STRESS $\div$ $pD_i/2t_e$ )	
Inner surface meridional	= 2.35 (2.19 on weld)
Outer surface meridional	= -0.72 (-1.28 on weld)
Inner surface circumferential	= -1.99 (-2.29 on weld)
Outer surface circumferential	= -2.82 (-3.78 on weld)
<u>IMPORTANT PRESSURES</u> (lbf/in <sup>2</sup> )	
* Pressure for first yield in cylinder (von Mises)	= 90
+ Pressure for first yield in cylinder (Experimental)	= 84
* Pressure for first yield in end (von Mises)	= 27
+ Pressure for first yield in end (Experimental)	= -
Limit pressure (Shield and Drucker)	= 33
Elastic buckling pressure (Thurston and Holston)	= 270
Measured buckling pressure	= 70
Maximim test pressure	= 94
(* Assumed yield stress 18.0 tonf/in <sup>2</sup> ) (+ 0.1% proof pressure)	
<u>CIRCUMFERENTIAL STRAINS IN CYLINDER</u>	
At buckling pressure	= 0.13%
At maximum test pressure	= 0.38%

UNIVERSITY OF NOTTINGHAM

INTERNAL PRESSURE TESTING OF VERY THIN

TORISPHERICAL PRESSURE VESSEL ENDS

SUMMARY SHEET

END NO. 9

DATE May 1973

MATERIAL: HIGH PROOF STRESS 304 AUSTENITIC STAINLESS STEEL

MANUFACTURE: PRESSED AND SPUN

NOMINAL DIMENSIONS AND SHAPE PARAMETERS

Diameter ( $D_i$ )	=	108.0 in	
Knuckle radius ( $r_i$ )	=	8.0 in	$r_i/D_i = 0.074$
Crown radius ( $R_i$ )	=	108.0 in	$R_i/D_i = 1.000$
End height ( $h_i$ )	=	19.21 in	$h_i/D_i = 0.178$
Thickness of end ( $t_e$ )	=	0.128 in	$t_e/D_i = 0.00119$
Thickness of cylinder ( $t_c$ )	=	0.104 in	$t_c/D_i = 0.00096$

MEASURED THICKNESS OF END

Minimum thickness at k/cyl	=	0.089 in
Thickness at centre of knuckle	=	0.119 in (0.112 in on weld)

PEAK ELASTIC STRESS INDICES IN KNUCKLE (STRESS  $\div pD_i/2t_e$ )

Inner surface meridional	=	2.63 (2.59 on weld)
Outer surface meridional	=	-1.22 (-1.84 on weld)
Inner surface circumferential	=	-3.53 (-3.91 on weld)
Outer surface circumferential	=	-4.15 (-5.83 on weld)

IMPORTANT PRESSURES (lbf/in<sup>2</sup>)

* Pressure for first yield in cylinder (von Mises)	=	90
+ Pressure for first yield in cylinder (Experimental)	=	-
* Pressure for first yield in end (von Mises)	=	18
+ Pressure for first yield in end (Experimental)	=	45
Limit pressure (Shield and Drucker)	=	25
Elastic buckling pressure (Thurston and Holston)	=	160
Measured buckling pressure	=	62
Maximum test pressure	=	78
(* Assumed yield stress 18.0 tonf/in <sup>2</sup> )(+ 0.1% proof pressure)		

CIRCUMFERENTIAL STRAINS IN CYLINDER

At buckling pressure	=	0.11%
At maximum test pressure	=	0.14%

UNIVERSITY OF NOTTINGHAM

INTERNAL PRESSURE TESTING OF VERY THIN

TORISPHERICAL PRESSURE VESSEL ENDS

SUMMARY SHEET

END NO. 10	DATE August 1973
MATERIAL: HIGH PROOF STRESS 304 AUSTENITIC STAINLESS STEEL	
MANUFACTURE: PRESSED AND SPUN	
<u>NOMINAL DIMENSIONS AND SHAPE PARAMETERS</u>	
Diameter ( $D_i$ )	= 108.0 in
Knuckle radius ( $r_i$ )	= 8.0 in <span style="float:right"><math>r_i/D_i = 0.074</math></span>
Crown radius ( $R_i$ )	= 90.0 in <span style="float:right"><math>R_i/D_i = 0.833</math></span>
End height ( $h_i$ )	= 22.1 in <span style="float:right"><math>h_i/D_i = 0.205</math></span>
Thickness of end ( $t_e$ )	= 0.128 in <span style="float:right"><math>t_e/D_i = 0.00119</math></span>
Thickness of cylinder ( $t_c$ )	= 0.104 in <span style="float:right"><math>t_c/D_i = 0.00096</math></span>
<u>MEASURED THICKNESS OF END</u>	
Minimum thickness at k/cyl.	= 0.088 in
Thickness at centre of knuckle	= 0.119 in (0.114 in on weld)
<u>PEAK ELASTIC STRESS INDICES IN KNUCKLE</u> (STRESS $\div pD_i/2t_e$ )	
Inner surface meridional	= 2.11 (2.11 on weld)
Outer surface meridional	= -1.24 (-1.21 on weld)
Inner surface circumferential	= -3.32 (-3.54 on weld)
Outer surface circumferential	= -4.12 (-4.19 on weld)
<u>IMPORTANT PRESSURES</u> (lbf/in <sup>2</sup> )	
* Pressure for first yield in cylinder (von Mises)	= 90
+ Pressure for first yield in cylinder (Experimental)	= -
* Pressure for first yield in end (von Mises)	= 20
+ Pressure for first yield in end (Experimental)	= 68
Limit pressure (Shield and Drucker)	= 30
Elastic buckling pressure (Thurston and Holston)	= -
Measured buckling pressure	= 78
Maximum test pressure	= 86
(* Assumed yield stress 18.0 tonf/in <sup>2</sup> ) (+0.1% proof pressure)	
<u>CIRCUMFERENTIAL STRAINS IN CYLINDER</u>	
At buckling pressure	= 0.14%
At maximum test pressure	= 0.23%



UNIVERSITY OF NOTTINGHAM

INTERNAL PRESSURE TESTING OF VERY THIN  
TORISPHERICAL PRESSURE VESSEL ENDS

SUMMARY SHEET

END NO.	11	DATE	December 1973
MATERIAL: HIGH PROOF STRESS 304 AUSTENITIC STAINLESS STEEL			
MANUFACTURE: PRESSED AND SPUN			
<u>NOMINAL DIMENSIONS AND SHAPE PARAMETERS</u>			
Diameter ( $D_i$ )	=	108.0 in	
Knuckle radius ( $r_i$ )	=	8.0 in	$r_i/D_i = 0.074$
Crown radius ( $R_i$ )	=	78.0 in	$R_i/D_i = 0.722$
End height ( $h_i$ )	=	25.23 in	$h_i/D_i = 0.234$
Thickness of end ( $t_e$ )	=	0.128 in	$t_e/D_i = 0.00119$
Thickness of cylinder ( $t_c$ )	=	0.104 in	$t_c/D_i = 0.00096$
<u>MEASURED THICKNESS OF END</u>			
Minimum thickness at k/cyl	=	0.094 in	
Thickness at centre of knuckle	=	0.105 in (0.103 in on weld)	
<u>PEAK ELASTIC STRESS INDICES IN KNUCKLE</u> (STRESS $\div$ $pD_i/2t_e$ )			
Inner surface meridional	=	1.99 (2.38 on weld)	
Outer surface meridional	=	-1.23 (-1.80 on weld)	
Inner surface circumferential	=	-2.98 (-3.14 on weld)	
Outer surface circumferential	=	-3.48 (-4.07 on weld)	
<u>IMPORTANT PRESSURES</u> (lbf/in <sup>2</sup> )			
* Pressure for first yield in cylinder (von Mises)	=	90	
+ Pressure for first yield in cylinder (Experimental)	=	88	
* Pressure for first yield in end (von Mises)	=	23	
+ Pressure for first yield in end (Experimental)	=	78	
Limit pressure (Shield and Drucker)	=	36	
Elastic buckling pressure (Thurston and Holston)	=	-	
Measured buckling pressure	=	86	
Maximum test pressure	=	98	
(* Assumed yield stress 18.0 tonf/in <sup>2</sup> )(+ 0.1% proof pressure)			
<u>CIRCUMFERENTIAL STRAINS IN CYLINDER</u>			
At buckling pressure	=	0.19%	
At maximum test pressure	=	0.45%	

UNIVERSITY OF NOTTINGHAM

INTERNAL PRESSURE TESTING OF VERY THIN  
TORISPHERICAL PRESSURE VESSEL ENDS

SUMMARY SHEET

END NO.	12	DATE	November 1973
MATERIAL: HIGH PROOF STRESS 304 AUSTENITIC STAINLESS STEEL			
MANUFACTURE: PRESSED AND SPUN			
<u>NOMINAL DIMENSIONS AND SHAPE PARAMETERS</u>			
Diameter ( $D_i$ )	=	108.0 in	
Knuckle radius ( $r_i$ )	=	6.0 in	$r_i/D_i = 0.056$
Crown radius ( $R_i$ )	=	108.0 in	$R_i/D_i = 1.000$
End height ( $h_i$ )	=	18.13 in	$h_i/D_i = 0.167$
Thickness of end ( $t_e$ )	=	0.128 in	$t_e/D_i = 0.00119$
Thickness of cylinder ( $t_c$ )	=	0.104 in	$t_c/D_i = 0.00096$
<u>MEASURED THICKNESS OF END</u>			
Minimum thickness at k/cyl	=	0.087 in	
Thickness at centre of knuckle	=	0.119 in (0.117 in on weld)	
<u>PEAK ELASTIC STRESS INDICES IN KNUCKLE</u> (STRESS $\div pD_i/2t_e$ )			
Inner surface meridional	=	2.74 (3.21 on weld)	
Outer surface meridional	=	-1.40 (-1.94 on weld)	
Inner surface circumferential	=	-3.43 (-3.84 on weld)	
Outer surface circumferential	=	-4.66 (-5.51 on weld)	
<u>IMPORTANT PRESSURES</u> (lbf/in <sup>2</sup> )			
* Pressure for first yield in cylinder (von Mises)	=	90	
+ Pressure for first yield in cylinder (Experimental)	=	-	
* Pressure for first yield in end (von Mises)	=	16	
+ Pressure for first yield in end (Experimental)	=	35	
Limit pressure (Shield and Drucker)	=	21	
Elastic buckling pressure (Thurston and Holston)	=	110	
Measured buckling pressure	=	66	
Maximim test pressure	=	78	
(* Assumed yield stress 18.0 tonf/in <sup>2</sup> ) (+ 0.1% proof pressure)			
<u>CIRCUMFERENTIAL STRAINS IN CYLINDER</u>			
At buckling pressure	=	0.12%	
At maximum test pressure	=	0.16%	

UNIVERSITY OF NOTTINGHAM

INTERNAL PRESSURE TESTING OF VERY THIN  
TORISPHERICAL PRESSURE VESSEL ENDS

SUMMARY SHEET

END NO. 13

DATE February 1974

MATERIAL: HIGH PROOF STRESS 304 AUSTENITIC STAINLESS STEEL

MANUFACTURE: CROWN AND SEGMENT

NOMINAL DIMENSIONS AND SHAPE PARAMETERS

Diameter ( $D_i$ )	=	108.0 in	
Knuckle radius ( $r_i$ )	=	18.0 in	$r_i/D_i = 0.167$
Crown radius ( $R_i$ )	=	108.0 in	$R_i/D_i = 1.000$
End height ( $h_i$ )	=	25.51 in	$h_i/D_i = 0.236$
Thickness of end ( $t_e$ )	=	0.128 in	$t_e/D_i = 0.00119$
Thickness of cylinder ( $t_c$ )	=	0.104 in	$t_c/D_i = 0.00096$

MEASURED THICKNESS OF END

Minimum thickness at k/cyl = 0.081 in

Thickness at centre of knuckle = 0.133 in

PEAK ELASTIC STRESS INDICES IN KNUCKLE (STRESS  $\div pD_i/2t_e$ )

Inner surface meridional	=	1.58 (1.46 on weld)
Outer surface meridional	=	-0.12 (-0.23 on weld)
Inner surface circumferential	=	-1.59 (-1.80 on weld)
Outer surface circumferential	=	-1.77 (-2.32 on weld)

IMPORTANT PRESSURES (lbf/in<sup>2</sup>)

* Pressure for first yield in cylinder (von Mises)	=	90
+ Pressure for first yield in cylinder (Experimental)	=	89
* Pressure for first yield in end (von Mises)	=	34
+ Pressure for first yield in end (Experimental)	=	-
Limit pressure (Shield and Drucker)	=	47
Elastic buckling pressure (Thurston and Holston)	=	430
Measured buckling pressure	=	82
Maximum test pressure	=	102
(* Assumed yield stress 18.0 tonf/in <sup>2</sup> )(+ 0.1% proof pressure)		

CIRCUMFERENTIAL STRAINS IN CYLINDER

At buckling pressure	=	0.15%
At maximum test pressure	=	0.59%

UNIVERSITY OF NOTTINGHAM

INTERNAL PRESSURE TESTING OF VERY THIN  
TORISPHERICAL PRESSURE VESSEL ENDS

SUMMARY SHEET

END NO.	14	DATE	March 1974
MATERIAL: HIGH PROOF STRESS 304 AUSTENITIC STAINLESS STEEL			
MANUFACTURE: CROWN AND SEGMENT			
<u>NOMINAL DIMENSIONS AND SHAPE PARAMETERS</u>			
Diameter ( $D_i$ )	=	81.0 in	
Knuckle radius ( $r_i$ )	=	13.5 in	$r_i/D_i = 0.167$
Crown radius ( $R_i$ )	=	81.0 in	$R_i/D_i = 1.000$
End height ( $h_i$ )	=	19.14 in	$h_i/D_i = 0.236$
Thickness of end ( $t_e$ )	=	0.128 in	$t_e/D_i = 0.00158$
Thickness of cylinder ( $t_c$ )	=	0.104 in	$t_c/D_i = 0.00128$
<u>MEASURED THICKNESS OF END</u>			
Minimum thickness at k/cyl	=	0.106 in	
Thickness at centre of knuckle	=	0.130 in	
<u>PEAK ELASTIC STRESS INDICES IN KNUCKLE</u> (STRESS $\div$ $pD_i/2t_e$ )			
Inner surface meridional	=	1.80 (1.90 on weld)	
Outer surface meridional	=	-0.78 (-0.51 on weld)	
Inner surface circumferential	=	-1.29 (-1.73 on weld)	
Outer surface circumferential	=	-2.23 (-2.29 on weld)	
<u>IMPORTANT PRESSURES</u> (lbf/in <sup>2</sup> )			
* Pressure for first yield in cylinder (von Mises)	=	-	
+ Pressure for first yield in cylinder (Experimental)	=	-	
* Pressure for first yield in end (von Mises)	=	-	
+ Pressure for first yield in end (Experimental)	=	93	
Limit pressure (Shield and Drucker)	=	65	
Elastic buckling pressure (Thurston and Holston)	=	950	
Measured buckling pressure	=	120	
Maximim test pressure	=	239	
(* Assumed yield stress 18.0 tonf/in <sup>2</sup> )(+ 0.1% proof pressure)			
<u>CIRCUMFERENTIAL STRAINS IN CYLINDER</u>			
At buckling pressure	=	-	
At maximum test pressure	=	-	

UNIVERSITY OF NOTTINGHAM

INTERNAL PRESSURE TESTING OF VERY THIN

TORISPHERICAL PRESSURE VESSEL ENDS

SUMMARY SHEET

END NO. 15

DATE July 1974

MATERIAL: HIGH PROOF STRESS 304 AUSTENITIC STAINLESS STEEL

MANUFACTURE: CROWN AND SEGMENT

NOMINAL DIMENSIONS AND SHAPE PARAMETERS

Diameter ( $D_i$ )	=	81.0 in	
Knuckle radius ( $r_i$ )	=	13.5 in	$r_i/D_i = 0.167$
Crown radius ( $R_i$ )	=	81.0 in	$R_i/D_i = 1.000$
End height ( $h_i$ )	=	19.14 in	$h_i/D_i = 0.236$
Thickness of end ( $t_e$ )	=	0.128 in	$t_e/D_i = 0.00158$
Thickness of cylinder ( $t_c$ )	=	0.104 in	$t_c/D_i = 0.00128$

MEASURED THICKNESS OF END

Minimum thickness at k/cyl	=	0.092 in
Thickness at centre of knuckle	=	0.128 in

PEAK ELASTIC STRESS INDICES IN KNUCKLE (STRESS  $\div pD_i/2t_e$ )

Inner surface meridional	=	2.09 (2.76 on weld)
Outer surface meridional	=	-0.97 (-0.53 on weld)
Inner surface circumferential	=	-1.58 (-2.11 on weld)
Outer surface circumferential	=	-2.29 (-2.12 on weld)

IMPORTANT PRESSURES (lb/in<sup>2</sup>)

* Pressure for first yield in cylinder (von Mises)	=	120
+ Pressure for first yield in cylinder (Experimental)	=	-
* Pressure for first yield in end (von Mises)	=	37
+ Pressure for first yield in end (Experimental)	=	82
Limit pressure (Shield and Drucker)	=	65
Elastic buckling pressure (Thurston and Holston)	=	950
Measured buckling pressure	=	107
Maximum test pressure	=	239
(* Assumed yield stress 18.0 tonf/in <sup>2</sup> ) (+ 0.1% proof pressure)		

CIRCUMFERENTIAL STRAINS IN CYLINDER

At buckling pressure	=	0.13%
At maximum test pressure	=	-

UNIVERSITY OF NOTTINGHAM

INTERNAL PRESSURE TESTING OF VERY THIN

TORISPHERICAL PRESSURE VESSEL ENDS

SUMMARY SHEET

END NO. 16	DATE March 1974
MATERIAL: HIGH PROOF STRESS 304 AUSTENITIC STAINLESS STEEL	
MANUFACTURE: PRESSED AND SPUN	
<u>NOMINAL DIMENSIONS AND SHAPE PARAMETERS</u>	
Diameter ( $D_i$ )	= 81.0 in
Knuckle radius ( $r_i$ )	= 6.0 in <span style="float: right;"><math>r_i/D_i = 0.074</math></span>
Crown radius ( $R_i$ )	= 81.0 in <span style="float: right;"><math>R_i/D_i = 1.000</math></span>
End height ( $h_i$ )	= 14.41 in <span style="float: right;"><math>h_i/D_i = 0.178</math></span>
Thickness of end ( $t_e$ )	= 0.128 in <span style="float: right;"><math>t_e/D_i = 0.00158</math></span>
Thickness of cylinder ( $t_c$ )	= 0.104 in <span style="float: right;"><math>t_c/D_i = 0.00128</math></span>
<u>MEASURED THICKNESS OF END</u>	
Minimum thickness at k/cyl	= 0.086 in
Thickness at centre of knuckle	= 0.118 in (0.115 in on weld)
<u>PEAK ELASTIC STRESS INDICES IN KNUCKLE</u> (STRESS $\div pD_i/2t_e$ )	
Inner surface meridional	= 3.10 (3.57 on weld)
Outer surface meridional	= -1.76 (-2.30 on weld)
Inner surface circumferential	= -3.55 (-3.65 on weld)
Outer surface circumferential	= -4.15 (-5.79 on weld)
<u>IMPORTANT PRESSURES</u> (lbf/in <sup>2</sup> )	
* Pressure for first yield in cylinder (von Mises)	= 120
+ Pressure for first yield in cylinder (Experimental)	= -
* Pressure for first yield in end (von Mises)	= 23
+ Pressure for first yield in end (Experimental)	= 77
Limit pressure (Shield and Drucker)	= 36
Elastic buckling pressure (Thurston and Holston)	= 230
Measured buckling pressure	= 95
Maximum test pressure	= 119
(* Assumed yield stress 18.0 tonf/in <sup>2</sup> ) (+0.1% proof pressure)	
<u>CIRCUMFERENTIAL STRAINS IN CYLINDER</u>	
At buckling pressure	= 0.12%
At maximum test pressure	= 0.16%

UNIVERSITY OF NOTTINGHAM

INTERNAL PRESSURE TESTING OF VERY THIN  
TORISPHERICAL PRESSURE VESSEL ENDS

SUMMARY SHEET

END NO.    17	DATE    May 1974	
MATERIAL:    HIGH PROOF STRESS 304 AUSTENITIC STAINLESS STEEL		
MANUFACTURE:    PRESSED AND SPUN		
<u>NOMINAL DIMENSIONS AND SHAPE PARAMETERS</u>		
Diameter ( $D_i$ )	= 81.0 in	
Knuckle radius ( $r_i$ )	= 6.0 in	$r_i/D_i = 0.074$
Crown radius ( $R_i$ )	= 67.5 in	$R_i/D_i = 0.833$
End height ( $h_i$ )	= 16.59 in	$h_i/D_i = 0.205$
Thickness of end ( $t_e$ )	= 0.128 in	$t_e/D_i = 0.00158$
Thickness of cylinder ( $t_c$ )	= 0.104 in	$t_c/D_i = 0.00128$
<u>MEASURED THICKNESS OF END</u>		
Minimum thickness at k/cyl.	= 0.095 in	
Thickness at centre of knuckle	= 0.118 in (0.113 in on weld)	
<u>PEAK ELASTIC STRESS INDICES IN KNUCKLE</u> (STRESS $\div$ $pD_i/2t_e$ )		
Inner surface meridional	= 2.53 (2.78 on weld)	
Outer surface meridional	= -1.76 (-1.70 on weld)	
Inner surface circumferential	= -2.76 (-3.02 on weld)	
Outer surface circumferential	= -4.15 (-4.71 on weld)	
<u>IMPORTANT PRESSURES</u> (lbf/in <sup>2</sup> )		
* Pressure for first yield in cylinder (von Mises)	= 120	
+ Pressure for first yield in cylinder (Experimental)	= -	
* Pressure for first yield in end (von Mises)	= 28	
+ Pressure for first yield in end (Experimental)	= 84	
Limit pressure (Shield and Drucker)	= 43	
Elastic buckling pressure (Thurston and Holston)	= -	
Measured buckling pressure	= 107	
Maximim test pressure	= 199	
(* Assumed yield stress 18.0 tonf/in <sup>2</sup> ) (+ 0.1% proof pressure)		
<u>CIRCUMFERENTIAL STRAINS IN CYLINDER</u>		
At buckling pressure	= 0.15%	
At maximum test pressure	= -	